frontiers | Research Topics

Leaf functional traits: Ecological and evolutionary implications

Edited by
Peijian Shi, Johan Gielis, Karl J. Niklas, Ülo Niinemets and Julian Schrader

Published in
Frontiers in Plant Science

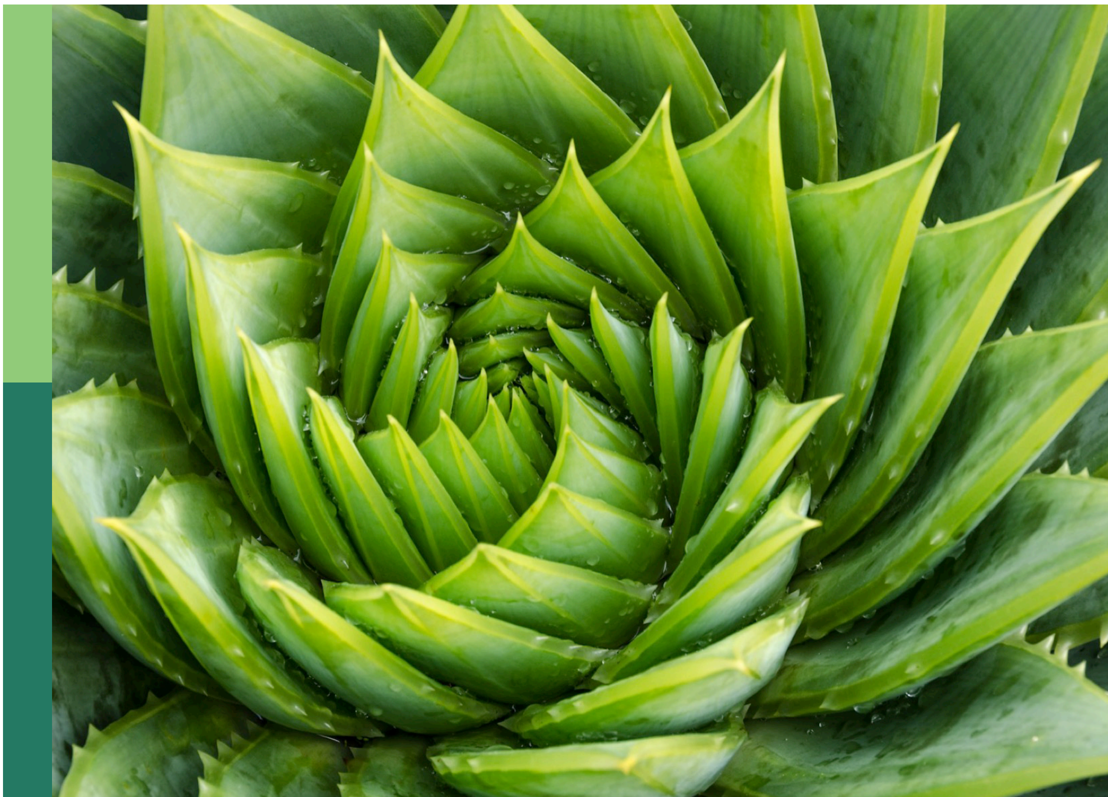

ISSN 1664-8714
ISBN 978-2-83252-086-4
DOI 10.3389/978-2-83252-086-4

About Frontiers

Frontiers is more than just an open access publisher of scholarly articles: it is a pioneering approach to the world of academia, radically improving the way scholarly research is managed. The grand vision of Frontiers is a world where all people have an equal opportunity to seek, share and generate knowledge. Frontiers provides immediate and permanent online open access to all its publications, but this alone is not enough to realize our grand goals.

Frontiers journal series

The Frontiers journal series is a multi-tier and interdisciplinary set of open-access, online journals, promising a paradigm shift from the current review, selection and dissemination processes in academic publishing. All Frontiers journals are driven by researchers for researchers; therefore, they constitute a service to the scholarly community. At the same time, the *Frontiers journal series* operates on a revolutionary invention, the tiered publishing system, initially addressing specific communities of scholars, and gradually climbing up to broader public understanding, thus serving the interests of the lay society, too.

Dedication to quality

Each Frontiers article is a landmark of the highest quality, thanks to genuinely collaborative interactions between authors and review editors, who include some of the world's best academicians. Research must be certified by peers before entering a stream of knowledge that may eventually reach the public - and shape society; therefore, Frontiers only applies the most rigorous and unbiased reviews. Frontiers revolutionizes research publishing by freely delivering the most outstanding research, evaluated with no bias from both the academic and social point of view. By applying the most advanced information technologies, Frontiers is catapulting scholarly publishing into a new generation.

What are Frontiers Research Topics?

Frontiers Research Topics are very popular trademarks of the *Frontiers journals series*: they are collections of at least ten articles, all centered on a particular subject. With their unique mix of varied contributions from Original Research to Review Articles, Frontiers Research Topics unify the most influential researchers, the latest key findings and historical advances in a hot research area.

Find out more on how to host your own Frontiers Research Topic or contribute to one as an author by contacting the Frontiers editorial office: frontiersin.org/about/contact

Leaf functional traits: Ecological and evolutionary implications

Topic editors
Peijian Shi — Nanjing Forestry University, China
Johan Gielis — University of Antwerp, Belgium
Karl J. Niklas — Cornell University, United States
Ülo Niinemets — Estonian University of Life Sciences, Estonia
Julian Schrader — Macquarie University, Australia

Citation
Shi, P., Gielis, J., Niklas, K. J., Niinemets, Ü., Schrader, J., eds. (2023). *Leaf functional traits: Ecological and evolutionary implications*. Lausanne: Frontiers Media SA.
doi: 10.3389/978-2-83252-086-4

Table of contents

frontiers | Frontiers in Plant Science

TYPE Editorial
PUBLISHED 21 March 2023
DOI 10.3389/fpls.2023.1169558

EDITED AND REVIEWED BY
Paolo Giordani,
University of Genoa, Italy

*CORRESPONDENCE
Karl J. Niklas
✉ kjn2@cornell.edu

SPECIALTY SECTION
This article was submitted to Functional Plant Ecology, a section of the journal Frontiers in Plant Science

RECEIVED 19 February 2023
ACCEPTED 09 March 2023
PUBLISHED 21 March 2023

CITATION
Niklas KJ, Shi P, Gielis J, Schrader J and Niinemets Ü (2023) Editorial: Leaf functional traits: Ecological and evolutionary implications. *Front. Plant Sci.* 14:1169558. doi: 10.3389/fpls.2023.1169558

Editorial: Leaf functional traits: Ecological and evolutionary implications

Karl J. Niklas[1]*, Peijian Shi[2], Johan Gielis[3], Julian Schrader[4] and Ülo Niinemets[5,6]

[1]School of Integrative Plant Science, Cornell University, Ithaca, NY, United States, [2]Bamboo Research Institute, Nanjing Forestry University, Nanjing, China, [3]Department of Biosciences Engineering, University of Antwerp, Antwerp, Belgium, [4]School of Natural Sciences, Macquarie University, Sydney, NSW, Australia, [5]Institute of Agricultural and Environmental Sciences, Estonian University of Life Sciences, Tartu, Estonia, [6]Estonian Academy of Sciences, Tallinn, Estonia

KEYWORDS

elevation, lamina centroid, leaf dry mass per area, leaf shape, leaf size, leaf stoichiometry, plant intraspecific trait variation, urbanization

Editorial on the Research Topic
Leaf functional traits: Ecological and evolutionary implications

Foliage provides the primary photosynthetic surfaces of terrestrial vascular plants. Consequently, quantifying and understanding the relationships among the functional traits of leaves are critical to our understanding of terrestrial ecosystem dynamics, nutrient cycles, responses to current global climate change, and the evolutionary trajectories of foliage form and function. Numerous prior studies have investigated relationships among critical leaf functional traits, such as leaf mass, area, shape, nutrient contents, photosynthesis and respiration, stomatal density, stomatal size, leaf vein density, leaf vein length, leaf vein area, areole area (Niklas, 1999; Franks and Farquhar, 2007; Milla and Reich, 2007; Franks and Beerling, 2009; Fiorin et al., 2016; Shi et al., 2021; Shi et al., 2022). However, much remains to be learned, particularly about the functional scaling of leaf characteristics with the traits of other plant organs, with whole plant traits such as plant height and total mass, and how variation in key environmental drivers shape leaf functional traits. The goal of this Research Topic in Frontiers of Plant Science was to bring together a group of ecophysiologists to provide fresh insight into how critical leaf traits respond to environmental variability and what are the implications of environmental-driven variation in leaf traits on plant performance. The Research Topic consists of 15 papers spanning a broad spectrum of research areas ranging from the effects of elevation and water stress on leaf size and shape, urbanization effects, and the influence of a mass extinction event on viable leaf-economic strategies.

Different perspectives on the allometry of leaf scaling

Leaf shape and size play important roles in photosynthetic efficiency of plants through the growing season, and this Research Topic includes four papers looking at fundamental leaf scaling relationships focusing on the effects of plant size, leaf shape, and leaf age that address whether there is disproportionality in mass and area scaling relationships, a phenomenon called "diminishing returns". Ma et al. studied 60 trees of an alpine evergreen oak (*Quercus pannosa*) to test whether tree size affects leaf shape, size, and leaf dry mass per unit area, and to test whether the proportional relationship between leaf area and the product of leaf length and width is a valid metric for calculating the leaf area of the leaves of trees differing in size (Figure 1). They found that tree size significantly influenced leaf shape, size, and leaf dry mass per unit area. Larger trees had larger and broader leaves with lower leaf dry mass per unit area, with lamina centroids closer to the leaf apex than the leaf base. Nevertheless, the proportional relationship between leaf area and the product of leaf length and width was independent of tree size.

To test whether the position of leaf lamina centroid is correlated with the allocation of biomass to the leaf lamina and petiole, Li et al. used a general ovate leaf-shape model to fit the leaf boundary coordinate data of two Lauraceae species, *Cinnamomum camphora* and *Machilus leptophylla*, using >290 leaves for each species. They found that a higher distance from the lamina centroid to the leaf base that connects the petiole and lamina does not necessarily result in a greater investment of mass to the petiole relative to lamina. In fact, the petiole/lamina mass ratio depends on the characteristics of the petiole (which is either short and thick or long and thin).

"Diminishing returns" in leaf economics occurs when lamina mass disproportionately increases with increasing leaf surface area (Niklas et al., 2007). Guo et al. tested whether both leaf fresh and dry mass manifest diminishing returns using a total of 4271 leaves from ten deciduous and two evergreen tree species. The authors demonstrate that leaf fresh mass scales more strongly with leaf area and that deciduous species tend to invest less biomass per unit leaf light-harvesting area than evergreen species. Another paper on leaf allometry by Jiao et al. examines if lamina mass vs. area scaling relationships are influenced by leaf age. They measured the leaf functional traits of five leaf-age groups of the evergreen broad-leaves shrub *Photinia* × *fraseri* using a total of 1,736 leaves, and observed that leaf area, and the ratio of lamina dry mass to lamina fresh mass increases with increasing leaf age. Their data indicate that leaves undergo a transition from resource acquisition to resource conservation during their development and growth.

Leaf economics spectrum: trait relationships and ecological implications through environmental gradients

The leaf economics spectrum includes two easily-assessed traits, specific leaf area (SLA) and leaf dry matter content (LDMC), that scale with the plant resource harvesting strategy of the leaf economics spectrum (Wright et al., 2004). Fast-return species have high SLA and low LDMC, whereas slow-return species have the opposite combination of these traits (Wright et al., 2004). Thus, efforts to characterize the variation in these traits over large scales are very useful to map the functional characteristics of vegetation. Wang et al. investigated the effects of climatic and soil factors on plant resource utilization strategies using data collected from 926 plots across 163 forests in China and confirm the presence of significant differences in SLA and LDMC among plant functional types. In addition, they show that SLA decreases with increasing temperature and decreasing rainfall amount, and vegetation growing in these conditions exhibit conservative resource utilization. These findings are useful for predicting the effect of increasing global temperatures on plant resource utilization in the studied ecosystems.

The functional traits of leaves and the traits of other plant organs change in a correlated manner because the plant body is an integrated phenotype. In addition, annual and perennial species often manifest different traits. In general, annual species are characterized by a more rapid resource acquisition strategy compared to perennials (e.g., short leaf life-spans, higher specific leaf area, and leaf nutrient concentrations) (Lusk, 2019; Niinemets, 2020). However, there are fewer comparisons among root traits between annuals and perennials (Roumet et al., 2006), particularly in arid and semi-arid areas. Ning et al. examined 12 leaf and root traits of 54 dominant species from Northeastern China and report, among other differences, that annuals have higher individual leaf area and specific root length, but lower leaf dry matter content, leaf tissue density, and leaf and fine root dry matter content compared to perennials. Their findings indicate that annuals and perennials are characterized by distinct suites of leaf and root traits, and biomass allocation strategies, leading to differences in resource acquisition. These differences collectively provide an explanation for variation in species adaptability to water limitations in dry grasslands.

The large-scale effects of global climate change on grassland productivity remain poorly understood, and studies of leaf traits can provide important insights into how vegetation may likely respond to global changes. Using 182 grassland samples established in 17 alpine meadows (AM) and 21 desert steppes (DS) in China, Wang et al. show that the net primary productivity (NPP) of alpine meadows is higher than that of desert steppes and that NPP increases with increasing leaf nitrogen content and leaf phosphorus content, but decreases with increasing leaf dry matter content. These and other findings provide additional insights for predicting the effects of global climate change on the NPP of grasslands.

Elevation is one of the driving factors leading to leaf trait variation (Midolo et al., 2019). Yang et al. measured six leaf traits of 257 woody species at 26 elevations ranging from 1,050 to 3,500 m within the Tibetan Plateau and analyzed the scaling relationships among leaf fresh and dry mass, and area. Their analyses indicate that plants respond to differences in elevation by changing leaf area and biomass investment and coordinating scaling relationships among traits, although leaf trait variation along the elevation gradient had a

FIGURE 1
Quercus pannosa growing in Shangri-la, Yunnan Province, China (Provided by Dr. Jianzhong Ma). Environmental factors and tree size can significantly affect the leaf functional traits (see Ma et al. in this special issue).

minor effect on the numerical values of scaling exponent. In two other studies of the effects of altitude on plant functioning, Zhang et al. and Li et al. looked at plant intraspecific trait variation (ITV) along elevational gradients. Zhang et al. compared the leaf stoichiometry of the Northern hemisphere generalist perennial species *Potentilla anserina* growing at different elevations in the Middle-Eastern part of Qilian Mountains. With an increase in elevation, leaf carbon concentrations were observed to decrease, whereas leaf nitrogen concentration and leaf nitrogen to phosphorous concentration ratio increase, indicating that phosphorus imposes a stronger limitation of growth on *P. anserina* at higher elevations. Overall, this study confirms that plants acclimate to changes in elevation by altering the stoichiometry of their leaves to enhance carbon gain during shorter and cooler growing seasons. However, in this specific setting, acclimation to shorter and cooler growing conditions was limited by phosphorus availability. Li et al. studied ITV in the endangered dioecious *Taxus fuana* in small isolated populations endemic to the Himalayas region. They examined 18 leaf traits from 179 ovulate and pollen bearing trees along an elevational gradient in Gyirong County, Tibet, China, and they assessed ITV and sources of variation in leaf traits. Pollen bearing ("male") plants were more tolerant to the environmental stresses at higher elevation, whereas the leaf traits of ovulate ("female") plants were more responsive to elevation. However, the stronger plasticity of "females" was not associated with improved fitness. Unfortunately, these differences are likely to be detrimental to the maintenance of *T. fuana* populations.

The papers in this section significantly enlarge our understanding of leaf trait correlations, trait correlations across plants, and highlight multiple opportunities to study how leaf traits can be used to understand how plants interact with the environment and current and future climates.

Role of leaf traits in environmental stress responses

Plants have evolved an array of mechanisms to deal with environmental stress. Among different environmental stresses, water availability is a key environmental factor affecting plant species distributions. However, the adaptive responses of congeneric species among sites differing in soil water availabilities remains unclear. Zhang et al. examined leaf economics and stem hydraulic traits in two *Quercus wutaishanica* dominated forests, a humid site in Qinling Mountains and a dry site in Loess Plateau, asking whether congeneric species have different economic and hydraulic traits across regions. They observed greater hydraulic safety and a stronger coordination of leaf economics and stem hydraulic traits in the dry site, and a greater hydraulic efficiency in the humid site. These results demonstrate that congeneric species utilize different types of adaptation mechanisms to maximize fitness in environments with different water availability. To further extend our understanding of the role of traits explaining species success along water availability gradients, Wang and Wen established two transects in the grasslands of Losses Plateau (LP) and Inner Mongolia Plateau (MP) to examine the distribution of intrinsic leaf water use efficiency (i.e., the ratio of net assimilation rate per unit stomatal conductance to water vapor) in coexisting species along aridity gradients. Intrinsic water use efficiency (iWUE) is a critical ecophysiological trait that characterizes the capacity of plants to cope with water- and nutrient-limited habitats in arid and semi-arid regions. The relationships between iWUE and a multi-dimensional functional trait spectrum indicated that species have evolved species-specific strategies to adapt to aridity by partitioning limiting resources. Thus far, the ranges of variation of iWUE in coexisting species along aridity gradients and the factors controlling the magnitude of interspecific variation have been poorly known. These findings highlight the interactive effects of limiting resources and leaf functional traits on plant adaptation strategies exploited to enhance iWUE.

In this Research Topic, Luo et al. have taken a biochemical approach to gain insight into acclimation responses to excess and limited water availabilities. In particular, they examined the time-dependent changes in ascorbate (AsA) and glutathione (GSH) contents, and the activities of enzymes involved in the AsA-GSH cycle in the perennial grass *Deschampsia caespitosa* in response to waterlogging and drought stresses. The authors reported that, in general, the activity of the AsA-GSH metabolic pathway increased with increasing both waterlogging and drought stress severity to reduce oxidative stress. Their findings provide information of biochemical responses of *D. caespitosa* to changes in water regimes, and as such constitute an important step for accelerating ecological restoration of degradation alpine marshes in the Qinghai-Tibetan Plateau.

Urbanization affects a range of morphological and physiological plant traits. However, plants can adopt different strategies to acclimate to urbanization pressures (Calfapietra et al., 2015). Xiao et al. examined the physiological and photosynthetic properties and heavy metal concentrations of four different plant functional groups (i.e., herbs, shrubs, subcanopy trees, and canopy trees, with eight species in total) located in urban, suburban, and rural areas. The authors report that canopy and subcanopy species acclimated to urbanization by reducing resource acquisition, but improving defense capacity, whereas the herb and shrub species improve resource acquisition as an acclimation response to urbanization. The evidence that different plant functional groups respond differently to urbanization is a valuable addition to our understanding plant adaptability to highly stressful urban environments and of high practical value for urban forestry.

The plant stress papers in this Research Topic jointly indicate that leaf traits are highly informative for assessing the severity of stress, and the degree of and capacity for stress acclimation.

Application of leaf traits to understand patterns in the past

Finally, we turn to using leaf functional traits to inform us about the distant past. The Chicxulub bolide impact has been linked to a mass extinction of plants at the Cretaceous—Paleogene boundary (KPB) approximately 66 Mya, but how this event affected the evolution of plant ecological strategies has been understudied. Butrim et al. studied 1303 fossil leaves from KPB sediments in the Denver Basin, Colorado. Using a leaf allometry-based method to estimate leaf dry mass per area (LMA), they found no evidence for a shift in LMA across the KPB. However, in the Denver Basin, local environmental conditions appear to have played a larger role in determining viable leaf-economic strategies than any potential global signal associated with the Chicxulub bolide impact.

Outlook

This collection of papers covers a broad range of topics that nevertheless all focus on the central question of how leaf functional traits inform our understanding of plant performance at different levels of biological organization. This collection emphasizes that we have only begun to fully uncover the many complex interrelationships among leaf traits, and their relationships to the traits of other plant organs, particularly roots. This suite of papers also highlights a number of broad and unique variation patterns in leaf traits in response to environmental limitations across gradients of water availability and along elevational gradients. It also demonstrates that different combinations of traits determine plant adaptability to specific environmental conditions. Although broad-scale variation patterns among key leaf traits have been identified in the past, the papers in this collection demonstrate that it is highly relevant to analyze the trait relationships in specific environmental contexts to draw inferences of plant performance, and to accurately predict changes in future vegetation. We hope that this Research Topic inspires future research in this challenging but vital and fruitful field of study.

Author contributions

KN conceived and produced the first draft. ÜN reorganized, revised, and extended the subsequent version of the MS, and PS, JG, and JS edited the final draft. All authors contributed to the article and approved the submitted version.

Acknowledgments

We thank Drs. Ze-Xin Fan, Raquel Lobo-do-Vale, Boris Rewald, and Ji Zhang for participating in handling some manuscripts in this Research Topic.

Conflict of interest

The authors declare that the research was conducted in the absence of any commercial or financial relationships that could be construed as a potential conflict of interest.

Publisher's note

References

Calfapietra, C., Peñuelas, J., and Niinemets, Ü. (2015). Urban plant physiology: Adaptation-mitigation strategies under permanent stress. *Trends Plant Sci.* 20, 72–75. doi: 10.1016/j.tplants.2014.11.001

Fiorin, L., Brodribb, T. J., and Anfodillo, T. (2016). Transport efficiency through uniformity: Organization of veins and stomata in angiosperm leaves. *New Phytol.* 209, 216–227. doi: 10.1111/nph.13577

Franks, P. J., and Beerling, D. J. (2009). Maximum leaf conductance driven by CO_2 effects on stomatal size and density over geologic time. *Proc. Natl. Acad. Sci. U.S.A.* 106, 10343–10347. doi: 10.1073/pnas.0904209106

Franks, P. J., and Farquhar, G. D. (2007). The mechanical diversity of stomata and its significance in gas-exchange control. *Plant Physiol.* 143, 78–87. doi: 10.1104/pp.106.089367

Lusk, C. H. (2019). Leaf functional trait variation in a humid temperate forest, and relationships with juvenile tree light requirements. *Peer J.* 7, e6855. doi: 10.7717/peerj.6855

Midolo, G., De Frenne, P., Hölzel, N., and Wellstein, C. (2019). Global patterns of intraspecific leaf trait responses to elevation. *Glob. Change Biol.* 25, 2485–2498. doi: 10.1111/gcb.14646

Milla, R., and Reich, P. B. (2007). The scaling of leaf area and mass: The cost of light interception increases with leaf size. *Proc. R. Soc Biol. Sci.* 274, 2109e2114. doi: 10.1098/rspb.2007.0417

Niinemets, Ü. (2020). Leaf trait plasticity and evolution in different plant functional types. *Ann. Plant Rev.* 3, 473–522. doi: 10.1002/9781119312994.apr0714

Niklas, K. J. (1999). A mechanical perspective on foliage leaf form and function. *New Phytol.* 143, 19–31. doi: 10.1046/j.1469-8137.1999.00441.x

Niklas, K. J., Cobb, E. D., Niinemets, Ü, Reich, P. B., Sellin, A., and Shipley, B. (2007). "Diminishing returns" in the scaling of functional leaf traits across and within species groups. *Proc. Natl. Acad. Sci. U.S.A.* 104, 8891–8896. doi: 10.1073/pnas.0701135104

Roumet, C., Urcelay, C., and Diaz, S. (2006). Suites of root traits differ between annual and perennial species growing in the field. *New Phytol.* 170, 357–368. doi: 10.1111/j.1469-8137.2006.01667.x

Shi, P., Jiao, Y., Diggle, P. J., Turner, R., Wang, R., and Niinemets, Ü. (2021). Spatial distribution characteristics of stomata at the areole level in *Michelia cavaleriei* var. *platypetala* (Magnoliaceae). *Ann. Bot.* 128, 875–885. doi: 10.1093/aob/mcab106

Shi, P., Miao, Q., Niinemets, Ü., Liu, M., Li, Y., Yu, K., et al. (2022). Scaling relationships of leaf vein and areole traits versus leaf size for nine magnoliaceae species differing in venation density. *Amer J. Bot.* 109, 899–909. doi: 10.1002/ajb2.1856

Wright, I. J., Reich, P. B., Westoby, M., Ackerly, D. D., Baruch, Z., Bongers, F., et al. (2004). The worldwide leaf economics spectrum. *Nature* 428, 821–827. doi: 10.1038/nature02403

frontiers
in Plant Science

ORIGINAL RESEARCH
published: 30 November 2021
doi: 10.3389/fpls.2021.773676

Plant Functional Groups Dominate Responses of Plant Adaptive Strategies to Urbanization

Yihua Xiao[1], Shirong Liu[2], Manyun Zhang[3,4]*, Fuchun Tong[5], Zhihong Xu[4], Rebecca Ford[4], Tianlin Zhang[1], Xin Shi[1], Zhongmin Wu[1] and Tushou Luo[1]

[1] Research Institute of Tropical Forestry, Chinese Academy of Forestry, Guangzhou, China, [2] Research Institute of Forest Ecology, Environment and Protection, Chinese Academy of Forestry, Beijing, China, [3] College of Resources and Environment, Hunan Agricultural University, Changsha, China, [4] Environmental Futures Research Institute, School of Environment and Science, Griffith University, Brisbane, QLD, Australia, [5] College of Forestry and Landscape Architecture, South China Agricultural University, Guangzhou, China

Urbanization causes alteration in atmospheric, soil, and hydrological factors and substantially affects a range of morphological and physiological plant traits. Correspondingly, plants might adopt different strategies to adapt to urbanization promotion or pressure. Understanding of plant traits responding to urbanization will reveal the capacity of plant adaptation and optimize the choice of plant species in urbanization green. In this study, four different functional groups (herbs, shrubs, subcanopies, and canopies, eight plant species totally) located in urban, suburban, and rural areas were selected and eight replicated plants were selected for each species at each site. Their physiological and photosynthetic properties and heavy metal concentrations were quantified to reveal plant adaptive strategies to urbanization. The herb and shrub species had significantly higher starch and soluble sugar contents in urban than in suburban areas. Urbanization decreased the maximum photosynthetic rates and total chlorophyll contents of the canopies (*Engelhardtia roxburghiana* and *Schima superba*). The herbs (*Lophatherum gracile* and *Alpinia chinensis*) and shrubs (*Ardisia quinquegona* and *Psychotria rubra*) species in urban areas had significantly lower nitrogen (N) allocated in the cell wall and leaf δ^{15}N values but higher heavy metal concentrations than those in suburban areas. The canopy and subcanopy (*Diospyros morrisiana* and *Cratoxylum cochinchinense*) species adapt to the urbanization via reducing resource acquisition but improving defense capacity, while the herb and shrub species improve resource acquisition to adapt to the urbanization. Our current studies indicated that functional groups affected the responses of plant adaptive strategies to the urbanization.

Keywords: urbanization, plant functional groups, maximum photosynthetic rate, heavy metal, leaf N allocation

Edited by:
Peijian Shi,
Nanjing Forestry University, China

Reviewed by:
Shidan Zhu,
Guangxi University, China
Faming Wang,
South China Botanical Garden,
Chinese Academy of Sciences (CAS),
China

***Correspondence:**
Manyun Zhang
manyunzhang@126.com

Specialty section:
This article was submitted to
Functional Plant Ecology,
a section of the journal
Frontiers in Plant Science

Received: 10 September 2021
Accepted: 20 October 2021
Published: 30 November 2021

Citation:
Xiao Y, Liu S, Zhang M, Tong F,
Xu Z, Ford R, Zhang T, Shi X, Wu Z
and Luo T (2021) Plant Functional
Groups Dominate Responses of Plant
Adaptive Strategies to Urbanization.
Front. Plant Sci. 12:773676.
doi: 10.3389/fpls.2021.773676

INTRODUCTION

Urbanization, through conversions of natural or agricultural environments to urban environments and population mobility from rural to urban areas, has generated overwhelming impacts on the territorial ecological system (Sala et al., 2000; Zhao et al., 2016). Globally, the geographical areas that are influenced by urbanization are estimated to triple in size from 2000 to 2030

(Seto et al., 2012). Relative to suburban areas, high population densities and intensive anthropogenic activities in urban areas have led to marked alterations in atmospheric, soil, and hydrological environmental factors (Sala et al., 2000; Beaumont et al., 2008; Zhao et al., 2016). Urbanization also resulted in an increase in environmental pollution originating from fossil fuel burning, gas emissions of vehicles, and industrial production. At the same time, urban heat islands have caused large effects from elevated temperatures on surrounding suburbia and hinterlands (Ferguson and Woodbury, 2007; Beaumont et al., 2008). These negative effects may be decreased partially through enhancing urban vegetation surface and density. For instance, urban vegetation tremendously reduced nitrogen dioxide, particulate matter, heavy metals, and heat island effects (Qiu et al., 2009; Pugh et al., 2012; Janhäll, 2015; Livesley et al., 2016). Understanding how urban vegetation responses and adapts to the urban environment is crucial for plant species choice or selection in urban green practice.

Within the urban vegetation communities, influential ecological factors to which an individual plant must adapt include water availability, atmospheric nitrogen (N) and phosphorus (P) dispositions, and pollutant exposure. Without these adaptive abilities, an individual plant would not leave descendants or clades to flourish (Wiens et al., 2010). Plant functional types can significantly influence the leaf traits (Shi et al., 2020) and the light, heat, and N dispositions and pollutant exposure could directly affect the photosynthesis, leaf properties, plant physiology, and, thereby, the vegetation community (Quigley, 2002; Zhao et al., 2016; Liu et al., 2020). For instance, Quigley (2002, 2004) suggested that trees in urban areas grew slower than those in rural areas due to environmental stresses such as higher temperature and water limitation. Conversely, tree seedlings in New York City grew twice as fast compared to those in the rural areas (Gregg et al., 2003), and Zhao et al. (2016) also demonstrated that an urban environment accelerates vegetation growth. In addition, urbanization might affect a range of morphological and physiological plant traits, and correspondingly, the plants might adopt different strategies to adapt to the urbanization promotion or pressure (Gregg et al., 2003; Hahs and Mcdonnell, 2007; Zhao et al., 2016). However, to the best of our knowledge, few studies have been conducted to reveal the physiological responses of different plants to the urbanization.

The plants could be divided into different functional groups: herbs, shrubs, subcanopies, and canopies according to their heights and external sizes. We hypothesized that the urbanization might discrepantly affect the different fictional plant groups. Moreover, the plants could remove urban environmental pollution, and therefore, it was also hypothesized that the urbanization might exert negative impacts on the subcanopies and canopies with large external sizes. Functional trait provides an opportunity to optimize urban vegetation species choice. To assess these issues, we conducted a study in the Pearl River Delta region, Southern China, to quantify the responses of different functional group plants to urbanization. The Pearl River Delta region is urbanizing rapidly, and currently, it is also one of the largest urban areas worldwide (Cai et al., 2017). Four different functional groups (eight plant species totally) located in urban and suburban areas were selected and their adaptive strategies to urbanization were assessed via leaf traits, heavy metal content, photosynthesis, and N status. Results from this study will benefit our understandings of the physiological responses to the urbanizations and the species selections in urban green practice and managements.

MATERIALS AND METHODS

Experimental Design and Sampling

Three different sites were selected to study the impacts of urbanization on plants (**Supplementary Figure 1**): the Urban Forest Park (UFP), the Suburban Forest Park (SFP), and the Rural Nature Reserve (RNR), which served as the three different treatments. The UFP (23°16′N, 113°22′E) was located in Baiyun District, Guangzhou, and served as the reference setting in this study, with a subtropical monsoon climate. In the UFP, the average annual temperature was 21.8°C and the average annual precipitation was 1,860 mm, with more than 80% of the rainfall being concentrated from April to September. The SFP (23°32′N, 113°45′E) and the RNR (24°07′N, 114°08′E) sites were approximately 70 and 150 km away from the UFP, respectively. They had similar subtropical monsoon climates: average annual temperatures were 20.7 and 19.5°C and average annual precipitations were 1,625 and 1,690 mm. The nitrogen (N) deposition and soil heavy metal concentration of the UFP were always the highest among the three sites, and more details are demonstrated in **Supplementary Table 1**. Eight common plant species at the three sites were selected: the herb species *Lophatherum gracile* and *Alpinia chinensis*, the shrub species *Ardisia quinquegona* and *Psychotria rubra*, the subcanopy species *Diospyros morrisiana* and *Cratoxylum cochinchinense*, and the canopy species *Engelhardtia roxburghiana* and *Schima superba*. Each treatment had eight replicated plants for each species at each site, with the total plant number being 192 (3 sites × 8 species × 8 replications of each species).

The healthy and mature leaves of the selected plant species were sampled for photosynthetic rate, light respiration rate, and other photosynthetic parameters measurement on sunny days (9:00–12:00 am) of August. After measurement, the leaves were collected to divide into three parts: one for leaf morphology and element concentration analysis; one for starches, sugars, and lipids determination; and the last one was frozen in liquid N_2 and stored at −80°C for chlorophyll, ribulose-1, 5-bisphosphate carboxylase/oxygenase (Rubisco), and cell N contents determination.

Leaf Traits Measurements

A total of 10 healthy leaves from each species were quantified with an electronic balance. Leaf thickness and surface area were measured with a thickness meter (Expolt, Expolt Ltd., PRC, Taiwan, China) and leaf area scanner (Biosciences, Lincoln, NE, United States), respectively. The leaves were dried at 105°C for 30 min and then at 70°C until they achieved a constant mass. The dry biomass was recorded.

The dried leaves were ground and passed through a 0.15-mm mesh sieve and digested with $HClO_4$-H_2SO_4. The carbon (C) and N contents in the digested fractions were quantified with an elemental analyzer (Elementar Vario EL III, Hanau, Germany), and P content was assessed with the molybdenum antimony colorimetric method (Lu, 2000; Zhang et al., 2018). Abundances of ^{13}C and ^{15}N in the dried leaves were analyzed with an IsoPrime 100 mass spectrometer (Cheadle Hulme, United Kingdom), and intrinsic water use efficiency was also calculated based on the abundances of ^{13}C (Osmond et al., 1980; Huang et al., 2016).

Leaf Heavy Metal Concentration and Organic Matter Determination

Concentrations of heavy metals such as cadmium (Cd), chromium (Cr), copper (Cu), nickel (Ni), lead (Pb), and zinc (Zn) were determined by using an acid digestion method at atmospheric pressure. The dried leaf samples were placed in a 150-ml Erlenmeyer flask, mixed with hydrofluoric acid and nitric acid, and digested at 190°C. The mixtures were filtered and the concentrations of heavy metals in the solution were determined by the ICP-OES (Palo Alto, CA, United States). Data quality was also checked with national standard reference material (ESS-3) supplied by the China National Environmental Monitoring Centre. Heavy metal concentrations were expressed as an oven-dried mass.

The concentrations of starch in the leaves were determined according to the method of Smith and Zeeman (2006). Approximately, 0.2 g of dried leaf powder was extracted by 80% ethanol (80°C water bath) three times and the starch was quantified by measuring the hydrolyzed glucose content. Plant leaves were also extracted with a mixed solution (water, methanol, and chloroform), and then the contents of soluble sugar and soluble phenolic and lipid in the leaves were determined according to the method of Liu et al. (2016). After the extraction, the residue leaf samples were boiled in 3% hydrochloric acid (HCl) (v/v) for 3 h and the insoluble sugars in the supernatants were determined according to the method of Liu et al. (2016). The results of starch, soluble sugar, soluble phenol, lipid, and insoluble sugar contents were all converted and recorded as mg g^{-1} dry leaf.

Leaf Photosynthetic Parameter Determination

Intact and healthy leaves were selected from the branches to construct photosynthetic light and carbon dioxide (CO_2) response curves and determine stomatal conductance, intercellular CO_2 concentration, and transpiration rate with a Li-6400XT portable photosynthetic system (Biosciences, Lincoln, NE, United States). In order to determine maximum photosynthetic rate, light component point, saturation irradiance, and respiration rate, the light response curves were constructed and fitted by using 14 different photosynthetic photon flux density (PPFD) gradients (1,500, 1,200, 1,000, 800, 500, 300, 200, 120, 100, 80, 60, 50, 20, and 0 μmol m^{-2} s^{-1}); 400 μmol mol^{-1} CO_2; 55–65% air humidity; 30°C leaf temperature; 1.5 kPa vapor pressure; and 30 min of induction time. The maximum carboxylation rate and maximum electron transport rate were quantified from the CO_2 response curve with the methods of previous studies (Farquhar and von Caemmerer, 1982; Loustau et al., 1999). The CO_2 curve was constructed under the conditions of 400, 300, 260, 200, 180, 150, 120, 100, 80, 60, 50, and 20 μmol·mol^{-1} CO_2. Prior to this, the leaves were exposed to saturated PPFD for 30 min to reach full photosynthetic induction. Subsequently, stomatal conductance, intercellular CO_2 concentrations, and transpiration rates were determined under saturated PPFD for each sample. Instantaneous water use efficiency was calculated by the ratio of the maximum photosynthetic rate and transpiration rate. Photosynthetic N or P use efficiency was calculated as follows (Hidaka and Kitayama, 2009):

$$\text{Photosynthetic N (or P) use efficiency} = \frac{\text{Maximum photosynthetic rate}}{total\ N\ (or\ P)\ content/leaf\ surface}$$

Leaf Chlorophyll Content and N Allocation Determination

Leaf chlorophyll content was determined within 24 h after fresh leaf sampling according to existing methods with minor modifications (Lichtenthaler and Buschmann, 2001; He et al., 2018). A leaf puncher was employed to cut three pieces (1 cm^2) from the center blade of each fresh leaf and 30 pieces of the blade (10 leaves × 3 pieces of each leaf) were mixed together, ground, and extracted with 80% acetone in the dark. After filtering, chlorophyll a and b concentrations were calculated (Lichtenthaler and Buschmann, 2001; He et al., 2018).

Leaf Rubisco content was determined by the method of Makino et al. (1986). Approximately, 0.5 g of the leaf blade was ground, mixed with Tris-HCl buffer, and centrifuged at 4°C for 30 min. The supernatant was electrophoresed on sodium dodecyl sulfate (SDS)-polyacrylamide gel, stained with Coomassie Brilliant Blue for 12 h, and then decolorized. The gel band containing Rubisco was cut and eluted in a 50°C water bath. The Rubisco concentration was determined at 595 nm with a spectrophotometer, and bovine serum albumin was used as the standard. The N contents of cell walls were determined with the method of Harrison et al. (2009). Freeze-dried leaves (approximately 100 mg) were mixed with 15 ml buffer containing 1% polyvinyl pyrrolidine and centrifuged for 5 min. Precipitates were resuspended in 1% SDS buffer, heated to 90°C for 5 min, centrifuged for 5 min, washed with KOH, ddH_2O, and ethanol, and dried at 80°C. The N content in the remaining matter was quantified with the elemental analyzer and recorded as the N contents of leaf cell walls. Area-based N content was calculated with the leaf N content to leaf surface ratio. The proportions of leaf N allocated to the photosynthetic system, Rubisco, carboxylation, bioenergetics, light-harvesting component, and cell wall were calculated according to the formula described in previous studies (Niinemets and Tenhunen, 1997; Xiao et al., 2018).

Statistical Analysis

The two-way ANOVA was employed to determine the effect of urbanization and species on the test parameters and significant differences of urbanization for the same species among different sites were quantified by Duncan's multiple range test. The Pearson's correlation was used to quantify the linear correlations among the maximum photosynthetic rate and leaf area, leaf thickness, heavy metal concentration, and leaf N status. Leaf parameters were divided into four different groups: resource acquisition (specific leaf area, total N and P, maximum photosynthetic rate, and photosynthetic N use efficiency); adaption (water use efficiency, ^{13}C, and^{15}N); defense (leaf thickness and soluble sugar and starch); and resistance (soluble phenol, liquid, and N allocation to cell wall) and they were analyzed with the confirmatory factor analysis to reveal their adaptive strategies to urbanization.

RESULTS

Plant Leaf Morphological Traits

The effects of urbanization on leaf appearances were also dominated by the plant functional group differentiation. Although the herbs located at the different sites had approximately similar leaf biomasses (**Supplementary Figure 2**), dry leaf biomass of the shrub *A. quinquegona* located in the UFR was significantly ($p < 0.05$) lower than that in the SFR (**Supplementary Figure 2b**). There were also significant differences in the dry leaf biomasses of the subcanopies, with the lowest being in the species located in the UFP. The leaves of herbs or shrubs located in the UFR were thinner but larger compared to those of their suburban and rural counterparts (**Supplementary Figures 2c,d**), but the canopies had the opposite trends (thicker but smaller leaves). Meanwhile, the specific leaf area among the different sites had similar trends to those of leaf surface, with the values of herbs, shrubs, and subcanopies located in the UFP being significantly ($p < 0.05$) higher than those of their suburban and rural counterparts (**Supplementary Figure 2e**). However, relative to the UFP, the specific leaf areas of the canopies *E. roxburghiana* and *S. superba* in the RNR were 17.2 and 37.3% higher, respectively.

Leaf Stoichiometry, Isotope Composition, and Intrinsic Water Use Efficiencies

Compared with those grown in the RNR, the leaf C, N, and P contents of the shrub *A. quinquegona* in the UFP were 6.4, 68.7, and 25.4% higher, respectively, and the leaf C, N, and P contents of the shrub *P. rubra* grown in the UFP increased by 7.1, 67.0, and 37.7%, respectively (**Figures 1A–C**). However, the canopies of plants grown in the UFP had negligible variation in the leaf C contents but were significantly decreased in the leaf P contents relative to those grown in the RNR. The urban environment also tended to increase the ratios of leaf N to P (**Figure 1D**).

The eight plant species had significant differences in leaf δ^{13}C values among the three sites. The leaf δ^{13}C values of herbs and shrubs located in the UFP were significantly ($p < 0.05$) lower than their suburban counterparts, which are opposite to the situation in the canopies (**Figure 1E**). In the subcanopy species, the lowest leaf δ^{13}C values were detected in plants located in the SFR and the RNR, respectively. However, the δ^{15}N values of all the plants in the UFP were lowest among the three different sites and were significantly ($p < 0.05$) lower than those located in the RNR. The intrinsic water use efficiencies of the eight plant species were also significantly affected by urbanization and the herbs, shrubs, and canopies had different trends of the water use efficiencies among the three sites (urban > suburban in herbs and shrubs, but urban < suburban in canopies).

Organic Matter Content and Heavy Metal Concentration in Leaves

The effects of urbanization on the organic matter in leaves were also dominated by the plant functional group differentiation (**Supplementary Figure 3**). Compared with the suburban and rural counterparts, the herbs and shrubs grown in the urban areas had significantly higher starch and soluble sugar contents. However, the differences between the plants grown in urban *vs.* suburban areas gradually diminished and even changed to be negative as the plant height increased (**Supplementary Figures 3a,b**). The leaf starch and soluble content levels of the canopy *E. roxburghiana* grown in the UFP were 80.0 and 58.4% of those grown in the SFP. For the soluble phenol and lipid contents, the numerical value of the herbs and shrubs of the urban were lower than those of the suburban, but the canopies results were reversed (**Supplementary Figures 3c,d**). There were inconsistent trends in the insoluble sugar content of plants at different sites and the canopy *E. roxburghiana* of the urban site contained the highest insoluble sugar content among all the samples (**Supplementary Figure 3e**).

Heavy metal concentrations in the leaves of all the eight plant species grown in urban areas were higher than those grown in the suburban and rural areas, with the sole exception of Cd content in *A. quinquegona* (**Figure 2**). Significant differences in leaf Ni concentrations were detected among *L. gracile*, *A. quinquegona*, and *E. roxburghiana* (**Figure 2A**), and the shrubs, subcanopies, and canopies all had significant differences in leaf Cu concentration at different sites (**Figure 2B**). Also, significant differences in Pb and Cr concentrations were found among their subcanopies at different sites (**Figure 2C,D,F**).

Chlorophyll Content and Leaf Photosynthetic Properties

Leaf chlorophyll, a content of the herbs and shrubs grown in the UFP, was significantly higher than those grown in the suburban and rural areas; however, the total chlorophyll differences between the urban and suburban plants changed from positive to negative with the plant height increases (**Figures 3A,C**). The *L. gracile*, *E. roxburghiana*, and *S. superba* species were significantly different in their leaf chlorophyll b contents among the three sites assessed (**Figure 3B**). Relative to the UFP, leaf chlorophyll b contents of the SFP grown plants were 13.7, 14.2, and 13.8% lower for the *L. gracile*, *E. roxburghiana*, and

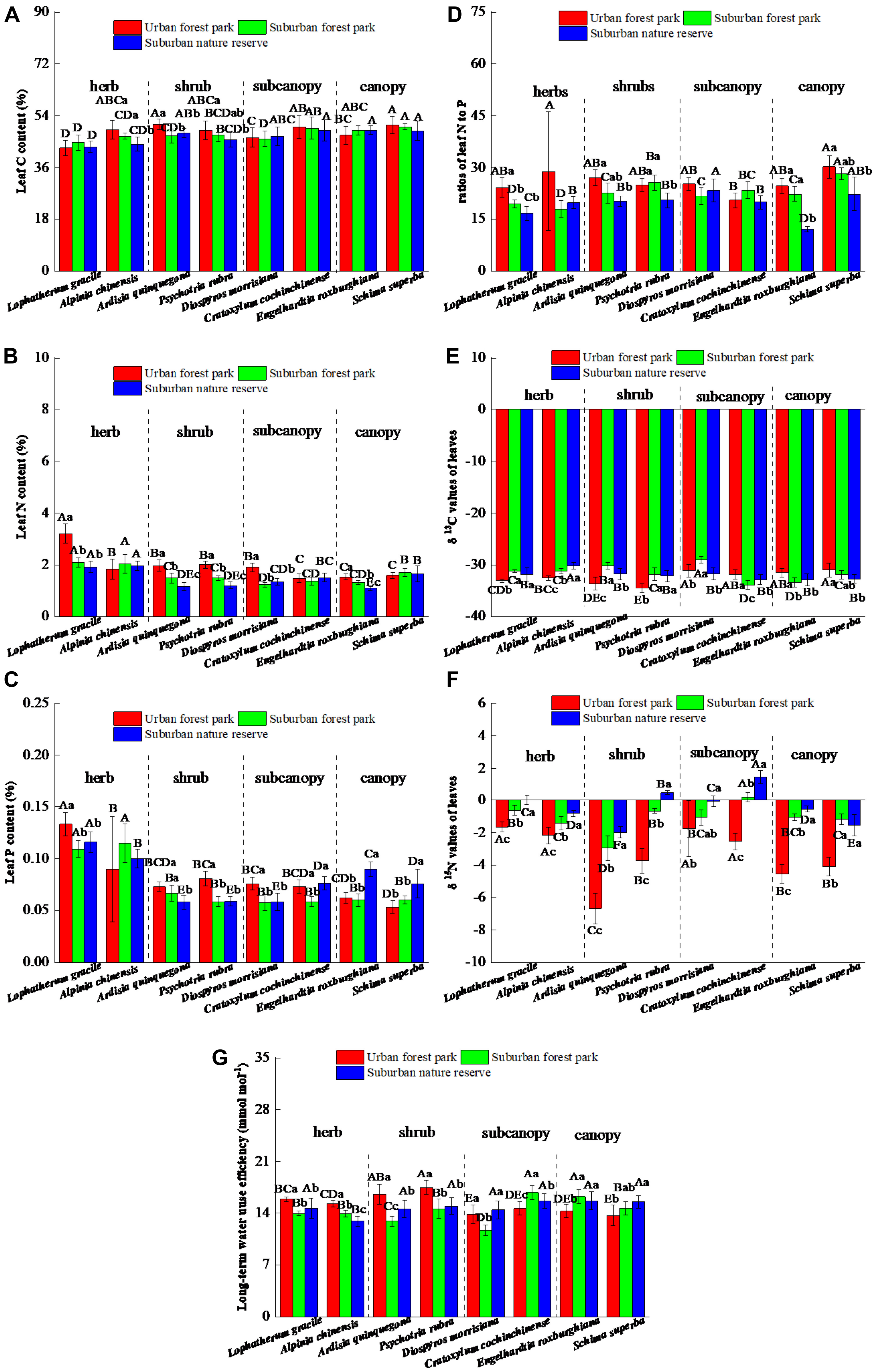

FIGURE 1 | Effects of growth environment on **(A)** C content, **(B)** N content, **(C)** P content, **(D)** ratios of N to P, **(E)** $\delta\ ^{13}$C, **(F)** $\delta\ ^{15}$N, and **(G)** long-term water use efficiency of leaves of eight plant species. The lowercase letters reveal the significant differences ($P < 0.05$) of the same species among different growth environments, and the capital letters reveal the significant differences ($P < 0.05$) of different species in the same growth environment.

S. superba, respectively. The trends of chlorophyll a to b ratios among the three different sites were similar to those of leaf chlorophyll a (**Figure 3D**).

The effects of urbanization on the photosynthetic properties of leaves were dominated by the plant functional group differentiation (**Figure 4**). Relative to the suburban counterparts, the herbs and shrubs in the urban area had higher maximum photosynthetic rates, but the canopies of the suburban areas had significantly ($p < 0.05$) higher maximum photosynthetic rates than their urban counterparts (**Figure 4A**). The differences in maximum carboxylation rate and maximum potential rate of electron transport between the plants grown in the urban and

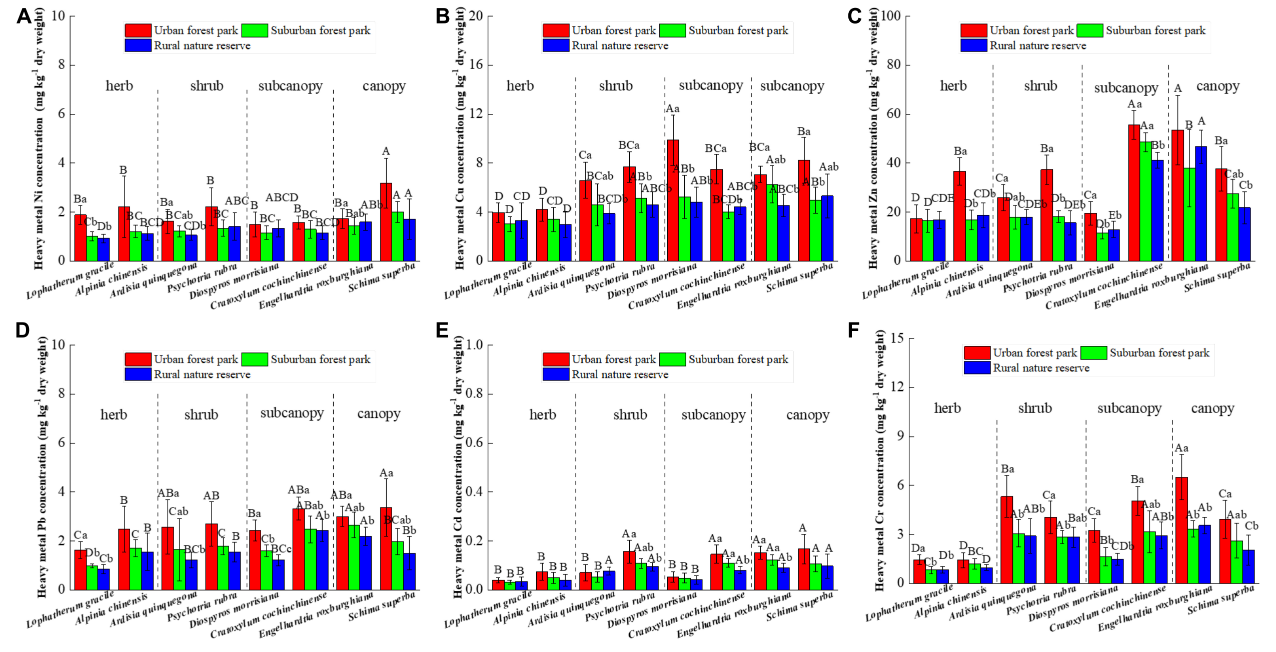

FIGURE 2 | Effects of growth environment on heavy metal **(A)** Ni, **(B)** Cu, **(C)** Zn, **(D)** Pb, **(E)** Cd, and **(F)** Cr concentrations of leaves of eight plant species. The lowercase letters reveal the significant differences ($P < 0.05$) of the same species among different growth environments, and the capital letters reveal the significant differences ($P < 0.05$) of different species in the same growth environment.

suburban areas were initially negative and gradually increased with the plant functional groups (**Figures 4B,C**). The trend of light respiration rates of plants grown among the different sites was similar to those of the photosynthetic rate (**Figure 4D**). The saturation irradiance and light compensation point of the shrub located at the RNR were significantly lower than those of the UFP (**Figures 4E,F**). The photosynthetic N use efficiencies of the canopies significantly ($p < 0.05$) differed among the three sites and decreased in the order of RNR > SFP > UFP (**Figure 4G**). Plant photosynthetic P use efficiency increased with the plant height and the photosynthetic P use efficiencies of the subcanopies of plants grown in the UFP were significantly lower than those grown in the RNR (**Figure 4H**). The maximum photosynthetic rates of the different plant species were also positively correlated with leaf area (**Table 1**).

Stomatal conductance, intercellular CO_2 concentration, transpiration rate, and instantaneous water use efficiency were significantly but erratically affected by the urbanization (**Supplementary Figure 4**). The highest stomatal conductances of *L. gracile* and *A. chinensis* were both present in the UFP plants, which were significantly ($p < 0.05$) higher than those from plants grown in the SFP (**Supplementary Figure 4a**). The average intercellular CO_2 concentration ranged from 206 to 270 μmol mol^{-1} and had erratic trends among all the plant species at the three sites (**Supplementary Figure 4b**). Significant differences in transpiration rates among the three sites were found among the herb, shrub, and subcanopy, but not found among the canopy samples (**Supplementary Figure 4c**). The responses of instantaneous water use efficiencies to the urbanization were dominated by the plant functional group differentiation. The instantaneous water use efficiency of the herbs, shrubs, and subcanopy plants located in the UFP were significantly ($p < 0.05$) lower than those grown in the RNR, which was opposite to the results of the canopies (**Supplementary Figure 4d**).

Leaf N Allocated to Different Components

The leaf N allocated to the Rubisco, bioenergetics, and light-harvesting components had similar trends among the same plant species sampled at different sites (**Figures 5B–D**). Significant differences in leaf N allocated to the photosynthetic and carboxylation systems were all detected among the same species at different sites (**Figures 5E,F**). Among the three sites, the canopies of the urban area had the lowest proportions of leaf N in the photosynthetic and carboxylation systems. Responses of leaf N allocated to plant cell wall were significantly ($p < 0.05$) affected by the urbanization, with significant differences among four plant functional groups (**Figure 5G**). The proportions of leaf N allocated in the cell wall of the UFP herbs, shrubs, and subcanopies were significantly ($p < 0.05$) lower than those of the suburban and rural counterparts in stark contrast to the canopies.

Adaptive Strategies and Plant Traits

The results showed that the canopies and subcanopies in the urban area suffered from environmental stress and they adapted to the stress via reducing resource acquisition, improving defense capacity, and enhancing resistance (**Figure 6**). For the canopies, the load of maximum photosynthetic rate in the

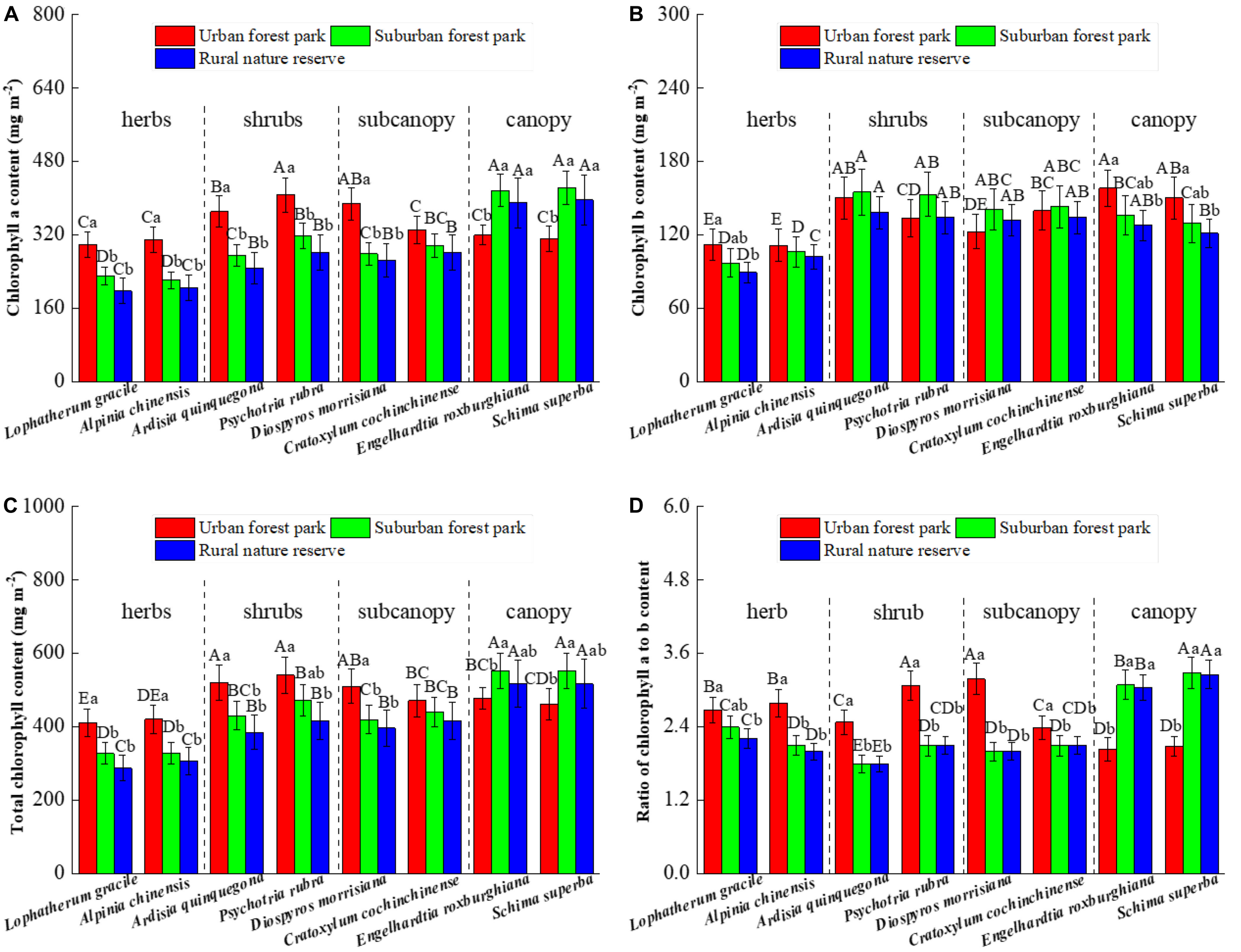

FIGURE 3 | Effects of growth environment on contents of **(A)** chlorophyll a, **(B)** chlorophyll b, and **(C)** total chlorophyll and **(D)** ratio of chlorophyll a to b of eight plant species. The lowercase letters reveal the significant differences ($P < 0.05$) of the same species among different growth environments, and the capital letters reveal the significant differences ($P < 0.05$) of different species in the same growth environment.

urban area was approximately the same as those grown in the suburban area and a load of specific leaf area decreased from 1.29 when grown in the urban area to 0.78 when grown in the suburban area (**Figures 6A,B**). Urbanization may improve environmental adaptability and the defense of understory plants by improving resource acquisition ability (**Figures 6C,D**). Leaf ^{13}C abundance (positive correlation) and water use efficiency (negative correlation) were the main characters related to plant adaptation. Soluble phenol and lipid concentrations may have contributed to resistance, with the load of soluble phenol < 1.0 under advantageous conditions.

DISCUSSION

Stimulation of Urbanization on Plants

Our results showed that it was the plant functional groups that dominated the stimulation or inhibition function of urbanization on plant species and that urbanization appeared to have negative impacts on the canopies. Previous studies suggested that the CO_2 concentration is higher in urban areas due to the proximity to additional emission sources. Since CO_2 is the substrate of photosynthesis, it is unsurprising that elevated CO_2 concentrations stimulate photosynthesis (Ainsworth and Rogers, 2007). Due to the heat island effect, the urban environment also has longer daytimes and higher air temperatures, promoting plant growth (Chapman et al., 2017). Moreover, relative to the urban areas, higher ozone (O_3) concentration in suburban and rural areas has a negative impact on plant growth (Galant et al., 2012; Xie et al., 2016). Therefore, increased light resources, higher CO_2 concentrations, atmospheric temperatures, and lower O_3 concentrations in the urban area theoretically stimulated photosynthesis, leaf soluble sugar and starch accumulations, and whole plant growth. At the same time, Pretzsch et al. (2017) also confirmed that urbanization accelerated tree growth in the subtropical zone after the 1960s. The discrepancy may be due to the pressure of environmental pollutants originating from urbanization.

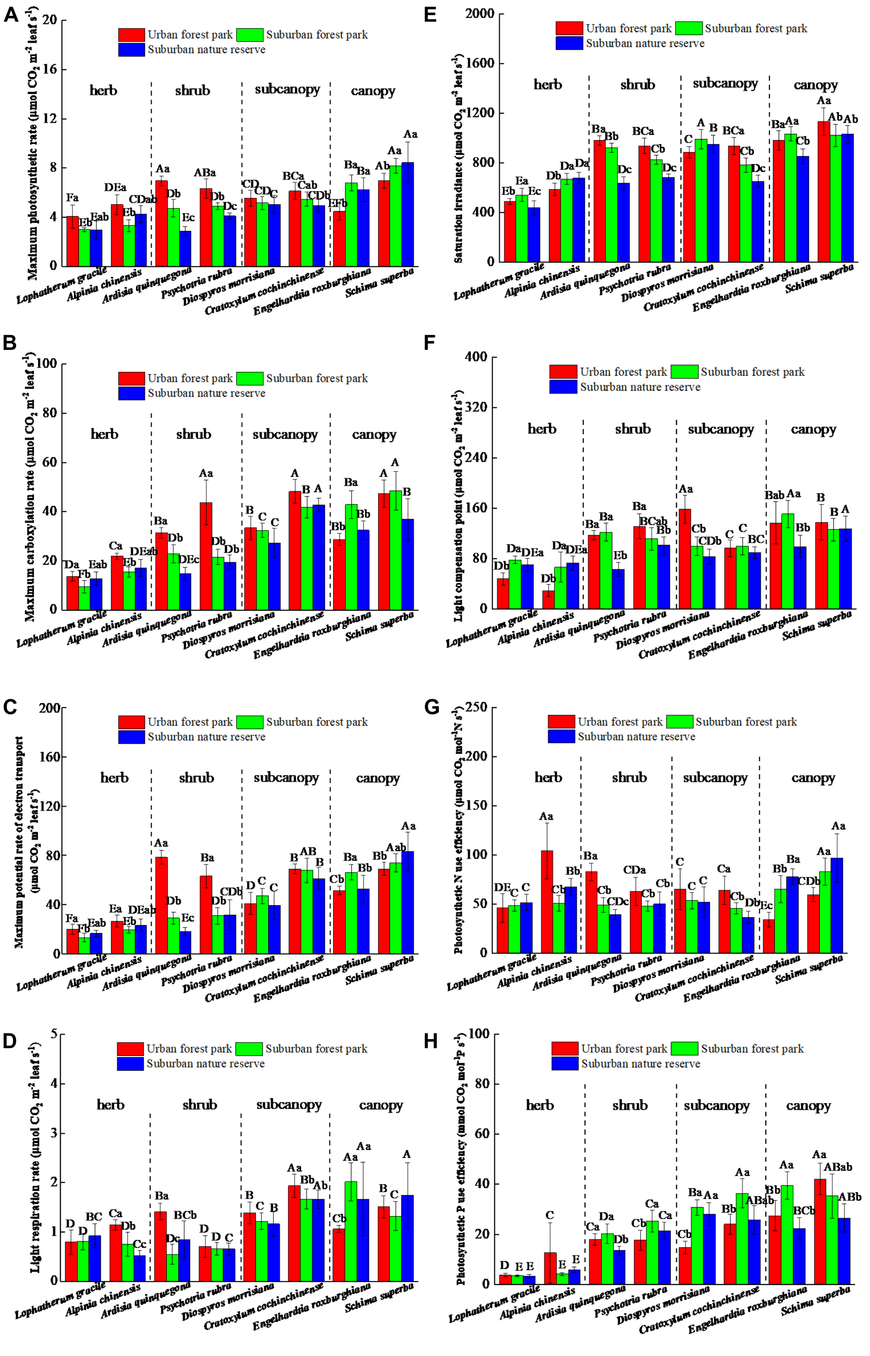

FIGURE 4 | Effects of growth environment on **(A)** maximum photosynthetic rate, **(B)** maximum carboxylation rate, **(C)** maximum potential rate of electron transport, **(D)** light respiration rate, **(E)** saturation irradiance, **(F)** light compensation point, **(G)** photosynthetic N use efficiency, and **(H)** photosynthetic P use efficiencies of eight plant species. The lowercase letters reveal the significant differences ($P < 0.05$) of the same species among different growth environments, and the capital letters reveal the significant differences ($P < 0.05$) of different species in the same growth environment.

Pressure of Urbanization on Plants

In this study, the negative correlations between heavy metal concentrations and maximum photosynthetic rates were all detected in the canopies (**Table 1**), which further implies that in the urban area, higher heavy metal concentrations in the leaves might offset the stimulating functions of urbanization on the canopies. It was also supported by previous studies, and Harrison (2018) also found that concentrations of traffic-generated pollutants in the urban background typically exceed the concentrations within suburban or rural areas. In the subtropical China area, all the concentrations of heavy metals in soils and dusts of the urban area were higher than their

TABLE 1 | Correlation coefficients and *P* levels of the Pearson's correlation among maximum photosynthetic rate and plant external size, leaf appearance, heavy metal concentration, and N allocated into different components.

	Lophatherum gracile	***Alpinia chinensis***	***Ardisia quinquegona***	***Psychotria rubra***	***Diospyros morrisiana***	***Cratoxylum cochinchinense***	***Engelhardtia roxburghiana***	***Schima superba***
Height	0.356	0.016	0.018	0.076	0.366	**0.481***	−0.376	−0.186
South-north crown width	0.125	**0.441***	**0.593****	**0.816****	−0.270	0.252	0.374	−0.018
East-west crown width	0.111	0.177	**0.436***	**0.705****	−0.078	−0.100	0.386	0.204
Leaf thickness	−0.293	−0.612**	−0.266	−0.301	**−0.474***	**−0.443***	**−0.651****	−0.197
Leaf surface	0.141	0.198	**0.731****	**0.514***	**0.547****	0.254	0.369	**0.409***
Specific area of leaves	**0.534****	0.211	**0.752****	**0.682****	**0.452***	**0.630****	0.247	**0.576****
Ni	**0.536****	**0.511***	**0.619****	**0.556****	0.055	**0.594****	−0.211	**−0.588****
Cu	**0.473***	0.157	**0.638****	**0.630****	0.075	**0.536****	−0.160	−0.149
Zn	−0.027	**0.603****	**0.547****	**0.843****	0.384	0.334	−0.366	**−0.437***
Pb	**0.496***	0.066	**0.445***	**0.693****	**0.539****	0.291	−0.250	−0.400
Cd	**0.608****	0.146	−0.148	**0.657****	0.340	0.279	**−0.447***	−0.275
Cr	**0.426***	0.158	**0.566****	**0.491***	0.358	0.270	**−0.745****	**−0.504***
Area-based leaf N	**0.539****	−0.306	0.346	0.218	−0.371	**−0.417***	−0.400	−0.206
Leaf N allocated to Rubisco	0.126	**0.622****	**0.831****	**0.848****	**0.618****	**0.613****	**0.731****	0.300
Leaf N allocated to bioenergetics	0.270	**0.713****	**0.850****	**0.758****	**0.663****	**0.660****	**0.657****	0.283
Leaf N allocated to light-harvesting components	**−0.535****	**0.483***	0.117	0.194	0.300	**0.452***	0.370	0.160
Leaf N allocated to photosynthetic system	0.143	**0.642****	**0.846****	**0.846****	**0.639****	**0.633****	**0.733****	0.350
Leaf N allocated to carboxylation system	−0.068	**0.604****	**0.730****	**0.774****	**0.572****	**0.610****	**0.641****	0.330
Leaf N allocated to cell wall	**−0.552****	−0.216	**−0.500***	**−0.619****	**−0.418***	**−0.468***	**−0.411***	**−0.628****

The bold values demonstrate the correlations are significant. $^{*}p < 0.05$ *and* $^{**}p < 0.01$.

background values (Wei and Yang, 2010). Relative to the herbs and shrubs, the canopies were generally exposed to higher amounts of pollution due to the heights and larger external sizes, and thereby, the significant differences in leaf heavy metal concentration were more frequently detected in the canopies between the urban and the suburban areas (**Figure 2**). The parameters of chlorophyll fluorescence were more vulnerable to heavy metal stress and that heavy metal Cd inhibited at least two different targets in photosystem II (Rocchetta and Küpper, 2009; Rajkumar et al., 2013). The Rubisco activity and CO_2 assimilation rate were also decreased in the presence of Cd (Cagno et al., 2008).

Effects of Urbanization on Leaf N Proportions

The urbanization also significantly influenced the leaf cell N allocations (**Figure 5**). The N distribution in leaf cells reflected the physiological characteristics and survival strategies of plants under different environmental conditions (Warren and Adams, 2001; Ridenour et al., 2008). Leaf N is generally distributed into the cell wall, membrane, nucleus, chloroplast, mitochondrion, and some free compounds, and more than 50% of leaf N is allocated to chloroplasts for photosynthesis and energy transformation systems (Warren and Adams, 2001). The ratio of leaf N allocated into the cell wall indicated the tenacity of leaves, which is also a basic self-defense strategy of plants (Ridenour et al., 2008). Amidst harsh abiotic conditions, more leaf N would be allocated in the cell wall, resulting in a decline in photosynthetic system N (Ridenour et al., 2008). Consequently, the maximum photosynthetic rate was positively correlated with the proportions of leaf N allocated to the photosynthetic system but had negative correlations with the proportions of leaf N allocated in the cell wall (**Table 1**).

In this study, the average leaf N:P ratios on a mass basis ranged from 12.0 to 30.2 (**Figure 1**), which is in the range of average ratios reported in global datasets (Reich and Oleksyn, 2004; Hättenschwiler et al., 2008). Although urbanization tended to increase the leaf N contents and N:P ratios, Townsend et al. (2007) demonstrated that relative to the N content, plant productivity was generally limited by the P content. As observed for leaf N status, the $\delta^{15}N$ value is a valuable parameter revealing long-term N sources of different plants (Hietz et al., 2011; Huang et al., 2016; Fu et al., 2020). Soil N saturation attributable to atmospheric N deposition influenced the plant $\delta^{15}N$ value by enhancing nitrification and leaching (Hietz et al., 2011), and thereby, the decline in leaf $\delta^{15}N$ of plants located in the urban was attributed to atmospheric N deposition. With reference to the studies conducted in different subtropical areas, atmospheric N deposition, including nitrogen oxides and ammonia, is frequently reported to be ^{15}N depleted (Battipaglia et al., 2010; Chen et al., 2011; Fu et al., 2020). The N deposition could also lead to

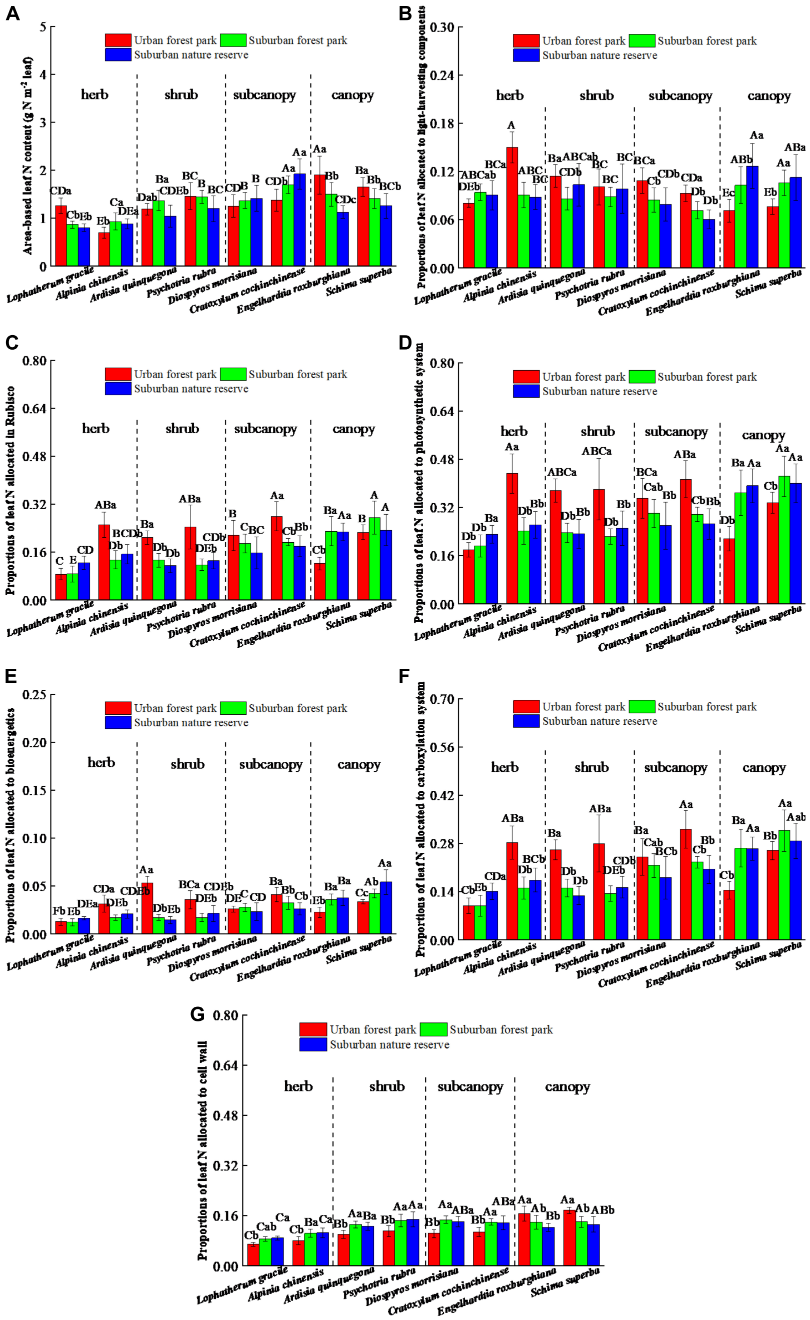

FIGURE 5 | Effects of growth environment on **(A)** area-based leaf N content and proportions of leaf N allocated to the **(B)** Rubisco, **(C)** bioenergetics, **(D)** light-harvesting components, **(E)** photosynthetic system, **(F)** carboxylation system, and **(G)** cell wall of eight plant species. The lowercase letters reveal the significant differences (*P* < *0.05*) of the same species among different growth environments, and the capital letters reveal the significant differences (*P* < *0.05*) of different species in the same growth environment.

plant P limitation by soil acidification, which reduces available P via being fixed by activated iron and aluminum (Hou et al., 2018). For the canopies in this study, atmospheric N disposition of urbanization tended to increase N content but decreased P content (**Figure 1**), which might cause an imbalance of plant N and P and generate side effects on other nutrient absorptions. Moreover, the leaf N allocations also imply that relative to the suburban and rural environment, the urbanization positively stimulated the herb growth but inhibited the canopies.

Adaptive Strategies of Plants

Apart from the inherent properties of the plant itself, plant growth is generally regulated by external environmental factors including light resource, temperature, fertilization, and pollutant

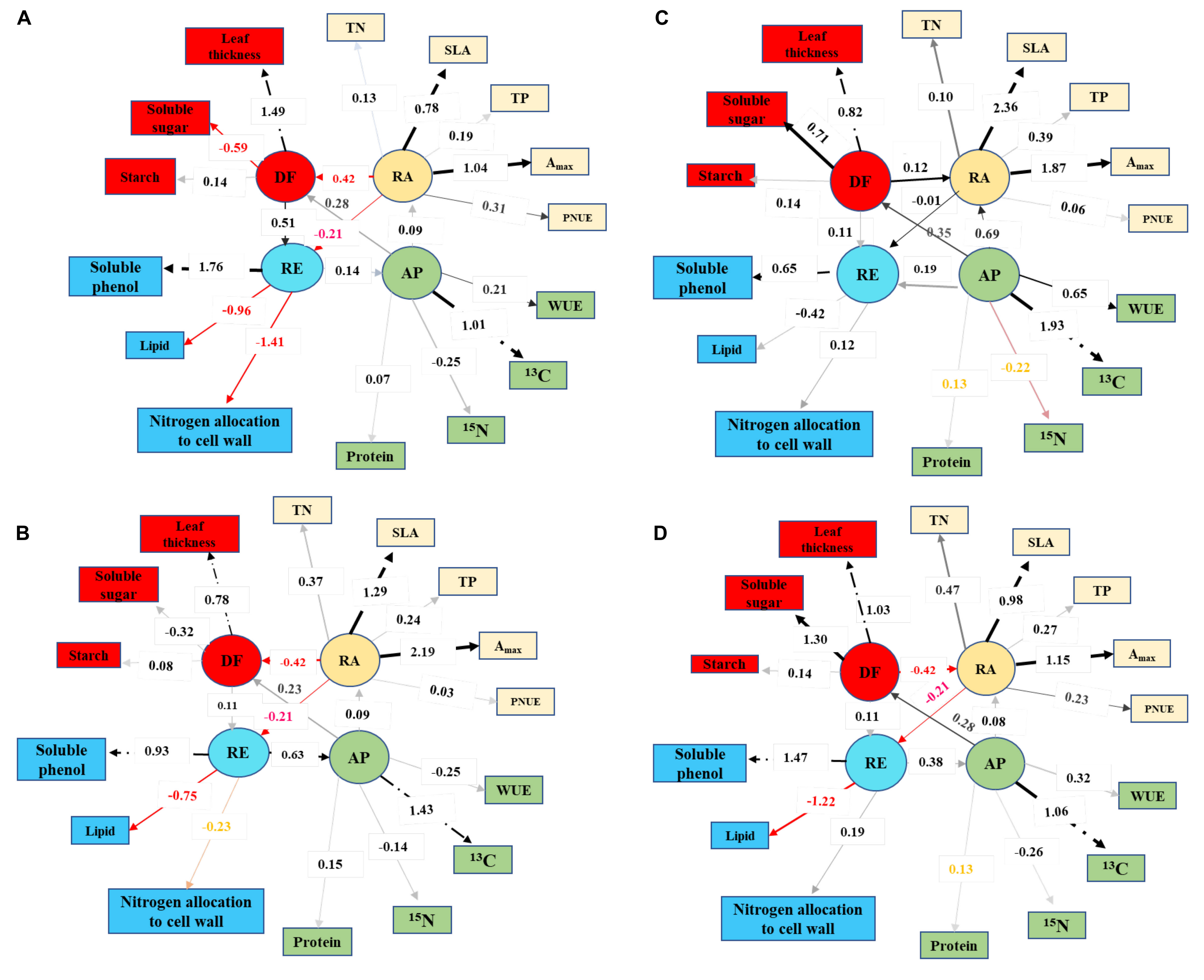

FIGURE 6 | Confirmatory factor analysis on the trait loading values per integrated functions (RA, resource acquisition; AP, adaptation; DF, defense; RE, resistance) and relationships between the functions for canopy and understory plants in urban and suburban habitat: **(A)** canopy plants in urban area; **(B)** canopy plants in suburban areas; **(C)** understory plants in urban area; and **(D)** understory plants in suburban areas. The numbers in the line between the latent variable and its observed variables denoted loading values, and the numbers in the line between four latent variables showed regression coefficients.

stress. All these environmental factors had positive or negative effects on plant growth, and these effects could be accumulated, which discrepantly influence the physiological property and growth of plants. The urban, suburban, and rural areas had a series of differences in these environmental factors. Relative to the suburban and rural counterparts, the urban environment differs in many aspects that may confound the responses of nutrient supplies and pollution. Consequently, plants appear to adopt different strategies, including photosynthetic rates and leaf N and P allocation, to adapt to these environments (**Figure 6**).

Photosynthesis is the primary assimilation process for most plants, which is also one of the key parameters affecting plant adaptive strategies to different environments (Houborg et al., 2013; Schliep et al., 2013). The plant photosynthetic capacity is quantified with the maximum photosynthetic rate under suitable conditions. In plants, the chlorophyll is responsible for absorbing and converting light energy, and thereby, the changes in chlorophyll contents directly demonstrated the advantages and disadvantages of urbanization on plant physiology at a molecular level (Wasielewski et al., 1981; Papageorgiou and Govindjee, 2004; Schliep et al., 2013). The primary pigment for plant photosynthesis is chlorophyll a and the chlorophyll b generally serves as an accessory pigment (Wasielewski et al., 1981; Schliep et al., 2013). The chlorophyll a absorbs light from the orange-red and violet-blue electromagnetic spectrum and the leaf contained more chlorophyll content with a higher efficient capture of photons and photosynthetic rate (Papageorgiou and Govindjee, 2004; Schliep et al., 2013). In this study, relative to the suburban and rural area, urbanization had positive effects on the total chlorophyll contents of the herbs and shrubs, namely, herbs and shrubs changed in their physiologies to adapt to stimulating roles of urbanization (**Figure 6**). For photosynthesis, light as an energy resource is essential to sustain plant growth and ensure long-term survival (Craine and Dybzinski, 2013). Compared to the suburban and rural environment, more artificial light sources exist in urban areas and it has been proved that artificial light could delay leaf senescence (Zhang et al., 2015).

CONCLUSION

Compared with the suburban and rural counterparts, the herbs and shrubs in the urban area had significantly higher starch and soluble sugar contents, but the canopies had significantly lower soluble sugar contents. Urbanization increased leaf heavy metal concentration and N content but decreased leaf δ^{15}N. The urbanization enhanced the maximum photosynthetic rate and total chlorophyll contents of the herbs and shrubs but decreased the maximum photosynthetic rate and total chlorophyll contents of the canopies. The proportions of leaf N allocated in the cell wall of urban herbs, shrubs, and subcanopies were significantly lower than those of the suburban and rural counterparts in stark contrast to the canopies. This study also demonstrated that plant functional groups dominated responses of adaptive strategies to urbanization and that urbanization tended to stimulate the herbs but inhibit the canopies. The canopies and subcanopies in the urban area suffered from environmental stress, and they adapted to the stress via reducing resource acquisition, improving defense capacity, and enhancing resistance. However, urbanization could improve environmental adaptability and the defense of understory plants by improving resource acquisition ability.

DATA AVAILABILITY STATEMENT

The original contributions presented in the study are included in the article/**Supplementary Material**, further inquiries can be directed to the corresponding author/s.

AUTHOR CONTRIBUTIONS

YX, SL, MZ, ZX, FT, XS, TL, TZ, and ZW were all involved in conceptualizing, designing, and implementing the project. YX and MZ prepared the manuscript. ZX and RF helped to revise the manuscript. YX carried out all the data collection and drafted the manuscript. All authors contributed to the article and approved the submitted version.

FUNDING

This study was jointly supported by the Central Public-interest Scientific Institution Basal Research Fund of Chinese Academy of Forestry (CAFYBB2016MA003), the Natural Science Foundation of Guangdong Province, China (2016A030313139), the Program of Forest Ecological Benefits Monitoring Network in Guangzhou (2019–2022), the Long-term Forest Ecological Benefits Monitoring Network of Guangdong Province (2019KJCX021), and the Guangdong Forestry Sci-Tech Innovation Platform Project (2019KJCX021 and 2020-KYXM-09).

ACKNOWLEDGMENTS

We are very grateful for the support from the Pearl River Delta Forest Ecosystem Research Station.

SUPPLEMENTARY MATERIAL

The Supplementary Material for this article can be found online at: https://www.frontiersin.org/articles/10.3389/fpls.2021.773676/full#supplementary-material

REFERENCES

Ainsworth, E. A., and Rogers, A. (2007). The response of photosynthesis and stomatal conductance to rising CO_2: mechanisms and environmental interactions. *Plant Cell Environ.* 30, 258–270. doi: 10.1111/j.1365-3040.2007.01641.x

Battipaglia, G., Marzaioli, F., Lubritto, C., Altieri, S., Strumia, S., Cherubini, P., et al. (2010). Traffic pollution affects tree-ring width and isotopic composition of *Pinus pinea*. *Sci. Total Environ.* 408, 586–593. doi: 10.1016/j.scitotenv.2009.09.036

Beaumont, L. J., Hughes, L., and Pitman, A. J. (2008). Why is the choice of future climate scenarios for species distribution modelling important? *Ecol. Lett.* 11, 1135–1146. doi: 10.1111/j.1461-0248.2008.01231.x

Cagno, R. D., Guidi, L., Gara, L. D., and Soldatini, G. F. (2008). Combined cadmium and ozone treatments affect photosynthesis and ascorbate-dependent defences in sunflower. *New Phytol.* 151, 627–636. doi: 10.1046/j.1469-8137.2001.00217.x

Cai, W., Gibbs, D., Zhang, L., Ferrier, G., and Cai, Y. (2017). Identifying hotspots and management of critical ecosystem services in rapidly urbanizing Yangtze River Delta Region, China. *J. Environ. Manage.* 191, 258–267. doi: 10.1016/j.jenvman.2017.01.003

Chapman, S., Watson, J. E. M., Salazar, A., Thatcher, M., and McAlpine, C. A. (2017). The impact of urbanization and climate change on urban temperatures: a systematic review. *Landscape Ecol.* 32, 1921–1935. doi: 10.1007/s10980-017-0561-4

Chen, N., Hong, H., Huang, Q., and Wu, J. (2011). Atmospheric nitrogen deposition and its long-term dynamics in a southeast China coastal area. *J. Environ. Manage.* 92, 1663–1667. doi: 10.1016/j.jenvman.2011.01.026

Craine, J. M., and Dybzinski, R. (2013). Mechanisms of plant competition for nutrients, water and light. *Funct. Ecol.* 27, 833–840. doi: 10.1111/1365-2435.12081

Farquhar, G. D., and von Caemmerer, S. (1982). "Modelling of photosynthetic response to environmental conditions," in *Physiological Plant Ecology II. Encyclopedia of Plant Physiology*, eds O. L. Lange, P. S. Nobel, C. B. Osmond, and H. Ziegler (Berlin: Springer).

Ferguson, G., and Woodbury, A. D. (2007). Urban heat island in the subsurface. *Geophys. Res. Lett.* 34, L23713.

Fu, L., Xu, Y., Xu, Z., Wu, B., and Zhao, D. (2020). Tree water-use efficiency and growth dynamics in response to climatic and environmental changes in a temperate forest in Beijing, China. *Environ. Int.* 134:105209. doi: 10.1016/j.envint.2019.105209

Galant, A., Koester, R. P., Ainsworth, E. A., Hicks, L. M., and Jez, J. M. (2012). From climate change to molecular response: redox proteomics of ozone-induced responses in soybean. *New Phytol.* 194, 220–229. doi: 10.1111/j.1469-8137.2011.04037.x

Gregg, J. W., Jones, C. G., and Dawson, T. E. (2003). Urbanization effects on tree growth in the vicinity of New York City. *Nature* 424, 183–187. doi: 10.1038/nature01728

Hahs, A. K., and Mcdonnell, M. J. (2007). Composition of the plant community in remnant patches of grassy woodland along an urban-rural gradient in

Melbourne, Australia. *Urban Ecosys.* 10, 355–377. doi: 10.1007/s11252-007-0034-7

Harrison, M. T., Edwards, E. J., Farquhar, G. D., Nicotra, A. B., and Evans, J. R. (2009). Nitrogen in cell walls of sclerophyllous leaves accounts for little of the variation in photosynthetic nitrogen-use efficiency. *Plant Cell Environ.* 32, 259–270. doi: 10.1111/j.1365-3040.2008.01918.x

Harrison, R. M. (2018). Urban atmospheric chemistry: a very special case for study. *npj Clim. Atmos. Sci.* 1:20175.

Hättenschwiler, S., Aeschlimann, B., Coûteaux, M.-M., Roy, J., and Bonal, D. (2008). High variation in foliage and leaf litter chemistry among 45 tree species of a neotropical rainforest community. *New Phytol.* 179, 165–175. doi: 10.1111/j.1469-8137.2008.02438.x

He, Y., Ma, Y., Du, Y., and Shen, S. (2018). Differential gene expression for carotenoid biosynthesis in a green alga *Ulva prolifera* based on transcriptome analysis. *BMC Genomics* 19:916. doi: 10.1186/s12864-018-5337-y

Hidaka, A., and Kitayama, K. (2009). Divergent patterns of photosynthetic phosphorus-use efficiency versus nitrogen-use efficiency of tree leaves along nutrient-availability gradients. *J. Ecol.* 97, 984–991. doi: 10.1111/j.1365-2745.2009.01540.x

Hietz, P., Turner, B. L., Wanek, W., Richter, A., Nock, C. A., and Wright, S. J. (2011). Long-term change in the nitrogen cycle of tropical forests. *Science* 334, 664–666. doi: 10.1126/science.1211979

Hou, E., Wen, D., Kuang, Y., Jing, C., and Zhang, Y. (2018). Soil pH predominantly controls the forms of organic phosphorus in topsoils under natural broadleaved forests along a 2500 km latitudinal gradient. *Geoderma* 315, 65–74. doi: 10.1016/j.geoderma.2017.11.041

Houborg, R., Cescatti, A., Migliavacca, M., and Kustas, W. P. (2013). Satellite retrievals of leaf chlorophyll and photosynthetic capacity for improved modeling of GPP. *Agric. Forest Meteorol.* 177, 10–23. doi: 10.1016/j.agrformet.2013.04.006

Huang, Z., Liu, B., Davis, M., Sardans, J., Peñuelas, J., and Billings, S. (2016). Long-term nitrogen deposition linked to reduced water use efficiency in forests with low phosphorus availability. *New Phytol.* 210, 431–442. doi: 10.1111/nph.13785

Janhäll, S. (2015). Review on urban vegetation and particle air pollution – Deposition and dispersion. *Atmos. Environ.* 105, 130–137. doi: 10.1016/j.atmosenv.2015.01.052

Lichtenthaler, H. K., and Buschmann, C. (2001). "Chlorophylls and carotenoids: measurement and characterization by UV-VIS spectroscopy," in *Current Protocols in Food Analytical Chemistry (CPFA). Spectroscopy. Supplement 1*, ed. H. K. Lichtenthaler (Hoboken, NJ: John Wiley and Sons, Inc). doi: 10.1016/j.chroma.2005.03.055

Liu, M., Niklas, K. J., Niinemets, Ü, Hölscher, D., Chen, L., and Shi, P. (2020). Comparison of the scaling relationships of leaf biomass versus surface area between spring and summer for two deciduous tree species. *Forests* 11:1010. doi: 10.3390/f11091010

Liu, N., Guo, Q., Ren, H., and Sun, Z. (2016). Schima superba outperforms other tree species by changing foliar chemical composition and shortening construction payback time when facilitated by shrubs. *Sci. Rep.* 6:19855. doi: 10.1038/srep19855

Livesley, S. J., Mcpherson, G. M., and Calfapietra, C. (2016). The urban forest and ecosystem services: impacts on urban water, heat, and pollution cycles at the tree, street, and city scale. *J. Environ. Qual.* 45:119. doi: 10.2134/jeq2015.11.0567

Loustau, D., Brahim, M. B., Gaudillere, J.-P., and Dreyer, E. (1999). Photosynthetic responses to phosphorus nutrition in two-year-old maritime pine seedlings. *Tree Physiol.* 19, 707–715. doi: 10.1093/treephys/19.11.707

Lu, R. K. (2000). *Analytical Methods of Soil Agrochemistry*. Beijing: China Agricultural Science and Technology Press.

Makino, A., Mae, T., and Ohira, K. (1986). Colorimetric measurement of protein stained with coomassie brilliant blue R on sodium dodecyl sulfate-polyacrylamide gel electrophoresis by eluting with formamide. *Agri. Biol. Chem.* 50, 1911–1912. doi: 10.1271/bbb1961.50.1911

Niinemets, Ü, and Tenhunen, J. D. (1997). A model separating leaf structural and physiological effects on carbon gain along light gradients for the shade-tolerant species *Acer saccharum*. *Plant Cell Environ.* 20, 845–866. doi: 10.1046/j.1365-3040.1997.d01-133.x

Osmond, C. B., Björkman, O., and Anderson, D. J. (1980). *Physiological Processes in Plant Ecology. Toward a Synthesis With Atriplex. Ecological Studies*. Berlin: Springer-Verlag.

Papageorgiou, E., and Govindjee, G. C. (2004). *Chlorophyll a Fluorescence-a Signature of Photosynthesis. Advances in Photosynthesis and Respiration*. Dordrecht: Springer.

Pretzsch, H., Biber, P., Uhl, E., Dahlhausen, J., Schütze, G., Perkins, D., et al. (2017). Climate change accelerates growth of urban trees in metropolises worldwide. *Sci. Rep.* 7:15403. doi: 10.1038/s41598-017-14831-w

Pugh, T. A. M., MacKenzie, A. R., Whyatt, J. D., and Hewitt, C. N. (2012). Effectiveness of green infrastructure for improvement of air quality in urban street canyons. *Environ. Sci. Technol.* 46, 7692–7699.

Qiu, Y., Guan, D., Song, W., and Huang, K. (2009). Capture of heavy metals and sulfur by foliar dust in urban Huizhou, Guangdong Province, China. *Chemosphere* 75, 447–452. doi: 10.1016/j.chemosphere.2008.12.061

Quigley, M. F. (2002). Franklin Park: 150 years of changing design, disturbance, and impact on tree growth. *Urban Ecosys.* 6, 223–235.

Quigley, M. F. (2004). Street trees and rural conspecifics: will long-lived trees reach full size in urban conditions? *Urban Ecosys.* 7, 29–39. doi: 10.1023/b:ueco.0000020170.58404.e9

Rajkumar, M., Prasad, M. N., Swaminathan, S., and Freitas, H. (2013). Climate change driven plant–metal–microbe interactions. *Environ. Int.* 53, 74–86. doi: 10.1016/j.envint.2012.12.009

Reich, P. B., and Oleksyn, J. (2004). Global patterns of plant leaf N and P in relation to temperature and latitude. *Proc. Natl. Acad. Sci. U.S.A.* 101, 11001–11006. doi: 10.1073/pnas.0403588101

Ridenour, W. M., Vivanco, J. M., Feng, Y., Horiuchi, J., and Callaway, R. M. (2008). No evidence for trade-offs: centaurea plants from America are better competitors and defenders. *Ecol. Monogr.* 78, 369–386. doi: 10.1890/06-1926.1

Rocchetta, I., and Küpper, H. (2009). Chromium- and copper-induced inhibition of photosynthesis in Euglena gracilis analysed on the single-cell level by fluorescence kinetic microscopy. *New Phytol.* 182, 405–420. doi: 10.1111/j.1469-8137.2009.02768.x

Sala, O. E., Chapin, F. S. III, Armesto, J. J., Berlow, E., Bloomfield, J., Dirzo, R., et al. (2000). Global biodiversity scenarios for the year 2100. *Science* 287, 1770–1774. doi: 10.1126/science.287.5459.1770

Schliep, M., Cavigliasso, G., Quinnell, R. G., Stranger, R., and Larkum, A. W. D. (2013). Formyl group modification of chlorophyll a: a major evolutionary mechanism in oxygenic photosynthesis. *Plant Cell Environ.* 36, 521–527. doi: 10.1111/pce.12000

Seto, K. C., Güneralp, B., and Hutyra, L. R. (2012). Global forecasts of urban expansion to 2030 and direct impacts on biodiversity and carbon pools. *Proc. Natl. Acad. Sci. U.S.A.* 109, 16083–16088. doi: 10.1073/pnas.1211658109

Shi, P., Li, Y., Hui, C., Ratkowsky, D. A., Yu, X., and Niinemets, U. (2020). Does the law of diminishing returns in leaf scaling apply to vines? – Evidence from 12 species of climbing plants. *Glob. Ecol. Conserv.* 21:e00830. doi: 10.1016/j.gecco.2019.e00830

Smith, A. M., and Zeeman, S. C. (2006). Quantification of starch in plant tissues. *Nat. Protoc.* 1, 1342–1345. doi: 10.1038/nprot.2006.232

Townsend, A. R., Cleveland, C. C., Asner, G. P., and Bustamante, M. M. C. (2007). Controls over foliar N: P ratios in tropical rain forests. *Ecology* 88, 107–118. doi: 10.1890/0012-9658(2007)88[107:cofnri]2.0.co;2

Warren, C. R., and Adams, M. A. (2001). Distribution of N, Rubisco and photosynthesis in Pinus pinaster and acclimation to light. *Plant Cell Environ.* 24, 597–609. doi: 10.1046/j.1365-3040.2001.00711.x

Wasielewski, M. R., Norris, J. R., Shipman, L. L., Lin, C. P., and Svec, W. A. (1981). Monomeric chlorophyll a enol: evidence for its possible role as the primary electron donor in photosystem I of plant photosynthesis. *Proc. Natl. Acad. Sci. U.S.A.* 78, 2957–2961. doi: 10.1073/pnas.78.5.2957

Wei, B., and Yang, L. (2010). A review of heavy metal contaminations in urban soils, urban road dusts and agricultural soils from China. *Microchem. J.* 94, 99–107.

Wiens, J. J., Ackerly, D. D., Allen, A. P., Anacker, B. L., Buckley, L. B., Cornell, H. V., et al. (2010). Niche conservatism as an emerging principle in ecology and conservation biology. *Ecol. Lett.* 13, 1310–1324. doi: 10.1111/j.1461-0248.2010.01515.x

Xiao, Y., Liu, S., Tong, F., Chen, B., and Kuang, Y. (2018). Dominant species in subtropical forests could decrease photosynthetic N allocation to carboxylation and bioenergetics and enhance leaf construction costs during forest succession. *Front. Plant Sci.* 9:117. doi: 10.3389/fpls.2018.00117

Xie, M., Zhu, K., Wang, T., Chen, P., Han, Y., Li, S., et al. (2016). Temporal characterization and regional contribution to O3 and NOx at an urban and a suburban site in Nanjing, China. *Sci. Total Environ.* 551-552, 533–545. doi: 10.1016/j.scitotenv.2016.02.047

Zhang, G., Shanqi, S., Michiko, T., Toyoki, K., and Wataru, Y. (2015). Supplemental upward lighting from underneath to obtain higher Marketable Lettuce (*Lactuca sativa*). leaf fresh weight by retarding senescence of outer leaves. *Front. Plant Sci.* 6:1110. doi: 10.3389/fpls.2015.01110

Zhang, H., Guo, W., Yu, M., Wang, G. G., and Wu, T. (2018). Latitudinal patterns of leaf N, P stoichiometry and nutrient resorption of *Metasequoia glyptostroboides* along the eastern coastline of China. *Sci. Total Environ.* 618, 1–6. doi: 10.1016/j.scitotenv.2017.11.030

Zhao, S., Liu, S., and Zhou, D. (2016). Prevalent vegetation growth enhancement in urban environment. *Proc. Natl. Acad. Sci. U.S.A.* 113, 6313–6318. doi: 10.1073/pnas.1602312113

Conflict of Interest: The authors declare that the research was conducted in the absence of any commercial or financial relationships that could be construed as a potential conflict of interest.

frontiers in Plant Science

ORIGINAL RESEARCH
published: 17 January 2022
doi: 10.3389/fpls.2021.822907

Application of an Ovate Leaf Shape Model to Evaluate Leaf Bilateral Asymmetry and Calculate Lamina Centroid Location

Yirong Li[1]†, Yiwen Zheng[1]†, David A. Ratkowsky[2]†, Hailin Wei[3]* and Peijian Shi[1]*

[1] Bamboo Research Institution, College of Science, Nanjing Forestry University, Nanjing, China, [2] Tasmanian Institute of Agriculture, University of Tasmania, Hobart, TAS, Australia, [3] Hunan Academy of Forestry, Changsha, China

Leaf shape is an important leaf trait, with ovate leaves common in many floras. Recently, a new leaf shape model (referred to as the MLRF equation) derived from temperature-dependent bacterial growth was proposed and demonstrated to be valid in describing leaf boundaries of many species with ovate leaf shape. The MLRF model's parameters can provide valuable information of leaf shape, including the ratio of lamina width to length and the lamina centroid location on the lamina length axis. However, the model wasn't tested on a large sample of a single species, thereby limiting its overall evaluation for describing leaf boundaries, for evaluating lamina bilateral asymmetry and for calculating lamina centroid location. In this study, we further test the model using data from two Lauraceae species, *Cinnamomum camphora* and *Machilus leptophylla*, with $>$290 leaves for each species. The equation was found to be credible for describing those shapes, with all adjusted root-mean-square errors (RMSE) smaller than 0.05, indicating that the mean absolute deviation is smaller than 5% of the radius of an assumed circle whose area equals lamina area. It was also found that the larger the extent of lamina asymmetry, the larger the adjusted RMSE, with approximately 50% of unexplained variation by the model accounted for by the lamina asymmetry, implying that this model can help to quantify the leaf bilateral asymmetry in future studies. In addition, there was a significant difference between the two species in their centroid ratio, i.e., the distance from leaf petiole to the point on the lamina length axis associated with leaf maximum width to the leaf maximum length. It was found that a higher centroid ratio does not necessarily lead to a greater investment of mass to leaf petiole relative to lamina, which might depend on the petiole pattern.

Keywords: centroid ratio, lamina area, leaf petiole, Lobry-Rosso-Flandrois equation, model validity

Edited by:
Ji Zhang,
Yunnan Academy of Agricultural Sciences, China

Reviewed by:
Sergey Baranov,
Vladimir State University, Russia
Danijela P. Miljkovic,
University of Belgrade, Serbia

***Correspondence:**
Hailin Wei
hailinwei82@163.com
Peijian Shi
pjshi@njfu.edu.cn

†These authors have contributed equally to this work

Specialty section:
This article was submitted to Functional Plant Ecology, a section of the journal Frontiers in Plant Science

Received: 26 November 2021
Accepted: 23 December 2021
Published: 17 January 2022

Citation:
Li Y, Zheng Y, Ratkowsky DA, Wei H and Shi P (2022) Application of an Ovate Leaf Shape Model to Evaluate Leaf Bilateral Asymmetry and Calculate Lamina Centroid Location. Front. Plant Sci. 12:822907. doi: 10.3389/fpls.2021.822907

INTRODUCTION

A leaf of a woody plant usually consists of a lamina, a petiole (or a pseudo-petiole) and a sheath. In the literature, leaf shape often refers just to the lamina shape and does not involve the morphological characteristics of the leaf petiole. As an important photosynthetic organ of plants, the leaf has always been a research hotspot, and leaf traits including lamina size (mass and area), lamina thickness, leaf shape, and lamina vein patterns are widely studied because those measures are intimately associated with the responses of plants to climate and environmental stress (Wright et al., 2004, 2017; Chitwood and Sinha, 2016; Baird et al., 2021). The leaf is crucial to the growth and development of plants, with the characteristics and variation of leaf structure directly affecting absorption and utilization of light energy and nutrients (Smith et al., 1997; Daas-Ghrib et al., 2011). Previous studies have shown that there is a tradeoff between the photosynthetic returns from increasing lamina area and the investment in leaf physical support and hydraulic systems from increasing lamina mass (Niklas et al., 2007; Huang et al., 2019a,b, 2020; Guo et al., 2021). Lamina thickness and leaf shape have been demonstrated to affect such a tradeoff (Niinemets et al., 2007; Lin et al., 2018, 2020). There is a large variation in leaf shape among different species and conspecfics, and it is often used to assist in identifying and classifying plants. Leaf shape is controlled by genetic, physiological, and ecological factors (Nicotra et al., 2011). Leaf shape and leaf venation pattern are closely related, and interact with each other in formation (Dengler and Kang, 2001; Runions et al., 2017). The ratio of lamina width to lamina length is usually used as the leaf shape indicator (Lin et al., 2020). The ovate leaf shape is common in many floras. The centroids of ovate leaves are closer to the lamina base than those of elliptical and obovate leaves, and thus the support costs of petioles for ovate leaves tend to be lower (Niinemets et al., 2007).

Lamina bilateral symmetry can be regarded as one of the leaf shape features (Shi et al., 2020a). How to measure the bilateral symmetry of the lamina is an important scientific issue. The standardized index (SI) was proposed to quantify the extent of lamina bilateral asymmetry based on the relative area differences of different sub-regions between both sides of the lamina (Shi et al., 2018a). The heterogeneity of light in the tree crown contributes to lamina bilateral asymmetry to a great degree (Wang et al., 2018; Guo et al., 2020). The two sides of some laminas might expose light in an irregular pattern because of the architectural structure of trees. Relative to leaf length, leaf width has a smaller variation for broad-leaved plants, especially those with hierarchical reticulate leaf venation (Shi et al., 2018b). For many plants, the bilateral symmetry is often slightly influenced by a skewed lamina apex. Wang et al. (2020) verified that a skewed lamina apex is likely to be beneficial to drainage on the lamina surface.

It is valuable to construct a parametric model to describe leaf shape. There are many models for calculating leaf size based on leaf length and width, using these two one-dimensional measures to reflect the influence of leaf shape on the calculation of leaf size (Dornbusch et al., 2011; Shi et al., 2015, 2019; Yu et al., 2020; Schrader et al., 2021). The principle of similarity suggests that an object's area is proportional to the square of its length (Thompson, 1917); however, the validity of this principle is demonstrated to be largely affected by the variation in the ratio of lamina width to length (Shi et al., 2019; Yu et al., 2020). In other words, the square relationship between lamina area and lamina length depends on the variation in leaf shape. There are linear, lanceolate, and elliptical leaf shape models (Dornbusch et al., 2011; Shi et al., 2015; Li et al., 2021). Although the ovate leaf shape is very common in many floras, this leaf shape was mathematically modeled only recently (Shi et al., 2021). Dornbusch et al. (2011) proposed a step model to describe the linear and lanceolate leaf shape of plants, especially crops, but this model could not produce a round lamina base. Shi et al. (2015) developed a simplified Gielis equation based on its original version (Gielis, 2003) to describe the shape of bamboo leaves. The validity of the simplified Gielis equation has been confirmed using the leaves of 42 bamboo species (Lin et al., 2016). Nevertheless, the simplified Gielis equation cannot produce concave curves close to the lamina apex that a typical ovate leaf shape usually has (Shi et al., 2021). The original Lobry-Rosso-Flandrois (LRF) equation was used to describe the relationship between developmental (or growth) rate and temperature of poikilotherms and microbes (Lobry et al., 1991; Rosso et al., 1993; Ratkowsky and Reddy, 2017). To increase the flexibility of curve fitting, Shi et al. (2017) proposed the modified LRF equation (referred to as MLRF model hereafter for convenience) by adding a parameter δ, which was then able to describe actual ovate leaf shapes (Shi et al., 2021). The resulting modified leaf shape equation has four parameters, all with geometrical meanings: the first one is half lamina maximum width (y_c); the second one is the distance from lamina base to a point on the lamina length axis associated with leaf maximum width (x_c); the third one is lamina length (x_2); the last one (i.e., δ) controls the curvature of a curve (**Figure 1**). These parameters can be potentially applied to reflect leaf shape, e.g., the quotient of x_c and x_2, which is referred to as the centroid ratio, can reflect the location of the lamina centroid on the lamina length axis for an ovate or obovate leaf shape. If the quotient is smaller than 0.5, this denotes that the lamina centroid is closer to the lamina base (i.e., an ovate leaf shape); if the quotient is larger than 0.5, this means that the lamina centroid is closer to the lamina apex (i.e., an obovate leaf shape); if the quotient is equal or approximate to 0.5, this indicates that the lamina centroid tends to be located at the midpoint of the lamina length. However, the influence of the location of the lamina centroid on the allocation of mass between the leaf petiole and the leaf lamina is unknown. The MLRF model provides an approach for examining whether the lamina centroid ratio can affect the ratio of leaf petiole mass to lamina mass. It is mistaken to directly use the maximum distance between two points on the lamina edge as lamina length, because lamina bilateral asymmetry can lead to an inaccuracy using such an approach. The estimate of the parameter x_2 is better as a candidate leaf length, because lamina apex might largely deviate from the midvein axis for some leaves, leading to an over-estimation or under-estimation for the lamina length defined from lamina base to lamina apex (Schrader et al., 2021). The MLRF equation predicts perfectly a bilateral symmetrical leaf shape, so the theoretical lamina length (x_2) is on the midvein length.

Regardless of the increase of support cost, the larger the leaf size, the greater the photosynthetic returns. However, there is a trade off between leaf size and support cost (Milla and Reich, 2007; Niklas et al., 2007). In addition, increases in leaf size also require increases in the investment of the leaf petiole (Niklas, 1991). The bilateral symmetry of leaf shape is helpful to reduce the cost of development at the earlier stage of leaf

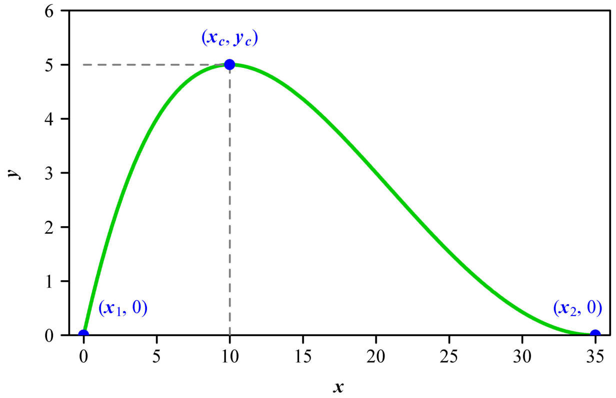

FIGURE 1 | The curve generated by the modified Lobry-Rosso-Flandrois (MLRF) equation, which represents a side of a lamina. Here, x_1 and x_2 represent the lamina base and lamina apex, respectively; x_c represents the point on the lamina length axis associated with the lamina maximum width $2y_c$; δ controls the curvature of this curve. In this study, the location of lamina base (i.e., x_1) is fixed to be 0. This means that the MLRF equation only has four parameters: y_c, x_c, x_2, and δ.

formation and also matches the evolution of the leaf venation system (Smith et al., 1997; Runions et al., 2017; Kierzkowski et al., 2019). Thus, it is valuable to explore the association of leaf size and structure with the corresponding functions. In this study, we use two Lauraceae species, *Cinnamomum camphora* (CC) and *Machilus leptophylla* (ML), both of which have an ovate leaf shape (**Figure 2**), to test: (i) whether the MLRF equation is valid for describing the leaves of the two species, (ii) whether leaf shape (represented by the lamina centroid ratio) can affect the allocation of mass between leaf petiole and lamina, and (iii) whether the extent of lamina bilateral asymmetry can affect the validity of the MLRF equation.

MATERIALS AND METHODS

Leaf Collection and Measurement

From two Lauraceae species, *Cinnamomum camphora* (L.) Presl, and *Machilus leptophylla* Hand.-Mazz., which will be referred to as CC and ML for convenience, more than 600 leaves were sampled from three trees for each species from early- to mid-August 2020 at the Nanjing Forestry University Campus (32°07′59″N, 118°81′37″E) and the Nanjing Botanical Garden of the Chinese Academy of Sciences (32°05′12″N, 118°83′47″E). Based on 100 randomly sampled leaves for each species, the ratio of leaf petiole length to lamina length is 0.26 ± 0.04 for CC, and 0.14 ± 0.02 for ML; the diameter of the leaf petiole is 0.15 ± 0.02 cm for CC, and 0.28 ± 0.03 cm for ML. On average, leaf petiole length is ca. 1/4 of lamina length for CC, and ca. 1/7 of lamina length for ML; CC has a longer and slenderer petiole than ML. Mature and intact leaves with leaf petioles were randomly sampled from the middle canopy between 8 am and 9 am. To reduce water loss, the sampled leaves were put into plastic self-sealing bags (28 cm × 20 cm), and quickly brought back to the laboratory at the Nanjing Forestry University Campus to measure lamina mass and leaf petiole mass, the total time lapse being less than two hours from the collection sites to the laboratory.

Lamina mass and leaf petiole mass were measured using an electronic balance (ME204/02, Mettler Toledo Company, Greifensee, Switzerland; measurement accuracy 0.0001 g), and the lamina image was scanned with an Epson scanner (V550, Epson Indonesia, Batam, Indonesia) at 600 dpi resolution. The images were converted to black–white images and saved as bitmap images at a 600 dpi resolution by Adobe Photoshop (version: 13.0). Then, the MATLAB (version ≥ 2009a) procedure developed by Shi et al. (2018b) was used to extract the planar coordinates of the leaf edges, and the R (based on R version 3.6.1; R Core Team, 2019) script proposed by Su et al. (2019) was used to measure lamina length, width, and area.

Statistical Methods

Lobry et al. (1991) proposed a model (i.e., LRF equation) to describe the effect of temperature on the growth rate of microbial populations. Shi et al. (2017) modified the LRF equation (i.e., MLRF equation) by adding a parameter δ to improve the fitting elasticity and used its integral to develop a new sigmoid growth equation. After adjusting the curves generated by the MLRF equation to make them more bilaterally symmetrical along the *x*-axis, we found that the following equation validly described ovate leaf shapes of many plants (Shi et al., 2021):

$$y = y_c\left[\frac{(x-x_1)(x-x_2)^2}{(x_2-x_c)\left[(x_2-x_c)(x-x_c)-(x_1-x_c)(x_c+x_2-2x)\right]}\right]^{\delta},$$

where, x_1 and x_2 represent, respectively, the lamina base as the starting point and the lamina apex as the ending point, x_c represents the point on the lamina length axis associated with lamina maximum width, y_c represents half lamina maximum width, and δ is a parameter influencing the curvature of the curve. The curvature of the lamina edge can be directly represented by the parameter δ of the ovate leaf shape model. A large δ value signifies a large curvature for the lamina edge [see Figure 1C of Shi et al. (2021)]. This equation produces half an ovate leaf shape, with the other half generated by $f(x) = -y$. In order to estimate the parameters of the MLRF equation, the Nelder-Mead optimization (Nelder and Mead, 1965) method was used to minimize the residual sum of squares (RSS):

$$\mathrm{RSS} = \sum_{j=1}^{n}\left(y_j - \hat{y}_j\right)^2,$$

where, n represents the number of data points on the lamina edge, the subscript j represents the jth point, and y_j with a circumflex represents the fitted response variable. For comparing the goodness of fit of the model to the lamina edge data of the two species, we calculated the adjusted root-mean-square error ($\mathrm{RMSE_{adj}}$) of each lamina (Wei et al., 2019; Shi et al., 2020b):

$$\mathrm{RMSE_{adj}} = \frac{\sqrt{\mathrm{RSS}/n}}{\sqrt{A/\pi}},$$

FIGURE 2 | Leaf examples of *Cinnamomum camphora* (L.) Presl and *Machilus leptophylla* Hand.-Mazz. (Lauraceae).

where, A is the lamina area. This indicator accounts for the proportion of the mean absolute deviation in the y values to the radius of an assumed circle whose area equals lamina area.

To measure the extent of lamina bilateral asymmetry, the standardized index (SI) proposed by Shi et al. (2018a) was calculated for each leaf. The indicator took a certain number of equidistant strips (rectangles) to intersect with a leaf, as shown in **Figure 3**. To obtain a more accurate value, we actually used 1,000 strips, but to conveniently show this approach only five strips were used in this figure. In each strip, the intersection between the strip and the lamina was divided into upper and lower parts, and their areas were represented by L_i and R_i respectively, where, i represents the ith strip. The mathematical expression of SI is as follows:

$$\mathrm{SI} = \frac{1}{1000}\sum_{i=1}^{1000}\frac{|\,Li - Ri|}{Li + Ri}.$$

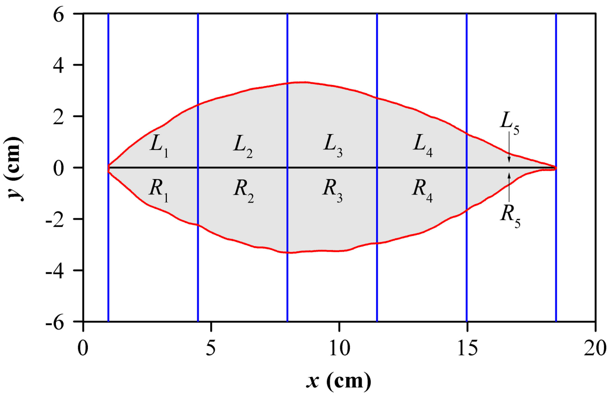

FIGURE 3 | Illustration for lamina bilateral asymmetry measure. For clarity, five equidistant strips are exhibited here, but 1000 strips were used in the actual calculation.

The smaller the SI, the smaller the degree of the bilateral asymmetry of a lamina. A prior study showed the log-transformation of SI made its distribution more normal (Shi et al., 2020a). Thus, we used the natural logarithm, i.e., ln SI, in the interspecific comparison.

To compare the significance of the difference in the extent of lamina bilateral asymmetry between the two species studied, leaf shape (reflected by the ratio of lamina width to lamina length, and the ratio of x_{c} to x_2), and the ratio of leaf petiole mass to lamina mass, the analysis of variance was carried out at the 0.05 significance level. The Pearson correlation coefficient test was used to test the significance of the correlation between the ratio of leaf petiole mass to lamina mass and the centroid ratio, and the correlation between the goodness of fit using the leaf shape model (reflected by $\mathrm{RMSE_{adj}}$) and the extent of lamina bilateral asymmetry. All statistical analyses were performed using R (version 3.6.1) (R Core Team, 2019).

RESULTS

The adjusted RMSEs of the MLRF equation for all laminas were smaller than 0.05, which verifies the validity of the MLRF equation in describing the ovate leaf shapes studied here. This shows that the mean absolute deviation between the observed and predicted y values is less than 5% of the radius of an assumed circle whose area equals lamina area for each of the 616 leaves. **Figure 4** exhibits two leaf examples and the predicted leaf shapes using the MLRF equation. Whether it is necessary to introduce a parameter to control the curvature in the MLRF equation was answered here; **Figure 5A** showed that most estimates of δ for CC were larger than 1, and the mean estimated δ of CC was significantly larger that of ML. This means that the leaf shape of CC has a larger curvature than that of ML. However, there was no significant difference in the goodness of fit between the two species according to the calculated adjusted RMSE values (**Figure 5B**). See **Supplementary Table 1** for details.

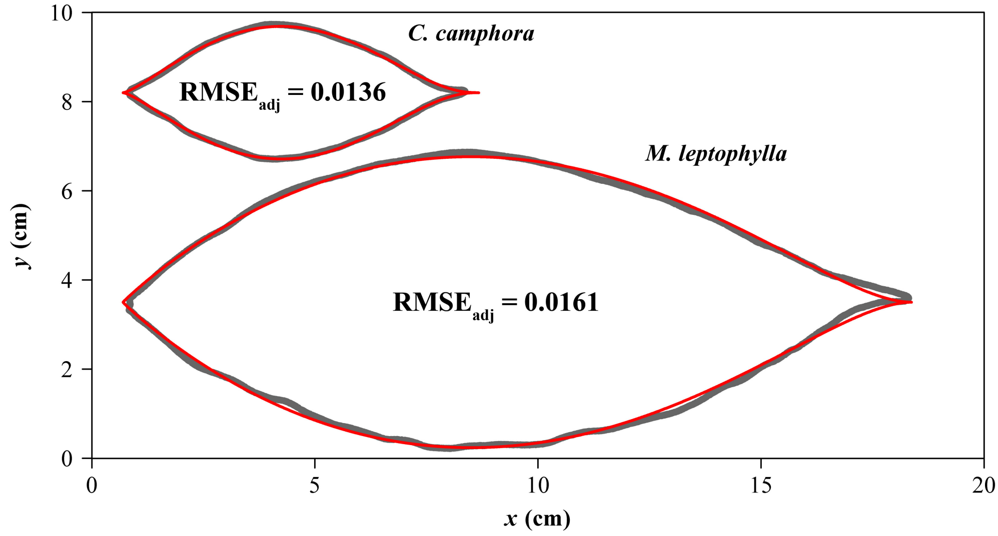

FIGURE 4 | Comparisons between the scanned leaf edges (gray curves) and the leaf edges predicted by the MLRF equation (red curves) for one leaf example each of *Cinnamomum camphora* (L.) Presl and *Machilus leptophylla* Hand.-Mazz. The adjusted root-mean-square error (RMSE$_{adj}$) is used to reflect the goodness of fit.

There were significant differences in leaf bilateral asymmetry (**Figure 5C**), the ratio of lamina width to length (**Figure 5D**), the ratio of leaf petiole mass to lamina mass (**Figure 5E**), and the centroid ratio (**Figure 5F**). CC has a more bilaterally symmetrical and broader leaf shape than ML; the lamina centroids are both close to the lamina bases for the two species, but the centroid of CC is closer to the lamina base; the ratio of leaf petiole mass to lamina mass of CC is significantly smaller than that of ML.

There was a significant negative correlation between the centroid ratio and that of leaf petiole mass to lamina mass for CC ($r = -0.14$; $P < 0.05$), but a significant positive correlation for ML ($r = 0.30$; $P < 0.05$). For the pooled data, a significant positive correlation was found ($r = 0.17$; $P < 0.05$).

There was a significant positive correlation between the adjusted RMSE values and the SI values for each species: the coefficient of correlation of *C. camphora* was 0.71 ($P < 0.01$), and that of *M. leptophylla* was 0.74 ($P < 0.01$) (**Figure 6**), which means that approximately 50% of the unexplained variation using the MLRF equation can be further accounted for by the extent of lamina bilateral asymmetry.

DISCUSSION

Link of the Validity of the Leaf Shape Equation to Lamina Bilateral Asymmetry

Although the extant leaf shape models (Dornbusch et al., 2011; Shi et al., 2015; Li et al., 2021) have been verified to be valid for plants with special leaf shapes, the question of lamina bilateral asymmetry has been little considered. The current study shows that the MLRF model has explained more than 95% of the mean absolute deviation in *y* values relative to the radius of an assumed circle whose area equals lamina area. The remaining prediction errors could be explained by the extent of leaf bilateral asymmetry, and the explained variation approximated 50%. This work implies that the validity of a leaf shape model is closely related to the extent of leaf bilateral asymmetry. For a leaf shape apparently deviating from a bilateral asymmetry hypothesis, it is necessary to introduce one or more parameter(s) to a model for reflecting such a deviation (Huang et al., 2020; Li et al., 2021). However, in the current study, the leaf shapes of two Lauraceae species are basically bilaterally symmetrical, and there is only a slight deviation in lamina apex from the lamina length axis (i.e., the symmetrical axis). This is a small but important functional modification for leaves to conveniently drain the water on the leaf surface (Wang et al., 2020). In future studies on developing other leaf shape models, investigators will have to consider whether it is necessary to introduce one or more parameter(s) to reflect the lamina asymmetry by checking whether the deviation from a perfect bilateral symmetry is large or negligible. Through the correlation analysis on RMSE$_{adj}$ and SI, we found that the degree of lamina asymmetry significantly influenced the goodness of fit of the model. The larger the degree of lamina asymmetry, the larger the RMSE$_{adj}$. Thus, the degree of lamina asymmetry can be quantified by the goodness of fit of the MLRF equation, which suggests that similar approaches are promising in quantifying or evaluating the degree of lamina bilateral asymmetry in future studies related to leaf asymmetry.

Apparently, the leaf shape characteristics including lamina bilateral symmetry or asymmetry are a result of the interactions for plants and environmental factors (Chitwood and Sinha, 2016). Plants growing in different environments show corresponding structural and physiological adaptabilities to external environmental conditions, such as moisture and carbon dioxide content (Ito et al., 2015; de Boer et al., 2016); light capture efficiency and the location of the leaves in the crown can both influence leaf shape (Reich et al., 1998). The leaf bilateral symmetry of CC was better than ML. The following reasons

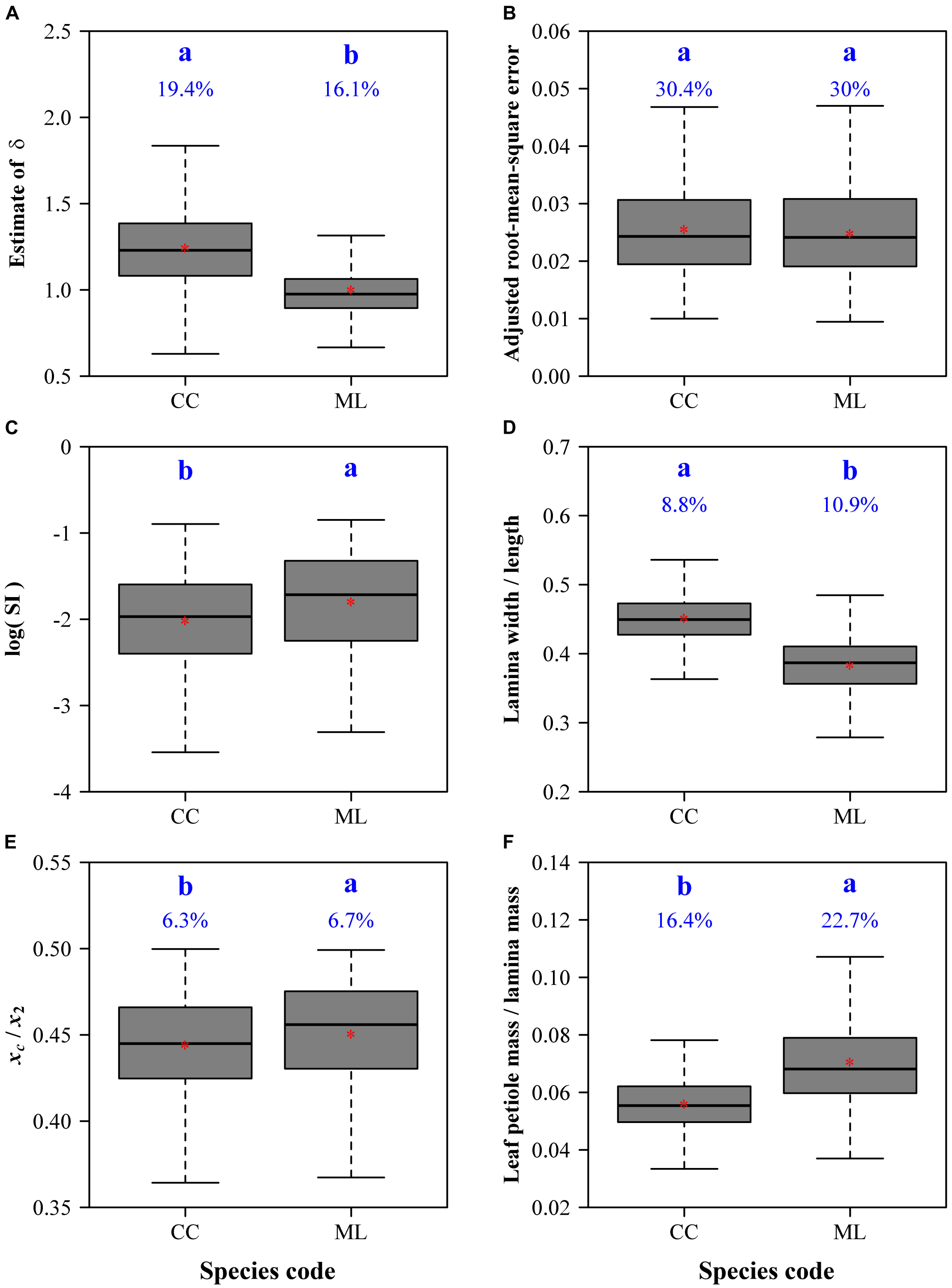

FIGURE 5 | Comparisons of the estimates of δ **(A)**, adjusted root-mean-square errors **(B)**, the natural logarithms of the standardized indices for lamina bilateral asymmetry **(C)**, ratios of lamina width to length **(D)**, centroid ratios (i.e., x_c/x_2) **(E)**, and ratios of leaf petiole mass to lamina mass **(F)** between *C. camphora* (represented by CC) and *M. leptophylla* (represented by ML). In each panel, the letters a and b are used to represent the significance of the differences between the two species, with species sharing a common letter not differing significantly at the 0.05 significance level; the percentage numbers at the top of the whiskers represent the coefficients of variation; the horizontal lines in boxes represent medians, and the asterisks in boxes represent means.

might have led to this result. For one thing, the lamina size of ML is larger, and it requires a more skewed lamina apex to rapidly drain the water on the leaf surface (Wang et al., 2020). Also, the ratio of lamina width to length of ML is significantly smaller than that of CC (**Figure 5D**), and the narrow leaf shape tends to cause large variations in the symmetrical distributions of hierarchical reticulate veins and in the cell division rates on both sides of the lamina (Dengler and Kang, 2001).

Influences of the Lamina Centroid Ratio and Leaf Petiole Pattern on the Investment of Mass to Leaf Petiole

The tradeoff between leaf photosynthetic investment and leaf support investment is always a study hotspot in botany (Niklas, 1991; Niinemets et al., 2007). Previous studies show that lamina mass positively correlates with lamina area, and leaf petiole mass also positively correlates with lamina mass on a log-log scale (Niklas, 1991; Li et al., 2008). Leaf shape has been demonstrated to affect the scaling relationship between lamina mass and lamina area (Lin et al., 2020), but few studies have been carried out to examine whether leaf shape can change the scaling relationship between leaf petiole mass and lamina mass. In this work, we analyzed the correlation between the lamina centroid ratio and the ratio of leaf petiole mass to lamina mass for two Lauraceae species, and found a negative correlation for the long and slender petiole (CC) and a positive correlation for the short and thick leaf petiole (ML).

The ratios of lamina width to length of CC and ML differ significantly. CC has a smaller and broader lamina, which greatly reduces the supporting requirement for the leaf petiole. Thus, smaller and broader leaves tend to have long and slender leaf petioles and are little influenced by the centroid ratio. ML has a larger and narrower lamina that increases the burden of the leaf petiole, so leaf petiole mass correlates with lamina mass. When the lamina centroid is far away from the lamina base, the plants tend to have short but thick leaf petioles to support laminas for maintaining the maximum light surface (Takenaka, 1994). Large laminas need the petiole to enhance the ability to conduct water, but also endure the role of external forces (Niklas, 1999), which requires increasing the investment of mass to the leaf petiole. The results indicated that lamina size and shape can significantly modulate the allocation of investment between the lamina mass and leaf petiole mass, thereby affecting leaf development patterns in different environments.

Fluctuating asymmetry is widely used as a measure of developmental stability (Palmer and Strobeck, 1986; Palmer, 1994). It regards the difference in a trait of interest between two sides of a sample as a developmental "noise." There are many indices to measure the level of fluctuating asymmetry, and the SI can be deemed as one indicator of fluctuating asymmetry [compared with FA2 of Palmer (1994)]. This is to say, the indicator here measured the extent of leaf fluctuating asymmetry. It is somewhat valuable to compare different fluctuating asymmetry indices for recommending the best one. However, the present work mainly focuses on: (i) the description of the ovate leaf shape using a known parametric model, i.e., the MLRF model, based on a large sample size, and (ii) whether the centroid ratio, which is obtained from the parameters of the ovate leaf shape model, can have a significant influence on the allocation of biomass to the petiole and lamina. Although we quantified the extent of lamina bilateral asymmetry using SI, it was used only to explore whether the goodness of fit of the ovate leaf shape model is associated with the extent of lamina bilateral asymmetry. The results showed that lamina bilateral asymmetry (which reflects SI) accounted for ca. 50% of the unexplained variation of the MLRF model. Our ovate leaf shape model actually hypothesizes (predicts) a perfectly bilateral symmetrical leaf shape, i.e., an ideal norm without developmental instability, so any existing asymmetry for laminas will more or less weaken the model's power. Fortunately, given developmental stability of leaves, the studied laminas are of nice bilateral symmetry except a minor deviation (which we can regard as a 'modification' from a bilateral symmetry) at the lamina apex for a functional drainage requirement. It is necessary to point out that fluctuating asymmetry is a population parameter rather than a sample parameter (Graham, 2021), so it requires using a large sample size to reflect an accurate asymmetrical trait of interest. To serve our study aim of testing whether the validity of the MLRF model is related to the extent of lamina bilateral asymmetry based on individual leaves (samples), for the two studied species, 320 and 296 leaves were used respectively,

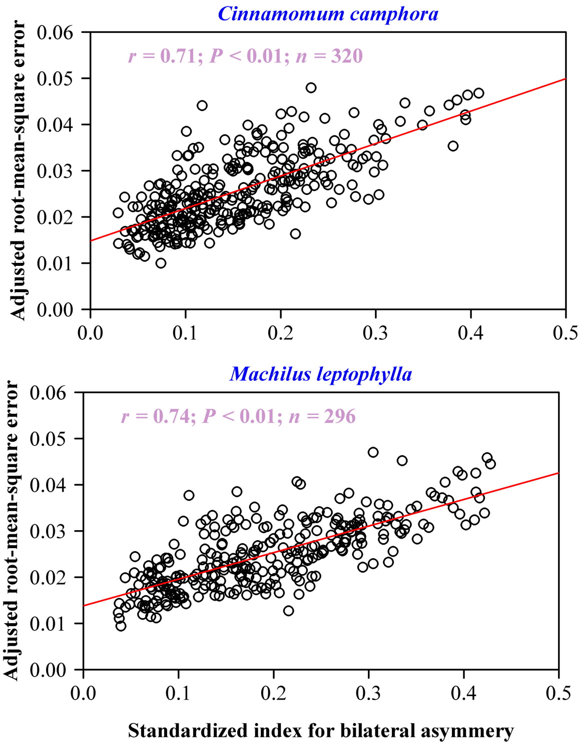

FIGURE 6 | Correlation between the adjusted root-mean-square error and standardized index for lamina bilateral asymmetry. In each panel, the open circles represent the observations; the red straight line represents the regression line; r is the coefficient of correlation; n is the sample size.

which should represent the general traits of lamina structure including lamina bilateral asymmetry.

CONCLUSION

In this study, we tested the validity of the MLRF model for describing leaf shapes of two species of Lauraceae using a large sample for each species. The equation was confirmed to be credible to describe the actual shapes, and all adjusted root-mean-square errors (RMSEs) were smaller than 0.05. This means that the mean absolute deviation is smaller than 5% of the radius of an assumed circle whose area is equal to the lamina area. We also found that the goodness of fit of the MLRF model relied on the extent of lamina bilateral asymmetry. The prediction error can be further accounted for by the lamina bilateral asymmetry, and it explained ca. 50% of the unexplained variation of the MLRF model. In addition, we did not find consistent evidence that the centroid ratio is positively correlated with the ratio of leaf petiole mass to lamina mass, which is perhaps associated with leaf petiole patterns. A long and slender leaf petiole tends to correspond to a small and broad leaf, regardless of the centroid ratio; a short and thick leaf petiole tends to correspond to a large and narrow leaf, and the ratio of leaf petiole mass to lamina mass is more likely to positively correlate with the lamina centroid ratio. This work provides important insights into the link between leaf structure and function.

DATA AVAILABILITY STATEMENT

The original contributions presented in the study are included in the article/**Supplementary Material**, further inquiries can be directed to the corresponding authors.

AUTHOR CONTRIBUTIONS

DR, HW, and PS designed the work, analyzed the data, and revised the manuscript. YL and YZ carried out the experiment and wrote the initial draft. All authors commented on and agreed with this submission.

ACKNOWLEDGMENTS

We thank Karl J. Niklas, Yabing Jiao, Mengdi Liu, Rong Wang, and Kexin Yu for their valuable help in the preparation of this manuscript.

SUPPLEMENTARY MATERIAL

The Supplementary Material for this article can be found online at: https://www.frontiersin.org/articles/10.3389/fpls.2021.822907/full#supplementary-material

REFERENCES

Baird, A. S., Taylor, S. H., Pasquet-Kok, J., Vuong, C., Zhang, Y., Watcharamongkold, T., et al. (2021). Developmental and biophysical determinants of grass leaf size worldwide. *Nature* 592, 242–247. doi: 10.1038/s41586-021-03370-0

Chitwood, D. H., and Sinha, N. R. (2016). Evolutionary and environmental forces sculpting leaf development. *Curr. Biol.* 26, 297–306. doi: 10.1016/j.cub.2016.02.033

Daas-Ghrib, C., Montpied, P., Ksontini, M., and Dreyer, E. (2011). Functional relationships between leaf structure and photosynthetic traits as modulated by irradiance and nutrient availability in a sclerophyllous and a non-sclerophyllous mediterranean oak species. *Eur. J. For. Res.* 130, 503–512. doi: 10.1007/s10342-010-0438-4

de Boer, H. J., Price, C. A., Wagner-Cremer, F., Dekker, S. C., Franks, P. J., and Veneklaas, E. J. (2016). Optimal allocation of leaf epidermal area for gas exchange. *New Phytol.* 210, 1219–1228. doi: 10.1111/nph.13929

Dengler, N. G., and Kang, J. (2001). Vascular patterning and leaf shape. *Curr. Opin. Plant Biol.* 4, 50–56. doi: 10.1016/s1369-5266(00)00135-7

Dornbusch, T., Watt, J., Baccar, R., Fournier, C., and Andrieu, B. (2011). A comparative analysis of leaf shape of wheat, barley and maize using an empirical shape model. *Ann. Bot.* 107, 865–873. doi: 10.1093/aob/mcq181

Gielis, J. (2003). A general geometric transformation that unifies a wide range of natural and abstract shapes. *Am. J. Bot.* 90, 333–338. doi: 10.3732/ajb.90.3.333

Graham, J. H. (2021). Fluctuating asymmetry and developmental instability, a guide to best practice. *Symmetry* 13:9. doi: 10.3390/sym13010009

Guo, X., Reddy, G. V. P., He, J., Li, J., and Shi, P. (2020). Mean-variance relationships of leaf bilateral asymmetry for 35 species of plants and their implications. *Glob. Ecol. Conserv.* 23:e01152.

Guo, X., Shi, P., Niinemets, Ü, Hölscher, D., Wang, R., Liu, M., et al. (2021). Leaf diminishing returns of five different age-groups of moso bamboo (*Phyllostachys edulis*) culms. *Am. J. Bot.* 108, 1662–1672. doi: 10.1002/ajb2.1738

Huang, W., Ratkowsky, D. A., Hui, C., Wang, P., Su, J., and Shi, P. (2019a). Leaf fresh weight versus dry weight: which is better for describing the scaling relationship between leaf biomass and leaf area for broad-leaved plants? *Forests* 10:256.

Huang, W., Reddy, G. V., Li, Y., Larsen, J. B., and Shi, P. (2020). Increase in absolute leaf water content tends to keep pace with that of leaf dry mass-evidence from bamboo plants. *Symmetry* 12:1345.

Huang, W., Su, X., Ratkowsky, D. A., Niklas, K. J., Gielis, J., and Shi, P. (2019b). The scaling relationships of leaf biomass vs. leaf surface area of 12 bamboo species. *Glob. Ecol. Conserv.* 20:e00793. doi: 10.1016/j.gecco.2019.e00793

Ito, F., Komatsubara, S., Shigezawa, N., Morikawa, H., Murakami, Y., Yoshino, K., et al. (2015). Mechanics of water collection in plants via morphology change of conical hairs. *Appl. Phys. Lett.* 106:133701. doi: 10.1063/1.4916213

Kierzkowski, D., Runions, A., Vuolo, F., Strauss, S., Lymbouridou, R., Routier-Kierzkowska, A.-L., et al. (2019). A growth-based framework for leaf shape development and diversity. *Cell* 177, 1405–1418.e17. doi: 10.1016/j.cell.2019.05.011

Li, G., Yang, D., and Sun, S. (2008). Allometric relationships between lamina area, lamina mass and petiole mass of 93 temperate woody species vary with leaf habit, leaf form and altitude. *Funct. Ecol.* 22, 557–564.

Li, Y., Niklas, K. J., Gielis, J., Niinemets, Ü, Schrader, J., Wang, R., et al. (2021). An elliptical blade is not a true ellipse, but a superellipse – Evidence from two Michelia species. *J. Fore. Res.* (in press). doi: 10.1007/s11676-021-01385-x

Lin, S., Niklas, K. J., Wan, Y., Hölscher, D., Hui, C., Ding, Y., et al. (2020). Leaf shape influences the scaling of leaf dry mass vs. area: a test case using bamboos. *Ann. For. Sci.* 77:11.

Lin, S., Shao, L., Hui, C., Song, Y., Reddy, G. V. P., Gielis, J., et al. (2018). Why does not the leaf weight-area allometry of bamboos follow the 3/2-power law? *Front. Plant Sci.* 9:583. doi: 10.3389/fpls.2018.00583

Lin, S., Zhang, L., Reddy, G. V. P., Hui, C., Gielis, J., Ding, Y., et al. (2016). A geometrical model for testing bilateral symmetry of bamboo leaf with a simplified Gielis equation. *Ecol. Evol.* 6, 6798–6806. doi: 10.1002/ece3.2407

Lobry, J. R., Rosso, L., and Flandrois, J. P. (1991). A FORTRAN subroutine for the determination of parameter confidence limits in non-linear models. *Binary* 3, 86–93.

Milla, R., and Reich, P. B. (2007). The scaling of leaf area and mass: the cost of light interception increases with leaf size. *Proc. R. Soc. Biol. Sci.* 274:2109e2114. doi: 10.1098/rspb.2007.0417

Nelder, J. A., and Mead, R. (1965). A simplex algorithm for function minimization. *Comput. J.* 7, 308–313.

Nicotra, A. B., Leigh, A., Boyce, C. K., Jones, C. S., Niklas, K. J., Royer, D. L., et al. (2011). The evolution and functional significance of leaf shape in the angiosperms. *Funct. Plant Biol.* 38, 535–552. doi: 10.1071/FP11057

Niinemets, Ü, Portsmuth, A., and Tobias, M. (2007). Leaf shape and venation pattern alter the support investments within leaf lamina in temperate species, a neglected source of leaf physiological differentiation. *Funct. Ecol.* 21, 28–40.

Niklas, K. J. (1991). The elastic moduli and mechanics of *Populus tremuloides* (Salicaceae) petioles in bending and torsion. *Am. J. Bot.* 78, 989–996.

Niklas, K. J. (1999). A mechanical perspective on foliage leaf form and function. *New Phytol.* 143, 19–31. doi: 10.1046/j.1469-8137.1999.00441.x

Niklas, K. J., Cobb, E. D., Niinemets, Ü, Reich, P. B., Sellin, A., and Shipley, B. (2007). Diminishing returns" in the scaling of functional leaf traits across and within species groups. *Proc. Natl. Acad. Sci. U.S.A.* 104, 8891–8896. doi: 10.1073/pnas.0701135104

Palmer, A. R. (1994). "Fluctuating asymmetry analyses: a primer," in *Developmental Instability: Its Origins and Evolutionary Implications*, ed. T. A. Markow (Netherlands: Kluwer), 335–364. doi: 10.1007/978-94-011-0830-0_26

Palmer, A. R., and Strobeck, C. (1986). Fluctuating asymmetry: measurement, analysis, patterns. *Ann. Rev. Ecol. Syst.* 17, 391–421. doi: 10.1146/annurev.es.17.110186.002135

R Core Team (2019). *R: A Language and Environment for Statistical Computing.* Vienna: R Foundation for statistical computing.

Ratkowsky, D. A., and Reddy, G. V. P. (2017). Empirical model with excellent statistical properties for describing temperature-dependent developmental rates of insects and mites. *Ann. Entomol. Soc. Am.* 110, 302–309.

Reich, P. B., Walters, M. B., Tjoelker, M. G., Vanderklein, D., and Buschena, C. (1998). Photosynthesis and respiration rates depend on leaf and root morphology and nitrogen concentration in nine boreal tree species differing in relative growth rate. *Funct. Ecol.* 12, 395–405. doi: 10.1046/j.1365-2435.1998.00209.x

Rosso, L., Lobry, J. R., and Flandrois, J. P. (1993). An unexpected correlation between cardinal temperatures of microbial growth high-lighted by a new model. *J. Theor. Biol.* 162, 447–463. doi: 10.1006/jtbi.1993.1099

Runions, A., Tsiantis, M., and Prusinkiewicz, P. (2017). A common developmental program can produce diverse leaf shapes. *New Phytol.* 216, 401–418. doi: 10.1111/nph.14449

Schrader, J., Shi, P., Royer, D. L., Peppe, D. J., Gallagher, R. V., Li, Y., et al. (2021). Leaf size estimation based on leaf length, width and shape. *Ann. Bot.* 128, 395–406. doi: 10.1093/aob/mcab078

Shi, P., Fan, M., Ratkowsky, D. A., Huang, J., Wu, H., Chen, L., et al. (2017). Comparison of two ontogenetic growth equations for animals and plants. *Ecol. Model.* 349, 1–10. doi: 10.1016/j.ecolmodel.2017.01.012

Shi, P., Liu, M., Ratkowsky, D. A., Gielis, J., Su, J., Yu, X., et al. (2019). Leaf area-length allometry and its implications in leaf-shape evolution. *Trees Struct. Funct.* 33, 1073–1085. doi: 10.1007/s00468-019-01843-4

Shi, P., Niinemets, Ü, Hui, C., Niklas, K. J., Yu, X., and Hölscher, D. (2020a). Leaf bilateral symmetry and the scaling of the perimeter vs. the surface area in 15 vine species. *Forests* 11:246. doi: 10.3390/f11020246

Shi, P., Ratkowsky, D. A., and Gielis, J. (2020b). The generalized Gielis geometric equation and its application. *Symmetry* 12:645. doi: 10.3390/sym12040645

Shi, P., Ratkowsky, D. A., Li, Y., Zhang, L., Lin, S., and Gielis, J. (2018b). General leaf area geometric formula exists for plants—evidence from the simplified Gielis equation. *Forests* 9:714. doi: 10.3390/f9110714

Shi, P., Xu, Q., Sandhu, H. S., Gielis, J., Ding, Y., Li, H., et al. (2015). Comparison of dwarf bamboos (*Indocalamus* sp.) leaf parameters to determine relationship between spatial density of plants and total leaf area per plant. *Ecol. Evol.* 5, 4578–4589. doi: 10.1002/ece3.1728

Shi, P., Yu, K., Niklas, K. J., Schrader, J., Song, Y., Zhu, R., et al. (2021). A general model for describing the ovate leaf shape. *Symmetry* 13:1524. doi: 10.3390/sym13081524

Shi, P., Zheng, X., Ratkowsky, D. A., Li, Y., Wang, P., and Cheng, L. (2018a). A simple method for measuring the bilateral symmetry of leaves. *Symmetry* 10:118. doi: 10.3390/sym10040118

Smith, W. K., Vogelmann, T. C., DeLucia, E. H., Bell, D. T., and Shepherd, K. A. (1997). Leaf form and photosynthesis: do leaf structure and orientation interact to regulate internal light and carbon dioxide? *BioScience* 47, 785–793.

Su, J., Niklas, K. J., Huang, W., Yu, X., Yang, Y., and Shi, P. (2019). Lamina shape does not correlate with lamina surface area: an analysis based on the simplified Gielis equation. *Glob. Ecol. Conserv.* 19:e00666. doi: 10.1016/j.gecco.2019.e00666

Takenaka, A. (1994). Effects of leaf blade narrowness and petiole length on the light capture efficiency of a shoot. *Ecol. Res.* 9, 109–114. doi: 10.1007/BF02347485

Thompson, D. W. (1917). *On Growth and Form.* London: Cambridge University Press.

Wang, P., Ratkowsky, D. A., Xiao, X., Yu, X., Su, J., Zhang, L., et al. (2018). Taylor's power law for leaf bilateral symmetry. *Forests* 9:500. doi: 10.3390/f9080500

Wang, T., Si, Y., Dai, H., Li, C., Gao, C., Dong, Z., et al. (2020). Apex structures enhance water drainage on leaves. *Proc. Natl. Acad. Sci. U.S.A.* 117, 1890–1894. doi: 10.1073/pnas.1909924117

Wei, H. L., Li, X. M., and Huang, H. (2019). Leaf shape simulation of castor bean and its application in nondestructive leaf area estimation. *Int. J. Agric. Biol. Eng.* 12, 135–140. doi: 10.25165/j.ijabe.20191204.4040

Wright, I. J., Dong, N., Maire, V., Prentice, I. C., Westoby, M., Díaz, S., et al. (2017). Global climatic drivers of leaf size. *Science* 357, 917–921. doi: 10.1126/science.aal4760

Wright, I. J., Reich, P. B., Westoby, M., Ackerly, D. D., Baruch, Z., Bongers, F., et al. (2004). The worldwide leaf economics spectrum. *Nature* 428, 821–827.

Yu, X., Shi, P., Schrader, J., and Niklas, K. J. (2020). Nondestructive estimation of leaf area for 15 species of vines with different leaf shapes. *Am. J. Bot.* 107, 1481–1490. doi: 10.1002/ajb2.1560

Conflict of Interest: The authors declare that the research was conducted in the absence of any commercial or financial relationships that could be construed as a potential conflict of interest.

frontiers in Plant Science

ORIGINAL RESEARCH
published: 04 February 2022
doi: 10.3389/fpls.2021.778547

Comparison of Leaf and Fine Root Traits Between Annuals and Perennials, Implicating the Mechanism of Species Changes in Desertified Grasslands

Zhiying Ning[1,2], Yulin Li[1], Xueyong Zhao[1]*, Dan Han[3] and Jin Zhan[1,2]*

[1] Naiman Desertification Research Station, Northwest Institute of Eco-Environment and Resources, Chinese Academy of Sciences, Lanzhou, China, [2] University of Chinese Academy of Sciences, Beijing, China, [3] Yangling Agricultural Hi-Tech Industries Demonstration Zone, Xi'an, China

OPEN ACCESS

Edited by:
Ülo Niinemets,
Estonian University of Life Sciences,
Estonia

Reviewed by:
Agnieszka Piernik,
Nicolaus Copernicus University
in Toruń, Poland
Shimon Rachmilevitch,
Ben-Gurion University of the Negev,
Israel

***Correspondence:**
Zhiying Ning
ningzhiying125@163.com
Xueyong Zhao
zhaoxy@lzb.ac.cn

Specialty section:
This article was submitted to
Functional Plant Ecology,
a section of the journal
Frontiers in Plant Science

Received: 17 September 2021
Accepted: 31 December 2021
Published: 04 February 2022

Citation:
Ning Z, Li Y, Zhao X, Han D and
Zhan J (2022) Comparison of Leaf
and Fine Root Traits Between Annuals
and Perennials, Implicating
the Mechanism of Species Changes
in Desertified Grasslands.
Front. Plant Sci. 12:778547.
doi: 10.3389/fpls.2021.778547

Annual species show traits, such as shortleaf lifetimes, higher specific leaf area, and leaf nutrient concentrations, that provided a more rapid resource acquisition compared to perennials. However, the comparison of root traits between the annuals and perennials is extremely limited, as well as the trade-offs of leaf and fine root traits, and resource allocation between leaf and root, which may provide insight into the mechanism of species changes in arid and semi-arid areas. With lab analysis and field observation, 12 traits of leaf and fine root of 54 dominant species from Horqin Sandy Land, Northeastern China were measured. The organization of leaf and fine root traits, and coordination between leaf and fine root traits of annual and perennial plants were examined. Results showed that there were differences between annuals and perennials in several leaves and fine root traits important in resource acquisition and conservation. Annuals had higher leaf area (LA), specific LA (SLA), and specific root length (SRL) but lower leaf dry-matter content (LDMC), leaf tissue density (LTD), leaf carbon concentration (LC), and fine root dry-matter content (FRDMC) than perennials. Leaf nitrogen (LN) concentration and fine root nitrogen concentration (FRN) were negatively related to LTD and FRDMC in annuals, while FRN was positively related to FRTD and fine root carbon concentration (FRC), and LA was positively related to LN in perennials. These implied that annuals exhibited tough tissue and low palatability, but perennials tend to have smaller leaves to reduce metabolism when N is insufficient. Annuals showed significant positive correlations between FRC/FRDMC and LDMC/LTD/LC, suggesting a proportional allocation of photosynthate between leaf and fine root. In perennials, significant negative correlations were detected between LN, LC, and SRL, fine root tissue density (FRTD), as well as between LA and FRTD/FRC. These indicated that perennials tend to allocate more photosynthate to construct a deeper and rigid roots system to improve resource absorption capacity in resource-limited habitats. Our findings suggested that annuals and perennials differed considerably in terms of adaptation, resource acquisition, and allocation strategies, which might be partly responsible for species changes in desertified grasslands. More broadly, this work might be conducive to understand the mechanism of species changes and could also provide support to the management and restoration of desertified grassland in arid and semi-arid areas.

Keywords: leaf, fine root, plant functional traits, annuals, perennials, species changes, arid and semi-arid area

INTRODUCTION

Species changes are universal in degraded ecosystems, especially in desertified grassland in arid and semi-arid areas (Kerley and Whitford, 2009; Pfeiffer et al., 2019). Dominant species in grassland changed from perennial grasses to annual forbs and grasses after grazing in western Oklahoma, United States (Collins et al., 1988). Herbaceous species, especially grasses, were lost and replaced by xerophytic shrubs or semi-shrubs during the degradation development in the cold semi-arid grasslands of Qinghai-Tibet Plateau, North-west China (Li et al., 2006). Understanding the mechanisms underlying these changes has been a challenge for ecologists. Previous studies suggested that the species changes during grassland desertification are the results of the interaction between species adaptation and environmental changes (D'Odorico et al., 2013; Zhang et al., 2020). Plant growth is often limited by drought stress and nutrient deficiency in arid and semi-arid areas, which have been exacerbated due to grassland desertification (Bennett and Adams, 2001; Yair and Kossovsky, 2002; Dong et al., 2009). Generally, functional traits have been used as indicators of plant species response to environmental change for characterizing plant survival and resource use strategies under stress conditions (Dyer et al., 2001; Reich et al., 2003). Previous studies compared photosynthetic, leaf morphology, and chemistry traits in annuals and perennials (Jaikumar et al., 2013; González-Paleo and Ravetta, 2018; González-Paleo et al., 2019). Nonetheless, few have specialized in the differences in coordination and organization in leaf and fine root traits between annuals and perennials, and very few have linked these with species changes. This study explores the plant adaptive mechanisms and species assembly rules by addressing the question as to whether there are differences in trade-offs of leaf and fine root traits between annuals and perennials.

Abundant pieces of evidence suggested that for plants, annual and perennial life histories exhibit leaf traits trade-offs between the rapid acquisition of resources and conservation of resources (Diaz et al., 2004; Wright et al., 2004a; Monroe et al., 2019). Annuals with shortleaf lifetimes, high SLA and leaf N concentrations, and fast returns to light and CO_2 generally capture resources and complete their life cycles more rapidly (Wright et al., 2004b), while perennials exhibit robustness and low palatability allow continued leaf function to maximize resource conservation and have adaptive advantages in resource-limited conditions (González-Paleo et al., 2019). However, compared to leaf traits, fewer studies have focused on traits of underground organs of annuals and perennials (Roumet et al., 2006; DuPont et al., 2014). It is not clear whether traits of root exhibit similar trade-offs (between below-ground resource acquisition and resource conservation, and root persistence) to leaf. Yet, there is some evidence suggesting that suites of correlated root traits are linked to plant growth strategies. Fort et al. (2012) found that drought-sensitive species have higher SRL, revealing more opportunistic root strategies than drought-tolerant species. Laughlin et al. (2021) demonstrated that forest species in warm climates tend to have low SRL and high root tissue density (RTD), but species in cold climates exhibit a high SRL and low RTD. In addition, roots directly access underground resources (nutrients and water) and hence better reflect plant underground components in response to the environmental changes and the adaptive strategy of plants to stressed conditions in desertified grassland (Hodge, 2004; Bardgett et al., 2014). The most obvious changes during grassland desertification are the decrease in productivity and selective loss of nutrient-rich fine soil particles which lead to seriously coarse-textured soil, poor soil nutrients, and soil water retention (McLendon and Redente, 1992; Zuo et al., 2009). Plant growth is mainly limited by drought stress and nutrient deficiency rather than light and CO_2 in desertified grassland in arid and semi-arid grasslands. We, therefore, tested whether fine root traits and organization of fine root traits differ between annuals and perennials, which might give insights in understanding species assembly in arid and semi-arid areas.

If root traits between annuals and perennials are subjected to the same trade-offs as leaf traits (resource acquisition and resource conservation), differences in leaf-root traits coordination between annuals and perennials are expected, with leaf-root traits exhibiting extravagant resource allocation strategy between above- and belowground components in annuals, and resource conservation allocation strategy in perennials. Growing evidence of consistent trait syndromes between leaf and root indicates coordination between above- and belowground organs in terms of the acquisition and allocation of limited resources (Liu et al., 2010; de la Riva et al., 2016). However, there are more reasons to expect that trade-offs between leaf and fine root traits of annual species might differ considerably from those of perennials. Literature demonstrated that this coordination varied between growth forms and strategies. For example, Valverde-Barrantes et al. (2021) found that among woody plants, high LN is associated with low RTD, whereas among non-woody plants, low SRL is associated with high LN. Fort et al. (2012) showed that for the same SLA, drought-tolerant species exhibit higher root mass and lower SRL than drought-sensitive species, to develop and maintain a coarser and deeper root system. These trade-offs are the result of plant species adapting to resource-poor habitats by improving their resource-acquisition ability. In addition, trade-offs between leaf and root traits might be also altered due to changes in the environment owing to climatic or edaphic shifts. Results from Liu et al. (2010) suggested that the ratio of leaf

N per area root N per length increased, but the ratios of SLA to SRL and leaf N to root N decreased from semi-arid to arid environment. These changes are associated with the allocation of photosynthates and N to root, likely reflecting that those plants tend to allocate more resources to the construction of root systems due to extremely dry conditions (Craine, 2006; Morales et al., 2015). We surmised that different patterns of resource allocation between leaf and root might be observed in annuals and perennials, in response to stressed habitat, which might be conducive to further understanding of adaptation strategies of annual and perennial species in desertified grassland.

This study investigated 12 traits of leaf and fine root of 54 dominant species in Horqin Sandy Land, Northeastern China, to analyze leaf and fine root traits organization and leaf-root traits coordination in annuals and perennials, respectively. Horqin Sandy Land is one of the four well-known Sandy Lands in northern China, has been subjected to serious desertification in the last 40 years (Duan et al., 2014). Studies in this area have found that the dominance of annual species decreased but that of perennial species increased with the desertification development (Zhang et al., 2004; Zuo et al., 2009; Ning et al., 2021). These might be attributed to the adaptation of plant species to environmental changes, as well as different resource use strategies. Our objective is to explore plant strategies of resource use and allocation in annuals and perennials, by using a functional approach, thereby implicating the mechanism of species changes in desertified grassland. Specifically, we hypothesize that: (a) Annual species differ from perennial species in fine root traits organization in desertified grassland in arid and semi-arid areas; (b) The coordination between leaf and fine root traits of the annuals and perennials differs in ways that may reflect different resource allocation strategies.

MATERIALS AND METHODS

Study Area

The study was conducted in the Horqin Sandy Land (118.4°E to 123.5°E, 42.7°N to 45.8°N, 180 to 650 masl), which covers an area of 12.90×10^4 km^2 in the northeastern part of Inner Mongolia, China. The area has a continental semi-arid to a semi-humid monsoon climate. The mean annual temperature ranges from 5.8°C to 6.4°C, with mean monthly temperatures from −12.6°C in January to 23.5°C in August, and mean annual precipitation from 343 mm to 451 mm, of which approximately 70% falls from June to August. The mean annual potential evaporation ranges from 1,500 to 2,500 mm. The mean annual wind velocity ranges from 3.5 to 4.5 m s^{-1}, and the mean wind velocity in spring (the season with the lowest vegetation cover and thus, the greatest vulnerability to erosion) ranges from 4.2 to 5.9 m s^{-1}. Windy days with a velocity greater than 17 m s^{-1} is from 25 to 40 days per year, which results in 10 to 15 days of sandstorms and dust storms, mainly (more than 70% of the total) in the spring.

The Horqin Sandy Land is a sandy dune landscape due to desertification, with a mosaic distribution of flat or undulating sandy land, mobile dunes, semi-fixed dunes, fixed dunes, and interdune lowlands. The soil in the study area is classified as a Cambic Arenosol (FAO and ISRIC, 1988), in which coarse sand with a particle size of 0.25 to 1 mm accounts for 20 to 58% of the mass, fine sand with a particle size of 0.05 to 0.25 mm accounts for 40 to 67%, and clay and silt with a particle size <0.05 mm accounts for 0.1 to 15%. The soil organic matter content is 0.08 to 0.49%. The dominant species in this area are *Agriophyllum squarrosum* (annual forb), *Setaria viridis* (annual grass), *Artemisia halodendron* (sub-shrub), *Caragana microphylla* (shrub), *Bassia dasyphylla* (annual forb), *Artemisia annua* (annual forb), *Chenopodium acuminatum* (annual forb), *Artemisia frigid* (annual forb), *Periploca sepium* (shrub), and *Cynanchum thesioides* (annual forb).

Leaf and Fine Root Traits Measurement

In August 2018, we investigated the traits of leaf and fine root of 54 dominant plants on a sand streak in Horqin Sandy Land. We measured leaf and fine root traits on five samples for each species, and at least five healthy and mature individuals were collected as one sample. To obtain intact fine roots, we excavated each plant by digging soil range 25 cm diameter and 25 cm deep, and wider and deeper when necessary to obtain fine roots for deeper-rooted species or taprooted species. For some sand-fixing shrubs, such as *A. halodendron* and *C. microphylla*, it was necessary to excavate to a depth of 1 m to obtain complete fine root tissue. Plants were transported to the laboratory and cleaned with distilled water to remove adherent soil, debris, and root of surrounding plants. For leaves, intact and mature leaves were collected for each sample. Part of the collection was oven-dried at 65°C for chemical analysis, while the other (10 leaves, or more for microphyllous species) was placed in a plastic bag for traits analysis. For fine root, we extracted undamaged fine root (<2 mm) of each sample. Part of the collection was oven-dried at 65°C for chemical analysis, while the other was placed in a plastic bag for traits analysis. Then, the collection of leaves and fine roots of each sample were put in the water in the dark for 24 h at 4°C to allow water saturation. For the leafless species *Ephedra sinica*, the plant part functionally similar to the leaf was measured.

Before measurement, fresh and water-saturated leaf and fine root were dried with clean filter paper gently and weighted for water-saturated leaf and fine root. The leaf and fine root of each sample were then scanned with a scanner (Epson, Japan) for the digital image. Image analysis was conducted with WinRHIZO software (Regent Instruments, Quebec, Canada) to measure the LA, length, and volume of the fine root. After scanning, these materials were oven-dried at 65°C to a constant weight and weighted. Leaf thickness (LT) was measured with a digital caliper as the mean of 3 measurements for each leaf, and 10 leaves were measured for each sample. SLA and SRL were calculated as the ratio between leaf area and leaf dry mass, and between root length and root dry mass, respectively. LDMC and FRDMC were calculated as the ratio between leaf and fine root dry mass and their water-saturated mass, respectively. LTD and FRTD were calculated as the ratio between leaf dry mass and leaf volume, and between fine root dry mass and root volume, respectively. The leaf and fine root of each sample were ground into a fine powder using a ball mill (GT300 Ball Mill, POWTEQ, Beijing, China). The C and N concentrations of leaf and fine root (LC, LN, FRC, and FRN) were measured by an elemental analyzer (ECS4010, Costech, Milan, Italy).

Calculations and Data Analysis

Phylogenetic signal (Blomberg's K) in all leaf and fine root traits was tested using the K statistic, where K is calculated as the ratio of the observed phylogenetically correct mean-square error divided by the mean-square error of the data, standardized by the expectation under Brownian motion (Blomberg et al., 2003). When measuring functional traits with phylogenetic signals, the species in the phylogenetic tree are usually randomly permuted 999 times to calculate the K statistic. The higher the K-value, the stronger the phylogenetic signal is and suggested the tendency of close relatives to have similar traits due to their common ancestor. The K-value and associated P-value were calculated with 3.5.3 of R[1], using the 'picante' package.

When the statistical analysis is conducted at the species level, traits of plant species are not statistically independent because species have a common ancestor and with different degrees of genetic relationship among species (Felsenstein, 1985). Thus, the phylogenetically independent contrasts (PIC) are essential to enhance the reliability of statistical analysis and reveal the potential importance of evolutional history in determining the current traits of species. A phylogenetic tree was recovered for 54 species by using the Phylo-matic tree[2] (Webb and Donoghue, 2005), based on the phylogenetic hypothesis for relationships among angiosperm families. For this analysis, branch lengths were estimated from a set of dated nodes based on fossil calibrations of vascular plants (Webb et al., 2011). PIC of each trait was calculated as the difference in mean trait values for pairs of sister species and nodes. We calculated the PIC of leaf and fine root traits of 54 species using the 'ape' package in R.

Coefficients of variation (CV) in leaf and fine root traits were calculated using Equation 1:

$$\mathrm{CV}\ (\%) = \mathrm{SD}/\mathrm{mean} \times 100 \qquad (1)$$

The 54 species in Horqin Sandy Land were classified into two categories: annuals (27) and perennials (27) (**Supplementary Table A. 1**). For all the variables measured, the distribution of values was tested for normality (Kolmogorov–Smirnov test, $P = 0.05$) and the homogeneity of error variance (using Levene's test, $P = 0.05$). An independent-sample t-test was used to test for the differences in leaf and fine root traits between annuals and perennials. The Pearson correlation tests were used to analyze the correlations among leaf and fine root traits. We repeated this correlation analysis using PIC of traits to test the effect of species evolutional history in the correlation of leaf and fine root traits. To test the correlations both within and among traits defining leaf and fine root, a principal component analysis (PCA) was performed on 12 traits (with 'vegan' package in R). To account for the influence of species evolutionary histories, we conducted PCA both with and without the PIC. Both PIC correlations and PCA with PIC were analyzed based on standardized contrasts, calculating relationships through the origin and adjusting degrees of freedom.

RESULTS

Variation of Leaf and Fine Root Traits

The LT and LA showed large variation (CV) among species, while FRDMC, LC, FRC, LN, and FRN had low variation in 54 dominant species in Horqin Sand Land (**Table 1**). Significant phylogenetic signals in LDMC, SLA, FRTD, and FRC were found ($P < 0.05$), suggesting that these traits were strongly influenced by their evolutionary history. However, the K values of these traits were relatively small ($K < 1$).

Annuals showed significantly higher SLA and SRL than perennials (**Figure 1**, $P < 0.05$). But the perennial species had higher LDMC, LTD, LC, FRN, and FRC than annual species significantly ($P < 0.05$). Unexpectedly, there was no significant LN difference between annuals and perennials, as well as LT, LA, FRDMC, and FRTD ($P > 0.05$).

Correlations Among Leaf and Fine Root Traits

Pairwise correlation among leaf and fine root traits of overall species were analyzed, significant correlations were found (**Table 2**, $P < 0.05$). LDMC was positively related to LTD and LC but negatively related to SLA and LN ($P < 0.05$). The correlation of fine root traits had a similar pattern as the leaf. FRDMC was positively related to FRTD but negatively related to SRL ($P < 0.05$). When PIC was included in the analysis of pairwise correlation of leaf and fine root traits, the different patterns of correlation were observed (**Table 2**). The correlations between LDMC and SLA, between LTD and LC, LN, and between SLA and FRTD disappeared after considering evolutionary relationships among species. But the SLA, FRTD, and FRDMC were associated with FRN ($P < 0.05$).

Both for annuals and perennials, species with high LT tend to low LDMC and LTD, and species with high SRL means low FRTD (**Tables 3**, **4**). However, annuals and perennials showed different patterns of correlation among leaf traits or fine root traits. In annuals, LN was negatively related to LTD, and FRN was negatively related to FRTD (**Table 4**, $P < 0.05$). But in perennials, LN was positively correlated with LA (**Table 3**, $P < 0.05$). And FRN is positively correlated with FRTD and FRC.

Coordination Between Leaf and Fine Root Traits

Looking at the relationship between leaf and fine root traits for overall species, there was a positive correlation between LDMC and FRDMC, as well as between LN and FRN, and between LC and FRC (**Table 2**, $P < 0.05$). However, SLA and LTD did not correlate to SRL and FRTD, respectively ($P > 0.05$). When PIC was included, the SLA and SRL were still not correlated, while the relationship between LN and FRN exhibited concordant patterns

---

[1] https://www.r-project.org/

[2] http://camwebb.info/doc/phylomatic.html

TABLE 1 | Traits of leaf and fine root of 54 dominant species in Horqin Sandy Land and their phylogenetic signal (*K*).

Traits	Traits	Mean ± SE	Minimum	Maximum	CV (%)	*K*	*P*
Leaf thickness (mm)	LT	0.26 ± 0.03	0.09	1.45	92.31	0.24	0.19
Leaf area (cm^2)	LA	6.69 ± 1.50	0.08	60.07	164.57	0.11	0.09
Leaf dry-matter content (g/g)	LDMC	0.24 ± 0.01	0.07	0.47	41.67	0.06	0.02
Specific leaf area (cm^2/g)	SLA	219.74 ± 11.53	31.83	498.56	38.56	0.08	0.08
Leaf tissue density (g/cm^3)	LTD	0.03 ± 0.00	0.01	0.06	33.33	0.06	0.02
Fine root dry-matter content (g/g)	FRDMC	0.34 ± 0.01	0.13	0.60	26.47	0.04	0.12
Specific root length (cm/g)	SRL	1258.20 ± 107.15	375.90	4147.92	62.58	0.03	0.46
Fine root tissue density (g/cm^3)	FRTD	0.23 ± 0.01	0.09	0.55	39.13	0.08	0.01
Leaf nitrogen concentration (%)	LN	2.36 ± 0.09	0.75	3.87	28.39	0.02	0.59
Leaf carbon concentration (%)	LC	43.56 ± 0.47	35.63	49.89	7.85	0.05	0.13
Fine root nitrogen concentration (%)	FRN	1.03 ± 0.07	0.11	2.46	24.27	0.04	0.27
Fine root carbon concentration (%)	FRC	45.73 ± 0.24	41.65	50.76	3.94	0.06	0.04

K, phylogenetic signal.

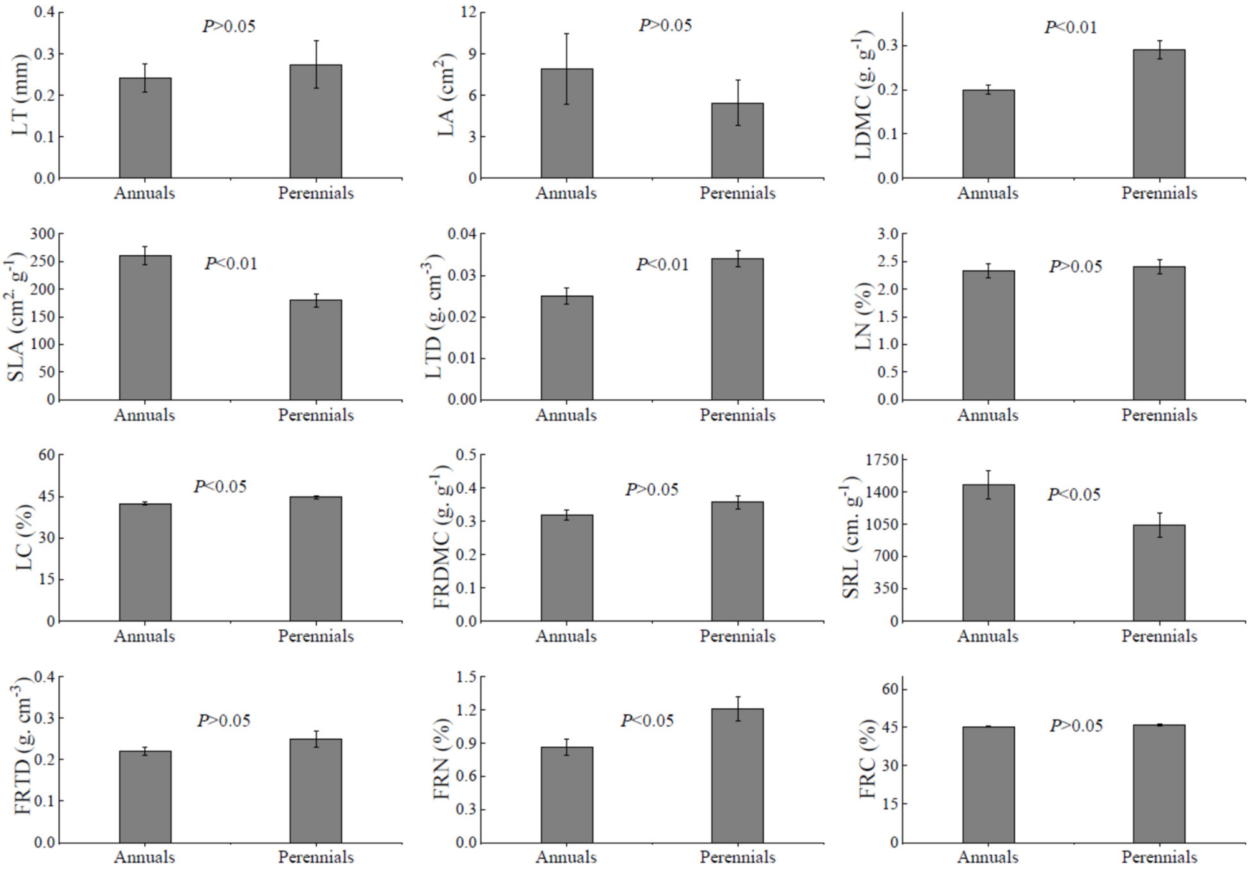

FIGURE 1 | Traits of leaf and fine root of 54 dominant species. LT, leaf thickness; LA, leaf area; LDMC, leaf dry-matter content; SLA, specific leaf area; LTD, leaf tissue density; FRDMC, fine root dry-matter content; SRL, specific root length; FRTD, fine root tissue density; LN, leaf nitrogen concentration; LC, leaf carbon concentration; FRN, fine root nitrogen concentration; FRC, fine root carbon concentration. Values are mean ± SE. Independent-sample *t*-test, $P < 0.05$ represents a significant difference between annuals and perennials.

as ahistorical correlations, although the magnitude was increased. The LTD was positively correlated with FRTD, but the LDMC was decoupled from FRDMC. Somewhat unexpected was the positive relationship between LC and FRC in ahistorical correlations, while the negative relationship was observed in evolutionary correlations (**Table 2**).

The coordination between leaf and fine root traits of annuals differed from those of perennials. For annuals, LT was

TABLE 2 | Matrix of Pearson's correlation coefficients for the relationships between leaf and fine root traits of 54 dominant species ($n = 54$).

Trait	LT	LA	LDMC	SLA	LTD	LN	LC	FRDMC	SRL	FRTD	FRN	FRC
LT		−0.34*	**−0.57****	−0.04	**−0.45****	−0.18	**−0.85****	**0.36***	−0.14	0.00	−0.06	0.13
LA	−0.10		0.22	0.01	0.02	**0.53****	**0.29***	**−0.44****	0.25	**−0.48****	**0.42****	**−0.44****
LDMC	**−0.31***	−0.23		−0.18	**0.31***	**0.40****	**0.70****	−0.17	−0.15	−0.14	**0.40****	**−0.49****
SLA	**−0.27***	−0.04	**−0.43****		**−0.68****	0.19	0.14	0.13	−0.03	−0.21	0.06	−0.09
LTD	**−0.52****	−0.00	**0.76****	**−0.41****		−0.12	0.18	−0.24	0.22	**0.35****	−0.14	0.17
LN	0.10	0.10	−0.14	0.10	**−0.33***		**0.34***	**−0.52****	**0.29***	**−0.58****	**0.80****	**−0.66****
LC	**−0.30***	−0.16	**0.52****	−0.07	**0.39****	0.18		−0.26	0.11	−0.12	0.25	**−0.35****
FRDMC	**−0.34***	**−0.27***	**0.64****	−0.10	**0.51****	−0.19	0.28		−0.24	**0.45****	**−0.46****	0.23
SRL	−0.17	0.14	−0.04	0.17	0.20	**−0.35****	**−0.31***	0.06		−0.22	**0.42****	−0.20
FRTD	0.04	−0.18	0.10	**−0.28***	−0.02	**0.32***	0.14	**0.34***	**−0.57****		**−0.66****	**0.48****
FRN	0.18	−0.00	0.08	−0.21	0.09	**0.62****	0.22	−0.12	−0.26	**0.31***		**−0.78****
FRC	−0.14	**−0.32***	**0.35****	−0.15	0.23	0.10	**0.42****	0.22	−0.25	0.19	0.18	

$^{*}P < 0.05$; $^{**}P < 0.01$.

Below-diagonal values and above-diagonal values indicate correlations without and with phylogenetically independent contrasts, respectively.

LT, leaf thickness; LA, leaf area; LDMC, leaf dry-matter content; SLA, specific leaf area; LTD, leaf tissue density; FRDMC, fine root dry-matter content; SRL, specific root length; FRTD, fine root tissue density; LN, leaf nitrogen concentration; LC, leaf carbon concentration; FRN, fine root nitrogen concentration; FRC, fine root carbon concentration.

TABLE 3 | Matrix of Pearson's correlation coefficients for the relationships between leaf and fine root traits in perennials ($n = 32$).

Trait	LT	LA	LDMC	SLA	LTD	LN	LC	FRDMC	SRL	FRTD	FRN
LA	−0.05										
LDMC	−0.39	−0.12									
SLA	−0.34	−0.27	−0.27								
LTD	−0.62**	0.18	**0.74****	−0.24							
LN	0.10	**0.42***	−0.09	0.08	0.37						
LC	0.09	−0.39	**0.48***	−0.18	0.19	0.35					
FRDMC	**−0.43***	−0.38	0.35	0.11	0.40	−0.06	0.30				
SRL	−0.15	**0.42***	−0.05	0.02	0.20	**−0.51****	**−0.47***	−0.06			
FRTD	0.15	**−0.44***	0.18	−0.22	0.13	**−0.42***	0.37	**0.50****	**−0.51****		
FRN	0.21	−0.22	0.05	−0.36	−0.13	**0.70****	0.30	−0.07	−0.29	**0.39***	
FRC	−0.09	**−0.50****	0.16	−0.18	0.02	0.29	0.31	0.04	−0.38	0.25	**0.39***

$^{*}P < 0.05$; $^{**}P < 0.01$.

LT, leaf thickness; LA, leaf area; LDMC, leaf dry-matter content; SLA, specific leaf area; LTD, leaf tissue density; FRDMC, fine root dry-matter content; SRL, specific root length; FRTD, fine root tissue density; LN, leaf nitrogen concentration; LC, leaf carbon concentration; FRN, fine root nitrogen concentration; FRC, fine root carbon concentration.

negatively related to FRDMC and FRC (**Table 4**, $P < 0.05$). And the LDMC and LTD were related to FRDMC and FRC positively ($P < 0.05$). The LN and LC were related to FRN and FRC, respectively, suggesting the proportional distribution of photosynthate and nutrients between the aboveground and belowground components in annuals. But for perennials, the LN was positively related to FRN, but negatively related to SRL and FRTD (**Table 3**, $P < 0.05$). A positive relationship between LA and SRL and a negative relationship between LA and FRTD and FRC were also detected in perennials ($P < 0.05$).

Principal Component Analysis of Leaf and Fine Root Traits

The PCA of trait correlations was performed in leaf and fine root traits in 54 dominant species (**Figures 2A,B**). The first two axes of the PCA performed with leaf and fine root traits accounted for 50% of the variance. The first PCA axis (PC1) was a structural axis defined by LDMC, LTD, LC, and FRDMC; the second PCA axis (PC2) was defined by SRL and LN, FRN, and FRTD, but the SRL and other traits (LN, FRN, and FRTD) were in an opposite direction (**Supplementary Table A. 3**). Although there was a little overlap, traits of annuals and perennials were clustered and separated from each other. The annuals were mostly distributed on the left half of the PCA axis 2, while the perennials were mainly distributed on the right half of the PCA axis 2. Perennials had higher LTD, LDMC, LC, FRDMC, FRTD, and FRC than perennials. When including PIC in the PCA, the patterns of correlations among leaf and fine root traits were completely inconsistent, confirming that species evolutionary history influenced the observed correlations among leaf and fine root traits. The first and second PCA axis explained 58% of the total variation of all 12 leaf and fine root traits (**Figure 2A**). The LN, FRN, LA, and FRTD were loaded on the PCA axis 1, while

TABLE 4 | Matrix of Pearson's correlation coefficients for the relationships between leaf and fine root traits in annuals (*n* = 22).

Trait	LT	LA	LDMC	SLA	LTD	LN	LC	FRDMC	SRL	FRTD	FRN
LA	–0.16										
LDMC	–0.41*	–0.28									
SLA	–0.24	–0.04	–0.26								
LTD	**–0.63****	–0.04	**0.74****	–0.33							
LN	0.10	0.30	–0.33	0.19	**–0.38***						
LC	**–0.70****	–0.01	**0.42****	0.28	**0.38***	0.04					
FRDMC	**–0.42***	–0.18	**0.66****	–0.10	**0.51****	–0.33	0.09				
SRL	–0.19	0.11	0.27	0.06	0.32	–0.21	–0.09	**0.39***			
FRTD	**0.47***	–0.11	–0.23	–0.28	–0.34	0.18	–0.20	–0.04	**–0.66****		
FRN	0.07	0.31	–0.38	0.33	–0.33	**0.60****	–0.08	**–0.49****	–0.04	–0.00	
FRC	–0.31	–0.37	**0.48***	0.09	**0.42***	–0.20	**0.48***	**0.40***	0.00	–0.03	–0.49**

**P < 0.05; **P < 0.01.*

LT, leaf thickness; LA, leaf area; LDMC, leaf dry-matter content; SLA, specific leaf area; LTD, leaf tissue density; FRDMC, fine root dry-matter content; SRL, specific root length; FRTD, fine root tissue density; LN, leaf nitrogen concentration; LC, leaf carbon concentration; FRN, fine root nitrogen concentration; FRC, fine root carbon concentration.

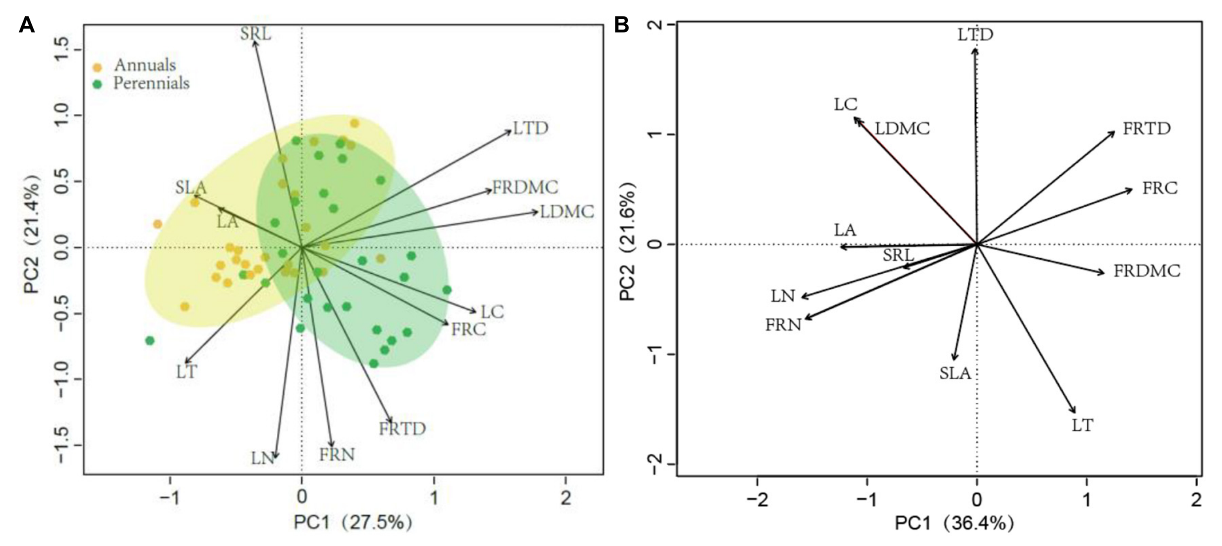

FIGURE 2 | Principal component analysis (PCA) on traits in 54 dominant species in Horqin Sandy Land. Data: **(A)** without and **(B)** with phylogenetically independent contrasts. LT, leaf thickness; LA, leaf area; LDMC, leaf dry-matter content; SLA, specific leaf area; LTD, leaf tissue density; FRDMC, fine root dry-matter content; SRL, specific root length; FRTD, fine root tissue density; LN, leaf nitrogen concentration; LC, leaf carbon concentration; FRN, fine root nitrogen concentration; FRC, fine root carbon concentration.

the LT, LDMC, and LC were loaded on the PCA axis 2 (**Supplementary Table A. 3**).

DISCUSSION

Annuals Differed From Perennials in Leaf and Fine Root Traits Important in Resource Uptake and Conservation

Differences in leaf and fine root traits between annuals and perennials followed the pattern of the gradient (from acquisitive to conservative) in carbon-use strategies previously reported (Wright et al., 2004b; González-Paleo and Ravetta, 2018). As expected, the annuals exhibited higher LA, SLA, and SRL but showed lower LDMC, LTD, and LC and FRDMC than perennials (**Figure 1**). These results suggested that annuals have traits that demonstrated a more acquisitive strategy than perennials since higher SLA and SRL have usually been associated with large leaf area and leaf gas exchange, rapid rates of root elongation, and high resource uptake capacities (Hodge, 2004; Roumet et al., 2006). By contrast, perennials leaf and fine root traits were characterized by high LDMC, LTD, LC, and FRDMC, which are associated with longer-lived leaf and root (Ryser, 1996; Tjoelker et al., 2005). Theoretically, the annuals have higher LN and FRN than perennials, implying that a higher proportion of the energy allocated to leaf and root construction is used for 'expensive' proteins for rapid exploitation and assimilation of resources (Eissenstat and Yanai, 1997; Martínez et al., 2002). However, there was no significant difference in

LN between annuals and perennials. Perennials had a higher FRN than annuals unexpectedly (**Figure 1**). This might be due to the fact that 7 of the 22 perennials we investigated in this area were legumes, which are characterized by biological N fixation.

High LA, SLA, and SRL might have been selected to maximize leaf and root surface area in annuals, enabling a greater acquisition of carbon and resource which is crucial to grow fast and to complete their life cycle in a short period of time (Hodge, 2004; Roumet et al., 2006). However, high N and the combination of high SLA may increase leaf vulnerability to herbivory and physical hazards in annuals. By contrast, in perennials, the diversion of photosynthate promotes persistence, tolerates herbivory, and resists environmental stress *via* higher tissue density and dry matter content, which is the advantage of survival in harsh conditions of desertified grassland (González-Paleo et al., 2016). And perennials with higher FRDMC may be advantageous in terms of more efficient soil exploration and the ability to better penetrate the soil matrix, reflecting an adaptation to survive and water stress tolerance in environments where the competition is strong (Beyer et al., 2013; Liu et al., 2019). Meanwhile, higher FRDMC in perennials is associated with the longer-lived roots, which means a greater carbon storage capacity, and enough total carbon available for the next vegetation season (Munné-Bosch, 2014). PCA analysis also showed considerable differences in leaf and fine root traits between annuals and perennials (**Figure 2**), suggesting that annuals and perennials have different adaptation and resource acquisition strategies.

The Annual Species Differed From Perennial Species in Leaf and Fine Root Traits Organization in Arid and Semi-Arid Grasslands

Surprisingly, significant relationships existed neither between SLA and LN nor between SRL and FRN in arid and semi-arid desertification in our study. The observed unwonted patterns of leaf and fine root traits in our study might be attributed to two reasons. First, functional trade-offs of traits and resource acquisition strategies were differed among functional groups due to their ecological specialization (**Supplementary Table A. 2**). For instance, the grasses (annual grasses and perennial grasses) had the highest SLA and SRL but the lowest LN and FRN, while the perennial forbs had the highest LN, FRN, and FRTD but the lowest SLA and SRL. The coexistence in desertified grassland of species with a multifaceted array of resource acquisition strategies was the key determinant of maintaining a range of niche conditions and system stability (Kong et al., 2014; Diaz et al., 2015; Kraft et al., 2015). Second, our principal component analysis failed to identify LN and FRN (**Figure 2A**), which support enzyme functioning and economy of resource capture in plant tissues, as significant contributors to the primary axis of leaf and fine root traits variation (Valverde-Barrantes et al., 2017). Instead, leaf and fine root traits were most significantly explained by structural traits. However, these were significantly explained by FRN and LN after considering PIC (**Figure 2B**), probably implying that the evolutionary history overshadowed the central role of nitrogen in metabolic activity in desertified grassland.

Negative correlations between FRTD and SRL, as well as between LT and LTD, and LC were observed both in annuals and perennials (**Tables 3**, **4**). A general tendency for species inhabiting arid and semi-arid areas to have thick leaf blades, leathery leaves have been reported, which is beneficial for plants to withstand drought by reducing water loss, excessive irradiance, and heat load, and facilitating retention of water (Sobrado and Medina, 1980; Niinemets, 2001; Wright et al., 2001). And species with higher SRL in dry habitats are able to avoid drought by accessing deep water, as confirmed by their deep root system (Morales et al., 2015). Yet, it appears that annuals did not follow similar patterns to perennials when we explored the organization of leaf and fine root traits of annuals and perennials. In annuals, LN and FRN were negatively correlated with LTD and FRDMC, respectively (**Table 4**), probably due to the fact that species with high protein content (typically high-SLA leaf and/or high-SRL root) tend to have lower concentrations of other 'expensive' compounds, such as lignin, phenols, and lipids (Martínez et al., 2002). Perennials, however, showed a positive correlation between FRN and FRTD/FRC. A possible explanation for this unexpected result is that 7 of the 22 perennials we investigated were legumes (such as *Caragana microphylla*, *Lespedeza bicolor*), which capture additional N through biological N fixation. These legumes would have a growth advantage in N limited desertified grassland, which is theoretically one of the reasons why these species could colonize in desertified grassland. Furthermore, a positive correlation between LA and LN was observed in perennials. Leaf nitrogen is integral to protein factors in photosynthetic machinery, especially Rubisco (Wright et al., 2004a). This implied that as a natural basis for light interception and substance exchange of plants, leaves tend to be smaller to reduce metabolism, such as photosynthesis, when N is insufficient. And small leaf areas may cause a reduction of transpiration to protect against water loss, which is probably the plant's adaptation to water scarcity in our study area (Bacelar et al., 2004). This trade-off of leaf traits might be contributed by adapting perennials in a resource-poor environment in arid and semi-arid areas.

The Coordination Between Leaf and Fine Root Traits of Annuals and Perennials Differed in Ways in an Arid and Semi-Arid Grassland

Studies have examined the coordination between leaf and root traits for characterizing resource economic trade-offs and allocation, such as SLA and SRL, leaf and root nutrients concentrations (e.g., Tjoelker et al., 2005; Hajek et al., 2013). Contrary to previous studies (Withington et al., 2006; Geng et al., 2014), the SLA-SRL relation was not significant in our study regardless of whether the PIC was considered, even though we investigated 54 dominant species in our study area. The missing SLA-SRL relationship might be due to the inconsistent effects of environmental and evolutionary pressures on the plant above- and belowground components (Liu et al., 2010). LN was inversely correlated with FRN, and the correlation coefficient has increased by 90% after considering PIC, demonstrating that the nutrient allocation between leaf and fine root was the outcome of plant specialization toward soil fertility, instead of species common lineages. And no significant phylogenetic signal was detected in traits related to resource acquisition (SRL, SLA, FRN, and LN), probably implying that these traits were less affected by the degree of phylogenetic relatedness, and their phenotypic plasticity obscure phylogenetic signal. We also tested for coordination of structural traits between leaf and fine root. The LDMC was decoupled from FRDMC, the LTD was positively correlated with FRTD, and the LC-FRC correlation shifted from positive to negative when including PIC. Meanwhile, a significant phylogenetic signal was detected in structural traits (LDMC, LTD, FRTD, and FRC), suggesting the conservative evolution of these traits in desertified grassland, despite the presence of environmental variation and resource limitation. Ma et al. (2018) found that the variation in morphological traits (root diameter and SRL) was strongly influenced by evolutionary history at the global scale, while chemical traits did not show a significant phylogenetic signal. These results indicated that plants may show differentiation in plant traits depending on environmental conditions. Pfennig et al. (2006) proposed that divergence between species arising from trait plasticity could contribute to species coexistence. In desertified grassland, the differentiation in plant traits was occurred in resource-limited conditions, as a result of the ability of plasticity and adaptation to the environment.

When we explored the coordination between leaf and fine root traits of annuals and perennials, respectively, it appears that annuals did not follow similar patterns to perennials. Annuals showed significant positive correlations between FRC, FRDMC and LDMC, LTD and LC, suggesting a proportional allocation of photosynthate between leaf and fine root in annuals. However, a significant negative correlation was detected between LN, LC, and SRL, FRTD in perennials, as well as between LA and FRTD/FRC. These results implied a conservative resource allocation strategy that more photosynthate has been allocated to roots when leaf N is insufficient in desertified grassland, to maximize root length and resource capture and decrease potential growth rates. And perennials tend to have small leaves, to allocate more photosynthate to root establishment. Likewise, Fort et al. (2012) proposed that drought-tolerant species may allocate more biomass to root and invest more in vessel clarification to ensure water acquisition and transport in dry conditions. Drenovsky et al. (2008) have found that invasive perennial forbs allocated more biomass to roots and allocated proportionately more root length to nutrient-rich microsites than did natives, which might contribute to the success of invasive forbs in low-nutrient environments. These pieces of evidence altogether suggested that a deeper and rigid root system and small leaves for the same level of investment for unit mass in perennials might be produced and maintained, as well as a conservative strategy and competitive advantage in desertified grassland.

Implications for Species Changes in Desertified Grassland in Arid and Semi-Arid Areas

In Horqin Sandy Land, a large amount of clay and silt particles have been removed by strong wind erosion resulting in coarse-textured soil, which is conducive to the infiltration of precipitation and replenishing of water into the deep soil layer (Cheng et al., 2020). The precipitation regimes that characterize arid and semi-arid grasslands are largely composed of small-sized precipitation events (<10 mm), which effectively improved shallow soil moisture, but only be accounted for a small proportion of the total rainfall (17%). The large-sized precipitation events (>30 mm), which mainly affect deep soil moisture, are account for 48% of the total rainfall during the growing season (Liu et al., 2011). Walter's two-layer model proposed that water in the deep layers of the soil is ineffective for grasses with shallow roots, and shrubs with deep roots have exclusive access to a source of water in relatively deep layers (Walter, 1979; Walker et al., 1981). Based on this model, we believed that annuals with a more opportunistic strategy, could utilize the short-term availability of water in upper soil layers and rapidly grow to complete their life cycle once the rainfall event occurs in arid and semi-arid areas. Perennial, however, tend to develop a deeper and rigid root system to have access to deeper soil water resources in drier areas as water stress intensifies, and establish smaller leaves to reduce metabolism and leaf gas exchange, as well as to allocate more photosynthate to root build when nutrients are insufficient. With these conservative strategies, perennials have less response to the fluctuation of rainfall in arid and semi-arid areas and are gradually colonized in desertified grassland.

On the vertical direction, vertical resource partitioning interacted with annuals-perennials resource utilization strategy differences, to realize the diversification of soil water resources utilization, which is the driving force behind annuals-perennials coexistence (Holdo, 2013). Furthermore, the colonization of perennial plants in desertified grassland increases resource heterogeneity by forming fertile islands beneath their canopies (Ding and Eldridge, 2021). The perennial patches could act as nurse plants for annuals in arid and semi-arid areas, protecting annuals from windy, dusty, and herbivores (Dohn et al., 2013). On the horizontal direction, spatial differences in resource utilization (e.g., nutrients, moisture, light) resulted in niche partitioning (and therefore coexistence) between annuals and perennials. Therefore, annuals and perennials could coexist stably due to the diversification of their both vertical and horizontal spatial resource utilization in undisturbed habitat, which provides necessary conditions for the colonization of perennials in desertified grassland. However, if the persistently external disturbance is removed, some perennial species may gradually vanish as vegetation succession progressed in the late stage of desertified grassland restoration. For example, the establishment of the protective system of artificial vegetation in Shapotou, China, led to an increase in the percentage of annual herbaceous species, but a decrease in the abundance of others, such as restored (artificial) planted shrubs, as succession progressed. These changes were related to a thickened sand surface crust, the reduced moisture content in the deep layer, and the limited reproduction of deep-rooted shrubs and perennial herbaceous plants (Li et al., 2003).

In the last 40 years, Horqin Sandy Land has been subjected to serious desertification, accompanied by a sharp decline in soil nutrients and marked changes in the vegetation. The dominant species *Cleistogenes squarrosa*, *Chenopodium acuminatum, Tribulus terrester*, *Chloris virgata*, etc., were observed in the early stage of desertification. Then, *Aneurolepidium dasystachys*, *Caragana microphylla*, *Artemisia halodendron*, *Bassia dasyphylla*, *Lespedeza bicolor*, *Pennisetum centrasiaticum* gradually colonized (Ning et al., 2021). This process was closely related to the adaptation and resource utilization strategies of these species. But in the most extreme cases, resulting from continuous disturbances, shrub or thicket (*Artemisia halodendron*) and/or *Agriophyllum squarrosum* dominated the final state, virtually excluding other species (Zhang et al., 2004).

The differences in adaptation, resource acquisition, and allocation strategies between annuals and perennials can also provide guidance for the restoration and management of desertified grassland. In severely desertified grassland, it is necessary to establish artificial sand-fixing vegetation with perennial plants, which have a conservative strategy, such as smaller leaves and a deeper and rigid roots system, and thus can gradually colonize in desertified grassland. The colonization of perennials can create better conditions for the recolonization of annuals, which adopt an opportunistic strategy. Annuals can utilize the short-term availability of water in upper soil layers and rapidly grow to complete their life cycle once the rainfall events occur. Annuals and perennials might show a dynamically balanced state and coexist stably, due to diversification of their both vertical and horizontal spatial resource utilization. Thus, a new artificial-natural ecosystem might be established in the former moving dune-dominated landscape, which is important to the mitigation of desertification and restoration of desertified grassland in arid and semi-arid areas.

CONCLUSION

Our study shows important implications for an in-depth understanding of the mechanism of species changes in desertified grassland in arid and semi-arid areas. Annuals and perennials differed considerably in terms of adaptation, resource acquisition, and allocation strategies, which might be partly responsible for species changes in desertified grassland. First, annuals differed from perennials in terms of several leaves and fine root traits important in resource uptake and conservation. Annuals displayed an opportunistic strategy associated with enhanced resource acquisition *via* the presence of large leaves, high SLA and SRL, low-density leaf and fine root, and high N concentration, while perennials exhibited a conservative strategy relatively. Second, annuals tend to establish tough tissue and low palatability, but perennials tend to have smaller leaves to reduce metabolism and water loss in resource-limited conditions. Third, there was a proportional allocation of photosynthate between leaf and fine root in annuals. But perennials showed a conservative resource allocation strategy that species tend to allocate more photosynthate to roots to improve resource absorption capacity in resource-limited habitats, resulting in a deeper and rigid roots system and smaller leaves. Perennials gradually colonized and coexisted with annuals in desertified grassland in arid and semi-arid areas, due to their different conservative adaptation and resource acquisition strategies, as well as their diversified use of spatial resources. These different strategies of annuals and perennials might be useful for the prediction of the succession of vegetation community in desertified grassland in arid and semi-arid areas, and thus provide support for the management and restoration of desertified grassland. We suggest the establishment of artificial sand-fixing vegetation with perennials in desertified grassland, which would facilitate the recolonization of annuals, and is expected to form a stable artificial-natural ecosystem.

DATA AVAILABILITY STATEMENT

The original contributions presented in the study are included in the article/**Supplementary Material**, further inquiries can be directed to the corresponding authors.

AUTHOR CONTRIBUTIONS

XZ conceived and designed the study based on discussions involving ZN and YL. ZN, YL, DH, and JZ performed the experiments. ZN and YL analyzed the results. ZN drafted the manuscript. All co-authors had a chance to review the manuscript before submission and contributed to discussion and interpretation of the data. All authors contributed to the article and approved the submitted version.

FUNDING

This work was supported by the National Natural Science Foundation of China (Y911021001).

SUPPLEMENTARY MATERIAL

The Supplementary Material for this article can be found online at: https://www.frontiersin.org/articles/10.3389/fpls.2021.778547/full#supplementary-material

Supplementary Table A. 1 | The 54 species surveyed in the study in Horqin Sandy Land.

Supplementary Table A. 2 | Traits of leaf and fine root for 54 species to different functional groups.

Supplementary Table A. 3 | Principal Components Analysis of the 54 species with respect to leaf and fine root traits.

Supplementary Table 2 | Data.

REFERENCES

Bacelar, E. A., Correia, C. M., Moutinho-Pereira, J. M., Gonçalves, B. C., Lopes, J. I., and Torres-Pereira, J. M. (2004). Sclerophylly and leaf anatomical traits of five field-grown olive cultivars growing under drought conditions. *Tree Physiol.* 24, 233–239. doi: 10.1093/treephys/24.2.233

Bardgett, R. D., Mommer, L., and Vries, F. T. (2014). Going underground: root traits as drivers of ecosystem processes. *Trends Ecol. Evol.* 29, 692–699. doi: 10.1016/j.tree.2014.10.006

Bennett, L. T., and Adams, M. A. (2001). Response of a perennial grassland to nitrogen and phosphorus additions in sub-tropical, semi-arid Australia. *J. Arid Environ.* 48, 289–308. doi: 10.1006/jare.2000.0759

Beyer, F., Hertel, D., and Leuschner, C. (2013). Fine root morphological and functional traits in Fagus sylvatica and Fraxinus excelsior saplings as dependent on species, root order and competition. *Plant Soil* 373, 143–156. doi: 10.1007/s11104-013-1752-7

Blomberg, S. P., Garland, T. Jr., and Ives, A. R. (2003). Testing for phylogenetic signal in comparative data: behavioral traits are more labile. *Evolution* 57, 717–745. doi: 10.1111/j.0014-3820.2003.tb00285.x

Cheng, Y. B., Yang, W. B., Zhan, H. B., Jiang, Q. O., Shi, M. C., and Wang, Y. Q. (2020). On the origin of deep soil water infiltration in the arid sandy region of China. *Water* 12:2409. doi: 10.3390/w12092409

Collins, S. L., Bradford, J. A., and Sims, P. L. (1988). Succession and fluctuation in Artemisia dominated grassland. *Plant Ecol.* 73, 89–99. doi: 10.1007/BF00031856

Craine, J. M. (2006). Competition for nutrients and optimal root allocation. *Plant Soil* 285, 171–185. doi: 10.1007/s11104-006-9002-x

de la Riva, E. G., Tosto, A., Pérez-Ramos, I. M., Navarro-Fernández, C. M., Olmo, M., Anten, N. P. R., et al. (2016). A plant economics spectrum in Mediterranean forests along environmental gradients: is there coordination among leaf, stem and root traits? *J. Veg. Sci.* 27, 187–199. doi: 10.1111/jvs.12341

Diaz, S., Hodgson, J. G., Thompson, K., Cabido, M., Cornelissen, J. H., Jalili, A., et al. (2004). The plant traits that drive ecosystems: evidence from three continents. *J. Veg. Sci.* 15, 295–304. doi: 10.1111/j.1654-1103.2004.tb02266.x

Diaz, S., Kattge, J., Cornelissen, J. H., Wright, I. J., Lavorel, S., Dray, S., et al. (2015). The global spectrum of plant form and function. *Nature* 529, 167–171. doi: 10.1038/nature16489

Ding, J., and Eldridge, D. J. (2021). The fertile island effect varies with aridity and plant patch type across an extensive continental gradient. *Plant Soil* 459, 173–183. doi: 10.1007/s11104-020-04731-w

D'Odorico, P., Bhattachan, A., Davis, K. F., Ravi, S., and Runyan, C. W. (2013). Global desertification: drivers and feedbacks. *Adv. Water Resour.* 51, 326–344. doi: 10.1016/j.advwatres.2012.01.013

Dohn, J., Dembélé, F., Karembé, M., Moustakas, A., Amévor, K. A., and Hanan, N. P. (2013). Tree effects on grass growth in savannas: competition, facilitation and the stress-gradient hypothesis. *J. Ecol.* 101, 202–209. doi: 10.1111/1365-2745.12010

Dong, Z. B., Hu, G. Y., Yan, C. Z., Wang, W. L., and Lu, J. F. (2009). Aeolian desertification and its causes in the Zoige Plateau of China's Qinghai-Tibetan Plateau. *Environ. Earth Sci.* 59, 1731–1740. doi: 10.1007/s12665-009-0155-9

Drenovsky, R. E., Martin, C. E., Falasco, M. R., and James, J. J. (2008). Variation in resource acquisition and utilization traits between native and invasive perennial forbs. *Am. J. Bot.* 95, 681–687. doi: 10.3732/ajb.2007408

Duan, H. C., Wang, T., Xue, X., Liu, S. L., and Guo, J. (2014). Dynamics of aeolian desertification and its driving forces in the Horqin Sandy Land, Northern China. *Environ. Monit. Assess*. 186, 6083–6096. doi: 10.1007/s10661-014-3841-3

DuPont, S. T., Beniston, J., Glover, J. D., Hodson, A., Culman, S. W., Lal, R., et al. (2014). Root traits and soil properties in harvested perennial grassland, annual wheat, and never-tilled annual wheat. *Plant Soil* 381, 405–420. doi: 10.1007/s11104-014-2145-2

Dyer, A. R., Goldberg, D. E., Turkington, R., and Sayre, C. (2001). Effects of growing conditions and source habitat on plant traits and functional group definition. *Funct. Ecol.* 15, 85–95. doi: 10.1046/j.1365-2435.2001.00487.x

Eissenstat, D. M., and Yanai, R. D. (1997). The ecology of root lifespan. *Adv. Ecol. Res.* 27, 1–60. doi: 10.1016/S0065-2504(08)60005-7

FAO and ISRIC (1988). *Revised Legend of the FAO-UNESCO SoilMap of the world. ISRIC-World Soil Information*. Available online at: https://www.isric.org/sites/default/files/isric_report_1988_01.pdf

Felsenstein, J. (1985). Phylogenies and the comparative method. *Am. Nat.* 125:284325. doi: 10.1086/284325

Fort, F., Jouany, C., and Cruz, P. (2012). Root and leaf functional trait relations in Poaceae species: Implications of differing resource-acquisition strategies. *J. Plant Ecol.* 6, 211–219. doi: 10.1093/jpe/rts034

Geng, Y., Wang, L., Jin, Dong, M., Liu, H. Y., and He, J. S. (2014). Alpine climate alters the relationships between leaf and root morphological traits but not chemical traits. *Oecologia* 175, 445–455. doi: 10.1007/s00442-014-2919-5

González-Paleo, L., Pastor-Pastor, A., Rajnoch, G., and Ravetta, D. A. (2019). Mechanisms of nitrogen conservation at the leaf-level in annual and perennial desert forbs: implications for perennial crops domestication. *Flora* 252, 62–68. doi: 10.1016/j.flora.2019.02.008

González-Paleo, L., and Ravetta, D. A. (2018). Relationship between photosynthetic rate, water use and leaf structure in desert annual and perennial forbs differing in their growth. *Photosynthetica* 56, 1177–1187. doi: 10.1007/s11099-018-0810-z

González-Paleo, L., Vilela, A. E., and Ravetta, D. A. (2016). Back to perennials: does selection enhance tradeoffs between yield and longevity? *Ind. Crop Prod.* 91, 272–278. doi: 10.1016/j.indcrop.2016.07.018

Hajek, P., Hertel, D., and Leuschner, C. (2013). Intraspecific variation in root and leaf traits and leaf-root trait linkages in eight aspen demes (*Populus tremula* and *P. tremuloides*). *Front. Plant Sci.* 4:415. doi: 10.3389/fpls.2013.00415

Hodge, A. (2004). The plastic plant: root responses to heterogeneous supplies of nutrients. *New Phytol.* 162, 9–24. doi: 10.1111/j.1469-8137.2004.01015.x

Holdo, R. (2013). Revisiting the two-layer hypothesis: coexistence of alternative functional rooting strategies in *Savannas*. *PLoS One* 8:e69625. doi: 10.1371/journal.pone.0069625

Jaikumar, N. S., Snapp, S. S., and Sharkey, T. D. (2013). Life history and resource acquisition: photosynthetic traits in selected accessions of three perennial cereal species compared with annual wheat and rye. *Am. J. Bot.* 100, 2468–2477. doi: 10.3732/ajb.1300122

Kerley, G. I., and Whitford, W. G. (2009). Impact of grazing and desertification in the Chihuahuan Desert: plant communities, granivores and granivory. *Am. Midl. Nat.* 144, 78–91.

Kong, D., Ma, C. G., Zhang, Q., Li, L., Chen, X. Y., Zeng, H., et al. (2014). Leading dimensions in absorptive root trait variation across 96 subtropical forest species. *New Phytol.* 203, 863–872. doi: 10.1111/nph.12842

Kraft, N. J., Godoy, O., and Levine, J. M. (2015). Plant functional traits and the multidimensional nature of species coexistence. *Proc. Natl. Acad. Sci. U.S.A.* 112, 797–802. doi: 10.1073/pnas.1413650112

Laughlin, D. C., Mommer, L., Sabatini, F. M., Bruelheide, H., Kuyper, T. W., Mccormack, M. L., et al. (2021). Root traits explain plant species distributions along climatic gradients yet challenge the nature of ecological trade-offs. *Nat. Ecol. Evol.* 5, 1–12. doi: 10.1038/s41559-021-01471-7

Li, X. R., Jia, X. H., and Dong, G. R. (2006). Influence of desertification on vegetation pattern variations in the cold semi-arid grasslands of Qinghai-Tibet Plateau, North-West China. *J. Arid Environ.* 64, 505–522. doi: 10.1016/j.jaridenv.2005.06.011

Li, X. R., Zhang, J. G., Liu, L. C., Chen, H. S., and Shi, Q. H. (2003). *Plant Diversity and Succession of Artificial Vegetation Types and Environment in an Arid Desert Region of China//Conserving Biodiversity in Arid Regions*. Boston, MA: Springer, 179–188.

Liu, C., Xiang, W. H., Zou, L. M., Lei, P. F., Zeng, Y. L., and Shuai, O. Y. (2019). Variation in the functional traits of fine roots is linked to phylogenetics in the common tree species of Chinese subtropical forests. *Plant Soil* 436, 1–18. doi: 10.1007/s11104-019-03934-0

Liu, G. F., Freschet, G., Pan, X., Cornelissen, J., Li, Y., and Dong, M. (2010). Coordinated variation in leaf and root traits across multiple spatial scales in Chinese semi-arid and arid ecosystems. *New Phytol.* 188, 543–553. doi: 10.1111/j.1469-8137.2010.03388.x

Liu, X. P., He, Y. H., and Zhao, X. Y. (2011). Characteristics of precipitation in Naiman region of Horqin Sandy Land (in Chinese with English summary). *Res. Soil Water Conserv.* 18, 155–158. doi: 10.3724/SP.J.1146.2006.01085

Ma, Z. Q., Guo, D. L., Xu, X. L., Lu, M. Z., Bardgett, R., and Eissenstat, D. (2018). Evolutionary history resolves global organization of root functional traits. *Nature* 555, 94–97. doi: 10.1038/nature25783

Martínez, F., Lazo, Y. O., Fernández-Galiano, R. M., and Merino, J. A. (2002). Chemical composition and construction cost for roots of Mediterranean trees, shrub species and grassland communities. *Plant Cell Environ.* 25, 601–608. doi: 10.1046/j.1365-3040.2002.00848.x

McLendon, T., and Redente, E. F. (1992). Effects of nitrogen limitation on species replacement dynamics during early secondary succession on a semiarid sagebrush site. *Oecologia* 91, 312–317. doi: 10.1007/BF00317618

Monroe, J. G., Gill, B., Turner, K. G., and Mckay, J. K. (2019). Drought regimens predict life history strategies in Heliophila. *New Phytol.* 223, 2054–2062. doi: 10.1111/nph.15919

Morales, J., Squeo, F. A., Tracol, Y., Armas, C., and Gutiérrez, J. R. (2015). Resource economics and coordination among above-and below-ground functional traits of three dominant shrubs from the Chilean coastal desert. *J. Plant Ecol.* 8, 70–78. doi: 10.1093/jpe/rtu010

Munné-Bosch, S. (2014). Perennial roots to immortality. *Plant Physiol.* 166, 720–725. doi: 10.1104/pp.114.236000

Niinemets, Ü (2001). Global-scale climatic controls of leaf dry mass per area, density, and thickness in trees and shrubs. *Ecology* 82, 453–469.

Ning, Z. Y., Zhao, X. Y., Li, Y. L., Wang, L. L., Lian, J., Yang, H. L., et al. (2021). Plant community C:N:P stoichiometry is mediated by soil nutrients and plant functional groups during grassland desertification. *Ecol. Eng.* 162:106179. doi: 10.1016/j.ecoleng.2021.106179

Pfeiffer, M., Langan, L., Linstädter, A., Martens, C., Gaillard, C., Ruppert, J. C., et al. (2019). Grazing and aridity reduce perennial grass abundance in semi-arid rangelands – Insights from a trait-based dynamic vegetation model. *Ecol. Model.* 395, 11–22. doi: 10.1016/j.ecolmodel.2018.12.013

Pfennig, D. W., Rice, A. M., and Martin, R. A. (2006). Ecological opportunity and phenotypic plasticity interact to promote character displacement and species coexistence. *Ecology* 87, 769–779. doi: 10.1890/05-0787

Reich, P., Wright, I. J., Cavender-Bares, J., Craine, J. M., Oleksyn, J., Westoby, M., et al. (2003). The evolution of plant functional variation: traits, spectra, and strategies. *Int. J. Plant Sci.* 164, S143–S164. doi: 10.1086/374368

Roumet, C., Urcelay, C., and Diaz, S. (2006). Suites of root traits differ between annual and perennial species growing in the field. *New Phytol.* 170, 357–368. doi: 10.1111/j.1469-8137.2006.01667.x

Ryser, P. (1996). The importance of tissue density for growth and life span of leaves and roots: a comparison of five ecologically contrasting grasses. *Funct. Ecol.* 10:717. doi: 10.2307/2390506

Sobrado, M. A., and Medina, E. (1980). General morphology, anatomical structure, and nutrient content of sclerophyllous leaves of the 'bana' vegetation of amazonas. *Oecologia* 45, 341–345. doi: 10.1007/BF00540202

Tjoelker, M. G., Craine, J. M., Wedin, D., Reich, P. B., and Tilman, D. (2005). Linking leaf and root trait syndromes among 39 grassland and savannah species. *New Phytol.* 167, 493–508. doi: 10.1111/j.1469-8137.2005.01428.x

Valverde-Barrantes, O. J., Authier, L., Schimann, H., and Baraloto, C. (2021). Root anatomy helps to reconcile observed root trait syndromes in tropical tree species. *Am. J. Bot.* 108, 744–755. doi: 10.1002/ajb2.1659

Valverde-Barrantes, O. J., Freschet, G. T., Roumet, C., and Blackwood, C. B. (2017). A worldview of root traits: the influence of ancestry, growth form, climate and mycorrhizal association on the functional trait variation of fine-root tissues in seed plants. *New Phytol.* 215, 1562–1573. doi: 10.1111/nph.14571

Walker, B. H., Ludwig, D., Holling, C. S., and Peterman, R. M. (1981). Stability of semi-arid savanna grazing systems. *J. Ecol.* 69, 473–498. doi: 10.2307/2259679

Walter, H. (1979). *Vegetation of the Earth: Second Edition*. New York, NY: Springer-Verlag.

Webb, C. O., Ackerley, D. D., and Kembel, S. W. (2011). *Software for the Analysis of Phylogenetic Community Structure and Character Evolution (With Phylomatic and Ecovolve). User's Manual Version 4.2.*

Webb, C. O., and Donoghue, M. J. (2005). Phylomatic: tree assembly for applied phylogenetics. *Mol. Ecol. Notes* 5, 181–183. doi: 10.1111/j.1471-8286.2004.00829.x

Withington, J. M., Reich, P. B., Oleksyn, J., and Eissenstat, D. M. (2006). Comparison of structure and life span in roots and leaves among temperate trees. *Ecol. Monogr.* 76, 381–397.

Wright, I. J., Groom, P. K., Lamont, B. B., Poot, P., Prior, L. D., Reich, P. B., et al. (2004b). Leaf trait relationships in Australian plant species. *Funct. Plant Biol.* 31, 551–558. doi: 10.1071/FP03212

Wright, I. J., Reich, P. B., and Westoby, M. (2001). Strategy shifts in leaf physiology, structure and nutrient content between species of high- and low- rainfall and high- and low-nutrient habitats. *Funct. Ecol.* 15, 423–434. doi: 10.1046/j.0269-8463.2001.00542.x

Wright, I. J., Reich, P. B., Westoby, M., Ackerly, D. D., Baruch, Z., Bongers, F., et al. (2004a). The world-wide leaf economics spectrum. *Nature* 428, 821–827. doi: 10.1038/nature02403

Yair, A., and Kossovsky, A. (2002). Climate and surface properties: hydrological response of small and semi-arid watersheds. *Geomorphology* 42, 43–57. doi: 10.1016/S0169-555X(01)00072-1

Zhang, J. Y., Zhao, H. L., Cui, J. H., Li, Y. L., and Yang, J. D. (2004). Development process of the vegetation and the change of species composition in the Horqin Sandland. *Arid Zone Res.* 27, 425–435. doi: 10.1017/S0140525X04520095

Zhang, S., Zhang, Y., Xiong, K., Yu, Y., and Min, X. (2020). Changes of leaf functional traits in karst rocky desertification ecological environment and the driving factors. *Glob. Ecol. Conserv.* 24:e01381. doi: 10.1016/j.gecco.2020.e01381

Zuo, X. A., Zhao, H. L., Zhao, X. Y., Guo, Y. R., Yun, J. Y., Wang, S. K., et al. (2009). Vegetation pattern variation, soil degradation and their relationship along a grassland desertification gradient in Horqin Sandy Land, northern China. *Environ. Geol.* 58, 1227–1237. doi: 10.1007/s00254-008-1617-1

Conflict of Interest: The authors declare that the research was conducted in the absence of any commercial or financial relationships that could be construed as a potential conflict of interest.

frontiers | Frontiers in Plant Science

ORIGINAL RESEARCH
published: 08 April 2022
doi: 10.3389/fpls.2022.860206

Influence of Leaf Age on the Scaling Relationships of Lamina Mass vs. Area

Yabing Jiao[1], Karl J. Niklas[2], Lin Wang[1], Kexin Yu[1], Yirong Li[1] and Peijian Shi[1]**

[1] College of Biology and the Environment, Bamboo Research Institution, Nanjing Forestry University, Nanjing, China, [2] Plant Biology Section, School of Integrative Plant Science, Cornell University, Ithaca, NY, United States

Leaf lamina mass and area are closely correlated with the photosynthetic capacity and competitive ability of plants, whereas leaf age has been demonstrated to affect physiological processes such as photosynthesis. However, it remains unknown whether the lamina mass vs. area scaling relationship is influenced by leaf age, which is important for understanding plant adaptive strategies and, more broadly, resource utilization and growth. We measured the leaf functional traits of five leaf-age groups of *Photinia* × *fraseri* for a total of 1,736 leaves. ANOVA followed by Tukey's honestly significant difference test was used to compare the functional traits among the five leaf-age groups. Reduced major axis regression protocols were used to fit the scaling relationship between lamina mass and area, and the bootstrap percentile method was used to compare the lamina mass vs. area scaling relationships among the leaf-age groups. Lamina area, and the ratio of lamina dry mass to lamina fresh mass increased with increasing leaf age. Lamina fresh mass per unit area, and lamina dry mass per unit area both exhibited a parabolic-like trend as leaf age increased, i.e., at the leaf maturation stage, it showed a slight but significant decline. The phenomenon called diminishing returns were confirmed by each of the five leaf-age groups, i.e., all of the numerical values of the scaling exponents of lamina mass vs. area were significantly greater than 1. There were significant differences in the scaling exponents of lamina mass vs. area for the leaves across different sampling times. The scaling exponents were lower at the early rapid growth stage, indicating a lower cost for increasing leaf area compared to the leaf maturation stage. These data are consistent with leaves undergoing a transition from resource acquisition to resource conservation in the process of their development and growth.

Keywords: diminishing returns, leaf development, leaf functional traits, LMA, resources utilization strategy

OPEN ACCESS

Edited by:
Ze-Xin Fan,
Xishuangbanna Tropical Botanical Garden (CAS), China

Reviewed by:
Eric R. Scott,
University of Florida, United States
Francesco Ferrini,
University of Florence, Italy

***Correspondence:**
Karl J. Niklas
kjn2@cornell.edu
Peijian Shi
pjshi@njfu.edu.cn

Specialty section:
This article was submitted to Functional Plant Ecology, a section of the journal Frontiers in Plant Science

Received: *22 January 2022*
Accepted: *14 March 2022*
Published: *08 April 2022*

Citation:
Jiao Y, Niklas KJ, Wang L, Yu K, Li Y and Shi P (2022) Influence of Leaf Age on the Scaling Relationships of Lamina Mass vs. Area. Front. Plant Sci. 13:860206. doi: 10.3389/fpls.2022.860206

INTRODUCTION

Photosynthesis plays an indispensable and critical role in maintaining the balance of carbon and oxygen in the atmosphere. Leaves provide the most important albeit not the only organ for photosynthesis. Consequently, the functional traits of leaves are of primary interest in understanding plant biology and ecosystem dynamics. In the context of the functional traits, the leaf lamina mass and area are important indexes to describe photosynthetic capacity as well as reflecting the trade-off between the investment ("cost") of leaf construction and photosynthetic return. Prior studies have shown that there is a significant allometric relationship between the lamina mass and area (Milla and Reich, 2007; Niklas et al., 2007; Huang et al., 2019; Liu et al., 2020) indicating that increases in the dry mass investment in lamina construction do not obtain a proportional increase in lamina area. This phenomenon has been described as diminishing returns (Niklas et al., 2007).

In addition to leaf lamina mass and area, the leaf lamina dry mass per unit area (LMA) is an important functional trait (Westoby et al., 2002; Poorter et al., 2009). Wright et al. (2004) concluded that the maximum photosynthetic capacity of leaves decreased significantly with increasing LMA such that species with faster resource utilization and return efficiency tend to have lower LMA, higher photosynthetic efficiency, and shorter leaf life spans. In a similar vein, some investigators (Niinemets, 2001; Westoby et al., 2002; Hikosaka and Shigeno, 2009) concluded that species with lower resource utilization rates and return efficiencies have high LMA, which is often used to reflect the adaptive abilities of plants to obtain carbon resources in different environments (Poorter et al., 2009; Cui et al., 2020). Therefore, the study of leaf functional traits can effectively reflect the photosynthetic capacity and competitiveness of plants.

Leaf age and leaf growth stages are crucial factors in morphological construction and physiological processes of many plants. For example, Niklas (1991) showed that the total leaf mass and total leaf area per plant are positively correlated with leaf age by comparing shoots with young and mature leaves of *Populus tremuloides* Michx. Mediavilla et al. (2014) contended that the interspecific differences in leaf longevity, morphology, and chemical composition of mature leaves are more notable compared to immature leaves. Ji et al. (2021) report that LMA and leaf dry matter content increase significantly during the development of leaves. In addition, previous studies have shown that leaf age is closely associated with photosynthetic capacity (Field and Mooney, 1983; Han et al., 2008). However, with increasing leaf age, photosynthetic capacity is known to gradually decrease (Kitajima et al., 1997). For example, Day et al. (2001) concluded that the leaves of the red spruce (*Picea rubens* Sarg.) manifest age-related trends in leaf morphology and physiology and that the decline in the productivity of old red spruce results from the age-related decline in photosynthetic rate.

However, prior research on the effects of leaf age on growth has mainly focused on conifers, e.g., *Pinus pinaster* Ait., *Pinus koraiensis* Sieb. et Zucc., and *Picea rubens* Sarg (Eimil-Fraga et al., 2015; Ji et al., 2021). To address this bias, we examined the shade-tolerant evergreen shrub species *Photinia* × *fraseri* to determine the effects of leaf age on leaf functional traits and the leaf (lamina) mass vs. area scaling relationship Specifically, we addressed the following two questions: (i) Do leaf functional traits change with leaf age? and (ii) Does the scaling relationship between leaf mass and area change with age? *Photinia* × *fraseri* is a hybrid between *Photinia glabra* and *Photinia serratifolia*. It is a nothospecies in the rose family, Rosaceae. *Photinia* × *fraseri* was selected for study because of its availability and because its evergreen leaves have a comparatively simple ovoid morphology, which makes measurements of lamina mass and area comparatively simple to make (**Figure 1**).

MATERIALS AND METHODS

Leaf Collection Protocols

The sampling site was located at the campus of Nanjing Forestry University (118°48′35″ E, 32°04′67″ N), Nanjing, Jiangsu Province, China, which has a subtropical monsoon climate. The mean annual precipitation is 1,156 mm, and the mean annual temperature is 15.6°C based on the climate data collected between 1951 and 2014.[1] The rainy season is from June to August, approximately accounting for half of the annual accumulated precipitation.

A total of 1,736 leaves were collected from 40-50 *Photinia* × *fraseri* "Red Robin" plants in 2021. Newly developed leaves in early March 2021 were collected in the middle of March, April, May, June, and July 2021. These collections are labeled as N3, N4, N5, N6, and N7, respectively (to denote "new" in each month) (**Figure 1** and **Table 1**).

Measures of Leaf Functional Traits

We measured the fresh mass of each lamina using an electronic balance (Type: ML 204; Mettler Toledo Company, Greifensee,

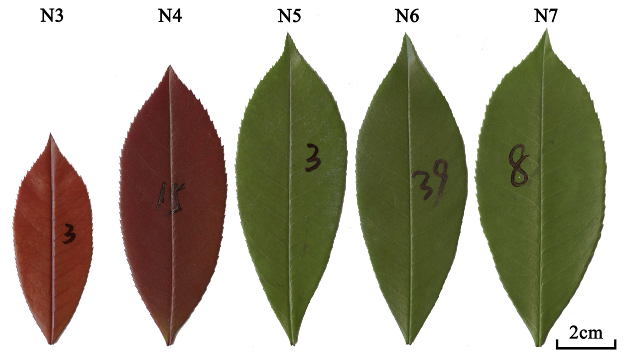

FIGURE 1 | Examples of leaves from the five leaf-age groups. Newly developed leaves in early March 2021 were harvested in the middle of March, April, May, June, and July 2021, which were denoted by N3-7, respectively. The numbers on written on leaves were used to mark leaves harvested in different months.

TABLE 1 | Leaf collection information for *Photinia* × *fraseri* "Red Robin".

Leaf-age group	Sampling date	Sample size	Leaf-unfolding time
N3	March 15, 2021	387	Early March 2021
N4	April 11, 2021	333	Early March 2021
N5	May 16, 2021	330	Early March 2021
N6	June 15, 2021	350	Early March 2021
N7	July 17, 2021	336	Early March 2021

---

[1] http://data.cma.cn

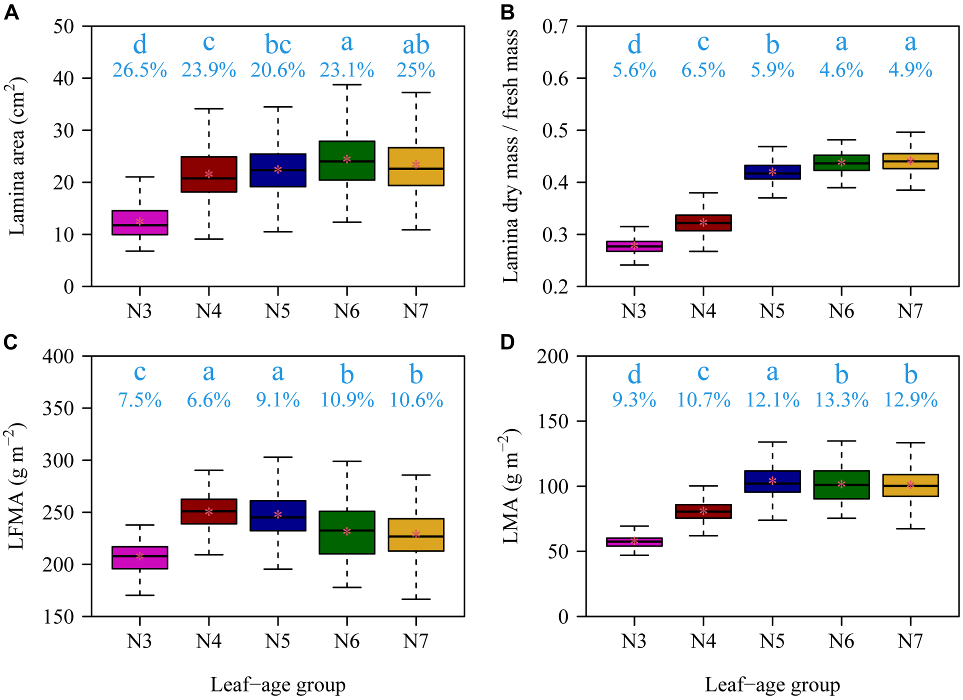

FIGURE 2 | Boxplots of lamina area **(A)**, the ratio of lamina dry mass to lamina fresh mass **(B)**, lamina fresh mass per unit area **(C)**, and lamina dry mass per unit area **(D)** for the five leaf-age groups. The lowercase letters indicate the significance of the difference between any two of the five groups; the numbers below the lowercase letters are the coefficients of variation. In each panel, there was a significant difference ($p \leq 0.05$) between any two leaf-age groups that did not share the same letter, and there was no significant difference ($p > 0.05$) between any two leaf-age groups that shared the same letter based on Tukey's HST test with the 0.05 significance level.

Switzerland; measurement accuracy 0.0001 g) and scanned the leaves to bitmap images at a 600-dpi resolution using a photo scanner (V550, Epson Indonesia, Batam, Indonesia). Adobe Photoshop (CS6, version: 13.0) was used to obtain a black and white image of each lamina. The M-file based on MatLab (version ≥ 2009a) developed by Shi et al. (2018) was used to extract the planar coordinates of each lamina. And then leaf *A* was calculated using an R script (version 4.0.3; R Core Team, 2020) developed by Shi et al. (2018) and Su et al. (2019). The fresh leaves were then dried to constant weight in an oven (Type: XMTD-8222; Jinghong Experimental Equipment Co., Ltd., Shanghai, China) at 80°C for 48 h to measure dry mass using the same electronic balance.

Statistical Methods

We used the analysis of variance (ANOVA) with a 0.05 significance level to test whether leaf age had a significant effect on the leaf lamina area, the ratio of lamina dry mass to lamina fresh mass (i.e., LDM/LFM), the lamina fresh mass per unit area (LFMA), and the lamina dry mass per unit area (LMA). Provided that a significant effect of leaf area on each of the measures was found, we used Tukey's honestly significance difference test with a significance level of 0.05 (Hsu, 1996) to test the significance of the difference between any two groups in the leaf lamina area, LDM/LFM, LFMA, and LMA. Additionally, we used a power-law function to fit the scaling relationship between any two variables of interest:

$$Y_1 = \beta Y_2^{\alpha},$$

where Y_1 and Y_2 represent the two interdependent variables, respectively, and α and β are the scaling exponent and the normalization constant, respectively. In order to stabilize the variance of leaf measures, both sides of the equation were log-transformed (Niklas, 1994; Niklas et al., 2007):

$$y = \gamma + \alpha x.$$

where $y = \ln Y_1$, $x = \ln Y_2$, and $\gamma = \ln \beta$. The numerical values of α and γ were obtained using reduced major axis regression protocols (Niklas, 1994; Smith, 2009). The bootstrap percentile method (Efron and Tibshirani, 1993; Sandhu et al., 2011) was used to compare the significance of the differences of the numerical values of α between any two leaf-age groups. For any two leaf-age groups (denoted as groups A and B), we calculated 4,000 replicates of α for each group using the bootstrap method (Efron and Tibshirani, 1993). Denoting D as the differences in the replicates of α between groups A and B, we observed whether the 95% CI of D included 0. If the lower bound of the 95% CI of D is larger than 0, it indicates that the estimated α-value of group A is larger than that of group B; if the upper bound of the 95% CI of D is smaller than 0, it indicates that the estimated α-value of group A is smaller than that of group B; if the 95% CI of D includes 0, it indicates that there is no

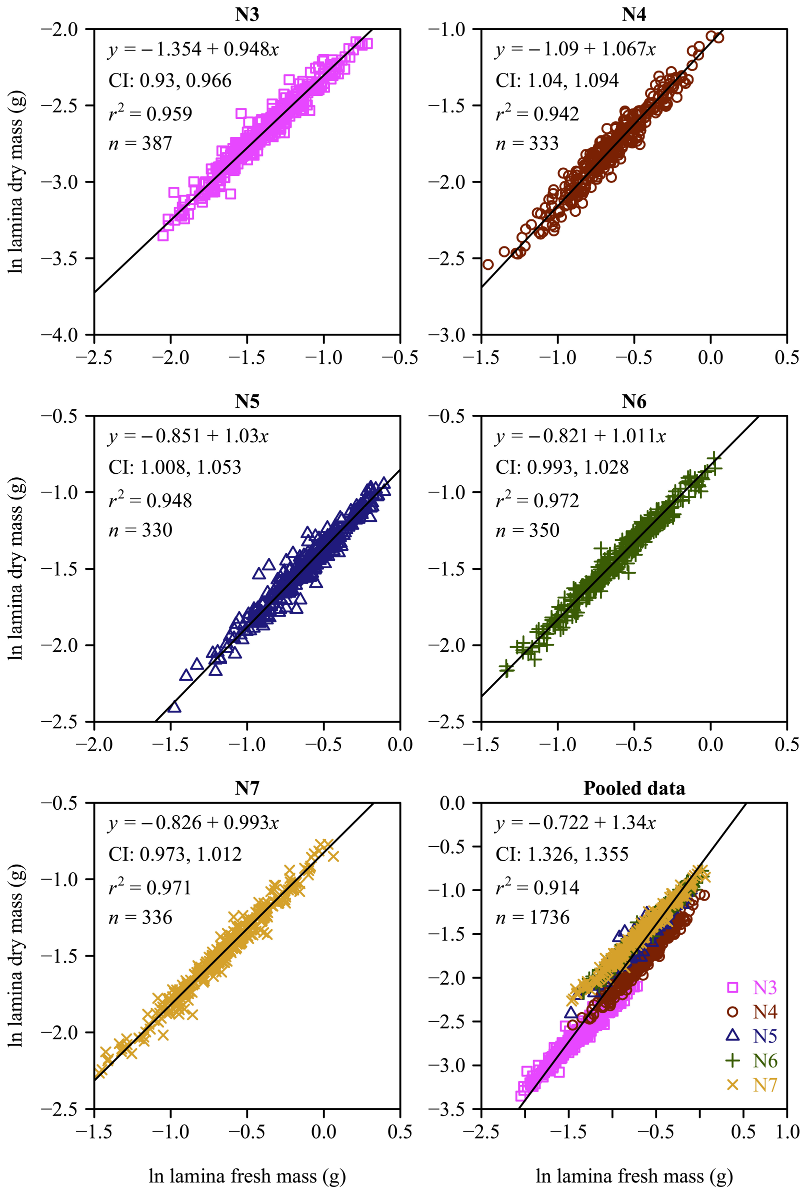

FIGURE 3 | Fitted scaling relationships between lamina dry mass and lamina fresh mass for the five leaf-age groups. The small open circles represent log-transformed values of lamina dry mass vs. lamina fresh mass; the red straight lines represent the regression lines; CI represents the 95% confidence intervals of the slope; r^2 is the coefficient of determination; and n is the sample size.

significant difference in the estimated α-values between groups A and B (see Sandhu et al., 2011 for details). To measure the goodness of fit, the root-mean-square error (RMSE = the square root of the quotient of residual sum of squares and sample size) was used. All statistical analyses were carried out using R (version 4.0.3; R Core Team, 2020).

RESULTS

There were significant effects of leaf age on the leaf lamina area, LDM/LFM, LFMA, and LMA among the five leaf-age groups (all p-values < 0.01). With increasing leaf age, both the lamina area and LDM/LFM significantly increased (**Figure 2**). The LMA and LFMA both exhibited a parabolic-like trend with increasing age, i.e., LMA and LFMA increased and then declined with increasing leaf age (**Figure 2**). All of the functional leaf traits examined over the course of this study were significantly correlated within each of the five leaf-age groups when the data were log-log transformed (**Figures 3–5**). Each of the coefficients of determination (r^2) equaled or exceeded 0.75 for each of the leaf-age groups. There was a statistically significant log-log linear relationship between LDM and LFM for each leaf-age group. The 95% confidence intervals for the N6 and N7 included unity,

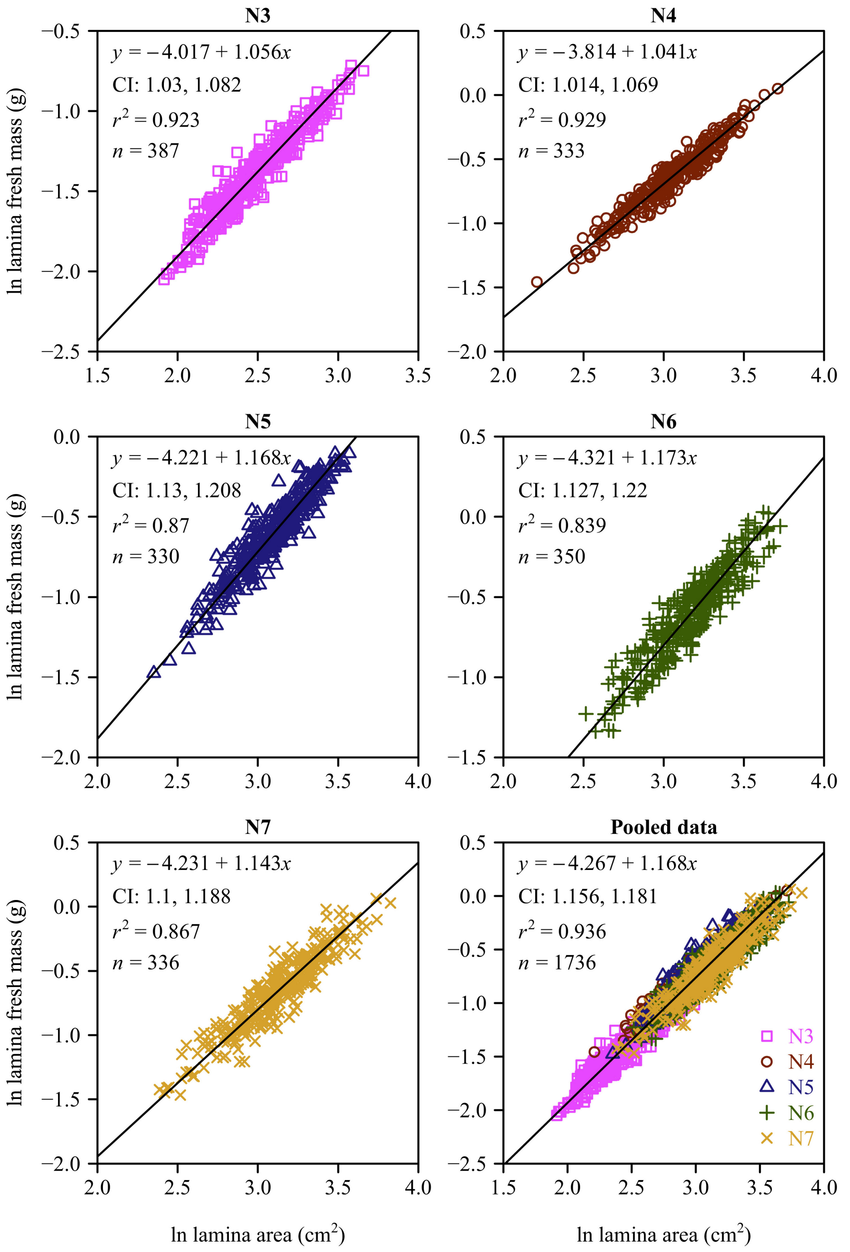

FIGURE 4 | Fitted scaling relationships between lamina fresh mass and lamina surface area for the five leaf-age groups. The small open circles represent the log-transformed values of lamina fresh mass vs. lamina surface area; the red straight lines represent the regression lines; CI represents the 95% confidence intervals of the slope; r^2 is the coefficient of determination; and *n* is the sample size.

and the lower bound of the 95% confidence intervals of the scaling exponents of LDM vs. LFM for N5 was approximately equal to 1 with a difference from 1 < 0.01. For N3 and N4, the difference between the upper bound of the 95 CIs of the slope and 1 and between the lower bound of the 95 CIs of the slope and 1 were slightly larger, with the absolute value of 0.04. This indicated that the mature leaves maintained an isometric scaling relationship, whereas the young leaves tended to slightly deviate from the isometric scaling. However, for the pooled data, the scaling exponent of LDM vs. LFM was overestimated because of the differences in water content across the different leaf-age groups (**Figure 3**).

There was a strong positive relationship between lamina mass and area for each leaf-age group (**Figures 4**, **5**). The lower bound of the 95% CIs of the lamina mass vs. area scaling relationship exceeded unity for each of the five leaf-age groups, indicating that the lamina mass vs. area scaling relationship is allometric. For each leaf-age group, the scaling exponents of LFM vs. lamina area and LDM vs. lamina area exceeded unity, and were therefore consistent with the hypothesis of "diminishing

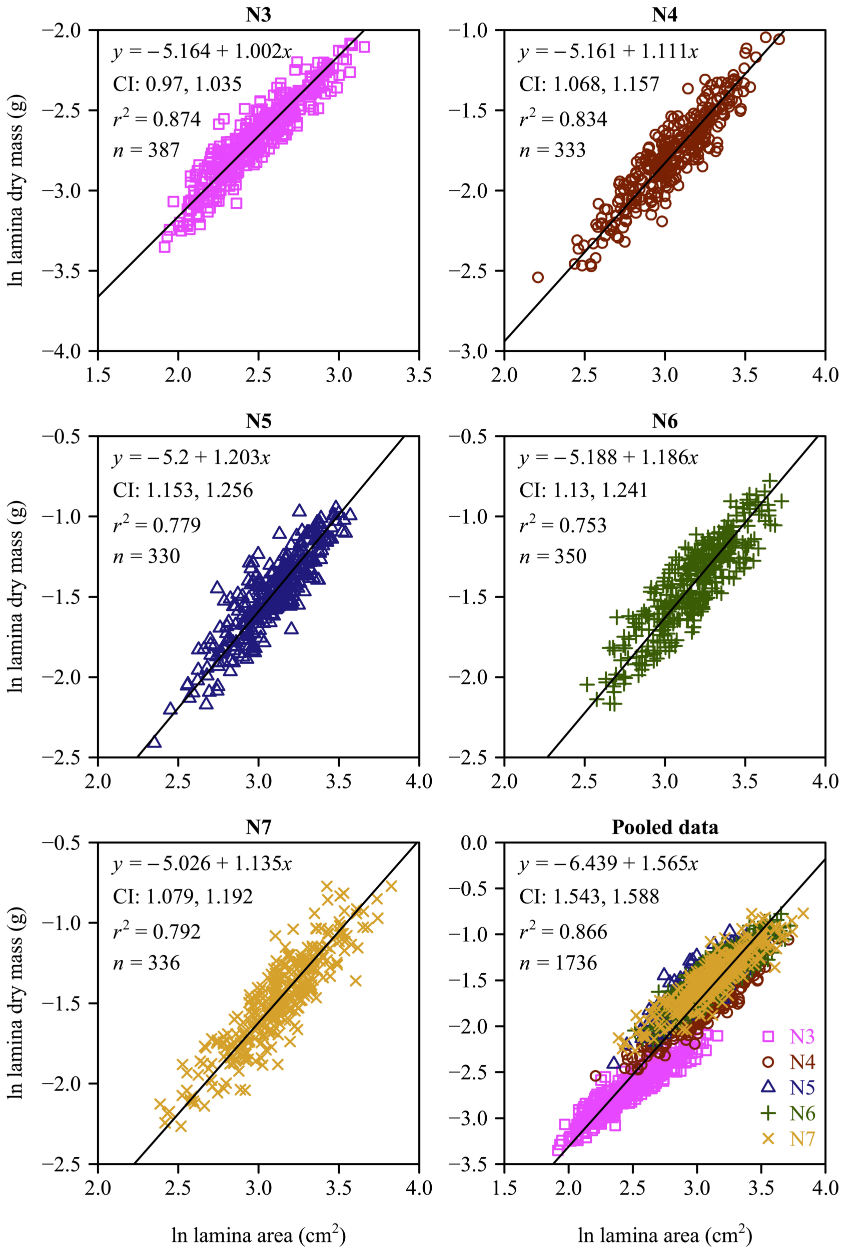

FIGURE 5 | Fitted scaling relationships between lamina dry mass and lamina surface area for the five leaf-age groups. The small open circles represent the log-transformed values of lamina dry mass vs. lamina surface area; the red straight lines represent the regression lines; CI represents the 95% confidence intervals of the slope; r^2 is the coefficient of determination; and *n* is the sample size.

returns." However, the r^2 value of the LDM vs. lamina area scaling relationship was lower than that of the LFM vs. lamina area scaling relationship for each leaf-age group (compare **Figure 4** with **Figure 5**). In addition, for the pooled data, the scaling exponent of LDM vs. lamina area was largely overestimated in comparison with that of LFM vs. lamina area.

With the exception of N3, the numerical values of the LDM vs. LFM scaling exponents decreased and converged onto a value of 1 with increasing leaf age (**Figure 6**). The scaling exponents of leaf *M* vs. lamina area for N3 and N4 were significantly smaller than those of N5, N6 and N7 (**Figure 6**), indicating that older leaves had larger costs of construction.

DISCUSSION

Variations in Leaf Functional Traits Across Leaf-Age Groups

Prior research has shown that the photosynthetic capacity of leaves decreases with increasing leaf age

(Horsley and Gottschalk, 1993; Bauerle et al., 2020), and that this might be associated with the changes in chemical composition, leaf nitrogen content, and CO_2 diffusion limitation (Zhang et al., 2008). Photosynthetic rates of fully expanded leaves generally show a decline with increasing leaf age due to the reallocation of resources to young leaves to optimize the overall systemic photosynthetic returns of an individual plant, rather than resulting from leaf functional degradation (Field and Mooney, 1983; Hikosaka et al., 1994). Moreover, the photosynthetic capacity of young leaves has been shown to be significantly lower than mature leaves (Hikosaka and Shigeno, 2009; Liu et al., 2020; Ji et al., 2021). Although leaf functional traits have been regarded as important references for understanding plant ecological and growth strategies (Westoby et al., 2000, 2002), there are trade-offs among different leaf functional traits (e.g., lamina area, LMA) under the limitation of resources. If plants increase their investment to one functional trait, they are likely to reduce their investment to other functional traits (Falster et al., 2018).

The data presented here show that the leaf lamina area, the ratio of LDM to LFM, and LMA generally increase with increasing leaf age, which is consistent with previous reports in other species (Niklas, 1991; He and Yan, 2018; Liu et al., 2020; Guo et al., 2021). In addition, LFMA decreased at the leaf maturation stage. There are two interrelated explanations for this phenomenology. First, over the course of leaf development, maturation, and subsequent senescence, the dry matter investment disproportionately increases with increasing age, and, second, the symplastic volume fraction (the living contents of a leaf, i.e., the protoplasmic contents) systematically decreases with increasing age. Both of these trends are reflected in the trends of lamina area, LDM/LFM, LFMA, and LMA reported here with increasing leaf age, and both are clearly and intrinsically interrelated, although the proximate mechanism(s) underlying each of these trends differs. During leaf expansion, leaves generally have a low cost of construction with increasing leaf area because leaf expansion involves the volumetric increase in cell size (and increase in the symplastic volume fraction) rather than the addition of significant amounts of cell wall (apoplastic) materials. The reverse is generally true during leaf maturation during which the apoplastic volume fraction increases relative to the symplasic volume fraction as a consequence of the deposition of secondary cell wall materials including the lignification of vascular tissues. This general phenomenology is consistent with the trends in our data (see **Figure 2**).

The aforementioned growth dynamic has obvious physiological and biomechanical consequences. For example, species with long versus short leaf longevities must adopt specific and different strategies to maintain growth (Mediavilla et al., 2014). It is not surprising therefore that previous studies have shown that variations in LMA are correlated across plant functional groups (such as trees, shrubs, herbs) as well as abiotic variables such as light, temperature, water and nutrient availability, and atmospheric composition (Ackerly, 1992; Poorter and de Jong, 1999; Niinemets, 2001; Poorter et al., 2009). In our study site, ambient temperature and precipitation gradually increase during the rainy season, especially in June, July, and August, over the course of leaf initiation, expansion, and maturation (see the online **Supplementary Material** in

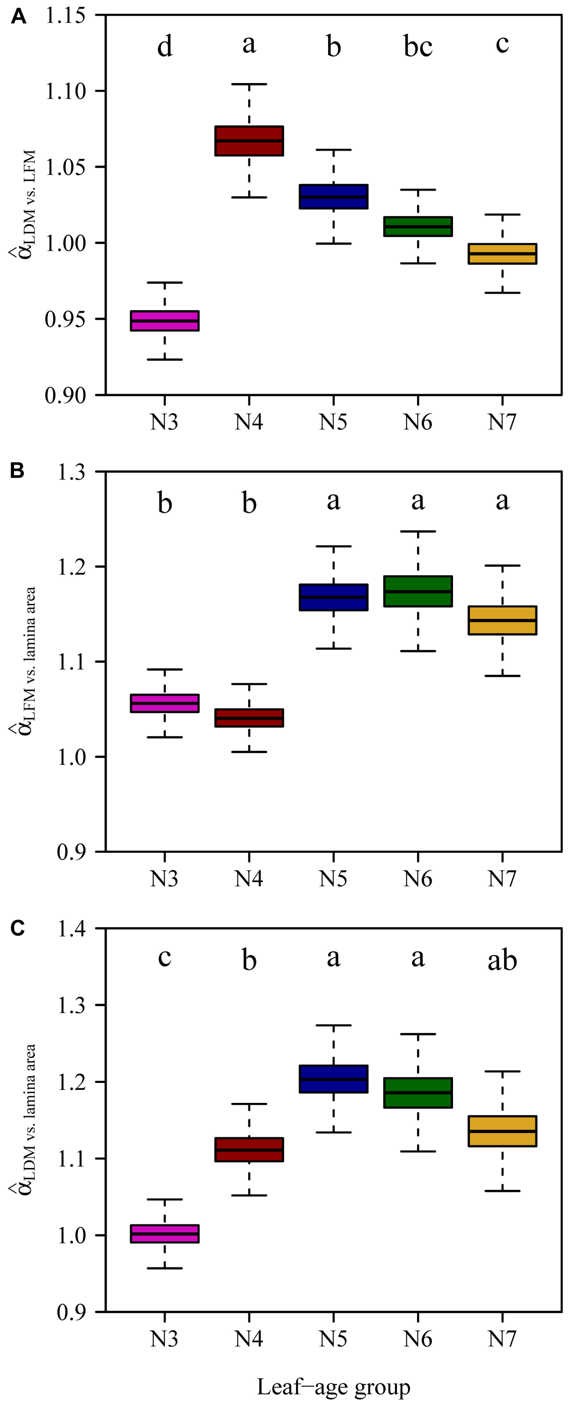

FIGURE 6 | Comparisons of the scaling exponents of LDM vs. LFM **(A)**, LFM vs. lamina area **(B)**, LDM vs. lamina area **(C)** for the five leaf-age groups. The lowercase letters indicate the significance of the difference between any two of the five leaf-age groups.

Li et al., 2022). LMA has been demonstrated to have plastic responses to climate, e.g., in arid environments plants can reduce water requirements, which results in a higher LMA relative to those in humid environments (Poorter et al., 2009). Similarly, at the leaf maturation stage, the ratio of lamina dry mass to fresh mass reached a stable status, and the precipitation might play an important role in affecting the numerical value of LMA. For example, June and July receive greater amount of rain than May, which perhaps to a certain degree accounts for why the LMAs in June and July are significantly but slightly lower than that in May (**Figure 2**). Thus, changing but predictable environmental conditions might have exerted an influence to a certain degree on the expression of leaf functional traits (Poorter et al., 2009). Nevertheless, it requires additional controlled experiments for testing whether the amount of precipitation can change LMA, i.e., a plasticity of LMA to weather, in future studies.

Influence of Leaf Age on Leaf Allometry

The scaling exponents of LDM vs. LFM were found to be significantly different between March and April, likely because new leaves were growing expanding at this time. **Figure 2** shows significant increases in both the lamina area and LDM/LFM between March and April. With the exception of March, the scaling exponents of LDM vs. LFM decreased toward 1 with increasing leaf age (**Figure 6**). We interpret these data to indicate that leaf water content and leaf dry mass tend to synchronously increase.

Liu et al. (2020) confirmed that for leaves of *Alangium chinense* (Lour.) Harm and *Liquidambar formosana* Hance, the scaling exponents of the lamina mass vs. area scaling relationship during the spring are significantly higher than during the summer. This is consistent with our results. In the case of N3 and N4, the numerical values of the lamina mass vs. area scaling exponents were significantly smaller compared to those for N5, N6, and N7 (**Figure 6**), indicating that the larger leaf area of mature leaves require greater apoplastic investments. Under any circumstances, it is obvious that the investment in leaf construction changed between the early rapid growth and leaf maturation stages. Changes in leaf investment may be related to photosynthetic returns (Day et al., 2001; Bielczynski et al., 2017), such that young leaves produce less photosynthates (Falster and Westoby, 2003) compared to more mature leaves (Pan et al., 2012).

The numerical values of the scaling exponents of the lamina mass vs. area scaling relationship for each of leaf-age groups were in excess of unity, and thus conform with the phenomenon called "diminishing returns" (see also Huang et al., 2019; Liu et al., 2020). In general, although larger leaf lamina area can yield a higher photosynthetic capacity, progressively larger leaves generally require a disproportionately greater investment in their mechanical support (Niklas, 1992, 1999; see also Gibert et al., 2016). This disproportionate investment in the apoplastic content relative to the symplastic content per unit leaf area can account for the numerical values of the lamina mass vs. area scaling relationship approaching and exceeding unity (i.e., $\alpha > 1.0$).

CONCLUSION

Our data indicate that both lamina area and ratio of lamina dry mass to lamina fresh mass increase with increasing leaf age, whereas LMA and LFMA manifest a parabolic-like trend. With the exception of leaves collected in March, the numerical values of the LDM vs. LFM scaling exponents decreased and converged onto 1, indicating a proportional (isometric) relationship between leaf dry mass and leaf absolute water content. All of the numerical values of the lamina mass vs. area scaling exponents exceeded 1, thereby confirming the phenomenon called diminishing returns. Based on these numerical values and the trends exhibited, we concluded that the costs of leaf construction increase and subsequently plateau as a consequence of an increase in the apoplastic volume fraction per unit leaf area over the course of leaf expansion, maturation, and early senescence over the course of leaf ontogeny. We believe that this ontogenetic pattern holds for the leaves of all plant species. Future research is necessary, however, to validate this speculation, and needs to be expanded to include the leaves of different functional and phyletic plant groups (e.g., ferns, cycads, and monocots).

DATA AVAILABILITY STATEMENT

The original contributions presented in the study are included in the article/**Supplementary Material**, further inquiries can be directed to the corresponding authors.

AUTHOR CONTRIBUTIONS

KN and PS designed this work, analyzed the data, and revised the manuscript. YJ, LW, KY, and YL carried out the experiment. YJ wrote the initial draft. All authors commented on and agreed with this submission.

FUNDING

This work was supported by the National Key Research and Development Program of China (Grant No. 2021YFD02200403).

ACKNOWLEDGMENTS

We thank all the members of our research group for their valuable help in this experiment. We also thank the associate editor, Z-XF, and two reviewers for their constructive comments.

SUPPLEMENTARY MATERIAL

The Supplementary Material for this article can be found online at: https://www.frontiersin.org/articles/10.3389/fpls.2022.860206/full#supplementary-material

REFERENCES

Ackerly, D. D. (1992). Light, leaf age, and leaf nitrogen concentration in a tropical vine. *Oecologia* 89, 596–600. doi: 10.1007/BF00317169

Bauerle, W. L., McCullough, C., Iversen, M., and Hazlett, M. (2020). Leaf age and position effects on quantum yield and photosynthetic capacity in hemp crowns. *Plants* 9:271. doi: 10.3390/plants9020271

Bielczynski, L. W., Łącki, M. K., Hoefnagels, I., Gambin, A., and Croce, R. (2017). Leaf and plant age affects photosynthetic performance and photoprotective capacity. *Plant Physiol.* 175, 1634–1648. doi: 10.1104/pp.17.00904

R Core Team (2020). *R: A Language and Environment for Statistical Computing*. Vienna: R Foundation for Statistical Computing.

Cui, E., Weng, E., Yan, E., and Xia, J. (2020). Robust leaf trait relationships across species under global environmental changes. *Nat. Commun.* 11:2999. doi: 10.1038/s41467-020-16839-9

Day, M. E., Greenwood, M. S., and White, A. S. (2001). Age-related changes in foliar morphology and physiology in red spruce and their influence on declining photosynthetic rates and productivity with tree age. *Tree Physiol.* 21, 1195–1204. doi: 10.1093/treephys/21.16.1195

Efron, B., and Tibshirani, R. J. (1993). *An Introduction to the Bootstrap*. London: Chapman and Hall.

Eimil-Fraga, C., Sánchez-Rodríguez, F., Álvarez-Rodríguez, E., and Rodríguez-Soalleiro, R. (2015). Relationships between needle traits, needle age and site and stand parameters in *Pinus pinaster*. *Trees* 29, 1103–1113. doi: 10.1007/s00468-015-1190-7

Falster, D. S., Duursma, R. A., and FitzJohn, R. G. (2018). How functional traits influence plant growth and shade tolerance across the life cycle. *Proc. Natl. Acad. Sci. U.S.A.* 115, E6789–E6798. doi: 10.1073/pnas.1714044115

Falster, D. S., and Westoby, M. (2003). Plant height and evolutionary games. *Trends Ecol. Evol.* 18, 337–343. doi: 10.1016/s0169-5347(03)00061-2

Field, C., and Mooney, H. A. (1983). Leaf age and seasonal effects on light, water, and nitrogen use efficiency in a California shrub. *Oecologia* 56, 348–355. doi: 10.1007/BF00379711

Gibert, A., Gray, E. F., Westoby, M., Wright, I. J., and Falster, D. S. (2016). On the link between functional traits and growth rate: meta-analysis shows effects change with plant size, as predicted. *J. Ecol.* 104, 1488–1503. doi: 10.1111/1365-2745.12594

Guo, X., Shi, P., Niinemets, Ü, Hölscher, D., Wang, R., Liu, M., et al. (2021). Leaf diminishing returns of five different age-groups of moso bamboo (*Phyllostachys edulis*) culms. *Am. J. Bot.* 108, 1662–1672. doi: 10.1002/ajb2.1738

Han, Q., Kawasaki, T., Nakano, T., and Chiba, Y. (2008). Leaf-age effects on seasonal variability in photosynthetic parameters and its relationships with leaf mass per area and leaf nitrogen concentration within a *Pinus densiflora* crown. *Tree Physiol.* 28, 551–558. doi: 10.1093/treephys/28.4.551

He, D., and Yan, E. R. (2018). Size-dependent variations in individual traits and trait scaling relationships within a shade-tolerant evergreen tree species. *Am. J. Bot.* 105, 1165–1174. doi: 10.1002/ajb2.1132

Hikosaka, K., and Shigeno, A. (2009). The role of rubisco and cell walls in the interspecific variation in photosynthetic capacity. *Oecologia* 160, 443–451. doi: 10.1007/s00442-009-1315-z

Hikosaka, K., Terashima, I., and Katoh, S. (1994). Effects of leaf age, nitrogen nutrition and photon flux density on the distribution of nitrogen among leaves of a vine (*Ipomoea tricolor* Cav.) grown horizontally to avoid mutual shading of leaves. *Oecologia* 97, 451–457. doi: 10.1007/BF00325881

Horsley, S. B., and Gottschalk, K. W. (1993). Leaf area and net photosynthesis during development of *Prunus serotina* seedlings. *Tree Physiol.* 12, 55–69. doi: 10.1093/treephys/12.1.55

Hsu, P. (1996). *Multiple Comparisons: Theory and Methods*. New York, NY: Chapman and Hall/CRC.

Huang, W., Su, X., Ratkowsky, D. A., Niklas, K. J., Gielis, J., and Shi, P. (2019). The scaling relationships of leaf biomass vs. leaf surface area of 12 bamboo species. *Glob. Ecol. Conserv.* 20:e00793. doi: 10.1016/j.gecco.2019.e00793

Ji, M., Jin, G., and Liu, Z. (2021). Effects of ontogenetic stage and leaf age on leaf functional traits and the relationships between traits in *Pinus koraiensis*. *J. For. Res.* 32, 2459–2471. doi: 10.1007/s11676-021-01308-w

Kitajima, K., Mulkey, S. S., and Wright, S. J. (1997). Decline of photosynthetic capacity with leaf age in relation to leaf longevities for five tropical canopy tree species. *Am. J. Bot.* 84, 702–708. doi: 10.2307/2445906

Li, Y., Shi, P., Niinemets, Ü, Song, Y., Yu, K., Schrader, J., et al. (2022). Diminishing returns among lamina fresh and dry mass, surface area, and petiole fresh mass among nine Lauraceae species. *Am. J. Bot.* doi: 10.1002/ajb2.1812

Liu, M., Niklas, K. J., Niinemets, Ü, Hölscher, D., Chen, L., and Shi, P. (2020). Comparison of the scaling relationships of leaf biomass versus leaf surface area between spring and summer for two deciduous tree species. *Forests* 11:1010. doi: 10.3390/f11091010

Mediavilla, S., Herranz, M., González-Zurdo, P., and Escudero, A. (2014). Ontogenetic transition in leaf traits: a new cost associated with the increase in leaf longevity. *J. Ecol.* 7, 567–575. doi: 10.1093/jpe/rtt059

Milla, R., and Reich, P. B. (2007). The scaling of leaf area and mass: the cost of light interception increases with leaf size. *Proc. Biol. Sci.* 274, 2109–2114. doi: 10.1098/rspb.2007.0417

Niinemets, Ü (2001). Global-scale climatic controls of leaf dry mass per area, density, and thickness in trees and shrubs. *Ecology* 82, 453–469. doi: 10.2307/2679872

Niklas, K. J. (1991). The elastic moduli and mechanics of *Populus tremuloides* (Salicaceae) petioles in bending and torsion. *Am. J. Bot.* 78, 989–996. doi: 10.1002/j.1537-2197.1991.tb14503.x

Niklas, K. J. (1992). Gravity-induced effects on material properties and size of leaves on horizontal shoots of *Acer saccharum* (Aceraceae). *Am. J. Bot.* 79, 820–827. doi: 10.1002/j.1537-2197.1992.tb13659.x

Niklas, K. J. (1994). *Plant Allometry: The Scaling of Form and Process*. Chicago, IL: University of Chicago Press.

Niklas, K. J. (1999). A mechanical perspective on foliage leaf form and function. *New Phytol.* 143, 19–31. doi: 10.1046/j.1469-8137.1999.00441.x

Niklas, K. J., Cobb, E. D., Niinemets, Ü, Reich, P. B., Sellin, A., Shipley, B., et al. (2007). "Diminishing returns" in the scaling of functional leaf traits across and within species groups. *Proc. Natl. Acad. Sci. U.S.A.* 104, 8891–8896. doi: 10.1073/pnas.0701135104

Pan, R., Wang, X., and Li, N. (2012). *Plant Physiology*. Beijing: Higher Education Press.

Poorter, H., and de Jong, R. (1999). A comparison of specific leaf area, chemical composition and leaf construction costs of field plants from 15 habitats differing in productivity. *New Phytol.* 143, 163–176. doi: 10.1046/j.1469-8137.1999.00428.x

Poorter, H., Niinemets, Ü, Poorter, L., Wright, I. J., and Villar, R. (2009). Causes and consequences of variation in leaf mass per area (LMA): a meta-analysis. *New Phytol.* 182, 565–588. doi: 10.1111/j.1469-8137.2009.02830.x

Sandhu, H. S., Shi, P., Kuang, X., Xue, F., and Ge, F. (2011). Applications of the bootstrap to insect physiology. *Fla. Entomol.* 94, 1036–1041. doi: 10.1653/024.094.0442

Shi, P., Ratkowsky, D. A., Li, Y., Zhang, L., Lin, S., and Gielis, J. (2018). General leaf area geometric formula exists for plants—evidence from the simplified Gielis equation. *Forests* 9:714. doi: 10.3390/f9110714

Smith, R. J. (2009). Use and misuse of the reduced major axis for line-fitting. *Am. J. Phys. Anthropol.* 140, 476–486. doi: 10.1002/ajpa.21090

Su, J., Niklas, K. J., Huang, W., Yu, X., Yang, Y., and Shi, P. (2019). Lamina shape does not correlate with lamina surface area: an analysis based on the simplified Gielis equation. *Glob. Ecol. Conserv.* 19:e00666. doi: 10.1016/j.gecco.2019.e00666

Westoby, M., Falster, D. S., Moles, A. T., Vesk, P. A., and Wright, I. J. (2002). Plant ecological strategies: some leading dimensions of variation between species. *Annu. Rev. Ecol. Syst.* 33, 125–159. doi: 10.1146/annurev.ecolsys.33.010802.150452

Westoby, M., Warton, D., and Reich, P. B. (2000). The time value of leaf area. *Am. Nat.* 155, 649–656. doi: 10.1086/303346

Wright, I. J., Reich, P. B., Westoby, M., Ackerly, D. D., Baruch, Z., Bongers, F., et al. (2004). The worldwide leaf economics spectrum. *Nature* 428, 821–827. doi: 10.1038/nature02403

Zhang, S., Hu, H., and Li, Z. (2008). Variation of photosynthetic capacity with leaf age in an alpine orchid, *Cypripedium flavum*. *Acta Physiol. Plant* 30, 381–388. doi: 10.1007/s11738-008-0135-9

Conflict of Interest: The authors declare that the research was conducted in the absence of any commercial or financial relationships that could be construed as a potential conflict of interest.

frontiers | Frontiers in Plant Science

ORIGINAL RESEARCH
published: 12 April 2022
doi: 10.3389/fpls.2022.824461

Varying Relationship Between Vascular Plant Leaf Area and Leaf Biomass Along an Elevational Gradient on the Eastern Qinghai-Tibet Plateau

Ketong Yang[1], Guopeng Chen[1], Junren Xian[2] and Weiwei Chen[1]*

[1] College of Forestry, Gansu Agricultural University, Lanzhou, China, [2] College of Environmental Sciences, Sichuan Agricultural University, Chengdu, China

The altitudinal gradient is one of the driving factors leading to leaf trait variation. It is crucial to understand the response and adaptation strategies of plants to explore the variation of leaf traits and their scaling relationship along the altitudinal gradient. We measured six main leaf traits of 257 woody species at 26 altitudes ranging from 1,050 to 3,500 m within the eastern Qinghai-Tibet Plateau and analyzed the scaling relationships among leaf fresh weight, leaf dry weight, and leaf area. The results showed that leaf dry weight increased significantly with elevation, while leaf fresh weight and leaf area showed a unimodal change. Leaf dry weight and fresh weight showed an allometric relationship, and leaf fresh weight increased faster than leaf dry weight. The scaling exponent of leaf area and leaf fresh weight (or dry weight) was significantly greater than 1, indicating that there have increasing returns for pooled data. For α and normalization constants (β), only β of leaf area vs. leaf fresh weight (or dry weight) had significantly increased with altitude. All three paired traits had positive linear relationships between α and β. Our findings suggest that plants adapt to altitudinal gradient by changing leaf area and biomass investment and coordinating scaling relationships among traits. But leaf traits variation had a minor effect on scaling exponent.

Keywords: scaling relationship, leaf trait, elevational gradient, arid valley, alpine plant

OPEN ACCESS

Edited by:
Peijian Shi,
Nanjing Forestry University, China

Reviewed by:
Guoyong Li,
Henan University, China
Xin Jia,
Beijing Forestry University, China

****Correspondence:***
Guopeng Chen
chgp1986@gmail.com

Specialty section:
This article was submitted to
Functional Plant Ecology,
a section of the journal
Frontiers in Plant Science

Received: *29 November 2021*
Accepted: *07 March 2022*
Published: *12 April 2022*

Citation:
Yang K, Chen G, Xian J and Chen W (2022) Varying Relationship Between Vascular Plant Leaf Area and Leaf Biomass Along an Elevational Gradient on the Eastern Qinghai-Tibet Plateau.
Front. Plant Sci. 13:824461.
doi: 10.3389/fpls.2022.824461

INTRODUCTION

Leaves are crucial for plant metabolic performance, have significant functions in biogeochemical cycles (Cui et al., 2020; Cubino et al., 2021), and influence global climate change (Niinemets, 2001; Li et al., 2008; Cubino et al., 2021). Previous studies have confirmed that leaf size spans six orders of magnitude (Milla and Reich, 2007; Wright et al., 2017), and this variation in leaf size is the basis for maintaining biodiversity (Mi et al., 2021). For leaves, abiotic factors (e.g., altitude) are one of the driving forces of variation (Chen et al., 2021; Jiang et al., 2021; Ren et al., 2021). The scaling relationship between leaf traits caused by leaf size may affect leaf biomass and element allocation, and this relationship has also been proven to be one of the strategies for species to acquire resources, and even affect species coexistence and community construction (Li et al., 2008; Ren et al., 2021). Although variations in leaf and scaling relationships between different climatic regions and life forms have been widely documented (Niklas et al., 2007; Li et al., 2008), how they vary along elevation gradient remains unclear.

Plant leaves have abundant phenotypic variation. Milla and Reich's (2011) study showed that leaves gradually became thicker and water content decreased with elevation, and Guo et al.'s (2018) study showed that the leaves gradually became smaller with altitude. These variations are thought to be better adapted to the environment, with smaller, thicker leaves that can endure mechanical damage from intense radiation, freezing, and wind (Xiang et al., 2009; Pan et al., 2013). However, at present, many studies only focus on the changes of leaf traits along the elevation gradient, and such static changes only represent the leaves' current situation, while the dynamic changes among traits, such as allometric relationship (or scaling relationship), are ignored. Another very important aspect is that although Sun et al. (2017) and Guo et al. (2018) have done some work on allometric variation along elevation gradients, a single species (bamboo) is not a good representative plant for the whole community. Therefore, it is urgent to explore whether leaves allometric growth at the community level is affected by altitude.

Elevational gradient represents a combination of various changing environmental factors, namely, colder climate, decreasing soil depth, and less fertile soil, but also reduced human disturbance with increasing altitude (Kühn et al., 2021). Meanwhile, the elevation gradient is known as a "natural platform" for studying plant variation (Thakur et al., 2019). With increasing altitude, most functional traits, namely, leaf area (LA), leaf dry weight (LDW), leaf fresh weight (LFW), and water content, decreased significantly (Guo et al., 2018). Because most traits are correlated, these will further lead to variation in the scaling relationship. For instance, Pan et al. (2013) found that the scaling exponent between LA with LDW gradually increased from 0.859 to 1.258 along the elevational gradient for 121 vascular species ranging from 414 to 1,462 m on Mt. Tianmu, and they attributed the reason to environmental variations that cause different leaf biomass allocation. However, Thakur et al. (2019) showed that the scaling exponent of LA and LDW decreased significantly from 1.08 to 0.85 with increasing elevation with the altitude from 3,350 to 5,150 m in the western Himalaya. Therefore, we attempted to further summarize the general relationship between LDW–LFW, LA–LFW, and LA–LDW through a larger elevation scale, and test the relationship between leaf size and scaling exponent to systematically elucidate the variation mechanism of leaf traits and their internal relationships with altitudes. These will help to expand our understanding of plant light capture cost mechanisms and their response and adaptation to elevation gradient.

The eastern region of the Qinghai-Tibet Plateau has diverse native flora and is significant for protecting biodiversity and ecosystem balance (Chen et al., 2021; Liu et al., 2021). Some vegetation of this region has been severely disturbed in the past. After decades of restoration and conservation, most of the vegetation is recovering (Yan et al., 2013; Chen et al., 2021). Therefore, the region is one of the most powerful "natural laboratories" for studying the elevation responses of the plant (Thakur et al., 2019). To explore changes of scaling exponents and normalization constants along the elevation gradient, we set 26 plots in different altitudes along 1,050–3,500 m located at the eastern Qinghai-Tibet Plateau. In this research, we measured leaf traits—i.e., LA, LFW, LDW, specific leaf area (SLA), and leaf dry matter content (LDMC)—of 257 woody plant species with the following objectives: (1) How do the leaf traits change along the altitudinal gradient? (2) Whether elevation gradient will affect the variation of scaling exponent and normalization constant?

MATERIALS AND METHODS

Study Sites

The study sites located in Gongbahe of Bailong River (GBR) in Zhouqu County, Southern Gansu Province, P.R. China (103° 57′ 05″–104° 42′ 05″ E, 33° 14′ 32″–33° 53′ 52″ N, 998–3,600 m a.s.l.), which is the transition zone of temperate monsoon, subtropical monsoon, and plateau montane climate zones, and at the boundary between semihumid and semiarid regions (Chen et al., 2021). According to the last 30 years of climatic data, the mean annual rainfall, evaporation of GBR, relative humidity, and mean annual temperature are 951 mm, 918 mm, 82%, and 4.3°C, respectively. The mean temperature of the coldest month (January) is −13.3°C; the mean temperature of the hottest month (July) is 20.8°C; and the annual frost-free period is about 96.7 days. The annual sunshine duration is 1,398.4 h, and the sunshine percentage is 32.0%. The old-growth vegetation of GBR had been logged several decades ago and the regrowth of restored vegetation is well underway (Yang et al., 2021).

During previous *in situ* surveys, we found that vegetation gradually changed from arid valley dwarf xerophytic shrubs, deciduous broad-leaved forests, to the evergreen coniferous forest and evergreen broad-leaved shrubs from 1,050 to 3,500 m (Chen et al., 2021; Yang et al., 2021). We set up a transect along an elevational gradient and surveyed 26 plots of 20 m × 20 m at different altitudes (Appendix 1).

Sampling and Measurement of Leaves

We identified a total of 257 woody plant species (some plants were found in multiple plots), belonging to 55 families and 115 genera (Appendix 2) according to *Flora of China*,[1] selected three healthy branches of each woody species, and collected five leaves from the middle-upper canopy of each plant at 10:00–14:00. Then, put the leaves into plastic self-sealing bags in a portable incubator with ice bags (to prevent blades from deforming and losing water), and then brought them to the forest research station to measure.

Each leaf was scanned, and images were saved as bitmap images at a 480-dpi resolution using a scanner (EPSON V39, Indonesia). Image J software (version 1.48)[2] was used to obtain a leaf profile in a black and white image. Then, the length, width, and area of the blade were measured by the Image J. We then measured LFW and dried the leaves in a ventilated oven at 105°C for 15 min and turned to 75°C

---

[1] http://www.iplant.cn/frps

[2] https://imagej.net/software/fiji/

until achieving a constant dry weight (i.e., LDW) (Huang et al., 2019a; Guo et al., 2021; Jiang et al., 2021). LFW and LDW were both measured using an electronic balance (0.0001 g, Zhuojing Experimental Equipment Co. Ltd., BMS, Shanghai, China).

Data Analysis

The arithmetic mean value is often used to represent the average of a series of measurements. But when data are not normally distributed, the median may be more representative. Thus, we tested the normality of the dataset, and five out of six traits showed non-normal distribution (**Figure 1**). So, we first calculated the mean for every individual leaf trait as a species traits value, then, for each altitude (plot), we calculated each plot species median traits value as a community traits value. Some previous studies found that LFW is better for describing the scaling relationship between leaf biomass and LA (Huang et al., 2019b; Shi et al., 2020). So, we calculated SLA by LFW and LDW, which were used by SLA_F and SLA_D, respectively.

We established scaling relationships between traits based on species at each altitude (plot). The relationships of LDW–LFW, LA–LFW, and LA–LDW can be described as $y = \beta\, x^{\alpha}$, linearized under the form $\log(y) = \log(\beta) + \alpha \log(x)$. The values of α determine whether the relationship is isometric ($\alpha = 1.0$) or allometric ($\alpha > 1.0$ or $\alpha < 1.0$). The term β is the *y*-intercept of the relationship (Xiang et al., 2009; Pan et al., 2013). Its value does not determine the form of the relationship and, if two lines of the same slope are compared, the difference between their respective values of β indicates the difference independent of parameters. The 95% CIs of α and β were calculated using the SMATR Version 2.0 (Falster et al., 2006). For the three paired traits, we compared its α with 1.0 to test the difference. If the slope is not significantly different from 1.0, the relationship between the two indexes represents roughly isometric growth; and if the slope is greater or less than 1.0, the relationship between the two indexes is allometric growth (Xiang et al., 2009; Sun et al., 2017). We used the coefficient of determination (R^2) to determine the goodness of fit. The images describing scaling exponents and normalization constants were analyzed by the *mgcv* (2011) package and of R 4.0.5 software (R Core Team, 2021).

RESULTS

Leaf Traits Variation Along the Altitudinal Gradient

Leaf fresh weight (LFW) and LA showed significant unimodal variation across the elevational gradient (**Figures 2A,D**) and ranged from 0.024 g and 1.456 cm^2 to 0.366 g and 24.619 cm^2, respectively. LDW gradually increased and then decreased ($p < 0.05$) at 3,200 m (**Figure 2B**). LDMC ranged from 24.21 to 48.96% and had no obvious relationship with altitude (**Figure 2C**). SLA_F and SLA_D ranged from 41.686 and 116.582 $\text{cm}^2 \cdot \text{g}^{-1}$ to 112.179 and 437.291 $\text{cm}^2 \cdot \text{g}^{-1}$, respectively (**Figures 2E,F**). They neither showed a significant relationship with elevations, but had a maximum unimodal at 2,500 m.

Scaling Relationship Between Leaf Traits for Pooled Data

The log-transformed relationships of LDW–LFW, LA–LFW, and LA–LDW exhibited strong linear (**Figure 3**). The scaling exponent of LDW–LFW was 0.962 (95% CI, 0.951–0.973) (**Figure 3A**), which was significantly less than 1.0 ($p < 0.001$). The scaling exponents of LA–LFW and LA–LDW were 1.066 (95% CI, 1.044–1.088) and 1.108 (95% CI, 1.082–1.136) (**Figures 3B,C**), both significantly greater than 1.0 ($p < 0.001$).

Scaling Exponent and Normalization Constant Variation Along the Altitudes

All α of LDW–LFW, LA–LFW, and LA–LDW showed no relationship with altitudinal gradient (**Figures 4A,C,E**). For LA–LFW and LA–LDW, the β first increased and then slowly converged with altitude (**Figures 4B,D,F**).

The Relationship Between Leaf Traits and Scaling Parameters

The relationships among two scaling parameters (i.e., α and β) and other derived parameters were very complex (**Figures 5–7**). Overall, only the α and β of the three paired traits had a significant quadratic relationship (all $p < 0.001$) (**Figures 5H**, **6H**, **7H**), other traits and scaling parameters had no clear linear relationship (**Figures 5A–G**, **6A–G**, **7B–G**). Even so, we still detected a weakly relationship between α of LA-LDW with LA ($R^2 = 0.351$, $p = 0.088$) (**Figure 7A**).

DISCUSSION

Plant traits response and adaptation to the environment are critical for plant survival. Combining with scaling relationship to explore the connection between leaf traits provides a theoretical basis for leaf variations with altitudinal gradient. Based on this study, we have found that plants adapt to altitude gradient mainly by adjusting LA and leaf mass, and the change of area and mass further affects scaling relationships.

Effects of Altitude on Leaf Traits

Plants can produce adaptive strategies to cope with the environmental variation caused by the elevational gradient (Rudgers et al., 2019; Cui et al., 2020; Cubino et al., 2021). Previous studies had suggested that as elevation increases, the temperature always lowers, heat and energy supply limited LA expansion (Pan et al., 2013; Sun et al., 2017). But our study showed that the LA gradually increased up to 2,500 m. This non-intuitive pattern might be caused by the influence of precipitation on LA. The lowest elevation of our plots was located in a dry valley, where plants exhibited smaller leaves (Niinemets, 2001; Rudgers et al., 2019; Sun et al., 2020). As the altitude increased, precipitation and atmospheric humidity gradually increased, and LA also increased. Beyond a critical altitude (in our case, perhaps 2,500 m), temperature and heat may have limited LA increasing (Nikita et al., 2018). At low temperatures, smaller leaves reduce thermal convection in the boundary layer, which

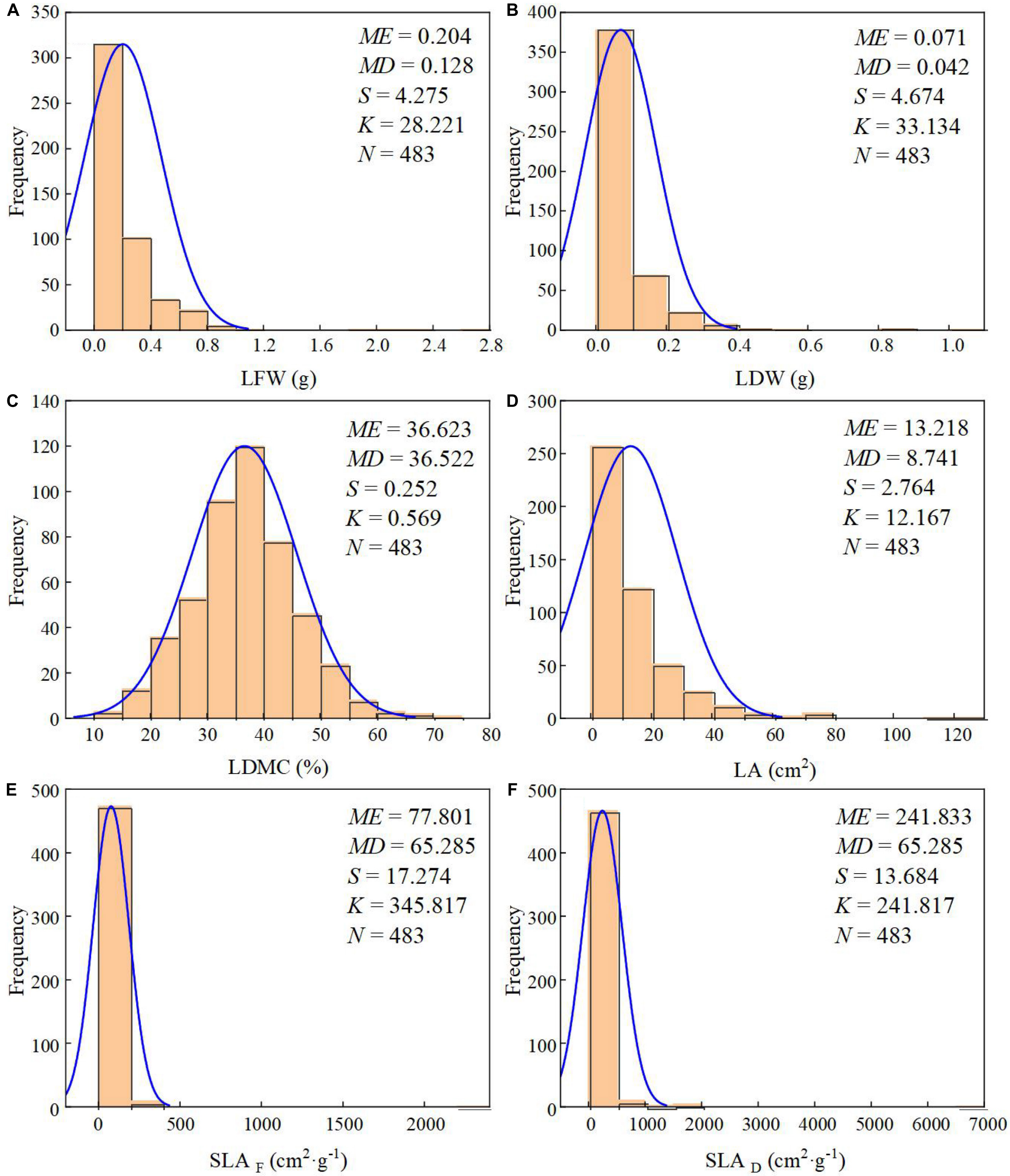

FIGURE 1 | Frequency distribution histogram and normality test of leaf traits. **(A)** LFW; **(B)** LDW; **(C)** LDMC; **(D)** LA; **(E)** SLA$_F$-based fresh weight; and **(F)** SLA$_D$-based dry weight. ME, mean value; MD, median value; S, skewness; K, kurtosis; N, total number.

is very important for maintaining leaf heat and keeping the appropriate temperature of photosynthesis (Cubino et al., 2021; Lyu et al., 2021). LFW and LA have the same variation model. By comparison, LDW increased continuously with the altitude, and then gradually convergent. The increase of leaf biomass with altitude may reflect the conservative strategy of leaves, that is, the harsher the environment, the more investment in leaf biomass (Pan et al., 2013; Zhang et al., 2020; Yang et al., 2021). Abundant

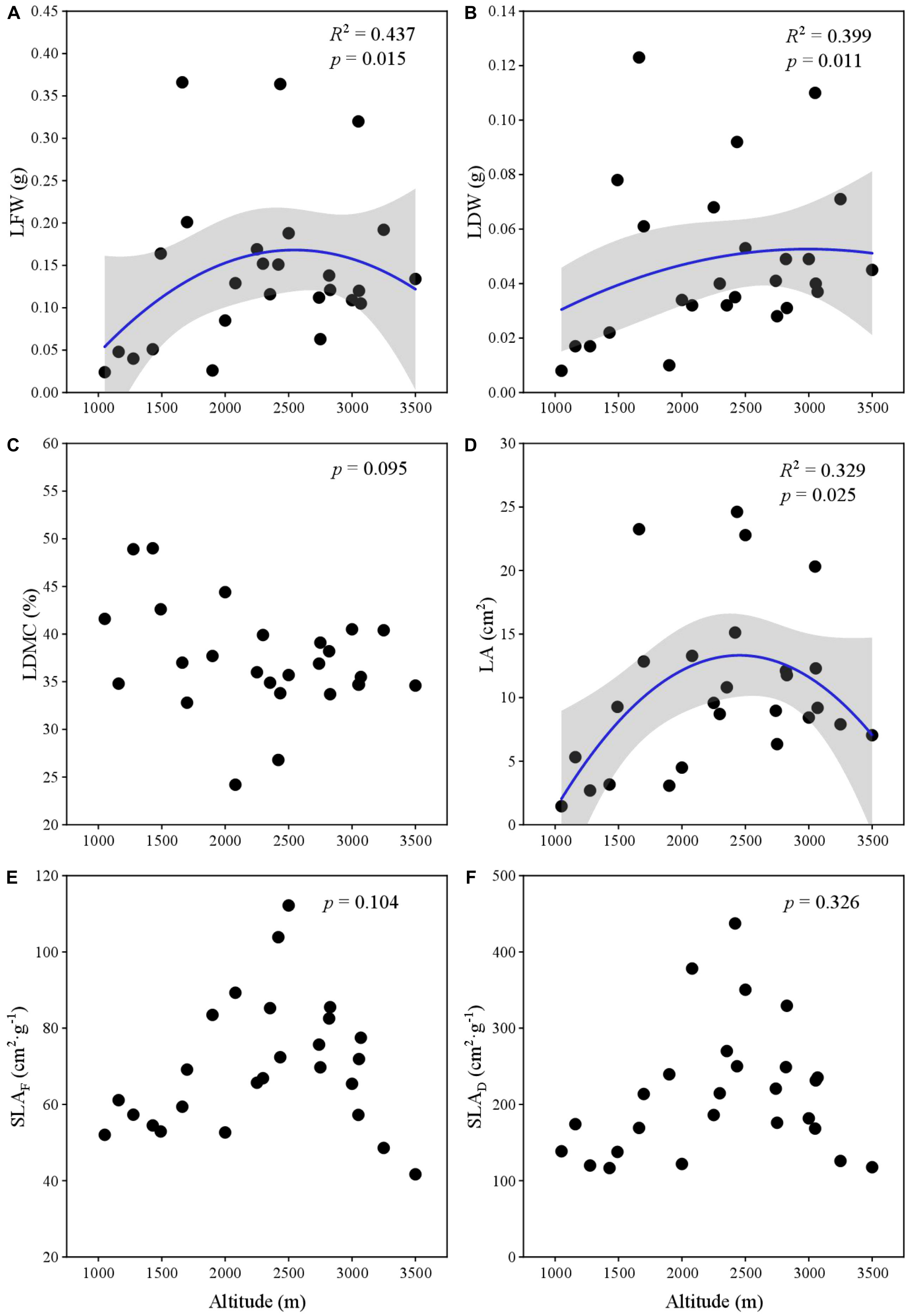

FIGURE 2 | The variation of leaf traits along elevation gradient. **(A)** LFW; **(B)** LDW; **(C)** LDMC; **(D)** LA; **(E)** SLA$_F$-based fresh weight; and **(F)** SLA$_D$-based dry weight.

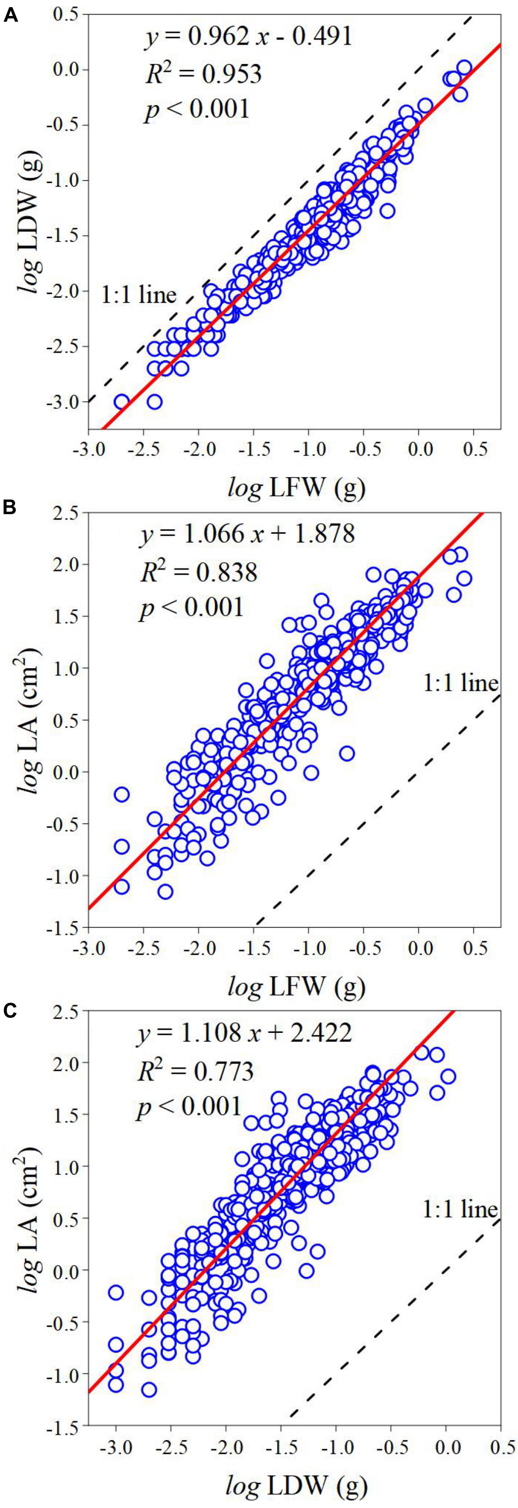

FIGURE 3 | The scaling relationship between leaf traits. **(A)** The scaling relationship between LFW and LDW. **(B)** The scaling relationship between LFW and LA. **(C)** The scaling relationship between LDW and LA. The blue circle represents observed values, the red line represents the SMA regression line, and the black-dotted line represents the 1:1 line; R^2 is the coefficient of determination that is used to measure the goodness of fit; *p* represents the significant level of goodness of fit at 0.05 level.

investment of leaf biomass promotes the denser mesophyll tissue, this not only helps prevent freezing injury but also reduces mechanical damage (Niinemets, 2001; Nikita et al., 2018).

In this study, SLA showed a unimodal change with altitude, the result is inconsistent with Umaña and Swenson (2019), who found that SLA of four out of six species decreased with elevation. This difference may cause by the relatively limited range of altitudes in their study (only ranged from 250 to 1,075 m a.s.l.). In addition, Costa et al. (2018) researched trait patterns along tropical elevation gradient ranging from 1,620 to 3,060 m also found that LA, SLA, and LDMC showed different patterns along their elevational gradient—sometimes decreasing, increasing, or showing no clear changes. Unimodal patterns of leaf traits may also reflect changes in biodiversity. Many studies have linked changes in leaf traits to species richness (Costa et al., 2018; Chen et al., 2021; Liu et al., 2021); competition among species may increase as species abundance increases. Furthermore, increased species abundance may promote niche differentiation, which can also influence the leaf traits pattern (Costa et al., 2018; Zhu et al., 2019; Guo et al., 2021). The biotas and succession along the altitudinal gradient may be one of the main factors leading to the variation of leaf traits.

For plants, leaf water content is associated with photosynthesis and light capture efficiency. Many studies have shown this for bamboos, climbing plants, and alpine plant taxa (Huang et al., 2019a, 2020; Wang et al., 2021). The goodness of fit between LFW (R^2 = 0.437) with altitude is greater than that LDW (R^2 = 0.399) with altitude, which is consistent with the findings of other research. It may be due to the different leave shapes. Compared with broad leaves, narrow leaves require dense tissue (lower water content) to resist static loads. In other words, even given the same leaf fresh mass, different plants will have a great difference in leaf dry mass. Huang et al. (2019a) thought that the studies of leaf allometry had to consider the influence of foliar water content on the scaling relationship. However, in the field sampling process, it is difficult to obtain the leaves' fresh weight in time, so there are still many operational difficulties.

Effects of Altitude on α and β

Allometric relationships among leaf traits reflect their priority needs and dynamic growth. Based on the pooled data, the LDW did not keep pace with LFW, and as the leaf size gradually increased there was more biomass investment per unit area. The result of this study did not support the law of diminishing returns, which was inconsistent with Huang et al. (2019a, 2020). This implied that with the increasing of LFW, leaf water content gradually increased or leaf dry matter content gradually decreased. It may be because larger LA transpiration more water and therefore need to store more water, and plenty of water keeps photosynthesis going. So, leaf water content and dry matter content will gradually increase, and the increased rate of water content is higher than that of dry matter content. Consistent with Yang et al.'s (2021) study, the fitness of LA–LFW is better than that of LA–LDW. Most plant—like evergreen and deciduous species have different hydraulic strategies and photosynthetic efficiency (Niinemets, 2001; Cubino et al., 2021; Wang et al., 2021), which may lead to differences in leaf water

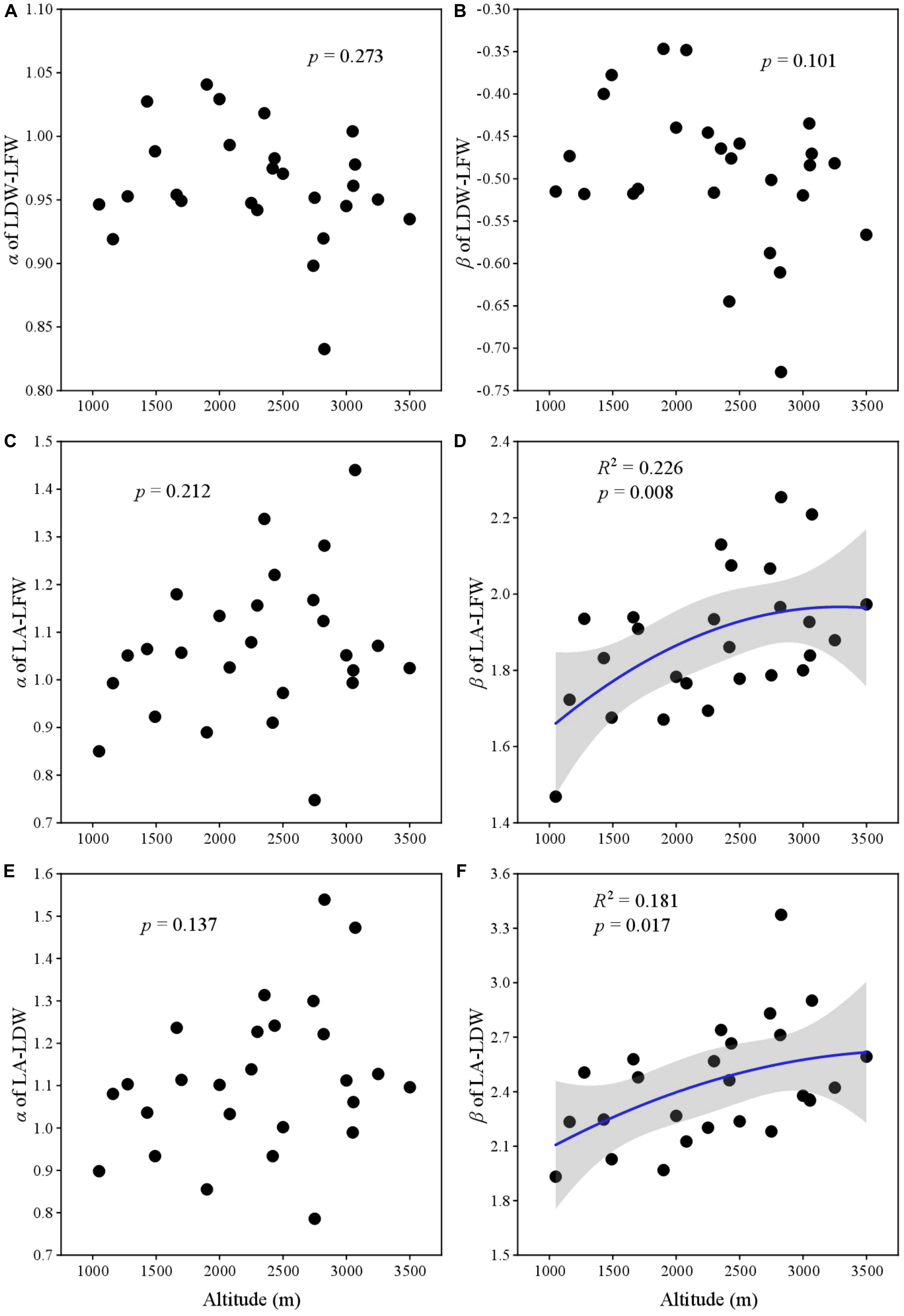

FIGURE 4 | The relationship between scaling exponent and normalization constant with elevation gradient. **(A)** Scaling exponent of LDW and LFW; **(B)** normalization constant of LDW and LFW; **(C)** scaling exponent of LA and LFW; **(D)** normalization constant of LA and LFW; **(E)** scaling exponent of LA and LDW; and **(F)** normalization constant LA and LDW.

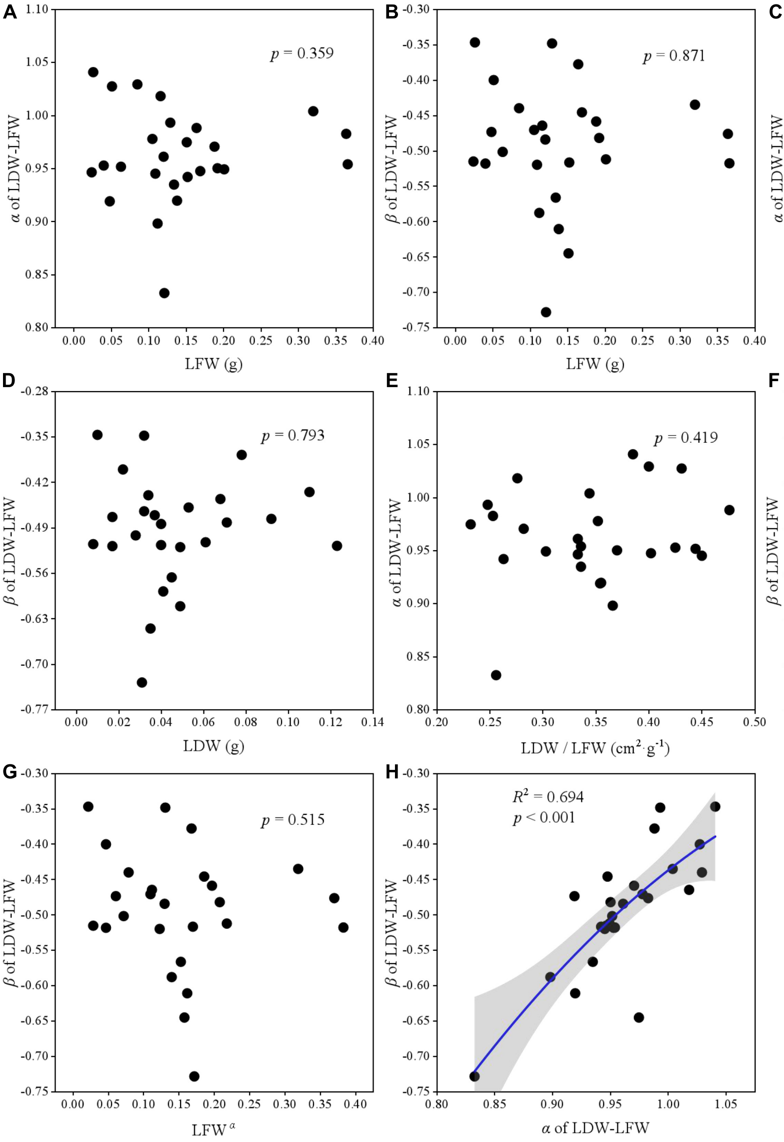

FIGURE 5 | The correlation relationship of parameters of LDW and LFW. **(A)** The relationship between α and LFW; **(B)** the relationship between β and LFW; **(C)** the relationship between α and LDW; **(D)** the relationship between β and LDW; **(E)** the relationship between α and LDW/LFW; **(F)** the relationship between β and LDW/LFW; **(G)** the relationship between β and LFW^{α}; and **(H)** the relationship between β and α.

content or dry matter content, and thus lead to divergences in LDW per unit area.

To our knowledge, few studies reveal the variation of scaling parameters (i.e., scaling exponent and normalization constant) for leaf traits at such a large scale. Scaling relationships among leaf traits can reveal how the material allocation at leaf level as they grow. We found that most scaling exponents and normalization constants had no significant relationship between altitudes, except for the β of LA–LFW and LA–LDW. Our results were inconsistent with Pan et al. (2013) and Sun et al. (2017), who reported that scaling exponents for leaf mass and area significantly increased or was the V-shape with altitudinal gradient. These might be different vegetation types. Their study sites were located in subtropical monsoon regions, where most plants were evergreen. Previous studies indicate that evergreen and deciduous plants have different strategies to adapt to their habitat. The evergreen plants are resource-conserved and have greater leaf thickness and mass, lower SLA and water content, and longer leaf life span; and the deciduous are resource-acquisitive, with thinner leaves, greater SLA and lower dry matter content, and shorter leaf life (Li et al., 2008; Wu et al., 2013). Generally, evergreen plants have a higher biomass investment per unit area than deciduous plants (Lyu et al., 2021; Zhang et al., 2021). Another plausible explanation for this discrepancy may be because of the elevation range; the other studies included only 3 or 6 altitudes (Pan et al., 2013; Sun et al., 2017). If we

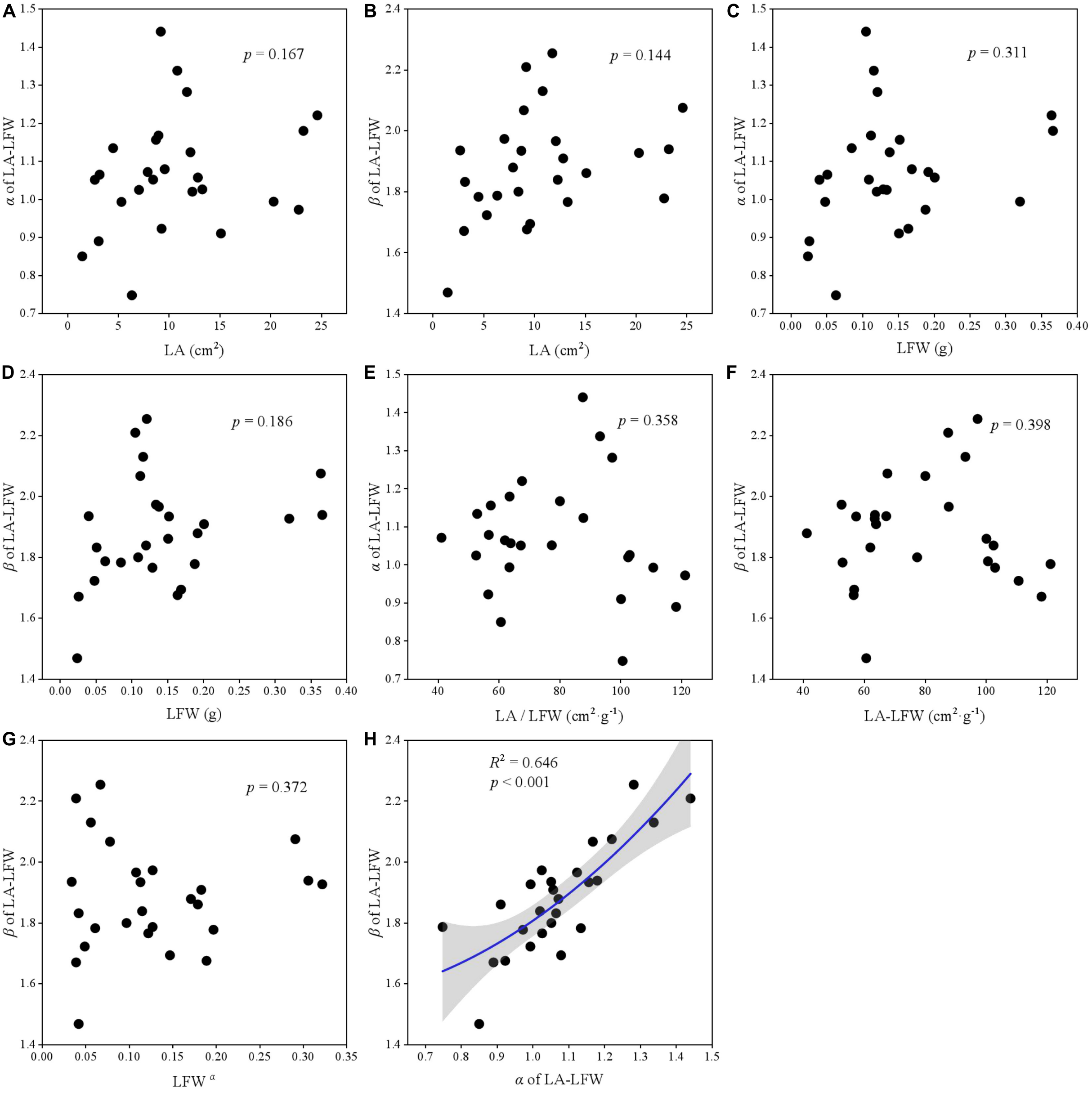

FIGURE 6 | The correlation relationship of parameters of LA and LFW. **(A)** The relationship between α and LA; **(B)** the relationship between β and LA; **(C)** the relationship between α and LFW; **(D)** the relationship between β and LFW; **(E)** the relationship between α and LA/LFW; **(F)** the relationship between β and LA/LFW; **(G)** the relationship between β and LFW^{α}; and **(H)** the relationship between β and α.

had selected only a few elevations, we would found a significant linear relationship, too. In future studies, we suggest researchers consider elevation amplitude and study variation across more altitudes, vegetation types, and climatic regions.

Leaf mass and area are two important leaf traits for the most vascular plants. The relative changes of leaf mass and area reveal the metabolic activity and photosynthesis potential, which are not invariable (Liu et al., 2016; Umaña and Swenson, 2019; Sun et al., 2020). The scaling exponent and normalization constant for LDW–LFW, LA–LFW, and LA–LDW of this study were significant positive correlations. The altitude shifted leaf traits and affected α and β, it is not clear whether altitude, leaves, or their coupling relationship changes α and β. Along the altitudinal gradient, the environment changes rapidly over a short distance. Plants are subject to a lower temperature and higher irradiance and strong wind at higher altitudes (Nikita et al., 2018; Zhang et al., 2020; Kühn et al., 2021). However, in the middle altitude, most plants are understory, a few dominant species may be in the canopy. In other words, understory plants are rarely exposed to wind and strong light irradiance (Pan et al., 2013; Costa et al., 2018). Environmental variation at different stages of altitudinal gradient (high, middle, and low altitude) may be the

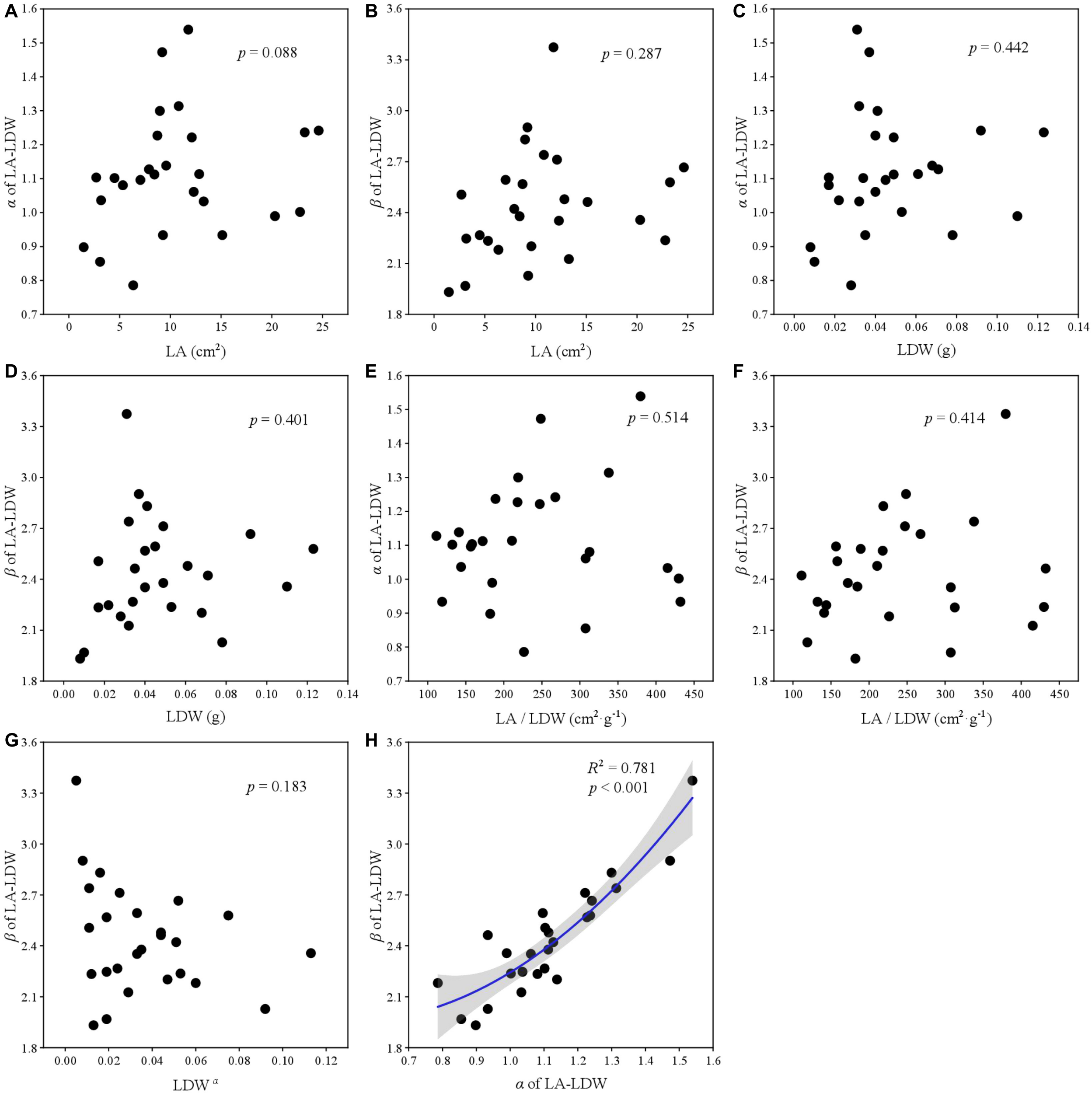

FIGURE 7 | The correlation relationship of parameters of LA and LDW. **(A)** The relationship between α and LA; **(B)** the relationship between β and LA; **(C)** the relationship between α and LDW; **(D)** the relationship between β and LDW; **(E)** the relationship between α and LA/LDW; **(F)** the relationship between β and LA/LDW; **(G)**, the relationship between β and LDW^{α}; and **(H)** the relationship between β and α.

main factors leading to the change of many traits that showed unimodal patterns.

The Relationship Between α and β With Derived Parameters

Scaling relationships for leaves quantifies the allometry of resource allocation at the leaf scale and helps to interpret correlations among traits and scaling parameters (Thakur et al., 2019; Zhang et al., 2020). Our data showed close relationships between scaling exponent and normalization constant for all leaf traits. However, contrary to previous studies (Milla and Reich, 2007; Sun et al., 2017), LA did not affect α of LA–LFW and LA–LDW, LFW also did not affect α of LDW–LFW. The reason might be that our target plant species included conifer species such as *Abies fabri*, *Pinus bungeana*, and *Cupressus chengiana*, and our results were the pooled data rather than life-form or plant-specific.

In our study, we included conifer species, whose unusual leaf morphology may have influenced the results of our analysis.

For example, they have very small LA (needle or scale leaf), specific LA, and water content, but have large leaf mass. They may be a very strong disturbance when compared with broad-leaved species, and we recommend that future studies treat broad-leaved and coniferous species separately.

CONCLUSION

With the increase of altitude, the LFW and LA showed a unimodal change, while the LDW was a slow increase. LA with LFW and LDW showed an increasing returns relationship. Our study demonstrates that there is no fixed variation pattern of scaling relationship with altitude, and leaf traits had little effect on the variation of scaling relationship. Therefore, the coordination of leaf trait variation and scaling relationship may be the positive response of plants to the elevation gradient. These provide a possible biological explanation for the plant adaptation to high radiation, freezing, and strong wind on altitude gradient.

DATA AVAILABILITY STATEMENT

The original contributions presented in the study are included in the article/**Supplementary Material**, further inquiries can be directed to the corresponding author.

AUTHOR CONTRIBUTIONS

KY, GC, and WC designed the experiments, were responsible for field collections, and analyzed the data. KY, GC, JX, and WC wrote and revised the manuscript. All authors contributed to the article and approved the submitted version.

FUNDING

This work was supported by the National Natural Science Foundation of China (31800352), the Youth Talents Supporting Program of Gansu Province (GXH20210611-11), the Science and Technology Innovation Fund of Gansu Agricultural University (GSAU-RCZX201708), the Star of Innovation Project for Outstanding Graduate Students of Gansu Education Department (2021CXZX-398), and the National College Students' Innovative Entrepreneurial Training Plan Program (201710733029 and 202010733027).

SUPPLEMENTARY MATERIAL

The Supplementary Material for this article can be found online at: https://www.frontiersin.org/articles/10.3389/fpls.2022.824461/full#supplementary-material

REFERENCES

Costa, D. S., Zotz, G., Hemp, A., and Kleyer, M. (2018). Trait patterns of epiphytes compared to other plant life-forms along a tropical elevation gradient. *Funct. Ecol.* 32, 2073–2084. doi: 10.1111/1365-2435.13121

Cui, E. Q., Weng, E. S., Yan, E. R., and Xia, J. Y. (2020). Robust leaf trait relationships across species under global environmental changes. *Nat. Commun.* 11:2999. doi: 10.1038/s41467-020-16839-9

Chen, G. P., Yang, K. T., Zhang, J. W., Wang, L., and Xian, J. R. (2021). Effects of succession stages and altitudinal gradient on leaf surface area and biomass allocation of typical plants in the subalpine of Eastern Tibetan Plateau. *Glob. Ecol. Conserv.* 27:e01590. doi: 10.1016/j.gecco.2021.e01590

Cubino, J. P., Biurrun, I., Bonari, G., Braslavskaya, T., Font, X., Jandt, U., et al. (2021). The leaf economic and plant size spectra of European forest understory vegetation. *Ecography* 44, 1311–1324. doi: 10.1111/ecog.05598

Falster, D., Warton, D., and Wright, I. (2006). *User's guide to SMATR: standardized major axis tests and routines version 2.0, copyright 2006*. Available: http://www.bio.mq.edu.au/ecology/SMATR/. (Accessed on 3 2013).

Guo, Z. W., Lin, H., and Yang, Q. P. (2018). Altitudinal patterns of leaf traits and leaf allometry in bamboo *Pleioblastus amarus*. *Front. Plant Sci.* 9:1110. doi: 10.3389/fpls.2018.01110

Guo, J. W., Zhao, C. C., Zhang, L. N., Han, Y. Y., Cao, R., Liu, Y. Z., et al. (2021). Water table decline alters arthropod community structure by shifting plant communities and leaf nutrients in a Tibetan peatland. *Sci. Total Environ.* 814:151944. doi: 10.1016/j.scitotenv.2021.151944

Huang, W. W., Ratkowsky, D. A., Hui, C., Wang, P., Su, J. L., and Shi, P. J. (2019a). Leaf fresh weight versus dry weight: which is better for describing scaling relationship between leaf biomass and leaf area for broad-leaved plants? *Forests* 10:256. doi: 10.3390/f10030256

Huang, W. W., Su, X. F., Ratkowsky, D. A., Niklas, K. J., and Shi, P. J. (2019b). The scaling relationships of leaf biomass vs. leaf surface area of 12 bamboo species. *Glob. Ecol. Conserv.* 20:e00793. doi: 10.1016/j.gecco.2019.e00793

Huang, W. W., Reddy, G. V. P., Li, Y. Y., Larsen, J. B., and Shi, P. J. (2020). Increase in absolute leaf water content tends to keep pace with that of leaf dry mass-evidence from bamboo plants. *Symmetry* 12:1345. doi: 10.3390/sym12081345

Jiang, X. Y., Jia, X., Gao, S. J., Jiang, Y., Wei, N. N., Han, C., et al. (2021). Plant nutrient contents rather than physical traits are coordinated between leaves and roots in a desert shrubland. *Front. Plant Sci.* 12:734775. doi: 10.3389/fpls.2021.734775

Kühn, P., Backes, A. M., Römermann, C., Bruelheide, H., and Haider, S. (2021). Contrasting patterns of intraspecific trait variability in native and non-native plant species along an elevational gradient on Tenerife. *Canary Islands. Ann. Bot.* 127, 565–576. doi: 10.1093/aob/mcaa067

Li, G. Y., Yang, D. M., and Sun, S. C. (2008). Allometric relationships between lamina area, lamina mass and petiole mass of 93 temperate woody species vary with leaf habit, leaf form and altitude. *Funct. Ecol.* 22, 557–564. doi: 10.1111/j.1365-2435.2008.01407.x

Liu, Y. J., Dawson, W., Prati, D., Haeuser, E., Feng, Y. H., and Kleuuen, M. (2016). Does greater specific leaf area plasticity help plants to maintain a high performance when shaded? *Ann. Bot.* 118, 1329–1336. doi: 10.1093/aob/mcw180

Liu, Y. Z., Li, G. Y., Wu, X. W., Niklas, K. J., Yang, Z. L., and Sun, S. C. (2021). Linkage between species traits and plant phenology in an alpine meadow. *Oecologia* 195, 409–419. doi: 10.1007/s00442-020-04846-y

Lyu, M., Sun, M. K., Penuelas, J., Sardans, J., Sun, J., Chen, X. P., et al. (2021). Temperature controls growth of *Pinus taiwanensis* along an elevational gradient. *Trees* 35, 433–440. doi: 10.1007/s00468-020-02045-z

Milla, R., and Reich, P. B. (2007). The scaling of leaf area and mass: the cost of light interception increases with leaf size. *P. Roy. Soc. B Biol. Sci.* 274, 2109–2114. doi: 10.1098/rspb.2007.0417

Milla, R., and Reich, P. B. (2011). Multi-trait interactions, not phylogeny, fine-tune leaf size reduction with increasing altitude. *Ann. Bot* 107, 455–465. doi: 10.1093/aob/mcq261

Mi, X. C., Feng, G., Hu, Y. B., Zhang, J., Chen, L., Corlett, R. T., et al. (2021). The global significance of biodiversity science in China: an overview. *Natl. Sci. Rev.* 8:nwab032. doi: 10.1093/nsr/nwab032

Niinemets, Ü (2001). Global-scale climatic controls of leaf dry mass per area, density, and thickness in trees and shrubs. *Ecology* 82, 453–469. doi: 10.2307/2679872

Niklas, K. J., Cobb, E. D., Niinemets, Ü, Reich, P. B., Sellin, A., Shipley, B., et al. (2007). Diminishing returns in the scaling of functional leaf traits across and within species groups. *Proc. Natl. Acad. Sci.U.S.A.* 104, 8891–8896. doi: 10.1073/pnas.0701135104

Nikita, R., Dinesh, T., and Amit, C. (2018). Seasonal variations coupled with elevation gradient drives significant changes in eco-physiological and biogeochemical traits of a high altitude evergreen broadleaf shrub. *Rhododendron anthopogon*. *Plant Physiol. Biochem.* 132, 708–719. doi: 10.1016/j.plaphy.2018.08.009

Pan, S., Liu, C., Zhang, W. P., Xu, S. S., Wang, N., Li, Y., et al. (2013). The scaling relationships between leaf mass and leaf area of vascular plant species change with altitude. *Plos One* 8:e76872. doi: 10.1371/journal.pone.0076872

Ren, T. T., He, N. P., Liu, Z. G., Li, M. X., Zhang, J. H., Li, A., et al. (2021). Environmental filtering rather than phylogeny determines plant leaf size in three floristically distinctive plateaus. *Ecol. Indic.* 130:108049. doi: 10.1016/j.ecolind.2021.108049

R Core Team. (2021). *R: a Language and Environment for Statistical Computing.* Vienna, Aus.: R Foundation for Statistical Computing.

Rudgers, J. A., Hallmark, A., Baker, S. R., Baur, L., Hall, K. M., Litvak, M. E., et al. (2019). Sensitivity of dryland plant allometry to climate. *Funct. Ecol.* 33, 2290–2303. doi: 10.1111/1365-2435.13463

Shi, P. J., Li, Y. R., Hui, C., Ratkowsky, D. A., Yu, X. J., and Niinemets, Ü (2020). Does the law of diminishing returns in leaf scaling apply to vines? - Evidence from 12 species of climing plants. *Glob. Ecol. Conserv.* 21:e00830. doi: 10.1016/j.gecco.2019.e00830

Sun, J., Fan, R. R., Niklas, K. J., Zhong, Q. L., Yang, F. C., Li, M., et al. (2017). "Diminishing returns" in the scaling of leaf area vs. dry mass in Wuyi Mountain bamboos. *Southeast China. Am. J. Bot.* 104, 993–998. doi: 10.3732/ajb.1700068

Sun, J., Chen, X. P., Wang, M. T., Li, J. L., Zhong, Q. L., and Cheng, D. L. (2020). Application of leaf size and leafing intensity scaling across subtropical trees. *Ecol. Evol.* 10, 13395–13402. doi: 10.1002/ece3.6943

Thakur, D., Rathore, N., and Chawla, A. (2019). Increases in light interception cost and metabolic mass component of leaves are coupled for efficient resource use in the high altitude vegetation. *Oikos* 128, 254–263. doi: 10.1111/oik.05538

Umaña, M. N., and Swenson, N. G. (2019). Intraspecific variation in traits and tree growth along an elevational gradient in a subtropical forest. *Oecologia* 191, 153–164. doi: 10.1007/s00442-019-04453-6

Wu, J. B., Hong, J. T., Wang, X. D., Sun, J., Lu, X. Y., Fan, J. H., et al. (2013). Biomass partitioning and its relationship with the environmental factors at the alpine steppe in northern Tibet. *Plos One* 8:e81986. doi: 10.1371/journal.pone.0081986

Wright, I. J., Dong, N., Maire, V., Prentice, I. C., Westoby, M., Díaz, S., et al. (2017). Global climatic drivers of leaf size. *Science* 357, 917–921. doi: 10.1126/science.aal4760

Wang, R. M., He, N. P., Li, S. G., Xu, L., and Li, M. X. (2021). Spatial variation and mechanisms of leaf water content in grassland plants at the biome scale: evidence from three comparative transects. *Sci. Rep.* 11:9281. doi: 10.1038/s41598-021-88678-7

Xiang, S., Wu, N., and Sun, S. C. (2009). Within-twig biomass allocation in subtropical evergreen broad-leaved species along an altitudinal gradient: allometric scaling analysis. *Trees* 23, 637–647. doi: 10.1007/s00468-008-0308-6

Yan, E. R., Wang, X. H., Chang, S. X., and He, F. L. (2013). Scaling relationships among twig size, leaf size and leafing intensity in a successional series of subtropical forests. *Tree Physiol.* 33, 609–617. doi: 10.1093treephys/tpt042

Yang, K. T., Chen, G. P., Xian, J. R., Yu, X. Y., and Wang, L. (2021). Scaling relationship between leaf mass and leaf area: A case study using six alpine Rhododendron species in the Eastern Tibetan Plateau. *Glob. Ecol. Conserv.* 30:e01754. doi: 10.1016/j.gecco.2021.e01754

Zhang, L., Yang, L., and Shen, W. (2020). Dramatic altitudinal variations in leaf mass per area of two plant growth forms at extreme heights. *Ecol. Indic.* 110:105890. doi: 10.1016/j.ecolind.2019.105890

Zhang, L. L., Khamphilavong, K., Zhu, H. C., Li, H., He, X. J., Shen, X. F., et al. (2021). Allometric scaling relationships of *Larix pataninii* subsp. chinensis traits across topographical gradients. *Ecol. Indic.* 125:107492. doi: 10.1016/j.ecolind.2021.107492

Zhu, G. J., Niklas, K. J., Li, M., Sun, J., and Cheng, D. L. (2019). "Diminishing returns" in the scaling between leaf area and twig size in three forest communities along an elevation gradient of Wuyi mountain. *China. Forests* 10:1138. doi: 10.3390/f10121138

Conflict of Interest: The authors declare that the research was conducted in the absence of any commercial or financial relationships that could be construed as a potential conflict of interest.

frontiers | Frontiers in Plant Science

ORIGINAL RESEARCH
published: 26 May 2022
doi: 10.3389/fpls.2022.902509

Effects of Water Availability on the Relationships Between Hydraulic and Economic Traits in the *Quercus wutaishanica* Forests

Yuhan Zhang[1†], Jiale Zhao[1†], Jinshi Xu[1], Yongfu Chai[1], Peiliang Liu[1], Jiaxin Quan[1], Xipin Wu[1], Cunxia Li[1] and Ming Yue[1,2*]

[1]Key Laboratory of Resource Biology and Biotechnology in Western China, Northwest University, Xi'an, China, [2]Xi'an Botanical Garden of Shaanxi Province/Institute of Botany of Shaanxi Province, Xi'an, China

Edited by:
Boris Rewald,
University of Natural Resources and Life Sciences Vienna, Austria

Reviewed by:
Maria Conceição Caldeira,
University of Lisbon, Portugal
Manuel Esperon-Rodriguez,
Western Sydney University, Australia

***Correspondence:**
Ming Yue
yueming@nwu.edu.cn

†These authors have contributed equally to this work and share first authorship

Specialty section:
This article was submitted to Functional Plant Ecology, a section of the journal Frontiers in Plant Science

Received: *23 March 2022*
Accepted: *03 May 2022*
Published: *26 May 2022*

Citation:
Zhang Y, Zhao J, Xu J, Chai Y, Liu P, Quan J, Wu X, Li C and Yue M (2022) Effects of Water Availability on the Relationships Between Hydraulic and Economic Traits in the Quercus wutaishanica Forests.
Front. Plant Sci. 13:902509.
doi: 10.3389/fpls.2022.902509

Water availability is a key environmental factor affecting plant species distribution, and the relationships between hydraulic and economic traits are important for understanding the species' distribution patterns. However, in the same community type but within different soil water availabilities, the relationships in congeneric species remain ambiguous. In northwest China, *Quercus wutaishanica* forests in the Qinling Mountains (QM, humid region) and Loess Plateau (LP, drought region) have different species composition owing to contrasting soil water availability, but with common species occurring in two regions. We analyzed eight hydraulic traits [stomatal density (SD), vein density (VD), wood specific gravity (WSG_{branch}), lower leaf area: sapwood area (Al: As), stomatal length (SL), turgor loss point (Ψ_{Tlp}), maximum vessel diameter (Vd_{max}) and height (Height)] and five economic traits [leaf dry matter content (LDMC), leaf tissue density (TD), leaf dry mass per area (LMA), Leaf thickness (LT) and maximum net photosynthetic rate (P_{max})] of congeneric species (including common species and endemic species) in *Q. wutaishanica* forests of QM and LP. We explored whether the congeneric species have different economic and hydraulic traits across regions. And whether the relationship between hydraulic and economic traits was determined by soil water availability, and whether it was related to species distribution and congeneric endemic species composition of the same community. We found that LP species tended to have higher SD, VD, WSG_{branch}, Al: As, SL, Ψ_{Tlp} and Vd_{max} than QM species. There was a significant trade-off between hydraulic efficiency and safety across congeneric species. Also, the relationships between hydraulic and economic traits were closer in LP than in QM. These results suggested that relationships between hydraulic and economic traits, hydraulic efficiency and safety played the role in constraining species distribution across regions. Interestingly, some relationships between traits changed (from significant correlation to non-correlation) in common species across two regions (from LP to QM), but not in endemic species. The change of these seven pairs of relationships might be a reason for common species' wide occurrence in the two *Q. wutaishanica* forests with different soil water availability. In drought or humid conditions, congeneric species developed different types of adaptation mechanisms. The study helps to understand the environmental adaptive strategies of plant species, and the results improve our understanding of the role of both hydraulic and economic traits during community assembly.

Keywords: functional trait, congeneric species, trade-off, species distribution, temperate forest

INTRODUCTION

Water availability is an essential resource for plants survival, growth and distribution (Toledo et al., 2012; Poorter et al., 2017; Ramírez-Valiente and Cavender-Bares, 2017; Ali et al., 2018; Granato-Souza et al., 2018; Rodríguez-Ramírez et al., 2019). The long-term adaptation of plants to different water conditions will originate different water regulation strategies (Aguilar-Romero et al., 2017; Luo et al., 2017; Liu et al., 2021a) and functional traits (Rita et al., 2016). Different strategies of plants in response to the environment, such as water transport, mechanical support, and defense strategies, combine to determine the survival and distribution of plants (Bucci et al., 2012; Reich, 2014). Therefore, the relationships between functional traits and species distribution in multiple dimensions of traits should be studied (Laughlin, 2014; Liu et al., 2021c). Previous studies have focused on economic traits (Zheng and Shangguan, 2007a,b,c; Tanaka-Oda et al., 2010; Suter and Edwards, 2013; Chai et al., 2015; Zhang et al., 2017; Han et al., 2020; Ji et al., 2020), which reflect trade-offs between acquisition and investment of resources (Wright et al., 2004). Economic traits are related to CO_2 and water exchange and light capture, such as maximum net photosynthetic rate (P_{max}; Li et al., 2015). However, it is of great ecological significance to explore the water limitation in vegetative growth through hydraulic traits, which could reflect these resource allocation strategies as well (von Arx et al., 2012). Economic and hydraulic traits reveal different response levels of plants to environmental changes (Yin et al., 2018; Zhao et al., 2021). Hydraulic traits are related to water transport and loss, which affect plants' water transport efficiency and gas exchange and thus affect economic traits (i.e., the rate of photosynthesis; Liu et al., 2021b). Hydraulic traits play a key role in limiting species' growth, competition and distribution (Meinzer et al., 1999; Brodribb et al., 2005; Tomasella et al., 2008; Villagra et al., 2013; Cosme et al., 2017), which are more directly reflection of water availability.

Species may exhibit a combination of hydraulic traits under different soil water availability, which can be related to the ability to tolerate drought or wetness (von Arx et al., 2012). The combination of divergent species hydraulic traits suggests a trade-off between hydraulic efficiency and safety (Tyree et al., 1994; Cosme et al., 2017). Normally, the combination follows biophysical rules, that is, hydraulic efficiency (i.e., large and grouped vascular bundles) and hydraulic safety (i.e., narrow and isolated vascular bundles) cannot coexist (Litvak et al., 2012; Liu et al., 2020b). In low soil water availability, plants must take a conservative strategy to ensure hydraulic safety by investing in traits that can improve water-resistance, avoid cavitation, minimize the risk of embolism (i.e., to conduct water with narrow vessels; Zhao et al., 2021). By contrast, plants must invest in traits that confer high hydraulic efficiency in humid regions (i.e., to conduct water with wide vessels) to reduce the resistance of water flow and to increase conductivity (Cosme et al., 2017). A recent integrated analysis, however, has shown only weak support for the trade-off between hydraulic efficiency and safety (Gleason et al., 2016b; Schuldt et al., 2016; Zhu et al., 2017; Santiago et al., 2018), causing some controversy (Bittencourt et al., 2016; Brodersen, 2016; Gleason et al., 2016a). The combinations of hydraulic traits for species under different soil water availability remain unclear. Cosme et al. (2017) argued that there was hydraulic safety vs. efficiency trade-off in different water conditions, which affects species co-occurrence. The results were obtained in congeneric endemic species mostly restricted to plateaus (drought) or valleys (humid). However, Zhu et al. (2017) showed the opposite results: in two forests with different water conditions, the relationships of congeneric common species remained decoupled, which have high hydraulic efficiency and safety at the same time. Therefore, the relationships between hydraulic efficiency and safety should be tested closely. Both congeneric endemic species and common species should be considered.

Previous studies found that hydraulic traits and economic traits were decoupled (Li et al., 2015; Zhang et al., 2015; Liu et al., 2020a). The decoupled relationships brought greater freedom for more combinations of leaf traits to adapt to different environments (Li et al., 2015). But Yin et al. (2018) indicated hydraulic and economic traits may be coupled in semi-arid regions and the relationships depend on water availability. Similar results were also found in Li et al. (2018) and Males and Griffiths (2018). However, the physiological effects of the different relationships are unknown. In addition, Zhu et al. (2017) showed that common species can be found commonly in two regions owing to escaping hydraulic trade-off. Whether the relationships between hydraulic and economic traits would affect plant species distribution is still unclear. Exploring the relationships between hydraulic and economic traits under different water availability may help reveal how water availability shapes plant communities (Kraft et al., 2008).

Since the Middle Pleistocene, *Quercus wutaishanica* forest has become the dominant and stable community in specific areas of Qinling Mountains (QM, humid region) and Loess Plateau (LP, drought region; Zhu, 1982). *Quercus wutaishanica* forests in QM and LP have different species composition owing to different soil water availability (Yue, 1998; Zhao et al., 2021), but with some species that can be found commonly in two forests. There are congeneric endemic species with complementary distributions (For each genus, a species mostly restricted to LP and a species mostly restricted to QM) and congeneric common species distributed in two regions. It is necessary to explore the causes of the distribution patterns through economic and hydraulic traits.

In the present study, we investigated the relationships between hydraulic and economic traits of congeneric species (common and endemic species) in *Q. wutaishanica* forests which are disjunctively distributed in QM and LP. We aim to understand why species composition differs within the same community type, revealing the physiological and ecological mechanisms of species niche differentiation. We hypothesized that in soils with different water availability, (1) there was a trade-off between hydraulic safety and efficiency across congeneric species (common species and endemic species), which might affect species co-occurrence at the regional scale. (2) The relationships between hydraulic and economic traits were closer in drought region than in humid region, which might be a type of adaptation mechanism. (3) Common species might change the relationships between hydraulic and economic traits, which might provide an explanation for their common occurrence in the two *Q. wutaishanica* forests.

MATERIALS AND METHODS

Study Sites and Plant Materials

The present study was performed in natural *Q. wutaishanica* forests in Shaanxi province, northwest China. Based on our previous work, both Ziwuling region (35°41′–35°44′ N, 109°00′–109°02′ E) on the middle section of LP and Taibaishan Nature Reserve (33°84′–33°86′ N, 108°82′–108°87′ E) in the north slope of QM were selected as the sampling sites. The climate of *Q. wutaishanica* forests in LP is semiarid, temperate, continental monsoon, with a mean annual temperature of 9°C–11°C (Chai et al., 2014). The mean annual precipitation is approximately 560–650 mm. The soil type is cinnamon soil (Liang et al., 2010). The northern boundary of its distribution is determined by water (Meng et al., 2011; Yin et al., 2018). The climate of *Q. wutaishanica* forests in QM is temperate monsoon, with a mean annual temperature of 6.5°C, and its upper limit of distribution is determined by temperature (Zhu et al., 1982). The mean annual precipitation is approximately 900–1,000 mm, which is relatively humid. The soil type is brown soil (Zhu et al., 1982). There are also significant differences in soil water content under such different climatic conditions (**Supplementary Figure S1**; Zhao et al., 2021).

This research was surveyed in July 2019, three plots (50 × 50 m) were established in the *Q. wutaishanica* forests of LP (35°37′–35°49′N, 109°00′–109°11′E; at 1100–1112 m) and QM (33°84′–34°41′N, 107°45′–108°83′E; 1900–1958 m), and the geographic information is the same as our previous work (Table 1 in Zhao et al., 2021). The total number of common species in the two communities is less than 15% (Zhao and Yue, 1996; Yue, 1998). The species selected in this study are the most abundant species of *Q. wutaishanica* communities in the two regions. After sampling investigation, we sort out and selected 20 pairs of congeneric common species (20 species on LP and 20 species in QM) and 11 pairs of congeneric endemic species (11 species on LP and 11 species in QM), a total of 31 pairs of congeneric species (62 species in two regions; **Figure 1**) in six plots across two regions. Because of the interaction between environmental gradients and species, the interspecific differences in traits may offset or strengthen the effects of environmental gradients on traits. Therefore, it is necessary to exclude the influence of genetic background. The control of phylogenetic relatedness is included in the sampling design to exclude the influence of genetic background as much as possible (Fine et al., 2006; Baraloto et al., 2007). In particular, we selected 18 special congeneric species in six genera (*Crataegus*, *Cotoneaster*, *Quercus*, *Euonymus*, *Acer*, and *Lonicera*) from the total 62 species, that is, three species in each genus, including a common species in the two regions and two endemic species limited to LP or QM (**Figure 1**). We tested the first hypothesis by 18 special congeneric species to accurately exclude the influence of genetic background.

Within each plot, three to five healthy and mature individuals were randomly selected from each target species. Three to five sun-exposed branches with well-developed leaves were collected. The diameter of the base of the cut branches was 6–8 mm, and the length was 15–30 cm. After cutting, branches were immediately sealed in opaque plastic bags, humidified by moist paper towels and transported back to the laboratory for measurements of economic traits and physiological hydraulic traits. Three to five leaves and branches (5–7 cm) were immediately fixed in FAA70 (formaldehyde, acetic acid, and 70% ethanol) for analyses of hydraulic traits (stomatal, veinal traits and anatomical structures; **Table 1**).

Trait Selection

We measured 13 functional traits (eight hydraulic traits and five economic traits) of 62 species growing in *Q. wutaishanica* forests on LP and in QM (**Table 1**). Eight hydraulic traits include stomatal density [stomatal density (SD), vein density (VD), wood-specific gravity (WSG_{branch}), lower leaf area: sapwood area (Al: As), stomatal length (SL), turgor loss point (Ψ_{Tlp}), maximum vessel diameter (Vd_{max}) and height (Height)]. Five economic traits include [leaf dry matter content (LDMC), leaf tissue density (TD), leaf dry mass per area (LMA), Leaf thickness (LT) and maximum net photosynthetic rate (P_{max})].

Economic Traits

We scanned and measured surface areas of each fresh leaf with Motic Images Plus 6.0 software (Motic China group, Xiamen, China). The fresh mass was measured with electronic balance (one ten-thousandth). Thereafter, samples were oven-dried for 72 h at 70°C and weighed as leaf dry mass. Leaf mass per area (LMA, $g\,m^{-2}$) was calculated as the ratio of dry mass to leaf surface area (Yin et al., 2018). Leaf dry matter content (LDMC, $g\,g^{-1}$) was calculated as the ratio between leaf dry mass and fresh mass (Zhao et al., 2021). Leaf thickness (LT, μm) was measured through transverse sections using Image-Pro Plus 6.0, avoiding the influence of major veins. Ten to twenty measurements were made for each leaf. Leaf tissue density (TD, $g\,cm^{-3}$) was calculated as the ratio of LMA to LT (Yin et al., 2018). The photosynthetic rate was determined using the portable photosynthesis system (Li-6,800, Li-Cor, Lincoln, NE, United States) between 9:00 and 11:00 in the

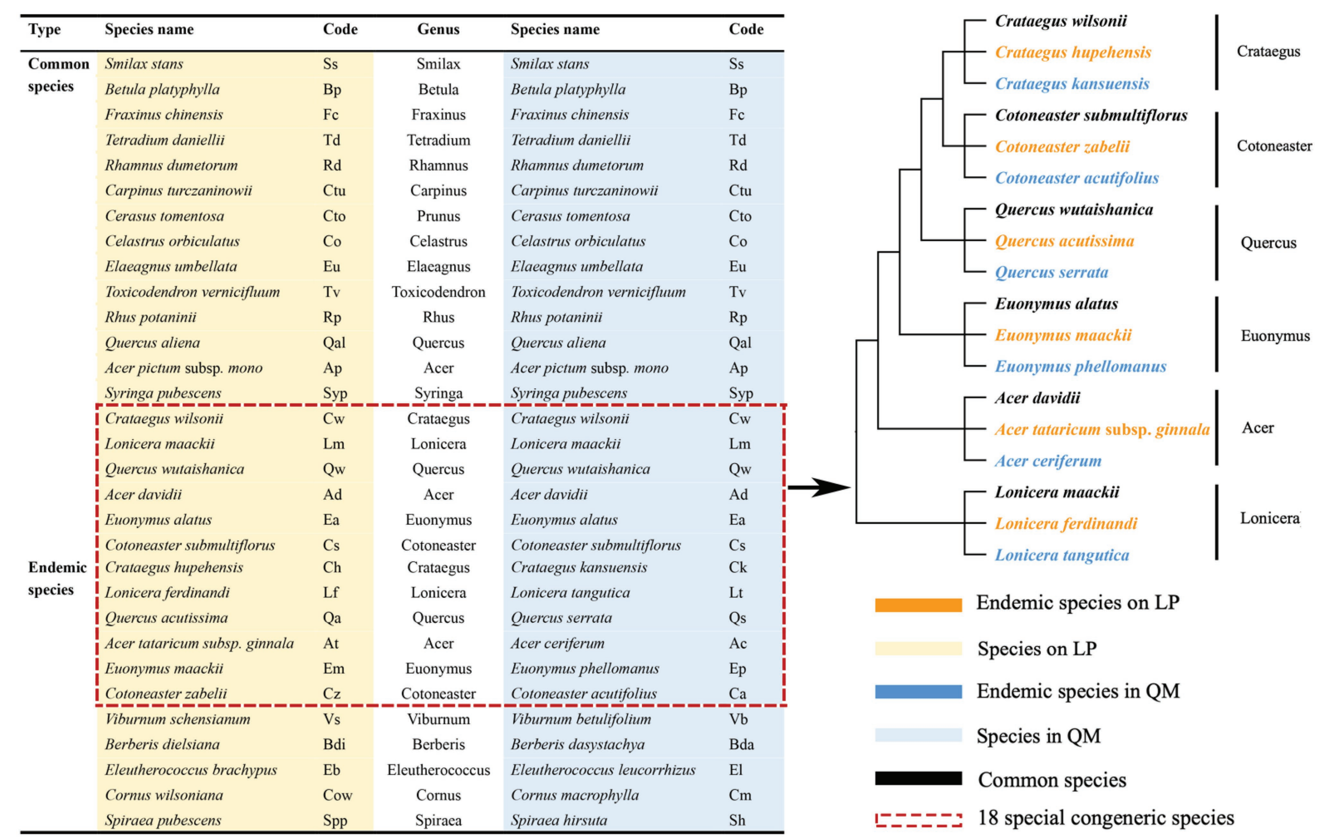

Type	Species name	Code	Genus	Species name	Code
Common species	*Smilax stans*	Ss	Smilax	*Smilax stans*	Ss
	Betula platyphylla	Bp	Betula	*Betula platyphylla*	Bp
	Fraxinus chinensis	Fc	Fraxinus	*Fraxinus chinensis*	Fc
	Tetradium daniellii	Td	Tetradium	*Tetradium daniellii*	Td
	Rhamnus dumetorum	Rd	Rhamnus	*Rhamnus dumetorum*	Rd
	Carpinus turczaninowii	Ctu	Carpinus	*Carpinus turczaninowii*	Ctu
	Cerasus tomentosa	Cto	Prunus	*Cerasus tomentosa*	Cto
	Celastrus orbiculatus	Co	Celastrus	*Celastrus orbiculatus*	Co
	Elaeagnus umbellata	Eu	Elaeagnus	*Elaeagnus umbellata*	Eu
	Toxicodendron vernicifluum	Tv	Toxicodendron	*Toxicodendron vernicifluum*	Tv
	Rhus potaninii	Rp	Rhus	*Rhus potaninii*	Rp
	Quercus aliena	Qal	Quercus	*Quercus aliena*	Qal
	Acer pictum subsp. *mono*	Ap	Acer	*Acer pictum* subsp. *mono*	Ap
	Syringa pubescens	Syp	Syringa	*Syringa pubescens*	Syp
	Crataegus wilsonii	Cw	Crataegus	*Crataegus wilsonii*	Cw
	Lonicera maackii	Lm	Lonicera	*Lonicera maackii*	Lm
	Quercus wutaishanica	Qw	Quercus	*Quercus wutaishanica*	Qw
	Acer davidii	Ad	Acer	*Acer davidii*	Ad
	Euonymus alatus	Ea	Euonymus	*Euonymus alatus*	Ea
	Cotoneaster submultiflorus	Cs	Cotoneaster	*Cotoneaster submultiflorus*	Cs
Endemic species	*Crataegus hupehensis*	Ch	Crataegus	*Crataegus kansuensis*	Ck
	Lonicera ferdinandi	Lf	Lonicera	*Lonicera tangutica*	Lt
	Quercus acutissima	Qa	Quercus	*Quercus serrata*	Qs
	Acer tataricum subsp. ginnala	At	Acer	*Acer ceriferum*	Ac
	Euonymus maackii	Em	Euonymus	*Euonymus phellomanus*	Ep
	Cotoneaster zabelii	Cz	Cotoneaster	*Cotoneaster acutifolius*	Ca
	Viburnum schensianum	Vs	Viburnum	*Viburnum betulifolium*	Vb
	Berberis dielsiana	Bdi	Berberis	*Berberis dasystachya*	Bda
	Eleutherococcus brachypus	Eb	Eleutherococcus	*Eleutherococcus leucorrhizus*	El
	Cornus wilsoniana	Cow	Cornus	*Cornus macrophylla*	Cm
	Spiraea pubescens	Spp	Spiraea	*Spiraea hirsuta*	Sh

FIGURE 1 | List of 31 pairs of congeneric species (including 20 pairs of congeneric common species and 11 pairs of congeneric endemic species) in *Quercus wutaishanica* forests across two regions and evolutionary relationship for 18 special congeneric species in six genera selected for this study.

TABLE 1 | List of 13 functional traits measured at the branch, leaf, and whole-plant level for this study with corresponding abbreviations and units.

	Plant traits	Abbreviation	Unit	Organ
Hydraulic traits	Height	Height	m	Whole plant
	Wood specific gravity	WSG_{branch}	$g·cm^{-3}$	Branch
	Leaf area: sapwood area	Al:As		Branch
	Maximum vessel diameter	Vd_{max}	μm	
	Turgor loss point	Ψ_{tlp}	MPa	Leaf
	Vein density	VD	$mm·mm^{-2}$	Leaf
	Stomatal density	SD	mm^{-2}	Leaf
	Stomatal length	SL	μm	Leaf
Economic traits	Maximum net photosynthetic rate	P_{max}	$mmol·m^{-2}·s^{-1}$	Leaf
	Leaf dry matter content	LDMC	$g·g^{-1}$	Leaf
	Leaf dry mass per area	LMA	$g·m^{-2}$	Leaf
	Leaf thickness	LT	μm	Leaf
	Leaf tissue density	TD	$g\ cm^{-3}$	Leaf

field. The temperature was controlled at 20°C–25°C in ambient CO_2, and the airflow rate was set at 500 μmol s^{-1}. The photosynthetically active radiation (PAR) gradients were 1800, 1,500, 1,200, 1,000, 800, 600, 400, 200 and 0 μmol m^{-2} s^{-1}. Maximum net photosynthetic rate (P_{max}, μmol m^{-2} s^{-1}) was obtained by fitting the empirical equation of the least square method adopted by Bassman and Zwier (1991).

Hydraulic Traits

For vein density assessments, 2 cm^2 of leaf area were sampled in the central region, immersed in 10% NaOH in an oven at 65°C for 4–12 h. Samples were repeatedly washed with deionized water for about 30 min, immersed and bleached in 10% H_2O_2 for 10–30 min and then, washed again in deionized water. Sections were next stained with safranin for 30 min. The sections were then dehydrated using graded ethanol series and immersed in xylene/ethanol absolute (1:1) solution and xylene. Stained sections were mounted, photographed and then, analyzed using Image-Pro Plus 6.0 (Media Cybernetics, United States). The total length of veins per unit area was measured as vein density (VD, mm mm^{-2}; Zhao et al., 2021).

Leaf stomatal density (SD, mm^{-2}) and stomatal length (SL, μm) were measured on three leaves for one by the nail-polish imprint method (Zhao et al., 2016; Yin et al., 2018). Stomatal prints were observed and photographed under a Classica SK200 digital light microscope (at ×10 magnification; Motic ChinaGroup Co., Ltd., China). More than 20 fields randomly were selected per leaf and a photograph of 200 × 200 μm in the area was selected for analyses using Image-Pro Plus 6.0. The density of stomata (SD, mm^{-2}) was calculated by counting all stomata for each specified area ($200 \times 200\,\mu m$) and dividing this number by the area. We measured the length of the guard cells as stomatal length (SL, μm).

We used the paraffin method to get a transverse section of the petiole vessel (Zhao et al., 2021). The paraffin sections were observed and photographed under a light microscope at ×40 magnification equipped with a digital camera. Using Image-Pro Plus 6.0, we assessed the diameter of petiole conduits as described by Schulte (1999) to get the maximum vessel diameter (Vd_{max}, μm).

Leaf water potential (Ψ_{leaf}, MPa) was measured using a 3,115 portable plant water potential pressure chamber (SEC., Ltd., United States) in consecutive sunny days of mid-July 2019. Leaf samples from three individuals of each species were collected and immediately sealed in opaque plastic bags, humidified by moist paper towels, and transported back to the laboratory. First, leaves were weighed to obtain the initial fresh mass and then placed in a pressure chamber to determine the initial water potential. We measured leaf mass and water potential periodically during slow desiccation of the sample in the natural condition. Samples were oven-dried for 72 h at 70°C and weighed as leaf dry mass. Finally, pressure–volume curves were elaborated according to Tyree and Hammel (1972) to calculate the leaf turgor loss point (Ψ_{Tlp}, MPa).

For one individual, 5 cm long branches were cut from the base of the annual branches on the upper part of the species under good light conditions. Then, we removed the bark and determined the wood density (WSG_{branch}; Zhao et al., 2021). We used the drainage method to get the volume of the branches, and the dry mass was obtained by weighing scales with an accuracy of 0.0001 g after oven-drying at 70°C for 72 h. The WSG_{branch} is the dry mass of the annual branch divided by the volume of the branch (Zhao et al., 2021). We measured the diameter of the branches by digital calipers (HITEC MESSTECHNIK., Ltd., Germany). Heartwood and pulp were subtracted, and the sapwood area (As) of the branches was obtained. Then, all the leaves on the branches were collected to calculate the total leaf area (Al) and the ratio of total leaf area to sapwood area (Al: As). We estimated the total height of all trees by laser rangefinder. The mean height per species was the average of the five individuals sampled for that species.

Data Analysis

We used paired *t*-tests (SPSS, Chicago, IL, United States) to evaluate whether 18 special congeneric species (common species and endemic species) in six genera have divergent hydraulic and economic traits. Relationships between economic and hydraulic traits were analyzed with Pearson's correlation (SPSS, Chicago, IL, United States). Linear regression analyses were used to examine the correlations of traits (SigmaPlot, SPSS Inc., Chicago, IL, United States). Standardized major axis (SMA) estimation (R 3.2.2 statistical platform) was used to determine whether the correlations between economic and hydraulic traits changed with environmental water availability. Multivariate associations of leaf traits were analyzed with a principal component analysis (PCA) in CANOCO software for Windows 4.5 (Microcomputer Power, Ithaca, NY, United States).

RESULTS

Congeneric Species Differ in Hydraulic Traits Across Regions

The results showed significant differences in hydraulic traits among 18 special congeneric species in six genera under different soil water availability. Within each genus, common species on LP had lower values of A_l: A_s, SL (except for *Crataegus wilsonii*), Vd_{max}, and more negative Ψ_{Tlp} values, but higher values of SD, VD and WSG_{branch} values than in QM (**Figure 2**). For example, the common species of *Quercus* is *Q. wutaishanica*. The SD of *Q. wutaishanica* on LP was higher than that in QM (**Figure 2B**). There was non-significant difference for Height (**Figure 2E**). For economic traits, LDMC, LMA, LT, and TD of common species did not differ significantly across regions, except that P_{max} showed significant differences (higher in QM than on LP; **Figure 3**).

In each of six genera, the congeneric endemic species had similar results with the common species. Except for Height, the other seven hydraulic traits differ significantly across regions (**Figure 2**). Compared with species in QM, species on LP tended to have lower values of A_l: A_s, SL, Vd_{max} and more negative Ψ_{Tlp} values. SD, VD and WSG_{branch} values were higher in QM than on LP. For example, the endemic species of *Quercus* are *Q. acutissima* on LP and *Q. serrata* in QM. The SD of *Q. acutissima* was higher than that of *Q. serrata*. Similarly, most of the five economic traits (LDMC, LMA, LT (except for *Acer* spp.) and TD) showed no significant differences between the two regions, except that the differences of P_{max} were significant (higher in QM than on LP; **Figure 3**).

Relationships Between Hydraulic and Economic Traits Differ Across Two Regions

The PCA of 20 common species on LP showed that economic traits could be divided into three groups and were coupled with some hydraulic traits, respectively. P_{max} and TD, coupled with Vd_{max}; LDMC and LT, coupled with WSG_{branch} and A_l: A_s; LMA, coupled with VD, SD, height, and Ψ_{Tlp}. But these were less obvious for 20 common species in QM (**Figure 4A**). We found similar results in total 31 pairs of species and 11 pairs of endemic species (**Figures 4B,C**), that is, the relationships between hydraulic and economic traits were closer on LP than in QM.

Relationships Between Hydraulic and Economic Traits Changed in Common Species

According to linear regression and SMA analysis, most relationships between hydraulic and economic traits differed between LP and QM, which were closer on LP than in QM for 20 pairs of congeneric common species, 11 pairs of congeneric endemic species and total 31 pairs of congeneric

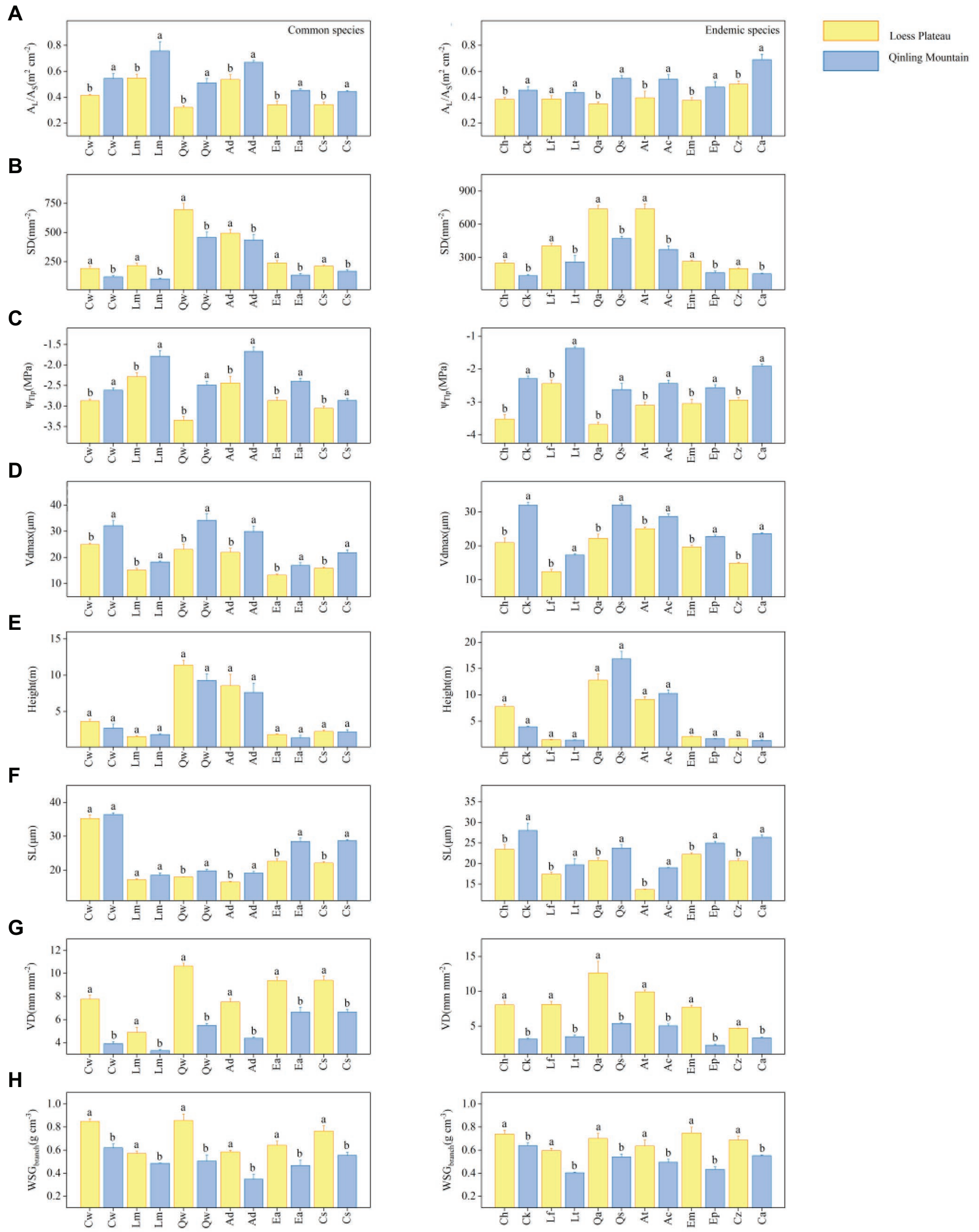

FIGURE 2 | Eight hydraulic traits: **(A)** leaf area: sapwood area (A_l: A_s), **(B)** Stomatal density (SD), **(C)** Turgor loss point (Ψ_{Tlp}), **(D)** Maximum vessel diameter (Vd_{max}), **(E)** Height (height), **(F)** Stomatal length (SL), **(G)** Vein density (VD), and **(H)** Wood specific gravity (WSG_{branch}) for 18 special congeneric pairs of species (common species and endemic species in six genera) in Loess plateau (LP; low soil water availability) and Qinling Mountain (high soil water availability). The species abbreviations are shown in **Figure 1**. Error bars represent 1 SE, and different letters indicate significant differences between regions ($p < 0.05$).

species (**Figure 5**; **Supplementary Figures S2–S6**). There was a negative relationship between VD and LMA in common species across regions. LMA decreased with increasing VD, and LMA decreased more on LP than in QM. In addition, some relationships were only found on LP, but not in QM. For instance, the relationships between LDMC and VD were positive on LP, but no relationships were found in QM (**Figure 5**).

Interestingly, by sorting out the results of linear regression and SMA analysis of all the relationships (**Figure 5**; **Supplementary Figures S2–S6**) we found some relationships between hydraulic and economic traits changed (from significant correlation to non-correlation) in common species across regions (from LP to QM), but not in endemic species. For example, Al: As, VD and LDMC; VD and TD; WSG_{branch} and LMA; SD, Ψ_{Tlp}, VD, and P_{max} (**Table 2**).

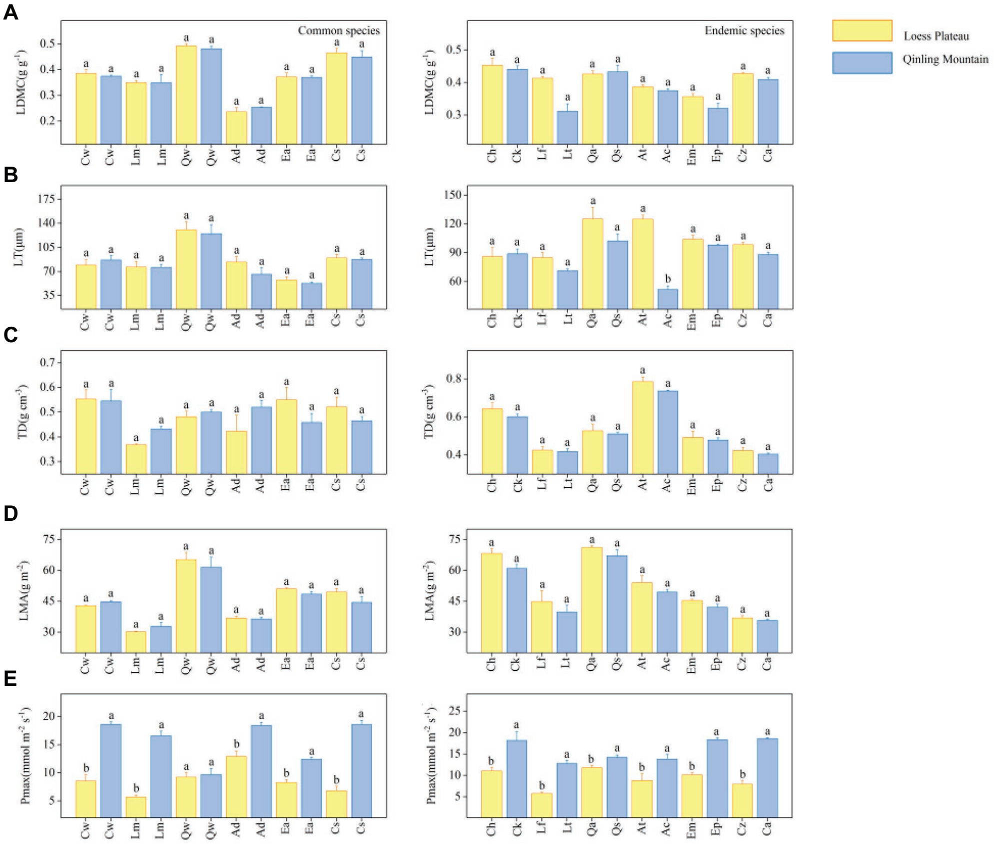

FIGURE 3 | Five economic traits: **(A)** Leaf dry matter content (LDMC), **(B)** Leaf thickness (LT), **(C)** Leaf tissue density (TD), **(D)** Leaf mass per area (LMA), and **(E)** Maximum net photosynthetic rate (P_{max}) for 18 special congeneric pairs of species (common species and endemic species in six genera) in Loess plateau (low soil water availability) and Qinling Mountain (high soil water availability). The species abbreviations are shown in **Figure 1**. Error bars represent 1 SE, and different letters indicate significant differences between regions ($p < 0.05$).

DISCUSSION

The Trade-Off Between Hydraulic Efficiency and Safety in Congeneric Species

Here, we focused on 18 special congeneric species (common species and endemic species) in six genera in *Q. wutaishanica* forests within different soil water availabilities (LP and QM), considering the control of species genetic background. We found significant differences in most hydraulic traits. Across congeneric species, the different combination of hydraulic traits values within each environmental condition showed a significant trade-off between hydraulic efficiency and safety. The result was consistent with our hypothesis that safety vs. efficiency trade-off might affect species co-occurrence at the regional scale. Compared with species in QM, congeneric species on LP tend to adopt conservative water-use strategies and invest in hydraulic traits associated with water transport safety, which indicated a better adaptation to drought environment (Zhao et al., 2021). Both endemic species and common species on LP had higher values of SD, VD, and WSG_{branch}, lower Vd_{max}, SL, A_l: A_s, and more negative Ψ_{Tlp} values, indicating that species on LP invest in higher hydraulic safety at the expense of efficiency, whereas congeneric species in QM had contrasting trait values, suggesting more investment in water transport efficiency. The similar results of endemic species and common species in the same genera fully indicated that differences in hydraulic traits were caused by soil water availability.

Highly embolism resistance is an important feature for species to adapt to low soil water availability (Barigah et al., 2013; Pfautsch et al., 2016; Zhu et al., 2017). Low values of Al: As are associated with hydraulic safety. Because low leaf areas reduce transpiration and ensure water supply, and narrow xylem vessels reduce embolism risk by increasing sapwood area (Togashi et al., 2015; Anderegg and Hillerislambers, 2016; Sande et al., 2019). Also, high values of WSG_{branch} mean thick conduit walls or a great proportion of mechanical tissue, which increase the implosion-resistance (Hacke et al., 2001; Lens et al., 2011; Markesteijn et al., 2011). In low soil water availability, species are favorable to regulate the two traits (WSG_{branch} and A_l: A_s) at the branch level to improve the water-resistance (Pratt et al., 2007; Fortunel et al., 2014) and increase hydraulic safety (Cosme et al., 2017). At the leaf level, species can

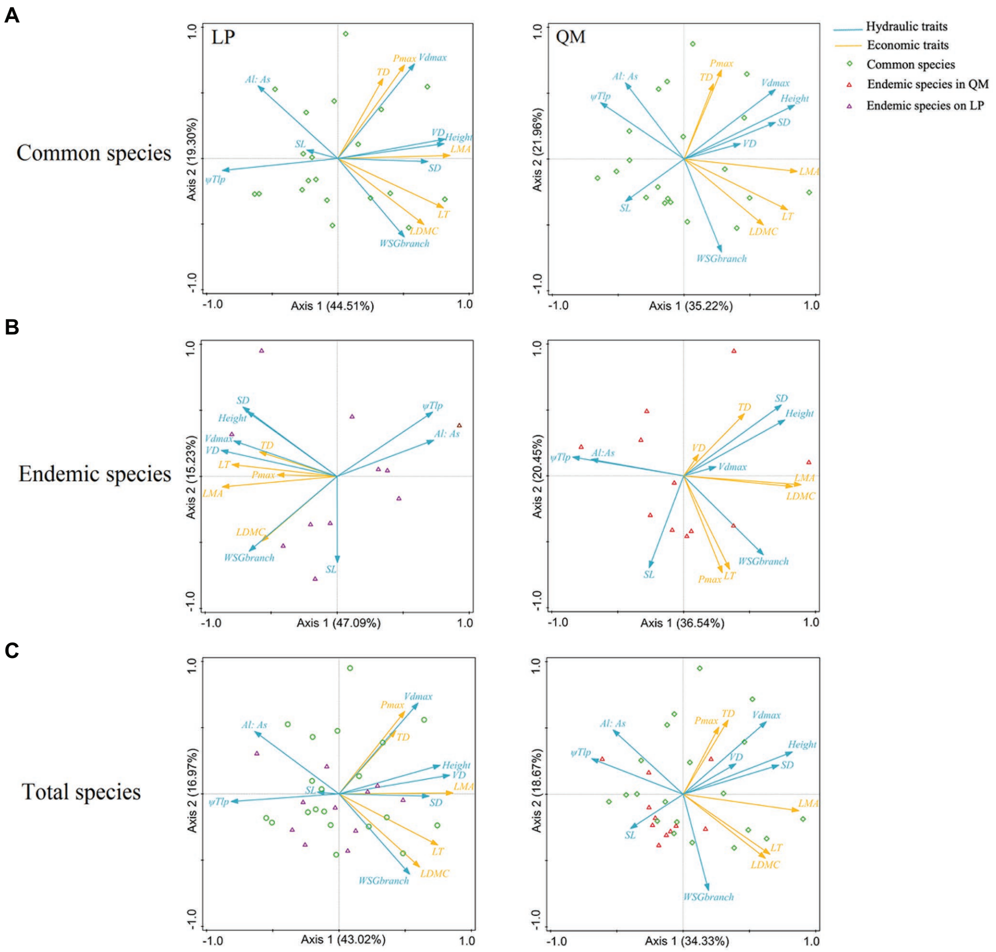

FIGURE 4 | Principal component analysis (PCA) between hydraulic and economic traits on cross-species means among congeneric species **(A)** (20 pairs of congeneric common species, **(B)** 11 pairs of congeneric endemic species and **(C)** 31 pairs of congeneric species). Values in parentheses in the axis labels are percentages explained by the first two components. Eight hydraulic traits were included: SD, stomatal density; SL, stomatal guard cell length; Vd_{max}, maximum vessel diameter; Height; Al:As, leaf area: sapwood area ratio in the branch; VD, vein density; WSG_{branch}, wood specific gravity of branch; Ψ_{Tlp}, turgor loss point. Five economic traits were included: LMA, leaf dry mass per area; LT, leaf thickness; TD, leaf tissue density; LDMC, leaf dry matter content; and P_{max}, maximum net photosynthesis rate.

minimize embolism risk by reducing diameters of the maximum vessels in leaf petioles. In low soil water availability, species with narrow vessels appear to be at low risk of air seeding into the water column to ensure water transport safety (Zhao et al., 2021). Increasing leaf vein density is also an effective adaptation to cope with drought (Xiong et al., 2017). The high values of VD increase the paths of water transportation to ensure hydraulic safety (Sack and Scoffoni, 2013). Besides, small and dense stomata (high values of SD and low values of SL) can be more flexible to deal with drought, i.e., close stomata to reduce water loss in time (Franks et al., 2009). Ψ_{Tlp} is also a key factor to determine the tolerance of leaves to drought stress (Bartlett et al., 2012; Maréchaux et al., 2015). It can be used as a proxy of leaf hydraulic vulnerability (Meinzer et al., 2016, 2017; Zhu et al., 2018). Compared with species in QM, species on LP with more negative Ψ_{Tlp} values can maintain positive turgor pressure, certain stomatal conductance, hydraulic conductivity, and photosynthetic gas exchange in low soil water availability (Brodribb and Holbrook, 2003). Therefore, species on LP were more drought resistant. In previous studies, adjustments in Ψ_{Tlp} have also been observed in different water availability (Mitchell and O'Grady, 2015; Farrell et al., 2017; Johnson et al., 2018). There was no significant difference in Height. One possible reason is that species in QM suffer from disturbances caused by winds, heavy rains and animals (Hu et al., 2014; Zhang et al., 2019), which might limit tree growth.

Our results indicated that within-genus variation in hydraulic traits was caused by soil water availability. Different combinations of hydraulic traits for congeneric species (including common species and endemic species) across two regions with different soil water availability supported the trade-off between hydraulic efficiency and safety, which might affect species co-occurrence at the regional scale. The results were different from Zhu et al. (2017), who found that hydraulic efficiency and safety were decoupled in common species. Zhu et al. (2017) mainly discussed

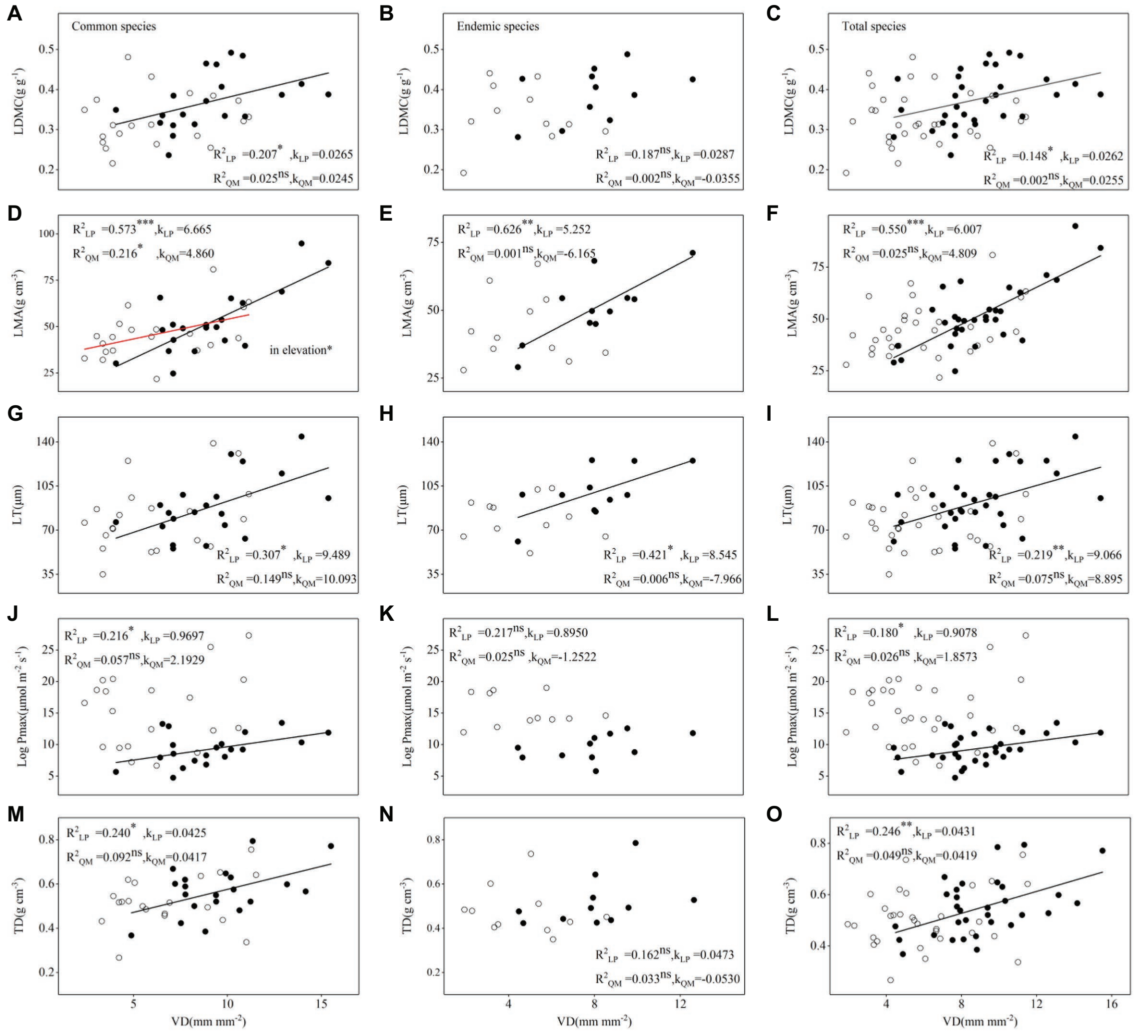

FIGURE 5 | Relationships between VD and **(A-C)** LDMC, **(D-F)** LMA, **(G-I)** LT, **(J-L)** P_{max}, **(M-O)** TD of congeneric species (20 pairs of congeneric common species, 11 pairs of congeneric endemic species and 31 pairs of congeneric species) in Loess plateau (low soil water availability; closed circles) and Qinling Mountain (high soil water availability; open circles). Linear regressions were fitted to the data (black regression lines, LP; red regression lines, QM). Values of R^2 are followed by significance level (*, $p < 0.05$; **, $p < 0.01$; ***, and $p < 0.001$). Values of *K* represent slopes of lines.

TABLE 2 | According to **Figure 5, Supplementary Figures S1–S5**, list the relationships between hydraulic and economic traits of 20 pairs of congeneric common species and 11 pairs of congeneric endemic species, which changed with soil water availability [O, significant correlation ($p < 0.05$); \, no correlation ($p > 0.05$)].

Hydraulic-economic	Common species		Endemic species	
	LP	QM	LP	QM
Al: As-LDMC	O	\	\	\
SD-P_{max}	O	\	\	\
Ψ_{Tlp}-P_{max}	O	\	\	\
VD-LDMC	O	\	\	\
VD-P_{max}	O	\	\	\
VD-TD	O	\	\	\
WSG_{branch}-LMA	O	\	\	\

that distinctive dimorphic xylem vessels (extremely large vessels and many small vessels) may assure both hydraulic efficiency and safety, which are the reasons of decoupled relationships between hydraulic efficiency and safety in common species. The extremely large vessels allow for high hydraulic efficiency, while the many small vessels allow for high hydraulic safety (Rosell and Olson, 2014). However, many other hydraulic traits can confer hydraulic efficiency or safety in addition to xylem vessels, such as vein density (Sack and Holbrook, 2006; Brodribb et al., 2007). It is obviously not convincing to only considering xylem vessels. No significant differences were found in most economic traits. Our results suggested that hydraulic traits are important in determining the mechanisms of species' response to drought and may be important for predictions of future species distribution (Anderegg et al., 2012).

Relationships Were Closer in Drought Region (LP) Than in Humid Region (QM)

Relationships between economic and hydraulic traits were coupled in two regions but were closer couple on LP than in QM. The results were different from previous studies (Li et al., 2015; Zhang et al., 2015; Liu et al., 2020), which showed that hydraulic traits and economic traits were decoupled. The closely relationships of species on LP indicated the principle of optimization in water transportation and CO_2 assimilation (Wright et al., 2004) and the adaptation mechanism in low water availability (Yin et al., 2018).

We found three groups (TD and P_{max}; LT and LDMC; LMA) that were, respectively, coupled to several hydraulic traits on LP, but were not obvious in QM. TD has an important influence on the structure and function of leaves (Kitajima and Poorter, 2010). Under low soil water availability, high values of TD can reduce water loss and increase photosynthetic capacity (Mediavilla et al., 2001; Niinemets, 2001; Elizabeth et al., 2014). Therefore, TD and P_{max} are closely related and coupled with Vd_{max}. The diameters of vessels affect water transport capacity (Zhu et al., 2017). According to Hagen–Poiseuille's law, hydraulic conductance efficiency is proportional to the sum of the vessel diameters to the fourth power (Zimmermann, 1983). High values of LDMC and LT indicated that species have high resource utilization and strong resistance to external water stress and retain water (Garnier et al., 2001). LDMC and LT were coupled with WSG_{branch} and A_l: A_s, which indicated that drought-resistant plants improve their hydraulic safety (WSG_{branch} and Al: As, as the discussion in the first part) at the cost of increasing the carbon investment in leaf tissue construction (LDMC and LT; Simonin et al., 2012). LMA is an important leaf carbon economic trait and the core of complex and diversified relational network among leaf economics spectrum (Osnas et al., 2013). On one hand, high values of LMA represent strong wilting resistance and competitiveness against water stress (Baltzer et al., 2008; Rose and Hertel, 2013). VD, Ψ_{Tlp}, and stomatal characteristics (such as SD, SL) are also important indexes to measure drought resistance (Martínez-Vilalta et al., 2014). Thus, the coupled relationships between LMA and VD, Ψ_{Tlp}, SD, SL confer the extremely strong resistance against hydraulic failure (Blonder et al., 2011; Kardiman and Ræbild, 2017). On the other hand, leaf structural trait (LMA) and leaf hydraulic traits (VD, Ψ TLP, SD, SL) were coupled, indicating that there is a trade-off between the carbon investment allocated to the leaf water transport system and the carbon investment allocated to the construction of leaf structure (Villagra et al., 2013).

Water transport and CO_2 diffusion are the key processes that determine the assimilation efficiency of terrestrial plants (Flexas et al., 2013). As many studies showed that for plants species the greatest biophysical barrier to survival is the ability to maintain high carbon gain while avoiding desiccation (Nardini and Luglio, 2014). Through the close relationships, species on LP tended to improve photosynthetic carbon assimilation efficiency and the resistance to low soil water availability, then form corresponding morphological structures and strategies (Zhao et al., 2021). Similar results were also found in woody angiosperms on the LP (Yin et al., 2018). By comparison, species in QM with high soil water availability tend to form more flexible combinations in adaption to the environment. Like the relationships between hydraulic efficiency and safety, the results suggested that relationships between hydraulic and economic traits also played a role in constraining species distribution across regions.

Common Species Changed Relationships Within Different Soil Water Availability

Species distribution is greatly related to water conditions (Cosme et al., 2017). Changes in soil water availability can lead to changes in species composition of communities, which are determined through the process of species migration and substitution (Parmesan and Yohe, 2003; Zhao et al., 2021). Zhu et al. (2017) reported that the reason for common species occurrence in two forests with contrasting soil water conditions was that they could escape the hydraulic trade-off. In our study, there was hydraulic trade-off in common species. Therefore, the causes for common species' wide occurrence in two forests need further research.

The hydraulic safety and efficiency, water transportation and CO_2 assimilation trade-offs affect species co-occurrence at the region scale. Species on LP had strong drought-resistant ability and maximize their survival at the expense of hydraulic efficiency and CO_2 assimilation efficiency. Through sorting out all the relationships between hydraulic and economic traits, we found that seven pairs of relationships (Al: As, VD and LDMC; VD and TD; WSG_{branch} and LMA; SD, Ψ_{Tlp}, VD, and P_{max}) changed (from significant correlation to non-correlation) in common species across regions (from LP to QM), but not in endemic species. The changes in relationships might be a reason for common species' wide occurrence in the two *Q. wutaishanica* forests with different water availability and for endemic species only distinctly occurring in either LP or QM.

Common species can be found in two regions, which indicates a stronger ecological adaptability to different water availability than endemic species. We found that common species were sensitive to water availability and capable of changing the hydraulic and economic traits trade-offs in time. On LP with low soil water availability, the significant correlations make common species to adapt to the environment by "increasing resources and reducing expenditure" (Wright et al., 2004; Yin et al., 2018). Whereas in QM with high water availability, non-correlation indicated that common species adapt to the environment by flexible combinations. Endemic species were similar in morphology but were different in ecological and adaptive strategies to occupy the most suitable region in *Q. wutaishanica* forests within different water conditions. On LP with low soil water availability, the development of community is sensitive to water (Xu et al., 2016; Yin et al., 2018). Long-term adaptations to drought allow drought-tolerant species to survive. On the other hand, water stress may also limit species migration and thus accelerate the process of the formation of LP regional endemic species (Parmesan and Yohe, 2003). By contrast, QM with abundant water inhibited the dominance of drought-tolerant species to some extent but met water demand of acquired species and improved their competitiveness to inhibit the development of other species in the community. Thus, endemic species on LP are unable to establish. Therefore, endemic species can only be distributed in a certain region without the change of the relationships between traits.

CONCLUSION

This study showed significant differences in hydraulic traits and not in most economic traits of congeneric species across two regions. The different hydraulic traits combinations indicated the trade-off between hydraulic safety and efficiency. We also found the trade-off between hydraulic and economic traits, which were more closely on LP than in QM. The two trade-offs affect species co-occurrence at the regional scale. Seven pairs of relationships changed in common species across regions, but not in endemic species, which may be the reason for differences in the species composition of the same community type. The changes in common species might explain their distributions across regions, but endemic species can only be distributed in a certain region because they lack variation. The results are helpful to understand distributions and adaptive strategies of species, as well as the importance of both hydraulic and economic traits during community assembly.

DATA AVAILABILITY STATEMENT

The original contributions presented in the study are included in the article/**Supplementary Material**, further inquiries can be directed to the corresponding author.

AUTHOR CONTRIBUTIONS

YZ and MY conceived and designed the experiments and wrote the manuscript. YZ, JZ, JX, YC, PL, JQ, XW, and CL performed the experiments. YZ and JZ analyzed the data. All authors contributed to the article and approved the submitted version.

FUNDING

This study was financially supported by the National Science Foundation of China (41871036), the Shaanxi Science and Technology Program (2020JQ-580), China Postdoctoral Science Foundation (2018M643717).

SUPPLEMENTARY MATERIAL

The Supplementary Material for this article can be found online at: https://www.frontiersin.org/articles/10.3389/fpls.2022.902509/full#supplementary-material

Supplementary Figure S1 | Barplot comparing soil water content (SWC) among per plot between LP and QM. Error bars represent 1 SE, and different letters indicate significant differences between regions ($p < 0.05$).

Supplementary Figure S2 | Relationships between Al: As and LDMC, LMA, LT of congeneric species (20 pairs of congeneric common species, 11 pairs of congeneric endemic species and 31 pairs of congeneric species) in Loess plateau (LP; low soil water availability; closed circles) and Qinling Mountain (QM; high soil water availability; open circles). Linear regressions were fitted to the data (black regression lines, LP; red regression lines, QM). Values of R2 are followed by significance level (*, $p < 0.05$; **, $p < 0.01$; and ***, $p < 0.001$). Values of K represent slopes of lines.

Supplementary Figure S3 | Relationships between SD and LMA, LT, Pmax.

Supplementary Figure S4 | Relationships between ΨTlp and LDMC, LMA, LT, Pmax.

Supplementary Figure S5 | Relationships between Vdmax and LMA, TD.

Supplementary Figure S6 | Relationships between WSGbranch and LDMC, LMA, LT.

REFERENCES

Aguilar-Romero, R., Pineda-Garcia, F., Paz, H., González-Rodríguez, A., and Oyama, K. (2017). Differentiation in the water-use strategies among oak species from Central Mexico. *Tree Physiol.* 37, 915–925. doi: 10.1093/treephys/tpx033

Ali, A., Lin, S. L., He, J. K., Kong, F. M., Yu, J. H., and Jiang, H. S. (2018). Climatic water availability is the main limiting factor of biotic attributes across large-scale elevational gradients in tropical forests. *Sci. Total Environ.* 647, 1211–1221. doi: 10.1016/j.scitotenv.2018.08.072

Anderegg, W. R. L., Berry, J. A., Smith, D. D., Sperry, J. S., Anderegg, L. D. L., and Field, C. B. (2012). The roles of hydraulic and carbon stress in a widespread climate-induced forest die-off. *Proc. Natl. Acad. Sci.* 109, 233–237. doi: 10.1073/pnas.1107891109

Anderegg, L. D. L., and Hillerislambers, J. (2016). Drought stress limits the geographic ranges of two tree species via different physiological mechanisms. *Glob. Chang. Biol.* 22, 1029–1045. doi: 10.1111/gcb.13148

Anderegg, W. R. L., Klein, T., Bartlett, M., Sack, L., Pellegrini, A. F. A., Choat, B., et al. (2016). Meta-analysis reveals that hydraulic traits explain cross-species patterns of drought-induced tree mortality across the globe. *Proc. Natl. Acad. Sci. U. S. A.* 113, 5024–5029. doi: 10.1073/pnas.1525678113

Baltzer, J. L., Davies, S. J., Bunyavejchewin, S., and Noor, N. S. M. (2008). The role of desiccation tolerance in determining tree species distributions along the Malay-Thai peninsula. *Funct. Ecol.* 22, 221–231. doi: 10.1111/j.1365-2435.2007.01374.x

Balvanera, P., Quijas, S., and Pérez-Jiménez, A. (2011). Distribution patterns of tropical dry forest trees along a mesoscale water availability gradient. *Biotropica* 43, 414–422. doi: 10.1111/j.1744-7429.2010.00712.x

Baraloto, C., Morneau, F., Bonal, D., Blanc, L., and Ferry, B. (2007). Seasonal water stress tolerance and habitat associations within four Neotropical tree genera. *Ecology* 88, 478–489. doi: 10.1890/0012-9658(2007)88[478:SWSTAH]2.0.CO;2

Barigah, T. S., Charrier, O., Douris, M., Bonhomme, M., Herbette, S., Ameglio, T., et al. (2013). Water stress-induced xylem hydraulic failure is a causal factor of tree mortality in beech and poplar. *Ann. Bot.* 112, 1431–1437. doi: 10.1093/aob/mct204

Bartlett, M. K., Scoffoni, C., and Sack, L. (2012). The determinants of leaf turgor loss point and prediction of drought tolerance of species and biomes: a global meta-analysis. *Ecol. Lett.* 15, 393–405. doi: 10.1111/j.1461-0248.2012.01751.x

Bassman, J. H., and Zwier, J. C. (1991). Gas exchange characteristics of *Populus trichocarpa*, *Populus deltoides* and *Populus trichocarpa* x *P. deltoides* clones. *Tree Physiol.* 8, 145–159. doi: 10.1093/treephys/8.2.145

Bittencourt, P. R. L., Pereira, L., and Oliveira, R. S. (2016). On xylem hydraulic efficiencies, wood space-use and the safety-efficiency tradeoff. *New Phytol.* 211, 1152–1155. doi: 10.1111/nph.14044

Blonder, B., Violle, C., Bentley, L. P., and Enquist, B. J. (2011). Venation networks and the origin of the leaf economics spectrum. *Ecol. Lett.* 14, 91–100. doi: 10.1111/j.1461-0248.2010.01554.x

Brodersen, C. R. (2016). Finding support for theoretical tradeoffs in xylem structure and function. *New Phytol.* 209, 8–10. doi: 10.1111/nph.13763

Brodribb, T. J., Feild, T. S., and Jordan, G. J. (2007). Leaf maximum photosynthetic rate and venation are linked by hydraulics. *Plant Physiol.* 144, 1890–1898. doi: 10.1104/pp.107.101352

Brodribb, T. J., and Holbrook, N. M. (2003). Stomatal closure during leaf dehydration, correlation with other leaf physiological traits. *Plant Physiol.* 132, 2166–2173. doi: 10.1104/pp.103.023879

Brodribb, T. J., Holbrook, N. M., Zwieniecki, M. A., and Palma, B. (2005). Leaf hydraulic capacity in ferns, conifers and angiosperms: impacts on photosynthetic maxima. *New Phytol.* 165, 839–846. doi: 10.1111/j.1469-8137.2004.01259.x

Bucci, S. J., Scholz, F. G., Campanello, P. I., Montti, L., Jimenez-Castillo, M., Rockwell, F. A., et al. (2012). Hydraulic differences along the water transport system of south American *Nothofagus* species: do leaves protect the stem functionality? *Tree Physiol.* 32, 880–893. doi: 10.1093/treephys/tps054

Chai, Y., Liu, X., Yue, M., Guo, J., Wang, M., Wan, P., et al. (2014). Leaf traits in dominant species from different secondary successional stages of deciduous forest on the loess plateau of northern China. *Appl. Veg. Sci.* 18, 50–63. doi: 10.1111/avsc.12123

Choat, B., Brodribb, T. J., Brodersen, C. R., Duursma, R. A., Lopez, R., and Medlyn, B. E. (2018). Triggers of tree mortality under drought. *Nature* 558, 531–539. doi: 10.1038/s41586-018-0240-x

Cosme, L. H. M., Schietti, J., Costa, F. R. C., and Oliveira, R. S. (2017). The importance of hydraulic architecture to the distribution patterns of trees in a central Amazonian Forest. *New Phytol.* 215, 113–125. doi: 10.1111/nph.14508

Farrell, C., Szota, C., and Arndt, S. K. (2017). Does the turgor loss point characterize drought response in dryland plants? *Plant Cell Environ.* 40, 1500–1511. doi: 10.1111/pce.12948

Fine, P. V. A., Miller, Z. J., Mesones, I., Irazuzta, S., Appel, H. M., Stevens, M. H. H., et al. (2006). The growth-defense trade-off and habitat specialization by plants in Amazonian forests. *Ecology* 87, S150–S162. doi: 10.1890/0012-9658(2006)87[150:TGTAHS]2.0.CO;2

Flexas, J., Scoffoni, C., Gago, J., and Sack, L. (2013). Leaf mesophyll conductance and leaf hydraulic conductance: an introduction to their measurement and coordination. *J. Exp. Bot.* 64, 3965–3981. doi: 10.1093/jxb/ert319

Fortunel, C., Ruelle, J., Fine, P. V. A., and Baraloto, C. (2014). Wood specific gravity and anatomy of branches and roots in 113 Amazonian rainforest tree species across environmental gradients. *New Phytol.* 202, 79–94. doi: 10.1111/nph.12632

Franks, P. J., Drake, P. L., and Beerling, D. J. (2009). Plasticity in maximum 1355 stomatal conductance constrained by negative correlation between stomatal 1356 size and density: an analysis using Eucalyptus globulus. *Plant Cell Environ.* 32, 1737–1748. doi: 10.1111/j.1365-3040.2009.002031.x

Garnier, E., Shipley, B., Roumet, C., and Laurent, G. (2001). A standardized protocol for the determination of specific leaf area and leaf dry mater content. *Funct. Ecol.* 15, 688–695. doi: 10.1046/j.0269-8463.2001.00563.x

Gleason, S. M., Westoby, M., Jansen, S., Choat, B., Brodribb, T. J., Cochard, H., et al. (2016a). On research priorities to advance understanding of the safety-efficiency tradeoff in xylem. *New Phytol.* 211, 1156–1158. doi: 10.1111/nph.14043

Gleason, S. M., Westoby, M., Jansen, S., Choat, B., Hacke, U. G., Pratt, R. B., et al. (2016b). Weak tradeoff between xylem safety and xylem-specific hydraulic efficiency across the world's woody plant species. *New Phytol.* 209, 123–136. doi: 10.1111/nph.13646

Granato-Souza, D., Adenesky-Filho, E., Barbosa, A. C. M. C., and Esemann-Quadros, K. (2018). Dendrochronological analyses and climatic signals of *Alchornea triplinervia* in subtropical forest of southern Brazil. *Austral Ecol.* 43, 385–396. doi: 10.1111/aec.12576

Han, T. T., Ren, H., Wang, J., Lu, H. F., Song, G. M., and Chazdon, R. L. (2020). Variations of leaf eco-physiological traits in relation to environmental factors during forest succession. *Ecol. Indic.* 117:106511. doi: 10.1016/j.ecolind.2020.106511

Hu, L., Su, J., Sang, Y. Z., Zhang, W. J., and Wang, Q. (2014). Spatial and temporal characteristics of rainfall erosivity in Shaanxi province. *Arid Land Geography* 37, 1101–1107. doi: 10.13826/j.cnki.cn65-1103/x.2014.06.002

Ji, W. L., LaZerte, S. E., Waterway, M. J., and Lechowicz, M. J. (2020). Functional ecology of congeneric variation in the leaf economics spectrum. *New Phytol.* 225, 196–208. doi: 10.1111/nph.16109

Johnson, D. M., Berry, Z. C., Baker, K. V., Smith, D. D., McCulloh, K. A., and Domec, J. C. (2018). Leaf hydraulic parameters are more plastic in species that experience a wider range of leaf water potentials. *Funct. Ecol.* 32, 894–903. doi: 10.1111/1365-2435.13049

Kardiman, R., and Ræbild, A. (2017). Relationship between stomatal density, size and speed of opening in Sumatran rainforest species. *Tree Physiol.* 38, 696–705. doi: 10.1093/treephys/tpx149

Kitajima, K., and Poorter, L. (2010). Tissue-level leaf toughness, but not lamina thickness, predicts sapling leaf lifespan and shade tolerance of tropical tree species. *New Phytol.* 186, 708–721. doi: 10.1111/j.1469-8137.2010.03212.x

Kraft, N. J., Valencia, R., and Ackerly, D. D. (2008). Functional traits and niche-based tree community assembly in an Amazonian Forest. *Science* 322, 580–582. doi: 10.1126/science.1160662

Lamont, B. B., and Lamont, H. C. (2000). Utilizable water in leaves of 8 arid species as derived from pressure-volume curves and chlorophyll fluorescence. *Physiol. Plant.* 110, 64–71. doi: 10.1034/j.1399-3054.2000.110109.x

Laughlin, D. C. (2014). The intrinsic dimensionality of plant traits and its relevance to community assembly. *J. Ecol.* 102, 186–193. doi: 10.1111/1365-2745.12187

Lens, F., Sperry, J. S., Christman, M. A., Choat, B., Rabaey, D., and Jansen, S. (2011). Testing hypotheses that link wood anatomy to cavitation resistance and hydraulic conductivity in the genus Acer. *New Phytol.* 190, 709–723. doi: 10.1111/j.1469-8137.2010.03518.x

Li, X. M., Blackman, C. J., Choat, B., Duursma, R. A., Rymer, P. D., Medlyn, B. E., et al. (2018). Tree hydraulic traits are coordinated and strongly linked to climate-of-origin across a rainfall gradient. *Plant Cell Environ.* 41, 646–660. doi: 10.1111/pce.13129

Li, L., McCormack, M. L., Ma, C., Kong, D., Zhang, Q., Chen, X., et al. (2015). Leaf economics and hydraulic traits are decoupled in five species-rich tropical-subtropical forests. *Ecol. Lett.* 18, 899–906. doi: 10.1111/ele.12466

Liang, J., Wang, X., Yu, Z., Dong, Z., and Wang, J. (2010). Effects of vegetation succession on soil fertility within farming-plantation ecotone in Ziwuling Mountains of the loess plateau in China. *Agric. Sci. China* 9, 1481–1491. doi: 10.1016/S1671-2927(09)60241-8

Litvak, E., McCarthy, H. R., and Pataki, D. E. (2012). Transpiration sensitivity of urban trees in a semi-arid climate is constrained by xylem vulnerability to cavitation. *Tree Physiol.* 32, 373–388. doi: 10.1093/treephys/tps015

Liu, C., Li, Y., Zhang, J., Baird, A. S., and He, N. (2020a). Optimal community assembly related to leaf economic-hydraulic-anatomical traits. *Front. Plant Sci.* 11:341. doi: 10.3389/fpls.2020.00341

Liu, H., Ye, Q., Gleason, S. M., He, P., and Yin, D. (2021a). Weak tradeoff between xylem hydraulic efficiency and safety: climatic seasonality matters. *New Phytol.* 229, 1440–1452. doi: 10.1111/nph.16940

Liu, X., Li, Q., Wang, F., Sun, X., Wang, N., Song, H., et al. (2020b). Weak tradeoff and strong segmentation among plant hydraulic traits during seasonal variation in four woody species. *Front. Plant Sci.* 11:585674. doi: 10.3389/fpls.2020.585674

Liu, X., Wang, N., Cui, R., Song, H., Wang, F., Sun, X., et al. (2021b). Quantifying key points of hydraulic vulnerability curves from drought-rewatering experiment using differential method. *Front. Plant Sci.* 12:627403. doi: 10.3389/fpls.2021.627403

Liu, X., Zhang, Q., Song, M., Wang, N., Fan, P., Wu, P., et al. (2021c). Physiological responses of Robinia pseudoacacia and Quercus acutissima seedlings to repeated drought-rewatering under different planting methods. *Front. Plant Sci.* 12:760510. doi: 10.3389/fpls.2021.760510

Luo, D. D., Wang, C. K., and Jin, Y. (2017). Plant water-regulation strategies: isohydric versus anisohydric behavior. *Chin. J. Plant Ecol.* 41, 1020–1032.

Males, J., and Griffiths, H. (2018). Economic and hydraulic divergences underpin ecological differentiation in the Bromeliaceae. *Plant Cell Environ.* 41, 64–78. doi: 10.1111/pce.12954

Maréchaux, I., Bartlett, M. K., Sack, L., Baraloto, C., Engel, J., Joetzjer, E., et al. (2015). Drought tolerance as predicted by leaf water potential at turgor loss point varies strongly across species within an Amazonian Forest. *Funct. Ecol.* 29, 1268–1277. doi: 10.1111/1365-2435.12452

Markesteijn, L., Poorter, L., Paz, H., Sack, L., and Bongers, F. (2011). Ecological differentiation in xylem cavitation resistance is associated with stem and leaf structural traits. *Plant Cell Environ.* 34, 137–148. doi: 10.1111/j.1365-3040.2010.02231.x

Martínez-Vilalta, J., Poyatos, R., Aguadé, D., Retana, J., and Mencuccini, M. (2014). A new look at water transport regulation in plants. *New Phytol.* 204, 105–115. doi: 10.1111/nph.12912

Mclean, Q. H., Prober, S. M., Stock, W. D., Steane, D. A., Potts, B. M., Vaillancourt, R. E., et al. (2014). Plasticity of functional traits varies clinally along a rainfall gradient in *eucalyptus tricarpa*. *Plant Cell Environ.* 37, 1440–1451. doi: 10.1111/pce.12251

Mediavilla, S., Escudero, A., and Heilmeier, H. (2001). Internal leaf anatomy and photosynthetic resource-use efficiency: interspecific and intraspecific comparisons. *Tree Physiol.* 21, 251–259. doi: 10.1093/treephys/21.4.251

Meinzer, F. C., Andrade, J. L., Goldstein, G., Holbrook, N. M., Cavelier, J., and Wright, S. J. (1999). Partitioning of soil water among canopy trees in a seasonally dry tropical forest. *Oecologia* 121, 293–301. doi: 10.1007/s004420050931

Meinzer, F. C., Smith, D. D., Woodruff, D. R., Marias, D. E., McCulloh, K. A., Howard, A. R., et al. (2017). Stomatal kinetics and photosynthetic gas exchange along a continuum of isohydric to anisohydric regulation of plant water status. *Plant Cell Environ.* 40, 1618–1628. doi: 10.1111/pce.12970

Meinzer, F. C., Woodruff, D. R., Marias, D. E., Smith, D. D., McCulloh, K. A., Howard, A. R., et al. (2016). Mapping 'hydroscapes' along the iso- to anisohydric continuum of stomatal regulation of plant water status. *Ecol. Lett.* 19, 1343–1352. doi: 10.1111/ele.12670

Meng, Q. C., Zhang, X. F., Liu, X., and Yue, M. (2011). Photosynthetic mechanisms of northern boundary formation of *Quercus wutaishanica* forest in loess plateau of northern Shaanxi Province. *Chin. J. Appl. Ecol.* 22, 1409–1415. doi: 10.3724/SP.J.1011.2011.00353

Mitchell, P. J., and O'Grady, A. P. (2015). Adaptation of leaf water relations to climatic and habitat water availability. *Forests* 6, 2281–2295. doi: 10.3390/f6072281

Nardini, A., and Luglio, J. (2014). Leaf hydraulic capacity and drought vulnerability: possible trade-offs and correlations with climate across three major biomes. *Funct. Ecol.* 28, 810–818. doi: 10.1111/1365-2435.12246

Niinemets, Ü. (2001). Global-scale climatic controls of leaf dry mass per area, density and thickness in trees and shrubs. *Ecology* 82, 453–469. doi: 10.1890/0012-9658(2001)082[0453:GSCCOL]2.0.CO;2

Osnas, J. L. D., Lichstein, J. W., Reich, P. B., and Pacala, S. W. (2013). Global leaf trait relationships: mass, area, and the leaf economics spectrum. *Science* 340, 741–744. doi: 10.1126/science.1231574

Parmesan, C., and Yohe, G. (2003). A globally coherent fingerprint of climate change impacts across natural systems. *Nature* 421, 37–42. doi: 10.1038/nature01286

Pfautsch, S., Harbusch, M., Wesolowski, A., Smith, R., Macfarlane, C., Tjoelker, M. G., et al. (2016). Climate determines vascular traits in the ecologically diverse genus eucalyptus. *Ecol. Lett.* 19, 240–248. doi: 10.1111/ele.12559

Poorter, L., Van der Sande, M. T., Arets, E. J. M. M., Ascarrunz, N., Enquist, B. J., Finegan, B., et al. (2017). Biodiversity and climate determine the functioning of Neotropical forests. *Glob. Ecol. Biogeogr.* 26, 1423–1434. doi: 10.1111/geb.12668

Pratt, R. B., Jacobsen, A. L., Ewersä, F. W., and Davis, S. D. (2007). Relationships among xylem transport, biomechanics and storage in stems and roots of nine Rhamnaceae species of the California chaparral. *New Phytol.* 174, 787–798. doi: 10.1111/j.1469-8137.2007.02061.x

Ramírez-Valiente, J. A., and Cavender-Bares, J. (2017). Evolutionary trade-offs between drought resistance mechanisms across a precipitation gradient in a seasonally dry tropical oak (*Quercus oleoides*). *Tree Physiol.* 37, 889–901. doi: 10.1093/treephys/tpx040

Reich, P. B. (2014). The world-wide 'fast-slow' plant economics spectrum: a traits manifesto. *J. Ecol.* 102, 275–301. doi: 10.1111/1365-2745.12211

Rita, A., Borghetti, M., Todaro, L., and Saracino, A. (2016). Interpreting the climatic effects on xylem functional traits in two Mediterranean oak species: the role of extreme climatic events. *Front. Plant Sci.* 7:1126. doi: 10.3389/fpls.2016.01126

Rodríguez-Ramírez, E. C., Terrazas, T., and Luna-Vega, I. (2019). The influence of climate on the masting behavior of Mexican beech: growth rings and xylem anatomy. *Trees* 33, 23–35. doi: 10.1007/s00468-018-1755-3

Rose, R., and Hertel, L. (2013). Management alters interspecific leaf trait relationships and trait-based species rankings in permanent meadows. *J. Veg. Sci.* 24, 239–250. doi: 10.1111/j.1654-1103.2012.01455.x

Rosell, J. A., and Olson, M. E. (2014). Do lianas really have wide vessels? Vessel diameter–stem length scaling in non-self-supporting plants. *Perspect. Plant Ecol. Evol. Syst.* 16, 288–295. doi: 10.1016/j.ppees.2014.08.001

Rowland, L., da Costa, A. C. L., Galbraith, D. R., Oliveira, R. S., Binks, O. J., Oliveira, A. A. R., et al. (2015). Death from drought in tropical forests is triggered by hydraulics not carbon starvation. *Nature* 528, 119–122. doi: 10.1038/nature15539

Sack, L., and Holbrook, N. M. (2006). Leaf hydraulics. *Annu. Rev. Plant Biol.* 57, 361–381. doi: 10.1146/annurev.arplant.56.032604.144141

Sack, L., and Scoffoni, C. (2013). Leaf venation: structure, function, development, evolution, ecology and applications in the past, present and future. *New Phytol.* 198, 983–1000. doi: 10.1111/nph.12253

Sande, M. T. V. D., Poorter, L., Schnitzer, S. A., Engelbrecht, B. M. J., and Markesteijn, L. (2019). The hydraulic efficiency-safety trade-off differs between lianas and trees. *Ecology* 100:e02666. doi: 10.1002/ecy.2666

Santiago, L. S., De Guzman, M. E., Baraloto, C., Vogenberg, J. E., Brodie, M., Hérault, B., et al. (2018). Coordination and trade-offs among hydraulic safety, efficiency and drought avoidance traits in amazonian rainforest canopy tree species. *New Phytol.* 218, 1015–1024. doi: 10.1111/nph.15058

Schuldt, B., Knutzen, F., Delzon, S., Jansen, S., Müller-Haubold, H., Burlett, R., et al. (2016). How adaptable is the hydraulic system of european beech in the face of climate change-related precipitation reduction? *New Phytol.* 210, 443–458. doi: 10.1111/nph.13798

Schulte, P. J. (1999). Water flow through a 20-pore perforation plate in vessels of *Liquidambar styraciflua*. *J. Exp. Bot.* 50, 1179–1187. doi: 10.1093/jxb/50.336.1179

Suter, M., and Edwards, P. J. (2013). Convergent succession of plant communities is linked to species' functional traits. *Perspect. Plant Ecol. Evol. Syst.* 15, 217–225. doi: 10.1016/j.ppees.2013.05.001

Tanaka-Oda, A., Kenzo, T., Koretsune, S., and Fukuda, K. (2010). Ontogenetic changes in water-use efficiency ($\delta^{13}C$) and leaf traits differ among tree species growing in a semiarid region of the loess plateau, China. *For. Ecol. Manag.* 259, 953–957. doi: 10.1016/j.foreco.2009.11.037

Togashi, H. F., Prentice, I. C., Evans, B. J., Forrester, D. I., Drake, P., Feikema, P., et al. (2015). Morphological and moisture availability controls of the leaf area-to-sapwood area ratio: analysis of measurements on australian trees. *Evol. Ecol.* 5, 1263–1270. doi: 10.1002/ece3.1344

Toledo, M., Peña-Claros, M., Bongers, F., Alarcón, A., Balcázar, J., Chuviña, J., et al. (2012). Distribution patterns of tropical woody species in response to climatic and edaphic gradients. *J. Ecol.* 100, 253–263. doi: 10.1111/j.1365-2745.2011.01890.x

Tomasella, J., Hodnett, M. G., Cuartas, L. A., Nobre, A. D., Waterloo, M. J., and Oliveira, S. M. (2008). The water balance of an Amazonian micro-catchment: the effect of interannual variability of rainfall on hydrological behaviour. *Hydrol. Process.* 22, 2133–2147. doi: 10.1002/hyp.6813

Tyree, M. T., Davis, S. D., and Cochard, H. (1994). Biophysical perspectives of xylem evolution: is there a tradeoff of hydraulic efficiency for vulnerability to dysfunction? *IAWA J.* 15, 335–360. doi: 10.1163/22941932-90001369

Tyree, M. T., and Hammel, H. T. (1972). The measurement of the turgor pressure and the water relations of plants by the pressure-bomb technique. *J. Exp. Bot.* 23, 267–282. doi: 10.1093/jxb/23.1.267

Villagra, M., Campanello, P. I., Bucci, S. J., and Goldstein, G. (2013). Functional relationships between leaf hydraulics and leaf economic traits in response to nutrient addition in subtropical tree species. *Tree Physiol.* 33, 1308–1318. doi: 10.1093/treephys/tpt098

Wright, I. J., Reich, P. B., Westoby, M., Ackerly, D. D., Baruch, Z., Bongers, F., et al. (2004). The worldwide leaf economics spectrum. *Nature* 428, 821–827. doi: 10.1038/nature02403

Xiong, D., Flexas, J., Yu, T., Peng, S., and Huang, J. (2017). Leaf anatomy mediates coordination of leaf hydraulic conductance and mesophyll conductance to CO_2 in Oryza. *New Phytol.* 213, 572–583. doi: 10.1111/nph.14186

Xu, X., Medvigy, D., Powers, J. S., Becknell, J. M., and Guan, K. (2016). Diversity in plant hydraulic traits explains seasonal and inter-annual variations of vegetation dynamics in seasonally dry tropical forests. *New Phytol.* 212, 80–95. doi: 10.1111/nph.14009

Yin, Q., Wang, L., Lei, M. L., Dang, H., Quan, J. X., Tian, T. T., et al. (2018). The relationships between leaf economics and hydraulic traits of woody plants depend on water availability. *Sci. Total Environ.* 621, 245–252. doi: 10.1016/j.scitotenv.2017.11.171

Yue, M. (1998). Species diversity of higher plant of *Quercus wutaishanica* forests in Qinling Mountain and loess plateau. *Acta Botan. Boreali-Occiden. Sin.* 18, 124–131.

Zhang, Y. J., Cao, K. F., Sack, L., Li, N., Wei, X. M., and Goldstein, G. (2015). Extending the generality of leaf economic design principles in the cycads, an ancient lineage. *New Phytol.* 206, 817–829. doi: 10.1111/nph.13274

Zhang, L., Di, M., Xu, J. S., Quan, J. X., and Yue, M. (2017). Economic trade-offs of hydrophytes and neighbouring terrestrial herbaceous plants based on plant functional traits. *Basic Appl. Ecol.* 22, 11–19. doi: 10.1016/j.baae.2017.06.004

Zhang, Y., Liu, X., Lv, Z., Zhao, X., and Zhu, Y. (2019). Animal diversity responding to different forest restoration schemes in the Qinling Mountains, China. *Ecol. Eng.* 136, 23–29. doi: 10.1016/j.ecoleng.2019.05.020

Zhang, S. B., Sun, M., Cao, K. F., Hu, H., Zhang, J. L., and Ng, C. (2014). Leaf photosynthetic rate of tropical ferns is evolutionarily linked to water transport capacity. *PLoS One* 9:e84682. doi: 10.1371/journal.pone.0084682

Zhao, W. L., Chen, Y. J., Brodribb, T. J., and Cao, K. F. (2016). Weak co-ordination between vein and stomatal densities in 105 angiosperm tree species along altitudinal gradients in Southwest China. *Funct. Plant Biol.* 43, 1126–1133. doi: 10.1071/FP16012

Zhao, J. B., and Yue, M. (1996). Oak forest and climate in Qinling Mountain and loess plateau. *J. Earth Sci. Environ.* 18, 67–73.

Zhao, J. L., Zhang, Y. H., Xu, J. S., Chai, Y. F., Liu, P. L., Cao, Y., et al. (2021). Strong environmental filtering based on hydraulic traits occurring in the lower water availability of temperate forest communities. *Front. Plant Sci.* 12:698878. doi: 10.3389/fpls.2021.698878

Zheng, S., and Shangguan, Z. (2007a). Spatial patterns of foliar stable carbon isotope compositions of C_3 plant species in the loess plateau of China. *Ecol. Res.* 22, 342–353. doi: 10.1007/s11284-006-0024-x

Zheng, S., and Shangguan, Z. (2007b). Spatial patterns of leaf nutrient traits of the plants in the loess plateau of China. *Trees* 21, 357–370. doi: 10.1007/s00468-007-0129-z

Zheng, S., and Shangguan, Z. (2007c). Spatial patterns of photosynthetic characteristics and leaf physical traits of plants in the loess plateau of China. *Plant Ecol.* 191, 279–293. doi: 10.1007/s11258-006-9242-0

Zhu, Z. C. (1982). A preliminary studies on the *Quercus liaotungensis* forests in the Qinling Mountain and the loess plateau of northern part of the Shanxi Province. *Chin. J. Plant Ecol.* 6, 95–104.

Zhu, S. D., Chen, Y. J., Fu, P. L., and Cao, K. F. (2017). Different hydraulic traits of woody plants from tropical forests with contrasting soil water availability. *Tree Physiol.* 37, 1469–1477. doi: 10.1093/treephys/tpx094

Zhu, S. D., Chen, Y. J., Ye, Q., He, P. C., Liu, H., Li, R. H., et al. (2018). Leaf turgor loss point is correlated with drought tolerance and leaf carbon economics traits. *Tree Physiol.* 38, 658–663. doi: 10.1093/treephys/tpy013

Zimmermann, M. H. (1983). *Xylem Structure and the Ascent of Sap*. Berlin, Germany, New York, USA: Springer-Verlag.

Conflict of Interest: The authors declare that the research was conducted in the absence of any commercial or financial relationships that could be construed as a potential conflict of interest.

Frontiers in Plant Science

ORIGINAL RESEARCH
published: 09 June 2022
doi: 10.3389/fpls.2022.850203

Tree Size Influences Leaf Shape but Does Not Affect the Proportional Relationship Between Leaf Area and the Product of Length and Width

*Jianzhong Ma[1,2], Karl J. Niklas[3], Leyi Liu[4], Zhendong Fang[5], Yirong Li[2] and Peijian Shi[2]**

[1] Yunnan Academy of Forestry and Grassland, Kunming, China, [2] Bamboo Research Institute, Nanjing Forestry University, Nanjing, China, [3] Plant Biology Section, School of Integrative Plant Science, Cornell University, Ithaca, NY, United States, [4] College of Landscape Architecture and Horticulture Science, Southwest Forestry University, Kunming, China, [5] Shangri-la Alpine Botanical Garden, Shangri-la, China

The Montgomery equation predicts leaf area as the product of leaf length and width multiplied by a correction factor. It has been demonstrated to apply to a variety of leaf shapes. However, it is unknown whether tree size (measured as the diameter at breast height) affects leaf shape and size, or whether such variations in leaf shape can invalidate the Montgomery equation in calculating leaf area. Here, we examined 60 individual trees of the alpine oak (*Quercus pannosa*) in two growth patterns (trees growing from seeds vs. growing from roots), with 30 individuals for each site. Between 100 and 110 leaves from each tree were used to measure leaf dry mass, leaf area, length, and width, and to calculate the ellipticalness index, ratio of area between the two sides of the lamina, and the lamina centroid ratio. We tested whether tree size affects leaf shape, size, and leaf dry mass per unit area, and tested whether the Montgomery equation is valid for calculating leaf area of the leaves from different tree sizes. The diameters at breast height of the trees ranged from 8.6 to 96.4 cm (tree height ranged from 3 to 32 m). The diameter at breast height significantly affected leaf shape, size, and leaf dry mass per unit area. Larger trees had larger and broader leaves with lower leaf dry mass per unit area, and the lamina centroid was closer to the leaf apex than the leaf base. However, the variation in leaf size and shape did not negate the validity of the Montgomery equation. Thus, regardless of tree size, the proportional relationship between leaf area and the product of leaf length and width can be used to calculate the area of the leaves.

Keywords: bilateral symmetry, centroid ratio, DBH, growth patterns, leaf ellipticalness index, Montgomery equation

Edited by:
Raquel Lobo-do-Vale,
University of Lisbon, Portugal

Reviewed by:
Danijela P. Miljkovic,
University of Belgrade, Serbia
Radu E. Sestras,
University of Agricultural Sciences and Veterinary Medicine of Cluj-Napoca, Romania

****Correspondence:***
Peijian Shi
pjshi@njfu.edu.cn

Specialty section:
This article was submitted to Functional Plant Ecology, a section of the journal Frontiers in Plant Science

Received: *07 January 2022*
Accepted: *23 May 2022*
Published: *09 June 2022*

Citation:
Ma J, Niklas KJ, Liu L, Fang Z, Li Y and Shi P (2022) Tree Size Influences Leaf Shape but Does Not Affect the Proportional Relationship Between Leaf Area and the Product of Length and Width. Front. Plant Sci. 13:850203. doi: 10.3389/fpls.2022.850203

INTRODUCTION

Leaf shape has been demonstrated to be important for light interception, evapotranspiration, and mechanics (Niklas, 1988, 1999; Nicotra et al., 2008, 2011), and thus to affect the tradeoff between the leaf support cost and photosynthetic returns (Niinemets et al., 2007; Lin et al., 2020). For example, using computer simulations, Niklas (1988, 1989) reported that the extent of leaf lobing affected the capacity to intercept light, whereas Santiago and Kim (2009) found that *Sonchus* species from exposed habitats have smaller, more dissected leaves with greater photosynthetic rates compared with those of *Sonchus* species from shaded habitats. Thus, leaf shape can often be used as a predictor of photosynthetic capacity of leaves, such as rates of carbon uptake (Ölçer et al., 2001; Royer and Wilf, 2006). In this context, Shi et al. (2021a) showed that the ratio of leaf width to length (RWL) is significantly positively correlated with the fractal dimension of leaf shape, which means that RWL is a good indicator of the geometric characteristics of leaf shape. Using 101 bamboo taxa, Lin et al. (2020) demonstrated that the scaling exponent of leaf dry mass vs. leaf surface area decreases toward 1 as RWL increases, thereby indicating that broader leaves tend to have lower support cost with increasing unit leaf area compared to narrower leaves.

In addition to RWL, other leaf shape indices are available, i.e., the leaf roundness index and its reciprocal, the leaf dissection index (Kincaid and Schneider, 1983; Thomas and Bazzaz, 1996; Niinemets, 1998; Santiago and Kim, 2009; Peppe et al., 2011). However, an accurate quantification of many elliptical, oval, and oboval leaves significantly deviates from circular leaves. Consequently, Li et al. (2021b) proposed a new index, the leaf ellipticalness index (EI), based on the Montgomery equation (ME; see Montgomery, 1911), which assumes that leaf area is proportional to the product of leaf length and width. In contrast to the leaf roundness index, the EI reflects the extent to which an elliptical leaf deviates from an ellipse, and can be used to calculate leaf area provided that leaf length and width are known. In theory, the EI value can be larger or smaller than 1 depending on leaf shape. It cannot be used to accurately evaluate the degree of leaf bilateral asymmetry, or predict the leaf centroid from the base of an oval or oboval leaf shape. In order to cope with this limitation, Shi et al. (2021b) developed an ovate and obovate leaf shape model using leaf length and width and a third parameter representing the distance from the leaf base to the point on the leaf length axis associated with maximum leaf width. Consequently, Li et al. (2021c) defined the "centroid ratio" (as the ratio of this third parameter to leaf length) to quantify the extent of the deviation of the leaf centroid from the midpoint of leaf length. Using this model, Li et al. (2021c) found that the centroid ratio is significantly correlated with the ratio of leaf petiole mass to lamina mass for two Lauraceae species (*Cinnamomum camphora*, and *Machilus leptophylla*). Therefore, the centroid ratio is a potentially a good quantitative index of leaf shape. It is necessary to point out the difference between the centroid ratio (as the ratio of the distance, from the leaf base to a point on the leaf length axis associated with the maximum leaf width, to the leaf length) and centroid size in geometric morphometrics (Mitteroecker et al., 2013; Klingenberg, 2016). The latter is equal to the Euclidean distance between the landmarks on the boundary of a planar polygon to their centroid, which the centroid is the geometric centre of the polygon. In the present work, the definition of the "centroid" is the point on the leaf length axis associated with the maximum leaf width, which is not the geometric center in geometric morphometrics methods. The reason is that it is difficult to find landmarks on the boundary of a completely or approximately entire leaf.

A critical and as yet unanswered question is whether plant size (which is often but not invariably correlated with the age of perennial plant species) affects leaf shape or size. Tree populations usually consist of different age- and size-groups. For evergreen tree species, leaves are in a constant state of renewal, and limited research has shown that leaf and overall plant age can to a large extent determine overall photosynthetic capacity (Küppers, 1989; Bielczynski et al., 2017). In addition, tree height, which is often correlated with age, is important because water transport from roots to the highest elevated leaves becomes progressively more difficult (Becker et al., 2000). Thus, the leaf size, shape, leaf-level cost of light-interception (which can be quantified by leaf dry mass per unit area, LMA, or its reciprocal specific leaf area, SLA) can vary significantly within a canopy (Sack et al., 2006; He and Yan, 2018). Nevertheless, whether leaf shape varies significantly across tree size has not been tested.

Quercus pannosa was selected for study because it is an important evergreen tree species, which usually forms a single forest or a mixed forest with other *Quercus* species typically growing at altitudes of 3,300–4,200 m in China. The species also produces leaves that are elliptical or oboval in shape (**Figure 1**) with a high dry mass per unit area (LMA). The leaf structure and shape of this species allows it to tolerate low temperatures and to grow closer to the climatic conifer treeline (He et al., 1994; Yang et al., 2020). He et al. (1994) explored the relationship between leaf anatomical structures and elevation of alpine oaks, and found that at high altitudinal areas the quadrangular and pentagonal epidermis in leaves are frequently observed, and that the stomatal density decreases at high elevations. However, there are no studies that have quantified the leaf-shape of this species, or that have related leaf-shape and LMA to tree size.

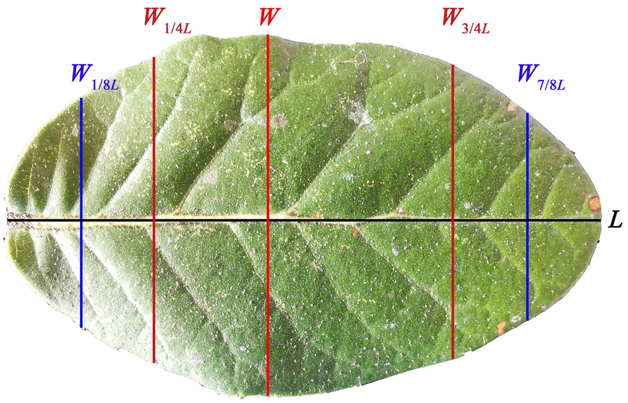

FIGURE 1 | Adaxial surface (i.e., the upper image) of a representative leaf of *Quercus pannosa*. L represents the leaf length; W represents the maximum leaf width; $W_{1/4L}$ represents the leaf width associated with 1/4L from leaf base; $W_{3/4L}$ represents the leaf width associated with 3/4L from leaf base; $W_{1/8L}$ represents the leaf width associated with 1/8L from leaf base; $W_{7/8L}$ represents the leaf width associated with 7/8L from leaf base.

To address this question, we sampled >6,500 leaves from 60 naturally growing individual trees of *Quercus pannosa* Hand.-Mazz. at two sites (representing two growth patterns, i.e., trees growing from seeds vs. trees growing from roots) in south-western China to test: (i) whether tree size and growth pattern affects leaf shape, size, and leaf-level cost of light interception, (ii) whether the ME is valid for calculating the leaf area of different tree sizes at the individual tree level and for the pooled data across all individuals, and (iii) whether the EI differs from other leaf-shape indices including the leaf RWL and centroid ratio. In general, although the diameter at breast height (DBH) is positively correlated tree height, in practice, DBH is easier to accurately measure tree size. Therefore, in the present study, DBH is used as a measure of tree size.

MATERIALS AND METHODS

Sampling Sites and Leaf Collection

Two sites (see **Table 1** for details) measuring 100 m × 100 m in naturally growing tree communities were selected for study in Shangri-la, Yunnan Province, China. The annual accumulated precipitation for Shangri-la from 2000 to 2019 is 624 ± 124 mm; the mean annual temperature is 6.8°C ± 0.4°C; the annual duration of sunshine is 2,182 ± 149 h; the number of days for frosts per year is 152 ± 12 days (China Meteorological Data Service Centre).[1] Thirty trees were randomly selected from the first site (S1), and another 30 trees were randomly selected from the second site (S2). For S1, *Q. pannosa* was intermixed with *Q. pseudosemecarpifolia*, and the coverage of either oak species accounted for *ca.* 25%–35%. For S2, *Q. pannosa* dominated the forest community, and accounted for *ca.* 85%–95% of the total forest coverage. Most trees grew from seeds in S1; most trees in S2 grew from roots. Most trees growing from seeds in S2 were cut down by local farmers, and the following trees growing from roots were usually shorter and the trunks near the ground are most curved, which is easy to distinguish between the trees of two growing patterns by observing tree size and simultaneously checking how bent the trunks are. In addition, S1 is far away from villages, and it is difficult for local farmers to arrive; however, S1 is closer to villages, and local farmers used to go to this site and the surrounding area to cut firewood. There were 22 out of the 30 trees whose DBH values ≥ 30 cm in S1, but were only 2 out of the 30 trees whose DBH values ≥ 30 cm in S2. Our experimental design is to choose 30 trees from each site, representing the smallest big sample size in statistics. In each site, we randomly sampled 30 trees in the range of 100 m × 100 m, and there is no need to sample more trees given the heavy workload required. We used a quadrat of 20 m × 20 m around the center of each site to measure the site information (**Table 1**).

TABLE 1 | Site information.

Information	Site 1 (S1)	Site 2 (S2)
Location	27° 37′33.05″	99°34′0.68″
Elevation (m)	3,202	3,716
Size (m^2)	20 × 20	20 × 20
Slope (°)	27	24
Aspect (°)	172	158
Soil type	Brown soil	Brown soil
Soil depth (m)	0.5–1.0	0.1–0.2
Dominant species of the community	*Quercus pannosa* *Quercus pseudosemecarpifolia* *Rhododendron decorum* *Fragaria nilgerrensis*	*Quercus pannosa* *Rhododendron Rubiginosum* *Ainsliaea fragrans*
Coverage of *Q. pannosa* (%)	25–35	85–95
Human disturbance	Weak	Strong
Main growth pattern of *Q. pannosa*	Growing from seeds	Growing from roots

The trees are all native species for both S1 and S2, and are naturally distributed in Site 1. Local farmers often cut down trees in and around S2 for daily use. However, it is difficult to accurately estimate tree age for each individual. We randomly sampled 30 trees from each site of 100 m × 100 m, and we calculated the site information in this table using one quadrat of 20 m × 20 m around the center of each site.

On 25 September 2021, we randomly sampled 100–110 leaves from the lower canopy of each of the 30 trees in S1, and on 1 October 2021, we sampled leaves from S2. Because of the difference in height among different individual trees, we defined "the lower canopy" as the positions of ≤1/4 of a tree crown height, and sampled leaves without distinguishing directions and between the shade and sun leaves given that a large sample can well reflect general characteristics of leaf shape and size. All leaves were wrapped in wet newspaper to reduce tissue dehydration.

Indices for Measuring Leaf Shape

To quantify leaf shape, we used six indices.

(i) The ratio of leaf width to length (RWL)

$$\mathrm{RWL} = W/L,$$

where W denotes leaf maximum width, and L denotes leaf length.

(ii) The leaf ellipticalness index (EI; Li et al., 2021a,b)

$$\mathrm{EI} = \frac{A}{\left(\pi/4\right)LW},$$

where A denotes leaf area.

(iii) The ratio of the W associated with $1/4L$ from leaf base to the leaf width associated with $3/4L$ from leaf base, which is referred to as the proximal ratio index (PRI). To normalize this parameter, we used its log-transformed value, i.e.,

$$\ln \mathrm{PRI} = \ln \frac{W_{1/4L}}{W_{3/4L}}.$$

---

[1] http://data.cma.cn/

(iv) The ratio of the W associated with $1/8\,L$ from the leaf base to the width associated with $7/8\,L$ from the leaf base. This ratio is referred to as the distal ratio index (DRI). To normalize this parameter, we also used its log-transformed value, i.e.,

$$\ln \mathrm{DRI} = \ln \frac{W_{1/8L}}{W_{7/8L}}$$

(v) The area ratio of the two sides of a leaf (AR). We used a log-transformed form to normalize this parameter, i.e.,

$$\ln \mathrm{AR} = \ln \frac{A_{\mathrm{Left}}}{A_{\mathrm{Right}}},$$

where A_{Left} and A_{Right} represent the areas of the left and right sides of a leaf, respectively.

(vi) The centroid ratio (CR), which is the ratio of the distance from leaf base to a point on the leaf length axis associated with leaf maximum width (L_{W}) to leaf length (L), i.e.,

$$\mathrm{CR} = \frac{L_W}{L}.$$

We did not take mathematically transformed forms (i.e., the log-transformation) of RWL, EI, or CR because the log-transformation did not improve the normality of these data, and because the tails of the histograms of those variables did not exhibit skewness.

Image Processing and Data Acquisition

After taking leaves back to the laboratory of Shangri-la Alpine Botanical Garden, we used three photo scanners (Type: CanoScan LiDE 220, Cannon, Vietnam) to scan all leaves to JPE images at 600 dpi resolution. The leaves were then dried using an oven (DHG 9070A, SoodKing, Suzhou, China) at 108°C for 48 h until achieving constant dry mass. We used an electric balance (BSA 124S, Sartorius Scientific Instruments Ltd., Beijing, China; measurement accuracy: 10^{-4} g) to measure leaf dry mass.

The scanned images were transformed to black–white BMP images, and we used the protocols proposed by Shi et al. (2018) to obtain the planar coordinates of each leaf edge. We used the statistical software R (version 4.2.0; R Core Team, 2022) to run the R script developed by Su et al. (2019) to calculate leaf area, length and width. To calculate PRI, DRI and CR, the slightly modified R script of Su et al. (2019) was used to provide values, which has been combined into the “bilat” function in a special R package “biogeom” (Shi et al., 2022a) was used to calculate the parameters related to leaf shape and size.

Statistical Analyses

The ANOVA followed by the Tukey’s honest significant difference (HSD) test at the 0.05 significance level (Hsu, 1996) was used to test the significance of the differences between any two individual trees in their leaf size, shape, and LMA.

To check the influence of DBH on leaf shape, size, and LMA, linear mixed-effects models (Bates et al., 2015) were used. For each tree, there was one DBH value, and 100–110 measurements for leaf shape, size, and LMA (i.e., those of 100–100 leaves). DBH was regarded as a fixed effect, and site (representing the levels of the two growth patterns, i.e., trees from seeds vs. trees from roots) as a random effect. The intraclass correlation coefficient was calculated to check the extent of variation between the levels:

$$\rho = \frac{\sigma_{\alpha}^2}{\sigma_{\alpha}^2 + \sigma_{\varepsilon}^2},$$

where σ_{α} and σ_{ε} represent the standard errors between the levels and within the levels, respectively. When there is no variation between the levels, $\sigma_{\alpha} = 0$ and $\rho = 0$; when the variation between the levels is much larger than that within the levels, ρ will approach 1 (Faraway, 2006).

To check whether tree size affected leaf area, the Montgomery equation (ME; Montgomery, 1911) was used:

$$A = \mathrm{MP} \cdot LW,$$

where MP is the Montgomery parameter, i.e., the proportionality coefficient to be estimated. We used the log-transformation of this equation to stabilize the variance of leaf area, i.e.,

$$\ln A = a + \ln LW,$$

where a is the natural logarithm of MP. When the ME held true, EI could be used as an indicator of leaf shape (Li et al., 2021b). The MP has a relationship with EI as:

$$\mathrm{MP} = \frac{\pi}{4}\mathrm{EI}.$$

According to the principle of similarity (Thompson, 1917), the area of an object is usually proportional to the square of its length. However, the empirical estimates for the scaling exponent of leaf area vs. leaf length for complex leaf shapes (especially those with lobes) can deviate from 2 (Shi et al., 2019; Yu et al., 2019, 2020). However, for elliptical, oval, and oboval leaf shapes, the principle of similarity has been confirmed (Shi et al., 2022b). Because the leaves of *Q. pannosa* exhibit elliptical and oboval shapes, it was nevertheless necessary to check whether it follows the principle of similarity. If and when it is confirmed, it can simplify the calculation of leaf area only using one leaf length dimension. We also checked whether the extent of variation in RWL influenced the validity of the principle of similarity. We calculated the root-mean-square error (RMSE) of fitting the following equation

$$\ln A = c + 2 \ln L,$$

and checked whether RMSE increases with the increase of the coefficient of variation (CV) in RWL. If it increases with increasing CV in RWL, it signifies the extent to which the principle of similarity depends on the variation in RWL. All analyses were carried out using the statistical software R (version 4.2.0; R Core Team, 2022).

RESULTS

The DBHs of the trees examined over the course of this study ranged from 8.6 to 96.4 cm. Tree height ranged from 3 to 32 m. **Table 2** shows the influence of DBH and site on leaf size, shape, and LMA. Leaf size and the ratio of leaf width to length (RWL) tend to increase with increasing DBH (**Figures 2A,C**), whereas LMA decreases with increasing DBH (**Figure 2B**). DBH did not significantly affect the leaf ellipticalness index (EI; **Figure 2D**; **Table 2**), which appears to result from a random effect. There were large variations among the sites for EI, leaf area, LMA, and RWL, with ρ ranging from 0.1832 to 0.5056 (**Table 2**). For other leaf shape indices, DBH had a statistically significant effect on the proximal ratio index (PRI), and the random site effect was very minor (**Figures 3A–C**; **Table 2**). With increasing DBH, the leaf centroid did not shift closer to the leaf apex or to the leaf base (**Figure 3D**; **Table 2**), that is, leaves morphologically maintain an oboval shape rather than an elliptical shape regardless of tree size. The DBH did not significantly affect the distal ratio index (DRI) or the area ratio of the two sides of leaves (AR), and the random site effect was very minor, with $\rho < 0.1$. The intercept of ln AR was not significant ($p > 0.05$), which indicated that there was no significant difference in area between the two sides of leaves (**Table 2**).

The Montgomery equation (ME) was found to be valid for the leaves of each tree with a correlation coefficient r ranging from 0.985 to 0.999. The estimated Montgomery parameter (MP) ranged from 0.7 to 0.8, and exceeded $\pi/4$ for 13 out of the 60 trees examined (**Figure 4**). Using the pooled data of the 60 trees, there was a significant log–log linear relationship between leaf area and leaf length on a log–log scale, and that between leaf area and the product of leaf length and width (**Figure 5**). However, the latter had a higher goodness of fit for a < 0.05 RMSE than the former with a > 0.13 RMSE. The 95% confidence intervals of the slope did not include 2 (**Figure 5A**), which indicated that the principle of similarity did not hold true for this oak species. There was a strong correlation between the goodness of the fit of the A vs. L^2 data on a log–log scale and the coefficient of variation of RWL (**Figure 6**). A smaller RMSE corresponded to a better goodness of fit and a lower coefficient of variation in RWL. Therefore, overall, the ME was found to be valid for calculating leaf area both at the individual tree level and for the pooled data across all individuals that were examined. Although the estimated MP values differ across individual trees, these values varied over a small range, which resulted in a < 0.05 RMSE by fitting the pooled leaf data of the 60 trees.

DISCUSSION

Leaf Size and LMA of *Quercus pannosa*

The data presented here reveals a trend in which leaf size increases with increasing tree size (as measured by DBH), which is not in accord with previous reports of the opposite trend (England and Attiwill, 2006). A number of possible explanations for this contradiction become apparent. However, we believe that it might result from the differences in the conduit sizes (vessel diameters) with increasing overall tree size reflecting an adaptation to extreme alpine environments. The number of days of frosts per year is more than 150 days in the study area. *Quercus pannosa* has evolved a special diffuse porous anatomy with more comparatively small diameter conduits capable of avoiding fatal winter embolism across multi-year vessel cohorts (Yang et al., 2020), since freezing can cause xylem cavitation for alpine trees (Mayr et al., 2007). However, narrower vessels also have a greater resistance to water transport, which limits the rate at which water can be delivered to leaves high in the canopy. The mean vessel diameter of newly formed vessels in larger *Q. pannosa* trees tends to be larger than that of newly formed vessels in smaller trees. It is possible therefore that this ontogenetic anatomical shift in vessel size permits the development of larger leaves (see **Figure 2A**). Future research in this area is required.

TABLE 2 | Fitted results of the linear mixed model to eight leaf size and shape indices.

Item	Estimate		Significance (*P*)		Standard deviation		Intraclass correlation coefficient
	Intercept	DBH	Intercept	DBH	Site	Residual	
Leaf area (m^{-2})	6.780850	0.107641	<0.05	<0.05	3.5449	5.6104	0.2853
LMA ($g\,m^{-2}$)	189.151290	−0.151780	<0.05	<0.05	14.9116	31.4880	0.1832
Leaf width/length	0.676246	0.000298	<0.05	<0.05	0.0437	0.0871	0.2009
Leaf ellipticalness index	0.984667	−0.000079	<0.05	>0.05	0.0382	0.0377	0.5065
$\ln W_{1/4L}/W_{3/4L}$	−0.031559	−0.000278	<0.05	<0.05	0.0134	0.1179	0.0128
$\ln W_{1/8L}/W_{7/8L}$	−0.011575	0.000253	>0.05	>0.05	0.0305	0.1977	0.0233
$\ln A_{\text{Left}}/A_{\text{Right}}$	0.027439	0.000183	>0.05	>0.05	0.0224	0.1611	0.0190
Centroid ratio	0.523712	0.000041	<0.05	>0.05	0.0053	0.0692	0.0059

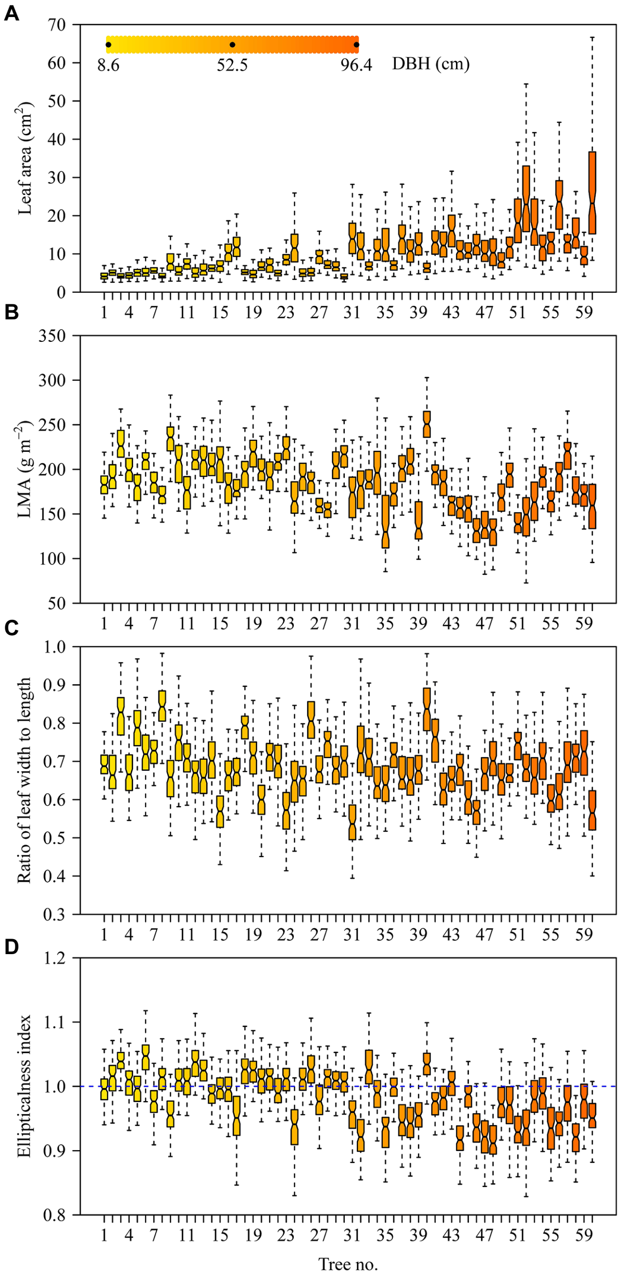

FIGURE 2 | Boxplots of leaf area **(A)**, leaf dry mass per unit area **(B)**, ratio of leaf width to length **(C)**, and leaf ellipticalness index **(D)**. The notches of boxes represent the medians, and the colors of boxes reflect their DBH values (see panel **A**).

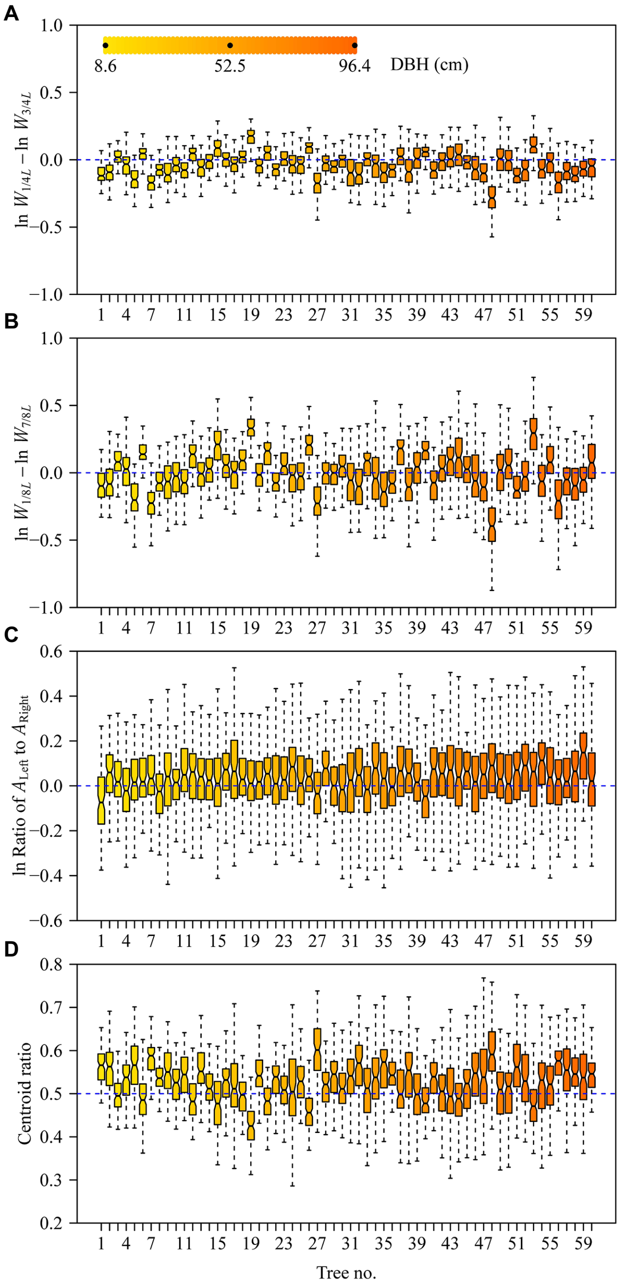

FIGURE 3 | Boxplots of the logarithm of leaf proximal ratio index **(A)**, logarithm of leaf distal ratio index **(B)**, logarithm of the area ratio of the left side to the right side **(C)**, and centroid ratio **(D)**. The notches of boxes represent the medians, and the colors of boxes reflect their DBH values (see panel **A**).

Turning attention to the morphometrics of leaves, it is important to note that LMA reflects the leaf-level cost of light interception (Poorter et al., 2009), and serves as an important indicator of plant ecological strategies (Westoby et al., 2002). A high LMA and long leaf lifespan dimension signifies slow turnover of plant components, long nutrient residence times, and slow response to favorable growth conditions (Westoby et al., 2002). In light of the extreme growth environment of *Q. pannosa*, we speculate that the leaves of this species are typically in a state of water deficiency as a consequence of the comparative narrow vessels in their wood. A drought environment usually correlates with large LMA values (Poorter et al., 2009), and the mean LMA of *Q. pannosa* ranges between 100 and 250 g m^{-2} (**Figure 2B**), which is larger than that previously reported for other evergreen trees, that is, 50–50 g m^{-2} as is reported by Poorter et al. (2009).

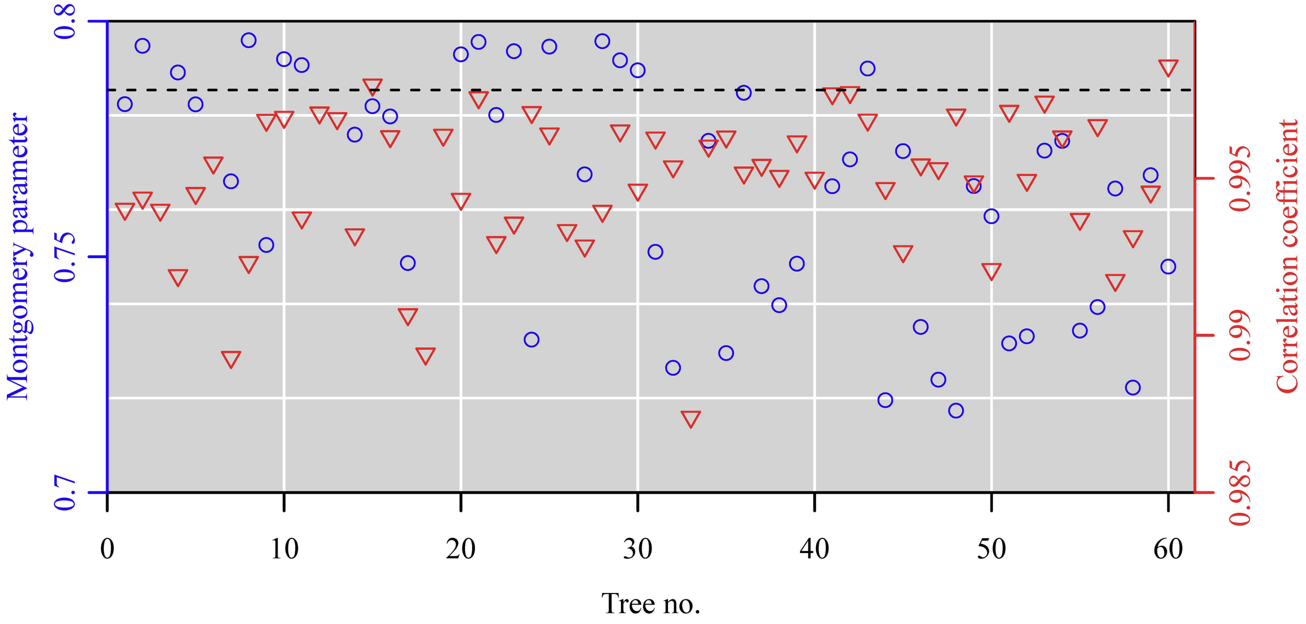

FIGURE 4 | The estimates of the Montgomery parameters (blue open circles) and correlation coefficients (red open lower triangles) for the leaves sampled from each of the 60 trees. Each Montgomery parameter (MP) was estimated as a proportionality coefficient for leaf area = MP × leaf length × length width on a log–log scale, and the correction coefficient was used to reflect the linear degree between leaf area and the product of leaf length and width on a log–log scale.

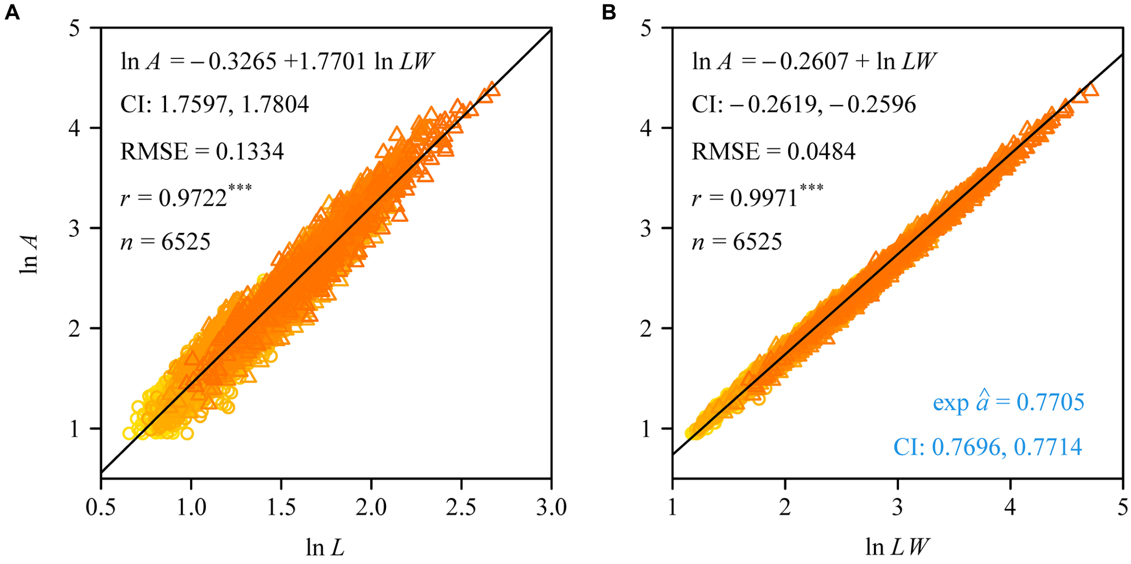

FIGURE 5 | Fitted results to the data of leaf area vs. leaf length **(A)**, and the data of leaf area vs. the product of leaf length and width **(B)**. In panel **(A)**, CI represents the 95% confidence intervals of the slope; in panel **(B)**, CI represents the 95% confidence intervals of the exponential of the intercept, i.e., the Montgomery parameter's CI. RMSE is the root-mean-square error of the linear regression; *r* is the correlation coefficient, with three asterisks indicating $p < 0.001$; *n* is the sample size, i.e., the number of the pooled data.

Our results are inconsistent with those of England and Attiwill (2006) who found that SLA (the reciprocal of LMA) of a *Eucalyptus* species decreases with increasing tree age, which translates in a trend of increasing LMA. The present work shows that LMA decreases with increasing DBH. This can be explained based on the differences in the conduit sizes (vessel diameters) with increasing overall tree size reflecting an adaptation to an extreme alpine environment. Because larger trees have larger mean vessel diameters in their newly formed vessels than smaller trees, water transport in larger

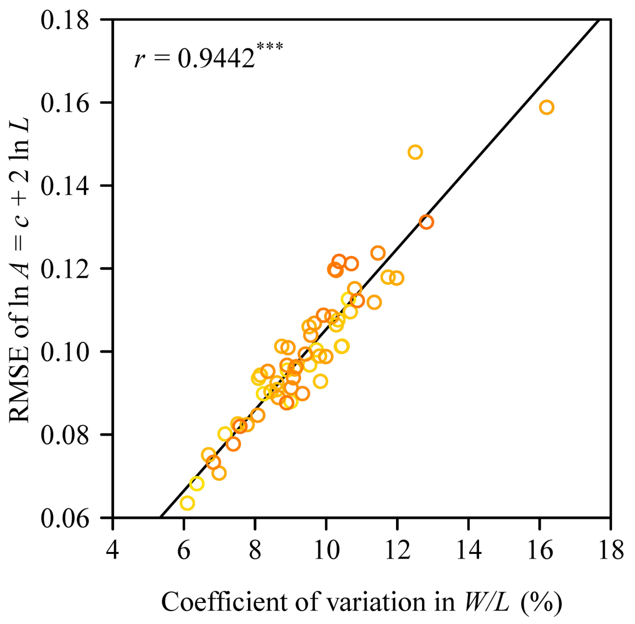

FIGURE 6 | Correlation between the goodness of fit based on the principle of similarity (assuming a square relationship between leaf area and leaf length) and the coefficient of variation in the ratio of leaf width to length. The *y*-label represents the root-mean-square error of the linear regression for the relationship between leaf area and the square of leaf length on a log–log scale; and *r* is the correlation coefficient, with three asterisks indicating $p < 0.001$.

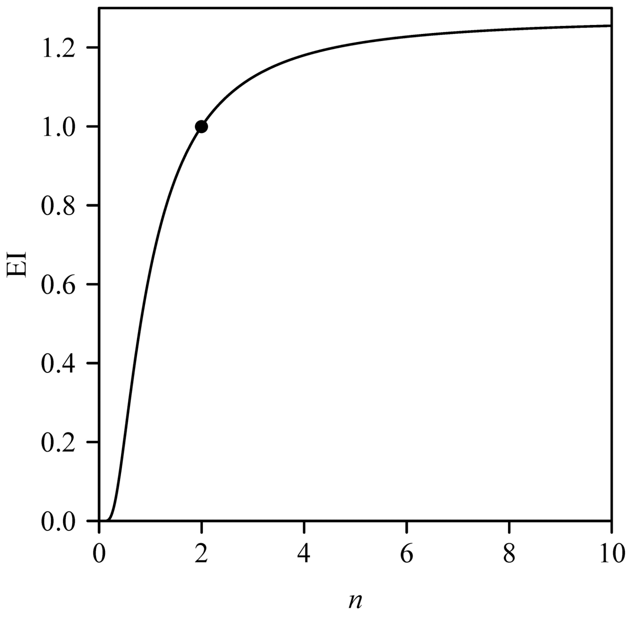

FIGURE 7 | Leaf ellipticalness index (EI) varying with the *n* values in the superellipse. The point corresponds to the EI when $n = 2$.

trees is relatively better than in younger trees, i.e., the leaves of small trees are in a state of water deficiency, and thus have larger LMA values.

Leaf Shape of *Quercus pannosa*

Previous studies have shown that the Montgomery parameter (MP) of most leaves ranges from 1/2 to π/4 (Shi et al., 2019; Yu et al., 2020; Schrader et al., 2021). Even in the case of the oblong and oblate leaf-shapes examined by Schrader et al. (2021), MP tends to be <π/4. However, in the present study, 13 out of a total of 60 MP values were larger than π/4 (**Figure 4**). In addition, most of the mean centroid ratios were numerically >0.5 (**Figure 3D**). These features indicate that the leaf shape of *Q. pannosa* is not a standard ellipse. Indeed, visual inspection (**Figure 2D**) shows that the leaves of this species are not ellipses, a feature that is numerically quantifiable by virtue of the leaf ellipticalness index (EI), which is either >1 or <1. Thus, the leaf-shape of *Q. pannosa* may be a superellipse rather than an ellipse (Gielis, 2003; Li et al., 2021a), as defined by the formula

$$\left|x/\alpha\right|^{n} + \left|y/\beta\right|^{n} = 1,$$

where x and y are the planar coordinates of a superellipse, and n is a parameter determining the shape of the superellipse. The area formula of a superellipse (Huang et al., 2020) is

$$A = \frac{4^{-1/n}\sqrt{\pi}\,\Gamma\left(1+1/n\right)}{\Gamma\left(0.5+1/n\right)} LW,$$

where Γ is the gamma function. With $n \rightarrow \infty$, the superellipse will approximate a rectangle, so MP −>1 and EI −>MP/(π/4) ≈ 1.27. **Figure 7** shows that EI is a sigmoid function of n, and has an asymptotic value. This suggests that *Q. pannosa* might produce approximately superelliptical leaves. In this regard, Li et al. (2021a) have demonstrated the existence of superelliptical leaves in nature for two Magnoliaceae species.

Finally, it is noteworthy that the ratio of leaf width to length (RWL) increases with tree size (**Figure 2C**; **Table 2**), which differs from the leaves produced by other tree species (England and Attiwill, 2006). This phenomenology might be related to water deficiency. The relationship between conduit size and tree size with the corresponding influences on leaf size and shape deserves further investigation.

CONCLUSION

Bigger trees (as measured by DBH) of *Q. pannosa* tend to have larger and broader leaves. The LMAs for the 60 trees are much larger than those reported for other evergreen tree species. We conclude that this phenomenology reflects hydraulic limitations resulting from adaptions to the cold alpine environment in which this species of oak grows. The mean leaf centroid position exceeds the midpoint of leaf length, but the centroid does not shift closer to the leaf apex with increasing tree size. There is no significant difference in the lamina area of the two sides of leaves, which indicates a bilateral symmetry for *Q. pannosa* leaves. The relationship between leaf area and length does not support the principle of similarity, which postulates that the area of an object is proportional to the square of its length. Our results show that the principle of similarity depends on the extent of variation in the ratio of leaf width to length (RWL). A larger coefficient of variation in RWL obtains a larger prediction error when the principle of similarity is used to calculate leaf area. In contrast, the variation in leaf shape does not affect the validity of the Montgomery equation in calculating leaf area based on leaf length and width. The effect of tree size on leaf area can be neglected when using the Montgomery equation could be better related to the altitudes at which *Q. pannosa* grows and its hydraulic limitations resulting from adaptions to the cold alpine environment.

DATA AVAILABILITY STATEMENT

The original contributions presented in the study are included in the article/**Supplementary Material**, further inquiries can be directed to the corresponding author.

AUTHOR CONTRIBUTIONS

JM, KN, and PS designed this work, analyzed the data, and wrote the manuscript. JM, LL, ZF, and YL carried out the experiment. All authors contributed to the article and approved the submitted version.

FUNDING

JM was supported by the Economic Research Center of State Forestry and Grassland Administration of China (No. JYC2020-YN01) and National Natural Science Foundation of China (No. 32171539).

ACKNOWLEDGMENTS

We thank Drolma, Xian Hai, Xu He, and Cong Li for their valuable help in the field investigation. We also thank the associate editor, Raquel Lobo-do-Vale, and two reviewers for their valuable comments.

SUPPLEMENTARY MATERIAL

The Supplementary Material for this article can be found online at: https://www.frontiersin.org/articles/10.3389/fpls.2022.850203/full#supplementary-material

REFERENCES

Bates, D., Mächler, M., Bolker, B. M., and Walker, S. C. (2015). Fitting linear mixed-effects models using lme4. *J. Stat. Softw.* 67, 1–48. doi: 10.18637/jss.v067.i01

Becker, P., Meinzer, F. C., and Wullschleger, S. D. (2000). Hydraulic limitation of tree height: a critique. *Funct. Ecol.* 14, 4–11. doi: 10.1046/j.1365-2435.2000.00397.x

Bielczynski, L. W., Łącki, M. K., Hoefnagels, I., Gambin, A., and Croce, R. (2017). Leaf and plant age affects photosynthetic performance and photoprotective capacity. *Plant Physiol.* 175, 1634–1648. doi: 10.1104/pp.17.00904

England, J. R., and Attiwill, P. M. (2006). Changes in leaf morphology and anatomy with tree age and height in the broadleaved evergreen species, *Eucalyptus regnans* F. *Muell. Trees Struct. Funct.* 20, 79–90. doi: 10.1007/s00468-005-0015-5

Faraway, J. F. (2006). *Extending the Linear Model With R*. Baca Raton, FL, USA: Chapman & Hall/CRC.

Gielis, J. (2003). A general geometric transformation that unifies a wide range of natural and abstract shapes. *Am. J. Bot.* 90, 333–338. doi: 10.3732/ajb.90.3.333

He, J., Chen, W., and Wang, X. (1994). Morphological and anatomical features of *Quercus* section *Suber* and its adaption to the ecological environment. *Acta Phytoecol. Sin.* 18, 219–227.

He, D., and Yan, E.-R. (2018). Size-dependent variations in individual traits and trait scaling relationships within a shade-tolerant evergreen tree species. *Am. J. Bot.* 105, 1165–1174. doi: 10.1002/ajb2.1132

Hsu, P. (1996). *Multiple Comparisons: Theory and Methods*. Boca Raton, FL, USA: Chapman and Hall/CRC.

Huang, W., Li, Y., Niklas, K. J., Gielis, J., Ding, Y., Cao, L., et al. (2020). A superellipse with deformation and its application in describing the cross-sectional shapes of a square bamboo. *Symmetry* 12:2073. doi: 10.3390/sym12122073

Kincaid, D. T., and Schneider, R. B. (1983). Quantification of leaf shape with a microcomputer and Fourier transform. *Can. J. Bot.* 61, 2333–2342. doi: 10.1139/b83-256

Klingenberg, C. P. (2016). Size, shape, and form: concepts of allometry in geometric morphometrics. *Dev. Genes Evol.* 226, 113–137. doi: 10.1007/s00427-016-0539-2

Küppers, M. (1989). Ecological significance of above-ground architectural patterns in woody plants: a question of cost-benefit relationships. *Trends Ecol. Evol.* 4, 375–379. doi: 10.1016/0169-5347(89)90103-1

Li, Y., Niklas, K. J., Gielis, J., Niinemets, Ü., Schrader, J., Wang, R., et al. (2021a). An elliptical blade is not a true ellipse, but a superellipse – evidence from two Michelia species. *J. Fore. Res.* doi: 10.1007/s11676-021-01385-x (in press).

Li, Y., Quinn, B.K., Niinemets, Ü., Schrader, J., Gielis, J., Liu, M., et al. (2021b). *Ellipticalness index — a simple Measure for the Complexity of oval leaf Shape*. *Pak. J. Bot*. doi: 10.30848/PJB2022-6(44) (in press).

Li, Y., Zheng, Y., Ratkowsky, D. A., Wei, H., and Shi, P. (2021c). *Application of an ovate leaf shape model to evaluate leaf bilateral asymmetry and calculate lamina centroid location. Front. Plant Sci. 12*:822907. doi: 10.3389/fpls.2021.822907

Lin, S., Niklas, K. J., Wan, Y., Hölscher, D., Hui, C., Ding, Y., et al. (2020). Leaf shape influences the scaling of leaf dry mass vs. area: a test case using bamboos. *Ann. For. Sci.* 77:11. doi: 10.1007/s13595-019-0911-2

Mayr, S., Cochard, H., Améglio, T., and Kikuta, S. (2007). Embolism formation during freezing in the wood of *Picea abies*. *Plant Physiol.* 143, 60–67. doi: 10.1104/pp.106.085704

Mitteroecker, P., Gunz, P., Windhager, S., and Schaefer, K. (2013). A brief review of shape, form, and allometry in geometric morphometrics, with applications to human facial morphology. *Hystrix Italian J. Mammal.* 24, 59–66. doi: 10.4404/hystrix-24.1-6369

Montgomery, E. G. (1911). "Correlation studies in corn," in *Annual Report no. 24. Agricultural Experimental Station* (Lincoln, NB), 108–159.

Nicotra, A. B., Cosgrove, M. J., Cowling, A., Schlichting, C. D., and Jones, C. S. (2008). Leaf shape linked to photosynthetic rates and temperature optima in South African Pelargonium species. *Oecologia* 154, 625–635. doi: 10.1007/s00442-007-0865-1

Nicotra, A. B., Leigh, A., Boyce, C. K., Jones, C. S., Niklas, K. J., Royer, D. L., et al. (2011). The evolution and functional significance of leaf shape in the angiosperms. *Funct. Plant Biol.* 38, 535–552. doi: 10.1071/fp11057

Niinemets, Ü. (1998). Adjustment of foliage structure and function to a canopy light gradient in two co-existing deciduous trees. Variability in leaf inclination angles in relation to petiole morphology. *Trees Struct. Funct.* 12, 446–451. doi: 10.1007/s004680050173

Niinemets, Ü., Portsmuth, A., and Tobias, M. (2007). Leaf shape and venation pattern alter the support investments within leaf lamina in temperate species, a neglected source of leaf physiological differentiation. *Funct. Ecol.* 21, 28–40. doi: 10.1111/j.1365-2435.2006.01221.x

Niklas, K. J. (1988). The role of phyllotactic pattern as a "developmental constraint," on the interception of light by leaf surfaces. *Evolution* 42, 1–16. doi: 10.1111/j.1558-5646.1988.tb04103.x

Niklas, K. J. (1989). The effect of leaf-lobing on the interception of direct solar radiation. *Oecologia* 89, 59–64.

Niklas, K. J. (1999). A mechanical perspective on foliage leaf form and function. *New Phytol.* 143, 19–31. doi: 10.1046/j.1469-8137.1999.00441.x

Ölçer, H., Lloyd, J. C., and Raines, C. A. (2001). Photosynthetic capacity is differentially affected by reductions in sedoheptulose-1,7-bisphosphatase activity during leaf development in transgenic tobacco plants. *Plant Physiol.* 125, 982–989. doi: 10.1104/pp.125.2.982

Peppe, D. J., Royer, D. L., Gariglino, B., Oliver, S. Y., Newman, S., Leight, E., et al. (2011). Sensitivity of leaf size and shape to climate: global patterns and paleoclimatic applications. *New Phytol.* 190, 724–739. doi: 10.1111/j.1469-8137.2010.03615.x

Poorter, H., Niinemets, Ü., Poorter, L., Wright, I. J., and Villar, R. (2009). Causes and consequences of variation in leaf mass per area (LMA): a meta-analysis. *New Phytol.* 182, 565–588. doi: 10.1111/j.1469-8137.2009.02830.x

R Core Team (2022). R: A Language and Environment for Statistical Computing. Vienna: R Foundation for Statistical Computing. Available at: https://www.r-project.org/ (Accessed October 10, 2020).

Royer, D. L., and Wilf, P. (2006). Why do toothed leaves correlate with cold climates? Gas exchange at leaf margins provides new insights into a classic paleotemperature proxy. *Int. J. Plant Sci.* 167, 11–18. doi: 10.1086/497995

Sack, L., Melcher, P. J., Liu, W. H., Middleton, E., and Pardee, T. (2006). How strong is intracanopy leaf plasticity in temperate deciduous trees? *Am. J. Bot.* 93, 829–839. doi: 10.3732/ajb.93.6.829

Santiago, L. S., and Kim, S.-C. (2009). Correlated evolution of leaf shape and physiology in the woody *Sonchus* alliance (Asteraceae: Sonchinae) in Macaronesia. *Int. J. Plant Sci.* 170, 83–92. doi: 10.1086/593044

Schrader, J., Shi, P., Royer, D. L., Peppe, D. J., Gallagher, R. V., Li, Y., et al. (2021). Leaf size estimation based on leaf length, width and shape. *Ann. Bot.* 128, 395–406. doi: 10.1093/aob/mcab078

Shi, P., Gielis, J., and Quinn, B. K. (2022a). biogeom: Biological Geometries. R package version 1.0.5. Available at: https://CRAN.R-project.org/package=biogeom (Accessed May 12, 2022).

Shi, P., Liu, M., Ratkowsky, D. A., Gielis, J., Su, J., Yu, X., et al. (2019). Leaf area-length allometry and its implications in leaf-shape evolution. *Trees Struct. Funct.* 33, 1073–1085. doi: 10.1007/s00468-019-01843-4

Shi, P., Miao, Q., Niinemets, Ü., Liu, M., Li, Y., Yu, K., et al. (2022b). Scaling relationships of leaf vein and areole traits versus leaf size for nine Magnoliaceae species differing in venation density. *Am. J. Bot.* doi: 10.1002/ajb2.1856 (in press).

Shi, P., Ratkowsky, D. A., Li, Y., Zhang, L., Lin, S., and Gielis, J. (2018). A general leaf area geometric formula exists for plants—eidence from the simplified Gielis equation. *Forests* 9:4. doi: 10.3390/f9110714

Shi, P., Yu, K., Niinemets, Ü., and Gielis, J. (2021a). Can leaf shape be represented by the ratio of leaf width to length? Evidence from nine species of *Magnolia* and *Michelia* (Magnoliaceae). *Forests* 12:41. doi: 10.3390/f12010041

Shi, P., Yu, K., Niklas, K. J., Schrader, J., Song, Y., Zhu, R., et al. (2021b). A general model for describing the ovate leaf shape. *Symmetry* 13:1524. doi: 10.3390/sym13081524

Su, J., Niklas, K. J., Huang, W., Yu, X., Yang, Y., and Shi, P. (2019). Lamina shape does not correlate with lamina surface area: an analysis based on the simplified Gielis equation. *Glob. Ecol. Conserv.* 19:e00666. doi: 10.1016/j.gecco.2019.e00666

Thomas, S. C., and Bazzaz, F. A. (1996). Elevated CO_2 and leaf shape: are dandelions getting toothier? *Am. J. Bot.* 83, 106–111. doi: 10.1002/j.1537-2197.1996.tb13882.x

Thompson, D. W. (1917). *On Growth and Form*. London: Cambridge University Press.

Westoby, M., Falster, D. S., Moles, A. T., Vesk, P. A., and Wright, I. J. (2002). Plant ecological strategies: some leading dimensions of variation between species. *Annu. Rev. Ecol. Syst.* 33, 125–159. doi: 10.1146/annurev.ecolsys.33.010802.150452

Yang, Y., Sun, H., and Körner, C. (2020). Explaining the exceptional 4270 m high elevation limit of an evergreen oak in th South-Eastern Himalayas. *Tree Physiol.* 40, 1327–1342. doi: 10.1093/treephys/tpaa070

Yu, X., Hui, C., Sandhu, H. S., Lin, Z., and Shi, P. (2019). Scaling relationships between leaf shape and area of 12 Rosaceae species. *Symmetry* 11:1255. doi: 10.3390/sym11101255

Yu, X., Shi, P., Schrader, J., and Niklas, K. J. (2020). Nondestructive estimation of leaf area for 15 species of vines with different leaf shapes. *Am. J. Bot.* 107, 1481–1490. doi: 10.1002/ajb2.1560

Conflict of Interest: The authors declare that the research was conducted in the absence of any commercial or financial relationships that could be construed as a potential conflict of interest.

frontiers | Frontiers in Plant Science

ORIGINAL RESEARCH
published: 16 June 2022
doi: 10.3389/fpls.2022.894690

No Consistent Shift in Leaf Dry Mass per Area Across the Cretaceous—Paleogene Boundary

Matthew J. Butrim[1,2]*, Dana L. Royer[1], Ian M. Miller[3], Marieke Dechesne[4], Nicole Neu-Yagle[3], Tyler R. Lyson[3], Kirk R. Johnson[5] and Richard S. Barclay[5]

[1] Department of Earth and Environmental Sciences, Wesleyan University, Middletown, CT, United States, [2] Department of Geology and Geophysics and Program in Ecology, University of Wyoming, Laramie, WY, United States, [3] Department of Earth Sciences, Denver Museum of Nature and Science, Denver, CO, United States, [4] U. S. Geological Survey, Denver, CO, United States, [5] Department of Paleobiology, Smithsonian Institution, National Museum of Natural History, Washington, DC, United States

The Chicxulub bolide impact has been linked to a mass extinction of plants at the Cretaceous—Paleogene boundary (KPB; ~66 Ma), but how this extinction affected plant ecological strategies remains understudied. Previous work in the Williston Basin, North Dakota, indicates that plants pursuing strategies with a slow return-on-investment of nutrients abruptly vanished after the KPB, consistent with a hypothesis of selection against evergreen species during the globally cold and dark impact winter that followed the bolide impact. To test whether this was a widespread pattern we studied 1,303 fossil leaves from KPB-spanning sediments in the Denver Basin, Colorado. We used the relationship between petiole width and leaf mass to estimate leaf dry mass per area (LMA), a leaf functional trait negatively correlated with rate of return-on-investment. We found no evidence for a shift in this leaf-economic trait across the KPB: LMA remained consistent in both its median and overall distribution from approximately 67 to 65 Ma. However, we did find spatio-temporal patterns in LMA, where fossil localities with low LMA occurred more frequently near the western margin of the basin. These western margin localities are proximal to the Colorado Front Range of the Rocky Mountains, where an orographically driven high precipitation regime is thought to have developed during the early Paleocene. Among these western Denver Basin localities, LMA and estimated mean annual precipitation were inversely correlated, a pattern consistent with observations of both fossil and extant plants. In the Denver Basin, local environmental conditions over time appeared to play a larger role in determining viable leaf-economic strategies than any potential global signal associated with the Chicxulub bolide impact.

Keywords: Cretaceous—Paleogene boundary, leaf mass per area (LMA), mass extinction, paleobotanical analysis, Denver Basin, Williston Basin, leaf economic spectrum (LES), Castle Rock

Edited by:
Julian Schrader,
University of Göttingen, Germany

Reviewed by:
Harald Schneider,
Xishuangbanna Tropical Botanical Garden (CAS), China
Keith Berry,
Hoehne School District RE-3, United States

***Correspondence:**
Matthew J. Butrim
mbutrim@uwyo.edu

Specialty section:
This article was submitted to Functional Plant Ecology, a section of the journal Frontiers in Plant Science

Received: 12 March 2022
Accepted: 10 May 2022
Published: 16 June 2022

Citation:
Butrim MJ, Royer DL, Miller IM, Dechesne M, Neu-Yagle N, Lyson TR, Johnson KR and Barclay RS (2022) No Consistent Shift in Leaf Dry Mass per Area Across the Cretaceous—Paleogene Boundary. Front. Plant Sci. 13:894690. doi: 10.3389/fpls.2022.894690

INTRODUCTION

More than 50% of plant species in mid-continental North America went extinct at the Cretaceous—Paleogene boundary (KPB; ~66 Ma; Wilf and Johnson, 2004; Nichols and Johnson, 2008; Lyson et al., 2019) in a mass extinction linked to the Chicxulub bolide impact (Alvarez et al., 1980; Vellekoop et al., 2014; Hull et al., 2020) and concurrent volcanism from the Deccan Traps (Courtillot et al., 1986; Schoene et al., 2019; Sprain et al., 2019). This event also caused the total extinction of non-avian dinosaurs (Le Loeuff, 2012) and led to significant ecological selection on insects and mammals (Labandeira et al., 2002; Grossnickle and Newham, 2016).

The nature of ecological selection on plants is less understood. Extinction at the family level was negligible (Cascales-Miñana et al., 2018), and angiosperm dominated ecosystems were already well established by the Late Cretaceous (i.e., Johnson et al., 2003; Carvalho et al., 2021), raising the question of how the mass extinction caused functional changes in plant communities, if at all. One hypothesis suggests that an impact winter triggered by the bolide favored deciduous plants (Wolfe and Upchurch, 1986; Wolfe, 1987). Impact generated aerosols could have imposed a regime of global dim light and low atmospheric temperatures for months to years (Vellekoop et al., 2014), giving deciduous plants, naturally disposed to periods of dormancy, a competitive advantage over their evergreen counterparts.

The signal for a shift toward deciduous strategies is difficult to pick up in the fossil record. However, a proxy for estimating the functional trait leaf dry mass per area (LMA) is well suited for making inference about shifts in plant strategy, including between deciduous and evergreen leaf habit (Royer et al., 2007). This is because LMA estimates can be mapped onto the leaf economics spectrum (LES), a continuum of viable leaf strategies that reflects tradeoffs in leaf resource allocation (Wright et al., 2004). One end of the LES represents fast-return strategies, which are manifested as thin, flimsy leaves (low LMA) that trade a short leaf lifespan (often deciduous) for high rates of photosynthesis. The other end of the LES represents slow-return strategies, manifested as thick, tough, long-lived leaves (high LMA), that due to a low rate of photosynthesis only slowly make a return on their initial carbon investment. These trait relationships are robust across the angiosperm phylogeny and although particular clades can have distinctive trait values (Ackerly and Reich, 1999), including LMA (Cornwell et al., 2014), the same fundamental leaf economic tradeoffs still occur (Wright et al., 2004). Thus, even in a mass extinction scenario in which there was significant taxonomic turnover, shifts in trait values represent shifts in leaf economic strategies.

Within this leaf economic framework, Blonder et al. (2014) studied Late Cretaceous and early Paleocene fossil plant localities from the Williston Basin, North Dakota (**Figure 1**), and found evidence for a loss of slow-return, high LMA species across the KPB; Wilson Deibel (2022) reports similar patterns further west in the basin. Both studies interpret their results to represent the increased survival of fast-return, likely deciduous, plants in response to an impact winter. This theory, reliant on a global-scale change in environment, suggests a global response. However, recent studies indicate that the angiosperm trait response to the mass-extinction event was geographically heterogeneous, highlighting different responses between South American floras and the North American Williston Basin flora (Stiles et al., 2020; Carvalho et al., 2021). Further, other hypotheses of selection across the KPB connect survival to traits not explicitly linked to the LES, such as non-recalcitrant seeds (Berry, 2020) and polyploidy (Fawcett et al., 2009; Moeglein et al., 2020; Wei et al., 2020).

In light of these recent findings, we test whether the shift toward fast-return strategies observed in the Williston Basin represents a common response to the global effects of the bolide impact. Following Blonder et al. (2014) we use LMA estimates to position fossil plant communities preserved in KPB-spanning sediments of the Denver Basin, Colorado (**Figure 1**) along the LES. The Denver Basin fossil record complements the Williston Basin well and offers new opportunities for interpreting LMA and the broader LES across the KPB. First, while the Late Cretaceous fossil record in the Williston Basin is better represented than the Paleocene record (Wilf and Johnson, 2004), the reverse is true in the Denver Basin (Johnson et al., 2003). Second, the Paleocene flora of the Williston Basin consists of a homogeneous low-diversity, basin-center flora within a broad, low-relief coastal plain (Johnson, 2002). In contrast, the synorogenic, KPB-spanning sediments in the Denver Basin, which were deposited adjacent to and during the uplift of the Colorado Front Range of the Rocky Mountains, contain a heterogeneous flora that includes both low-diversity basin-center localities and high-diversity mountain-proximal localities (Johnson et al., 2003). While the flora in the center of the Denver Basin provides a close taxonomic and ecological analog to the flora of the Williston Basin (i.e., the "Fort Union Flora," see Nichols and Johnson, 2008), the mountain proximal flora provides an opportunity to evaluate the ecological strategies and responses of different plant assemblages, such as the early rainforest flora at Castle Rock (Johnson and Ellis, 2002).

To understand trans-KPB shifts in LMA in the Denver Basin, we evaluate four scenarios following Blonder et al. (2014). These are (1) directional shift—a shift in LMA space associated with a shift in environmental conditions; (2) convergence—a narrowing in LMA space associated with a loss of viability of ecological strategies; (3) divergence—a widening in LMA space associated with the appearance of new environmental conditions supporting newly viable strategies; and (4) a lack of environmental filtering—no significant changes in LMA expression because environmental changes are unrelated to LMA. In the Williston Basin, the loss of slow-return strategies was a combination of a directional shift and a convergence toward low LMA values (Blonder et al., 2014). If this represents a global response to the bolide impact, the Denver Basin flora should also exhibit a downward directional shift and a convergence in LMA space across the KPB, regardless of taxonomic and environmental differences between the basins. A KPB spanning subset of 39 localities in the Corral Bluffs study area of the Denver Basin (**Figure 1**) showed a moderate downward shift in both minimum and maximum LMA values but no significant shift in median LMA (Lyson et al., 2019), leaving it unresolved whether plant communities in the Denver Basin responded similarly to those in the Williston Basin. We present here a Denver Basin LMA analysis on a larger scale, spanning four million years across the KPB and ranging from the low-diversity basin center to the taxonomically and environmentally diverse floras of the Denver Basin's mountain proximal western margin.

MATERIALS AND METHODS

Data Sources

We estimated LMA on 1,303 fossil leaves from 95 localities in the Denver Basin (paleolatitude: ∼44–46° N;

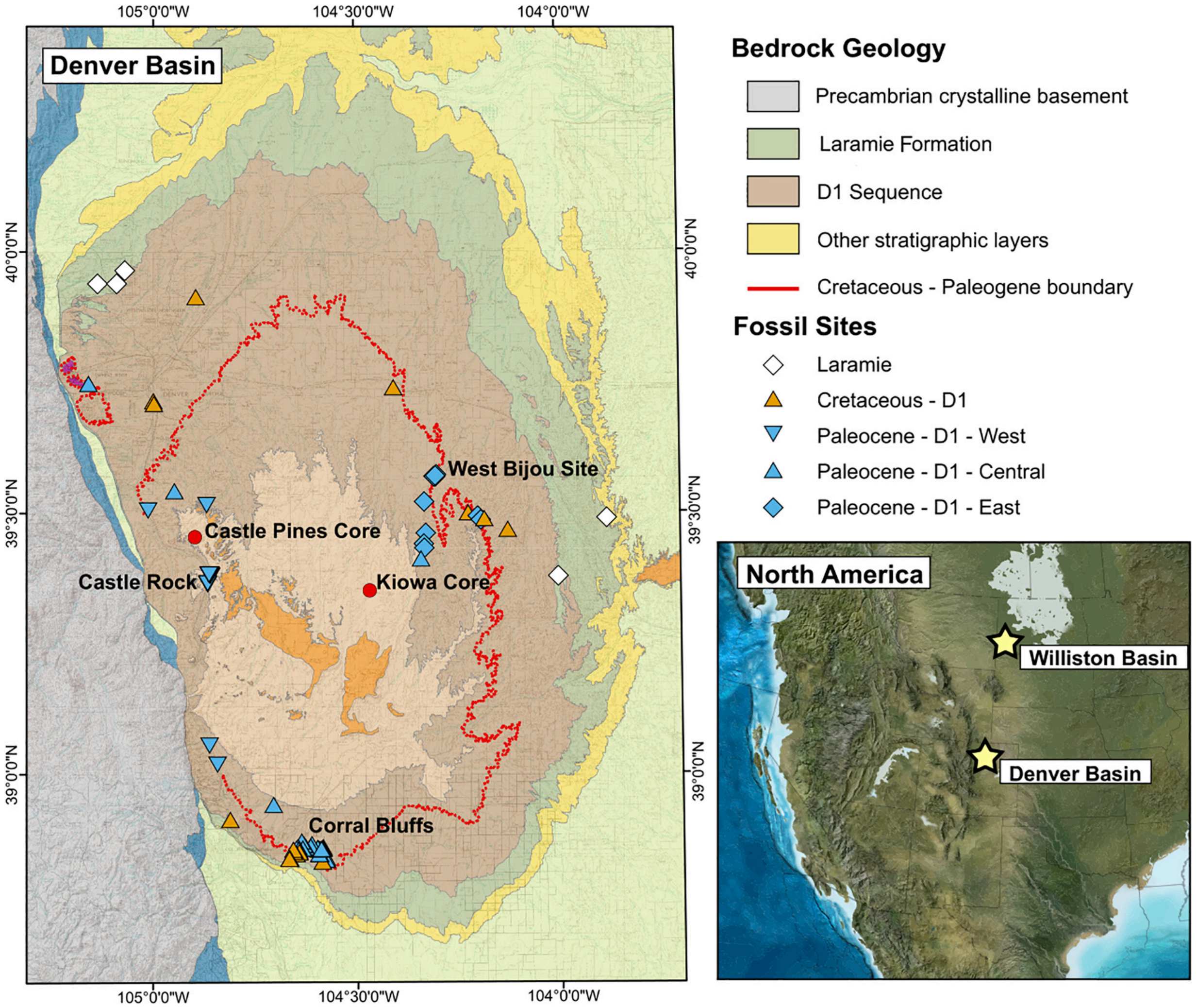

FIGURE 1 | Bedrock geology of the Denver Basin (modified from Dechesne et al., 2011) and locations of megafloral fossil sites. The D1 Sequence in yellow and the Laramie Formation in pink are the two fossil-bearing sediments considered in this study. The inset map [Paleogeography of the North America Western Interior at the KPB, from Ron Blakely, Colorado Plateau Geosystems, Arizona, United States (http://cpgeosystems.com/paleomaps.html)] shows the relative position of the Williston and Denver Basins; the stars are in the general region of the fossil sites used from each basin.

Van Hinsbergen et al., 2015), representing 551 species-site pairs. All measured leaves come from woody dicot angiosperms. Common taxa were described and many of the individual localities were listed by Johnson et al. (2003), with the remaining localities collected subsequently by the Denver Museum of Nature and Science (DMNS). The chronology of the Denver Basin is well constrained, with U-Pb dates for the KPB (66.021 ± 0.024 Ma) and the magnetochron boundaries C28 n through C30 n taken from the 688 m long Kiowa core near the center of the basin and along the West Bijou Creek escarpment (Clyde et al., 2016; **Figure 1**); individual localities within the basin can be constrained to ∼100 k.y. time bins or finer using radiometric dates and magnetochron boundaries (e.g., Clyde et al., 2016), combined with correlations between the Kiowa core, oil and water well logs throughout the basin, and surface outcrops (Raynolds et al., 2007; Dechesne et al., 2011). Many localities can be further constrained to ∼10 k.y. time bins by local sedimentation rates and a biostratigraphic framework derived from pollen, megaflora, and vertebrate fossils (Hicks et al., 2003; Johnson et al., 2003; Raynolds et al., 2007; Clyde et al., 2016; Lyson et al., 2019; see **Supplementary Material** for site age errors).

The measured fossils come from the Late Cretaceous Laramie Formation (∼69–68 Ma) and the KPB spanning D1 sequence of the Denver Basin Group (∼68–63.8 Ma; Johnson et al., 2003). The Laramie Formation consists of coal-bearing, backswamp floodplain facies associated with the withdrawal of the Western Interior Seaway (Raynolds and Johnson, 2003). The D1 sequence is an unconformity-bounded, synorogenic sedimentary package that contains the Arapahoe Formation (or Conglomerate; Raynolds, 2002), the Denver Formation, and the lower Dawson Formation (or Arkose). These interfingering formations, which were deposited adjacent to and during the uplift of the Colorado Front Range (Raynolds and Johnson, 2003), preserve floodplain facies deposited in environments that range from well- to poorly drained.

Cretaceous sediments of the D1 sequence are under-sampled compared to Paleocene sediments and contain a diverse and spatially heterogeneous flora (Johnson et al., 2003; Raynolds et al., 2007). As a result the characteristics of this flora are not fully understood, but it contains many species that appear to go extinct after the KPB, as well as many species also found in Cretaceous sediments of the Williston Basin (Johnson et al., 2003; Lyson et al., 2019).

Paleocene sediments of the D1 sequence are highly sampled and spatially heterogeneous. Much of the heterogeneity of the flora can be observed across a west-to-east profile shaped by proximity to the Colorado Front Range (Barclay et al., 2003; Ellis et al., 2003; Johnson et al., 2003). Based on this observation, Johnson et al. (2003) binned localities into three megafloral associations defined by geographic and stratigraphic occurrence (**Figure 1**): P-D1-West, P-D1-Central, and P-D1-East ("P" for Paleocene, "D1" for D1-sequence).

The P-D1-West floral association occurs in a narrow geographic band along the western margin of the basin close to the Front Range, and is generally found in high-energy floodplain systems associated with alluvial fans suggesting local topographic complexity. This association typically contains diverse floras with large leaves. A noteable site that falls within the P-D1-West association is Castle Rock (63.84 Ma; DMNH loc. 1,200, 2,689, 2,690, 2,698, 2,699, 2,716, 2,720, 2,723, 2,731, 2,733, 2,748, 2,763, 2,801, 2,802, 2,831, 2,966, 2,967, 2,968, 2,969, 2,994; Kowalczyk et al., 2018), an autochthonous leaf litter deposit which has been interpreted as an early Paleocene rainforest (Ellis and Johnson, 2013) very near to the Front Range (Ellis et al., 2003). The nearby Plum Creek Parkway (DMNH loc. 3,613, 3,618, 3,620) and Sick of Sycamores (DMNH loc. 2,339) localities (63.84 and ∼63.8 Ma, respectively) are not quite as diverse or as strongly diagnostic of rainforest physiognomies as Castle Rock, but are considered coeval floras found in different depositional settings on the floodplain (Ellis et al., 2003; Ellis and Johnson, 2013).

The P-D1-East floral association occurs in the eastern exposures of the basin, furthest from the Front Range. These localities are found in low-energy fluvial, lacustrine, or paludal systems indicating low paleo-relief, and the flora is typically low diversity (Barclay et al., 2003). The P-D1-East association shares a close taxonomic affinity with the Paleocene flora of the Williston Basin (Johnson et al., 2003) and is sometimes referred to as part of a widespread early Paleocene "Fort Union flora" (Nichols and Johnson, 2008), components of which can be found in similar swampy environments from the nearby Raton Basin (Wolfe and Upchurch, 1987) to the Ravenscrag Formation in Saskatchewan (West et al., 2021). Compared to the rest of the Paleocene D1, P-D1-East localities are sparse and do not represent as large of a temporal range, with most localities found nearer to the KPB (Johnson et al., 2003).

Last, the P-D1-Central floral association, while appearing geographically close to the western basin margin, is far enough from the Front Range that deposits are lower energy than the alluvial fan deposits characteristic of the P-D1-West floodplain systems. These P-D1-Central localities vary from low to high diversity and generally represent an intermediate flora with a smaller leaf size than is seen in the P-D1-West association but without the uniformly low diversity seen in the P-D1-East association. The Paleocene sites in the Corral Bluffs study area considered by Lyson et al. (2019; **Figure 1**) are part of the P-D1-Central association.

To evaluate changes across the KPB, we compared the Cretaceous D1 sequence floras (67.5–66.02 Ma; $n = 17$ localities) to the Paleocene D1 sequence floras that occur during the first one million years after the KPB (herein referred to as the "early Paleocene D1" flora; 66.02–65.02 Ma; $n = 44$). This categorization excludes the older Laramie Formation ($n = 5$) from the Cretaceous bin, and 29 younger Paleocene localities from between 64.75 and 63.8 Ma, including Castle Rock, from the Paleocene bin, resulting in a relatively continuous temporal sequence of measured fossils comparable in age range to fossils measured in the Williston Basin by Blonder et al. (2014).

Morphotypes

The Denver Basin flora was initially classified with the morphotype method developed by Johnson (1989), using a separate set of morphotypes for five different study areas in the basin (Castle Rock—CR, Scotty's Palm—SP, West Bijou Site—BC, Laramie Formation—LA, the remainder—JC; Johnson and Ellis, 2002; Barclay et al., 2003; Ellis et al., 2003; Johnson et al., 2003). The DMNS later partially integrated the five study areas into a single set of morphotypes covering the entire basin (Denver Basin—DB). The most common of these morphotypes were assigned to species and are typically found throughout the Denver Basin and sometimes in the Williston Basin as well (Johnson, 2002). The DMNS also made substantial collections at the Corral Bluffs study area in 2017 and 2018 (Lyson et al., 2019). These fossils have been assigned to a new morphotype series (Colorado Springs—CS) but are not integrated within the basin-wide DB system. Finally, a number of less-productive localities, along with many collected after Johnson et al. (2003), have not been integrated into either the DB or study area morphotype systems. Fossils from these localities have instead been assigned bin numbers, which are locality-specific classifications based on taxonomically important morphological characters (Ellis et al., 2009). Combined, the quality of taxonomy across these collections enables the analysis of morphospecies-site pairs (herein referred to as species-site pairs) with the understanding that bin numbers are not significant beyond their locality and that the morphotype series are only significant among the localities that the associated study area is comprised of.

Leaf Mass per Area Measurements

LMA estimates were made using the petiole width proxy of Royer et al. (2007), which depends on the mechanical relationship between the cross-sectional area of the petiole and leaf mass. We digitally photographed fossils at the DMNS using a Nikon D5300 digital camera with an af-s micro Nikkor 40 mm 1:2.8 g macrophotography lens, except for fossils from Castle Rock,

FIGURE 2 | An example of leaf dry mass per area (LMA) estimation. Petiole width (0.07 cm) was measured at the pink line; leaf area (12.3 cm^2) was estimated with a conservative reconstruction of the leaf apex. LMA = 60.5 g/m^2. Morphotype DB396, EPI 53397. Baptist Road DMNH 2177 (65.7 Ma). Scale bar = 1 cm.

which DMNS staff photographed using a Canon EOS Mark 5 d digital camera and 100 mm lens. We selected fossils with the petiole preserved widthwise at the base of the leaf blade and with enough of the leaf margin intact that we could confidently reconstruct the complete leaf area (**Figure 2**). Image manipulation and measurements were both done in Adobe Photoshop following Royer et al. (2007). Petiole width (PW) was measured with the ruler tool at the basal-most point of intersection between the petiole and the leaf blade. Leaf area (LA) was measured by tracing the margin of the leaf blade and petiole with the polygonal lasso tool, reconstructing any missing margin along the way, and then computing area with the measurement log toolbar (**Figure 2**). LMA was estimated with the linear regression derived by Royer et al. (2007) from a large set of leaves from 468 extant woody dicot species (Equation 1). 95% prediction intervals for each species site pair were derived following Sokal and Rohlf (2012) using the equation and coefficients provided by Royer et al. (2007; their Table 2). See **Supplementary Material** for all measurements.

$$\log_{10}\text{LMA} = 3.070 + 0.382 \times \log_{10}\left(\frac{\text{PW}^2}{\text{LA}}\right) \tag{1}$$

Climate Estimates

Estimates of mean annual temperature (MAT) and mean annual precipitation (MAP) for 77 and 11 localities respectively, come from previous reports (Ellis et al., 2003; Johnson et al., 2003; Lyson et al., 2019; see **Supplementary Material**). All MAT estimates used Wilf (1997) regression and all MAP estimates come from Johnson et al. (2003), preserving methodological continuity between locality climate estimates.

Statistical Analysis

The significance of directional shifts in LMA was tested using the Mann-Whitney *U*-test, a non-parametric test of the null hypothesis that populations have the same median, and the Kolmogorov-Smirnov two-sample-test, a non-parametric test of the null hypothesis that two samples have an identical distribution (Sokal and Rohlf, 2012). The significance of convergence or divergence of LMA between sites was assessed using the Brown-Forsythe test, a non-parametric test of the null hypothesis that two samples have equal variance (Sokal and Rohlf, 2012).

Comparison With Williston Basin

We also considered the 608 leaves representing 309 species-site pairs from the Williston Basin published by Blonder et al. (2014). Some morphotypes present in both basins have palmate venation with primary veins that converge beneath the point where the leaf margin intersects the outermost primary veins (**Figure 3**). Blonder et al. (2014) measured PW where the margin intersects these primaries; However, in many of these leaves, the primary veins are still separated from each other by laminar tissue at this point of intersection, causing an overestimation of PW and thus LMA. For this study, we measured PW directly below the point at which the primary veins fully converged. The difference in estimated LMA between these two methods was sometimes large, with the most extreme differences in excess of 100 g/m^2 (**Figure 4**). Thus to better compare the two data sets, we remeasured all leaves from Williston Basin morphotypes with the described vein architecture, plus one morphotype with lamina along the length of the petiole that was previously included

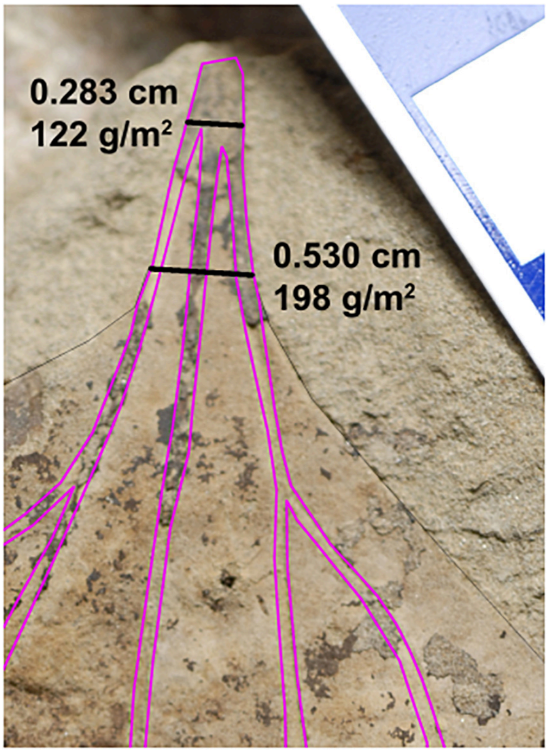

FIGURE 3 | Representative revision from the Williston Basin. The two black lines are the revised petiole width measurement used in this study (top) and original measurement of Blonder et al. (2014) (bottom). Primary and secondary veins are traced with magenta lines. For each number pair, the top number is the petiole width and bottom is the estimated leaf dry mass per area. Morphotype HC162, *Marmarthia pearsonii,* DMNH 21687. Scale bar = 1 cm.

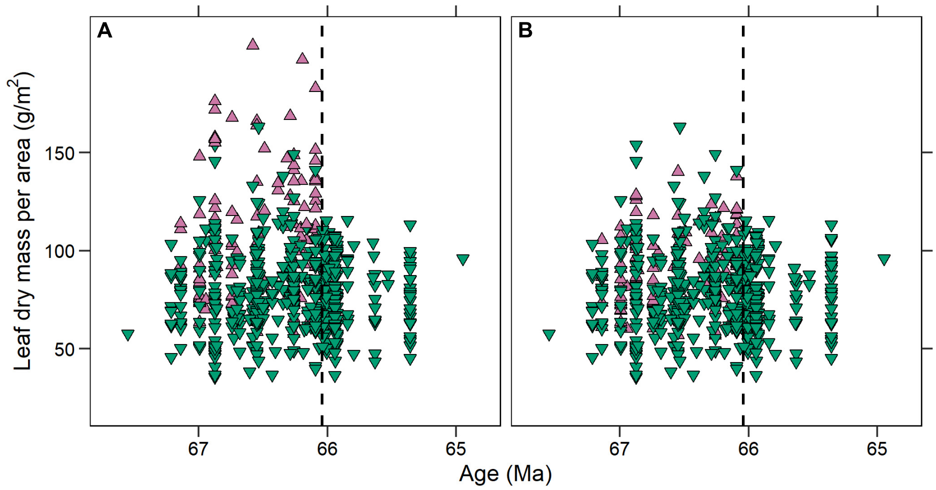

FIGURE 4 | Individual leaf dry mass per area (LMA) estimates for the Williston Basin **(A)** before and **(B)** after revision. Upward facing purple triangles represent fossils that we measured again. The convergence in LMA space across the Cretaceous—Paleogene boundary (black dashed line) observed by Blonder et al. (2014) is still apparent after revision, although the loss of high-LMA leaves is less stark.

in the PW measurement (see **Supplementary Material**). We also removed morphotypes that Blonder et al. (2014) labeled herbaceous, because they require a different LMA regression, and because we solely focused on woody angiosperms in the Denver Basin. All comparisons to the Williston Basin use the revised LMA estimates.

In Blonder et al. (2014), Williston Basin sites were plotted by stratigraphic distance (m) from the KPB. In order to compare with the Denver Basin, we applied an age model based on an assumption of constant sedimentation rates between the KPB and magnetochron boundaries C30 n/C29 r and C29 r/C29 n (Hicks et al., 2002; Wilf et al., 2003). Boundary ages come from the GPTS (Gradstein et al., 2012). This results in a chronological range of fossils between ~67.6 and 64.9 Ma.

RESULTS

Basin-Wide Trends: Leaf Mass per Area at the Cretaceous-Paleogene Boundary

We found no statistically significant differences in LMA between species-site pairs in the Denver Basin's Cretaceous D1 and early Paleocene D1 sediments (orange vs. blue symbols in **Figure 5A**). The median species-site pair LMA in Cretaceous D1 sediments (77.2 g/m^2; $n = 108$) was not significantly different from the median species-site pair LMA in early Paleocene D1 sediments (72.4 g/m^2; $n = 196$; $p = 0.13$). The distribution of species-site pairs in LMA did not significantly change across the KPB ($p = 0.08$), nor did the bounds of available LMA space as expressed by population variance ($p = 0.15$).

We estimated LMA of five KPB crossing morphotypes found in both Cretaceous and Paleocene sediments of the Denver Basin (**Table 1**). In the Cretaceous, the mean LMA of these boundary crossers ranged from 56.9 to 103.5 g/m^2, suggesting that species occupying both the faster and slower-return ends of the LES survived the mass extinction. Similarly in the Paleocene the boundary crossers ranged from 48.4 to 104.2 g/m^2, again spanning both ends of the spectrum. From the Cretaceous to the Paleocene, two of these morphotypes increased in LMA, while the other three decreased, but in all cases the 95% prediction intervals for the Cretaceous and Paleocene populations overlap suggesting that among the species that survived there was no unified leaf-economic response.

In the revised Williston Basin dataset (**Figure 5B**; see also section "Materials and Methods"), there was no significant shift ($p = 0.19$) in median LMA between the Cretaceous (83.0 g/m^2; $n = 237$) and Paleocene (82.3 g/m^2; $n = 62$) or in the distribution of LMA values ($p = 0.12$). Variance in LMA space however, decreased significantly across the KPB ($p = 0.02$); additionally, no Paleocene species-site pair had LMA greater than 110 g/m^2, a level commonly exceeded in the Cretaceous (**Figure 5B**). Our analysis of revised measurements thus supports the original interpretation of Blonder et al. (2014) of a convergence in LMA space in the Paleocene.

In comparison with the Williston Basin, species-site pairs from the Denver Basin had significantly lower LMA in both the Cretaceous and Paleocene by median (respectively, $p = 0.006$; $p = 0.005$) and distribution ($p = 0.04$; $p = 0.007$). Variance in LMA space did not significantly differ between the two basins in either the Cretaceous ($p = 0.54$) or the Paleocene ($p = 0.19$). Despite the generally lower LMA of species-site pairs from the Denver Basin Paleocene, we observed nine with LMA exceeding the ceiling of 110 g/m^2 observed in the Williston Basin Paleocene.

Influence of Denver Basin Geography on Temporal Patterns

We observed different temporal responses in LMA among the three megafloral associations of the Paleocene D1 sequence (**Figure 6**). In the P-D1-West association, along the western

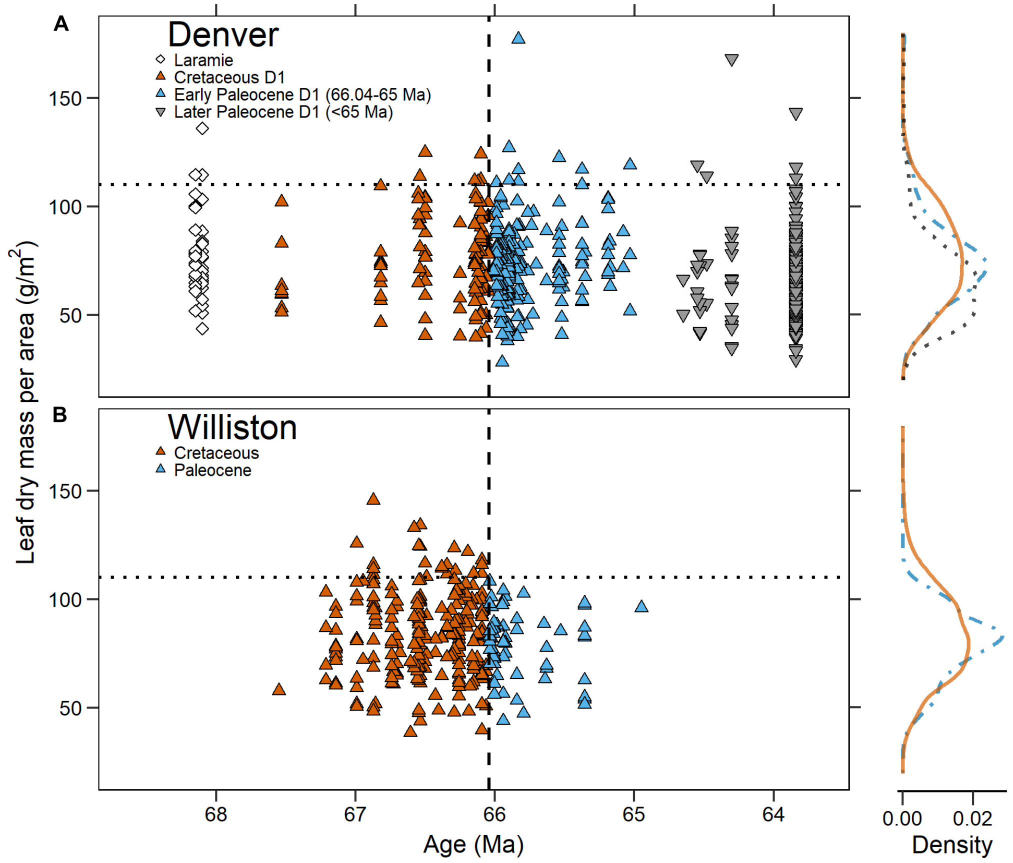

FIGURE 5 | Mean leaf dry mass per area (LMA) of species-site pairs plotted against time in the **(A)** Denver Basin and **(B)** Williston Basin. In both, the vertical dashed line is the Cretaceous-Paleogene boundary and the horizontal dotted line is the 110 g/m^2 cut-off for high LMA species observed in the Williston Basin. To the right are probability density functions for each basin. The solid orange line represents Cretaceous D1 species-site pairs in the Denver Basin and Cretaceous species-site pairs in the Williston. The blue dot-dash line represents early Paleocene D1 species-site pairs in the Denver Basin and Paleocene species-site pairs in the Williston. The black dotted line represents Later Paleocene D1 species-site pairs in the Denver Basin.

margin of the basin, LMA shifted downwards after the KPB and stayed low throughout the first 2.2 m.y. of the Paleocene (**Figures 6A,D**). Compared to the Cretaceous D1, the early P-D1-West (n = 46 species-site pairs; green triangles in **Figure 6A**) had a significantly lower median LMA (69.1 vs. 77.2 g/m^2; p = 0.03) and distribution (p = 0.03; **Figure 6D**), with no shift in variance (p = 0.12). Younger P-D1-West sites (gray triangles in **Figure 6A**)—Castle Rock, Sick of Sycamores, and Plum Creek Parkway (all ~63.8 Ma)—were not significantly different from the early P-D1-West by median (63.3 g/m^2; n = 167; p = 0.08), distribution (p = 0.19), or variance (p = 0.79).

The LMA of the early P-D1-Central association (n = 112) was not significantly different from the Cretaceous D1 by median (73.0 vs. 77.2 g/m^2; p = 0.29), distribution (p = 0.31), or variance (p = 0.65; **Figures 6B,E**). However, we observed a later downwards shift in LMA more than a million years after the KPB (gray triangles in **Figure 6B**). Species from younger localities in P-D1-Central (n = 28) had a significantly lower median LMA (62.9 vs. 73.0 g/m^2; p = 0.01) than the older early P-D1-Central assemblage, while distribution (p = 0.11) and variance (p = 0.44) were not significantly different.

The P-D1-East megafloral association showed no evidence of a downwards shift in LMA. The early P-D1-East (n = 38) did not differ from the Cretaceous D1 by median (74.1 vs. 77.2 g/m^2; p = 0.86) or distribution (p = 0.33; **Figures 6C,F**). However, as in the Williston Basin, variance significantly decreased across the KPB (p = 0.007). Direct comparison between P-D1-East and the Williston Paleocene shows no significant difference in median (p = 0.18), distribution (p = 0.18), or variance (p = 0.61).

TABLE 1 | Estimated mean leaf dry mass per area (LMA) of boundary crossing morphotypes found on both sides of the Cretaceous—Paleogene boundary (KPB).

KPB-crossing morphotypes	Cretaceous (g/m^2)	Paleocene (g/m^2)
Platanites marginata	$90.3 \pm^{16.4}_{13.8}$	$72.5 \pm^{8.0}_{7.2}$
"Zizyphus" fibrillosus	$103.5 \pm^{41.0}_{29.3}$	$104.2 \pm^{19.7}_{16.5}$
"Ficus" planicostata	$85.1 \pm^{23.8}_{18.6}$	$71.3 \pm^{12.5}_{10.7}$
DB 950	$73.9 \pm^{20.7}_{16.2}$	$83.6 \pm^{65.0}_{36.6}$
CSS 106	$56.9 \pm^{34.2}_{21.4}$	$48.4 \pm^{37.7}_{21.2}$

Uncertainties are 95% prediction intervals.

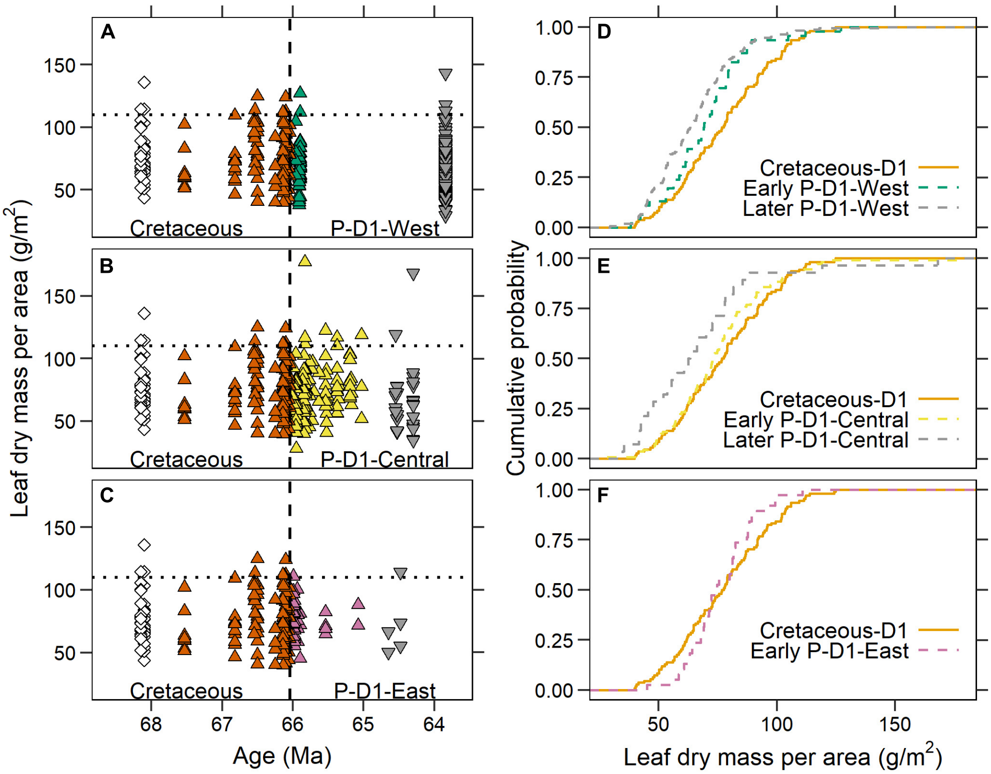

FIGURE 6 | Leaf dry mass per area (LMA) of the three Paleocene D1 megafloral associations. **(A–C)** Comparisons of LMA in the Denver Basin between the Cretaceous and **(A)** P-D1-West; **(B)** P-D1-Central; and **(C)** P-D1-East associations. The Cretaceous species-site pairs are identical to **Figure 5A** and are identical in all three panels. In the Paleocene, upward facing triangles = early Paleocene D1 (66.04–65 Ma); downward facing triangles = later Paleocene D1 (< 65 Ma). The sum of Paleocene data across all three panels is identical to **Figure 5A**. **(D–F)** Cumulative distribution functions of LMA from different temporal groupings in the Denver Basin in **(D)** P-D1-West; **(E)** P-D1-Central; and **(F)** P-D1-East.

Sparse sampling of species from younger sites in the P-D1-East association (n = 5; gray triangles in **Figure 6C**) makes it impossible to evaluate whether, like P-D1-Central, a downward shift in LMA occurred later.

Correlation With Climate

We found a significant inverse correlation in the Denver Basin between MAP and LMA (n = 137 species-site pairs; adjusted $R^2 = 0.05$; $p = 0.003$) and no correlation between MAT and LMA (n = 481; adjusted $R^2 = 0.01$; $p = 0.20$; **Figure 7**). The MAP correlation was even stronger when restricted to the four P-D1-West sites with precipitation estimates ($n = 70$; adjusted $R^2 = 0.14$; $p < 0.001$; green regression in **Figure 7B**).

DISCUSSION

We investigated over 1,000 leaves from nearly 100 localities temporally and spatially distributed throughout KPB-spanning Denver Basin sediments and found no evidence for a basin-wide change in plant ecological strategies. Our LMA estimates did not support a directional shift, convergence, or divergence across the KPB. Moreover, slow-return species with LMA greater than 110 g/m^2, conspicuously absent in the Williston Basin post-KPB (Blonder et al., 2014; **Figure 5B**), were present throughout the Denver Basin record, including within less than 200 k.y. after the KPB (**Figure 5A**). Together, this suggests that the Williston Basin's convergence in LMA after the KPB was not representative of a unified global, or even North American, response to the mass-extinction event.

Instead, our results indicate that shifts in LMA, even during this tumultuous time, were more reflective of smaller scale environmental factors. The P-D1-West megafloral association, located along the western basin margin next to the uplifting Front Range, experienced a directional shift toward lower LMA within the first 200 k.y. of the Paleocene and then persisted in that low LMA space through at least 63.8 Ma (**Figures 6A,D**). P-D1-Central, close to the basin margin but not directly adjacent to the uplifting Front Range, showed no significant change in LMA in relation to the KPB (**Figures 6B,E**; and see Lyson et al., 2019), but experienced a later directional shift toward lower LMA around 65–64 Ma. Finally, furthest from the basin margin, P-D1-East did not experience a directional shift in LMA at any point but did see a convergence in LMA within the first million years of the Paleocene (**Figures 6C,F**). This convergence in LMA without a corresponding directional shift closely matches what occurred in the Williston Basin during this same time span. The leaf-economic similarity is in keeping with

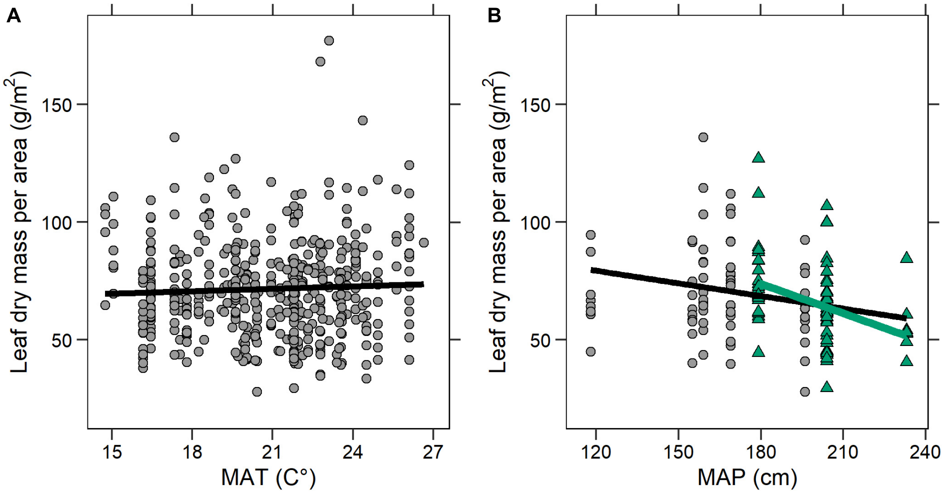

FIGURE 7 | Correlations between LMA and climate. Each point is a species-site pair. **(A)** LMA and mean annual temperature (MAT). LMA = 63.25 + 0.40 × MAT (Adjusted $R^2 = 0.001$; $p = 0.20$). **(B)** LMA and mean annual precipitation (MAP). Black line is the whole basin regression: LMA = 100.84 – 0.18 × MAP (Adjusted $R^2 = 0.05$; $p = 0.004$). Green triangles are P-D-West species-site pairs, and the green line is the P-D1-West regression: LMA = 148.81–0.42 × MAP (Adjusted $R^2 = 0.14$; $p < 0.001$).

a similarity in taxonomic composition and environmental setting (low-relief basin center).

We argue that the different temporal patterns observed in the western part of the basin (P-D1-West and P-D1-Central) could be a result of concurrent changes in precipitation. In the early Paleocene, surface relief generated during the uplift of the Colorado Front Range is thought to have initiated an orographic precipitation regime along the western margin of the basin (Sewall et al., 2000; Johnson et al., 2003; Sewall and Sloan, 2006). An inverse correlation between MAP and LMA is commonly observed in both extant (Wright et al., 2004, 2005) and fossil plants (Butrim and Royer, 2020). Thus, an increase in precipitation was likely one of the prevailing environmental factors most influencing plant strategies, and indeed we found a stronger inverse correlation between MAP and LMA among species-site pairs found in the P-D1-West association than elsewhere in the basin (**Figure 7B**). In the P-D1-Central and P-D1-East associations, we do not currently have enough MAP estimates to clearly link LMA to precipitation, but we hypothesize that a greater distance from the Front Range's locally high paleo-relief and its associated orographic precipitation effects could have delayed the shift toward lower LMA until the uplift progressed further. In the P-D1-Central association, we see the first indication of a downward shift in LMA values about one million years after the KPB, around the same time that we see an increase in regional MAP in P-D1-West sites. While we do not have MAP estimates for the later P-D1-Central sites, it is possible that an intensification of orographic precipitation reached more Front Range distal environments, driving a downward shift. In the case of P-D1-East, the shift toward lower LMA values may have never occurred or occurred beyond the temporal range of available leaf fossils.

An exploration of individual sites bears out these same themes. Castle Rock (63.84 Ma; P-D1-West association) is notable for being an early example of a tropical rainforest (Johnson and Ellis, 2002; Johnson et al., 2003). Compared to most of the Denver Basin, Castle Rock had a low LMA (median = 64 g/m^2) and a high MAP (204 cm), in-line with many present-day tropical rainforests (Royer et al., 2007; Poorter et al., 2009; Peppe et al., 2011). We found a similarly low LMA (median = 59 g/m^2) at the older Baptist Road locality (∼66.5 Ma; P-D1-West; no MAP estimate), which is high in diversity but has never been classified as a rainforest. On the other hand, at Scotty's Palm (∼66.5 Ma; P-D1-West), another high diversity locality found just after the KPB, LMA was higher (median = 80 g/m^2) and MAP was lower (179 cm), in keeping with our basin-wide inverse correlation between MAP and LMA. Perhaps the difference in LMA between Baptist Road and Scotty's Palm represents the beginnings of a transition to the later Castle Rock type rainforest, as changes in precipitation favored new leaf economic strategies. Future analyses incorporating taxonomy alongside these leaf-economic results should help reveal the nature and timing of this and other transitions by better describing the heterogeneity across localities and regions within the Denver Basin.

CONCLUSION

The Denver Basin provides an opportunity to evaluate leaf economic responses to the end-Cretaceous mass extinction. In contrast to the Williston Basin, we found no basin-wide response in LMA across the KPB. Instead, changes in LMA were correlated with shifts in proximity to the Colorado Front Range and local precipitation. At P-D1-West sites, defined by high-diversity floras living adjacent to the Front Range with its orographic precipitation regime, we found evidence that MAP and LMA were negatively correlated. At the relatively Front Range distal P-D1-East sites, defined by low-diversity floras in the swampy basin center, we saw a narrowing in occupied LMA space similar to what occurred in the swampy depositional environments of the Williston Basin Paleocene. In the Denver Basin, localized environmental conditions, rather than the catastrophic mass extinction event, seem to have played the most important role in setting the limits of viable LMA space.

DATA AVAILABILITY STATEMENT

The original contributions presented in this study are included in the article/**Supplementary Material**, further inquiries can be directed to the corresponding author/s.

AUTHOR CONTRIBUTIONS

All authors listed have made a substantial, direct, and intellectual contribution to the work, and approved it for publication.

FUNDING

Funding provided in part by NSF DEB (1556769) to DR.

ACKNOWLEDGMENTS

We thank Jennifer Kowalczyk for sharing GIS files; Matt Hess for assistance with photography; K. MacKenzie for collections assistance; and Barry Chernoff for discussions. We also thank Keith Berry and Harald Schneider for reviewing the manuscript, and Jeremiah Workman and Alejandra Angulo for their helpful comments. For fieldwork at Corral Bluffs we thank Norwood Properties, City of Colorado Springs, Waste Management, Aztec Family Raceway, J. Hawkins, J. Hilaire, J. Carner, W. Pendleton, the Bishop Family, H. Kunstle for land access; the State of Colorado, Office of the State Archaeologist, for issuing collection permits. Funding for work at Corral Bluffs was provided by The Lisa Levin Appel Family Foundation, M. Cleworth, Lyda Hill Philanthropies, David B. Jones Foundation, M. L. and S. R. Kneller, T. and K. Ryan, and J. R. Tucker as part of the Denver Museum of Nature and Science No Walls Community Initiative.

SUPPLEMENTARY MATERIAL

The Supplementary Material for this article can be found online at: https://www.frontiersin.org/articles/10.3389/fpls.2022.894690/full#supplementary-material

REFERENCES

Ackerly, D. D., and Reich, P. B. (1999). Convergence and correlations among leaf size and function in seed plants: a comparative test using independent contrasts. *Am. J. Bot.* 86, 1272–1281. doi: 10.2307/2656775

Alvarez, L. W., Alvarez, W., Asaro, F., and Michel, H. V. (1980). Extraterrestrial cause for the Cretaceous-Tertiary extinction. *Science* 208, 1095–1108. doi: 10.1126/science.208.4448.1095

Barclay, R. S., Johnson, K. R., Betterton, W. J., and Dilcher, D. L. (2003). Stratigraphy and megaflora of a K-T boundary section in the eastern denver basin Colorado. *Rocky Mt. Geol.* 38, 45–71. doi: 10.2113/gsrocky.38.1.45

Berry, K. (2020). Seed traits linked to differential survival of plants during the Cretaceous/Paleogene impact winter. *Acta Palaeobot.* 60, 307–322. doi: 10.35535/acpa-2020-0016

Blonder, B., Royer, D. L., Johnson, K. R., Miller, I., and Enquist, B. J. (2014). Plant ecological strategies shift across the Cretaceous–Paleogene boundary. *PLoS Biol.* 12:e1001949. doi: 10.1371/journal.pbio.1001949

Butrim, M. J., and Royer, D. L. (2020). Leaf-economic strategies across the eocene-oligocene transition correlate with dry season precipitation and paleoelevation. *Am. J. Bot.* 107, 1772–1785. doi: 10.1002/ajb2.1580

Carvalho, M. R., Jaramillo, C., de la Parra, F., Caballero-Rodríguez, D., Herrera, F., Wing, S., et al. (2021). Extinction at the end-Cretaceous and the origin of modern neotropical rainforests. *Science* 372, 63–68. doi: 10.1126/science.abf1969

Cascales-Miñana, B., Servais, T., Cleal, C. J., Gerrienne, P., and Anderson, J. (2018). Plants—the great survivors! Geol. *Today* 34, 224–229. doi: 10.1111/gto.12250

Clyde, W. C., Ramezani, J., Johnson, K. R., Bowring, S. A., and Jones, M. M. (2016). Direct high-precision U–Pb geochronology of the end-Cretaceous extinction and calibration of Paleocene astronomical timescales. *Earth Planet. Sci. Lett.* 452, 272–280. doi: 10.1016/j.epsl.2016.07.041

Cornwell, W. K., Westoby, M., Falster, D. S., Fitzjohn, R. G., O'Meara, B. C., Pennell, M. W., et al. (2014). Functional distinctiveness of major plant lineages. *J. Ecol.* 102, 345–356. doi: 10.1111/1365-2745.12208

Courtillot, V., Besse, J., Vandamme, D., Montigny, R., Jaeger, J. J., and Cappetta, H. (1986). Deccan flood basalts at the cretaceous/tertiary boundary? *Earth Planet. Sci. Lett.* 80, 361–374. doi: 10.1016/0012-821X(86)90118-4

Dechesne, M., Raynolds, R. G. H., Barkmann, P. E., and Johnson, K. R. (2011). *Notes on the Denver Basin geologic Maps: Bedrock Geology, Structure, and Isopach Maps of the Upper Cretaceous to Paleogene Strata Between Greeley and Colorado Springs, Colorado, Denver, Colorado, Colorado Geological Survey map Series scale 1:250,000*. Denver, Co: Colorado Geological Survey.

Ellis, B., Daly, D. C., Hickey, L. J., Johnson, K. R., Mitchell, J. D., Wilf, P., et al. (2009). *Manual of Leaf Architecture*. New York: Botanical Garden.

Ellis, B., and Johnson, K. R. (2013). Comparison of leaf samples from mapped tropical and temperate forests: implications for interpretations of the diversity of fossil assemblages. *Palaios* 28, 163–177. doi: 10.2110/palo.2012.p12-073r

Ellis, B., Johnson, K. R., and Dunn, R. E. (2003). Evidence for an in situ early Paleocene rainforest from Castle Rock, Colorado. *Rocky Mt. Geol.* 38, 73–100.

Fawcett, J. A., Maere, S., and Van De Peer, Y. (2009). Plants with double genomes might have had a better chance to survive the cretaceous-tertiary extinction event. *Proc. Natl. Acad. Sci. U.S.A.* 106, 5737–5742. doi: 10.1073/pnas.0900906106

Gradstein, F. M., Ogg, J. G., Schmitz, M., and Ogg, G. (eds) (2012). *The Geologic Time Scale*. Amsterdam: Elsevier.

Grossnickle, D. M., and Newham, E. (2016). Therian mammals experience an ecomorphological radiation during the Late Cretaceous and selective extinction at the K–Pg boundary. *Proc. R. Soc. B Biol. Sci.* 283, 1–8. doi: 10.1098/rspb.2016.0256

Hicks, J. F., Johnson, K. R., Obradovich, J. D., Miggins, D. P., and Tauxe, L. (2003). Magnetostratigraphy of upper Cretaceous (Maastrichtian) to lower eocene strata of the denver basin. *Colorado. Rocky Mt. Geol.* 38, 1–27. doi: 10.2113/gsrocky.38.1.1

Hicks, J. F., Johnson, K. R., Obradovich, J. D., Tauxe, L., and Clark, D. (2002). Magnetostratigraphy and geochronology of the Hell Creek and basal Fort Union formations of southwestern North Dakota and a recalibration of the age of the Cretaceous-Tertiary boundary. *Spec. Pap. Geol. Soc. Am.* 361, 35–55. doi: 10.1130/0-8137-2361-2.35

Hull, P. M., Bornemann, A., Penman, D. E., Henehan, M. J., Norris, R. D., Wilson, P. A., et al. (2020). On impact and volcanism across the cretaceous-paleogene boundary. *Science* 367, 266–272. doi: 10.1126/science.aay5055

Johnson, K. R. (1989). *A High-Resolution Megafloral Biostratigraphy Spanning the Cretaceous-Tertiary Boundary in the Northern Great Plains*. New Haven, CT: Yale University.

Johnson, K. R. (2002). Megaflora of the hell Creek and lower Fort Union Formations in the western Dakotas: vegetational response to climate change, the cretaceous-tertiary boundary event, and rapid marine transgression. *Spec. Pap. Geol. Soc. Am.* 361, 329–391. doi: 10.1130/0-8137-2361-2.329

Johnson, K. R., and Ellis, B. (2002). A tropical rainforest in colorado 1.4 million years after the Cretaceous-Tertiary boundary. *Science* 296, 2379–2383. doi: 10.1126/science.1072102

Johnson, K. R., Reynolds, M. L., Werth, K. W., and Thomasson, J. R. (2003). Overview of the late Cretaceous, early Paleocene, and early eocene megafloras of the denver basin, Colorado. *Rocky Mt. Geol* 38, 101–120.

Kowalczyk, J. B., Royer, D. L., Miller, I. M., Anderson, C. W., Beerling, D. J., Franks, P. J., et al. (2018). Multiple proxy estimates of atmospheric CO2 from an early Paleocene rainforest. *Paleoceanogr. Paleoclimatol.* 33, 1427–1438. doi: 10.1029/2018PA003356

Labandeira, C. C., Johnson, K. R., and Wilf, P. (2002). Impact of the terminal Cretaceous event on plant-insect associations. *Proc. Natl. Acad. Sci. U.S.A.* 99, 2061–2066. doi: 10.1073/pnas.042492999

Le Loeuff, J. (2012). Paleobiogeography and biodiversity of Late Maastrichtian dinosaurs: how many dinosaur species went extinct at the Cretaceous-Tertiary boundary? *Bull. Soc. Geol. Fr.* 183, 547–559. doi: 10.2113/gssgfbull.183.6.547

Lyson, T. R., Miller, I. M., Bercovici, A. D., Weissenburger, K., Fuentes, A. J., Clyde, W. C., et al. (2019). Exceptional continental record of biotic recovery after the Cretaceous-Paleogene mass extinction. *Science* 366, 977–983. doi: 10.1126/science.aay2268

Moeglein, M. K., Chatelet, D. S., Donoghue, M. J., and Edwards, E. J. (2020). Evolutionary dynamics of genome size in a radiation of woody plants. *Am. J. Bot.* 107, 1527–1541. doi: 10.1002/ajb2.1544

Nichols, D. J., and Johnson, K. R. (2008). *Plants and the KT Boundary*. Cambridge: Cambridge University Press.

Peppe, D. J., Royer, D. L., Cariglino, B., Oliver, S. Y., Newman, S., Leight, E., et al. (2011). Sensitivity of leaf size and shape to climate: global patterns and paleoclimatic applications. *New Phytol.* 190, 724–739. doi: 10.1111/j.1469-8137.2010.03615.x

Poorter, H., Niinemets, Ü, Poorter, L., Wright, I. J., and Villar, R. (2009). Causes and consequences of variation in leaf mass per area (LMA): a meta-analysis. *New Phytol* 182, 565–588. doi: 10.1111/j.1469-8137.2009.02830.x

Raynolds, R. G. (2002). Upper Cretaceous and Tertiary stratigraphy of the Denver Basin, Colorado. *Rocky Mt. Geol.* 37, 111–134.

Raynolds, R. G., and Johnson, K. R. (2003). Synopsis of the stratigraphy and paleontology of the uppermost Cretaceous and lower Tertiary strata in the Denver Basin, Colorado. *Rocky Mt. Geol.* 38, 171–181. doi: 10.2113/gsrocky.38.1.171

Raynolds, R. G., Johnson, K. R., Ellis, B., Dechesne, M., and Miller, I. M. (2007). Earth history along Colorado's Front Range: salvaging geologic data in the suburbs and sharing it with the citizens. *GSA Today* 17, 4–10.

Royer, D. L., Sack, L., Wilf, P., Lusk, C. H., Jordan, G. J., Niinemets, Ü, et al. (2007). Fossil leaf economics quantified: calibration, eocene case study, and implications. *Paleobiology* 33, 574–589. doi: 10.1666/07001.1

Schoene, B., Eddy, M. P., Samperton, K. M., Keller, C. B., Keller, G., Adatte, T., et al. (2019). U-Pb constraints on pulsed eruption of the Deccan traps across the end-Cretaceous mass extinction. *Science* 363, 862–866. doi: 10.1126/science.aau2422

Sewall, J. O., and Sloan, L. C. (2006). Come a little bit closer: a high-resolution climate study of the early Paleogene Laramide foreland. *Geology* 34, 81–84. doi: 10.1130/G22177.1

Sewall, J. O., Sloan, L. C., Huber, M., and Wing, S. (2000). Climate sensitivity to changes in land surface characteristics. *Glob. Planet. Change* 26, 445–465. doi: 10.1016/S0921-8181(00)00056-4

Sokal, R., and Rohlf, F. (2012). *Biometry*, 4th Edn. New York, NY: WH Freeman and Company.

Sprain, C. J., Renne, P. R., Vanderkluysen, L., Pande, K., Self, S., and Mittal, T. (2019). The eruptive tempo of deccan volcanism in relation to the cretaceous-paleogene boundary. *Science* 363, 866–870. doi: 10.1126/science.aav1446

Stiles, E., Wilf, P., Iglesias, A., Gandolfo, M. A., and Cuneo, N. R. (2020). Cretaceous-Paleogene plant extinction and recovery in Patagonia. *Paleobiology* 46, 445–469. doi: 10.1017/pab.2020.45

Van Hinsbergen, D. J. J., De Groot, L. V., Van Schaik, S. J., Spakman, W., Bijl, P. K., Sluijs, A., et al. (2015). A paleolatitude calculator for paleoclimate studies. *PLoS One* 10:e0126946. doi: 10.1371/journal.pone.0126946

Vellekoop, J., Sluijs, A., Smit, J., Schouten, S., Weijers, J. W. H., Sinninghe Damsté, J. S., et al. (2014). Rapid short-term cooling following the Chicxulub impact at the Cretaceous-Paleogene boundary. *Proc. Natl. Acad. Sci. U.S.A.* 111, 7537–7541. doi: 10.1073/pnas.1319253111

Wei, N., Du, Z., Liston, A., and Ashman, T. L. (2020). Genome duplication effects on functional traits and fitness are genetic context and species dependent: studies of synthetic polyploid Fragaria. *Am. J. Bot.* 107, 262–272. doi: 10.1002/ajb2.1377

West, C. K., Reichgelt, T., and Basinger, J. F. (2021). The Ravenscrag Butte flora: paleoclimate and paleoecology of an early Paleocene (Danian) warm-temperate deciduous forest near the vanishing inland Cannonball Seaway. *Palaeogeogr. Palaeoclimatol. Palaeoecol.* 576:110488. doi: 10.1016/j.palaeo.2021.110488

Wilf, P. (1997). When are leaves good thermometers? A new case for leaf margin analysis. *Paleobiology* 23, 373–390.

Wilf, P., and Johnson, K. R. (2004). Land plant extinction at the end of the Cretaceous: a quantitative analysis of the North Dakota megafloral record. *Paleobiology* 30, 347–368. doi: 10.1666/0094-83732004030<0347:lpeate<2.0.co;2

Wilf, P., Johnson, K. R., and Huber, B. T. (2003). Correlated terrestrial and marine evidence for global climate changes before mass extinction at the Cretaceous-Paleogene boundary. *Proc. Natl. Acad. Sci. U.S.A.* 100, 599–604. doi: 10.1073/pnas.0234701100

Wilson Deibel, P. K. (2022). *Vegetation and Environmental Changes Across the Cretaceous-Paleogene (K-Pg) Boundary in Northeastern Montana.* Seattle, WA: University of Washington.

Wolfe, J. A. (1987). Late Cretaceous-Cenozoic history of deciduousness and the terminal Cretaceous event. *Paleobiology* 13, 215–226. doi: 10.1017/S0094837300008769

Wolfe, J. A., and Upchurch, G. R. (1986). Vegetation, climatic and floral changes at the Cretaceous-Tertiary boundary. *Nature* 324, 148–152. doi: 10.1038/324148a0

Wolfe, J. A., and Upchurch, G. R. (1987). Leaf assemblages across the Cretaceous-Tertiary boundary in the Raton Basin, New Mexico and Colorado. *Proc. Natl. Acad. Sci.* 84, 5096–5100. doi: 10.1073/pnas.84.15.5096

Wright, I. J., Reich, P. B., Cornelissen, J. H. C., Falster, D. S., Groom, P. K., Hikosaka, K., et al. (2005). Modulation of leaf economic traits and trait relationships by climate. *Glob. Ecol. Biogeogr.* 14, 411–421. doi: 10.1111/j.1466-822x.2005.00172.x

Wright, I. J., Reich, P. B., Westoby, M., Ackerly, D. D., Baruch, Z., Bongers, F., et al. (2004). The worldwide leaf economics spectrum. *Nature* 428, 821–827. doi: 10.1038/nature02403

Conflict of Interest: The authors declare that the research was conducted in the absence of any commercial or financial relationships that could be construed as a potential conflict of interest.

The handling editor JS declared a past co-authorship with one of the authors DR.

frontiers | Frontiers in Plant Science

TYPE Original Research
PUBLISHED 29 July 2022
DOI 10.3389/fpls.2022.909603

*CORRESPONDENCE
Jing Wang
wangjing.15b@igsnrr.ac.cn
Xuefa Wen
wenxf@igsnrr.ac.cn

SPECIALTY SECTION
This article was submitted to
Functional Plant Ecology,
a section of the journal
Frontiers in Plant Science

RECEIVED 31 March 2022
ACCEPTED 29 June 2022
PUBLISHED 29 July 2022

CITATION
Wang J and Wen X (2022) Limiting resource and leaf functional traits jointly determine distribution patterns of leaf intrinsic water use efficiency along aridity gradients.
Front. Plant Sci. 13:909603.
doi: 10.3389/fpls.2022.909603

Limiting resource and leaf functional traits jointly determine distribution patterns of leaf intrinsic water use efficiency along aridity gradients

Jing Wang[1]* and Xuefa Wen[1,2,3,4]*

[1]Key Laboratory of Ecosystem Network Observation and Modeling, Institute of Geographic Sciences and Natural Resources Research, Chinese Academy of Sciences, Beijing, China, [2]Collaborative Innovation Center on Forecast and Evaluation of Meteorological Disasters (CIC-FEMD), Nanjing University of Information Science & Technology, Nanjing, China, [3]College of Resources and Environment, University of Chinese Academy of Sciences, Beijing, China, [4]Beijing Yanshan Earth Critical Zone National Research Station, University of Chinese Academy of Sciences, Beijing, China

Intrinsic water use efficiency (iWUE) is a critical eco-physiological function allowing plants to adapt to water- and nutrient-limited habitats in arid and semi-arid regions. However, the distribution of iWUE in coexisting species along aridity gradients and its controlling factors are unknown. We established two transects along an aridity gradient in the grasslands of Losses Plateau (LP) and Inner Mongolia Plateau (MP) to elucidate the patterns and underlying mechanisms of iWUE distribution in coexisting species along aridity gradient. We determined leaf carbon ($\delta^{13}C$) and oxygen ($\delta^{18}O$) stable isotopes, functional traits related to carbon fixation, and limiting resources. Bulk leaf $\delta^{13}C$ and $\delta^{18}O$ were used as proxies for time-integrated iWUE and stomatal conductance (gs) during the growing season. Our results showed that variability in iWUE within transect was primarily controlled by species, sampling sites and an interactive effect between species and sampling sites. Mean values of iWUE ($iWUE_{Mean}$) increased and coefficient of variation (CV) in iWUE ($iWUE_{CV}$) decreased with an increase in aridity, demonstrating that increases in aridity lead to conservative and convergent water use strategies. Patterns of $iWUE_{Mean}$ and $iWUE_{CV}$ were controlled primarily by the ratio of soil organic carbon to total nitrogen in LP and soil moisture in MP. This revealed that the most limited resource drove the distribution patterns of iWUE along aridity gradients. Interspecific variation in iWUE within transect was positively correlated with $\Delta^{18}O$, indicating that interspecific variation in iWUE was primarily regulated by gs. Furthermore, relationship between iWUE and multi-dimensional functional trait spectrum indicated that species evolved species-specific strategies to adapt to a harsh habitat by partitioning limiting resources. Overall, these findings highlighted the interactive effects of limiting resources and leaf functional traits on plant adaptation strategies for iWUE, and emphasized the importance of considering biological processes in dissecting the underlying mechanisms of plant adaptation strategies at large regional scales.

KEYWORDS

intrinsic water use efficiency, carbon stable isotope, oxygen stable isotope, environment filter, leaf economic spectrum

Introduction

Arid and semi-arid regions constitute ~41% of the global land area (Reynolds et al., 2007), and are predicted to expand in the future (Yao et al., 2020). Limited water and nutrient resources in these regions severely restrict plant growth, survival, and reproduction (Martin-StPaul et al., 2017). To avoid hydraulic failure and carbon starvation (Choat et al., 2018), plants open or close the stomata to balance carbon uptake and water losses (Galmes et al., 2007). Consequently, intrinsic water use efficiency (iWUE), the ratio of carbon gain in photosynthetic rate (A) to stomatal conductance (gs), is a critical eco-physiological strategy for plant water–carbon regulation in the process of adaptation to water- and nutrient-limited habitats (Moreno-Gutierrez et al., 2012; Querejeta et al., 2018; Wang et al., 2018).

Diverse trade-offs between carbon gain and water loss (iWUE) facilitate species coexistence in habitats with harsh and unpredictable environmental conditions (Moreno-Gutierrez et al., 2012; Bermúdez and Retuerto, 2014; Wang et al., 2018). In generally, plants with a conservative water use strategy (high iWUE) are better able to adapt to water-limited habitats than those with low iWUE (Flexas et al., 2016; Aparecido et al., 2020). However, opportunistic water-use strategy (low iWUE) is advantageous for nutrient acquisition (Querejeta et al., 2018). Along environmental gradients, limiting resources act as environmental filters, shape the expression of plant eco-physiological functions (Bahar et al., 2016), determine trait distribution of each species in the community, and theoretically drive species toward an "optimum" for a set of environmental conditions (Mitchell et al., 2018). However, understanding of iWUE distribution in coexisting species in response to aridity gradients, and its controlling factors remain incomplete.

Given that iWUE is regulated by a rapid response of A and gs to environmental variables (Prentice et al., 2014; Basu et al., 2021), time-integrated iWUE can reflect adaptability of plants to their environment, especially in areas with large environmental fluctuations (Maxwell et al., 2018; Guerrieri et al., 2019). Leaf carbon isotope discrimination during photosynthesis ($\Delta^{13}C$) is linearly related to the ratio of the partial pressures of intercellular (Ci) to ambient (Ca) CO_2 (Ci/Ca), and is influenced by both A and gs over a period when the leaf is produced (Farquhar et al., 1989; Maxwell et al., 2018; Prieto et al., 2018). Time integrated iWUE can be estimated independently from the carbon isotope ratios ($\delta^{13}C$) of leaf tissue, allowing for more extensive studies of plant water use strategies at broader spatial scales than traditional leaf gas exchange measurements (Prentice et al., 2014).

According to the least-cost theory (Wright et al., 2003), water and nitorgen (N) are expected to be the most important environmental filters shaping the distribution of iWUE in each species in communities along aridity gradients. Previous studies conducted in arid and semi-arid areas focused primarily on spatial patterns of iWUE in response to water variables. As expected, leaf iWUE in drylands increases with decreasing precipitation (Zheng and Shangguan, 2007; Liu et al., 2013; Wang et al., 2016) or soil moisture (SM) (Ale et al., 2018) to reduce water cost. Alternatively, iWUE may decrease to reduce N cost when low soil N increases the cost of soil N uptake (Wright et al., 2003). In general, soil N supply (i.e., mineralization and nitrification rates) exhibits a decreasing trend with increasing water stress (Feyissa et al., 2021). However, it is not clear whether water or N-limitation dominates the distribution of iWUE in co-occuring species in communities along aridity gradients. In addition, evidence is accumulating in support of diverse water use strategies in resource-limited ecosystems (Moreno-Gutierrez et al., 2012; Bermúdez and Retuerto, 2014; Wang et al., 2018). However, it has not been established how this diversity varies with the strength of environmental filtering.

Large interspecific differences in iWUE along environmental gradients may be driven by variability in leaf functional traits within species (Maxwell et al., 2018; Rumman et al., 2018; Tang et al., 2021), because leaf functional traits can determine species persistence against strong environmental filters along a resource-use strategies gradient (Maracahipes et al., 2018; Guo et al., 2021; Li et al., 2022). Theoretically, many leaf functional traits correlate with variability in iWUE, including leaf N per unit area (Prentice et al., 2014) and specific leaf area (SLA) (Maxwell et al., 2018; Prieto et al., 2018). However, these are likely secondary to the primary effects of A and gs (Roden and Farquhar, 2012). In general, the first response of plants to dryness stress is to reduce gs, and photosynthetic capacity begins to decrease with the increase in dryness stress (Utkhao and Yingjajaval, 2015). However, it is challenging to determine whether variability in time-integrated iWUE derived from $\Delta^{13}C$ is the result of changes in A, or gs, or both (Scheidegger et al., 2000; Farquhar et al., 2007). Given that the leaf oxygen isotope ($\delta^{18}O$) is unaffected by variability in A, oxygen isotope enrichment in leaf tissue above source water ($\Delta^{18}O$) may help in disentangling the independent effects of A and gs on iWUE (Guerrieri et al., 2019).

In this study, we aimed to gain insight into the response of iWUE distribution in coexisting species to aridity gradient, and elucidated the underlying mechanisms. The Loess Plateau (LP) and the Inner Mongolia Plateau (MP) are located mainly in arid and semi-arid regions in China. The preliminary limiting resource for plants is soil N in LP, and water in MP (Ren et al., 2021). Thus, LP and MP provide ideal conditions for an exploration of water use strategies in coexisting species in response to resource-limiting habitats. We hypothesized that (1) increased aridity may lead to a divergence in iWUE distribution, (2) distribution patterns of iWUE along an aridity gradient may be controlled by the most limited resource such as N in LP, and water in MP, and (3) interspecific variation in iWUE is influenced primarily by gs, rather than A, because high VPD and dry soil conditions can lead to severely reduced gs before

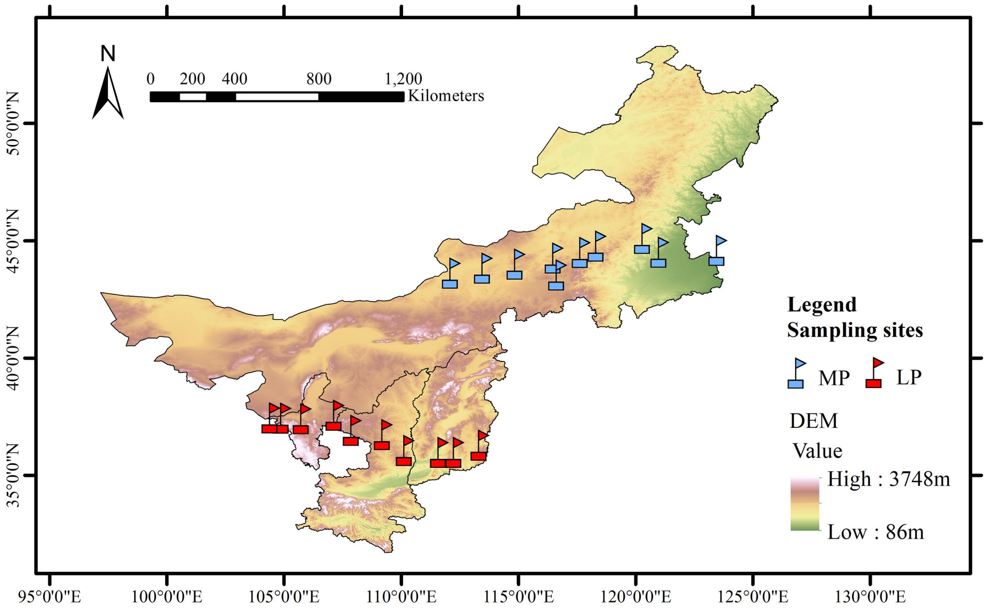

FIGURE 1
Geographic characteristics of the grassland transects in Loess Plateau (LP) and Inner Mongolia Plateau (MP).

manifesting in photosynthetic capacity (Utkhao and Yingjajaval, 2015). To test these hypotheses, we established two grassland transects along aridity gradients from east to west in LP and TP. We used bulk leaf $\delta^{13}C$ and $\delta^{18}O$ to calculate iWUE and $\Delta^{18}O$, respectively. The latter was used to reflect variability in gs among species.

Materials and methods

Description of study sites

This study was conducted along two grassland transects, one in the Loess Plateau (LP) and one in the Inner Mongolia Plateau (MP) (Figure 1). LP has a typical arid and semi-arid temperate continental monsoon climate, and an extremely fragmented hilly loess landscape due to severe soil and water erosion (Yue et al., 2019). MP experiences arid and semi-arid continental climate.

The LP transect was 600 km long from east (Lucheng District, 113.36°E, 36.29°N) to west (Shapotou District, 104.44°E, 37.46°N), with a wide range in annual total precipitation (189–599 mm) and aridity (0.51–0.63) (Figure 1). Aridity was calculated as 1- mean annual precipitation/ potential evapotranspiration. The MP transect was 1,200 km long from east (Changling County, 123.51°E, 44.59°N) to west (Erenhot, 112.15°E, 43.63°N), with a smaller range in precipitation (183–425 mm) and greater aridity (0.42–0.83). Each transect includes 10 sampling sites at an interval of about 60–150 km from east to west (Lyu et al., 2021). Grassland types include meadow grassland ($n = 3$), typical grassland ($n = 4$), and desert grassland ($n = 3$).

Sampling and measurements

Field survey and sample collection

Field sampling was carried out during the peak growing season (July–August) in 2018. We delineated a 1 km × 1 km sampling area within each sampling site, and tried to collected as many different species as possible (Zhang et al., 2019). Plant species were identified by experienced plant taxonomists. Overall, 574 and 433 plant species were found at LP and MP, respectively, including trees, shrubs, herbs and ferns (Supplementary Table S1).

At least 3 individuals per species per sampling area were selected as replicates. For trees and shrubs, we collected branches from the sunny-side of crowns. For herbs, we collected mature whole plants. Ten, fully expanded and mature leaves ($n = 50$) collected from each species were mixed uniformly into one sample for subsequent analyses. Soil samples were collected from the 0 to 10 cm layer using a soil auger, with eight replications at each site.

Leaf functional traits analysis

Leaf apparent morphology was determined using six to 10 fresh leaves per species. Leaf area (LA) was measured with a portable scanner (Cano Scan LIDE 110, Japan). LA values were obtained using an Image J software (Schneider et al., 2012). Leaf dry mass was determined after drying at 60°C. Specific leaf area (SLA) was obtained by dividing LA by leaf dry mass. Then, bulked dried leaf materials were finely ground for subsequent analyses.

Elemental analyzer (Vario Max CN Element Analyser, Elementar, Hanau, Germany) was used to determine bulk-leaf nitrogen (N) content. Leaf N per unit area (N_{area}) was calculated from N content and SLA. Elemental analyzer (Model Flash 2000HT, Thermo Fisher Scientific, Bremen, Germany) coupled to an isotope ratio mass spectrometer in continuous-flow mode (Model 253 plus, Thermo Fisher Scientific, Bremen, Germany) was used to analyze carbon ($\delta^{13}C$) and oxygen ($\delta^{18}O$) isotopes of bulk leaf samples. Isotope ratios are expressed as per mil deviations relative to Vienna Pee Dee Belemnite standard, VPDB for $\delta^{13}C$ and VSMOW for $\delta^{18}O$. Long-term precision for the instrument were $< 0.1‰$ for $\delta^{13}C$ and $< 0.2‰$ for $\delta^{18}O$.

There were 519 and 402 species with bulk leaf $\delta^{13}C < -20‰$ (C_3 species) (Supplementary Table S1), and 55 and 31 species with bulk leaf $\delta^{13}C > -20‰$ (C_4 species), respectively, in LP and MP. In generally, the iWUE of C_4 species is usually several times higher than that of the C_3 species (Pinto et al., 2014), and the iWUE of the C_3 and C_4 species is not distributed continuously when put together. Consequently, previous studies often investigated C_3 and C_4 species separately when analyzing plant water use strategies (Cornwell et al., 2018; Rumman et al., 2018). Given that the number of C_4 species in the two transects is relatively small, we only selected C_3 species to elucidated the patterns and underlying mechanisms of iWUE distribution in coexisting species along aridity gradient.

Calculation of iWUE and $\Delta^{18}O$

Time-integrated leaf intrinsic water use efficiency (iWUE, μmol mol^{-1}) during the growing season was derived from bulk leaf $\delta^{13}C$ based on the well-established theory linking CO_2 partial pressure of leaf intercellular space (Ci) to ambient (Ca) (Ci/Ca) with carbon isotopic carbon discrimination ($\Delta^{13}C$) during photosynthesis (Farquhar et al., 1989; Guerrieri et al., 2019). According to Fick's first law of diffusion, iWUE is linearly related to Ci/Ca, and can be expressed as:

$$\text{iWUE} = \text{A/gs} = \text{Ca}/1.6 \times (1 - \text{Ci/Ca}) \quad (1)$$

where A is the photosynthetic rate; gs is the stomatal conductance of CO_2. The $\Delta^{13}C$ can be calculated as Farquhar et al. (1989):

$$\Delta^{13}C = (\delta^{13}C_a - \delta^{13}C_L)/(1 + \delta^{13}C_L/1000) \quad (2)$$

where, $\delta^{13}C_a$ is $\delta^{13}C$ values of atmospheric CO_2; $\delta^{13}C_L$ is $\delta^{13}C$ values of bulk-leaf tissue. According to the "simple" form of isotopic discrimination that does not include effects due to mesophyll conductance and photorespiration (Farquhar et al., 1989; Guerrieri et al., 2019), Ci/Ca can be expressed as:

$$\text{Ci/Ca} = (\Delta^{13}\text{C-a})/(\text{b-a}) \quad (3)$$

where a is the isotope fractionation constant during CO_2 diffusion through stomata (4.4‰); b is the isotope fractionation constant during fixation by Rubisco (27‰). Combining Equation (1) and (3), iWUE can be calculated as follows:

$$\text{iWUE} = \text{Ca}/1.6 \times \left[1\text{-}(\Delta^{13}\text{C-a})/(\text{b-a})\right] \quad (4)$$

Oxygen isotope enrichment of leaf tissue above source water ($\Delta^{18}O$) was calculated using

Equation (5) (Barbour, 2007):

$$\Delta^{18}O = (\delta^{18}O_L - \delta^{18}O_S)/(1 + \delta^{18}O_S/1000) \quad (5)$$

where $\delta^{18}O_L$ and $\delta^{18}O_s$ are oxygen isotope values of bulk leaf and source water, respectively. We assumed that $\delta^{18}O$ in precipitation reflects that of soil water (i.e., source water), modified by evaporation (Guerrieri et al., 2019).

Auxiliary dataset

Climate variables for 1970–2000 were extracted from the meteorological database of the WorldClim at 0.1° spatial resolution (https://www.worldclim.org/). Mean annual precipitation and temperature, growing season (April to October) precipitation, temperature and actual water vapor pressure were calculated from monthly values. Aridity was obtained from CGIAR-CSI (https://cgiarcsi.community). Data for soil moisture (SM) (at ~10 cm depth) were obtained from a remote-sensing-based surface soil moisture dataset at 0.1° spatial resolution, and ~10-day temporal resolution (Chen et al., 2021). Vapor pressure deficit (VPD) was derived from actual water vapor pressure and temperature (Grossiord et al., 2020). Soil total N content (TN), and the ratio of soil organic carbon to TN (SOC/TN) were obtained from the "Functional Trait database of terrestrial ecosystems in China (China_Trait)."

Statistical analysis

Blomberg's K values were used to evaluate the phylogenetic signal of iWUE (Blomberg et al., 2003) using "phytools" and "Picante" package in R software (version 3.5.1, R Development Core version Team, Vienna, Austria), because phylogenetic relationships are an important source of inter-specific differences in leaf functional traits. A significant phylogenetic signal ($P < 0.05$) and large K value indicated that iWUE was constrained by phylogeny (Blomberg et al., 2003).

Our results showed that no significant phylogenetic signals of iWUE were observed, and the Blomberg's K values were small (Supplementary Table S2).

Normality of iWUE was tested using the Shapiro–Wilk test (SPSS, Chicago, IL, USA). One-way ANOVA with Duncan's *post hoc* multiple comparisons was used to compare the differences in iWUE among transects and communities, and to partition variances in iWUE within-site from among site (SPSS, Chicago, IL, USA). Multivariate analysis of covariance was used to partition the contribution of sampling site, species and their interaction to variances in iWUE (SPSS, Chicago, IL, USA).

All iWUE values of C_3 species in each sampling site were used to calculate frequency distribution characteristics, such as mean, variance, standard deviation, coefficients of variation, range, skewness and kurtosis (SPSS, Chicago, IL, USA). Simple linear regressions between frequency distribution characteristics of iWUE and aridity were conducted to test for the first hypothesis.

Pearson correlation analyses were used to test bivariate relationships between SOC/TN, SM, VPD and iWUE (SPSS, Chicago, IL). To test for the hypothesis (2), we conducted variation partitioning (R software, version 3.5.1, R Development Core version Team, Vienna, Austria) to quantify the relative contributions of water (SM and VPD) and SOC/TN to the spatial patterns of iWUE along aridity gradients, combining with the results of Pearson correlation analyses.

Simple linear regressions between iWUE and leaf functional traits ($\Delta^{18}O$, SLA and N_{area}) were conducted (R2018b, MathWorks, Inc). The result of simple linear regressions between iWUE and $\Delta^{18}O$ was used to test for hypothesis (3).

A multivariate associations among iWUE, $\Delta^{18}O$, SLA, and N_{area} were analyzed with principal component analysis (PCA) (R2018b, MathWorks, Inc) to understand the role of iWUE and $\Delta^{18}O$ in multidimensional leaf functional traits. Another PCA was performed excluding iWUE and using the remaining three traits ($\Delta^{18}O$, SLA, and N_{area}). Simple linear regressions between iWUE and axes scores of each species of second PCA were conducted to further explain the drivers of interspecific variation in iWUE along aridity gradient.

Results

Distribution of intrinsic water use efficiency

Intrinsic water use efficiency (iWUE) was distributed normally across all plant species in Loess (LP) and Inner Mongola (MP) Plateaus (Figures 2A,B). iWUE ranged from 28.17 to 141.97 μmol mol^{-1} in LP and from 47.30 to 152.00 μmol mol^{-1} in MP (Supplementary Table S3). iWUE was significantly lower in LP than in MP ($P < 0.001$).

Within transects, iWUE of co-existing species in each sampling site was distributed normally ($P > 0.05$), except for one sampling site in MP ($P = 0.03$) (Supplementary Table S3). iWUE varied widely within and across sampling sites, and over 60% of variability in iWUE originated from within-site (Supplementary Table S4). When treated as categorical variables, variability in iWUE was primarily controlled by species (46 and 63% in LP and MP, respectively), followed by sampling site (30 and 19% in LP and MP, respectively), and the interaction between species and sites (22 and 16% in LP and MP, respectively) (Figure 3). It indicated that interaction of leaf functional traits and environmental factors drove the patterns of iWUE.

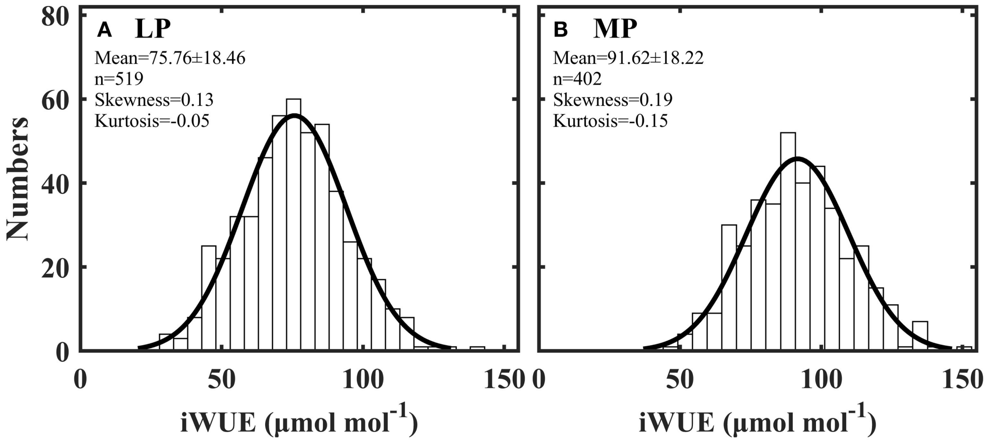

FIGURE 2
Frequency distribution of intrinsic water use efficiency (iWUE) in Loess Plateau (LP) **(A)** and Inner Mongola Plateau (MP) **(B)**.

Drivers of spatial patterns of intrinsic water use efficiency along aridity gradients

Mean values of iWUE ($\text{iWUE}_{\text{Mean}}$) significantly increased with aridity in LP and MP (Figures 4A,B). Coefficient of variation (CV) of iWUE (iWUE_{CV}) decreased with increasing aridity in LP and MP (Figures 4C,D). However, the variance, standard deviation, range, kurtosis, and skewness of iWUE did not show clear patterns along aridity gradients (Supplementary Table S3).

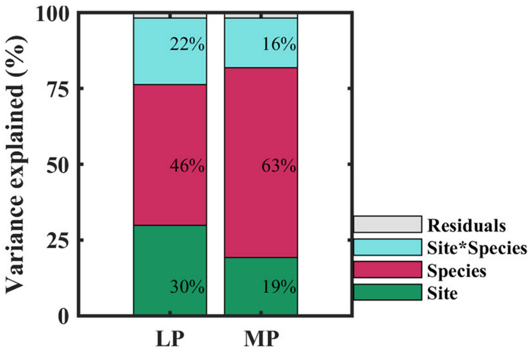

FIGURE 3
Contributions of species (red), site (green), and their interaction (blue) to variation in intrinsic water use efficiency. LP, Loess Pleateau; MP, Inner Mongolia Plateau.

$\text{iWUE}_{\text{Mean}}$ in LP was negatively related to soil moisture (SM) and to the ratio of soil organic carbon content to total nitrogen content (SOC/TN), and positively related to vapor pressure deficit (VPD) (Table 1). SOC/TN, SM, and VPD explained 94% of variation in $\text{iWUE}_{\text{Mean}}$, and the strongest predictor was SOC/TN (Figure 5A). iWUE_{CV} was negatively related to SM and SOC/TN (Table 1). SOC/TN and SM explained 76% of variation in iWUE_{CV}, and the strongest predictor was SOC/TN (Figure 5B).

In MP, $\text{iWUE}_{\text{Mean}}$ was negatively related to SM and SOC/TN (Table 1). SOC/TN and SM jointly explained 91% of variation in $\text{iWUE}_{\text{Mean}}$, and the strongest predictor was SM (Figure 5C). iWUE_{CV} was positively related to SM (Table 1). SM explained 57% of variation in iWUE_{CV} (Figure 5D).

Drivers of interspecific variation in intrinsic water use efficiency along aridity gradients

iWUE decreased with specific leaf area (SLA) ($P < 0.001$) (Figure 6A), and increased with leaf nitrogen per unit area (N_{area}) (Figure 6B) and with ^{18}O enrichment in leaf water above source water (Δ^{18}O) (Figure 6C).

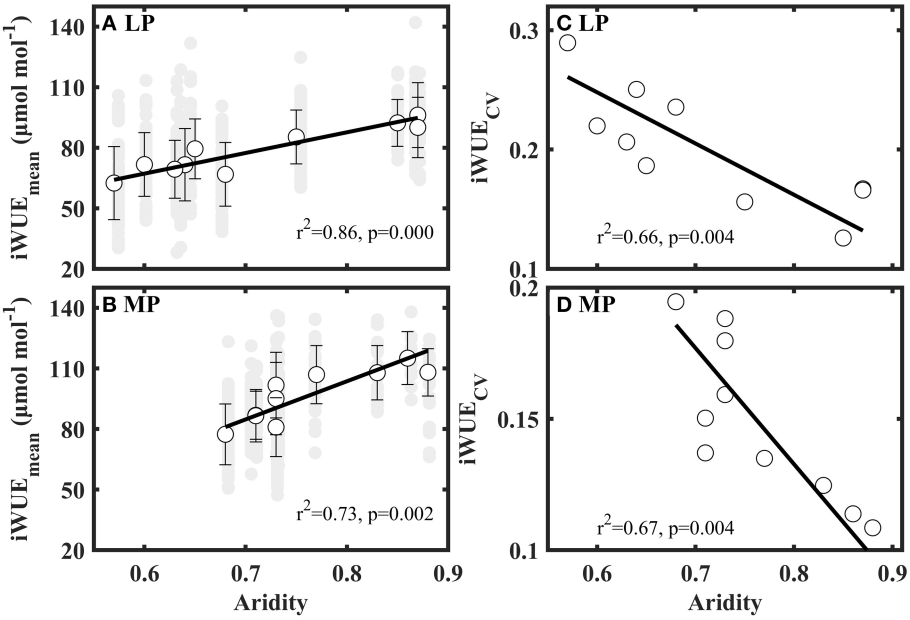

FIGURE 4
Patterns of mean value ($\text{iWUE}_{\text{mean}}$) **(A,B)** and coefficient of variation (iWUE_{CV}) **(C,D)** of intrinsic water use efficiency (iWUE) along aridity gradients in Loess Plateau (LP) and Inner Mongola Plateau (MP).

Principal component analysis (PCA) was conducted to quantify the effect of plant functional trait combinations on inter-specific variability in iWUE. The dominant leaf functional traits of Axis1 were SLA, Narea, $\Delta^{18}O$, and iWUE in LP (Figure 7A and Supplementary Table S5) and MP (Figure 7B and Supplementary Table S5). Axis2 was mainly loaded by N_{area} and iWUE in LP (Figure 7A), and SLA, $\Delta^{18}O$, and iWUE in MP (Figure 7B). Variability in iWUE was mainly controlled by Axis1 ($r^2 = 0.29$) in LP (Figure 7C), and by Axis1 ($r^2 = 0.30$) and Axis2 ($r^2 = 0.18$) in MP (Figure 7D).

TABLE 1 Pearson's correlation coefficients between intrinsic water use efficiency and environmental variables in Loess Plateau (LP) and Inner Mongola Plateau (MP).

		Loess plateau		Inner mongolia plateau	
		$iWUE_{Mean}$	$iWUE_{CV}$	iWUEmean	iWUEcv
Water	SM	−0.746*	0.718*	−0.828**	0.752*
	VPD	0.684*	−0.476	0.333	−0.496
Nutrient	SOC/TN	−0.905**	0.900**	−0.663*	0.375

iWUE, intrinsic water use efficiency; CV, coefficient of variation; SM, soil moisture; VPD, vapor pressure deficit, VPD; SOC/TN, the ratio of soil organic carbon content to soil total nitrogen content. ** and * represent a significant relationship at $p = 0.01$ and 0.05 levels, respectively.

Discussion

Most limited resource led to conservative and convergent water use strategies with an increase in aridity

Species in LP and MP adopt opportunistic water use strategies to cope with water- and nutrient-limiting habitats (Figure 2). Time-integrated iWUE in LP and MP were within the range but distributed at a relatively lower end of global values. For example, two multi-species datasets show that the instantaneous iWUE ranged from 5 to 324.00 μmol mol^{-1} (Flexas et al., 2016; Gago et al., 2016). Furthermore, leaf $\delta^{13}C$ of species in this study were also distributed at the relatively depleted end of the global $\delta^{13}C$ dataset (Supplementary Figure S1). The reason may be that an

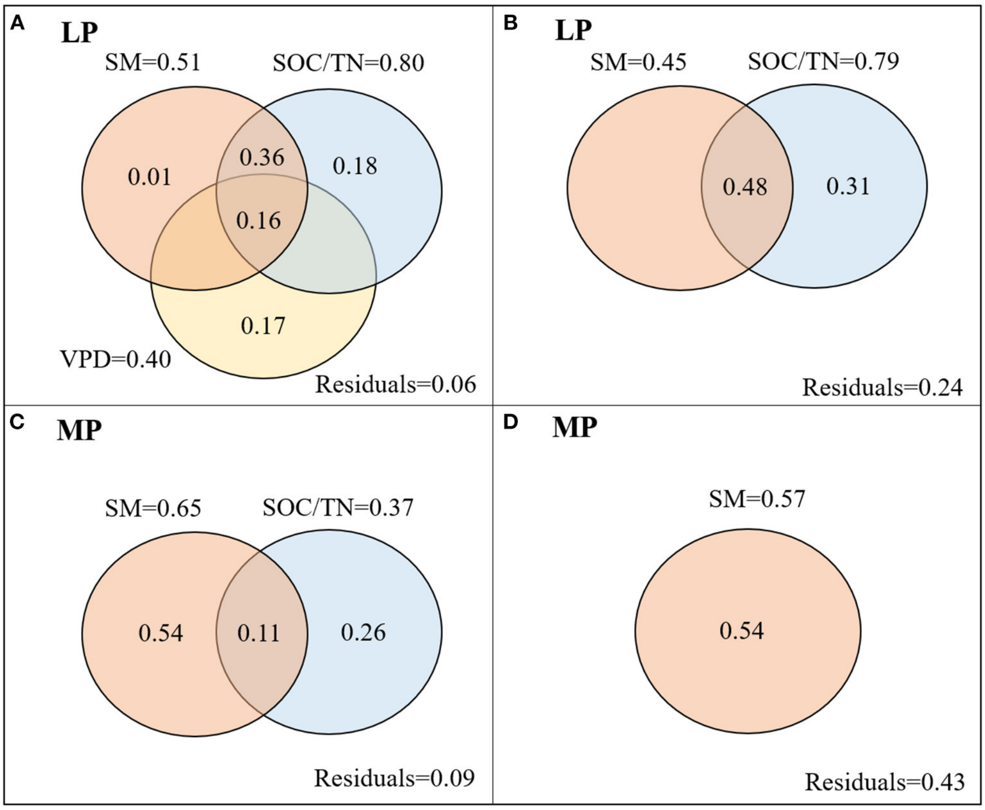

FIGURE 5
Variation partitioning (R^2) of environmental factors in mean **(A,C)** and coefficient of variation (CV) **(B,D)** of iWUE of co-occuring species in LP **(A,B)** and MP **(C,D)**. LP, Loess Pleateau; MP, Inner Mongolia Plateau; SM, soil moisture; VPD, vapor pressure deficit, VPD; SOC/TN, the ratio of soil organic carbon content to soil total nitrogen content.

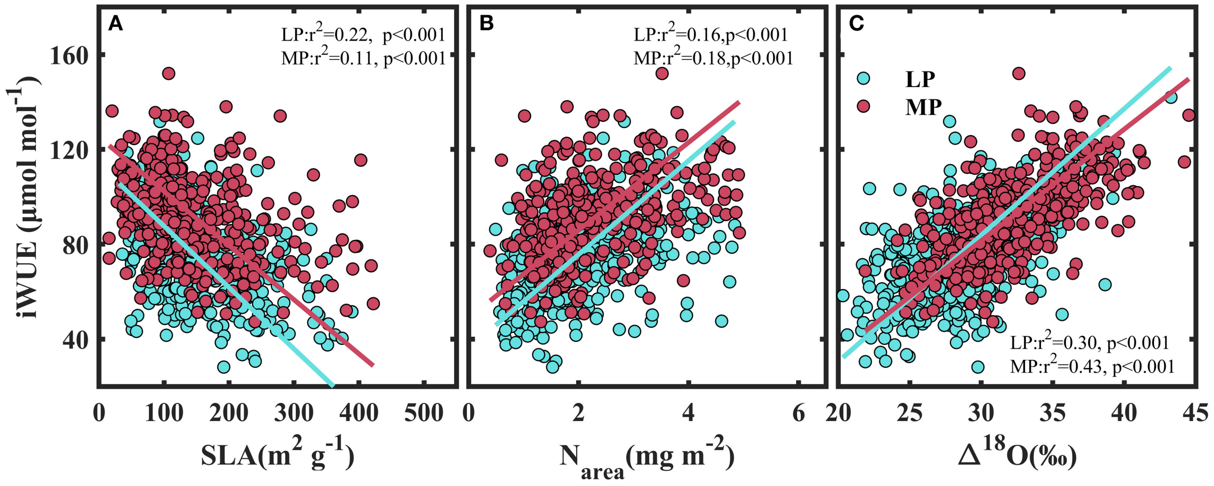

FIGURE 6
Relationships between intrinsic water use efficiency and specific leaf area (SLA) **(A)**, leaf nitrogen per unit area (N_{area}) **(B)**, and the ^{18}O enrichment in leaf water above source water ($\Delta^{18}O$) **(C)**. LP, Loess Pleateau; MP, Inner Mongolia Plateau.

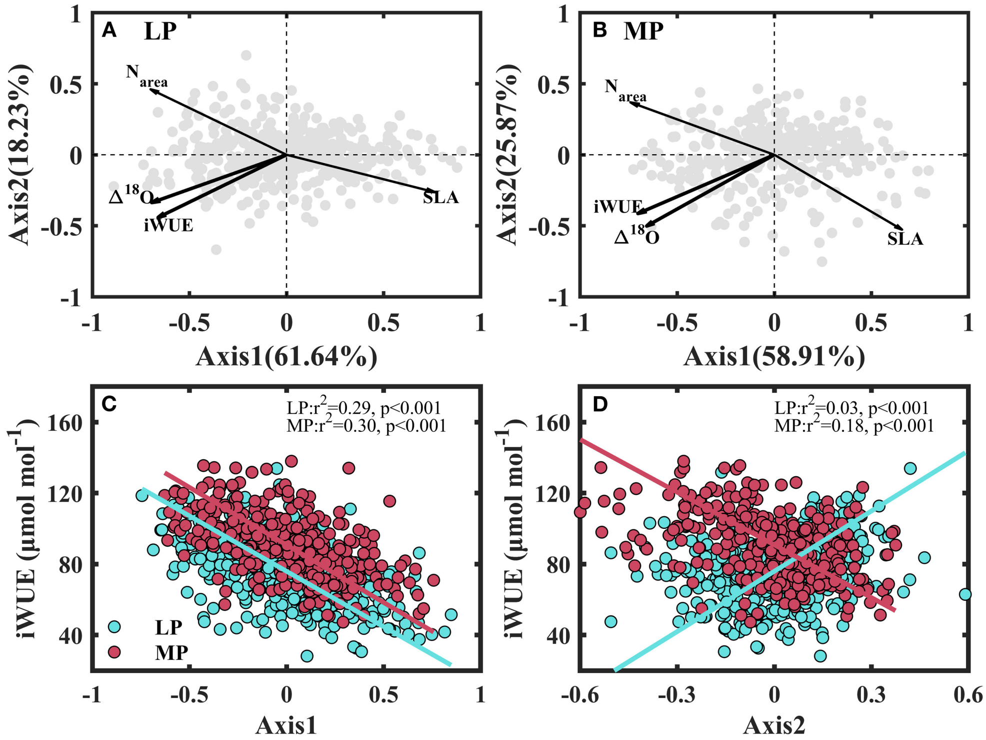

FIGURE 7
Principal component analysis (PCA) of intrinsic water use efficiency (iWUE) and leaf functional traits **(A,B)** and relationship between the principal component axes of PCA of leaf functional traits and iWUE **(C,D)**. SLA, specific leaf area; N_{area}, leaf nitrogen per unit area, and $\Delta^{18}O$, the ^{18}O enrichment in leaf water above source water. LP, Loess Pleateau; MP, Inner Mongolia Plateau.

opportunistic water use strategy is advantageous for maximizing nutrient capture (Querejeta et al., 2018; Salazar-Tortosa et al., 2018). Water and nutrient supply in arid and semi-arid habitats are highly heterogeneous in space and time due to the limited and variable rainfall (Chesson et al., 2004). Nutrient uptake from soil is tightly linked to the transpiration-driven mass flow of water (Salazar-Tortosa et al., 2018). Species with low iWUE always exhibit high stomatal conductance (gs) and transpiration rate (Moreno-Gutierrez et al., 2012), allowing rapid nutrient absorption when soil water and nutrients are available.

Within transect, we found that iWUE of co-occuring species in each sampling site exhibited high variability, however, functional convergence was observed along the aridity gradient (Figures 4C,D). This result is contrary to our first hypothesis. Species with diverse and contrasting water use stratergies are known to coexist in dry and nutrient-poor habitats, such as Karst (Wang et al., 2021), Mediterranean (Moreno-Gutierrez et al., 2012), coastal sand dunes (Bermúdez and Retuerto, 2014) and epiphytic (Querejeta et al., 2018) ecosystems. This demonstrates that species differences in eco-physiological function related to the use of resources facilitate species niche segregation (Moreno-Gutierrez et al., 2012; Bermúdez and Retuerto, 2014). There are two mechanisms that might explain the convergent water use strategies along aridity gradient: (1) Inter-specific competition decreased with increasing aridity (Wu et al., 2017). As the number of species (plant species richness) occuring within each community significantly decreases (Supplementary Table S1), available resources for each species may increase (Zhu et al., 2015). (2) The filtering effect of water stress on iWUE of species increased with increasing aridity. The reason is that species with similar physiological parameters can enter a given harsh habitats (Reich et al., 2003; Maracahipes et al., 2018). These results demonsteated that environmental filtering existed within transect, although species exhibited diverse water use strategies in water and nutrient-limited LP and MP.

Futhermore, we also found that co-occuring species within a sampling site shifted their water use strategies from opportunistic (low iWUE and high gs) to conservative (low iWUE and high gs) with an increase in aridity in LP and MP (Figures 4A,B), consistent with previous studies (Zheng and Shangguan, 2007; Liu et al., 2013; Wang et al., 2016; Ale et al., 2018). This reveals that plants lowered their water loss to adopt to the increasing water stress (i.e., low soil moisture and high water vapor pressure deficit) (Supplementary Table S3). However, the slope of the relationship between aridity and mean values of iWUE ($iWUE_{mean}$) in MP (Figure 4B, slope = 102.304) was steeper than that in LP (Figure 4A, slope = 188.901). This indicates that the negative effect of water stress on iWUE is higher in MP than in LP. We attribute this difference to dissimilarity in limited resources between the two transects.

The variability in $iWUE_{mean}$ along an aridity gradient was mainly determined by SOC/TN in LP, and by soil moisture in MP (Figure 5), which supports our second hypothesis. A previous study conducted in this study area demonstrated that plant N availability in LP was lower than that in MP, and increased with aridity in MP, but showed no clear trend in LP (Unpublished data). These results demonstrate that high plant N availability could meet N demand to reduce water cost across the transect in MP (high iWUE and low gs); however, plants in LP promoted N uptake to meet plant N demand at the expense of high water loss (low iWUE and high gs) (Wright et al., 2003). Our findings highlight the importance of balance between acquisitive and conservative strategies along the water and nitrogen gradients: opportunistic water use strategies allows species to established in habits with low soil N habitats due to their high nitorgen acquisition capacity, while conservative water use strategies promote resistance of species to water stress in relatively high soil N habitats (Wright et al., 2003; Maracahipes et al., 2018).

Interspecific variation in iWUE was primarily regulated by gs

Previous studies demonstrated that $\Delta^{18}O$ in co-existing species can be used as a reliable indicator of interspecific differences in gs in strongly water-limited ecosystems, and that leaf $\delta^{13}C$ and $\delta^{18}O$ can be used to separate the independent effects of photosynthetic rates and gs on iWUE (Moreno-Gutierrez et al., 2012; Querejeta et al., 2018). However, the effects of climatic (vapor pressure deficit [VPD] and temperature) variability and differences in $\delta^{18}O$ of plant source water on leaf $\delta^{18}O$ ($\Delta^{18}O$) should be considered across large spatial scales (Prieto et al., 2018). In this study, mean values of $\Delta^{18}O$ in C_3 species within a sampling site was not affected by VPD or temperature ($P > 0.05$) (Supplementary Table S6). The effect of source water across sites was corrected using $\delta^{18}O$ of precipitation at each site (Maxwell et al., 2018). However, the water source partitioning in C_3 species in each sampling site may attenuate the positive correlation between iWUE and $\Delta^{18}O$. The slopes of the linear regression between $\Delta^{18}O$ and iWUE across sites within transect did not differ statistically (Supplementary Figure S2 and Supplementary Table S7). Furthermore, water-source partitioning is not common in grassland communities (Bachmann et al., 2015). Consequently, differences in $\Delta^{18}O$ in co-occurring species within communities should be determined mainly by the interspecific variation in gs (Wang and Wen, 2022).

A positive relationship was found between $\Delta^{18}O$ and iWUE both within (Supplementary Figure S2 and Supplementary Table S7) and among sampling sites (Figure 6B), indicating that the variability in iWUE was determined mainly by stomatal regulation (Moreno-Gutierrez et al., 2012; Prieto et al., 2018; Querejeta et al., 2018). This conclusion supported our third hypothesis. Moreno-Gutierrez et al. (2012) found that the large interspecific difference in $\delta^{13}C$ in a Mediterranean ecosystem was controlled by $\Delta^{18}O$ rather than photosynthetic rate. However, in this study, a positive relationship between leaf nitrogen per unit area (N_{area}) and iWUE indicated that variability in iWUE was also affected by the interspecific variation in photosynthetic rate (Figure 6B), and that species invested more N to compensate for the negative effect of low gs on photosynthetic rates (Flexas et al., 2016). A previous study demonstrated that species with low leaf-specific leaf areas (SLA) had small and thick leaves, which benefit reductions in water loss (Wright et al., 2017). The negative relationship between iWUE and SLA demonstrated that species increased construction costs to prevent water loss (Maxwell et al., 2018).

In this study, the covariation of iWUE, $\Delta^{18}O$, SLA and N_{area} in LP and MP (Figure 7) demonstrates that water loss and carbon gain processes were tightly coupled in the study area. It also shows that iWUE and $\Delta^{18}O$ can be included in the traditional leaf economic spectrum in drylands (Reich, 2014; Prieto et al., 2018). This leaf economic spectrum defined a water use strategy gradient from conservative (high iWUE and low gs) with high N_{area} to profligate (low iWUE and high gs) with high SLA (Prieto et al., 2018). These results revealed that water losses and carbon gain processes in arid and semi-arid regions are tightly coupled (Prieto et al., 2018; Yin et al., 2018; Shi et al., 2021). A second dimension of trait space was observed in LP (N_{area}) (Figure 7A) and MP (SLA and $\Delta^{18}O$) (Figure 7B), demonstrating that the most limiting resource was N in LP and water in MP (Wang et al., 2021). The limiting-resource spectrum differentiated species along a uniform gradient from resource acquisition to high resource conservative traits (Baltzer and Thomas, 2010; Bermúdez and Retuerto, 2014). Variability in iWUE was mainly controlled by the leaf economic spectrum in LP, and by both—leaf economic spectrum and limiting resource spectrum in MP. This supports the idea that species evolved species-specific strategies to adapt to harsh habitats by partitioning limiting resources (Bermúdez and Retuerto, 2014).

Conclusions

In this study, we found that species adopted opportunistic water use strategies to adapt to water- and N-limited habitats in arid and semi-arid regions. Variability in iWUE was primarily controlled by species, followed by sampling site, and the interaction between species and sampling site. Within transect, co-occurring species within a sampling site shifted their water use strategies from opportunistic (low iWUE and high gs) to conservative (low iWUE and high gs) with an increase in aridity in LP and MP, and water use strategies of co-occurring species gradually converged. This distribution pattern was driven mainly by the most limited resource, i.e., SOC/TN in LP, and soil moisture in MP. High variability in iWUE mainly determined by stomatal regulation. Furthermore, variability in iWUE was mainly controlled by leaf economic spectrum in LP, and by both—leaf economic spectrum and limiting resource spectrum in MP, indicating that species evolved species-specific strategies to adapt to a limiting habitat by partitioning limiting resources. This study demonstrated that the limiting resource and leaf functional traits jointly determined the distribution patterns of water use strategies of species in LP and MP along an aridity gradient, and emphasized the importance of considering biological processes in dissecting the underlying mechanisms of plant adaptation strategies at large regional scales.

Data availability statement

The original contributions presented in the study are included in the article/Supplementary material, further inquiries can be directed to the corresponding author/s.

Author contributions

JW and XW conceived and designed the research. JW conducted stable isotope measurements, data analysis, and wrote the manuscript. XW revised the manuscript. All authors contributed to the article and approved the submitted version.

Funding

This work was funded by the Strategic Priority Research Program of the Chinese Academy of Sciences (XDA23070202) and National Natural Science Foundation of China (Grant No. 41991234).

Acknowledgments

We thank the members in grassland transect investigation for field sampling, and Functional Trait database of terrestrial ecosystems in China (China_Traits) for sharing all auxiliary plant and soil data.

Conflict of interest

The authors declare that the research was conducted in the absence of any commercial or financial relationships that could be construed as a potential conflict of interest.

Publisher's note

Supplementary material

The Supplementary Material for this article can be found online at: https://www.frontiersin.org/articles/10.3389/fpls.2022.909603/full#supplementary-material

References

Ale, R., Zhang, L., Li, X., Raskoti, B. B., Pugnaire, F. I., and Luo, T. X. (2018). Leaf delta C-13 as an indicator of water availability along elevation gradients in the dry Himalayas. *Ecol. Indic.* 94, 266–273. doi: 10.1016/j.ecolind.2018.07.002

Aparecido, L. M. T., Woo, S., Suazo, C., Hultine, K. R., and Blonder, B. (2020). High water use in desert plants exposed to extreme heat. *Ecol. Lett.* 23, 1189–1200. doi: 10.1111/ele.13516

Bachmann, D., Gockele, A., Ravenek, J. M., Roscher, C., Strecker, T., Weigelt, A., et al. (2015). No evidence of complementary water use along a plant species richness gradient in temperate experimental grasslands. *PLoS ONE* 10,e0116367. doi: 10.1371/journal.pone.0116367

Bahar, N. H., Ishida, F. Y., Weerasinghe, L. K., Guerrieri, R., O'Sullivan, O. S., Bloomfield, K. J., et al. (2016). Leaf-level photosynthetic capacity in lowland Amazonian and high-elevation Andean tropical moist forests of Peru. *New Phytol.* 214, 903–904. doi: 10.1111/nph.14079

Baltzer, J. L., and Thomas, S. C. (2010). A second dimension to the leaf economics spectrum predicts edaphic habitat association in a tropical forest. *PLoS ONE* 5:7. doi: 10.1371/journal.pone.0013163

Barbour, M. (2007). Stable oxygen isotope composition of plant tissue: a review. *Funct. Plant Biol.* 34, 83–94. doi: 10.1071/FP06228

Basu, S., Ghosh, S., and Chattopadhyay, D. (2021). Disentangling the abiotic versus biotic controls on C_3 plant leaf carbon isotopes: inferences from a global review. *Earth Sci. Rev.* 222,103839. doi: 10.1016/j.earscirev.2021.103839

Bermúdez, R., and Retuerto, R. (2014). Together but different: co-occurring dune plant species differ in their water- and nitrogen-use strategies. *Oecologia* 174, 651–663. doi: 10.1007/s00442-013-2820-7

Blomberg, S. P., Garland, T., and Ives, A. R. (2003). Testing for phylogenetic signal in comparative data: behavioral traits are more labile. *Evolution* 57, 717–745. doi: 10.1111/j.0014-3820.2003.tb00285.x

Chen, Y., Feng, X., and Fu, B. (2021). An improved global remote-sensing-based surface soil moisture (RSSSM) dataset covering 2003–2018. *Earth Syst. Sci. Data* 13, 1–31. doi: 10.5194/essd-13-1-2021

Chesson, P., Gebauer, R. L. E., Schwinning, S., Huntly, N., Wiegand, K., Ernest, M. S. K., et al. (2004). Resource pulses, species interactions, and diversity maintenance in arid and semi-arid environments. *Oecologia* 141, 236–253. doi: 10.1007/s00442-004-1551-1

Choat, B., Brodribb, T. J., Brodersen, C. R., Duursma, R. A., Lopez, R., and Medlyn, B. E. (2018). Triggers of tree mortality under drought. *Nature* 558, 531–539. doi: 10.1038/s41586-018-0240-x

Cornwell, W. K., Wright, I. J., Turner, J., Maire, V., Barbour, M. M., Cernusak, L. A., et al. (2018). Climate and soils together regulate photosynthetic carbon isotope discrimination within C_3 plants worldwide. *Glob. Ecol. Biogeogr.* 27, 1056–1067. doi: 10.1111/geb.12764

Farquhar, G., Ehleringer, J., and Hubick, K. (1989). Carbon isotope discrimination and photosynthesis. *Annu. Rev. Plant Physiol. Plant Mol. Biol.* 40, 503–537. doi: 10.1146/annurev.pp.40.060189.002443

Farquhar, G. D., Cernusak, L. A., and Barnes, B. (2007). Heavy water fractionation during transpiration. *Plant Physiol.* 143, 11–18. doi: 10.1104/pp.106.093278

Feyissa, A., Yang, F., Wu, J. J., Chen, Q., Zhang, D. D., and Cheng, X. L. (2021). Soil nitrogen dynamics at a regional scale along a precipitation gradient in secondary grassland of China. *Sci. Total Environ.* 781,146736. doi: 10.1016/j.scitotenv.2021.146736

Flexas, J., Díaz-Espejo, A., Conesa, M. A., Coopman, R. E., Douthe, C., Gago, J., et al. (2016). Mesophyll conductance to CO2 and Rubisco as targets for improving intrinsic water use efficiency in C-3 plants. *Plant Cell Environ.* 39, 965–982. doi: 10.1111/pce.12622

Gago, J., Daloso, D. D., Figueroa, C. M., Flexas, J., Fernie, A. R., and Nikoloski, Z. (2016). Relationships of leaf net photosynthesis, stomatal conductance, and mesophyll conductance to primary metabolism: a multispecies meta-analysis approach. *Plant Physiol.* 171, 265–279. doi: 10.1104/pp.15.01660

Galmes, J., Medrano, H., and Flexas, J. (2007). Photosynthetic limitations in response to water stress and recovery in Mediterranean plants with different growth forms. *New Phytol.* 175, 81–93. doi: 10.1111/j.1469-8137.2007.02087.x

Grossiord, C., Buckley, T. N., Cernusak, L. A., Novick, K. A., Poulter, B., Siegwolf, R. T. W., et al. (2020). Plant responses to rising vapor pressure deficit. *New Phytol.* 226, 1550–1566. doi: 10.1111/nph.16485

Guerrieri, R., Belmecheri, S., Ollinger, S. V., Asbjornsen, H., Jennings, K., Xiao, J. F., et al. (2019). Disentangling the role of photosynthesis and stomatal conductance on rising forest water-use efficiency. *Proc. Natl. Acad. Sci. U. S. A.* 116, 16909–16914. doi: 10.1073/pnas.1905912116

Guo, X. C., Shi, P. J., Niinemets, U., Holscher, D., Wang, R., Liu, M. D., et al. (2021). "Diminishing returns" for leaves of five age-groups of Phyllostachys edulis culms. *Am. J. Bot.* 108, 1662–1672. doi: 10.1002/ajb2.1738

Li, Y., Shi, P., Niinemets, Ü., Song, Y., Yu, K., Schrader, J., et al. (2022). Diminishing returns among lamina fresh and dry mass, surface area, and petiole fresh mass among nine Lauraceae species. *Am. J. Bot.* 109, 377–392. doi: 10.1002/ajb2.1812

Liu, Y. J., Niu, H. S., and Xu, X. L. (2013). Foliar delta C-13 response patterns along a moisture gradient arising from genetic variation and phenotypic plasticity in grassland species of Inner Mongolia. *Ecol. Evol.* 3, 262–267. doi: 10.1002/ece3.453

Lyu, S. D., Wang, J., Song, X. W. and Wen, X. F. (2021). The relationship of δD and $\delta^{18}O$ in surface soil water and its implications for soil evaporation along grass transects of Tibet, Loess, and Inner Mongolia Plateau. *J. Hydrol.* 600. doi: 10.1016/j.jhydrol.2021.126533

Maracahipes, L., Carlucci, M. B., Lenza, E., Marimon, B. S., Marimon, B. H., Guimarães, F. A. G., et al. (2018). How to live in contrasting habitats? Acquisitive and conservative strategies emerge at inter- and intraspecific levels in savanna and forest woody plants. *Perspect. Plant Ecol. Evol. Syst.* 34, 17–25. doi: 10.1016/j.ppees.2018.07.006

Martin-StPaul, N., Delzon, S., and Cochard, H. (2017). Plant resistance to drought depends on timely stomatal closure. *Ecol. Lett.* 20, 1437–1447. doi: 10.1111/ele.12851

Maxwell, T., Silva, L., and Horwath, W. (2018). Integrating effects of species composition and soil properties to predict shifts in montane forest carbon-water relations. *Proc. Natl. Acad. Sci. U. S. A.* 115, E4219–E4226. doi: 10.1073/pnas.1718864115

Mitchell, R. M., Wright, J. P., and Ames, G. M. (2018). Species' traits do not converge on optimum values in preferred habitats. *Oecologia* 186, 719–729. doi: 10.1007/s00442-017-4041-y

Moreno-Gutierrez, C., Dawson, T. E., Nicolas, E., and Querejeta, J. I. (2012). Isotopes reveal contrasting water use strategies among coexisting plant species in a Mediterranean ecosystem. *New Phytol.* 196, 489–496. doi: 10.1111/j.1469-8137.2012.04276.x

Pinto, H., Sharwood, R. E., Tissue, D. T., and Ghannoum, O. (2014). Photosynthesis of C_3, C_3-C_4, and C_4 grasses at glacial CO_2. *J. Exp. Bot.* 65, 3669–3681. doi: 10.1093/jxb/eru155

Prentice, I. C., Dong, N., Gleason, S. M., Maire, V., and Wright, I. J. (2014). Balancing the costs of carbon gain and water transport: testing a new theoretical framework for plant functional ecology. *Ecol. Lett.* 17, 82–91. doi: 10.1111/ele.12211

Prieto, I., Querejeta, J., Segrestin, J., Volaire, F., and Roumet, C. (2018). Leaf carbon and oxygen isotopes are coordinated with the leaf economics spectrum in Mediterranean rangeland species. *Funct. Ecol.* 32, 612–625. doi: 10.1111/1365-2435.13025

Querejeta, J. I., Iván, P., Torres, P., Campoya, M., Alguacila, M. M., and Roldán, A. (2018). Water-spender strategy is linked to higher leaf nutrient concentrations across plant species colonizing a dry and nutrient-poor epiphytic habitat. *Environ. Exp. Bot.* 153, 302–310. doi: 10.1016/j.envexpbot.2018.06.007

Reich, P. (2014). The world-wide 'fast-slow' plant economics spectrum: a traits manifesto. *J. Ecol.* 102, 275–301. doi: 10.1111/1365-2745.12211

Reich, P. B., Buschena, C., Tjoelker, M. G., Wrage, K., Knops, J., Tilman, D., et al. (2003). Variation in growth rate and ecophysiology among 34 grassland and savanna species under contrasting N supply: a test of functional group differences. *New Phytol.* 157, 617–631. doi: 10.1046/j.1469-8137.2003.00703.x

Ren, T., He, N., Liu, Z., Li, M., Zhang, J., Li, A., et al. (2021). Environmental filtering rather than phylogeny determines plant leaf size in three floristically distinctive plateaus. *Ecol. Indic.* 130,108049. doi: 10.1016/j.ecolind.2021.108049

Reynolds, J. F., Stafford Smith, D. M., Lambin, E. F., Turner, B. L., Mortimore, M., Batterbury, S. P. J., et al. (2007). Global desertification: building a science for dryland development. *Science* 316, 847–851. doi: 10.1126/science.1131634

Roden, J. S., and Farquhar, G. D. (2012). A controlled test of the dual-isotope approach for the interpretation of stable carbon and oxygen isotope ratio variation in tree rings. *Tree Physiol.* 32, 490–503. doi: 10.1093/treephys/tps019

Rumman, R., Atkin, O. K., Bloomfield, K. J., and Eamus, D. (2018). Variation in bulk-leaf ^{13}C discrimination, leaf traits and water-use efficiency-trait relationships along a continental-scale climate gradient in Australia. *Glob. Change Biol.* 24, 1186–1200. doi: 10.1111/gcb.13911

Salazar-Tortosa, D., Castro, J., Villar-Salvador, P., Vinegla, B., Matias, L., Michelsen, A., et al. (2018). The "isohydric trap": a proposed feedback between water shortage, stomatal regulation, and nutrient acquisition drives differential growth and survival of European pines under climatic dryness. *Glob. Change Biol.* 24, 4069–4083. doi: 10.1111/gcb.14311

Scheidegger, Y., Saurer, M., Bahn, M., and Siegwolf, R. (2000). Linking stable oxygen and carbon isotopes with stomatal conductance and photosynthetic capacity: a conceptual model. *Oecologia* 125, 350–357. doi: 10.1007/s004420000466

Schneider, C. A., Rasband, W. S., and Eliceiri, K. W. (2012). NIH Image to ImageJ: 25 years of image analysis. *Nat. Methods* 9, 671–675. doi: 10.1038/nmeth.2089

Shi, P. J., Jiao, Y. B., Diggle, P. J., Turner, R., Wang, R., and Niinemets, U. (2021). Spatial distribution characteristics of stomata at the areole level in *Michelia cavaleriei* var. platypetala (Magnoliaceae). *Ann. Bot.* 128, 875–885. doi: 10.1093/aob/mcab106

Tang, S. B., Lai, Y., Tang, X. L., Phillips, O. L., Liu, J. F., Chen, D. X., et al. (2021). Multiple environmental factors regulate the large-scale patterns of plant water use efficiency and nitrogen availability across China's forests. *Environ. Res. Lett.* 16,10. doi: 10.1088/1748-9326/abe3bb

Utkhao, W., and Yingjajaval, S. (2015). Changes in leaf gas exchange and biomass of Eucalyptus camaldulensis in response to increasing drought stress induced by polyethylene glycol. *Trees Struct. Funct.* 29, 1581–1592. doi: 10.1007/s00468-015-1240-1

Wang, C., Liu, D. W., Luo, W. T., Fang, Y. T., Wang, X. B., Lu, X. T., et al. (2016). Variations in leaf carbon isotope composition along an arid and semi-arid grassland transect in northern China. *J. Plant Ecol.* 9, 576–585. doi: 10.1093/jpe/rtw006

Wang, J., and Wen, X. (2022). Divergence and conservative of stomatal conductance in coexisting species in response to climatic stress in Tibetan Plateau. *Ecol. Indic.* 138,108843. doi: 10.1016/j.ecolind.2022.108843

Wang, J., Wen, X., Zhang, X., and Li, S. (2018). The strategies of water–carbon regulation of plants in a subtropical primary forest on karst soils in China. *Biogeosciences* 15, 4193–4203. doi: 10.5194/bg-15-4193-2018

Wang, J., Wen, X. F., Lyu, S. D., and Guo, Q. J. (2021). Transition in multi-dimensional leaf traits and their controls on water use strategies of co-occurring species along a soil limiting-resource gradient. *Ecol. Indic.* 128,107838. doi: 10.1016/j.ecolind.2021.107838

Wright, I. J., Dong, N., Maire, V., Prentice, I. C., Westoby, M., Diaz, S., et al. (2017). Global climatic drivers of leaf size. *Science* 357,917–21. doi: 10.1126/science.aal4760

Wright, I. J., Reich, P. B., and Westoby, M. (2003). Least-cost input mixtures of water and nitrogen for photosynthesis. *Am. Nat.* 161, 98–111. doi: 10.1086/344920

Wu, J., Chavana-Bryant, C., Prohaska, N., Serbin, S. P., Guan, K. Y., Albert, L. P., et al. (2017). Convergence in relationships between leaf traits, spectra and age across diverse canopy environments and two contrasting tropical forests. *New Phytol.* 214, 1033–1048. doi: 10.1111/nph.14051

Yao, J. Y., Liu, H. P., Huang, J. P., Gao, Z. M., Wang, G. Y., Li, D., et al. (2020). Accelerated dryland expansion regulates future variability in dryland gross primary production. *Nat. Commun.* 11,10. doi: 10.1038/s41467-020-15515-2

Yin, Q., Wang, L., Lei, M., Dang, H., Quan, J., Tian, T., et al. (2018). The relationships between leaf economics and hydraulic traits of woody plants depend on water availability. *Sci. Total Environ.* 621, 245–252. doi: 10.1016/j.scitotenv.2017.11.171

Yue, P., Zhang, Q., Zhang, L., Li, H. Y., Yang, Y., Zeng, J., et al. (2019). Long-term variations in energy partitioning and evapotranspiration in a semiarid grassland in the Loess Plateau of China. *Agric. For. Meteorol.* 278,107671. doi: 10.1016/j.agrformet.2019.107671

Zhang, J., He, N., Liu, C., Xu, L., Chen, Z., Li, Y., et al. (2019). Variation and evolution of C:N ratio among different organs enable plants to adapt to N-limited environments. *Glob. Change Biol.* 26, 2534–2543. doi: 10.1111/gcb.14973

Zheng, S. X., and Shangguan, Z. P. (2007). Spatial patterns of foliar stable carbon isotope compositions of C-3 plant species in the Loess Plateau of China. *Ecol. Res.* 22, 342–353. doi: 10.1007/s11284-006-0024-x

Zhu, J. T., Jiang, L., Zhang, Y. J., Jiang, Y. B., Tao, J., Tian, L., et al. (2015). Below-ground competition drives the self-thinning process of Stipa purpurea populations in northern Tibet. *J. Veg. Sci.* 26, 166–174. doi: 10.1111/jvs.12207

frontiers | Frontiers in Plant Science

TYPE Original Research
PUBLISHED 10 August 2022
DOI 10.3389/fpls.2022.990441

OPEN ACCESS

EDITED BY
Peijian Shi,
Nanjing Forestry University, China

REVIEWED BY
Yu Tao,
Beijing Forestry University, China
Wenchen Song,
Minzu University of China, China
Zhuoya Zhang,
Southwest Forestry University, China

*CORRESPONDENCE
Jie Gao
jiegao@pku.edu.cn

†These authors have contributed equally to this work

SPECIALTY SECTION
This article was submitted to Functional Plant Ecology, a section of the journal Frontiers in Plant Science

RECEIVED 10 July 2022
ACCEPTED 22 July 2022
PUBLISHED 10 August 2022

CITATION
Wang J, Wang X, Ji Y and Gao J (2022) Climate factors determine the utilization strategy of forest plant resources at large scales. *Front. Plant Sci.* 13:990441.
doi: 10.3389/fpls.2022.990441

Climate factors determine the utilization strategy of forest plant resources at large scales

Jiangfeng Wang[1†], Xianxian Wang[1†], Yuhui Ji[1†] and Jie Gao[1,2*]

[1]College of Life Sciences, Xinjiang Normal University, Ürümqi, China, [2]Key Laboratory of Earth Surface Processes of Ministry of Education, College of Urban and Environmental Sciences, Institute of Ecology, Peking University, Beijing, China

Plant functional traits are a representation of plant resource utilization strategies. Plants with higher specific leaf area (SLA) and lower leaf dry matter content (LDMC) exhibit faster investment-return resource utilization strategies. However, the distribution patterns and driving factors of plant resource utilization strategies at the macroscale are rarely studied. We investigated the relative importance of climatic and soil factors in shaping plant resource utilization strategies at different life forms in forests using data collected from 926 plots across 163 forests in China. SLA and LDMC of plants at different life forms (i.e., trees, shrubs, and herbs) differ significantly. Resource utilization strategies show significant geographical differences, with vegetation in the western arid regions adopting a slower investment-return survival strategy and vegetation in warmer and wetter areas adopting a faster investment-return survival strategy. SLA decreases significantly with increased temperature and reduced rainfall, and vegetation growing in these conditions exhibits conservative resource utilization. Mean annual precipitation (MAP) is a key climatic factor that controls the resource utilization strategies of plants at the macroscale. Plants use resources more conservatively as soil pH increases. The influence of climate and soil factors is coupled to determine the resource utilization strategies of plants occupying different life forms at the macroscale, but the relative contribution of each varies across life forms. Our findings provide a theoretical framework for understanding the potential impact of increasing global temperatures on plant resource utilization.

KEYWORDS

resource utilization strategies, vertical levels of communities, climatic factors, soil nutrient factors, macroscale

Introduction

Plant functional traits are physiological and morphological characteristics of plants that respond to environmental changes, significantly affecting the function of forest ecosystems (Cappelli et al., 2020; Li X. et al., 2021; Weemstra et al., 2021). Specific leaf area (SLA) and leaf dry matter content (LDMC) are significantly correlated with particular plant resource utilization strategies and are extremely sensitive to climate change (Kattge et al., 2020). SLA is the leaf area per unit of dry leaf mass (Worthy et al., 2020) which, to some extent, reflects the ability of plant leaves to capture light energy under different environmental conditions. SLA also reflects the survival strategy adopted by plants to maximize carbon capture and is positively correlated with potential growth rate and maximum photosynthetic rate (Liu et al., 2018). Plants living in barren, high-temperature, and arid environments allocate more resources to enhance the dry matter content of foliage, which buttresses leaves against adverse conditions. At the same time, plants growing in these environments reduce SLA and photosynthetic rate to prolong leaf lifespan (Dwyer et al., 2014; Gong and Gao, 2019). LDMC is the ratio of leaf dry weight to fresh weight, which measures vegetation's response to aridity and is closely related to the leaf water holding capacity (Smart et al., 2017). Smaller cell gaps and higher diffusion resistance in plants reduce leaf transpiration and total respiration, resulting in increased LDMC (Baribault et al., 2010). Studies have shown that plants with high SLA and low LDMC access resources more easily (Siefert and Ritchie, 2016), allowing for a faster investment-return survival strategy.

Plants adapt to local environmental conditions by modulating leaf functional traits to regulate their capacity to assimilate carbon and obtain nutrients (Yin et al., 2018). Mean annual precipitation (MAP) and mean annual temperature are the climate factors with the greatest impact on SLA (He et al., 2010), and both are strongly positively correlated to SLA (Firn et al., 2019). When rainfall is low, plant LDMC increases, reflecting vegetation's investment in leaf construction to improve survival odds (Jiang et al., 2017). Increases in precipitation result in enrichment of the soil solution in dissolved salts, which changes soil conductivity. Overall, increased precipitation supports plant growth due to its association with increased SLA, transpiration rate, and net photosynthetic rate and a decrease in LDMC (Pietsch et al., 2014; Gong and Gao, 2019). Plants with high LDMC conserve water more efficiently due to lower rates of transpiration (Suter and Edwards, 2013). Temperature and precipitation jointly determine the resource acquisition and utilization trade-offs of plant leaves. Within a given forest community, differences in vegetation type (i.e., tree, shrub, or herb) and nutrient uptake strategies make it difficult to determine the resource utilization strategies employed by different groups (Poorter et al., 2009). Therefore, it is particularly important to quantify the macroscale effects of climate factors on SLA and LDMC of plants occupying different life forms in forests.

The availability of soil nutrients influences spatiotemporal patterns of leaf functional traits as well as plant resource utilization (Newsham et al., 2016; Huang et al., 2021). Total nitrogen content and the ratio of carbon to nitrogen are positively correlated with SLA and negatively correlated with LDMC (Hodgson et al., 2011). The effects of N limitation on plant growth are mitigated in soils enriched in N, thereby increasing SLA and LDMC (Wang et al., 2022). The availability of phosphorus in the soil is pH-dependent and, under acidic conditions, plants can rapidly access P to maximize growth. They also tend to have higher SLA and lower LDMC (Tao et al., 2019). Though soil nutrients have an effect on plant growth, the main drivers affecting leaf resource utilization strategies have not yet been identified (Cochrane et al., 2016; Poorter et al., 2019).

Leaf functional traits indicate the survival strategies of plants under various environmental conditions (Li X. et al., 2021). Environmental variation is also reflected in the trade-offs between plant access and utilization of resources, with significant differences in resource utilization strategies appearing across environmental gradients (Storkey and Macdonald, 2022). Characteristics of community system diversity make community trait variation a more effective indicator of plant responses to environmental change than species traits alone (Poorter et al., 2009), which ignore interspecific interactions (Taylor et al., 2015). In general, community functional traits are a better indicator of the ability of plants to access resources than the traits of individual species (Liu et al., 2021). At the community level, the resource utilization strategies of plants occupying different life forms are significantly different (Cheng et al., 2022). When shrubs and herbs are shaded, they adopt a faster investment-return survival strategy by increasing SLA to produce more organic matter through more efficient light interception and enhanced photosynthetic rates (Rüger et al., 2012). In contrast, if the leaves of trees receive significant sunlight, intense respiration drives dry matter depletion, resulting in reduced LDMC. When exposed to continuous light, plants must decrease SLA to lower synthetic rate in order to minimize damage caused by solar radiation (Li Y. et al., 2021). SLA reduction is a survival strategy that allows plants to better capture light energy and increase LDMC to prolong leaf lifespan (Liu et al., 2018).

Numerous studies have found that plant resource utilization strategies are complex due to their regulation by a combination of environmental factors (Huang et al., 2021; Wang et al., 2022). Exploring the distribution patterns of key leaf functional traits at large scales is of great ecological importance to quantify the effects of environmental conditions on plant resource utilization strategies (Li et al., 2022). Based on field survey data from 163 sites in China, we sought to identify the key drivers affecting leaf resource utilization strategies at different vegetative levels in forest communities. We propose the following hypotheses: (1) at the macroscale, plant resource acquisition strategies vary between life forms; (2) average annual precipitation is the dominant factor affecting the resource utilization strategy of plants at different life forms; and (3) climatic conditions are the dominant environmental factors affecting leaf resource acquisition strategies at different life forms.

Materials and methods

Study area and sample data

China has a vast territory and diverse climate, with 23% of its area covered by a rich and diverse array of forest ecosystem types. Using 926 forest plots from 163 sites in China surveyed between 2005 and 2020 (**Supplementary Figure 1**), we explored the spatial distribution patterns and driving factors driving resource utilization strategies at different life forms of forest communities. Forest communities are divided into tree, shrub, and herb levels according to species composition, structure, and production, with each plant having its life form, and vertical differentiation provides a good indication of the community's adaptation to environmental conditions (Latham et al., 1998). We randomly selected at least four representative sample plots at each site and recorded the longitude, latitude, and altitude of each plot. Our study sites ranged from 19.1°N to 53.5°N, from 79.7°E to 129.3°E, and altitudes ranged from 1 to 4,000 m.

Functional data

Leaf traits are widely used to indicate the adaptation of plants to their environment (Yu et al., 2022). The functional traits selected were SLA and LDMC, which are closely related to light interception, resource utilization, growth, and development of plants (Brun et al., 2022).

The experiment used the Japanese Cano Scan LIDE 110 portable leaf area meter to measure the area of fresh single leaf leaves after petiole removal. The fresh leaf weight was measured by electronic balance (accuracy of 0.0001 g), and then the fresh leaves were placed in a drying box at 105°C for 15 min, after which the temperature was reduced to 60°C for 48 h. The leaf dry weight was measured by weighing with a 1/10,000 electronic balance after drying at (Nanes, 2015). SLA (m^2/kg) = leaf area/leaf dry weight; LDMC (g/g) = leaf dry weight/leaf fresh weight.

Functional traits vary between individuals due to intra- and inter-specific competition (Taylor et al., 2015). Thus, we used the community weighted mean trait (CWM_i) to represent the average trait value of the forest.

$$CWM_i = \frac{\sum_i^n D_i \times Trait}{\sum_i^n D_i} \qquad (1)$$

where CWM_i represents the weighted characteristic values of the functional traits of the community and D_i represents the abundance of the dominant tree species. $Trait_i$ represents the selected functional traits.

Environmental data

The study found that plant resource utilization strategies are related to climate (Wang and Ali, 2021). Mean annual temperature (MAT), mean coldest monthly temperature (MCMT), mean warmest monthly temperature (MWMT), and (MAP) were extracted from the WorldClim global climate database at a spatial resolution of 1 km. Light is a key environmental factor affecting photosynthesis (Kramer, 1981), and we hypothesized that both annual sunshine duration (ASD) and mean annual evaporation (MAE) may be key predictors affecting plant resource utilization strategies. Both ASD and MAE were extracted from the Meteorological Data Center of the China Meteorological Administration.[1]

Soil conditions in different areas may potentially affect plant resource utilization strategies, so We extracted soil pH, soil N,[2] and soil P[3] data from a 250 m resolution grid in the top 30 cm soil level.

Data analysis

The SLA and LDMC data we studied fit a continuous normal distribution. We used a significant difference test at the 0.05 significance level to test for significant differences between SLA and LDMC in the trees, shrubs, and herbs (**Figure 2**). Significant difference testing was performed using the R package *agricolae* (version 4.1.0, R Core Team, 2020).

The contribution of environmental factors to spatial variation within SLA and LDMC was investigated using a linear regression model. R^2 represents the goodness of fit of the model. Linear regression using the R package *lme4* (R Core Team, 2020).

Generalized additive models (GAMs) were used to evaluate the effects of various environmental factors on net primary productivity (NPP); this approach utilizes both parametric and non-parametric components to reduce model risks inherent to linear models (Zou et al., 2017). First, key environmental factors were selected using GAMs with a significance level of 0.05. Next, a single GAM was constructed to model how environmental factors were related to NPP; relationships were then visualized in a non-metric multidimensional scaling analysis (NMDS) (Sweeney et al., 2021). The model can be summarized as:

$$g[E(Y|X)] = \sum_i \beta iXi + \sum_j fi(Xi) + \varepsilon \qquad (2)$$

where g(•) represents the link function, of which the specific form depends on the Y variable distribution. ϵ is the random

---

[1] https://data.cma.cn/

[2] http://www.csdn.store

[3] https://www.osgeo.cn/data/wc137

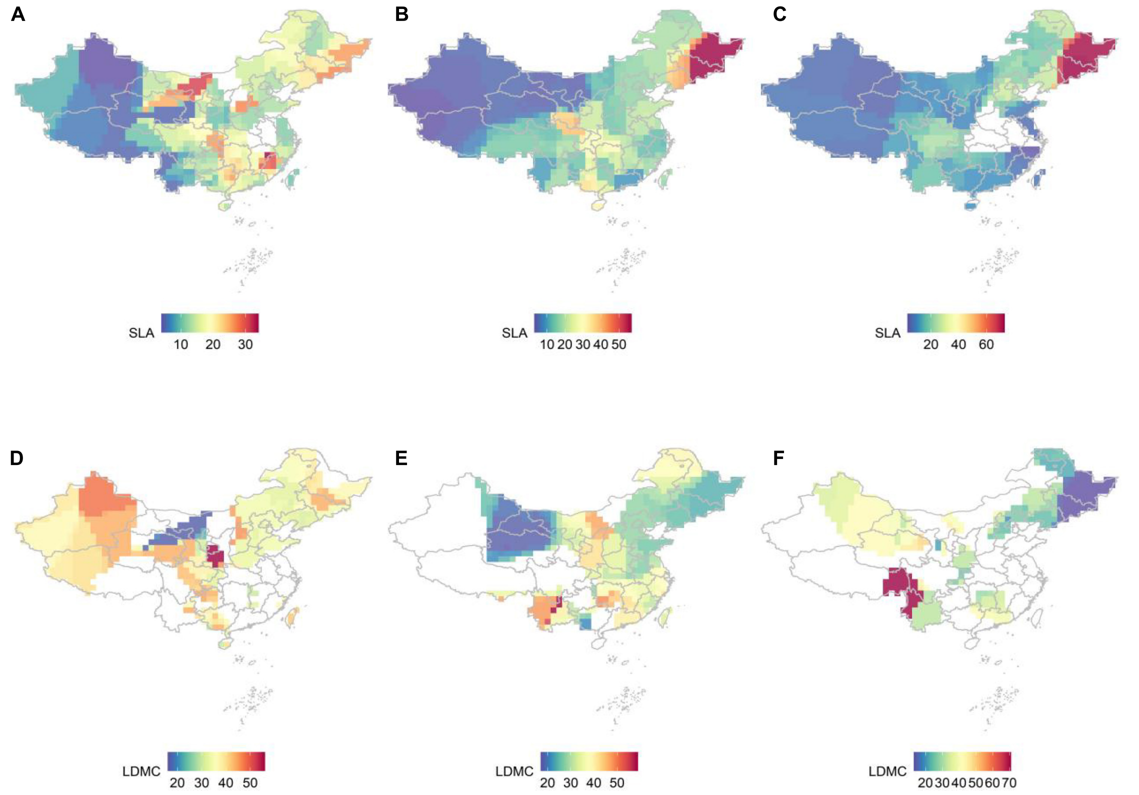

FIGURE 1
The distribution pattern of SLA and LDMC at different life forms in China, with a spatial resolution of 1 × 1 km, was studied by kernel density estimation. **(A)** SLA for trees; **(B)** SLA for shrubs; **(C)** SLA for herbs; **(D)** LDMC for trees; **(E)** LDMC for shrubs; **(F)** LDMC for herbs.

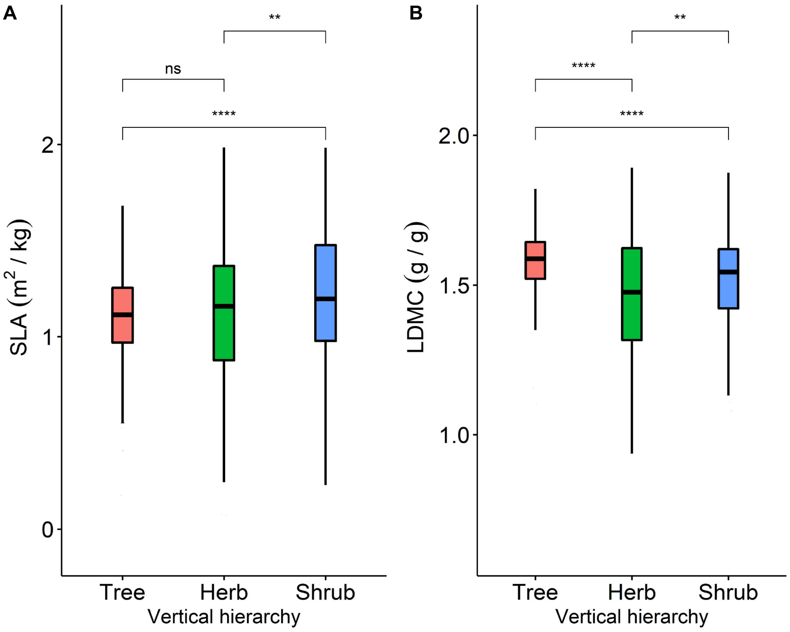

FIGURE 2
(A) Variability of SLA among trees, shrubs, and herbs; **(B)** variability of LDMC among trees, shrubs, and herbs. **Represents $P < 0.01$, ****represents $P < 0.0001$.

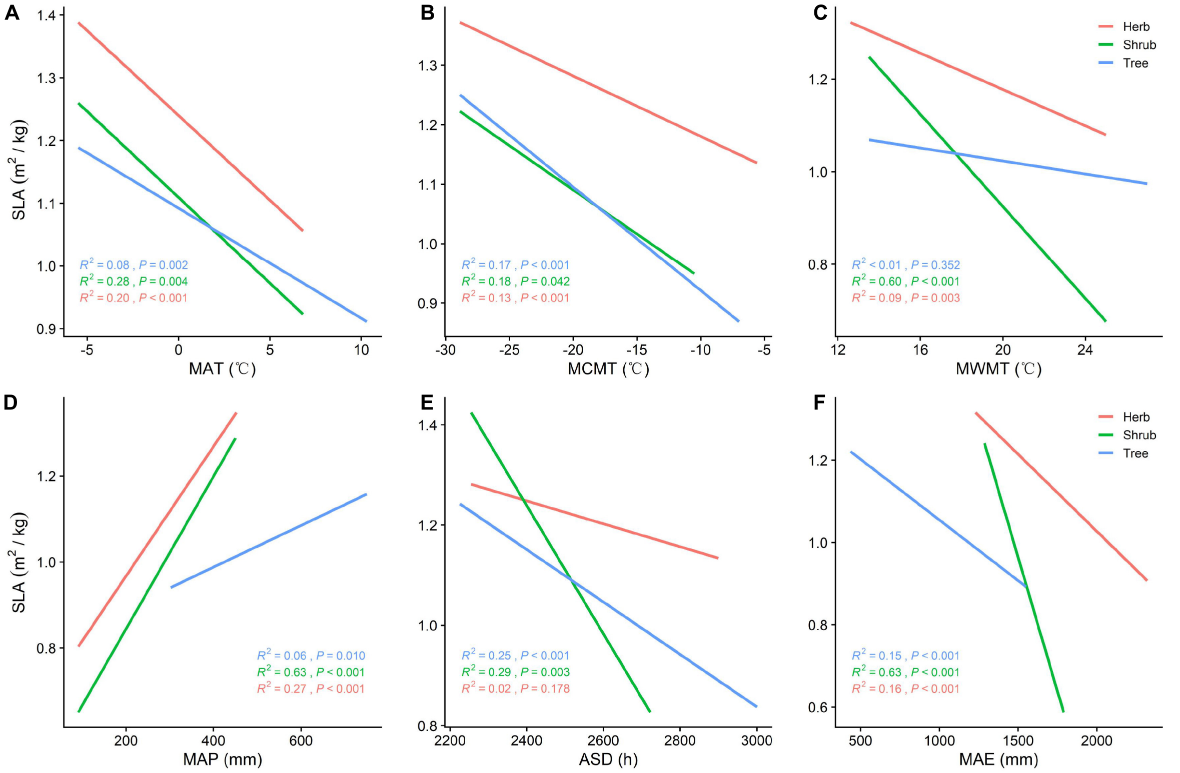

FIGURE 3

(A) General linear relationship between MAT and SLA of plants in the trees, shrubs, and herbs; **(B)** general linear relationship between MCMT and SLA of plants in the trees, shrubs, and herbs; **(C)** general linear relationship between MWMT and SLA of plants in the trees, shrubs, and herbs; **(D)** general linear relationship between MAP and SLA of plants in the trees, shrubs, and herbs; **(E)** general linear relationship between ASD and SLA of plants in the trees, shrubs, and herbs; **(F)** general linear relationship between MAE and SLA of plants in the trees, shrubs, and herbs.

error term; when a normal distribution function and identity-link are used, the errors are also normal. The link function is of the form g (u) = u, u = E (Y | X), E(ϵ | X) = 0. X_i is the explanatory variable, β_i is its corresponding parameter, and $f_j(\bullet)$ is a non-parametric smoothing function corresponding to the explanatory variable X_j. Here, a spline smoothing function S(•) (thin plate spline) was selected for function fitting between different nodes, and the penalty least square method was used to estimate each smoothing function S (•).

Results

Patterns of resource utilization strategies at different life forms in China

The resource utilization strategies of plants classified as trees, shrubs, and herbs show significant geographical differences but are highly consistent across similar latitude and longitude (Figure 1). As latitude and longitude increase, plant life strategy gradually changes from faster investment-return to slower investment-return, with SLA increasing from west to east and LDMC increasing from northeast to southwest at different verticals levels. Plants in the high mountains and high-altitude areas of the southwest tend to adopt a more conservative resource access strategy, while plants in the northeast obtain large amounts of available resources in the short term by improving SLA.

Differences in utilization strategies of plant resources at different life forms

The SLA and LDMC of plants at different life forms show significant differences (*, $P < 0.05$). Among the three life forms, shrub SLA and tree LDMC were higher (Figure 2). Moving across vegetation type from tree to shrub to herb, resource utilization strategies vary, gradually shifting from a slower (i.e., conservative) to a faster investment-return strategy. Shrub SLA was significantly higher than herb SLA, which was significantly higher than tree LDMC (Figure 2A). Tree LDMC was significantly higher than that of herbs and shrubs (Figure 2B).

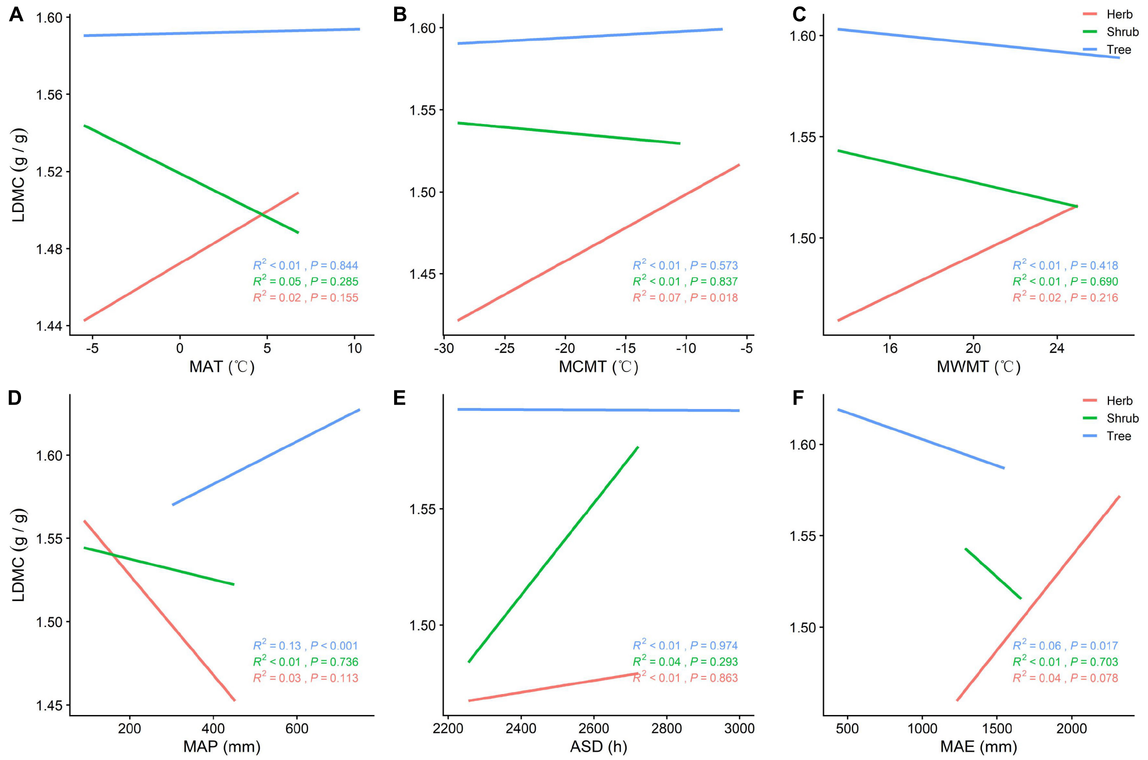

FIGURE 4

(A) General linear relationship between MAT and LDMC of plants in the trees, shrubs, and herbs; **(B)** general linear relationship between MCMT and LDMC of plants in the trees, shrubs, and herbs; **(C)** general linear relationship between MWMT and LDMC of plants in the trees, shrubs, and herbs; **(D)** general linear relationship between MAP and LDMC of plants in the trees, shrubs, and herbs; **(E)** general linear relationship between ASD and LDMC of plants in the trees, shrubs, and herbs; **(F)** general linear relationship between MAE and LDMC of plants in the trees, shrubs, and herbs.

Effects of environmental factors on plant resource utilization strategies at different life forms

SLA is positively correlated with MAP ($P < 0.05$) and negatively correlated with MAT, MCMT, ASD, and MAE across all vegetation types (Figures 3A–F). With increasing MAP, both SLA and tree LDMC increases, while SLA increases and LDMC decreases among herbs and shrubs (Figures 3D, 4D). The LDMC of herbs and shrubs increased significantly with increasing ASD (Figure 4E) and tree LDMC decreased significantly with increasing MAE (Figures 4D,F). Under better hydrothermal conditions, plants across life forms shift to a faster investment-return survival strategy, while plants exhibit a more conservative survival strategy as MAE and MAT increase. Of all the climatic factors, (Figure 3A–F, Figure 4A–F) ASD predicted SLA better for the trees and shrubs ($R^2 = 0.25, 0.29$, $P < 0.001$; Figure 3E) and MAP predicted LDMC best for the trees ($R^2 = 0.13$, $P < 0.001$; Figure 4D).

SLA is negatively correlated with soil pH at different life forms (Figure 5C), while LDMC increases with soil pH, with plants adopting a more conservative survival strategy. Tree and herb SLA and LDMC increase with increasing soil N and P, while shrubs exhibit increased SLA and decreased LDMC (Figures 5A,B,D,E). With increasing soil nutrients, plants switch to a faster investment-return survival strategy. Of all the soil nutrient factors, SLA was best predicted by soil pH for shrubs and trees ($R^2 = 0.27$, $P < 0.001$; Figure 5A–F).

Effects of environmental factors on changes in plant resource utilization strategies in different communities

We further analyzed the effects of environmental factors on SLA and LDMC at different life forms based on a generalized additive model (GAM) with non-metric multidimensional scaling (NMDS) ranking (Figure 6A–I; Figure 7A–I). Soil nutrient factors explained the variation in resource utilization strategies of plants at the tree level (Figure 6A, de = 19.0%; Figure 7A, de = 22.1%), while climatic factors best explained herb and shrub strategies (Figures 6E,F, de = 38.5%, 28%; Figures 7E,F, de = 12.2%, 27.7%). Climate and soil nutrient

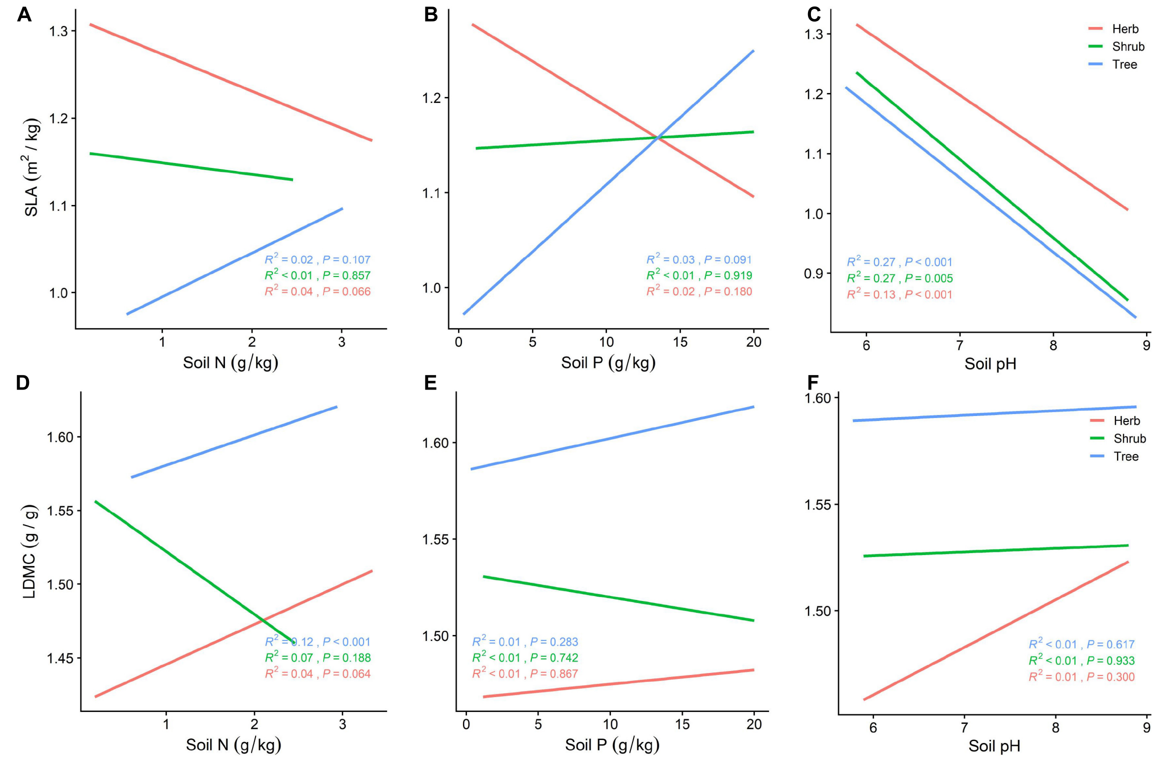

FIGURE 5

(A) General linear relationship between Soil N and SLA of plants in the trees, shrubs, and herbs; **(B)** general linear relationship between Soil P and SLA of plants in the trees, shrubs, and herbs; **(C)** general linear relationship between Soil pH and SLA of plants in the trees, shrubs, and herbs; **(D)** general linear relationship between Soil N and LDMC of plants in the trees, shrubs, and herbs; **(E)** general linear relationship between Soil P and LDMC of plants in the trees, shrubs, and herbs; **(F)** general linear relationship between Soil pH and LDMC of plants in the trees, shrubs, and herbs.

factors jointly shape the variation in SLA and LDMC of plants at different life forms.

Discussion

Significant differences exist among plant resource utilization strategies at different life forms in the forest community (Li Y. et al., 2021). SLA of understory plants is significantly higher than that of canopy plants and LDMC is significantly higher in canopy plants than in understory plants (Treml et al., 2019). There is a significant negative correlation between SLA and LDMC (Worthy et al., 2020). Shrubs and herbs, which are affected by the shading of tree foliage, adapt to low light conditions by increasing leaf area and SLA to capture more light energy, adopting a faster investment-return resource utilization strategy (Rüger et al., 2012).

There is a trade-off between leaf lifespan and photosynthetic productivity in plants (Yin et al., 2018). Understory plants increase photosynthetic efficiency at the expense of leaf lifespan, increasing SLA and reducing LDMC as the dry matter content of leaves decreases (Kröber et al., 2015). Due to the differences between species, herb plants are more adapted to understory shady environments, and the increase in SLA will be less than that of shrubs (Ma et al., 2021). Though tree leaves intercept light energy efficiently, their stomata close because of continuous and intense solar radiation. To reduce water loss due to transpiration, vegetation belonging to this life form enhance the amount of dry matter contained in their leaves (Baribault et al., 2010). Thus, the slower investment-return resource utilization strategy of tree leaves results in higher LDMC.

Habitat heterogeneity significantly affects the resource utilization strategy of plants (Guimarães et al., 2020). The SLA of plants at different life forms increases significantly with increasing longitude, while the LDMC increases with increasing latitude. From north to south and from west to east, precipitation and temperature increase (Wu et al., 2019). When plants experience water stress due to reduced precipitation, they close their stomata, reduce SLA, and compact their mesophyll cells to reduce water diffusion. These strategies enhance the amount of water retained in leaves, and high plant resource retention represents high plant survival (Galmés et al., 2013). The SLA of plant communities was significantly positively correlated with precipitation (Anderson et al., 2020). Similarly, temperature is an important factor

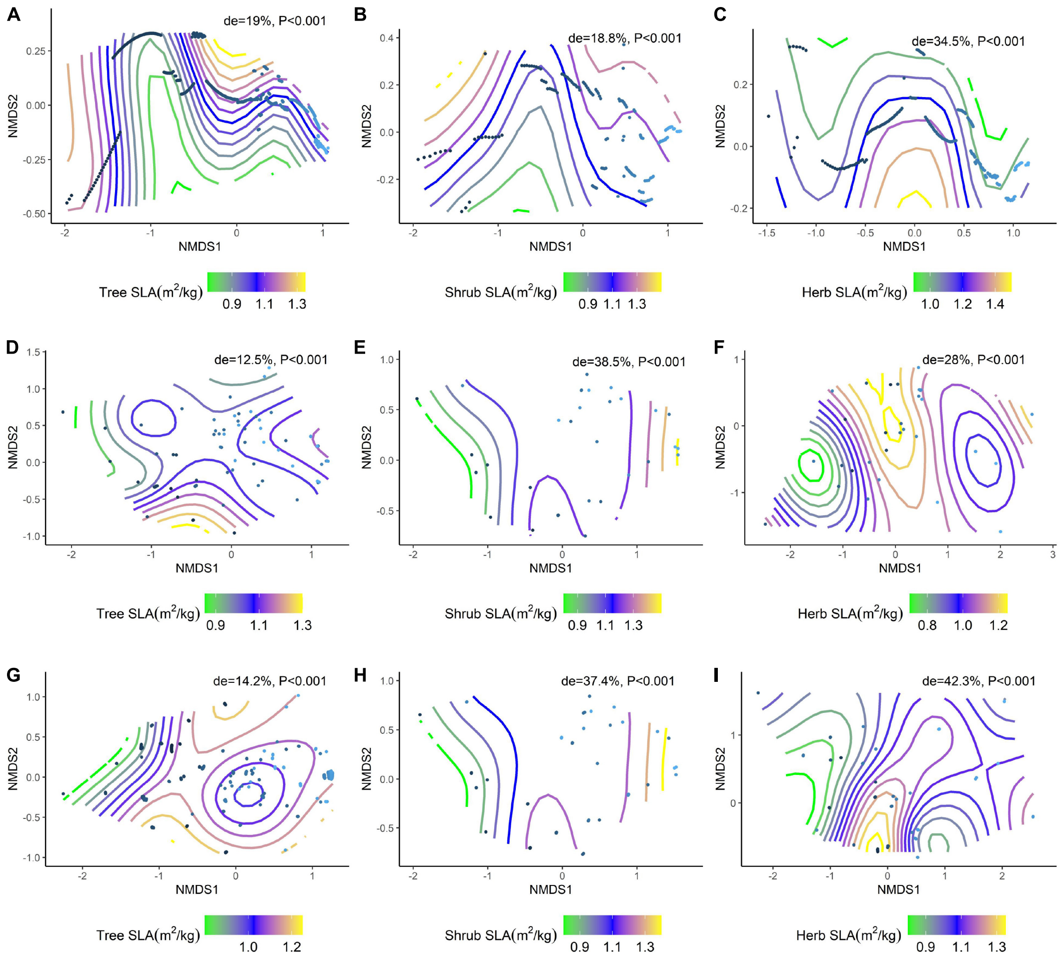

FIGURE 6

NMDS ranking of climatic and soil factors with different life forms of SLA. **(A)** NMDS ranking of soil factors with tree lSLA; **(B)** NMDS ranking of soil factors with shrub SLA; **(C)** NMDS ranking of soil factors with herb SLA; **(D)** NMDS ranking of climatic factors with tree SLA; **(E)** NMDS ranking of climatic factors with shrub SLA; **(F)** NMDS ranking of climate factors and herb SLA; **(G)** NMDS ranking of the sum of soil factors and climate factors and tree SLA; **(H)** NMDS ranking of the sum of soil factors and climate factors and shrub SLA; **(I)** NMDS ranking of the sum of soil factors and climate factors and herb SLA. Trait stacking indicates that abiotic factors, indicated by points on the NMD, are associated with higher or lower trait values, consistent with a colored trait gradient. Note that if the relationship between SLA and abiotic factors is linear, the gradient splines are parallel. Non-linear relationships between SLA and abiotic factors are represented by curve splines.

in the spatial and temporal distribution of plant resource utilization strategies, as it directly affects the activity of enzymes associated with photosynthesis and respiration (Descombes et al., 2020). Previous research has shown that, under low temperatures, plants adopt a slower investment-return strategy, reducing SLA and increasing LDMC to devote more dry matter to improving freezing tolerance. Similarly, under conditions high temperature and intense solar radiation, plants must increase dry matter and reduce SLA to reduce the photosynthetic rate and prevent water evaporation (Coble and Cavaleri, 2015). Trees in China are concentrated in southern regions where precipitation is high, and shrubs and herbs are concentrated in arid, semi-arid, and alpine high-altitude mountainous areas in the northwest (Zhao and Wu, 2014). This distribution explains the increasing trend of SLA and LDMC with increasing latitude and longitude (Tian et al., 2016). Herb and shrub LDMC decreases with MAP and in herb and shrub levels increases with ASD because understory growth is limited by the amount of light penetrating the canopy. Higher ASD raises ambient forest temperatures, but it also increases the amount of light energy reaching the understory, enhancing rates of photosynthesis. As ASD increases, so does LDMC as foliage accumulates dry matter, strengthening leaf structures (e.g., cell walls and microtubules) and prolonging leaf lifespan (Cheng et al., 2016). Excessive rainfall decreases soil conductivity and photosynthetically effective radiation, and understory herbs and shrubs in low light and rainy conditions tend to increase SLA and decrease LDMC to maximize resource access (Kröber et al., 2015). Therefore, at the community level, hydrothermal conditions (especially MAP) are

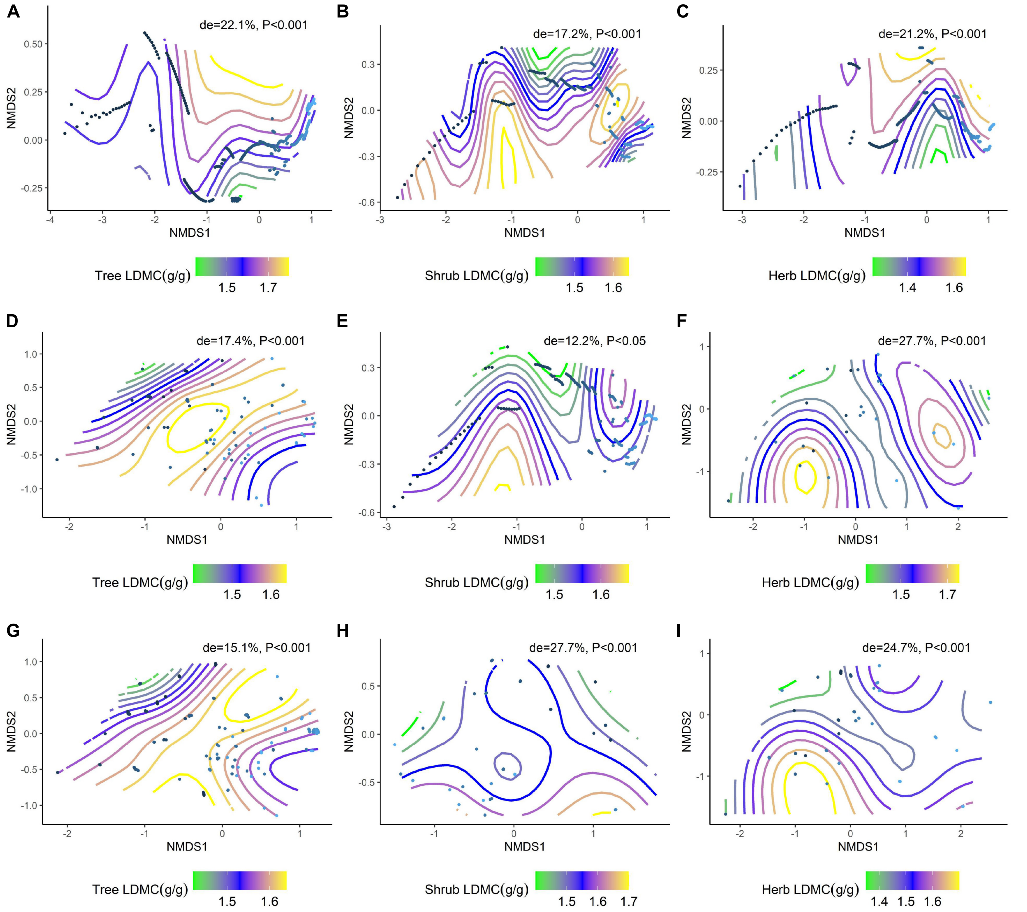

FIGURE 7

NMDS ranking of climatic and soil factors with different life forms of LDMC. **(A)** NMDS ranking of soil factors with tree LDMC; **(B)** NMDS ranking of soil factors with shrub LDMC; **(C)** NMDS ranking of soil factors with herb LDMC; **(D)** NMDS ranking of climatic factors with tree LDMC; **(E)** NMDS ranking of climatic factors with shrub LDMC; **(F)** NMDS ranking of climate factors and herb LDMC; **(G)** NMDS ranking of the sum of soil factors and climate factors and tree LDMC; **(H)** NMDS ranking of the sum of soil factors and climate factors and shrub LDMC; **(I)** NMDS ranking of the sum of soil factors and climate factors and herb LDMC. Trait stacking indicates that abiotic factors, indicated by points on the NMD, are associated with higher or lower trait values, consistent with a colored trait gradient. Note that if the relationship between LDMC and abiotic factors is linear, the gradient splines will be parallel. Non-linear relationships between LDMC and abiotic factors are represented by curve splines.

the principal factors driving plant resource utilization strategies (He et al., 2010).

Soil provides most of the nutrients required for plant growth, and soil nutrients are closely related to plant leaf resource utilization strategies (Gao et al., 2019). N and P are nutrients that are not only important for photosynthesis but that are also components of biomolecules such as nucleic acids and proteins (Yang et al., 2017). Soil N and P content directly affect plant leaf N (LN) and leaf P (LP) content, and LN and LP contribute to plant productivity and photosynthesis. Higher LN enhances the efficiency of carbon dioxide (CO_2) and N absorption, and higher LN is strongly correlated with improved stomatal conductance (Goedhart et al., 2010). The higher SLA of plants growing in high nutrient environments facilitates rapid access to soil resources; thus SLA is positively correlated with soil N and P content and negatively correlated with soil pH (Hodgson et al., 2011). This is consistent with our findings that tree, shrub, and herb SLA increases with increasing soil N and P content and decreases with increasing soil pH. The LDMC of plants in different life forms also increases with increasing soil N and P but, unlike SLA, LDMC also increases with soil pH. Other experiments have also shown that SLA, LN, and LP are lower and LDMC is higher in green leaves at higher pH (Tao et al., 2019), lending further support to the claim that plants growing in acidic conditions exhibit a slower investment-return survival strategy. Soil organic matter content is significantly and positively correlated with the resource utilization strategies of plants at different life forms (Niu et al., 2020).

Plant resource utilization strategies are influenced by environmental conditions, with temperature, precipitation, and soil nutrients acting together to influence plant leaf traits (Goll et al., 2017). Generalized additive model analysis shows that

SLA and LDMC across all life forms are mainly affected by soil nutrient factors, with climatic factors playing a key role in shaping the pattern of SLA and LDMC in the shrub and herb levels. Plants with higher SLA have a faster investment-return survival strategy, with efficient water and nutrient utilization supporting rapid growth (Pietsch et al., 2014). Higher LDMC in plants is associated with reduced leaf water holding capacity (Yu et al., 2009) and slower growth. Soil nutrient status, lower nutrient uptake and leaf water holding capacity, and low SLA and high LDMC of vegetation's topmost foliage is particularly critical for trees compared to shrubs and herbs factors on trees are particularly critical. In contrast, shrubs and herbs are more affected by light vs. shade.

Across vegetation types, differences in SLA and LDMC are primarily driven by hydrothermal conditions. Precipitation can accelerate the leaching and transformation of soil nutrients, while temperature provides a suitable environment for soil microorganisms to better decompose soil organic matter (Gao et al., 2021). Studies have found that soil nutrients are the main factors affecting plant resource utilization strategies, while the availability of soil nutrients depends on climatic factors and soil microorganisms (Jiao, 2021). Climate can directly act on soil nutrients and dominate plant resource utilization strategies. The significant differences in plant resource utilization strategies at different life forms of the community imply that plants have different growth strategies in response to different environmental factors (Madani et al., 2017). Thus, soil nutrient and climate factors combine to affect the distribution of resource utilization strategies associated with trees, shrubs, and herbs, and the contribution of climatic factors was greater than that of soil nutrient factors.

Conclusion

We used 926 forest plots from 163 sites in China surveyed between 2005 and 2020 to verify the driving effects of climatic and soil nutrient factors on forest resource utilization strategies. Our results show significant differences in the resource utilization strategies of plants classified as trees, shrubs, and herbs. Plants in the herb and shrub layers will mostly adopt a faster investment-return strategy, while plants at the tree level will choose to adapt to their environment in a more conservative way. MAP is a key factor in shaping the spatial pattern of resource utilization strategies of plants at different life forms. Both climate and soil significantly affect plant resource access and utilization strategies, but the relative contribution of climate factors is greater than that of soil nutrient factors. In the context of global environmental change, this study provides a theoretical framework for understanding the resource utilization strategies of plants.

Data availability statement

The original contributions presented in this study are included in the article/**Supplementary material**, further inquiries can be directed to the corresponding author.

Author contributions

JG: conceptualization, experiment implementation, visualization, and validation. XW and JW: formal analysis. XW: writing—original draft preparation. XW, JW, YJ, and JG: writing—review and editing. JG and YJ: project administration and funding acquisition. All authors have read and agreed to the published version of the manuscript.

Funding

This study was supported by the Xinjiang Normal University Landmark Achievements Cultivation Project, China.

Acknowledgments

We would like to thank the HighEdit company for assistance with English language editing of this manuscript.

Conflict of interest

The authors declare that the research was conducted in the absence of any commercial or financial relationships that could be construed as a potential conflict of interest.

Publisher's note

Supplementary material

The Supplementary Material for this article can be found online at: https://www.frontiersin.org/articles/10.3389/fpls.2022.990441/full#supplementary-material

References

Anderson, C. G., Bond-Lamberty, B., and Stegen, J. C. (2020). Active layer depth and soil properties impact specific leaf area variation and ecosystem productivity in a boreal forest. *PLoS One* 15:e0232506. doi: 10.1371/journal.pone.0232506

Baribault, T. W., Kobe, R. K., and Rothstein, D. E. (2010). Soil calcium, nitrogen, and water are correlated with aboveground net primary production in northern hardwood forests. *For. Ecol. Manag.* 260, 723–733. doi: 10.1016/j.foreco.2010.05.029

Brun, P., Violle, C., Mouillot, D., Mouquet, N., Enquist, B. J., and Munoz, F. (2022). Plant community impact on productivity: Trait diversity or key (stone) species effects? *Ecol. Lett.* 25, 913–925. doi: 10.1111/ele.13968

Cappelli, S. L., Pichon, N. A., Kempel, A., and Allan, E. (2020). Sick plants in grassland communities: A growth-defense trade-off is the main driver of fungal pathogen abundance. *Ecol. Lett.* 23, 1349–1359. doi: 10.1111/ele.13537

Cheng, J., Chu, P., Chen, D., and Bai, Y. (2016). Functional correlations between specific leaf area and specific root length along a regional environmental gradient in inner mongolia grasslands. *Funct. Ecol.* 30, 985–997. doi: 10.1111/1365-2435.12569

Cheng, X., Ping, T., Li, Z., Wang, T., Han, H., and Epstein, H. E. (2022). Effects of environmental factors on plant functional traits across different plant life forms in a temperate forest ecosystem. *New For.* 53, 125–142. doi: 10.1007/s11056-021-09847-0

Coble, A. P., and Cavaleri, M. A. (2015). Light acclimation optimizes leaf functional traits despite height-related constraints in a canopy shading experiment. *Oecologia* 177, 1131–1143. doi: 10.1007/s00442-015-3219-4

Cochrane, A., Hoyle, G. L., Yates, C. J., Neeman, T., and Nicotra, A. B. (2016). Variation in plant functional traits across and within four species of western australian banksia (proteaceae) along a natural climate gradient. *Austral. Ecol.* 41, 886–896. doi: 10.1111/aec.12381

Descombes, P., Pitteloud, C., Glauser, G., Defossez, E., Kergunteuil, A., and Allard, P. M. (2020). Novel trophic interactions under climate change promote alpine plant coexistence. *Science* 370, 1469–1473. doi: 10.1126/science.abd7015

Dwyer, J. M., Hobbs, R. J., and Mayfield, M. M. (2014). Specific leaf area responses to environmental gradients through space and time. *Ecology* 95, 399–410. doi: 10.1890/13-0412.1

Firn, J., McGree, J. M., Harvey, E., Flores-Moreno, H., Schütz, M., and Buckley, Y. M. (2019). Leaf nutrients, not specific leaf area, are consistent indicators of elevated nutrient inputs. *Nat. Ecol. Evol.* 3, 400–406. doi: 10.1038/s41559-018-0790-1

Galmés, J., Ochogavía, J. M., Gago, J., Roldán, E. J., Cifre, J., and Conesa, M. À (2013). Leaf responses to drought stress in mediterranean accessions of solanum lycopersicum: Anatomical adaptations in relation to gas exchange parameters. *Plant Cell Environ.* 36, 920–935. doi: 10.1111/pce.12022

Gao, J., Song, Z., and Liu, Y. (2019). Response mechanisms of leaf nutrients of endangered plant (*Acer catalpifolium*) to environmental factors varied at different growth stages. *Resour. Conserv. Recycl.* 17:e00521. doi: 10.1016/j.gecco.2019.e00521

Gao, X. L., Li, X. G., and Zhao, L. (2021). Shrubs magnify soil phosphorus depletion in Tibetan meadows: Conclusions from C: N: P stoichiometry and deep soil profiles. *Sci. Total Environ.* 785:147320. doi: 10.1016/j.scitotenv.2021.147320

Goedhart, C., Pataki, D., and Billings, S. (2010). Seasonal variations in plant nitrogen relations and photosynthesis along a grassland to shrubland gradient in owens valley, California. *Plant Soil* 327, 213–223. doi: 10.1007/s11104-009-0048-4

Goll, D. S., Winkler, A. J., Raddatz, T., Dong, N., Prentice, I. C., and Ciais, P. (2017). Carbon–nitrogen interactions in idealized simulations with jsbach (version 3.10). *Geosci. Model Dev.* 10, 2009–2030. doi: 10.5194/gmd-10-2009-2017

Gong, H., and Gao, J. (2019). Soil and climatic drivers of plant SLA (specific leaf area). *Resour. Conserv. Recycl.* 20:e00696. doi: 10.1016/j.gecco.2019.e00696

Guimarães, J. L., Hüther, C. M., Barros, A. R. D., Nogueira, L. T., Carvalho, D. L. F., and Borella, J. (2020). The specific leaf area of forest species subjected to different degrees of shading did not differ when detached and full leaflets were compared. *Semin. Cienc. Agrar.* 41, 1837–1848. doi: 10.5433/1679-0359.2020v41n5supl1p1837

He, J., Wang, X., Schmid, B., Flynn, D. F., Li, X., and Reich, P. B. (2010). Taxonomic identity, phylogeny, climate and soil fertility as drivers of leaf traits across chinese grassland biomes. *J. Plant Res.* 123, 551–561. doi: 10.1007/s10265-009-0294-9

Hodgson, J., Montserrat-Martí, G., Charles, M., Jones, G., Wilson, P., and Shipley, B. (2011). Is leaf dry matter content a better predictor of soil fertility than specific leaf area? *Ann. Bot.* 108, 1337–1345. doi: 10.1093/aob/mcr225

Huang, W., Wang, W., Cao, M., Fu, G., Xia, J., and Wang, Z. (2021). Local climate and biodiversity affect the stability of china's grasslands in response to drought. *Sci. Total Environ.* 768:145482. doi: 10.1016/j.scitotenv.2021.145482

Jiang, L., Bao, A., Guo, H., and Ndayisaba, F. (2017). Vegetation dynamics and responses to climate change and human activities in central asia. *Sci. Total Environ.* 599, 967–980. doi: 10.1016/j.scitotenv.2017.05.012

Jiao, F. (2021). Spatial distribution patterns and driving factors of plant biomass and leaf N, P stoichiometry on the loess plateau of china. *Plants* 10:2420. doi: 10.3390/plants10112420

Kattge, J., Bönisch, G., Díaz, S., Lavorel, S., Prentice, I. C., and Leadley, P. (2020). Try plant trait database–enhanced coverage and open access. *Global Change Biol.* 26, 119–188. doi: 10.1111/gcb.14904

Kramer, P. J. (1981). Carbon dioxide concentration, photosynthesis, and dry matter production. *Bioscience* 31, 29–33. doi: 10.2307/1308175

Kröber, W., Plath, I., Heklau, H., and Bruelheide, H. (2015). Relating stomatal conductance to leaf functional traits. *J. Vis. Exp.* 104:52738. doi: 10.3791/52738

Latham, P. A., Zuuring, H. R., and Coble, D. W. (1998). A method for quantifying vertical forest structure. *For. Ecol. Manag.* 4, 157–170. doi: 10.1016/S0378-1127(97)00254-5

Li, J., Chen, X., Niklas, K. J., Sun, J., Wang, Z., and Zhong, Q. (2022). A whole-plant economics spectrum including bark functional traits for 59 subtropical woody plant species. *J. Ecol.* 110, 248–261. doi: 10.1111/1365-2745.13800

Li, X., Song, X., Zhao, J., Lu, H., Qian, C., and Zhao, X. (2021). Shifts and plasticity of plant leaf mass per area and leaf size among slope aspects in a subalpine meadow. *Ecol. Evol.* 11, 14042–14055. doi: 10.1002/ece3.8113

Li, Y., Li, Q., Xu, L., Li, M., Chen, Z., and Song, Z. (2021). Plant community traits can explain variation in productivity of selective logging forests after different restoration times. *Ecol. Indic.* 131:108181. doi: 10.1016/j.ecolind.2021.108181

Liu, G., Wang, L., Jiang, L., Pan, X., Huang, Z., and Dong, M. (2018). Specific leaf area predicts dryland litter decomposition via two mechanisms. *J. Ecol.* 106, 218–229. doi: 10.1111/1365-2745.12868

Liu, Z., Dong, N., Zhang, H., Zhao, M., Ren, T., and Liu, C. (2021). Divergent long-and short-term responses to environmental gradients in specific leaf area of grassland species. *Ecol. Indic.* 130:108058. doi: 10.1016/j.ecolind.2021.108058

Ma, H., Mo, L., and Crowther, T. W. (2021). The global distribution and environmental drivers of aboveground versus belowground plant biomass. *Nat. Ecol. Evol.* 5, 1110–1122.

Madani, N., Kimball, J. S., and Running, S. W. (2017). Improving global gross primary productivity estimates by computing optimum light use efficiencies using flux tower data. *J. Geophys. Res. Biogeosci.* 122, 2939–2951. doi: 10.1002/2017JG004142

Nanes, B. A. (2015). Slide set: Reproducible image analysis and batch processing with ImageJ. *Biotechniques* 59, 269–278. doi: 10.2144/000114351

Newsham, K. K., Hopkins, D. W., Carvalhais, L. C., Fretwell, P. T., Rushton, S. P., and O'Donnell, A. G. (2016). Relationship between soil fungal diversity and temperature in the maritime antarctic. *Nat. Clim. Chang.* 6, 182–186. doi: 10.1038/nclimate2806

Niu, K., Zhang, S., and Lechowicz, M. J. (2020). Harsh environmental regimes increase the functional significance of intraspecific variation in plant communities. *Funct. Ecol.* 34, 1666–1677. doi: 10.1111/1365-2435.13582

Pietsch, K. A., Ogle, K., Cornelissen, J. H., Cornwell, W. K., Bönisch, G., and Craine, J. M. (2014). Global relationship of wood and leaf litter decomposability: The role of functional traits within and across plant organs. *Glob. Ecol. Biogeogr.* 23, 1046–1057. doi: 10.1111/geb.12172

Poorter, H., Niinemets, Ü, Ntagkas, N., Siebenkäs, A., Mäenpää, M., and Matsubara, S. (2019). A meta-analysis of plant responses to light intensity for 70 traits ranging from molecules to whole plant performance. *New Phytol.* 223, 1073–1105. doi: 10.1111/nph.15754

Poorter, H., Niinemets, Ü, Poorter, L., Wright, I. J., and Villar, R. (2009). Causes and consequences of variation in leaf mass per area (lma): A meta-analysis. *New Phytol.* 182, 565–588. doi: 10.1111/j.1469-8137.2009.02830.x

R Core Team (2020). *A language and environment for statistical computing.* Vienna: R Foundation for Statistical Computing.

Rüger, N., Wirth, C., Wright, S. J., and Condit, R. (2012). Functional traits explain light and size response of growth rates in tropical tree species. *Ecology* 93, 2626–2636. doi: 10.1890/12-0622.1

Siefert, A., and Ritchie, M. E. (2016). Intraspecific trait variation drives functional responses of old-field plant communities to nutrient enrichment. *Oecologia* 181, 245–255. doi: 10.1007/s00442-016-3563-z

Smart, S. M., Glanville, H. C., Blanes, M. D. C., Mercado, L. M., Emmett, B. A., and Jones, D. L. (2017). Leaf dry matter content is better at predicting above-ground net primary production than specific leaf area. *Funct. Ecol.* 31, 1336–1344. doi: 10.1111/1365-2435.12832

Storkey, J., and Macdonald, A. J. (2022). The role of long-term experiments in validating trait-based approaches to achieving multifunctionality in grasslands. *Front. Agric. Sci. Eng.* 9, 187–196. doi: 10.15302/J-FASE-2021438

Suter, M., and Edwards, P. J. (2013). Convergent succession of plant communities is linked to species' functional traits. *Perspect. Plant Ecol.* 15, 217–225. doi: 10.1016/j.ppees.2013.05.001

Sweeney, C. J., Vries, F. T., and Dongen, B. E. (2021). Root traits explain rhizosphere fungal community composition among temperate grassland plant species. *New Phytol.* 229, 1492–1507.

Tao, J., Zuo, J., He, Z., Wang, Y., Liu, J., and Liu, W. (2019). Traits including leaf dry matter content and leaf ph dominate over forest soil ph as drivers of litter decomposition among 60 species. *Funct. Ecol.* 33, 1798–1810. doi: 10.1111/1365-2435.13413

Taylor, P., Asner, G., Dahlin, K., Anderson, C., Knapp, D., and Martin, R. (2015). Landscape-scale controls on aboveground forest carbon stocks on the osa peninsula, costa rica. *PLoS One* 10:e0126748. doi: 10.1371/journal.pone.0126748

Tian, M., Yu, G., He, N., and Hou, J. (2016). Leaf morphological and anatomical traits from tropical to temperate coniferous forests: Mechanisms and influencing factors. *Sci. Rep.* 6, 1–10. doi: 10.1038/srep19703

Treml, V., Hejda, T., and Kašpar, J. (2019). Differences in growth between shrubs and trees: How does the stature of woody plants influence their ability to thrive in cold regions? *Agric. For. Meteorol.* 271, 54–63. doi: 10.1016/j.agrformet.2019.02.036

Wang, L. Q., and Ali, A. (2021). Climate regulates the functional traits–aboveground biomass relationships at a community-level in forests: A global meta-analysis. *Sci. Total Environ.* 761:143238. doi: 10.1016/j.scitotenv.2020.143238

Wang, X., Yan, X., Huang, K., Luo, X., Zhang, Y., and Zhou, L. (2022). Nitrogen enrichment and warming shift community functional composition via distinct mechanisms: The role of intraspecific trait variability and species turnover. *Funct. Ecol.* 36, 1230–1242. doi: 10.1111/1365-2435.14012

Weemstra, M., Zambrano, J., Allen, D., and Umaña, M. N. (2021). Tree growth increases through opposing above-ground and below-ground resource strategies. *J. Ecol.* 109, 3502–3512. doi: 10.1111/1365-2745.13729

Worthy, S. J., Laughlin, D. C., Zambrano, J., Umaña, M. N., Zhang, C., and Lin, L. (2020). Alternative designs and tropical tree seedling growth performance landscapes. *Ecology* 101:e03007. doi: 10.1002/ecy.3007

Wu, S. Y., Wu, Y., and Wen, J. (2019). Future changes in precipitation characteristics in china. *Int J. Climatol.* 39, 3558–3573. doi: 10.1002/joc.6038

Yang, S. Y., Huang, T. K., Kuo, H. F., and Chiou, T. J. (2017). Role of vacuoles in phosphorus storage and remobilization. *J. Exp. Bot.* 68, 3045–3055. doi: 10.1093/jxb/erw481

Yin, Q., Wang, L., Lei, M., Dang, H., Quan, J., and Tian, T. (2018). The relationships between leaf economics and hydraulic traits of woody plants depend on water availability. *Sci. Total Environ.* 621, 245–252. doi: 10.1016/j.scitotenv.2017.11.171

Yu, K., Wang, Y., Wei, J., Ma, Q., Yu, D., and Li, J. (2009). Improving rhizome yield and quality of Paris polyphylla through gibberellic acid-induced retardation of senescence of aerial parts. *Plant Signal. Behav.* 4, 413–415. doi: 10.4161/psb.4.5.8268

Yu, W., Wang, C., Huang, Z., Wang, D., and Liu, G. (2022). Variations in the traits of fine roots of different orders and their associations with leaf traits in 12 co-occuring plant species in a semiarid inland dune. *Plant Soil* 472, 193–206.

Zhao, D., and Wu, S. (2014). Responses of vegetation distribution to climate change in china. *Theor. Appl. Clim.* 117, 15–28. doi: 10.1007/s00704-013-0971-4

Zou, B., Chen, J., Zhai, L., Fang, X., and Zheng, Z. (2017). Satellite based mapping of ground pm2.5 concentration using generalized additive modeling. *Remote Sens.* 9:1. doi: 10.3390/rs9010001

frontiers | Frontiers in Plant Science

TYPE Original Research
PUBLISHED 09 September 2022
DOI 10.3389/fpls.2022.996313

OPEN ACCESS

EDITED BY
Peijian Shi,
Nanjing Forestry University, China

REVIEWED BY
Xiangjin Shen,
Northeast Institute of Geography and Agroecology (CAS), China
Romà Ogaya,
Ecological and Forestry Applications Research Center (CREAF), Spain
Zhuoya Zhang,
Southwest Forestry University, China
Yuyang Zhang,
Tarim University, China

*CORRESPONDENCE
Jie Gao
jiegao72@gmail.com

SPECIALTY SECTION
This article was submitted to Functional Plant Ecology, a section of the journal Frontiers in Plant Science

RECEIVED 17 July 2022
ACCEPTED 17 August 2022
PUBLISHED 09 September 2022

CITATION
Wang X, Wang R and Gao J (2022) Precipitation and soil nutrients determine the spatial variability of grassland productivity at large scales in China.
Front. Plant Sci. 13:996313.
doi: 10.3389/fpls.2022.996313

Precipitation and soil nutrients determine the spatial variability of grassland productivity at large scales in China

Xianxian Wang[1], Ru Wang[1] and Jie Gao[1,2]*

[1]College of Life Sciences, Xinjiang Normal University, Urumqi, China, [2]Institute of Ecology and Key Laboratory of Earth Surface Processes of Ministry of Education, College of Urban and Environmental Sciences, Peking University, Beijing, China

Changes in net primary productivity (NPP) to global change have been studied, yet the relative impacts of global change on grassland productivity at large scales remain poorly understood. Using 182 grassland samples established in 17 alpine meadows (AM) and 21 desert steppes (DS) in China, we show that NPP of AM was significantly higher than that of DS. NPP increased significantly with increasing leaf nitrogen content (LN) and leaf phosphorus content (LP) but decreased significantly with increasing leaf dry matter content (LDMC). Among all abiotic factors, soil nutrient factor was the dominant factor affecting the variation of NPP of AM, while the NPP of DS was mainly influenced by the changing of precipitation. All abiotic factors accounted for 62.4% of the spatial variation in the NPP of AM, which was higher than the ability to explain the spatial variation in the NPP of DS (43.5%). Leaf traits together with soil nutrients and climatic factors determined the changes of the grassland productivity, but the relative contributions varied somewhat among different grassland types. We quantified the effects of biotic and abiotic factors on grassland NPP, and provided theoretical guidance for predicting the impacts of global change on the NPP of grasslands.

KEYWORDS

grassland productivity, leaf traits, climate change, soil nutrients, desert steppe

Introduction

Grassland accounts for about a quarter of the global land area and is an important component of the terrestrial ecosystem (Pecina et al., 2019). Grasslands can not only effectively contributes to the global carbon cycle, but also plays a key role in regulating climate and soil conservation (Wang et al., 2019; Zhang et al., 2020). Grassland ecosystems are monospecific and structurally simple, making them more climate-sensitive than forest ecosystems (Liang and Gornish, 2019). Different types of grasslands (such as meadow steppe, typical steppe, desert steppe, and alpine steppe) also have obvious differences in ecosystem functions. Therefore, it is of great significance for us to investigate how environmental factors affect the functions of various grasslands in the context of global change (Anderegg et al., 2015; Seddon et al., 2016).

Net primary productivity (NPP) reflects the amount of carbon fixed by photosynthesis in a certain ecosystem per unit of time and space (Gang et al., 2018). NPP represents the energy that plants can use for growth, development, and reproduction, and is also the material basis for the survival and reproduction of biological groups (Sun and Du, 2017). Numerous studies have found that biological and abiotic factors jointly determine the temporal and spatial changes of NPP in grassland ecosystems (Shi et al., 2022). For example, Henry et al. (2018) found that precipitation controlled the spatio-temporal variation of grassland NPP, while Gong H. et al. (2020) believed that the availability of soil N and P content were the key factors that shaping the distribution pattern of grassland NPP. In recent years, with the development of functional trait research, leaf traits were widely used to predict the changes of NPP (Forrestel et al., 2017; Li et al., 2020; Schrader et al., 2021; Jiao et al., 2022). There remains no consensus on the dominant factors of spatial-temporal variation in grassland NPP (Henry et al., 2018; Wei et al., 2020).

Alpine meadows (AM) are mainly distributed in the alpine plateau region, which located at higher altitude regions. While desert steppes (DS) are mainly located in temperate regions with little mean annual precipitation (MAP) and are mainly distributed in northwest China (Zhou et al., 2020). Environmental factors driving the NPP of various grasslands vary considerably due to the difference in hydrothermal conditions and the altitude at which they are located (Sun et al., 2021). Drought stress significantly affects the photosynthesis and metabolism of the plants in DS (Grilli et al., 2017), therefore, precipitation is a key limiting factor of the NPP in DS. With the decline in MAP, the NPP of the DS decreased significantly (Chen et al., 2022). However, many studies have found that rainfall does not directly affect plant metabolism, but further influences plant uptake of soil nutrients by acting on soil microbial respiration and accelerating soil nutrient leaching and transformation (Gao et al., 2021). Soil is the direct living environment for plants. Plants absorb water and nutrients from the soil for photosynthesis. Soil nutrients control the photosynthesis of grass plants and affect the NPP of grasslands (Wieder et al., 2015). Soil N content can mitigate the effects on desert grassland NPP due to reduced precipitation, while soil P content is an essential element for plant energy transfer (Baldarelli et al., 2021), and soil pH represents soil fertility, which is a key soil factor to maintain NPP in desert grassland ecosystem (Zhang et al., 2021). Plants adapt to climate change by altering their traits (Wang et al., 2017b). Plants adapt to drought stress by reducing the leaf dry matter content (LDMC) and increased the leaf nitrogen content (LNC; Mahaut et al., 2020). Plants with lower specific leaf area (SLA) had a stronger ability to retain water and generally have a longer life span (Gong and Gao, 2019; Luo et al., 2020).

Compared with the DS, the structure and function of the AM are more sensitive to climate change (Pries et al., 2017). Zhang et al. (2019) found that light intensity significantly affects the NPP of the AM through the brightening experiment. NPP of the AM is also limited by low temperature and has no significant relationship with precipitation (Pan et al., 2021). Leaf traits represent the adaptability of alpine grassland function to low temperature, and plants with smaller leaf area (LA) are better able to avoid frost and heat damage (Dong et al., 2017). LN and LP are essential for plant growth and development (Heineman et al., 2016), and grassland NPP largely depends on plant availability to nitrogen and phosphorus (Wieder et al., 2015). LDMC is also closely related to grassland NPP, and Xu et al. (2018) found that grassland NPP is positively correlated with LDMC. The spatio-temporal variation of NPP of different grassland types is mainly influenced by a combination of environmental and biological factors, but there remains no consensus on the relative contribution of these factors (Gong Y. H. et al., 2020; Jochum et al., 2020; Shi et al., 2020).

Based on the field data from 182 grasslands in 17 AM and 21 DS in China, we sought to identify the main drivers of NPP in different grassland ecosystems. To answer this question, we proposed the following hypotheses: (1) The NPP of AM is significantly higher than DS. (2) Precipitation is the driving factor of NPP of DS, while NPP of AM is the combined effect of precipitation and temperature. (3) Climate factors are the key environmental factors dominating NPP of AM and that of DS, however, soil nutrient factors also play a non-negligible role.

Materials and methods

Study area and plot description

China has a vast territory and a diverse climate, with possesses many types of grasslands. These grasslands are mainly distributed in arid and semi-arid areas in northern China and the Qinghai-Tibet Plateau (Yu et al., 2021; Shen et al., 2022). The large spatial scale and the richness of climate types provide conditions for exploring the spatio-temporal variation of NPP of grasslands (Huang et al., 2021). The study used data from 182 grasslands in 17 AM in the southwest region and 21 DS in the north central region in China (**Figure 1A**). Our study sites range in latitude from 19.1° to 53.5° north and longitude from 79.72° to 121.1° east, with elevations ranging from 13 to 5,000 m.

Community leaf traits data

Leaf traits are widely used to detect the adaptability of plants to the living environment (Hikosaka et al., 2021). The

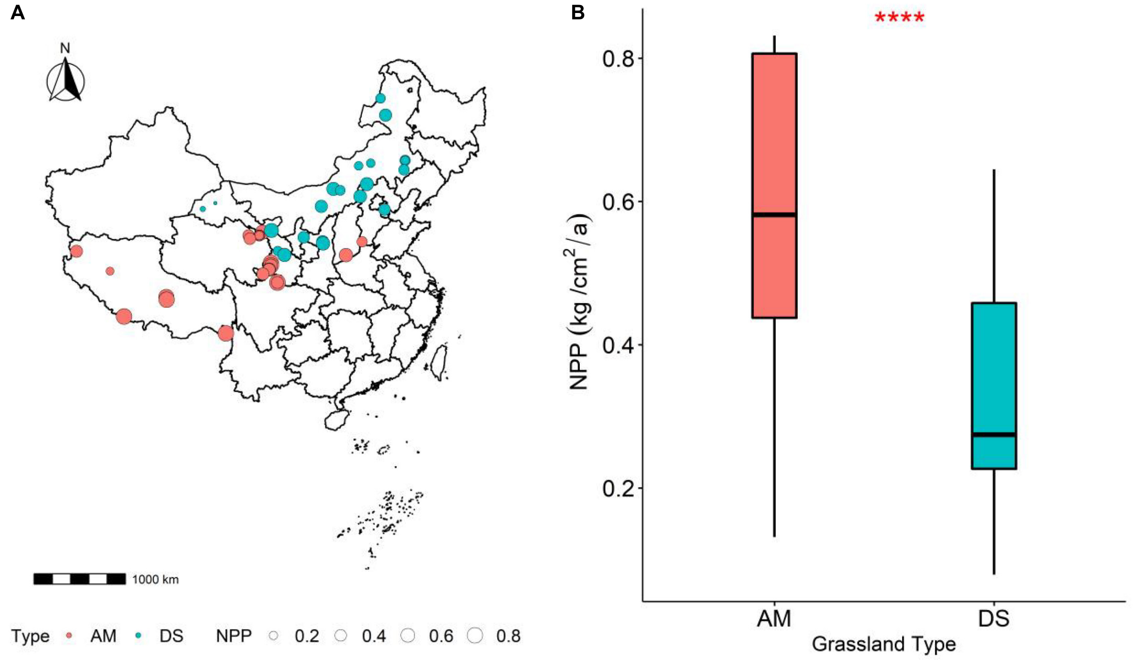

FIGURE 1
Comparison of the variability of different grassland NPP. **(A)** Geographical location of the grassland plots in this study; **(B)** variability of the NPP of AM and DS. AM represents alpine meadows and DS represents desert steppes. ****Represents $P < 0.0001$.

traits we selected included LA, SLA, LDMC, LN, LP, and leaf N/P ratio. These traits are closely related to light interception, resource utilization, growth, and development of plants (Brun et al., 2022). Previous studies at leaf traits usually focused on the species level (Butler et al., 2017). However, the effects of competitive asymmetry (i.e., the magnitude and consequences of competition affecting each party) related to interspecies functional characteristics has been neglected (Vázquez et al., 2007). We used community weighted average trait (CWM_i) to represent average trait values in grassland.

$$CWM = \sum_{i=1}^{S} Di \quad \times Traiti \tag{1}$$

where CWM_i represents the weighted trait value of the community, and D_i represents the abundance of the target species.

Environmental factors and net primary productivity data

Numerous studies have found that grassland NPP is influenced by climate factors, especially mean annual temperature (MAT) and MAP (Sloat et al., 2018). MAT, mean coldest monthly temperature (MCMT), mean warmest monthly temperature (MWMT), and MAP were extracted from the WorldClim global climate layer at a spatial resolution of 1 km (Conradi et al., 2020). Light is a key climatic factor affecting photosynthesis (Kramer, 1981). We hypothesized that annual sunshine hours (ASD) may be a key predictor of NPP. ASD and mean annual evaporation (MAE) were also obtained from the Meteorological Data Center of the China Meteorological Administration.[1]

We extracted from 250 m resolution of the grid in the top 30 cm soil layer soil pH, soil nitrogen,[2] and the content of soil effective phosphorus.[3]

NPP data from the national aeronautics and space administration (NASA[4]), the site offers from 2000 to 2015, a resolution of 250 m by 250 m of NPP. This dataset was derived from the widely used Medium Resolution Imaging Spectroradiometer (MOD13Q1) product, calculated using the C5 MOD17 algorithm, and verified by data from flflux towers (Li et al., 2020).

Data analysis

We used a significant difference test at the 0.05 significance level to test whether there was a significant difference between

---

[1] https://data.cma.cn/

[2] http://www.csdn.store

[3] https://www.osgeo.cn/data/wc137

[4] https://search.earthdata.NASA.gov/search

NPP in AM and DS (**Figure 1**). We also tested CWM_i differences between different grassland types at $\alpha = 0.05$ (Chen et al., 2020; **Supplementary Figure 1**). Significant difference tests were performed using the R package agricolae (version 4.1.0, R Core Team, 2020).

We tested the effects of environmental factors and community functional traits on NPP using general linearity. R^2 represents the goodness of fit of the model. Linear regression was performed using the R package lme4 (R Core Team, 2020).

Our preliminary results indicate that most functional traits have no significant linear relationship with NPP (**Figure 2**). Therefore, in subsequent studies, we mainly explore the impact of environmental factors on NPP.

We used a generalized additive model (GAM) to test the effects of climate and soil factors on NPP. This model is composed of parametric variables and non-parametric variables (Zou et al., 2016). Non-metric multidimensional scaling analysis (NMDS) was used to reflect the fit of GAM (Zou et al., 2016).

$$g[E(Y|X)] = \sum_i \beta i X i + \sum_j fi(Xi) + \varepsilon \tag{2}$$

where g(•) denotes the connection function, the form of which depends on the specific form and can be interpreted as the variable Y distribution. E is a random error term that can be interpreted as a normally distributed function named constant variable connection, and the connection function takes the form $g(u) = u$, $u = E(Y \mid X)$, $E(E|\ X) = 0$. X_i is the explanatory variable that strictly follows the parametric form of the explanatory variables, βi is the corresponding parameter, and f_j(•) is the smoothing function corresponding to the explanatory variable X_j that follows a non-parametric form. In our study, the spline smoothing function S(•) is chosen to fit, thin-slab spline smoothing is chosen to fit the function between different nodes, and least squares is used to estimate each smoothing function S(•).

Results

Effects of leaf traits on net primary productivity of grasslands

The NPP of AM was significantly higher than that of DS ($P < 0.001$), and most functional traits of AM and DS were also significantly different (**Figure 1B**). Except that the N/P of AM was lower than that of DS, other leaf traits were significantly higher than that of DS (**Supplementary Figure 1**). The NPP of different grassland types increased significantly with the increase of LDMC (**Figure 2C**), and decreased significantly with the increase of LN and LP (**Figures 2D,E**). NPP of AM and DS showed opposite trends with the increase of LA, SLA, and leaf N/P ratio (**Supplementary Figures 1A,B**). With the increase of the above leaf traits, NPP increased significantly of AM, while NPP decreased significantly of DS. Among all leaf traits, LDMC had better predictive power for NPP of AM ($R^2 = 0.35$, $P < 0.001$; **Figure 2C**) and LA had better predictive power for NPP of DS ($R^2 = 0.13$, $P < 0.001$; **Figure 2A**).

Effects of climate and soil nutrients on net primary productivity of grasslands

The NPP of AM was significantly positively correlated with MAT and MCMT and negatively correlated with MAE. The NPP of DS was significantly positively correlated with both MWMT and MAP (**Figure 3**). MAT ($R^2 = 0.28$, $P < 0.001$) was the best climate factor in predicting the change of NPP of AM. MAP ($R^2 = 0.22$, $P < 0.001$) was the best climate factor in predicting the change of NPP of DS.

We further analyzed the effects of soil nutrient factors on the NPP of different types of grasslands (**Figure 4**). The prediction ability of soil N, soil P, and soil pH on NPP of AM were 0.30, 0.30, and 0.40, respectively. Among all soil nutrient factors, except the positive correlation between soil N and the NPP of DS, the other factors have no significant effect ($P > 0.05$).

Soil factors dominate the variation of grassland net primary productivity

We analyzed the effects of abiotic factors on the NPP of AM and DS based on a generalized additive model with non-metric multidimensional scaling (NMDS) ordering. All environmental factors jointly explained 62.4% of NPP in AM and 43.5% of NPP in DS (**Figures 5C,F**). Among them, the soil factor explained the variation of NPP in different types of grasslands to a greater extent than the climate factor (**Figures 5A,B,D,E**). Soil factors are the dominant factors driving the spatial and temporal variation of NPP in grasslands, and climate factors also play an important role.

Discussion

There were significant spatial differences in NPP of different grassland types, and the NPP of AM was significantly higher than that of DS. Significant differences in NPP were closely related to habitat heterogeneity (Hikosaka et al., 2021). Due to the differences in biological or abiotic factors in different regions, there are significant differences in NPP of grassland in different regions (Li et al., 2019). AM are mainly distributed in the cold and high-altitude area of southwest China, with low temperature, strong radiation, thin soil layer, long soil freezing period, and neutral soil reaction. And DS are mainly distributed in the arid and semi-arid areas in the middle and north of China, which is characterized by lack of rainfall, strong

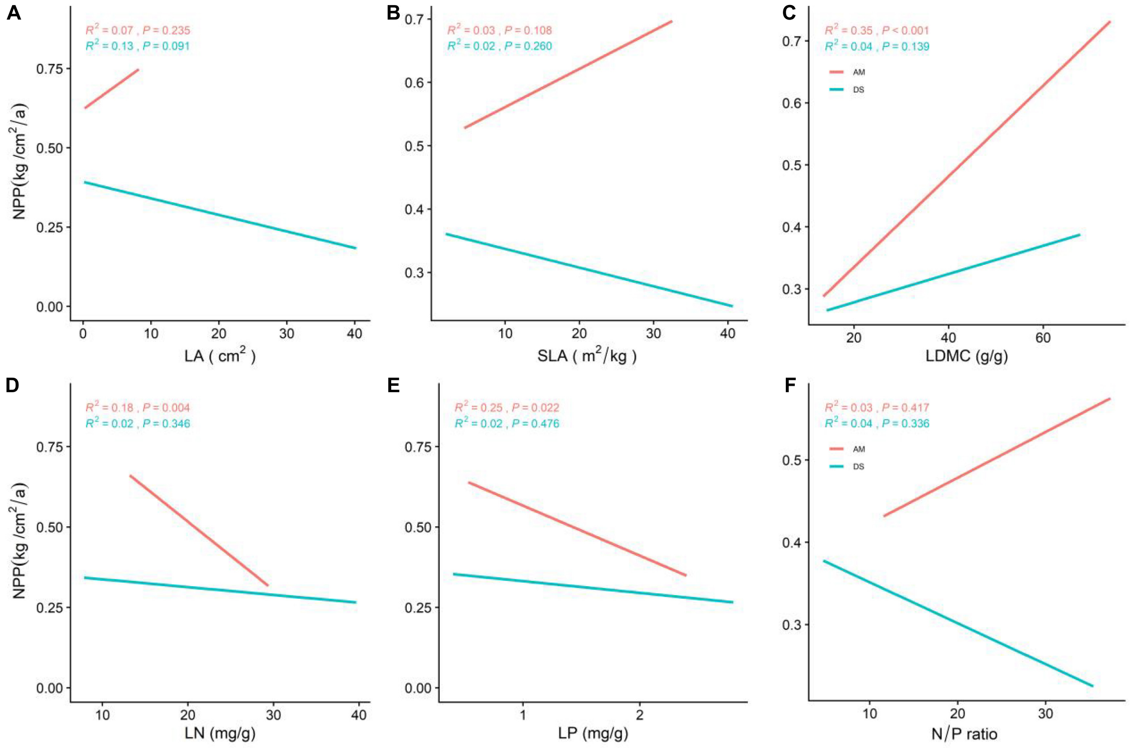

FIGURE 2
General linear correlations between community leaf traits and the NPP of AM and DS. **(A)** General linear relationship between LA and the NPP of AM and DS; **(B)** general linear relationship between SLA and the NPP of AM and DS; **(C)** general linear relationship between LDMC and the NPP of AM and DS; **(D)** general linear relationship between LN and the NPP of AM and DS; **(E)** general linear relationship between LP and the NPP of AM and DS; **(F)** general linear relationship between N/P and the NPP of AM and DS. LA represents leaf area; SLA represents specific leaf area; LDMC represents leaf dry matter content; LN represents leaf nitrogen content; LP represents leaf phosphorus content; N/P represents leaf nitrogen and phosphorus ratio. The red line represents the NPP of AM and the green line represents the NPP of DS; R^2 represents the fit of the model, and *P* represents the correlation.

evaporation, loose soil, lack of water, and low organic matter content. Therefore, differences in local hydrothermal conditions and community structure may be important reasons for the significant differences in NPP between AM and DS.

A large number of studies have found that the community leaf traits are closely related to the NPP of grasslands (Wang et al., 2017b). Our results found that the NPP of different grasslands increased significantly with the decreased of LN and LP, and increased significantly with the increase of LDMC. Nitrogen is the main component of chlorophyll, which is used to accumulate organic matter through light reactions. Phosphorus promotes the accumulation of glucose phosphate and organic matter through phosphorylation. Heineman et al. (2016) found that LN and LP limit the accumulation of plant organic matter. The NPP of the grasslands is largely determined by LN and LP contents (Oldroyd and Leyser, 2020). Studies have shown that LN is closely related to plant growth and defense, and that the relationship between grassland NPP and LN and LP is affected by the relative distribution of these nutrients among plant tissues (Zheng et al., 2022). The higher resource utilization and competitiveness of plants are beneficial to improve NPP, however, plants in arid, water-deficient, and alpine environments usually have lower LN and higher LDMC (Yang et al., 2022). Therefore, even with an increase in LN and LP, NPP did not increase with it (Xu et al., 2018), which explains our results well. We also found that NPP of grassland ecosystems was positively correlated with LDMC (Forrestel et al., 2017). As LDMC increases, free water required for plant growth and development is gradually converted to bound water, which is involved in plant metabolic processes (e.g., photosynthesis). The NPP of DS decreased significantly with the increase of LA and SLA. Plants with small and thick leaves (smaller SLA) have better drought tolerance and were more conducive to cell material transport rate and photosynthetic efficiency (Poorter and Markesteijn, 2008; Osnas et al., 2018). These traits reflect the optimal utilization of limited resources by plants (Gupta et al., 2020). Although MAT of AM was significantly lower than DS (**Supplementary Figure 2A**), MAP (**Supplementary Figure 2D**), soil nitrogen content (**Supplementary Figure 3A**) and soil phosphorus content (**Supplementary Figure 3B**) were significantly higher than DS. This reflects that relatively abundant rainwater and soil

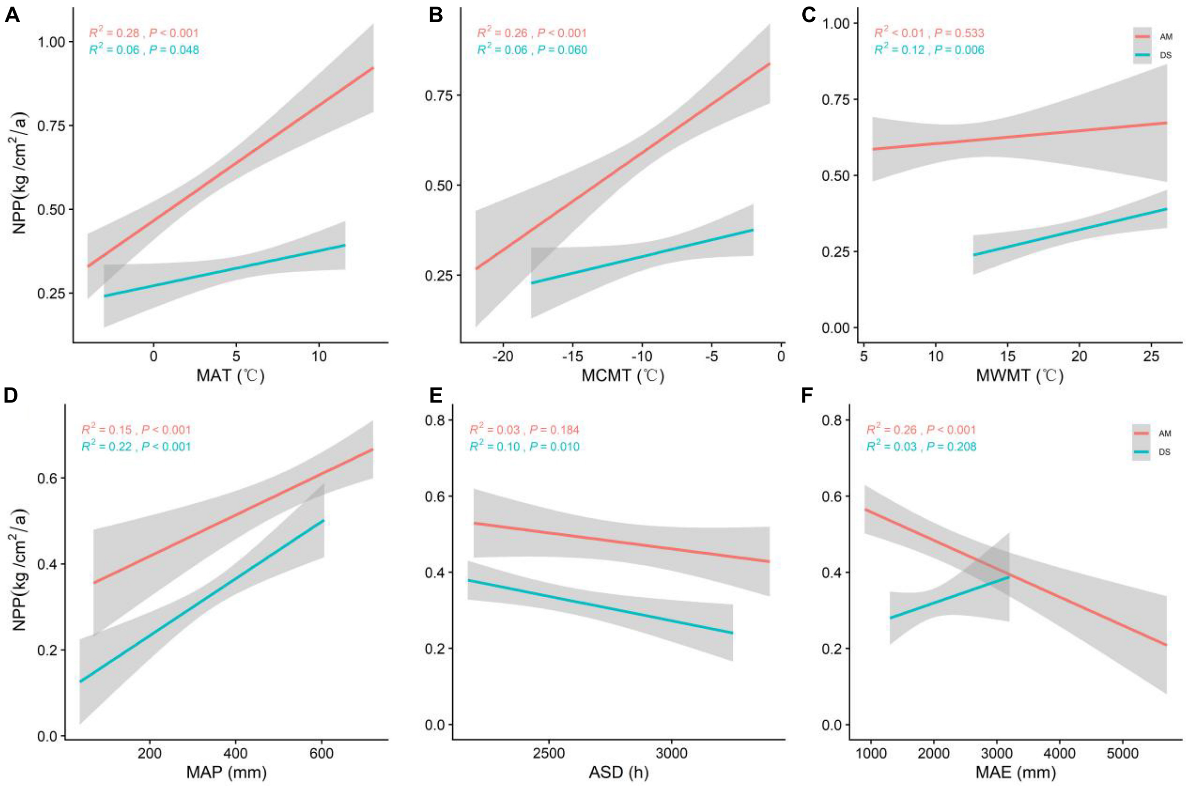

FIGURE 3
General linear regression analysis between climate factors and the NPP of AM and DS. **(A)** General linear relationship between MAT and the NPP of AM and DS; **(B)** general linear relationship between MCMT and the NPP of AM and DS; **(C)** general linear relationship between MWMT and the NPP of AM and DS; **(D)** general linear relationship between MAP and the NPP of AM and DS; **(E)** general linear relationship between ASD and the NPP of AM and DS; **(F)** general linear relationship between MAE and the NPP of AM and DS. MAT represents mean annual temperature; MCMT represents mean coldest monthly temperature; MWMT represents mean warmest monthly temperature; MAP represents mean annual precipitation; ASD represents annual sunshine hours; MAE represents mean annual evaporation. The shaded area shows a 95% confidence interval. The red line represents the NPP of AM, and the green line represents the NPP of DS; R^2 represents the model fit, and *P* represents the correlation.

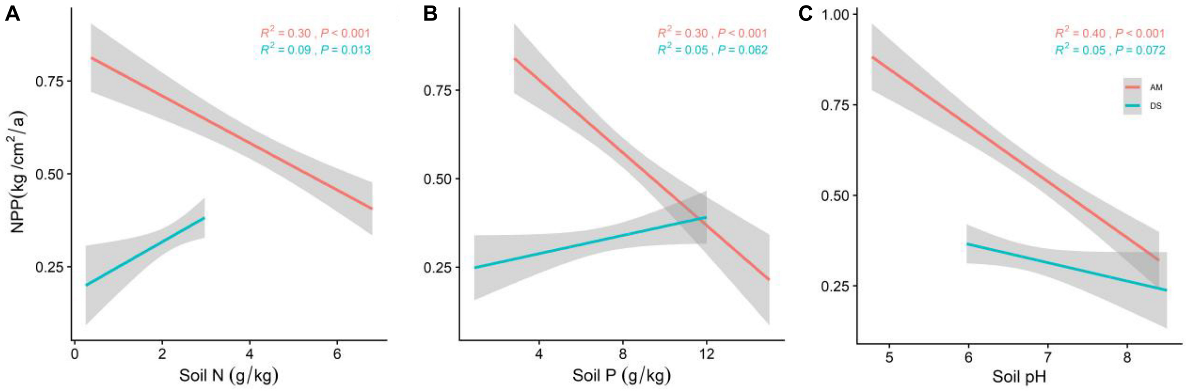

FIGURE 4
General linear regression analysis between soil nutrient factors and the NPP (soil N, soil P and soil PH) of AM and DS. **(A)** General linear relationship between soil N and the NPP of AM and DS; **(B)** general linear relationship between soil P and the NPP of AM and DS; **(C)** general linear relationship between soil pH and the NPP of AM and DS. The shaded area shows a 95% confidence interval. The red line represents the NPP of AM and the green line represents the NPP of DS; R^2 represents the model fit and *P* represents the correlation.

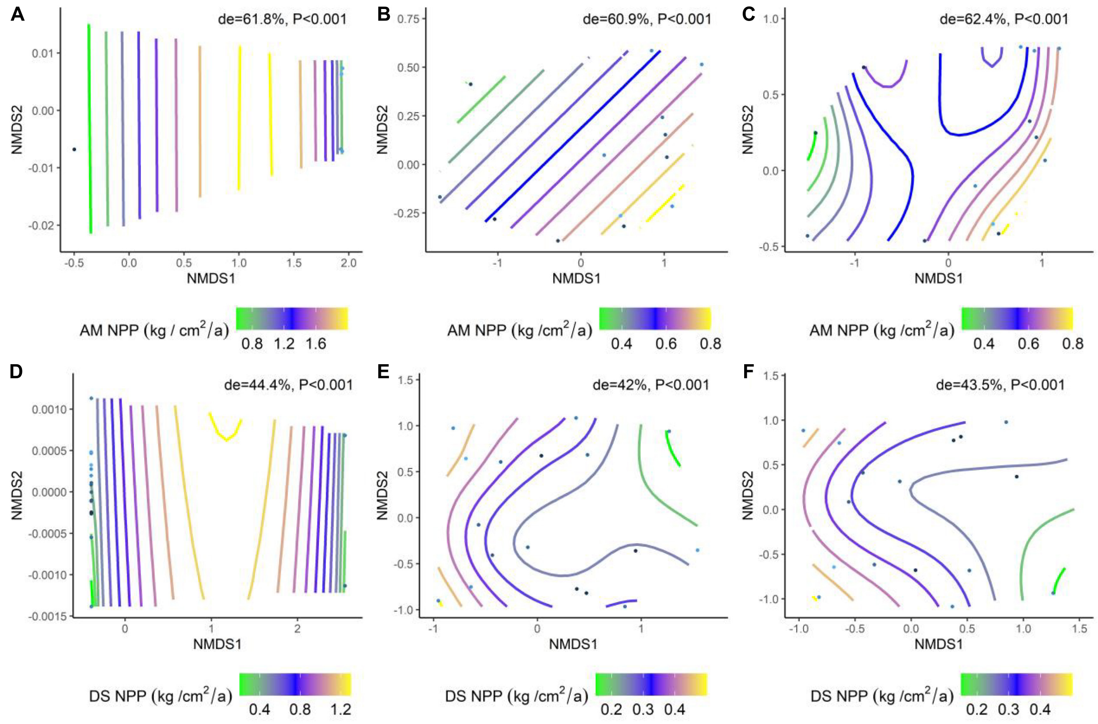

FIGURE 5
The results of the generalized additive model (GAM) fitted the effects of environmental factors and climate factors on grassland NPP. **(A)** NMDS ranking of soil factors and the NPP of AM; **(B)** NMDS ranking of climate factors and the NPP of AM; **(C)** NMDS ranking of environmental factors and the NPP of AM; **(D)** NMDS ranking of soil factors and the NPP of DS; **(E)** NMDS ranking of climate factors and the NPP of DS; **(F)** NMDS ranking of environmental factors with the NPP of DS. The color spline shows the fit of trait data from high (green) to low (yellow) values during the ranking. Trait overlays indicate that abiotic factors represented by points on the NMD are associated with higher or lower trait values, consistent with the colored trait gradient. Note that if the relationship between NPP and abiotic factors is linear, the gradient spline lines will be parallel. non-linear relationships between NPP and abiotic factors are represented by curve splines; de indicates the deviation explained by the corresponding model.

nutrients can alleviate the impact of low-temperature stress on NPP (Berdugo et al., 2020).

Climatic factors are the main driving factors of spatial variation of grassland NPP (Wang et al., 2017a). We found that NPP of AM was significantly positively correlated with MAT and MCMT, and significantly negatively correlated with MAE. Numerous studies have shown that changes in NPP of AM are strongly correlated with MAT and MCMT (Keenan and Riley, 2018; Sloat et al., 2018; Shi et al., 2022). Temperature can not only directly affect the enzyme activities related to photosynthesis and respiration of plants, but also affects the production of organic compounds such as starch, protein, and lipid. Niu et al. (2019) found that global warming can improve the productivity of grassland in alpine regions for a long time. For NPP of AM, the influence of solar radiation is no less than that of temperature (Zheng et al., 2020), and the intensity of solar radiation is also one of the important factors affecting plant photosynthesis, which is the energy source of the grassland ecosystem (Brun et al., 2022). However, excessive evaporation triggered by too high radiation zone intensity can weaken the positive response of plants to high temperatures, causing plant water deficit and thus reducing NPP. Therefore, with the increase of MAE, the NPP of AM decreased significantly, and precipitation was the main climate factor leading to the temporal and spatial variation of the NPP of DS. Our conclusion also has been verified by a large number of previous studies (Liang et al., 2015; Erb et al., 2018; Guo et al., 2022). As the MAP increases, the NPP of AM increases significantly. Water restriction will seriously reduce the material transport efficiency and photosynthetic productivity efficiency of plants in arid areas, and reduce the organic matter yield of leaves and significantly affecting the productivity of the whole region (Sun et al., 2021). Significant difference analysis of climate factors of different grassland types found that the differences in climate factors (e.g., MAT, MWMT, MAP, and MAE; **Supplementary Figure 2**) and the differences in NPP (**Figure 1B**) showed surprising consistency, which also indirectly indicated that climate factors were the key environmental factors affecting grassland NPP (Yang et al., 2016).

Soil is a natural "storage box," providing most of the nutrients needed for plants' growth and reproduction. Soil nutrient elements are closely related to plant leaf nutrient elements (Gao et al., 2019). Soil nutrient factors were significantly positively correlated with community leaf traits such as LA, SLA, and LDMC (Huang et al., 2021). Climate affects the function of grassland ecosystems by changing the physicochemical properties of the soil. These results indicate that soil factors interact with other environmental factors to jointly affect grasslands NPP (Gong and Gao, 2019). With the increase of soil N and P, the NPP of AM decreased significantly. Soil N and P are essential nutrients for plant growth and development, which limit plant productivity (Gong H. et al., 2020). The alpine environment limits the decomposition capacity of soil microorganisms, and relatively low soil mineralization rate and soil nutrient availability inhibits the NPP of AM (Wang et al., 2017c). Nitrogen addition has been found to inhibit microbial respiration and thus affect the rate of microbial decomposition (Wang et al., 2018). Soil nutrient availability, the main soil factor, leading to change the NPP of AM (Blowes et al., 2019). Higher pH reduces soil nutrient availability by affecting soil organic matter storage (Chen et al., 2018). The availability of soil water and soil nutrients limit the NPP of DS. Precipitation can promote mineralization and improve soil nutrients, thereby increasing plant NPP, which is the limiting factor for plants to absorb soil nutrients. Jiang et al. (2017) also showed that NPP in arid areas is positively correlated with precipitation, and soil water can promote the decomposition of soil organic matter and thus improve the availability of soil nutrients. These findings explain the weak predictive power of soil N, soil P and soil pH for NPP of DS. Water shortage and strong evaporation lead to slow soil development and high soil pH, resulting in insufficient soil fertility and water (Zhao et al., 2022).

The NPP of AM (de = 62.4%) has stronger environment plasticity than DS (de = 43.5%). Regardless of AM or DS, the contribution of soil nutrients in shaping the NPP pattern was slightly higher than that of climate factors (**Figure 5**). Climatic factors, especially MAP and MAT, have long been considered key factors in grassland NPP (Erb et al., 2018). However, more and more studies have proved that soil properties play a dominant role in grassland NPP (Radujković et al., 2021). Temperature and precipitation control plant growth by changing microbial activity and soil physicochemical properties, thus affecting the NPP of grassland ecosystems (Newsham et al., 2016). Drought and frozen soil will lead to the decrease of soil mineralization rate and soil fertility (Nogueira et al., 2018). Soil is the habitat for plants, where providing water, inorganic matter, and organic matter for plant growth and development, and is one of the core elements linking the entire ecosystem. Climate change directly affects the soil environment and indirectly affects grassland NPP. Therefore, soil factors dominated the temporal and spatial changes of NPP in different grassland types on a large scale.

The wide study area and large amount of data in this paper ensure the credibility of our experimental results. Our study quantifies the effects of plant functional traits and environmental factors on NPP of AM and DS, providing important theoretical guidance for addressing global climate change and better management of grasslands. In future research, we will further study and explore more soil factors, such as soil microorganisms and soil N and P effectiveness on grassland NPP.

Conclusion

We examined the relative roles of biological and abiotic factors in shaping NPP patterns using the data from 182 grassland plots in 17 DS and 21 AM in China. Our results confirmed that there are significant differences in productivity among different grasslands. Leaf traits, as well as climate and soil nutrient factors, jointly affect the changes of the grassland NPP. Among them, soil nutrients play the most critical role. Soil nutrient factors explained 61.8% of the spatial variation in NPP of AM and 44.4% of the spatial variation in NPP of DS. Quantifying the main driving factors of NPP of different grasslands is crucial for predicting future grassland dynamics and proposing reasonable management strategies.

Data availability statement

The original contributions presented in this study are included in the article/**Supplementary material**, further inquiries can be directed to the corresponding author.

Author contributions

JG: conceptualization, methodology, and investigation. XW, RW, and JG: formal analysis. XW: writing – original draft. All authors have read and agreed to the published version of the manuscript.

Acknowledgments

We thank reviewers for their valuable comments on this article. We also thank Xinjiang Normal University for providing scientific research funds for this research.

Conflict of interest

The authors declare that the research was conducted in the absence of any commercial or financial relationships that could be construed as a potential conflict of interest.

Publisher's note

Supplementary material

The Supplementary Material for this article can be found online at: https://www.frontiersin.org/articles/10.3389/fpls.2022.996313/full#supplementary-material

SUPPLEMENTARY FIGURE 1
Comparison of functional traits among different grassland types. **(A)** Variability between LA and the NPP of AM and DS; **(B)** variability between SLA and the NPP of AM and DS; **(C)** variability between LDMC and the NPP of AM and DS; **(D)** variability between LN and the NPP of AM and DS; **(E)** variability between LP and the NPP of AM and DS; **(F)** variability between N/P and the NPP of AM and DS. AM represents alpine meadows; DS represents deserts steppe; ns represents the insignificant difference; and *represents $0.01 < P < 0.05$. SLA represents specific leaf area; LDMC represents leaf dry matter content; LN represents leaf nitrogen content; LP represents leaf phosphorus content; N/P represents leaf nitrogen and phosphorus ratio.

SUPPLEMENTARY FIGURE 2
Comparison of AM and DS with different climate factors. **(A)** Variability between MAT and the NPP of AM and DS; **(B)** variability between MCMT and the NPP of AM and DS; **(C)** variability between MWMT and the NPP of AM and DS; **(D)** variability between MAP and the NPP of AM and DS; **(E)** variability between ASD and the NPP of AM and DS; **(F)** variability between MAE and the NPP of AM and DS. AM represents alpine meadows; DS represents desert steppes; ns represents no significant difference between them; and ****represents $P < 0.0001$. MAT represents annual mean temperature; MCMT represents mean coldest monthly temperature; MWMT represents mean warmest monthly temperature; MAP represents mean annual precipitation; ASD represents annual sunshine hours; MAE represents average annual evaporation.

SUPPLEMENTARY FIGURE 3
Comparison of different soil nutrient factors (soil N, soil P, and soil PH) between AM and DS. **(A)** Variability between soil N and the NPP of AM and DS; **(B)** variability between soil P and the NPP of AM and DS; **(C)** variability between soil pH and the NPP of AM and DS. AM represents alpine meadows; DS represents desert steppes; ns represents the insignificant difference between the two; and ****represents $P < 0.0001$.

References

Anderegg, W. R. L., Schwalm, C., Biondi, F., Camarero, J. J., Koch, G., and Litvak, M. (2015). Pervasive drought legacies in forest ecosystems and their implications for carbon cycle models. *Science* 349, 528–532. doi: 10.1126/science.aab1833

Baldarelli, L. M., Throop, H. L., Collins, S. L., and Ward, D. (2021). Nutrient additions have direct and indirect effects on biocrust biomass in a long-term Chihuahuan Desert grassland experiment. *J. Arid Environ.* 184:104317. doi: 10.1016/j.jaridenv.2020.104317

Berdugo, M., Delgado-Baquerizo, M., Soliveres, S., Hernández-Clemente, R., Zhao, Y. C., and Gaitán, J. J. (2020). Global ecosystem thresholds driven by aridity. *Science* 367, 787–790. doi: 10.1126/science.aay5958

Blowes, S. A., Supp, S. R., Antão, L. H., Bates, A., Bruelheide, H., and Chase, J. M. (2019). The geography of biodiversity change in marine and terrestrial assemblages. *Science* 366, 339–345. doi: 10.1126/science.aaw1620

Brun, P., Violle, C., Mouillot, D., Mouquet, N., Enquist, B. J., and Munoz, F. (2022). Plant community impact on productivity: Trait diversity or key (stone) species effects? *Ecol. Lett.* 25, 913–925. doi: 10.1111/ele.13968

Butler, E. E., Datta, A., Flores-Moreno, H., and Reich, P. B. (2017). Mapping local and global variability in plant trait distributions. *Proc. Natl. Acad. Sci. U.S.A.* 114:E10937–E10946. doi: 10.1073/pnas.1708984114

Chen, L., Hänninen, H., Rossi, S., Smith, N. G., Pau, S., and Liu, Z. Y. (2020). Leaf senescence exhibits stronger climatic responses during warm than during cold autumns. *Nat. Clim. Chang.* 10, 777–780. doi: 10.1038/s41558-020-0820-2

Chen, S. P., Wang, W. T., Xu, W. T., Wang, Y., Wan, H. W., and Bai, Y. F. (2018). Plant diversity enhances productivity and soil carbon storage. *Proc. Natl. Acad. Sci. U.S.A.* 115, 4027–4032. doi: 10.1073/pnas.1700298114

Chen, X. Y., Liu, P., Zhao, B., Zhang, J. W., Ren, B. Z., and Li, Z. (2022). Root physiological adaptations that enhance the grain yield and nutrient use efficiency of maize (Zea mays L) and their dependency on phosphorus placement depth. *Field Crops Res.* 276:108378. doi: 10.1016/j.fcr.2021.108378

Conradi, T., Meerbeek, K. V., Ordonez, A., and Svenning, J. C. (2020). Biogeographic historical legacies in the net primary productivity of Northern Hemisphere forests. *Ecol. Lett.* 23, 800–810. doi: 10.1111/ele.13481

Dong, N., Prentice, I. C., Harrison, S. P., Song, Q. H., and Zhang, Y. P. (2017). Biophysical homoeostasis of leaf temperature: A neglected process for vegetation and land-surface modelling. *Glob. Ecol. Biogeogr.* 26, 998–1007. doi: 10.1111/geb.12614

Erb, K. H., Kastner, T., Plutzar, C., Bais, A. L. S., Carvalhais, N., and Fetzel, T. (2018). Unexpectedly large impact of forest management and grazing on global vegetation biomass. *Nature* 553, 73–76. doi: 10.1038/nature25138

Forrestel, E. J., Donoghue, M. J., Edwards, E. J., Jetz, W., and Smith, M. D. (2017). Different clades and traits yield similar grassland functional responses. *Proc. Natl. Acad. Sci. U.S.A.* 114, 705–710. doi: 10.1073/pnas.1612909114

Gang, C. C., Zhao, W., Zhao, T., Zhang, Y., Gao, X. R., and Wen, Z. M. (2018). The impacts of land conversion and management measures on the grassland net primary productivity over the Loess Plateau. Northern China. *Sci. Total Environ.* 645, 827–836. doi: 10.1016/j.scitotenv.2018.07.161

Gao, J., Song, Z. P., and Liu, Y. H. (2019). Response mechanisms of leaf nutrients of endangered plant (Acer catalpifolium) to environmental factors varied at different growth stages. *Glob. Ecol. Conserv.* 17:e00521. doi: 10.1016/j.gecco.2019.e00521

Gao, X. L., Li, X. G., Zhao, L., and Kuzyakov, Y. (2021). Shrubs magnify soil phosphorus depletion in Tibetan meadows: Conclusions from C: N: P stoichiometry and deep soil profiles. *Sci. Total Environ.* 785:147320. doi: 10.1016/j.scitotenv.2021.147320

Gong, H., and Gao, J. (2019). Soil and climatic drivers of plant SLA (specific leaf area). *Glob. Ecol. Conserv.* 20:e00696. doi: 10.1016/j.gecco.2019.e00696

Gong, H., Li, Y. Y., Yu, T., Zhang, S. H., Gao, J., and Zhang, S. K. (2020). Soil and climate effects on leaf nitrogen and phosphorus stoichiometry along elevational gradients. *Glob. Ecol. Conserv.* 23:e01138. doi: 10.1016/j.gecco.2020.e01138

Gong, Y. H., Zhao, D. M., Ke, W. B., Fang, C., Pei, J. Y., and Ye, J. S. (2020). Legacy effects of precipitation amount and frequency on the aboveground plant biomass of a semi-arid grassland. *Sci. Total Environ.* 705:135899. doi: 10.1016/j.scitotenv.2019.135899

Grilli, J., Barabas, G., Michalska-Smith, M. J., and Allesina, S. (2017). Higher-order interactions stabilize dynamics in competitive network models. *Nature* 548, 210–213. doi: 10.1038/nature23273

Guo, X. X., Zuo, X. A., Yue, P. Li, X. Y., Hu, Y., and Chen, M. (2022). Direct and indirect effects of precipitation change and nutrients addition on desert steppe productivity in Inner Mongolia, Northern China. *Plant Soil* 471, 527–540. doi: 10.1007/s11104-021-05206-2

Gupta, A., Rico-Medina, A., and Caño-Delgado, A. I. (2020). The physiology of plant responses to drought. *Science* 368, 266–269. doi: 10.1126/science.aaz7614

Heineman, K. D., Turner, B. L., and Dalling, J. W. (2016). Variation in wood nutrients along a tropical soil fertility gradient. *New Phytol.* 211, 440–454. doi: 10.1111/nph.13904

Henry, H. A. L., Abedi, M., Alados, C. L., Beard, K. H., Fraser, L. H., and Jentsch, A. (2018). Increased soil frost versus summer drought as drivers of plant biomass responses to reduced precipitation: Results from a globally coordinated field experiment. *Ecosystems* 21, 1432–1444. doi: 10.1007/s10021-018-0231-7

Hikosaka, K., Kurokawa, H., Arai, T., Takayanagi, S., Tanaka, H. O., and Nagano, S. (2021). Intraspecific variations in leaf traits, productivity and resource use efficiencies in the dominant species of subalpine evergreen coniferous and deciduous broad-leaved forests along the altitudinal gradient. *J. Ecol.* 109, 1804–1818. doi: 10.1111/1365-2745.13603

Huang, W. J., Wang, W., Cao, M., Fu, G., Xia, J. Y., and Wang, Z. X. (2021). Local climate and biodiversity affect the stability of China's grasslands in response to drought. *Sci. Total Environ.* 768:145482. doi: 10.1016/j.scitotenv.2021.145482

Jiang, L. L., Jiapaer, G., Bao, A. M., Guo, H., and Ndayisaba, F. (2017). Vegetation dynamics and responses to climate change and human activities in Central Asia. *Sci. Total Environ.* 599, 967–980. doi: 10.1016/j.scitotenv.2017.05.012

Jiao, Y., Niklas, K. J., Wang, L., Yu, K., Li, Y., and Shi, P. (2022). Influence of leaf age on the scaling relationships of lamina mass vs. area. *Front. Plant Sci.* 13:860206. doi: 10.3389/fpls.2022.860206

Jochum, M., Fischer, M., Isbell, F., Roscher, C., Plas, F. V. D., and Boch, S. (2020). The results of biodiversity-ecosystem functioning experiments are realistic. *Nat. Ecol. Evol.* 4, 1485–1494. doi: 10.1038/s41559-020-1280-9

Keenan, T. F., and Riley, W. J. (2018). Greening of the land surface in the world's cold regions consistent with recent warming. *Nat. Clim. Chang.* 8, 825–828. doi: 10.1038/s41558-018-0258-y

Kramer, P. J. (1981). Carbon dioxide concentration, photosynthesis, and dry matter production. *Bioscience* 31, 29–33. doi: 10.2307/1308175

Li, F. R., Liu, L. L., Liu, J. L., and Yang, K. (2019). Abiotic and biotic controls on dynamics of labile phosphorus fractions in calcareous soils under agricultural cultivation. *Sci. Total Environ.* 681, 163–174. doi: 10.1016/j.scitotenv.2019.05.091

Li, Y. Q., Reich, P. B., Schmid, B., Shrestha, N., Feng, X., and Wang, Z. H. (2020). Leaf size of woody dicots predicts ecosystem primary productivity. *Ecol. Lett.* 23, 1003–1013. doi: 10.1111/ele.13503

Liang, M. W., and Gornish, E. S. (2019). Rainfall regulation of grazed grasslands. *Proc. Natl. Acad. Sci. U.S.A.* 116, 23887–23888. doi: 10.1073/pnas.1915399116

Liang, W., Yang, Y. T., Fan, D. M., Guan, H. D., Zhang, T., and Bai, D. (2015). Analysis of spatial and temporal patterns of net primary production and their climate controls in China from 1982 to 2010. *Agric. For. Meteorol.* 204, 22–36. doi: 10.1016/j.agrformet.2015.01.015

Luo, W. T., Zuo, X. A., Griffin-Nolan, R. J., Xu, C., Sardans, J., and Yu, Q. (2020). Chronic and intense droughts differentially influence grassland carbon-nutrient dynamics along a natural aridity gradient. *Plant Soil.* 473, 37–148. doi: 10.1007/s11104-020-04571-8

Mahaut, L., Fort, F., Violle, C., and Freschet, G. T. (2020). Multiple facets of diversity effects on plant productivity: Species richness, functional diversity, species identity and intraspecific competition. *Funct. Ecol.* 34, 287–298. doi: 10.1111/1365-2435.13473

Newsham, K. K., Hopkins, D. W., Carvalhais, L. C., Fretwell, P. T., Rushton, S. P. and O'Donnell, A. G. (2016). Relationship between soil fungal diversity and temperature in the maritime Antarctic. *Nat. Clim. Change* 6, 182–186. doi: 10.1038/nclimate2806

Niu, Y. J., Yang, S. W., Zhou, J. W., Chu, B., Ma, S. J., and Hua, L. M. (2019). Vegetation distribution along mountain environmental gradient predicts shifts in plant community response to climate change in alpine meadow on the Tibetan Plateau. *Sci. Total Environ.* 650, 505–514. doi: 10.1016/j.scitotenv.2018.08.390

Nogueira, C., Nunes, A., Bugalho, M. N., Branquinho, C., McCulley, R. L., and Caldeira, M. C. (2018). Nutrient addition and drought interact to change the structure and decrease the functional diversity of a Mediterranean grassland. *Front. Ecol. Evol.* 6:00155. doi: 10.3389/fevo.2018.00155

Oldroyd, G. E. D., and Leyser, O. (2020). A plant's diet, surviving in a variable nutrient environment. *Science* 368:eaba0196. doi: 10.1126/science.aba0196

Osnas, J. L., Katabuchi, M., Kitajima, K., Wright, S. J., Reich, P. B., and Lichstein, J. W. (2018). Divergent drivers of leaf trait variation within species, among species, and among functional groups. *Proc. Natl. Acad. Sci. U.S.A.* 115, 5480–5485. doi: 10.1073/pnas.1803989115

Pan, Q. M., Symstad, A. J., Bai, Y. F., Huang, J. H., Wu, J. G., and Han, X. G. (2021). Biodiversity–productivity relationships in a natural grassland community vary under diversity loss scenarios. *J. Ecol.* 110, 210–220. doi: 10.1111/1365-2745.13797

Pecina, M. V., Ward, R. D., Bunce, R. G. H., Sepp, K., Kuusemets, V., and Luuk, O. (2019). Country-scale mapping of ecosystem services provided by semi-natural grasslands. *Sci. Total Environ.* 661, 212–225. doi: 10.1016/j.scitotenv.2019.01.174

Poorter, L., and Markesteijn, L. (2008). Seedling traits determine drought tolerance of tropical tree species. *Biotropica* 40, 321–331. doi: 10.1111/j.1744-7429.2007.00380.x

Pries, C. H., Castanha, C., Porras, R. C., and Torn, M. S. (2017). The whole-soil carbon flux in response to warming. *Science* 355, 1420–1423. doi: 10.1126/science.aal1319

R Core Team. (2020). *A Language and Environment for Statistical Computing*. Vienna: R Foundation for Statistical Computing.

Radujković, D., Verbruggen, E., Seabloom, E. W., Bahn, M., Biederman, L. A., and Borer, E. T. (2021). Soil properties as key predictors of global grassland production: Have we overlooked micronutrients? *Ecol. Lett.* 24, 2713–2725. doi: 10.1111/ele.13894

Schrader, J., Shi, P. J., Royer, D. L., Peppe, D. J., Gallagher, R. V., and Li, Y. R. (2021). Leaf size estimation based on leaf length, width and shape. *Ann. Bot.* 128, 395–406. doi: 10.1093/aob/mcab078

Seddon, A. W., Macias-Fauria, M., Long, P. R., Benz, D., and Willis, K. J. (2016). Sensitivity of global terrestrial ecosystems to climate variability. *Nature* 531, 229–232. doi: 10.1038/nature16986

Shen, X. J., Liu, B. H., Henderson, M., Wang, L., Jing, M., and Lu, X. G. (2022). Vegetation greening, extended growing seasons, and temperature feedbacks in warming temperate grasslands of China. *J. Clim.* 35, 5103–5117. doi: 10.1175/JCLI-D-21-0325.1

Shi, F., Liu, M. X., Qiu, J., Zhang, Y. L., Su, H. Y., and Mao, X. P. (2022). Assessing land cover and ecological quality changes in the Forest-Steppe Ecotone of the Greater Khingan Mountains, Northeast China, from Landsat and MODIS observations from 2000 to 2018. *Remote Sens.* 14, 725–725. doi: 10.3390/rs14030725

Shi, P. J., Preisler, H. K., Quinn, B. K., Zhao, J., Huang, W., and Röll, A. (2020). Precipitation is the most crucial factor determining the distribution of moso bamboo in Mainland China. *Glob. Ecol. Conserv.* 22:e00924. doi: 10.1016/j.gecco.2020.e00924

Sloat, L. L., Gerber, J. S., Samberg, L. H., Smith, W. K., Herrero, M., and Ferreira, L. G. (2018). Increasing importance of precipitation variability on global livestock grazing lands. *Nat. Clim. Chang.* 8, 214–218. doi: 10.1038/s41558-018-0081-5

Sun, J., and Du, W. P. (2017). Effects of precipitation and temperature on net primary productivity and precipitation use efficiency across China's grasslands. *GIsci Remote Sens.* 54, 881–897. doi: 10.1080/15481603.2017.1351147

Sun, Y. F., Yang, Y. H., Zhao, X., Tang, Z. Y., Wang, S. P., and Fang, J. Y. (2021). Global patterns and climatic drivers of above-and belowground net primary productivity in grasslands. *Sci. China Life Sci.* 64, 739–751. doi: 10.1007/s11427-020-1837-9

Vázquez, D. P., Melián, C. J., Williams, N. M., Blüthgen, N., Krasnov, B. R., and Poulin, R. (2007). Species abundance and asymmetric interaction strength in ecological networks. *Oikos* 116, 1120–1127. doi: 10.1111/j.0030-1299.2007.15828.x

Wang, C., Liu, D. W., and Bai, E. (2018). Decreasing soil microbial diversity is associated with decreasing microbial biomass under nitrogen addition. *Soil Biol. Biochem.* 120, 126–133. doi: 10.1016/j.soilbio.2018.02.003

Wang, R. L., Wang, Q. F., Zhao, N., Yu, G. R., and He, N. P. (2017b). Complex trait relationships between leaves and absorptive roots: Coordination in tissue N concentration but divergence in morphology. *Ecol. Evol.* 7, 2697–2705. doi: 10.1002/ece3.2895

Wang, J., Dong, J., Yi, Y., Lu, G., Oyler, J., and Smith, W. K. (2017a). Decreasing net primary production due to drought and slight decreases in solar radiation in China from 2000 to 2012. *J. Geophys.Res. Biogeosci.* 122, 261–278. doi: 10.1002/2016JG003417

Wang, X., Xu, Z. E., Lü, X. T., Wang, R. Z., Cai, J. P., and Jiang, Y. (2017c). Responses of litter decomposition and nutrient release rate to water and nitrogen addition differed among three plant species dominated in a semi-arid grassland. *Plant Soil.* 418, 241–253. doi: 10.1007/s11104-017-3288-8

Wang, N., Quesada, B., Xia, L. L., Butterbach-Bahl, K., Goodale, C. L., and Kiese, R. (2019). Effects of climate warming on carbon fluxes in grasslands—A global meta-analysis. *Glob. Chang. Biol.* 25, 1839–1851. doi: 10.1111/gcb.14603

Wei, D., Zhao, H., Zhang, J. X., Qi, Y. H., and Wang, X. D. (2020). Human activities alter response of alpine grasslands on Tibetan Plateau to climate change. *J. Environ. Manag.* 262:110335. doi: 10.1016/j.jenvman.2020.110335

Wieder, W. R., Cleveland, C. C., Smith, W. K., and Todd-Brown, K. (2015). Future productivity and carbon storage limited by terrestrial nutrient availability. *Nat. Geosci.* 8, 441–444. doi: 10.1038/ngeo2413

Xu, Z. W., Li, M. H., Zimmermann, N. E., Li, S. P., Li, H., and Ren, H. Y. (2018). Plant functional diversity modulates global environmental change effects on grassland productivity. *J. Ecol.* 106, 1941–1951. doi: 10.1111/1365-2745.12951

Yang, Y. T., Chen, Z. F., Xu, B. C., Wei, J. Q., Zhu, X. X., and Yao, H. B. (2022). Using Trait-Based Methods to Study the Response of Grassland to Fertilization in the Grassland in Semiarid Areas in the Loess Plateau of China. *Plants* 11:2045. doi: 10.3390/plants11152045

Yang, Y., Wang, Z. Q., Li, J. L., Gang, C. C., Zhang, Y. Z., and Zhang, Y. (2016). Comparative assessment of grassland degradation dynamics in response to climate variation and human activities in China, Mongolia, Pakistan and Uzbekistan from 2000 to 2013. *J. Arid Environ.* 135, 164–172. doi: 10.1016/j.jaridenv.2016.09.004

Yu, H. L., Ding, Q. N., Meng, B. P., Lv, Y. Y., Liu, C., and Zhang, X. Y. (2021). The Relative Contributions of Climate and Grazing on the Dynamics of Grassland NPP and PUE on the Qinghai-Tibet Plateau. *Remote Sens.* 13:3424. doi: 10.3390/rs13173424

Zhang, D. Y., Peng, Y. F., Li, F., Yang, G. B., Wang, J., and Yu, J. C. (2019). Trait identity and functional diversity co-drive response of ecosystem productivity to nitrogen enrichment. *J. Ecol.* 107, 2402–2414. doi: 10.1111/1365-2745.13184

Zhang, Q. Y., Wang, Q. F., Zhu, J. X., Xu, L., Li, M. X., and Rengel, Z. (2021). Higher soil acidification risk in southeastern Tibetan Plateau. *Sci. Total Environ.* 755:143372. doi: 10.1016/j.scitotenv.2020.143372

Zhang, Z. C., Sun, J., Liu, M., Xu, M., Wang, Y., and Wei, T. X. (2020). Don't judge toxic weeds on whether they are native but on their ecological effects. *Ecol. Evol.* 10, 9014–9025. doi: 10.1002/ece3.6609

Zhao, Y. F., Wang, X., Jiang, S. L., Xiao, J. J., Li, J., and Zhou, X. H. (2022). Soil development mediates precipitation control on plant productivity and diversity in alpine grasslands. *Geoderma* 412, 115721. doi: 10.1016/j.geoderma.2022.115721

Zheng, S. X., Chi, Y. G., Yang, X. J., Li, W. H., Lan, Z. C., and Bai, Y. F. (2022). Direct and indirect effects of nitrogen enrichment and grazing on grassland productivity through intraspecific trait variability. *J. Appl. Ecol.* 59, 598–610. doi: 10.1111/1365-2664.14078

Zheng, Z. T., Zhu, W. Q., and Zhang, Y. J. (2020). Seasonally and spatially varied controls of climatic factors on net primary productivity in alpine grasslands on the Tibetan Plateau. *Glob. Ecol. Conserv.* 21:e00814. doi: 10.1016/j.gecco.2019.e00814

Zhou, W., Yang, H., Huang, L., Chen, C., Lin, X. S., and Hu, Z. J. (2020). Grassland degradation remote sensing monitoring and driving factors quantitative assessment in China from 1982 to 2010. *Ecol. Indic.* 83, 303–313. doi: 10.1016/j.ecolind.2017.08.019

Zou, B., Chen, J. W., Zhai, L., Fang, X., and Zheng, Z. (2016). Satellite based mapping of ground $PM_{2.5}$ concentration using generalized additive modeling. *Remote Sens.* 9, 2072–4292. doi: 10.3390/rs9010001

frontiers | Frontiers in Plant Science

TYPE Original Research
PUBLISHED 26 September 2022
DOI 10.3389/fpls.2022.941357

OPEN ACCESS

EDITED BY
Peijian Shi,
Nanjing Forestry University, China

REVIEWED BY
Xiangnan Li,
Northeast Institute of Geography and Agroecology (CAS), China
Feng Li,
Institute of Subtropical Agriculture (CAS), China
Jiahui Zhang,
Institute of Geographic Sciences and Natural Resources Research (CAS), China

*CORRESPONDENCE
Qi Feng
qifeng@lzb.ac.cn

SPECIALTY SECTION
This article was submitted to Functional Plant Ecology, a section of the journal Frontiers in Plant Science

RECEIVED 11 May 2022
ACCEPTED 25 August 2022
PUBLISHED 26 September 2022

CITATION
Zhang X, Feng Q, Cao J, Biswas A, Su H, Liu W, Qin Y and Zhu M (2022) Response of leaf stoichiometry of *Potentilla anserina* to elevation in China's Qilian Mountains. *Front. Plant Sci.* 13:941357. doi: 10.3389/fpls.2022.941357

Response of leaf stoichiometry of *Potentilla anserina* to elevation in China's Qilian Mountains

Xiaofang Zhang[1,2], Qi Feng[1]*, Jianjun Cao[3], Asim Biswas[4], Haohai Su[3], Wei Liu[1,5], Yanyan Qin[1,5,6] and Meng Zhu[1]

[1]Key Laboratory of Ecohydrology of Inland River Basin, Northwest Institute of Eco-Environment and Resources, Chinese Academy of Sciences, Lanzhou, China, [2]University of Chinese Academy of Sciences, Beijing, China, [3]College of Geography and Environmental Science, Northwest Normal University, Lanzhou, China, [4]School of Environmental Sciences, University of Guelph, Guelph, ON, Canada, [5]Qilian Mountains Eco-Environment Research Center in Gansu Province, Lanzhou, China, [6]Key Laboratory of Land Surface Process and Climate Change in Cold and Arid Regions, Northwest Institute of Eco-Environment and Resources, Chinese Academy of Sciences, Lanzhou, China

Plants adapt to changes in elevation by regulating their leaf ecological stoichiometry. *Potentilla anserina* L. that grows rapidly under poor or even bare soil conditions has become an important ground cover plant for ecological restoration. However, its leaf ecological stoichiometry has been given little attention, resulting in an insufficient understanding of its environmental adaptability and growth strategies. The objective of this study was to compare the leaf stoichiometry of *P. anserina* at different elevations (2,400, 2,600, 2,800, 3,000, 3,200, 3,500, and 3,800 m) in the middle eastern part of Qilian Mountains. With an increase in elevation, leaf carbon concentration $[(C)_{leaf}]$ significantly decreased, with the maximum value of 446.04 $g{\cdot}kg^{-1}$ (2,400 m) and the minimum value of 396.78 $g{\cdot}kg^{-1}$ (3,500 m). Leaf nitrogen concentration $[(N)_{leaf}]$ also increased with an increase in elevation, and its maximum and minimum values were 37.57 $g{\cdot}kg^{-1}$ (3,500 m) and 23.71 $g{\cdot}kg^{-1}$ (2,800 m), respectively. Leaf phosphorus concentration $[(P)_{leaf}]$ was the highest (2.79 $g{\cdot}kg^{-1}$) at 2,400 m and the lowest (0.91 $g{\cdot}kg^{-1}$) at 2,800 m. The $[C]_{leaf}/[N]_{leaf}$ decreased with an increase in elevation, while $[N]_{leaf}/[P]_{leaf}$ showed an opposite trend. The mean annual temperature, mean annual precipitation, soil pH, organic carbon, nitrogen, and phosphorus at different elevations mainly affected $[C]_{leaf}$, $[N]_{leaf}$, and $[P]_{leaf}$. The growth of *P. anserina* in the study area was mainly limited by P, and this limitation was stronger with increased elevation. Progressively reducing P loss at high elevation is of great significance to the survival of *P. anserina* in this specific region.

KEYWORDS

plant growth strategies, plant environmental adaptability, leaf traits, mountainous regions, nutrient limitation

Introduction

Ecological stoichiometry focuses on the balance of multiple elements in ecological interactions and processes, such as energy flow and nutrient cycling, and has become an important topic of research in recent years in ecology and biology (Moe et al., 2005; Sistla and Schimel, 2012; Yang et al., 2019; Zhu et al., 2020). It is an important tool to reveal organisms' responses to external disturbances and nutrient supply balance mechanisms in ecosystems (Zeng et al., 2016), mainly by analyzing changes in carbon (C), nitrogen (N), and phosphorus (P) (Cao et al., 2020), which are well-known as basic elements constituting plants and are closely linked to plant photosynthesis, respiration, and various ecosystem functions (Elser et al., 2010; Marschner and Marschner, 2012; Wang et al., 2015; Yan et al., 2016; Croft et al., 2017).

Leaves are the most active and primary photosynthetic plant organ (Elser et al., 2010; Yang et al., 2019), their size and structure exhibit a tradeoff between the support cost and photosynthetic returns during plant adaptation to environmental changes (Shi et al., 2020, 2022; Guo et al., 2021; Li et al., 2022a,b), and leaf stoichiometry can reflect the tradeoff formed in this evolution from the angle of leaf chemical elements and its spatio-temporal variations (Baxter and Dilkes, 2012; Cao et al., 2020; Zhu et al., 2020). Leaf C/N and C/P were widely accepted as effective indicators of plants' N and P use efficiency and growth rate, and their lower values indicated lower nutrient utilization efficiency and higher plant growth (Weidner et al., 2015; Sun et al., 2017; Cao et al., 2020; Zhang et al., 2020). Leaf N/P can reflect plant nutrient states and limitations (Tao et al., 2016). However, there remain questions about the N/P thresholds assessing plants' nutrient limitation during growth due to multiple factors (Crowley et al., 2012). For example, according to the study of Koerselman and Meuleman (1996) on wetland plant communities, when leaf N/P < 14, plant growth was limited by N; $14 \leq$ leaf N/P ≤ 16, plant growth has the common limit of N and P; and leaf N/P > 16, plant growth was limited by P, while the study of Güsewell (2004) on terrestrial plant communities found that when leaf N/P < 10, plant growth was limited by N; $10 \leq$ leaf N/P ≤ 20, plant growth has the common limit of N and P; and leaf N/P > 20, plant growth was limited by P. Nevertheless, leaf N/P is still considered to be a valuable tool for assessing potential patterns in nutrient limitation across broad landscapes (Crowley et al., 2012).

Relationships between leaf stoichiometry and environmental factors, including soil nutrients and geographical and climatic factors, were widely explored at various scales including regional and global scales (e.g., McGroddy et al., 2004; Reich and Oleksyn, 2004; Sardans et al., 2011; Du et al., 2017; Tian et al., 2018; Qin et al., 2021). Elevation is a crucial factor and can affect plant leaf stoichiometry by altering the combination of heat and water, soil properties, and vegetation community composition (Bo et al., 2020; Liu et al., 2021). However, there is little consensus on leaf stoichiometric characteristics as they change along an elevation gradient. Some studies observed that leaf C concentration $[(C)_{leaf}]$ increased but leaf N $[(N)_{leaf}]$ and leaf P concentration $[(P)_{leaf}]$ decreased with an increase in elevation (e.g., Zhao et al., 2014, 2018; Bo et al., 2020), while other studies reported an opposite trend (e.g., Macek et al., 2009; Li et al., 2018). Therefore, the response of plant leaf ecological stoichiometry to elevation should be investigated at regional and species-specific levels. Situated in the transition zone between the Qinghai–Tibetan Plateau and the arid region of northwestern China, the Qilian Mountains preserve a wide variety of plant species (Gui et al., 2020; Wang et al., 2022) and serve as an ideal region to study the impact of elevation on leaf stoichiometry of different plant species (Cao et al., 2020; Qin et al., 2021). *Potentilla anserina* L., a typical forb, is widely distributed in the Qilian Mountains. Due to its wide ecological amplitude and vegetative reproduction ability, *P. anserina* is an important species of degraded grasslands or secondary succession lands and is considered a prime species for ecological restoration in alpine regions (Sheng et al., 2004). Previous studies mainly focused on *P. anserina*'s chemical components (Zhao et al., 2020), pharmacological action (He et al., 2021), nutrient reabsorption (Li et al., 2020), and medicinal value (Cheng J. et al., 2021); information on its leaf stoichiometry remains unavailable. Exploring the leaf stoichiometry and growth nutrient limitation of *P. anserina* is of great significance for the ecological restoration and construction in the Qilian Mountains. It was found that the leaf stoichiometry of many dominant or common species in the Qilian Mountains was affected by elevation. For example, with increasing elevation, $[C]_{leaf}$ of *Oxytropis ochrocephala* first increased and then decreased, while $[N]_{leaf}$ and $[P]_{leaf}$ of the same species showed a trend of general increase in the identified soil organic carbon (SOC), the ratio of SOC to soil total phosphorus (STP), and the mean annual temperature (MAT) as dominant factors (Cao et al., 2020). $[C]_{leaf}$ and $[P]_{leaf}$ of *Potentilla fruticosa* first decreased and then increased with an increase in elevation, and SOC, STP, and soil pH were the main factors influencing the leaf stoichiometry (Qin et al., 2022). We hypothesized that elevation may also significantly influence leaf stoichiometry of *P. anserina* and leaf stoichiometry of *P. anserina* could be influenced by soil nutrients, MAT, and MAP. Previous studies have proposed that the soil P content of the Qilian Mountains was relatively low (Xu et al., 2018, 2019). Therefore, we hypothesized that P could be a limiting nutrient for *P. anserina* growth in this region.

This study attempted to: (i) explore how *P. anserina* changed leaf C/N/P stoichiometry to adapt to environmental changes along elevation (2,400–3,800 m) in the Qilian Mountains, (ii) identify the underlying mechanism of the effect of elevation on leaf C/N/P stoichiometry by building structural equation models, and (iii) determine the key nutrients limiting the growth of *P. anserina* in the Qilian Mountains.

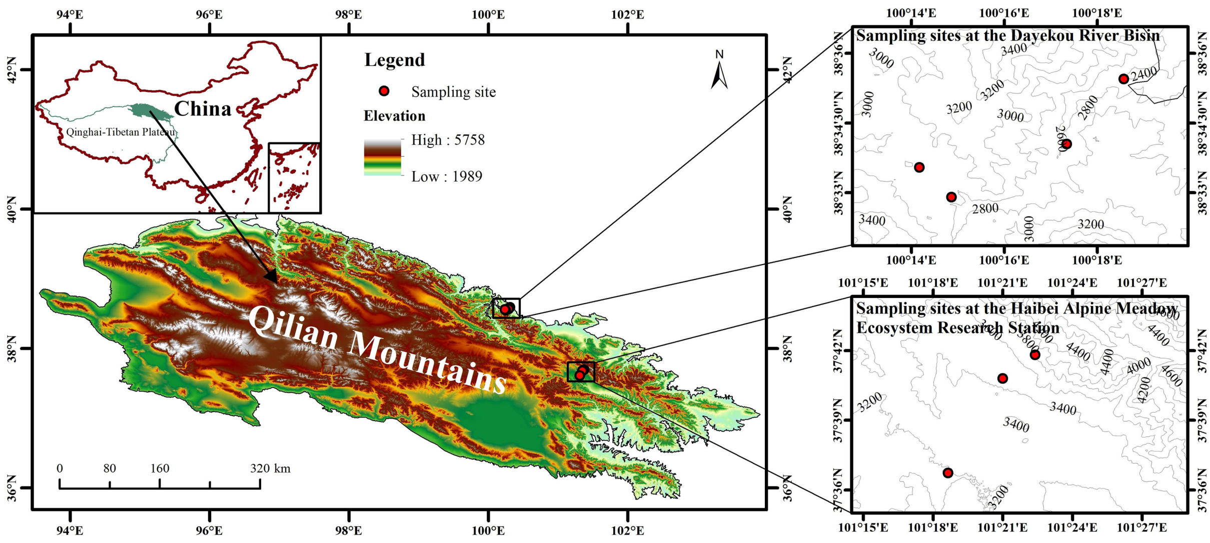

FIGURE 1
Sampling sites across elevations (2,400, 2,600, 2,800, 3,000, 3,200, 3,500, and 3,800 m) in the study area.

Materials and methods

Study area

A field study was conducted at the Dayekou River Basin and the Haibei Alpine Meadow Ecosystem Research Station in the Middle East of the Qilian Mountains (93°30′-103°30′ E, 36°30′-39°30′ N). The Qilian Mountains ranging from 2,000 to 5,500 m elevation belong to a typical plateau continental climate, with MAT and MAP of −0.4°C and 405 mm, respectively, from 2000 to 2015. Grasslands with *Carex tristachya*, *Stipa przewalskii*, *Leymus secalinus*, and *Polygonum viviparum* dominate the southern slopes, while Qinghai spruce (*Picea crassifolia* Kom.) forests dominate the northern slopes. Soils were classified as Haplic Kastanozems and Haplic Phaeozems on the southern and northern slopes, respectively (IUSS Working Group World Reference Base for Soil Resources, 2014).

Field sampling

In August and September 2018, samples of healthy fresh leaves of *P. anserina* were collected from the following seven elevations: 2,400, 2,600, 2,800, 3,000, 3,200, 3,500, and 3,800 m (Figure 1). Sampling at 2,400, 2,600, 2,800, and 3,000 m was conducted at the Dayekou River Basin, while sampling at 3,200, 3,500, and 3,800 m was conducted at the Haibei Alpine Meadow Ecosystem Research Station due to their distribution as well as accessibility of the sites. At each elevation, leaves were collected from three random plots (10 × 10 m) and then packed in paper bags. All the sampling plots were on the southern slopes with slope gradients between 27° and 33°. In each plot, three quadrats (1 × 1 m) were positioned evenly along a diagonal line. Soil samples from 0 to 0.10, 0.10 to 0.20, and 0.20 to 0.40 m were collected by using a 100-mm-diameter soil auger (Cao et al., 2020). A total of 21 sampling plots (seven elevations × three plots) and 63 sample quadrats (21 plots × three quadrats in each plot) were investigated.

Leaf and soil analyses

The leaves were firstly oven-dried at 80°C for 24 h and then ground to determine $[C]_{leaf}$, $[N]_{leaf}$, and $[P]_{leaf}$. Soil samples were air-dried and divided into two parts: One part was ground and sieved through a 100-mesh sieve for SOC, soil total nitrogen (STN), and STP determination, and the other part was ground and sieved through an 8-mesh sieve for soil pH determination. $[C]_{leaf}$ (g kg^{-1}) and SOC (g kg^{-1}), $[N]_{leaf}$ (g kg^{-1}) and STN (g kg^{-1}), and $[P]_{leaf}$ (g kg^{-1}) and STP (g kg^{-1}) were measured using the potassium bichromate titrimetric method (Nelson and Sommers, 1982), the Kjeldahl method (Bremmer and Mulvaney, 1982), and the molybdate blue method (Olsen and Sommers, 1982), respectively. Soil pH was measured by the potentiometric method with a soil–water ratio of 2:5.

Data analysis

MAT and MAP (Table 1) were calculated according to Zhao et al. (2005, 2006) as follows:

$$MAT = 20.96 - 5.49 \times 10^{-3} ELEV - 0.17 LAT + 8.9 \times 10^{-3} LONG, \; R^2 = 0.98 \quad (1)$$

TABLE 1 Sampling site coordinates, mean annual temperature (MAT), and precipitation (MAP) in the study area.

Parameter	**Elevation**						
	2,400 m	**2,600 m**	**2,800 m**	**3,000 m**	**3,200 m**	**3,500 m**	**3,800 m**
LONG	100°19′12″ E	100°17′18.5″ E	100°14′28″ E	100°14′26″ E	101°18′36″ E	101°21′00″ E	101°22′12″ E
LAT	38°35′24″ N	38°34′2.8″ N	38°33′9″ N	38°33′22″ N	37°36′36″ N	37°40′48″ N	37°41′24″ N
MAT (°C)	2.27	1.17	0.08	−1.02	−1.95	−3.61	−5.26
MAP (mm)	306.26	331.36	355.70	379.22	487.50	518.42	553.62

LAT, latitude; LONG, longitude; MAT, mean annual temperature; MAP, mean annual precipitation.

$$MAP = 1.68 \times 10^{3} + 0.12ELEV + 12.41LAT - 75.26LONG,\ R^{2} = 0.92 \quad (2)$$

where *ELEV* is the elevation, *LAT* is the latitude, *LONG* is the longitude, and R^2 is the regression coefficient.

All data were described by their average value and standard error (SE). Soil properties in the 0–0.40 m soil layer were expressed as an average of values in the 0–0.10, 0.10–0.20, and 0.20–0.40 m soil layers. The fixed effect (elevation) and random effect (experimental plots) on leaf stoichiometry of *P. anserina* and soil properties were tested by fitting linear mixed models (LMMs) in R3.3.1 (*nlme* vegan). The differences in soil properties among elevations were detected using the one-way ANOVA, followed by the least significant difference test to perform the significance analysis at $P < 0.05$ in SPSS 22.0 (SPSS Inc., Chicago, IL, USA). Pearson's correlation analysis was conducted to explore the correlations between the leaf stoichiometry of *P. anserina* and the topography-induced climatic factors and soil properties in SPSS 22.0. Path analysis was used in the structural equation modeling (SEM) to evaluate the direct and indirect effects of soil properties on leaf stoichiometry of *P. anserina* in Amos 22.0 (IBM SPSS Inc., Chicago, IL, USA).

Results

Variations in leaf stoichiometry of *Potentilla anserina* and soil properties with elevation

The results of LMMs showed that leaf stoichiometries of *P. anserina* and soil properties were significantly affected by elevation (Table 2). With increasing elevation, $[C]_{leaf}$ showed a generally decreasing trend (Figure 2A) and reached its maximum and minimum values at 2,400 m (446.04 ± 8.17 g kg^{-1}) and 3,500 m (396.78 ± 7.38 g kg^{-1}), respectively (Table 3). The $[N]_{leaf}$ showed a generally increasing trend (Figure 2B), with its maximum and minimum values at 3,500 m (37.57 ± 0.64 g kg^{-1}) and 2,800 m (23.71 ± 0.40 g kg^{-1}), respectively (Table 3). The $[P]_{leaf}$ decreased from 2,400 to 2,600 m elevation and reached the maximum and minimum values at 2,400 (2.79 ± 0.69 g kg^{-1}) and 3,800 m (0.97 ± 0.72 g kg^{-1}), respectively (Figure 2C, Table 3). However, there was no difference in $[P]_{leaf}$ at different elevations above 2,600 m (Table 3). In contrast to $[N]_{leaf}$, the $[C]_{leaf}/[N]_{leaf}$ showed a generally decreasing trend with an increase in elevation (Figure 2D), with a peak at 2,800 m (17.69 ± 0.46), and then reduced at 3,500 m (10.57 ± 0.27) (Table 3). The maximum and minimum values of $[C]_{leaf}/[P]_{leaf}$ were 842.36 ± 1,031.11 at 3,800 m and 173.03 ± 62.38 at 2,400 m, respectively. The $[N]_{leaf}/[P]_{leaf}$ showed a generally increasing trend with an increase in elevation (Figure 2F) and reached its maximum and minimum values at 3,800 m (69.40 ± 86.26) and at 2,400 m (10.05 ± 3.53), respectively (Table 3).

For soil properties, SOC and STN showed similar trends with their maximum values at 3,200 m (61.57 ± 3.15 g kg^{-1} and 6.09 ± 0.25 g kg^{-1}, respectively), and minimum values at 3,000 m (12.28 ± 0.61 g kg^{-1} and 1.35 ± 0.10 g kg^{-1}, respectively). The maximum and minimum values of STP were observed at 2,600 m (0.82 ± 0.05 g kg^{-1}) and 3,500 m (0.27 ± 0.05 g kg^{-1}), respectively. The maximum value of SOC/STN was observed at 2,800 m (20.45 ± 1.18), which was about two times that at other elevations. The values of SOC/STP and STN/STP at elevations ≥ 3,200 m were about two to seven times greater than those at elevations < 3,200 m. Soil pH at 3,000 m (8.51 ± 0.09) was the highest, while at 3,800 m (6.12 ± 0.10) it was the lowest.

Environmental factors influencing leaf ecological stoichiometry of *Potentilla anserina*

The SEM showed that the climatic and soil factors accounted for about 70, 91, 21, and 87% of the total variation in $[C]_{leaf}$, $[N]_{leaf}$, $[P]_{leaf}$, and $[C]_{leaf}/[N]_{leaf}$, respectively (Figure 3). Specifically, MAT had direct effects on $[C]_{leaf}$, $[N]_{leaf}$, and $[P]_{leaf}$ and an indirect effect on $[P]_{leaf}$ which may be from the positive influence on soil pH and negative influence on SOC (Figures 3A–C). MAP exerted direct effects on $[N]_{leaf}$ and $[C]_{leaf}/[N]_{leaf}$ and indirect effects on $[C]_{leaf}$, $[N]_{leaf}$,

TABLE 2 Summary of the generalized linear mixed models for leaf stoichiometry and soil properties (0–0.40 m) ($n = 9$).

Parameters	**Fixed effect (elevation)**			**Random effect (plot)**	**Fixed and random effects**	***df***
	F	***P***	***R*²**	***P***	***R*²**	
$[C]_{leaf}$	44.27	**<0.0001**	0.8107	0.9998	0.8107	6
$[N]_{leaf}$	774.79	**<0.0001**	0.9864	0.676	0.9868	6
$[P]_{leaf}$	7.5862	**<0.0001**	0.4053	0.4009	0.4479	6
$[C]_{leaf}/[N]_{leaf}$	341.89	**<0.0001**	0.9703	0.8819	0.9707	6
$[C]_{leaf}/[P]_{leaf}$	2.4541	**0.0377**	0.1899	0.8675	0.2005	6
$[N]_{leaf}/[P]_{leaf}$	2.6180	**0.0282**	0.2021	0.9998	0.2021	6
pH	674.41	**<0.0001**	0.9847	0.8551	0.9849	6
SOC	89.8473	**<0.0001**	0.8870	0.2683	0.8980	6
STN	158.795	**<0.0001**	0.9368	0.6607	0.9390	6
STP	10.3974	**<0.0001**	0.5015	0.9999	0.5015	6
SOC/STN	70.067	**<0.0001**	0.8715	0.9999	0.8715	6
SOC/STP	6.9747	**<0.0001**	0.4030	0.9998	0.4030	6
STN/STP	7.6212	**<0.0001**	0.4231	0.9413	0.4264	6

$[C]_{leaf}$, leaf carbon concentration; $[N]_{leaf}$, leaf nitrogen concentration; $[P]_{leaf}$, leaf phosphorus concentration; SOC, soil organic carbon; STN, soil total nitrogen; STP, soil total phosphorus. *F*, Fisher's test; *P*, probability value; *df*, degree of freedom. Significant values are in bold.

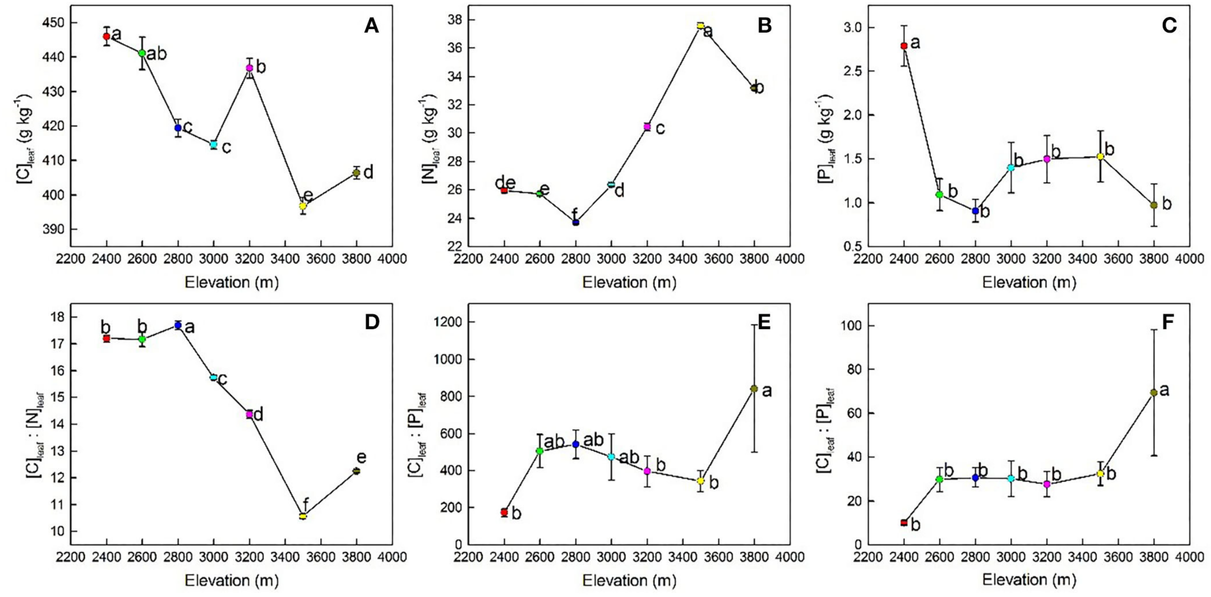

FIGURE 2
Changes in *Potentilla anserina*'s $[C]_{leaf}$ **(A)**, $[N]_{leaf}$ **(B)**, $[P]_{leaf}$ **(C)**, and their ratios **(D–F)** with an increase in elevation. $[C]_{leaf}$, leaf carbon concentration; $[N]_{leaf}$, leaf nitrogen concentration; $[P]_{leaf}$, leaf phosphorus concentration. Different lowercase letters indicate a significant difference in leaf stoichiometry and soil properties among elevations ($P < 0.05$).

and $[C]_{leaf}/[N]_{leaf}$ by influencing soil pH, STN, and STP (Figures 3A,B,D).

Soil pH and STP, which were both affected by MAP, exerted a direct positive effect on $[C]_{leaf}$ and $[C]_{leaf}/[N]_{leaf}$ and a negative effect on $[N]_{leaf}$ (Figures 3A,B,D). Soil pH also had a strong effect on $[P]_{leaf}$ (Figure 3C). The STN had not only a direct effect on $[C]_{leaf}$, but also an indirect effect as it positively influenced STP (Figure 3A). STN also indirectly affected $[N]_{leaf}$ by negatively influencing SOC/STN and positively influencing STP (Figure 3B). The SOC had a direct negative effect on $[P]_{leaf}$ and an indirect effect on $[P]_{leaf}$ by negatively influencing soil pH (Figure 3C).

TABLE 3 Variation of leaf stoichiometry of *Potentilla anserina* and soil properties (0–0.40 m) across elevations (mean ± standard error, $n = 9$).

Parameter	Elevation						
	2,400 m	**2,600 m**	**2,800 m**	**3,000 m**	**3,200 m**	**3,500 m**	**3,800 m**
$[C]_{leaf}$ (g kg^{-1})	446.04 ± 8.17a	441.17 ± 14.22ab	419.37 ± 7.66c	414.62 ± 3.66c	436.79 ± 8.58b	396.78 ± 7.38e	406.34 ± 5.37d
$[N]_{leaf}$ (g kg^{-1})	25.94 ± 0.55de	25.72 ± 0.46e	23.71 ± 0.40f	26.35 ± 0.38d	30.44 ± 0.82c	37.57 ± 0.64a	33.18 ± 0.41b
$[P]_{leaf}$ (g kg^{-1})	2.79 ± 0.69a	1.09 ± 0.54b	0.91 ± 0.38b	1.40 ± 0.87b	1.50 ± 0.82b	1.53 ± 0.87b	0.97 ± 0.72b
$[C]_{leaf}/[N]_{leaf}$	17.20 ± 0.41b	17.17 ± 0.79b	17.69 ± 0.46a	15.74 ± 0.29c	14.36 ± 0.46d	10.57 ± 0.27f	12.25 ± 0.19e
$[C]_{leaf}/[P]_{leaf}$	173.03 ± 62.38b	505.25 ± 266.91ab	542.76 ± 230.80ab	472.84 ± 374.58ab	395.71 ± 249.70b	343.74 ± 174.94b	842.36 ± 1031.11a
$[N]_{leaf}/[P]_{leaf}$	10.05 ± 3.53b	29.75 ± 16.70b	30.66 ± 12.98b	30.13 ± 24.11b	27.62 ± 17.23b	32.42 ± 16.26b	69.40 ± 86.26a
pH	8.25 ± 0.02b	8.03 ± 0.07c	8.10 ± 0.09c	8.51 ± 0.09a	7.75 ± 0.16d	6.44 ± 0.16e	6.12 ± 0.10f
SOC (g kg^{-1})	25.52 ± 0.15d	48.99 ±2.52b	36.42 ± 2.57c	12.28 ± 0.61e	61.57 ± 3.15a	58.64 ± 1.65a	50.14 ± 1.65b
STN (g kg^{-1})	2.67 ± 0.03d	4.48 ± 0.17c	1.82 ± 0.13e	1.35 ± 0.10f	6.09 ± 0.25a	5.24 ± 0.13b	4.72 ± 0.13c
STP (g kg^{-1})	0.64 ± 0.01b	0.82 ± 0.05a	0.46 ± 0.01ce	0.32 ± 0.03de	0.48 ± 0.07ace	0.27 ± 0.05d	0.53 ± 0.12ace
SOC/STN	9.56 ± 0.05cd	10.94 ± 0.44bc	20.45 ± 1.18a	9.22 ± 0.35d	10.09 ± 0.21bcd	11.19 ± 0.08b	10.62 ± 0.24bcd
SOC/STP	39.9 2± 0.32d	60.48 ± 3.05cd	80.05 ± 6.90bcd	40.81 ± 3.96d	174.70 ± 45.29b	307.11 ± 79.17a	147.41 ± 33.46bc
STN/STP	4.18 ± 0.06d	5.60 ± 0.36cd	3.95 ± 0.30d	4.38 ± 0.32d	16.75 ± 3.91b	27.24 ± 6.90a	13.99 ± 3.21bc

$[C]_{leaf}$, leaf carbon concentration; $[N]_{leaf}$, leaf nitrogen concentration; $[P]_{leaf}$, leaf phosphorus concentration; SOC, soil organic carbon; STN, soil total nitrogen; STP, soil total phosphorus. Different lowercase letters indicate a significant difference in leaf stoichiometry and soil properties among elevations ($P < 0.05$).

The SEM was not applicable for $[C]_{leaf}/[P]_{leaf}$ and $[N]_{leaf}/[P]_{leaf}$ because their models did not meet the requirement of P-values ($P > 0.05$). In this case, Pearson's correlation analysis was used to show their relationships with the environmental factors. Pearson's correlation analysis showed that the $[C]_{leaf}/[P]_{leaf}$ was only negatively correlated with MAT ($r = -0.250$, $P < 0.05$) and $[N]_{leaf}/[P]_{leaf}$ was positively correlated with MAP ($r = 0.315$, $P < 0.05$), but negatively correlated with MAT ($r = -0.360$, $P < 0.01$) and soil pH ($r = -0.325$, $P < 0.01$; Table 4).

Discussion

Effects of elevation on leaf ecological stoichiometry of *Potentilla anserina* and soil properties

The leaf stoichiometry of *P. anserina* changed due to heterogeneous habitat conditions with increased elevation. This agrees with the observations of van de Weg et al. (2009) and Hu et al. (2020) and supports our hypothesis that elevation would significantly influence leaf stoichiometry of *P. anserina*. However, Qin et al. (2022) found that elevation only significantly affected $[C]_{leaf}$, $[N]_{leaf}$, and $[C]_{leaf}/[N]_{leaf}$ of *Potentilla fruticosa*, while Su et al. (2022) reported that elevation was the key factor regulating the leaf stoichiometries of *Ligularia virgaurea* except $[P]_{leaf}$ and $[N]_{leaf}/[P]_{leaf}$ in the Qilian Mountains. This suggests diverse adaptation strategies of different species to environmental changes.

The $[C]_{leaf}$ of *P. anserina* showed a generally decreasing trend with an increase in elevation (Figure 2A), which is consistent with the study of Li et al. (2018) and Qin et al. (2022). This may be because photosynthesis was inhibited when the temperature dropped with an increase in elevation, which in turn weakened their carbon assimilation ability (Öquist, 1983). However, some studies (e.g., Zhao et al., 2018; Bo et al., 2020; Waigwa et al., 2020) reported that $[C]_{leaf}$ tended to be greater at higher elevations to balance cell osmotic pressure and improve the frost resistance of plants (Zhao et al., 2018). These conflicting results suggest that the response of $[C]_{leaf}$ to elevation still requires further studies based on species and at the regional level. The $[N]_{leaf}$ is an important indicator of plant adaptation to environmental changes (Li et al., 2014). It showed a generally increasing trend with an increase in elevation (Figure 2B), and this agrees with the observations of Cao et al. (2020). This may be because *P. anserina* could increase $[N]_{leaf}$ to offset the metabolic slowdown caused by a reduced enzymatic activity at low temperatures (McGroddy et al., 2004). The $[P]_{leaf}$ of *P. anserina* showed a significantly decreasing trend with an increase in elevation (Figure 2C), and this is in line with the observations of Waigwa et al. (2020). In the study area, the variation of *P. anserina*'s $[N]_{leaf}$ was consistent with the temperature–plant physiological hypothesis, while that of *P. anserina*'s $[P]_{leaf}$ was in contrast to this hypothesis. This may be because of the decoupling of N and P in plants under global changes (Yuan and Chen, 2015). Therefore, it is necessary to conduct targeted research on the mechanisms for their changes with elevation separately. The $[C]_{leaf}/[N]_{leaf}$ and $[C]_{leaf}/[P]_{leaf}$ reflected the nutrient utilization efficiency, and a lower value indicated a higher plant growth rate and a lower N utilization

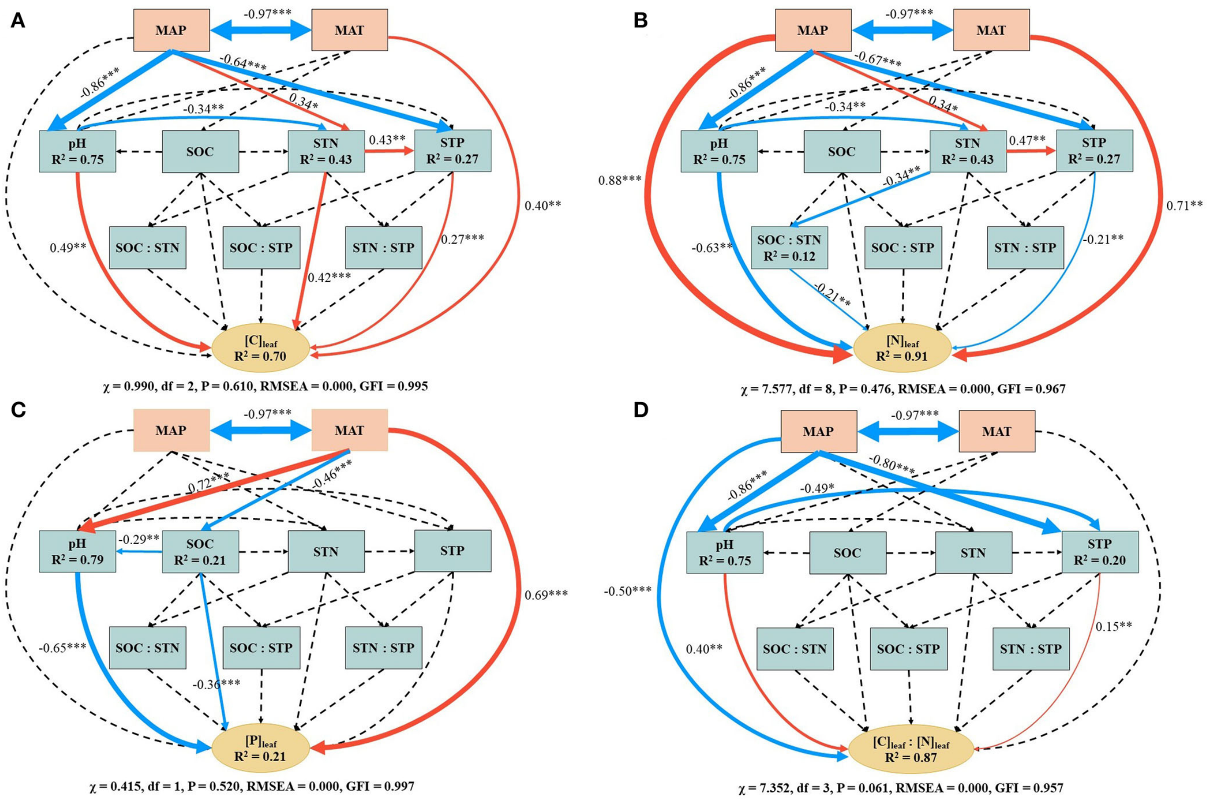

FIGURE 3
Structural equation modeling (SEM) examining the climatic and soil effects on leaf carbon concentration **(A)**, leaf nitrogen concentration **(B)**, leaf phosphorus concentration **(C)**, and the ratio of leaf carbon concentration and leaf nitrogen concentration **(D)**. $[C]_{leaf}$, leaf carbon concentration; $[N]_{leaf}$, leaf nitrogen concentration; $[P]_{leaf}$, leaf phosphorus concentration; SOC, soil organic carbon; STN, soil total nitrogen; STP, soil total phosphorus; MAT, mean annual temperature; MAP, mean annual precipitation. Single- and double-headed arrows represent the hypothesized causal direction and covarying variables, respectively. Continuous and dashed arrows indicate the relationships with ($^{*}P < 0.05$, $^{**}P < 0.01$, $^{***}P < 0.001$) and without statistical significance ($P > 0.05$), respectively. Numbers next to continuous arrows are standardized path coefficients, which indicate the effect size of the relationship. Red and blue arrows indicate the positive and negative relationships, respectively, and arrow width is scaled proportionally to their effect size. R^2 below variables indicates the proportion of variance explained.

TABLE 4 Pearson's correlations between environmental factors and leaf carbon-to-phosphorus ratio and the nitrogen-to-phosphorus ratio of *Potentilla anserina*.

	MAT	MAP	Soil pH	SOC	STN	STP	SOC:STN	SOC:STP	STN:STP
$[C]_{leaf}/[P]_{leaf}$	−0.250*	0.195	−0.197	0.118	0.067	−0.064	0.100	0.058	0.052
$[N]_{leaf}/[P]_{leaf}$	−0.360**	0.315*	−0.325**	0.176	0.154	−0.114	0.018	0.145	0.149

$[C]_{leaf}$, leaf carbon concentration; $[N]_{leaf}$, leaf nitrogen concentration; $[P]_{leaf}$, leaf phosphorus concentration; SOC, soil organic carbon; STN, soil total nitrogen; STP, soil total phosphorus; MAT, mean annual temperature; MAP, mean annual precipitation. $^{*}P < 0.05$, $^{**}P < 0.01$.

efficiency (Elser et al., 2003; Weidner et al., 2015; Sun et al., 2017). In the Qilian Mountains, $[C]_{leaf}/[N]_{leaf}$ of *P. anserina* decreased with elevation, consistent with the study of Zhang Q. et al. (2019) and Zhang Y. et al. (2019), but contrary to the study of Hu et al. (2020), indicating that the growth rate of *P. anserina* increased but N use efficiency decreased with elevation (Guo et al., 2016; Zhang et al., 2020). This was consistent with the adaptive growth hypothesis that under N-limited environments, plants adopt a survival-first strategy and maintain higher C/N to increase N use efficiency and ensure survival, while under less N-limited environments, plants adopt a growth-first strategy and maintain lower C/N to keep higher growth rates (Zhang et al., 2020). In the study area, compared with lower elevations (i.e., 2,400–3,000 m), STN was relatively higher at higher elevations (i.e., 3,200–3,800 m) (Table 3), resulting in a less N-limited condition. Therefore, $[C]_{leaf}/[N]_{leaf}$ of *P. anserina* decreased at higher elevations to benefit growth priority. The $[N]_{leaf}/[P]_{leaf}$ of *P. anserina* increased with elevation, similar to the study of Cao et al. (2020) on *Oxytropis ochrocephala* and the study of Wang et al. (2019) on *Sabina przewalskii* in the Qilian Mountains, while Su et al. (2022) found no significant changes in *Ligularia virgaurea*'s $[N]_{leaf}/[P]_{leaf}$ across elevation in the Qilian Mountains. The increasing $[N]_{leaf}/[P]_{leaf}$ of *P. anserina* with elevation indicates that the growth of *P. anserina* in the study area may be more susceptible to P-limitation at higher elevations.

In the study area, soil properties differ significantly with elevation (Tables 1, 2). Similar results were reported by Cao et al. (2020) and Niu et al. (2021), who found contrasting soil nutrient contents with elevation in the Qilian Mountains. The differences in soil properties may be from the variations in solar radiation, temperature, and precipitation at different elevations (Qin et al., 2022). Zonal climatic conditions could change soil nutrient flux and soil nutrient allocation by affecting vegetation composition, litter quality, and the exchange of matter and energy between the soil and the environment (Jiang et al., 2019). Likewise, under the combined influence of various factors, soil pH and SOC also changed with elevation (Yu et al., 2019; Zhu et al., 2019).

Mechanisms of elevation regulating leaf ecological stoichiometry of *Potentilla anserina*

As shown above, $[C]_{leaf}$, $[N]_{leaf}$, $[P]_{leaf}$, and their ratios of *P. anserina* showed inconsistent responses to elevation (Table 3, Figure 2), similar to the study of Müller et al. (2017) and Tong et al. (2021), indicating that the mechanisms of elevation regulating leaf ecological stoichiometry of *P. anserina* were different. In order to figure out how elevation affects leaf ecological stoichiometry, the underlying mechanisms of the variation in each element under elevation need to be explored individually (Weiher and Keddy, 1999; Suding et al., 2008).

Mechanisms of elevation regulating $[C]_{leaf}$ of *Potentilla anserina*

Temperature plays a key role in plant functions by influencing enzyme activity and membrane system fluidity as well as changing the absorption of nutrients and water and thus, in turn, affects the leaf ecological stoichiometry (Reich and Oleksyn, 2004; Hall et al., 2010; Liu et al., 2019). In the present study, MAT had a direct positive effect on $[C]_{leaf}$ (Figure 3A), similar to the study of Fang et al. (2019). Previous researchers found that when MAT declined and photosynthesis weakened, plants increased leaf thickness and reduced leaf area in order to prevent freezing damage, finally leading to a decrease in $[C]_{leaf}$ (Park and Day, 2007). With increasing elevation, the increased MAP can increase $[C]_{leaf}$ by impacting soil pH, STN, and STP (Figure 3A).

The STN and STP exerted positive effects on $[C]_{leaf}$ because high STN and STP were more conducive to the synthesis of enzymes that play key roles in carbon assimilation and accumulation (Zhang Q. et al., 2019). Soil pH exerted a positive influence on $[C]_{leaf}$, consistent with the study of Liu M. et al. (2021). However, most previous studies showed that higher soil pH had a significant negative impact on $[C]_{leaf}$ as it inhibits photosynthesis (e.g., He et al., 2016; Gong et al., 2018; Lin et al., 2022; Su et al., 2022). These results indicated that the impact of soil pH on $[C]_{leaf}$ was significant but varied with species.

Mechanisms of elevation regulating $[N]_{leaf}$ of *Potentilla anserina*

Elevation regulated $[N]_{leaf}$ by changing MAT, MAP, soil pH, SOC/STN, STN, and STP (Figure 3B). Persson et al. (2012) found that lower MAT could reduce $[N]_{leaf}$ by limiting the nutrient turnover rates. In the present study, MAT had a positive impact on $[N]_{leaf}$ (Figure 3B), consistent with the study of Li et al. (2021). However, with the decrease in MAT, $[N]_{leaf}$ showed a generally increasing trend (Table 3). This may be because the effect of MAT was weaker than the combined effects of MAP and soil physicochemical properties on $[N]_{leaf}$. In general, MAP changed plant nutrient absorption and photosynthesis by affecting soil water content and soil nutrient availability (Han et al., 2011; Liu et al., 2019). In this study, MAP affected $[N]_{leaf}$ either by directly changing its concentration, or by indirectly changing soil properties, further proved by the research of Reich (2005). MAP had a direct positive effect on $[N]_{leaf}$, similar to the research of Sardans et al. (2005) and Chen Y. H. et al. (2013). This may be because, with the increase in MAP, the increase in soil water content could improve the plant photosynthetic rate and sucrose synthase and nitrate reductase activities, thus resulting in increased $[N]_{leaf}$ (Patrick et al., 2009; Wang et al., 2011).

Decreased soil pH could promote the reabsorption of nitrogen to maintain plant growth, leading to increased $[N]_{leaf}$ (Su et al., 2022). Haynes (1986) found that when SOC/STN was ≤ 25, soil nitrogen was mineralized as available nitrogen for plant growth, while when it was > 25, microorganisms mineralized soil nitrogen for maintaining their own growth. In the present study, the SOC/STN was all < 25, suggesting that more soil available nitrogen was taken up by plants and increased $[N]_{leaf}$. However, this needs further research based on soil available nitrogen analysis. In addition, STP exerted a negative effect on $[N]_{leaf}$. This might be because the decreased STP reduced the availability of P and relatively weakened the limiting effect of available N on plants, thereby enhancing the competition of plants for available N and promoting the uptake and utilization of N by an individual plant (Li et al., 2017). However, some studies found that decreased STP could reduce $[N]_{leaf}$ (e.g., van Wijk et al., 2003; Mao et al., 2016). This was related to different responses of plant species to environmental changes due to their differentiation of niches based on functional attributes (Pontes et al., 2010; Adamidis et al., 2014; Li et al., 2017).

Mechanisms of elevation regulating $[P]_{leaf}$ of *Potentilla anserina*

MAT had a positive effect on $[P]_{leaf}$ (Figure 3C). This may be because the decrease in MAT restricted soil parent weathering, which led to a decrease in soil P absorption by plants (Tong et al., 2021). Besides, the decreased MAT can indirectly influence $[P]_{leaf}$ through decreasing soil pH and increasing SOC with an increase in elevation. Soil pH had a direct negative impact on $[P]_{leaf}$. This may be because the decrease in soil pH could release phosphate radicals and increase soil available P, thereby improving the uptake of P and $[P]_{leaf}$ (Chen D. M. et al., 2013), while high soil pH may facilitate P adsorption to soil particles (Qiao et al., 2018).

The SOC had a negative effect on $[P]_{leaf}$ (Figure 3C), contrary to what was observed by Liu et al. (2016) and Cao et al. (2020), suggesting that plants have their unique nutrient absorption mechanism in the processes of growth. The utilization of SOC by plants was extremely complex and may be controlled by a variety of soil physical and chemical properties (Pan et al., 2015; Rong et al., 2015).

Mechanisms of elevation regulating $[C]_{leaf}/[N]_{leaf}/[P]_{leaf}$ of *Potentilla anserina*

According to the SEM, decreased $[C]_{leaf}/[N]_{leaf}$ with an increase in elevation resulted from the positive impacts of soil pH and STP and the negative impact of MAP (Figure 3D). This suggests that the increase in soil pH and STP is beneficial to promote the growth of *P. anserina* within a certain range, while the increase in precipitation may inhibit the growth of *P. anserina* in the study area. The $[C]_{leaf}/[P]_{leaf}$ at 3,800 m was significantly higher than that at 2,400, 3,200, and 3,500 m, similar to the study of Qin et al. (2022). However, there was no clear variation trend of $[C]_{leaf}/[P]_{leaf}$ with elevation (Figure 2E). This may be because the similar variations of $[C]_{leaf}$ and $[P]_{leaf}$ with elevation weakened the relationship between $[C]_{leaf}/[P]_{leaf}$ and elevation. MAT was negatively correlated with $[N]_{leaf}/[P]_{leaf}$ (Table 4), which might be attributed to the positive effect of MAT on $[P]_{leaf}$ (Figure 3C), though MAT had a positive influence on $[N]_{leaf}$. This indicated a stronger influence of MAT on $[P]_{leaf}$ than on $[N]_{leaf}$. The positive relationship between MAP and $[N]_{leaf}/[P]_{leaf}$ (Table 4) may be related to the positive effects of MAP on $[N]_{leaf}$ (Figure 3B). However, the significantly increasing $[N]_{leaf}/[P]_{leaf}$ with elevation increase was mainly caused by significantly increasing $[N]_{leaf}$ rather than by decreasing $[P]_{leaf}$ in the study area.

Other factors impacting leaf ecological stoichiometry of *Potentilla anserina*

According to the SEM results, the environmental factors in the present study can only account for part of the total variation of leaf ecological stoichiometry of *P. anserina* (Figure 3). This indicates the possibility of effects of other factors, such as inheritance and genetic mutations of species (Luo et al., 2006), vegetation community structure and composition (Wang et al., 2014; Zhu et al., 2020), light (Zhu et al., 2020), soil microbial activity (Li et al., 2014), and intra- and inter-species competitions (Xu et al., 2015; Qin et al., 2016). As *P. anserina* is a pioneer species of degraded grassland, grassland management also needs to be taken into consideration in future research to fully understand the leaf ecological stoichiometry changes of *P. anserina* and provide basic information for ecological restoration in this region.

Nutrient limitation for *Potentilla anserina* growth across elevation

Due to the limited natural supply, N and P were the two most important elements to limit plant growth and functioning in a terrestrial ecosystem (Elser et al., 2000). Compared with the individual $[N]_{leaf}$ and $[P]_{leaf}$, $[N]_{leaf}/[P]_{leaf}$ was more reliable to identify plants' nutrient limitations (Li et al., 2018), although the thresholds were still controversial. In the present study area, the average $[N]_{leaf}/[P]_{leaf}$ (32.86) was significantly higher than that of global and Chinese vegetations (11.8 and 16.3, respectively) (Reich and Oleksyn, 2004; Han et al., 2005). This suggests that *P. anserina* was more P-limited than the averages of global and Chinese plants. According to the study of Güsewell (2004) on terrestrial plant communities, when $[N]_{leaf}/[P]_{leaf} < 10$, plants growth was limited by N; $10 \leq [N]_{leaf}/[P]_{leaf} \leq 20$, plant growth was co-limited by N and P; and $[N]_{leaf}/[P]_{leaf} > 20$, plant growth was limited by P. In the study area, the $[N]_{leaf}/[P]_{leaf}$ of *P. anserina* from 2,600 to 3,800 m was all > 20 and at 2,400 m was 10.05 (Table 3), suggesting that the growth of *P. anserina* was limited by P from 2,600 to 3,800 m and by both N and P at 2,400 m.

With increasing elevation, $[N]_{leaf}/[P]_{leaf}$ showed an increasing trend, indicating that the higher the elevation, the more severe the restriction of P element to the growth of *P. anserina*. This may be related to the decrease in MAT and soil pH and the increase in MAP (Tables 3, 4). Previous studies indicated that soil P deficiency was an important reason for P-limitation in plants in China (e.g., Han et al., 2005; Hu et al., 2017) and in the present study area (Cao et al., 2020; Qin et al., 2022). This also suggested that taking measures to increase soil available P and reduce P losses is of great importance for ecological restoration in the Qilian Mountains as well as in China.

Conclusion

According to the results of field sampling and experimental analysis, $[C]_{leaf}$, $[N]_{leaf}$, $[P]_{leaf}$, and the stoichiometric ratios of *P. anserina* fluctuated with elevation in the middle eastern part of the Qilian Mountains: from 2,400 to 3,800 m, $[C]_{leaf}$, $[P]_{leaf}$, and $[C]_{leaf}/[N]_{leaf}$ decreased, while $[N]_{leaf}$ and $[N]_{leaf}/[P]_{leaf}$ increased. Elevation played a significant role in the leaf ecological stoichiometry of *P. anserina* through the effects of MAT, MAP, and soil pH. Based on $[N]_{leaf}/[P]_{leaf}$ inference, P element was the restrictive resource that affected *P. anserina* growth in the study area, and it was particularly deficient with the increase in elevation.

As *P. anserina* is a useful species for restoring degraded grasslands, it is of great importance to increase soil available P and reduce P losses for the growth of *P. anserina*, especially at higher elevations. Due to the relatively small scale of the present study, further studies in the Qilian Mountains will ensure wider applicability of the observations in other areas.

Data availability statement

The original contributions presented in the study are included in the article/supplementary material, further inquiries can be directed to the corresponding author.

Author contributions

XZ, QF, and JC were involved in the conception and design of the research. XZ and HS were involved in the acquisition of data and drafted the manuscript. XZ and YQ analyzed and interpreted the data. XZ and WL performed the statistical analysis. AB, JC, and MZ were involved in the revision of the manuscript for important intellectual content. All authors have read and approved the final manuscript.

Funding

This work was supported by the National Natural Science Foundation of China (Grant No. 52179026), the Key R&D Program of Gansu Province, China (Grant No. 20YF8FA002), and the XPCC Science and Technique Foundation (Grant No. 2021AB021).

Conflict of interest

The authors declare that the research was conducted in the absence of any commercial or financial relationships that could be construed as a potential conflict of interest.

Publisher's note

References

Adamidis, G. C., Kazakou, E., Fyllas, N. M., and Dimitrakopoulos, P. G. (2014). Species adaptive strategies and leaf economic relationships across serpentine and non-serpentine habitats on Lesbos, eastern Mediterranean. *PLoS ONE* 9, e96034. doi: 10.1371/journal.pone.0096034

Baxter, I., and Dilkes, B. P. (2012). Elemental profiles reflect plant adaptations to the environment. *Science* 336, 1661–1663. doi: 10.1126/science.1219992

Bo, F., Zhang, Y., Chen, H. Y. H., Wang, P., Ren, X., and Guo, J. (2020). The C:N:P stoichiometry of planted and natural larix principis-rupprechtii stands along altitudinal gradients on the Loess Plateau, China. *Forests* 11, 363. doi: 10.3390/f11040363

Bremmer, J. M., and Mulvaney, C. S. (1982). "Nitrogen-total," in *Methods of Soil Analysis in Part 2-Chemical and Biochemical Methods*, eds H. R. Miller and D. R. Keeney (Madison, WI: American Society of Agronomy-Soil Science Society of America), 595–624.

Cao, J., Wang, X., Adamowski, J. F., Biswas, A., Liu, C., Chang, Z., et al. (2020). Response of leaf stoichiometry of *Oxytropis ochrocephala* to elevation and slope aspect. *Catena* 194, 104772. doi: 10.1016/j.catena.2020.104772

Chen, D. M., Lan, Z. C., Bai, X., Grace, J. B., and Bai, Y. F. (2013). Evidence that acidification-induced declines in plant diversity and productivity are mediated by changes in below-ground communities and soil properties in a semi-arid steppe. *J. Ecol.* 101, 1322–1334. doi: 10.1111/1365-2745.12119

Chen, Y. H., Han, W. X., Tang, L. Y., Tang, Z. Y., and Fang, J. Y. (2013). Leaf nitrogen and phosphorus concentrations of woody plants differ in responses to climate, soil and plant growth form. *Ecography* 36, 178–184. doi: 10.1111/j.1600-0587.2011.06833.x

Cheng, J., Liu, D., Zhao, L., Zhao, Q., Zhang, X., Wang, B., et al. (2021). *Potentilla anserine* L. polysaccharide inhibits cadmium-induced neurotoxicity by attenuating autophagy. *Neurochem. Int.* 147, 105045. doi: 10.1016/j.neuint.2021.105045

Croft, H., Chen, J., Luo, X., Bartlett, P., Chen, B., and Staebler, R. M. (2017). Leaf chlorophyll content as a proxy for leaf photosynthetic capacity. *Glob. Chang. Biol.* 23, 3513–3524. doi: 10.1111/gcb.13599

Crowley, K. F., Mcneil, B. E., Lovett, G. M., Canham, C. D., Driscoll, C. T., Rustad, L. E., et al. (2012). Do nutrient limitation patterns shift from nitrogen toward phosphorus with increasing nitrogen deposition across the northeastern united states?. *Ecosystems* 15, 940–957. doi: 10.1007/s10021-012-9550-2

Du, B. M., Ji, H. W., Peng, C., Liu, X. J., and Liu, C. J. (2017). Altitudinal patterns of leaf stoichiometry and nutrient resorption in quercus variabilis in the Baotianman mountains, China. *Plant Soil* 413, 193–202. doi: 10.1007/s11104-016-3093-9

Elser, J. J., Acharya, K., and Kyle, M. (2003). Growth rate-stoichiometry couplings in diverse biota. *Eco. Lett.* 6, 936–943. doi: 10.1046/j.1461-0248.2003.00518.x

Elser, J. J., Fagan, W. F., Denno, R. F., Dobberfuhl, D. R., Folarin, A., Huberty, A. F., et al. (2000). Nutritional constraints in terrestrial and freshwater food webs. *Nature* 408, 578–580. doi: 10.1038/35046058

Elser, J. J., Fagan, W. F., Kerkhoff, A. J., Swenson, N. G., and Enquist, B. J. (2010). Biological stoichiometry of plant production: metabolism, scaling and ecological response to global change. *New Phytol.* 186, 593–608. doi: 10.1111/j.1469-8137.2010.03214.x

Fang, Z., Li, D., Jiao, F., Yao, J., and Du, H. (2019). The latitudinal patterns of leaf and soil C:N:P stoichiometry in the Loess Plateau of China. *Front. Plant Sci.* 10, 85. doi: 10.3389/fpls.2019.00085

Gong, X., Xu, Z., Lu, W., Tian, Y., Liu, Y., Wang, Z., et al. (2018). Spatial patterns of leaf carbon, nitrogen, and phosphorus stoichiometry of aquatic macrophytes in the arid zone of northwestern China. *Front. Plant Sci.* 9, 1398. doi: 10.3389/fpls.2018.01398

Gui, J., Li, Z., Feng, Q., Yuan, R., Ning, T., Zhang, B., et al. (2020). Environmental effect and spatiotemporal pattern of stable isotopes in precipitation on the transition zone between the Tibetan Plateau and arid region. *Sci. Total Environ.* 749, 141559. doi: 10.1016/j.scitotenv.2020.141559

Guo, Q., Li, H., and Zhang, W. (2016). Variations in leaf functional traits and physiological characteristics of *Abies georgei* var. smithii along the altitude gradient in the Southeastern Tibetan Plateau. *J. Mount. Sci.* 13, 1818–1828. doi: 10.1007/s11629-015-3715-3

Guo, X., Shi, P., Niinemets, Ü., Hölscher, D., Wang, R., Liu, M., et al. (2021). "Diminishing returns" for leaves of five age-groups of *Phyllostachys edulis* culms. *Am. J. Bot.* 108, 1662–1672. doi: 10.1002/ajb2.1738

Güsewell, S. (2004). N: P ratios in terrestrial plants: variation and functional significance. *New Phytol.* 164, 243–266. doi: 10.1111/j.1469-8137.2004.01192.x

Hall, E. K., Singer, G. A., Kainz, M. J., and Lennon, J. T. (2010). Evidence for a temperature acclimation mechanism in bacteria: an empirical test of a membrane-mediated trade-off. *Funct. Ecol.* 24, 898–908. doi: 10.1111/j.1365-2435.2010.01707.x

Han, W. X., Fang, J. Y., Guo, D. L., and Zhang, Y. (2005). Leaf nitrogen and phosphorus stoichiometry across 753 terrestrial plant species in China. *New Phytol.* 168, 377–385. doi: 10.1111/j.1469-8137.2005.01530.x

Han, W. X., Fang, J. Y., Reich, P. B., Woodward, F. I., and Wang, Z. H. (2011). Biogeography and variability of eleven mineral elements in plant leaves across gradients of climate, soil and plant functional type in China. *Ecol. Lett.* 14, 788–796. doi: 10.1111/j.1461-0248.2011.01641.x

Haynes, R. J. (ed.). (1986). "The decomposition process: mineralization, immobilization, humus formation, and degradation," in *Mineral Nitrogen in the Plant-Soil* System (London: Academic Press), 52–126. doi: 10.1016/B978-0-12-334910-1.50006-6

He, L., Liu, N., Wang, K., Zhang, L., Li, D., Wang, Z., et al. (2021). Rosamultin from *Potentilla anserine* L. exhibits nephroprotection and antioxidant activity by regulating the reactive oxygen species/C/EBP homologous protein signaling pathway. *Phytother. Res.* 35, 6343–6358. doi: 10.1002/ptr.7285

He, Y., Chen, Y., Yu, C. L., Lu, K. X., Jiang, Q. S., Fu, J. L., et al. (2016). Photosynthesis and yield traits in different soybean lines in response to salt stress. *Photosynthetica* 54, 630–635. doi: 10.1007/s11099-016-0217-7

Hu, Q., Sheng, M., Bai, Y., Jie, Y., and Xiao, H. (2020). Response of C, N, and P stoichiometry characteristics of *Broussonetia papyrifera* to altitude gradients and soil nutrients in the karst rocky ecosystem, SW China. *Plant Soil* 475, 123–136. doi: 10.1007/s11104-020-04742-7

Hu, Y. K., Zhang, Y. L., Liu, G. F., Xu, P., and Ming, D. (2017). Intraspecific N and P stoichiometry of Phragmites australis: geographic patterns and variation among climatic regions. *Sci Rep.* 7, 43018. doi: 10.1038/srep43018

IUSS Working Group World Reference Base for Soil Resources (2014). *2014 International Soil Classification System for Naming Soils and Creating Legends for Soil Maps*. Rome: FAO.

Jiang, L., He, Z., Liu, J., Xing, C., Gu, X., Wei, C., et al. (2019). Elevation gradient altered soil C, N, and P stoichiometry of pinus taiwanensis forest on Daiyun mountain. *Forests* 10, 1089. doi: 10.3390/f10121089

Koerselman, W., and Meuleman, A. M. F. (1996). The vegetation N:P ratio: a new tool to detect the nature of nutrient limitation. *J. Appl. Ecol.* 33, 1441–1450. doi: 10.2307/2404783

Li, F., Hu, J., Xie, Y., Yang, G., Hu, C., Chen, X., et al. (2018). Foliar stoichiometry of carbon, nitrogen, and phosphorus in wetland sedge Carex brevicuspis along a small-scale elevation gradient. *Ecol. Indic.* 92, 322–329. doi: 10.1016/j.ecolind.2017.04.059

Li, H., Ye, D. D., Wang, X. G., Settles, M. L., Wang, J., Hao, Z. Q., et al. (2014). Soil bacterial communities of different natural forest types in Northeast China. *Plant Soil* 1–2, 203–216. doi: 10.1007/s11104-014-2165-y

Li, L., Gao, X., Gui, D., Liu, B., Zhang, B., and Li, X. (2017). Stoichiometry in aboveground and fine roots of *Seriphidium koroviniiin* desert grassland in response to artificial nitrogen addition. *J. Plant Res.* 130, 689–697. doi: 10.1007/s10265-017-0930-8

Li, W., Huang, G., and Zhang, H. (2020). Enclosure increases nutrient resorption from senescing leaves in a subalpine pasture. *Plant Soil* 457, 269–278. doi: 10.1007/s11104-020-04733-8

Li, Y., He, W., Wu, J., Zhao, P., Chen, Y., Zhu, L., et al. (2021). Leaf stoichiometry is synergistically-driven by climate, site, soil characteristics and phylogeny in karst areas, Southwest China. *Biogeochemistry* 155, 283–301. doi: 10.1007/s10533-021-00826-3

Li, Y., Shi, P., Niinemets, Ü., Song, Y., Yu, K., Schrader, J., et al. (2022a). Diminishing returns among lamina fresh and dry mass, surface area, and petiole fresh mass among nine *Lauraceae* species. *Am. J. Bot.* 109, 377–392. doi: 10.1002/ajb2.1812

Li, Y., Zheng, Y., Ratkowsky, D. A., Wei, H., and Shi, P. (2022b). Application of an ovate leaf shape model to evaluate leaf bilateral asymmetry and calculate lamina centroid location. *Front. Plant Sci.* 2, 822907. doi: 10.3389/fpls.2021.822907

Lin, Y., Lai, Y., Tang, S., and Qin, Z. (2022). Climatic and edaphic variables determine leaf C, N, P stoichiometry of deciduous *Quercus* species. *Plant Soil.* 474, 383–394. doi: 10.21203/rs.3.rs-900936/v1

Liu, D., Zheng, D., Xu, Y., Chen, Y., Wang, H., Wang, K., et al. (2021). Changes in the stoichiometry of *Castanopsis fargesii* along an elevation gradient in a Chinese subtropical forest. *PeerJ* 9, e11553. doi: 10.7717/peerj.11553

Liu, J. T., Gu, Z. J., Shao, H. B., Zhou, F., and Peng, S. Y. (2016). N-P stoichiometry in soil and leaves of *Pinus massoniana* forest at different stand ages in the subtropical soil erosion area of China. *Environ. Earth Sci.* 75, 1901. doi: 10.1007/s12665-016-5888-7

Liu, J. X., Fang, X., Tang, X. L., Wang, W. T., Zhou, G. Y., and Xu, S. (2019). Patterns and controlling factors of plant nitrogen and phosphorus stoichiometry across China's forests. *Biogeochemistry* 143, 191–205. doi: 10.1007/s10533-019-00556-7

Liu, M., Shen, Y., Li, Q., Xiao, W., and Song, X. (2021). Arbuscular mycorrhizal fungal colonization and soil pH induced by nitrogen and phosphorus additions affects leaf C:N:P stoichiometry in Chinese fir (*Cunninghamia lanceolata*) forests. *Plant Soil* 461, 421–440. doi: 10.1007/s11104-021-04831-1

Luo, J. X., Zang, R. G., and Li, C. Y. (2006). Physiological and morphological variations of *Picea asperata* populations originating from different altitudes in the mountains of southwestern. *For. Ecol. Manag.* 221, 285–290. doi: 10.1016/j.foreco.2005.10.004

Macek, P., Macková, J., and de Bello, F. (2009). Morphological and ecophysiological traits shaping altitudinal distribution of three polylepis treeline species in the dry tropical Andes. *Acta Oecol.* 35, 778–785. doi: 10.1016/j.actao.2009.08.013

Mao, R., Chen, H. M., Zhang, X. H., Shi, F., and Song, C. (2016). Effects of P addition on plant C: N: P stoichiometry in an N-limited temperate wetland of Northeast China. *Sci. Total Environ.* 559, 1–6. doi: 10.1016/j.scitotenv.2016.03.158

Marschner, H., and Marschner, P. (2012). *Marschner's Mineral Nutrition of Higher Plants*. London: Academic Press.

McGroddy, M. E., Daufresne, T., and Hedin, L. O. (2004). Scaling of C: N: P stoichiometry in forests worldwide: implications of terrestrial redfield-type ratios. *Ecology* 85, 2390–2401. doi: 10.1890/03-0351

Moe, S. J., Stelzer, R. S., Forman, M. R., Harpole, S. W., Daufresne, T., and Yoshida, T. (2005). Recent advances in ecological stoichiometry: insights for population and community ecology. *Oikos* 109, 29–39. doi: 10.1111/j.0030-1299.2005.14056.x

Müller, M., Oelmann, Y., Schickhoff, U., Böhner, J., and Scholten, T. (2017). Himalayan treeline soil and foliar C:N:P stoichiometry indicate nutrient shortage with elevation. *Geoderma* 291, 21–32. doi: 10.1016/j.geoderma.2016.12.015

Nelson, D. W., and Sommers, L. E. (1982). "Total carbon, organic carbon, and organic matter," in *Methods of Soil Analysis: Part 3 Chemical Methods,* eds D. L. Sparks, A. L. Page, P. A. Helmke, R. H. Loeppert, P. N. Soltanpour, M. A. Tabatabai, C. T. Johnston, and M. E. Sumner (Madison, WI: American Society of Agronomy), 539–579. doi: 10.2136/sssabookser5.3.c34

Niu, Y., Kang, J., Su, H., Adamowski, J. F., Biswas, A., Liu, C., et al. (2021). Elevation alone alters leaf N and leaf C to N ratio of *Picea Crassifolia* kom. in China's Qilian Mountains. *Forests* 12, 1325. doi: 10.3390/f12101325

Olsen, S. R., and Sommers, L. E. (1982). "Phosphorus, chemical and microbiological properties," in *Methods of Soil Analysis*, eds R. H. Miller and D.R. Keeney (Madison, WI: American Society of Agronomy), 403–430.

Öquist, G. (1983). Effects of low temperature on photosynthesis. *Plant Cell Environ*. 6, 281–300. doi: 10.1111/1365-3040.ep11612087

Pan, F., Zhang, W., Liu, S., Li, D. J., and Wang, K. L. (2015). Leaf N:P stoichiometry across plant functional groups in the karst region of southwestern China. *Trees* 29, 883–892. doi: 10.1007/s00468-015-1170-y

Park, J. H., and Day, T. A. (2007). Temperature response of CO_2 exchange and dissolved organic carbon release in a maritime Antarctic tundra ecosystem. *Polar Biol.* 30, 1535–1544. doi: 10.1007/s00300-007-0314-y

Patrick, L. D., Ogle, K., Bell, C. W., Zak, J., and Tissue, D. (2009). Physiological responses of two contrasting desert plant species to precipitation variability are differentially regulated by soil moisture and nitrogen dynamics. *Glob. Change Biol.* 15, 1214–1229. doi: 10.1111/j.1365-2486.2008.01750.x

Persson, I. L., Julkunen-Tiitto, R., Bergström, R., Wallgren, M., Suominen, O., and Danell, K. (2012). Simulated moose (*Alces alces* L.) browsing increases accumulation of secondary metabolites in bilberry (*Vaccinium myrtillus* L.) along gradients of habitat productivity and solar radiation. *J. Chem. Ecol.* 38, 1225–1234. doi: 10.1007/s10886-012-0209-4

Pontes, D. S. L., Louault, F., Carrère, P., Maire, V., Andueza, D., and Soussana, J. (2010). *The Role of Plant Traits and Their Plasticity in the Response of Pasture Grasses to Nutrients and Cutting Frequency*. London: Oxford University Press.

Qiao, Y., Yang, W., Zhao, Y., Jeelani, N., Xu, L., Zhao, H., et al. (2018). How Spartina alterniflora adapts to a new environment created by embankment reclamation through C-N-P stoichiometry in the coastal wetlands of eastern China. *Mar. Freshw. Res.* 69, 823–832. doi: 10.1071/MF17374

Qin, J., Xi, W., Rahmlow, A., Kong, H., Zhang, Z., and Shangguan, Z. (2016). Effects of forest plantation types on leaf traits of *Ulmus pumila* and *Robinia pseudoacacia* on the Loess Plateau, China. *Ecol. Eng.* 97, 416–425. doi: 10.1016/j.ecoleng.2016.10.038

Qin, Y., Feng, Q., Adamowski, J. F., Zhu, M., and Zhang, X. (2021). Community level response of leaf stoichiometry to slope aspect in a montane environment: a case study from the Central Qilian Mountains, China. *Glob. Ecol. Conserv*. 28, e01703. doi: 10.1016/j.gecco.2021.e01703

Qin, Y., Liu, W., Zhang, X., Adamowski, J. F., and Biswas, A. (2022). Leaf stoichiometry of *Potentilla fruticosa* across elevations in China's Qilian Mountains. *Front. Plant Sci.* 13, 814059. doi: 10.3389/fpls.2022.814059

Reich, P. B. (2005). Global biogeography of plant chemistry: filling in the blanks. *New Phytol.* 168, 263–266. doi: 10.1111/j.1469-8137.2005.01562.x

Reich, P. B., and Oleksyn, J. (2004). Global patterns of plant leaf N and P in relation to temperature and latitude. *Proc. Natl. Acad. Sci. U.S.A.* 101, 11001–11006. doi: 10.1073/pnas.0403588101

Rong, Q., Liu, J., Cai, Y., Lu, Z., Zhao, Z., Yue, W., et al. (2015). Leaf carbon, nitrogen and phosphorus stoichiometry of *Tamarix chinensis* Lour. in the Laizhou Bay coastal wetland, China. *Ecol Eng.* 76, 57–65. doi: 10.1016/j.ecoleng.2014.03.002

Sardans, J., Rivas-Ubach, A., and Penuelas, J. (2011). Factors affecting nutrient concentration and stoichiometry of forest trees in Catalonia (NE Spain). *For. Ecol. Manag.* 262, 2024–2034. doi: 10.1016/j.foreco.2011.08.019

Sardans, J., Rodà, F., and Peñuelas, J. (2005). Effects of water and a nutrient pulse supply on rosmarinus officinalis growth, nutrient content and flowering in the field. *Environ. Exp. Bot.* 53, 1–11. doi: 10.1016/j.envexpbot.2004.02.007

Sheng, H., Li, J., Yang, Y., and Li, H. (2004). Response of phenotypic plasticity of *Potentilla anserine* L. to soil moisture. *Agric. Res. Arid Areas* 3, 119–122.

Shi, P., Li, Y., Hui, C., Ratkowsky, D. A., Yu, X., and Niinemets, Ü. (2020). Does the law of diminishing returns in leaf scaling apply to vines?—Evidence from 12 species of climbing plants. *Glob. Ecol. Conserv.* 21, e00830. doi: 10.1016/j.gecco.2019.e00830

Shi, P., Miao, Q., Niinemets, Ü., Liu, M., Li, Y., Yu, K., et al. (2022). Scaling relationships of leaf vein and areole traits versus leaf size for nine *Magnoliaceae* species differing in venation density. *Am. J. Bot.* 109, 899–909. doi: 10.1002/ajb2.1856

Sistla, S. A., and Schimel, J. P. (2012). Stoichiometric flexibility as a regulator of carbon and nutrient cycling in terrestrial ecosystems under change. *New Phytol.* 196, 68–78. doi: 10.1111/j.1469-8137.2012.04234.x

Su, H., Cui, J., Adamowski, J. F., Zhang, X., Biswas, A., and Cao, J. (2022). Using leaf ecological stoichiometry to direct the management of *Ligularia virgaurea* on the Northeast Qinghai-Tibetan plateau. *Front. Environ. Sci.* 9, 805405. doi: 10.3389/fenvs.2021.805405

Suding, K. N., Lavorel, S., Chapin, F. S., Cornelissen, J. H. C., Díaz, S., Garnier, E., et al. (2008). Scaling environmental change through the community-level: a trait-based response-and-effect framework for plants. *Glob. Change Biol.* 14, 1125–1140. doi: 10.1111/j.1365-2486.2008.01557.x

Sun, L., Zhang, B., Wang, B., Zhang, G., and Zhang, W., Zhang, B., et al. (2017). Leaf elemental stoichiometry of *Tamarix Lour*. species in relation to geographic, climatic, soil, and genetic components in China. *Ecol. Eng.* 106, 448–457. doi: 10.1016/j.ecoleng.2017.06.018

Tao, Y., Wu, G. L., Zhang, Y. M., and Zhou, X. B. (2016). Leaf N and P stoichiometry of 57 plant species in the Karamori Mountain Ungulate Nature Reserve, Xinjiang. *China. J. Arid Land.* 8, 935–947. doi: 10.1007/s40333-016-0019-6

Tian, D., Reich, P. B., Chen, H., Xiang, Y., Luo, Y., Shen, Y., et al. (2018). Global changes alter plant multi-element stoichiometric coupling. *New Phytol.* 221, 807–817. doi: 10.1111/nph.15428

Tong, R., Zhou, B., Jiang, L., Ge, X., and Cao, Y. (2021). A typical forbs in alpine plant communities. *Catena* 201, 105221. doi: 10.1016/j.catena.2021.105221

van de Weg, M. J., Meir, P., Grace, J., and Atkin, O. K. (2009). Altitudinal variation in leaf mass per unit area, leaf tissue density and foliar nitrogen and phosphorus content along an Amazon-Andes gradient in Peru. *Plant Ecol. Divers.* 2, 243–254. doi: 10.1080/17550870903518045

van Wijk, M. T., Williams, M., Gough, L., Hobbie, S. E., and Shaver, G. R. (2003). Luxury consumption of soil nutrients: a possible competitive strategy in above-ground and below-ground biomass allocation and root morphology for slow-growing arctic vegetation? *J. Ecol.* 91, 664–676. doi: 10.1046/j.1365-2745.2003.00788.x

Waigwa, A. N., Mwangi, B. N., Wahiti, G. R., Omengo, F., Zhou, Y., and Wang, Q. (2020). Variation of morphological and leaf stoichiometric traits of two endemic species along the elevation gradient of Mount Kenya, East Africa. *J. Plant Ecol.* 13, 785–792. doi: 10.1093/jpe/rtaa067

Wang, F., Zhang, F., Guo, X., Zhang, J., Wang, Y., and Niu, H. (2019). Spatial and temporal variation of leaf nitrogen and phosphorus stoichiometry of Qilian juniper (*Sabina przewalskii*) in the middle section of the Qilian Mountains, northwest China. *J. Lanzhou Univer.* 55, 525–532. doi: 10.13885/j.issn.0455-2059.2019.04.016

Wang, W., Cai, Y. X., Yang, J. C., and Zhu, Q. S. (2011). Effects of soil water deficit on physiological causes of rice grain-filling. *Chin. J. Plant Ecol.* 35, 195–202. doi: 10.3724/SP.J.1258.2011.00195

Wang, W., He, Z., Du, J., Ma, D., and Zhao, P. (2022). Altitudinal patterns of species richness and flowering phenology in herbaceous community in Qilian Mountains of China. *Int. J. Biometeorol.* 66, 741–751. doi: 10.1007/s00484-021-02233-7

Wang, W. Q., Sardans, J., Wang, C., Zeng, C., Tong, C., Asensio, D., et al. (2015). Ecological stoichiometry of C, N, and P of invasive phragmites australis and native *Cyperus malaccensis* species in the Minjiang river tidal estuarine wetlands of China. *Plant Ecol.* 216, 809–822. doi: 10.1007/s11258-015-0469-5

Wang, X. G., Lü, X. T., and Han, X. G. (2014). Responses of nutrient concentrations and stoichiometry of senesced leaves in dominant plants to nitrogen addition and prescribed burning in a temperate steppe. *Ecol. Eng.* 70, 154–161. doi: 10.1016/j.ecoleng.2014.05.015

Weidner, S., Koller, R., Latz, E., Kowalchuk, G., Bonkowski, M., Scheu, S., et al. (2015). Bacterial diversity amplifies nutrient-based plant-soil feedbacks. *Funct. Ecol.* 29, 1341–1349. doi: 10.1111/1365-2435.12445

Weiher, E., and Keddy, P. A. (1999). *Ecological Assembly Rules: Perspectives, Advances, Retreats.* Cambridge: Cambridge University Press. doi: 10.1017/CBO9780511542237

Xu, S., Fan, X., Wang, L., Zhang, X., and An, L. (2015). The patterns of nitrogen and phosphorus stoichiometry across communities along altitudinal gradients in Qilian Mountains, China. *Biochem. Syst. Ecol.* 62, 58–65. doi: 10.1016/j.bse.2015.07.037

Xu, X. Y., Qin, Y. Y., and Cao, J. J. (2019). Variation characteristics of *Potentilla bifurca* leaf stoichiometry along the elevation gradient on the northeastern Qinghai-Tibetan Plateau. *Acta Ecol. Sin.* 39, 9041–9055. doi: 10.5846/stxb201805231128

Xu, X. Y., Qin, Y. Y., Cao, J. J., Li, M. T., Gong, Y. F., and Zhang, X. F. (2018). Elevational variations of leaf stochiometry in *Leontopodium leontopodioides* on the Qinghai-Tibetan Plateau, China. *Chin. J. Appl. Ecol.* 29, 3934–3940. doi: 10.13287/j.1001-9332.201812.021

Yan, W., Zhong, Y., Zheng, S., and Shangguan, Z. (2016). Linking plant leaf nutrients/stoichiometry to water use efficiency on the Loess Plateau in China. *Ecol. Eng.* 87, 124–131. doi: 10.1016/j.ecoleng.2015.11.034

Yang, D., Song, L., and Jin, G. (2019). The soil C:N:P stoichiometry is more sensitive than the leaf C:N:P stoichiometry to nitrogen addition: a four-year nitrogen addition experiment in a *Pinus koraiensis* plantation. *Plant Soil* 442, 183–198. doi: 10.1007/s11104-019-04165-z

Yu, M., Wang, Y., Jiang, J., Wang, C., Zhou, G., and Yan, J. (2019). Soil organic carbon stabilization in the three subtropical forests: importance of clay and metal oxides. *J. Geophys. Res. Biogeo.* 124, 2976–2990. doi: 10.1029/2018JG004995

Yuan, Z., and Chen, H. (2015). Decoupling of nitrogen and phosphorus in terrestrial plants associated with global changes. *Nat. Clim. Change* 5, 465–469. doi: 10.1038/nclimate2549

Zeng, Q., Xin, L., Dong, Y., An, S., and Darboux, F. (2016). Soil and plant components ecological stoichiometry in four steppe communities in the Loess Plateau of China. *Catena* 147, 481–488. doi: 10.1016/j.catena.2016.07.047

Zhang, J., He, N., Liu, C., Xu, L., Chen, Z., Li, Y., et al. (2020). Variation and evolution of C:N ratio among different organs enable plants to adapt to N-limited environments. *Glob. Change Biol.* 26, 2534–2543. doi: 10.1111/gcb.14973

Zhang, Q., Liu, Q., Yin, H., Zhao, C., Zhang, L., Zhou, G., et al. (2019). C:N:P stoichiometry of Ericaceae species in shrubland biomes across Southern China: influences of climate, soil and species identity. *J. Plant Ecol.* 12, 346–357. doi: 10.1093/jpe/rty033

Zhang, Y., Li, C., and Wang, M. (2019). Linkages of C: N: P stoichiometry between soil and leaf and their response to climatic factors along altitudinal gradients. *J. Soils Sediments* 19, 1820–1829. doi: 10.1007/s11368-018-2173-2

Zhao, B., Tao, F., Wang, J., and Zhang, J. (2020). The sulfated modification and antioxidative activity of polysaccharides from *Potentilla anserine L. New J. Chem.* 44, 4726–4735. doi: 10.1039/D0NJ00356E

Zhao, C. Y., Nan, Z. R., and Cheng, G. D. (2005). Methods for modelling of temporal and spatial distribution of air temperature at landscape scale in the southern Qilian mountains. *China. Ecol. Model* 189, 209–220. doi: 10.1016/j.ecolmodel.2005.03.016

Zhao, C. Y., Nan, Z. R., Cheng, G. D., Zhang, J. H., and Feng, Z. D. (2006). GIS-assisted modelling of the spatial distribution of Qinghai spruce (*Picea crassifolia*) in the Qilian Mountains, northwestern China based on biophysical parameters. *Ecol. Model* 191, 487–550. doi: 10.1016/j.ecolmodel.2005.05.018

Zhao, N., He, N., Wang, Q., Zhang, X., Wang, R., and Xu, Z. (2014). The altitudinal patterns of leaf C: N: P stoichiometry are regulated by plant growth form, climate and soil on Changbai Mountain, China. *PLoS ONE* 9, e95196. doi: 10.1371/journal.pone.0095196

Zhao, W., Reich, P. B., Yu, Q., Zhao, N., Yin, C., Zhao, C., et al. (2018). Shrub type dominates the vertical distribution of leaf C : N : P stoichiometry across an extensive altitudinal gradient. *Biogeosciences* 15, 2033–2053. doi: 10.5194/bg-15-2033-2018

Zhu, D., Hui, D., Wang, M., Yang, Q., and Yu, S. (2020). Light and competition alter leaf stoichiometry of introduced species and native mangrove species. *Sci. Total Environ.* 738, 40301. doi: 10.1016/j.scitotenv.2020.140301

Zhu, M., Feng, Q., Zhang, M., Liu, W., Deo, R. C., Zhang, C., et al. (2019). Soil organic carbon in semiarid alpine regions: the spatial distribution, stock estimation, and environmental controls. *J. Soil. Sediment* 19, 3427–3441. doi: 10.1007/s11368-019-02295-6

frontiers | Frontiers in Plant Science

TYPE Original Research
PUBLISHED 26 September 2022
DOI 10.3389/fpls.2022.987845

OPEN ACCESS

EDITED BY
Peijian Shi,
Nanjing Forestry University,
China

REVIEWED BY
Dongliang Han,
Lanzhou University,
China
Zhao Qingxia,
Guizhou University,
China
Xiaojun Yu,
Gansu Agricultural University,
China

*CORRESPONDENCE
Yushou Ma
mayushou@sina.com

SPECIALTY SECTION
This article was submitted to
Functional Plant Ecology,
a section of the journal
Frontiers in Plant Science

RECEIVED 06 July 2022
ACCEPTED 22 August 2022
PUBLISHED 26 September 2022

CITATION
Luo Q, Ma Y, Chen Z, Xie H, Wang Y,
Zhou L and Ma Y (2022) Biochemical
responses of hairgrass (*Deschampsia caespitosa*) to hydrological change.
Front. Plant Sci. 13:987845.
doi: 10.3389/fpls.2022.987845

Biochemical responses of hairgrass (*Deschampsia caespitosa*) to hydrological change

Qiaoyu Luo[1,2,3,4], Yonggui Ma[1,2,3], Zhi Chen[1,2,3], Huichun Xie[1,2,3], Yanlong Wang[4], Lianyu Zhou[1,2,3] and Yushou Ma[4]*

[1]School of Life Sciences, Qinghai Normal University, Xining, China, [2]Qinghai Provincial Key Laboratory of Medicinal Plant and Animal Resources of Qinghai-Tibet Plateau, Qinghai Normal University, Xining, China, [3]Academy of Plateau Science and Sustainability, Qinghai Normal University, Xining, China, [4]College of Agriculture and Animal Husbandry, Qinghai University, Xining, China

Plant growth and development are closely related to water availability. Water deficit and water excess are detrimental to plants, causing a series of damage to plant morphology, physiological and biochemical processes. In the long evolutionary process, plants have evolved an array of complex mechanisms to combat against stressful conditions. In the present study, the duration-dependent changes in ascorbate (AsA) and glutathione (GSH) contents and activities of enzymes involved in the AsA-GSH cycle in hairgrass (*Deschampsia caespitosa*) in response to water stress was investigated in a pot trial using a complete random block design. The treatments were as follows: (1) heavily waterlogging, (2) moderate waterlogging, (3) light waterlogging, (4) light drought, (5) moderate drought, (6) heavily drought, and (7) a control (CK) with plant be maintained at optimum water availability. The hairgrass plants were subjected to waterlogging or drought for 7, 14, 21 and 28days and data were measured following treatment. Results revealed that hairgrass subjected to water stress can stimulate enzymatic activities of ascorbate peroxidase (APX), glutathione peroxidase (GPX), glutathione reductase (GR), dehydroascorbate reductase (DHAR), monodehydroascorbate reductase (MDHAR) and L-galactono-1, 4-lactone dehydrogenase (GalLDH), switched on the ascorbate-glutathione (AsA-GSH) cycle and the L-galactose synthesis, up-regulated the contents of AsA and GSH, and maintained higher ratios of ascorbate to dehydroascorbate (AsA/DHA) and reduced glutathione to oxidized glutathione (GSH/GSSG) to alleviate potential oxidative damage. However, the light waterlogging did not induce hairgrass under stress to switch on the AsA-GSH pathway. In general, the critic substances and enzyme activities in AsA-GSH metabolic pathway increased as the increase of water stress intensity. As the increase of exposure duration, the critic antioxidant substances content and enzyme activities increased first and then maintained a relatively stable higher level. Our findings provide comprehensive information on biochemical responses of hairgrass to hydrological change, which would be a major step for accelerating ecological restoration of degradation alpine marshes in the Qinghai-Tibetan Plateau.

KEYWORDS

Deschampsia caespitosa, ascorbate-glutathione cycle, stress durations, antioxidant substance and enzyme, water-logging control, drought

Introduction

Water, one of the most critical abiotic factors limiting plant growth, participates in plant physiological and metabolic processes, and affects the survival, growth and distribution of plants. However, the demand of plants to water has a certain threshold. Water excess or water deficit are expected to exert negative effects on plant growth, development, and even plant production, because they may destroy the balance of water (Zupin et al., 2017) and that of reactive oxygen metabolism in plants (Fan et al., 2017; Zupin et al., 2017; Shan et al., 2020). During the long-term evolution, plants have evolved a series of complicated mechanisms, including morphological, physiological, biochemical changes to combat against imbalance of water metabolism and oxidative damage induced by water stress. For instance, plants display remarkably diverse leaf shapes and sizes in nature (Yu et al., 2020; Shi et al., 2021, 2022; Li et al., 2022), and there seems to be a tradeoff between the leaf support cost and photosynthetic returns (Ma et al., 2022; Peng et al., 2022). In addition, when exposed to water deficit, such as in arid and semiarid environment with poor resources, plants are usually with a lower leaf area (Yu et al., 2019; Huang et al., 2021) because water losses and carbon gain processes are tightly coupled (Guo et al., 2021). Although the adoption mechanisms of model plants such as *Arabidopsis thaliana* and important food crops such as *Oryza sativa* (e.g., Damanik et al., 2010) and *Triticum aestivum* (e.g., Lou et al., 2018) to water stress have been intensively studied, our understanding toward that of grass remains limited. Furthermore, numerous studies have revealed that the responses of plants to stress vary depending on plant species or even cultivars, plant development stage and metabolic state, as well as stress intensity and duration (Schneider et al., 2018; Anee et al., 2019; Nemeskéri et al., 2019; Nemeskéri and Helyes, 2019). Therefore, a depth understanding of the response and underlying mechanisms of a target species to water stress is still of paramount importance. The ascorbate-glutathione (AsA-GSH) cycle are found to be crucial in fighting against oxidative damage and keeping the redox balance of plants under water (Shan et al., 2020) or drought stress (Shan et al., 2018), whereas limited literatures have deciphered the responses of plants to alternation of drying and watering yet.

The Qinghai-Tibetan Plateau is the largest and highest highland in the world. In recent years, the Qinghai-Tibetan Plateau had been undergoing significant temperature changes (Yang et al., 2014), which have reshaped the local environment (Yang et al., 2014) and affected local atmospheric circulation and water cycles (Li et al., 2017). Under the background of global warming, drought event frequency, intensity and duration are also expected to increase in the near future due to the combined effects of the decrease in regional precipitation and the increase in evapotranspiration (Trenberth et al., 2013). Meanwhile, precipitation and soil water contents in permafrost region of the Qinghai-Tibetan Plateau are reported to have increased significantly during 1980–2018 (Zhao et al., 2019). In addition, extreme precipitation amount, intensity, frequency and duration have increased evidently (Feng et al., 2020; Guo, 2021). Therefore, the plants in Qinghai-Tibetan Plateau are likely to be subjected to drought and waterlogging stress concurrently. Due to the high altitude and unique alpine climate condition, such as low temperatures, strong evapotranspiration and large direct radiation, the alpine ecosystem is highly fragile and has been suffering from severe degradation due to climate change and anthropic activities during the last decades. The alpine grassland comprises 60% of the total area of the Qinghai-Tibetan Plateau, while about 70% of alpine grassland has been degraded in recent decades (Peng et al., 2019) due to combined effects of climate change and human disturbances (Wang et al., 2015; Zhan et al., 2020; Xu et al., 2022a). The deterioration of grassland greatly restricts the development of local economy and the improvement in living standard of herdsmen, and threats the stability and prosperity of regional society. Besides, grassland degradation undermines its capacity to support biodiversity, ecosystem services and human well-being (Bardgett et al., 2021). To reverse ecosystem deterioration, China has taken various ecological restoration practices, such as grassland cultivation and fencing since 2004. Meanwhile, combating degradation and promoting restoration of grasslands have become one of the most issues for ecological science and policy-making in China (Wang et al., 2015).

An earlier study shows that sowing grass seeds is a feasible and cost-effective way of degraded grassland restoration (Dong et al., 2020). Meanwhile, another study reports that water stress decreases biomass production of alpine grassland plants in autumn (Wang et al., 2020). Therefore, to develop a grass species with strong resilience to water stress maybe a promising alternative. Hairgrass (*Deschampsia caespitosa*) is widely distributed in various habitats, ranging from arid to wet habitats. It has shown highly seed production and germination rate in fields, and thus it is one of potential species used for vegetation restoration in degraded alpine grasslands. However, the physiological responses and underlying mechanisms to water stress remains elusive to date. The major objective of the present study is to investigate the biochemical responses of hairgrass to varying magnitudes and types of water stresses, including different intensities and durations of drought and waterlogging stresses. We specifically addressed the following questions: (1) will drought and waterlogging induced antioxidant response in hairgrass, (2) whether impacts of water stress on hairgrass varied greatly depending on stress duration. By answering these questions, we want to provide a scientific bias and some recommendation for grassland cultivation.

Materials and methods

Plant materials

The plant used in the present study is a hairgrass, which is a newly established strain after years of cultivation and domestication in the wild fields. Its seeds were provided by the Grassland Institute, Academy of Veterinary Sciences, Qinghai University. The seeds with highly seed vigor and germination rate and no disease symptom were selected. Selected seeds were surface-sterilized by immersion in a 2% aqueous solution of sodium hypochlorite for 10 min, and five rinses (each time for 5 min) with sterile deionized water.

Experimental design and growth conditions

The experimental site is located at the Chengbei Campus of the Qinghai Normal University, Xining, Qinghai, China (36°44′31.2′′ N，101°44′56.4′° E), at an altitude of 2390.6 m above mean sea level. The annual mean temperature of this region is 16.4°C. In September 2018, 20 homogenous seeds were sown in each pot (20 cm in diameter, 25 cm in height), which containing 3.0 kg of mixture of alpine meadow soil and sand (sand/soil at 1: 1 volume/volume). The soil was collected from alpine meadow in Dawu Town, Maqing County, Golog Tibetan Ethnic Minority Autonomous Prefecture, Qinghai Province. The alpine meadow soil was classified as Mat Cry-gelic Cambisols (according to the standard of Chinese soil taxonomy research group, 1995). Its chemical characteristics are as follows: total nitrogen 3.12 mg/g, total phosphorus 0.26 mg/g, total potassium 19.58 mg/g, soil organic matter 14.53 mg/g, pH 7.63 (water/soil at1: 1 volume/weight) and CEC 225.52 μS/cm (water/soil at 5: 1 volume/weight). Seeds emerged within 3–5 days later. Seedlings were kept at 10 plants each pot. The plants were kept in the greenhouse and normally watered since then, and were transferred to outdoor during mid-to-late April 2019. Water stress was carried out on July 25 when the grass grew to 25 cm. We applied a complete randomized block experiment design consisting of heavily waterlogging (HW), moderate waterlogging (MW), light waterlogging (LW), control check (CK), light drought (LD), moderate drought (MD) and heavily drought (HD) (Table 1). Each treatment was replicated for 10 times. For plants under drought and normal water demand, we put a basin holder on the bottom of each. For the plants under waterlogging, we place a bucket on the bottom of each basin to prevent water from flowing out. The CK was set as 70–80% of field water-holding capacity, which was measured by ring knife method. Representative undisturbed basin soil was collected with ring knife to absorb water to saturate soil moisture. Gravity water was removed and then dried and weighted. During the study, an awning is built *in situ* and ventilated on both sides of the awning without affecting temperature and humidity. Real-time monitoring of temperature and soil moisture was conducted using portable weather instrument (Hold-HED-SQ, China) and soil moisture sensor (ProCheck, United States), respectively. The water loss was estimated based on daily measurements of pot weight and was supplemented every 2 days. A pot soil without plants was set as a control, and the water loss of soil surface due to evaporation was estimated. Watering was conducted during 18: 00–19: 00. The study lasted for 28 days, and the leaves were collected at 7, 14, 21 and 28 days, respectively, since treatment. Two plants were randomly pruned from 10 pots in the first four times of sampling, and one plant was randomly pruned from 10 pots in the last two times of sampling. After rinsing with distilled water during sampling, the water on leaf surface was wiped. Then, and the leaves of each sample were put into an individual cryopreservation tube and was quickly frozen in liquid nitrogen, and all cryopreservation tubes stored in a refrigerator at-80°C before further proceeding.

Determination of the contents of AsA, DHA, GSH and GSSG

The contents of ascorbate (AsA), dehydroascorbate (DHA), reduced glutathione (GSH) and oxidized glutathione (GSSG) were measured as described previously (Hissin and Hilf, 1976; Takahama and Oniki, 1992; Turcsányi et al., 2000). Briefly, for determination of AsA and DHA, 0.5 g of tissue was homogenized on ice in 0.5 ml of 5% metaphosphoric acid and 6 ml of trichloroacetic acid. After centrifugation at 12000 × g for 20 min at 4°C, the supernatants were collected for substrate content determination. For AsA detection, 100 μl of clear homogenate was added with 2 ml of reaction mixture containing 100 mM KH_2PO_4 buffer (pH = 6.8) and one unite of ascorbic acid oxidase. The change in absorbance was estimated spectrophotometrically at 265 nm. For determination of DHA, 100 μl of clear homogenate was incubated with added with 2 ml of reaction mixture containing 100 mm KH_2PO_4 buffer (pH = 6.8) and 5 μl of 2 mM dithiothreitol (DTT; Sigma-Aldrich, United States), and changes in absorbance was estimated spectrophotometrically at 265 nm. The sum of AsA and DHA and the ratio of AsA/DHA were calculated.

For determination of GSH and GSSG, 0.5 g frozen tissue was ground with sand in mixture of 0.1 mol/l KH_2PO_4 buffer (pH = 8.0) containing 5 mm EDTA and 25% phosphoric acid with a mortar and pestle on ice. After centrifugation at 20000 × g for 30 min at 4°C, the supernatants were collected for substrate content determination. For GSH assay, 0.5 ml of original supernatant was mixed with 4.5 ml

0.1 M KH_2PO_4 buffer (pH = 8.0) containing 5 mm EDTA and 250 µl 0.1% o-phthalaldehyde (OPA). The mixture was mixed thorough and incubated at room temperature for 15 min. Then, 2 ml final assay solution was transferred to a quartz cuvette. The fluorescence at 420 nm was determined with the activation at 350 nm. For GSSG, 0.5 ml of original supernatant was incubated with 200 µl 0.04 M N-ethylmaleimide (NEM) at room temperature for 30 min. Then, 0.1 M NaOH was added into the mixture. Finally, a 100 µl of the resulted mixture was taken for GSSG measurement using the same procedure of GSH assay. The sum of GSH and GSSG and the ratio of GSH/GSSG were calculated.

Antioxidant enzyme activity assay

Ascorbate peroxidase (APX) activity was assayed according to standard protocols as described elsewhere (Nakano and Asada, 1981). Briefly, 0.1 g of tissue was homogenized on ice in 3 ml mixture containing 50 mm KH_2PO_4 buffer (pH = 7.0), 0.2 mm ethylenediaminetetraacetic acid (EDTA), 1% polyvinylpyrrolidone-4,000, 1% Triton X-100 and 5 mm AsA for 12 min. The resulted samples were centrifuged at 13000 × g for 15 min at 4°C, and the supernatants were collected for APX activity assays. The reaction mixture (3 ml) contains 2.6 ml 50 mm KH_2PO_4 buffer (including 0.1 Mm EDTA and 0.5 mm AsA), 0.1 ml enzyme extract and 0.3 ml 2 mm H_2O_2. The APX activity was determined by dynamically monitoring decreases in ascorbate concentration within 3 min at 290 nm as AsA was oxidized. One unit (nkat) of enzyme was defined as the oxidation of 1 µm AsA per min. The activity of dehydroascorbate reductase (DHAR) was assayed following Omar et al. (2013) with some modification. In brief, 0.5 g tissue was homogenized on ice in 3 ml 50 mm Tris–HCl buffer (pH = 7.2) comprising 0.3 M mannitol, 1 mm EDTA, 0.1% bovine serum albumin (BSA), 0.01% L-Cysteine. After centrifugation at 26000 × g for 20 min at 4°C to remove chloroplast and cell debris, the supernatants were collected. Then, 0.1 ml enzyme extract was added into 3 ml KH_2PO_4 buffer (pH = 6.3) containing l mm DHA. After blending thoroughly, the reaction was mixed with 0.1 ml 10 mm GSH. DHAR was assayed by dynamically monitoring changes in absorbance within 3 min at 290 nm. The monodehydroascorbate reductase (MDHAR) activity was assayed following (Miyake and Asada, 1992). The enzyme extract was prepared using the same procedure as described for the DHA extract. The reaction mixture consisted of 3 ml Tris–HCl buffer (pH = 7.2) comprising of 1 M AsA and 0.2 mM NADPH I, 0.1 ml enzyme extract and two units of ascorbic acid oxidase. The MDHAR activity was measured by dynamically monitoring decreases in NADPH I concentration for 3 min at 340 nm. The glutathione reductase (GR) activity was assayed according to Crace and Logan (1996). Specifically, 0.5 g of cells was homogenized on ice in 6 ml mixture containing 50 mm KH_2PO_4 buffer (pH = 7.5), 0.1 mm EDTA, 0.3% Triton X-100 and 1% polyvinylpyrrolidone-4,000. The resulted samples were centrifuged at 13000 × g for 15 min at 2°C, and the supernatants were collected for APX activity assays. The reaction mixture (3 ml) contains consisted of 3 ml Tris-KOH buffer (pH = 8.0) comprising 0.5 mm EDTA, 0.5 mm $MgCl_2$, 10 mm GSSG, 1 mm NADPH II and enzyme extract. The GR activity was determined by dynamically monitoring changes in absorbance within 3 min at 340 nm. One unit (nkat) of enzyme was defined as the reduction of 1 µm NADPH II per min. The glutathione peroxidase (GPX) was assayed following Khatun et al. (2008). Briefly, 0.50 g tissue was homogenized on ice in 5 ml 0.2 M KH_2PO_4 buffer (pH = 6.2) comprising 1 mM EDTA and 5% polyvinylpyrrolidone-4,000. After centrifugation at 8000 × g for 10 min at 4°C to remove chloroplast and cell debris, the supernatants were collected and centrifuged at 12000 × g for 5 min at 4°C. Then, enzyme extract was used to enzymatic activity assay. The GPX activity was assayed by at for 412 nm using H_2O_2 as a substrate. The L-galactono-1, 4-lactone dehydrogenase (GalLDH) activity was assayed according to the protocol as described by Li et al. (2009) with some modifications. In brief, 0.3 g tissues were homogenized on ice in 2 ml 100 mm KH_2PO_4 buffer (pH = 7.4) comprising 0.4 M sucrose, 10% glycerol (v/v), 1 mm EDTA, 0.3% mercaptoethanol (v/v) and 1% polyvinylpyrrolidone-4,000. After centrifugation at 500 × g for 10 min at 4°C to remove chloroplast and cell debris, the supernatants were collected. Then the supernatants were centrifuged at 12000 × g for 20 min at 4°C. The pellet was suspended in 2 ml 100 mm phosphate buffer (pH = 7.4) containing 5 mm glutathione, 1 mM EDTA and 10% (v/v) glycerol, and the supernatant used for assaying of GalLDH activity. GalLDH activity was assayed following the reduction of cytochrome c at 550 nm at 27°C. The reaction mixture (1 ml) containing 50 mM KH_2PO_4 buffer (pH = 7.8), 1.05 mg/ml cytochrome c, 5.6 mm L-galactono-1, 4-lactone and 0.1 ml enzyme extract. Reduction of cytochrome c was started up by adding L-galactono-1, 4-lactone and immediately monitored by the increase in absorbance at 550 nm. One unit (nkat) of enzyme was defined as the oxidation of 1 nm L-galactono-1, 4-lactone per min or the reduction of 2 nm cytochrome c per second.

Statistical analyses

Statistical analyses were performed with the software package SPSS 22.0 (IBM, Armonk, New York, United States). The data were presented as the mean ± standard error (SE). The assumptions of ANOVA were checked before analysis. Where possible, the effects of hydrological condition, treatment duration and their interactions on parameters were examined with linear mixed models. Differences between hydrological conditions and treatment duration were examined according to the Fisher's Least Significant Difference (LSD) tests, the significances ($p \leq 0.05$) were labeled with different uppercase letters or lowercase letters, respectively, in all figures. The figures were produced using OriginPro 2017 (OriginLab Corp, Northampton, United States). The correlations across parameters were examined with Spearman in R version 4.1.3, unless stated otherwise.

Results

Dynamic changes in non-enzymatic antioxidant contents

Hydrological regime significantly influenced all the parameters used to characterize ascorbic acids. Treatment duration greatly influenced the concentration of AsA and that of AsA + DHA. Meanwhile, the responses of all examined parameters characterizing ascorbic acids to hydrological regime were time-dependent, as revealed by significant interactive effects (Table 2). Hydrological regime, stress duration and their interactions significantly affected contents of GSH, GSSG and GSH + GSSG as well as GSH/GSSG ratio (Table 3). In general, antioxidant contents increased firstly and maintain a relative higher content during the experiment period (Figures 1, 2). The contents of antioxidants are positively correlated to stress magnitude. Neither light waterlogging nor light drought induced significant increase in antioxidant contents, whereas heavily water stress would trigger up-regulation of ascorbic acids within 7 days.

TABLE 1 Hydrological conditions used to examine the response of hairgrass (*Deschampsia caespitosa*).

Treatment	Method	Soil water content (%)
Heavily waterlogging, HW	The plants were completely immersed in water	–
Moderate waterlogging, MW	Less than 3 cm of aboveground plants were immersed in water	–
Light waterlogging, LW	The plants were kept at 100% of field water-holding capacity	40%
Control, CK	The plants were kept at 70–80% of field water-holding capacity	28–32%
Light drought, LD	The plants were kept at 50–60% of field water-holding capacity	20–24%
Moderate drought, MD	The plants were kept at 30–40% of field water-holding capacity	12–16%
Heavily drought, HD	The plants were kept at 20% of field water-holding capacity	7–9%

Dynamic changes in antioxidant enzymatic activities

Hydrological regime, exposure duration and their interactions significantly affected the activities of APX, DHAR, MDHAR, GalLDH, GR and GPX (Table 4). As shown in Figure 3, antioxidant enzymatic activities are positively correlated to stress magnitude. They increased significantly within 7 days of exposure and maintain a relative higher content during the experiment period. Light water stress did not induce up-regulation of defense enzymatic activity. Meanwhile, the response of antioxidant enzymatic activities to water stress depends on enzymatic identity.

Correlations between non-enzymatic antioxidant content and antioxidant enzymatic activity

As shown in Figure 4, AsA content is positively correlated to DHA content, T-AsA content, AsA/DHA, GSH content, GSSG content, T-GSH content, APX activity, DHAR activity, MDHAR activity, GalLDH activity, GR activity and GPX activity. DHA content is positively correlated to AsA content, T-AsA content and APX activity, whereas negatively correlated to AsA/DHA. AsA/DHA is positively correlated to AsA content, T-AsA content, GSH content, GSSG content, T-GSH content, APX activity, DHAR activity, MDHAR activity, GalLDH activity, GR activity and GPX activity, whereas negatively correlated to DHA content. GSH content is positively correlated to AsA content, T-AsA content, AsA/DHA, T-GSH content, GSH/GSSG, APX activity, DHAR activity, MDHAR activity, GalLDH activity, GR activity and

TABLE 2 Results of linear mixed models examining the effects of hydrological regime, stress exposure duration and their interactions on the contents of ascorbic acid in *Deschampsia caespitosa*.

Source of variation	*df*	AsA		DHA		T-AsA		AsA/DHA	
		F	*P*	F	*P*	F	*P*	F	*P*
Hydrological regime (H)	6	17.734	<0.0001	7.667	<0.0001	18.172	<0.0001	8.988	<0.0001
Stress duration (T)	4	16.711	<0.0001	1.168	0.333	17.151	<0.0001	4.647	0.002
H × T	23	7.875	<0.0001	2.416	0.003	8.093	<0.0001	3.386	<0.0001

AsA, ascorbic acid; DHA, dehydroascorbate; T-AsA, the sum of reduced and oxidized ascorbate; AsA/DHA, the ratio of reduced to oxidized ascorbate.

TABLE 3 Results of linear mixed models examining the effects of hydrological regime, stress duration and their interactions on the glutathione in *Deschampsia caespitosa*.

Source of variation	*df*	GSH		GSSG		T-GSH		GSH/GSSG	
		F	*P*	F	*P*	F	*P*	F	*P*
Hydrological regime (H)	6	8.310	<0.0001	8.525	<0.0001	7.568	<0.001	9.921	<0.0001
Stress duration (T)	4	16.227	<0.0001	17.957	<0.0001	21.323	<0.0001	7.701	<0.0001
H×T	23	5.591	<0.0001	4.090	<0.0001	6.202	<0.0001	4.304	<0.0001

GSH, glutathione; GSSG, glutathione oxidized; T-GSH, the sum of reduced and oxidized glutathione; GSH/GSSG, the ratio of reduced to oxidized glutathione.

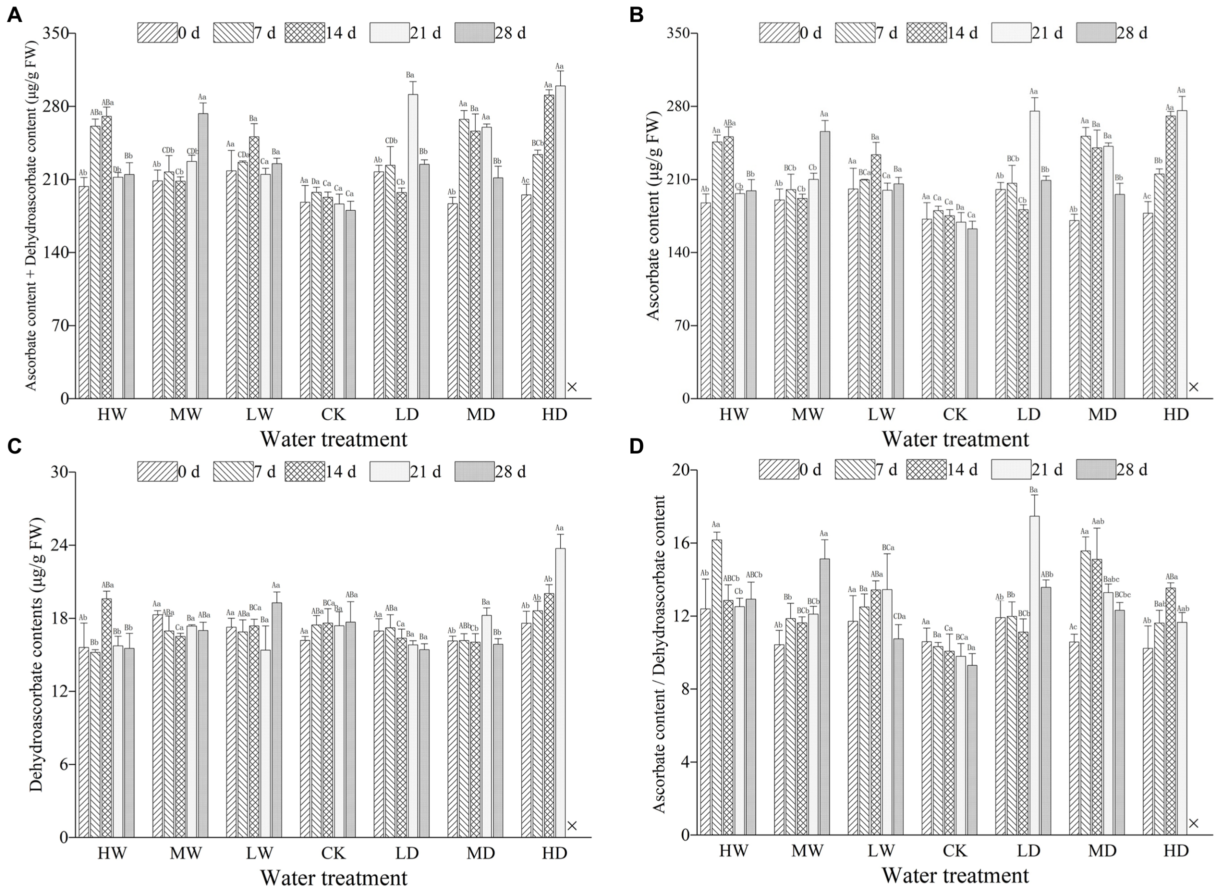

FIGURE 1
Total ascorbic acid content **(A)**, ascorbate content **(B)**, dehydroascorbate content **(C)** and ratio of ascorbate to dehydroascorbate **(D)** in leaves of hairgrass (*Deschampsia caespitosa*) under contrasting hydrological regimes and durations. Bar values are the mean±standard error (*N*=3). Different lowercase letters indicate that there are significant differences among stress exposure durations under the same hydrological treatment; and different capital letters indicate that there are significant differences across different water hydrological regimes at the same exposure duration. X represents the plant died, and thus not allows this parameter to be determined unless stated otherwise. Water treatment are as follows: HW, Heavily waterlogging; MW, Moderate waterlogging; LW, Light waterlogging; CK, Control; LW, Light drought; MW, Moderate drought; and HW, Heavily drought.

GPX activity. GSSG content is positively correlated to AsA content, T-AsA content, AsA/DHA, T-GSH content, GalLDH activity, DHAR activity, GR activity and GPX activity, whereas negatively correlated to GSH/GSSG. GSH/GSSG is positively correlated to GSH content, T-GSH content, MDHAR activity and GR activity, whereas negatively correlated to GSSG content, GalLDH activity and GPX activity.

Discussion

Since plant functional traits are correlated to many ecological processes (Cornwell and Cornelissen, 2008; Chin and Potts, 2018), deciphering the complex responses of plant functional traits under various environmental conditions was a better method to evaluate the potential impacts of global change. The

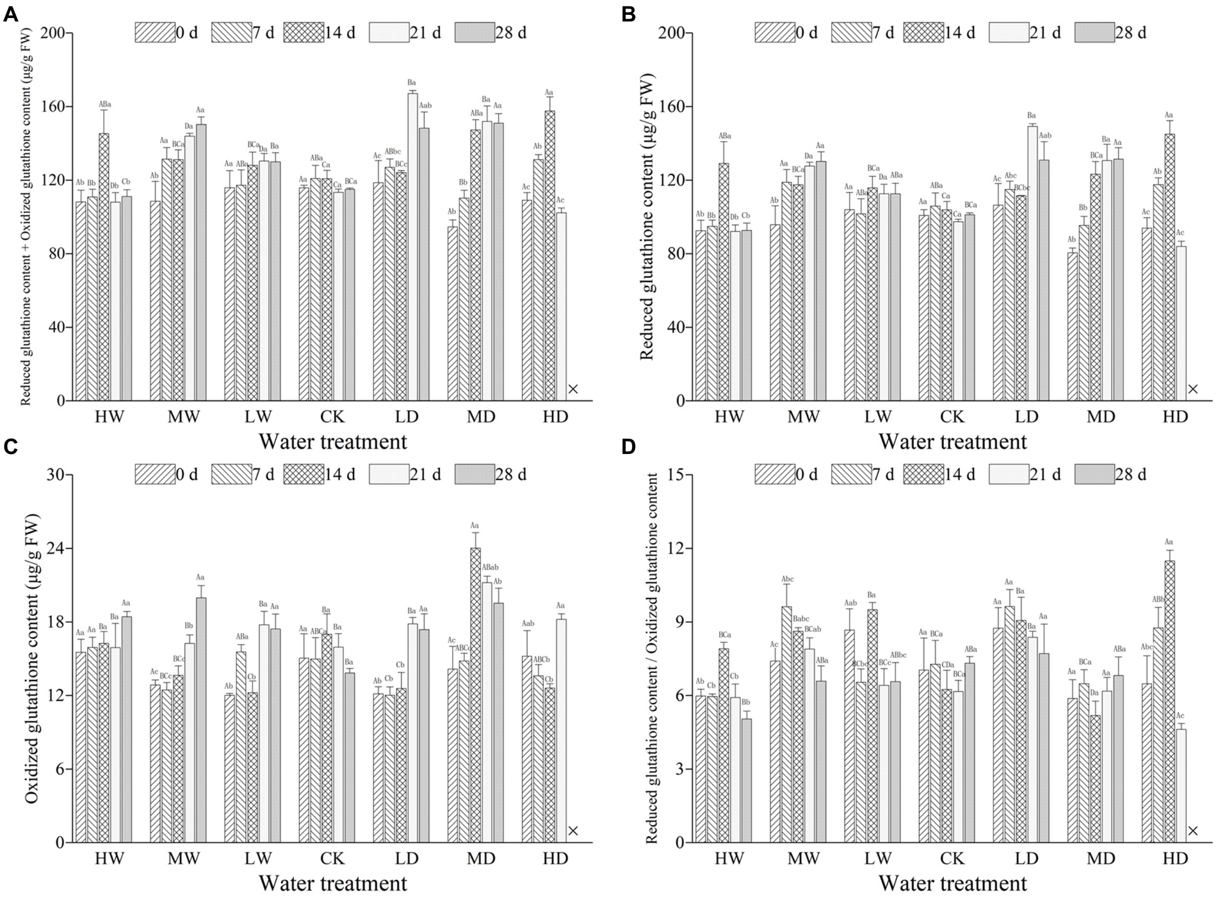

FIGURE 2
Total glutathione contents **(A)**, reduced glutathione **(B)**, oxidized glutathione **(C)** and ratio of reduced glutathione to oxidized glutathione **(D)** in leaves of hairgrass (*Deschampsia caespitosa*) under contrasting hydrological regimes and durations. Bar values are the mean±standard error (*N*=3). Different lowercase letters indicate that there are significant differences among stress exposure durations under the same hydrological treatment; and different capital letters indicate that there are significant differences across different water hydrological regimes at the same exposure duration. X represents the plant died, and thus not allows this parameter to be determined unless stated otherwise. Water treatment are as follows: HW, Heavily waterlogging; MW, Moderate waterlogging; LW, Light waterlogging; CK, Control; LW, Light drought; MW, Moderate drought; and HW, Heavily drought.

TABLE 4 Results of linear mixed models examining the effects of hydrological regime, stress duration and their interactions on the critical enzyme activities in AsA-GSH cycle of hairgrass (*Deschampsia caespitosa*).

Parameters	**Hydrological regime (H)**			**Stress duration (T)**			**H × T**		
	df	***F***	***P***	***df***	***F***	***P***	***df***	***F***	***P***
GalLDH	6	28.177	<0.0001	4	42.725	<0.0001	23	7.795	<0.0001
APX	6	46.745	<0.0001	4	18.445	0.001	23	8.363	<0.0001
DHAR	6	50.319	<0.0001	4	54.202	<0.0001	23	10.335	<0.0001
MDHAR	6	34.970	<0.0001	4	38.882	<0.0001	23	4.849	<0.0001
GR	6	30.041	<0.0001	4	24.275	<0.0001	23	3.085	<0.0001
GPX	6	37.712	<0.0001	4	72.324	<0.0001	23	9.032	<0.0001

GalLDH, L-galactono-1,4-lactone dehydrogenase, APX, Ascorbate peroxidase, DHAR, Dehydroascorbate reductase, MDHAR, Monodehydroascorbate reductase, GR, glutathione reductase, GPX, glutathione peroxidase.

current study examined the changes in non-enzymatic antioxidant contents and antioxidant enzyme activities under contrasting water stresses. On the whole, we observed that hairgrass enhanced non-enzymatic antioxidant accumulation and up-regulated antioxidant enzymatic activities in response to water stress. However, hairgrass exposed to light water stress did

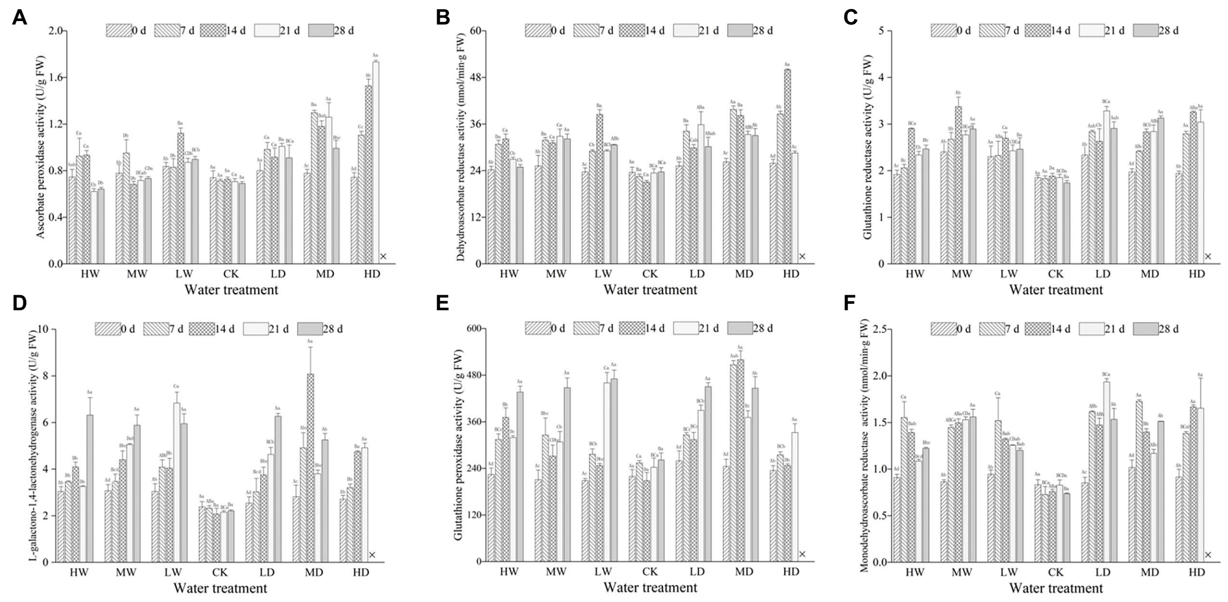

FIGURE 3
Enzymatic activities of ascorbate peroxidase **(A)**, dehydroascorbate reductase **(B)**, glutathione reductase **(C)**, L-galactono-1, 4-lactone dehydrogenase **(D)**, glutathione peroxidase **(E)** and monodehydroascorbate reductase **(F)** in leaves of hairgrass (*Deschampsia caespitosa*) under different hydrological regimes. Bar values are the mean±standard error (*N*=3). Different lowercase letters indicate that there are significant differences among stress exposure durations under the same hydrological treatment; and different capital letters indicate that there are significant differences across different water hydrological regimes at the same exposure duration. X represents the plant died, and thus not allows this parameter to be determined unless stated otherwise. Water treatment are as follows: HW, Heavily waterlogging; MW, Moderate waterlogging; LW, Light waterlogging; CK, Control; LW, Light drought; MW, Moderate drought; and HW, Heavily drought.

not innate defense response, indicating a trade-off between tolerance and oxidant damage defense. As reported, one functional trait would be strengthen at the expense of the construction and functional maintenance of other traits when plant resources are limited (e.g., Yu et al., 2019).

Contents of AsA, DHA, GSSG and GSH

AsA, an important water soluble non-enzymatic antioxidant with a low molecular weight, plays crucial roles in plant growth, metabolisms, development and stress response (Li et al., 2009; Anjum et al., 2014; Mostofa et al., 2015). At present, the contents of AsA are regulated by four synthesis pathways and one regeneration pathway. Specifically, the L-galactose pathway is recognized as the most important pathway for higher plants to synthesize AsA, the D-galacturonic acid pathway the auxiliary pathway, L-glucose pathway and inositol pathway the supplementary pathway, and AsA-GSH cycle pathway the regeneration pathway. The AsA/DHA ratio is an indicator of stress intensity experienced by plants (Kampfenkel et al., 1995), and changes in the AsA/DHA ratio are considered as an indicator of redox status in plants (Foyer and Noctor, 2011; Anjum et al., 2014). In the present study, the AsA and DHA contents of hairgrass plants under heavily waterlogging was increased in comparison with control after 7 days and 14 days. Our findings are in contrast with Anee et al. (2019), in which AsA and DHA of *Sesamum indicum* under waterlogging was steadily increased after 2, 4, 6, 8 days in comparison with control. In addition, the AsA and DHA contents of hairgrass plants under heavily drought were steadily increased in our study (Figure 1). Earlier studies reported that drought at 30% of field water-holding capacity evidently increased the accumulation non-enzymatic antioxidants (AsA and GSH), which are vital for ROS detoxification in the *Amaranthus tricolor* (Sarker and Oba, 2018). One plausible explanation for the discrepancy would be that the species-specific as well intensity and duration dependent of plants to water stress. Further studies are needed to decipher the short-term response of AsA and DHA to water stress.

GSH is a water-soluble thiol compound of low molecular weight, widely distributed in most plant tissues and participates directly or indirectly in detoxification of ROS (Foyer and Noctor, 2005). Besides, GSH is also an important component of antioxidant regeneration system, involved in recycling of AsA and regulating the redox homeostasis (de Carvalho, 2008; Szarka et al., 2012; Gruszka et al., 2018). Furthermore, GSH, a substrate for GPX, detoxifies lipid hydroperoxides together with GSTs, and the GSH/GSSG induces signals for abiotic stress adaptation (Hasanuzzaman et al., 2012). The accumulation of GSSG is often associated with tissue death or quiescence (Foyer and Noctor, 2005). In the present study, the changes in GSH and GSSG contents of plants did not show a regular change in response to waterlogging (Figure 2). Our findings are in contrast to the reported increased GSH and GSSG contents for plants whereas

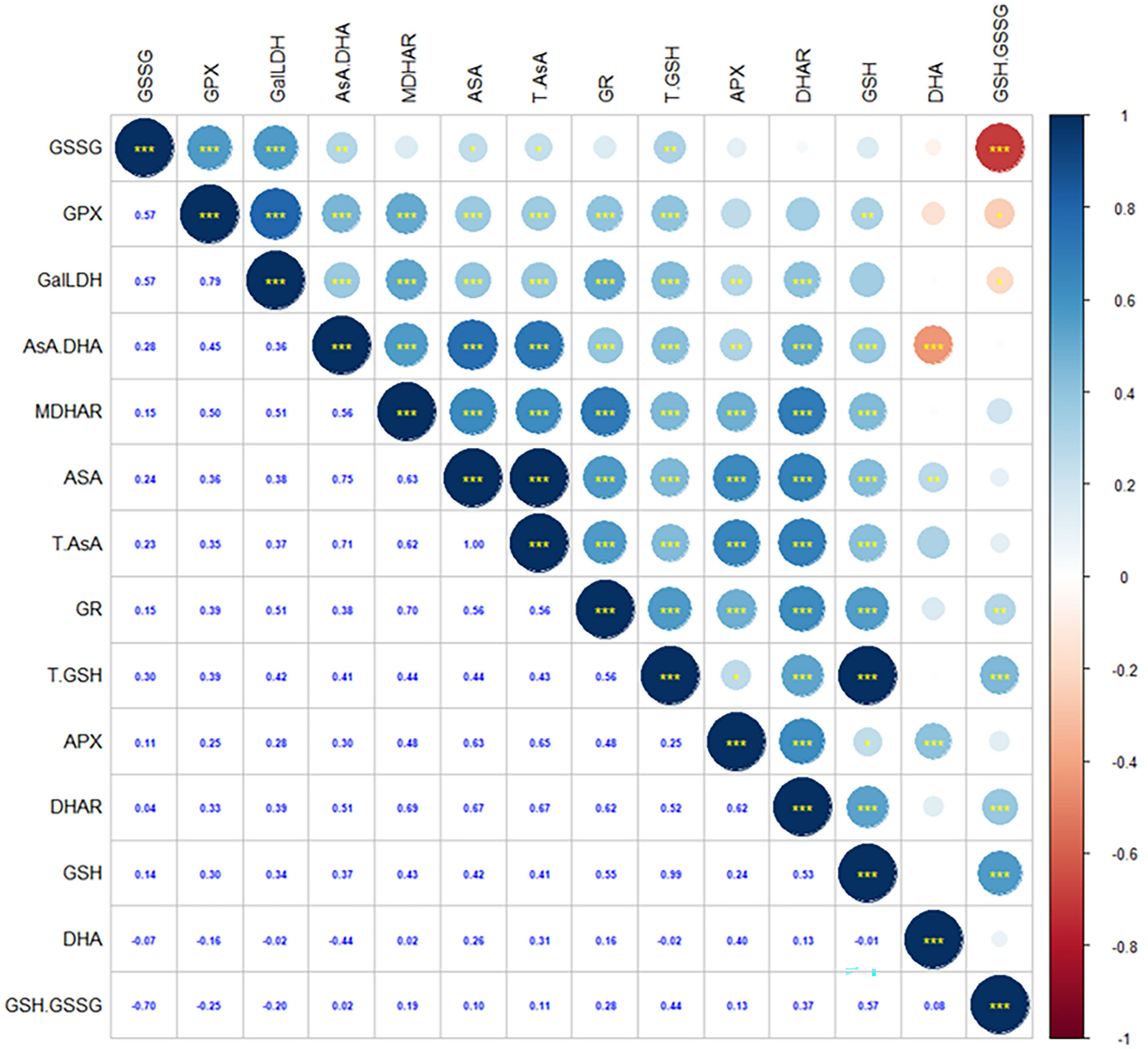

FIGURE 4
The Spearman's correlation coefficient between non-enzymatic substance accumlation and enzyme activities in AsA-GSH cycle of hairgrass (*Deschampsia caespitosa*) under different hydrological regimes. AsA---ascorbate, DHA---dehydroascorbate, T-AsA, the sum of ascorbate and dehydroascorbate; AsA/DHA, the ratio of ascorbate to dehydroascorbate; GSH, reduced glutathione; GSSG, oxidized glutathione; T-GSH, the sum of reduced glutathione and oxidized glutathione; GSH/GSSG, the ratio of reduced glutathione to oxidized glutathione; APX, ascorbate peroxidase; DHAR, dehydroascorbate reductase; GPX, glutathione peroxidase; GR, glutathione reductase; GalLDH, L-galactono-1; 4-lactone dehydrogenase; MDHAR, monodehydroascorbate reductase.

did not have affect GSH/GSSG under waterlogging (Anee et al., 2019). However, drought tend to increase GSH and GSSG contents (Figure 2). This result is in line with previous studies (e.g., Nahar et al., 2015; Gruszka et al., 2018; Lou et al., 2018). Drought exposure duration at 35–40% of field water-holding capacity is reported to result in reduced GSH/GSSG in the *Triticum aestivum* (Lou et al., 2018). Furthermore, drought increased the accumulation non-enzymatic antioxidants (AsA and GSH) of barley (Gruszka et al., 2018), but declined the ratios of AsA/DHA and GSH/GSSG in leaves of wheat seedling (Shan et al., 2018).

Collectively, we observed increased contents of AsA, DHA, AsA + DHA, GSH, GSSG and GSH + GSSG whereas reduced of AsA/DHA and GSH/GSSG of the hairgrass under water stress in the present study, indicating water stress can induce hairgrass to up-regulate non-enzymatic antioxidant contents to alleviate the negative impacts of water stress on plant growth (Gruszka et al., 2018; El-Beltagi et al., 2020).

Antioxidant enzyme activities

Previous studies have suggested that antioxidant enzymes of the AsA-GSH cycle, comprising the APX, MDHAR, DHAR and GR, play a vital role in detoxifying reactive oxygen species (Asada, 1999; Mostofa et al., 2015; Hasanuzzaman et al., 2019). APXs are heme-binding enzymes that reduce hydrogen peroxide to water utilizing AsA as an electron donor (Asada, 1999), participating in the AsA-GSH cycle or Foyer–Halliwell–Asada pathway (Anjum et al., 2016; Mukarram et al., 2021). Over-expression of APX has been shown to increase drought tolerance (Faize et al., 2011; Xu et al., 2022b). As a critical enzyme involved in AsA recycling (Liu et al., 2022), the DHAR reduces DHA to AsA using GSH as substrate. In addition, the MDHAR reduces MDHA to AsA, and the GR reduces the GSSG back to GSH (Anjum et al., 2014, 2016). GalLDH is a key enzyme in the last step of AsA biosynthesis in the Smifnoff-Wheeler pathway (Anjum et al., 2014).

Empirical studies have confirmed that up-regulation or over-expression of AsA-GSH pathway enzymes and the enhancement of the AsA and GSH levels conferred plants better tolerance to abiotic stresses by reducing the ROS (Anee et al., 2019; Hasanuzzaman et al., 2019; Wang et al., 2022). Drought up-regulated the enzymatic antioxidant activities of AsA-GSH pool (Hasanuzzaman et al., 2017; Bhuiyan et al., 2019), and enzymatic response of AsA-GSH pathways varied depending upon plant species (Gruszka et al., 2018) and plant developmental stage, as well as drought intensity and duration (Hasanuzzaman et al., 2017). Similarly, enzymatic response of AsA-GSH pathways to waterlogging stress also varied depending upon the plant species (Damanik et al., 2010; Sairam et al., 2010; Simova-Stoilova et al., 2012; Wang et al., 2019) and stress duration (Anee et al., 2019; Hasanuzzaman et al., 2019). In a Meta-analysis, water stress did not affect the activity of APX and GR (Sun et al., 2020). Anee et al. (2019) reported the APX and MDHAR activity increased with stress duration while DHAR and GR activity reduced when plants subjected to waterlogging. Xu et al. (2022b) found enhanced activities of APX and GR in response to drought. In our study a time-dependent pattern of antioxidant enzyme activities to water stress was observed (Figure 3).

Correlations between non-enzymatic antioxidant contents and antioxidant enzyme activities

As reported, AsA can be biosynthesized through L-galactose pathway (Li et al., 2009; Liao et al., 2021). MDHAR is critic for AsA regeneration; MDHAR and DHAR maintain the DHA pool and control the AsA/DHA (Anjum et al., 2014). Previous studies have demonstrated a positive correlation between the activities of MDHAR and DHAR, and between the contents of T-AsA and the AsA/DHA ratio in kiwifruit (Liao et al., 2021). AsA content is positively correlated APX activity, DHAR activity, MDHAR activity, GalLDH activity, GR activity and GPX activity (Figure 4). This is a logical conclusion. Similarly, GR is responsible for the regeneration of GSH (Shan et al., 2018), and thus maintains the GSH pool. Higher GPX activity may impose a threat to the level of GSH and the GSH/GGSG ratio in the absence of efficient recycling of GSSG (Mostofa et al., 2015). Taken together, our correlation analyses displayed intricate links between non-enzymatic antioxidants and antioxidant enzymes in protecting plants from potential damage posed by water stress.

Conclusion

In summary, the biochemical responses of hairgrass to hydrological changes depend on stress intensity and duration. Specifically, water stress induced increases in contents of AsA, DHA, AsA + DHA, GSH, GSSG and GSH + GSSG but reduced the ratios of AsA/DHA and GSH/GSSG. In addition, it enhanced the activities of APX, DHAR, GPX, GR, MDHAR and GalLDH, and switched on the AsA-GSH cycle pathway and the L-galactose synthesis pathway to mitigate potential oxidative damage posed by water stress. The light waterlogging did not induce hairgrass to initiate defense response, indicating that hairgrass has developed resistance against light waterlogging stress. Finally, the response of hairgrass to water stress (including waterlogging and drought) decreased with experimental duration; implying hairgrass has a great capacity to adapt to water stress.

Data availability statement

The original contributions presented in the study are included in the article/Supplementary material; further inquiries can be directed to the corresponding author.

Author contributions

YsM designed the experiments. QL and YgM collected the samples. QL, YW, and LZ performed the laboratory work. QL, HX, and ZC analyzed the data. QL wrote the first version of the manuscript, which was then edited by all co-authors. All authors contributed to the article and approved the submitted version.

Funding

This work was kindly supported by the Second Comprehensive Scientific Investigation and Research Project of Qinghai-Tibet Plateau (SQ2019QZKK2206), the National Key Research and Development Program of China (2016YFC0501903), Natural Science Foundation of Qinghai Province (2022-ZJ-941Q); University-level Young and Middle-aged Scientific Research Fund Project (KJQN2021003).

Conflict of interest

The authors declare that the research was conducted in the absence of any commercial or financial relationships that could be construed as a potential conflict of interest.

Publisher's note

References

Anee, T. I., Nahar, K., Rahman, A., Mahmud, J. A., Bhuiyan, T. F., Alam, M. U., et al. (2019). Oxidative damage and antioxidant defense in *Sesamum indicum* after different waterlogging durations. *Plan. Theory* 8:196. doi: 10.3390/plants8070196

Anjum, N. A., Gill, S. S., Gill, R., Hasanuzzaman, M., Duarte, A. C., Pereira, E., et al. (2014). Metal/metalloid stress tolerance in plants: role of ascorbate, its redox couple, and associated enzymes. *Protoplasma* 251, 1265–1283. doi: 10.1007/s00709-014-0636-x

Anjum, N. A., Sharma, P., Gill, S. S., Hasanuzzaman, M., Khan, E. A., Kachhap, K., et al. (2016). Catalase and ascorbate peroxidase-representative H_2O_2-detoxifying heme enzymes in plants. *Environ. Sci. Pollut. Res. Int.* 23, 19002–19029. doi: 10.1007/s11356-016-7309-6

Asada, K. (1999). The water-water cycle in chloroplasts: scavenging of active oxygens and dissipation of excess photons. *Annu. Rev. Plant Physiol. Plant Mol. Biol.* 50, 601–639. doi: 10.1146/annurev.arplant.50.1.601

Bardgett, R. D., Bullock, J. M., Lavorel, S., Manning, P., Schaffner, U., Ostle, N., et al. (2021). Combatting global grassland degradation. *Nat Rev Earth Env* 2, 720–735. doi: 10.1038/s43017-021-00207-2

Bhuiyan, T. F., Ahamed, K. U., Nahar, K., Al Mahmud, J., Bhuyan, M. B., Anee, T. I., et al. (2019). Mitigation of PEG-induced drought stress in rapeseed (*Brassica rapa* L.) by exogenous application of osmolytes. Biocatalysis Agri. *Australas. Biotechnol.* 20:101197. doi: 10.1016/j.bcab.2019.101197

Chin, C. S., and Potts, M. D. (2018). The role of plant functional traits in understanding forest recovery in wet tropical secondary forests. *Sci. Total Environ.* 642, 1252–1262. doi: 10.1016/j.scitotenv.2018.05.397

Chinese Soil Taxonomy Research Group. (1995). *Chinese Soil Taxonomy*. Beijing, China: Science Press, 58–147.

Cornwell, W. K., and Cornelissen, J. H. (2008). Plant species traits are the predominant control on litter decomposition rates within biomes worldwide. *Ecol. Lett.* 11, 1065–1071. doi: 10.1111/j.1461-0248.2008.01219.x

Crace, S. C., and Logan, B. A. (1996). Acclimation of foliar antioxidant systems to growth irradiance in three broad-leaved evergreen species. *Plant Physiol.* 112, 1631–1640.

Damanik, R. I., Maziah, M., Ismail, M. R., Ahmad, S., and Zain, A. M. (2010). Responses of the antioxidative enzymes in Malaysian rice (*Oryza sativa* L.) cultivars under submergence condition. *Acta Physiol. Plant.* 32, 739–747. doi: 10.1007/s11738-009-0456-3

de Carvalho, M. H. C. (2008). Drought stress and reactive oxygen species: production, scavenging and signaling. *Plant Signal. Behav.* 3, 156–165. doi: 10.4161/psb.3.3.5536

Dong, S., Shang, Z., Gao, J., and Boone, R. B. (2020). Enhancing sustainability of grassland ecosystems through ecological restoration and grazing management in an era of climate change on Qinghai-Tibetan plateau. *Agric. Ecosyst. Environ.* 287:106684. doi: 10.1016/j.agee.2019.106684

El-Beltagi, H. S., Mohamed, H. I., and Sofy, M. R. (2020). Role of ascorbic acid, glutathione and proline applied as singly or in sequence combination in improving chickpea plant through physiological change and antioxidant defense under different levels of irrigation intervals. *Molecules* 25:1702. doi: 10.3390/molecules25071702

Faize, M., Burgos, L., Faize, L., Piqueras, A., Nicolas, E., Barba-Espin, G., et al. (2011). Involvement of cytosolic ascorbate peroxidase and cu/Zn-superoxide dismutase for improved tolerance against drought stress. *J. Exp. Bot.* 62, 2599–2613. doi: 10.1093/jxb/erq432

Fan, H. F., Ding, L., Xu, Y. L., and Du, C. X. (2017). Antioxidant system and photosynthetic characteristics responses to short-term peg-induced drought stress in cucumber seedling leaves. *Russ. J. Plant Physiol.* 64, 162–173. doi: 10.1134/S1021443717020042

Feng, X., Shen, H., Li, W., Wang, Q., Duan, L., and Li, H. (2020). Spatiotemporal changes for extreme precipitation in wet season over the Qinghai-Tibetan plateau and the surroundings during 1961–2017. *Plateau Meteorology* 39, 694–705.

Foyer, C. H., and Noctor, G. (2005). Redox homeostasis and antioxidant signaling: A metabolic interface between stress perception and physiological responses. *Plant Cell* 17, 1866–1875. doi: 10.1105/tpc.105.033589

Foyer, C. H., and Noctor, G. (2011). Ascorbate and glutathione: the heart of the redox hub. *Plant Physiol.* 155, 2–18. doi: 10.1104/pp.110.167569

Gruszka, D., Janeczko, A., Dziurka, M., Pociecha, E., and Fodor, J. (2018). Non-enzymatic antioxidant accumulations in BR-deficient and BR-insensitive barley mutants under control and drought conditions. *Physiol. Plant.* 163, 155–169. doi: 10.1111/ppl.12674

Guo, X. S. (2021). *Study on the Changes in Extreme Precipitation and its Relationship with air Temperature on the Qinghai-Tibetan Plateau*. China. University of Geosciences, Beijing.

Guo, X., Shi, P., Niinemets, Ü., Hölscher, D., Wang, R., Liu, M., et al. (2021). "Diminishing returns" for leaves of five age-groups of Phyllostachys edulis culms. *Am. J. Bot.* 108, 1662–1672. doi: 10.1002/ajb2.1738

Hasanuzzaman, M., Bhuyan, M., Anee, T. I., Parvin, K., Nahar, K., Mahmud, J. A., et al. (2019). Regulation of ascorbate-glutathione pathway in mitigating oxidative damage in plants under abiotic stress. *Antioxidants (Basel)* 8:384. doi: 10.3390/antiox8090384

Hasanuzzaman, M., Hossain, M. A., da Silva, J. A. T., and Fujita, M. (2012). "Plant response and tolerance to abiotic oxidative stress: antioxidant defense is a key factor," in *Crop Stress and its Management: Perspectives and Strategies*. eds. B. Venkateswarlu, A. K. Shanker, C. Shanker and M. Maheswari, 261–315.

Hasanuzzaman, M., Nahar, K., Hossain, M. S., Mahmud, J. A., Rahman, A., Inafuku, M., et al. (2017). Coordinated actions of glyoxalase and antioxidant defense systems in conferring abiotic stress tolerance in plants. *Int. J. Mol. Sci.* 18:200. doi: 10.3390/ijms18010200

Hissin, P. J., and Hilf, R. (1976). A fluorometric method for determination of oxidized and reduced glutathione in tissues. *Anal. Biochem.* 74, 214–226. doi: 10.1016/0003-2697(76)90326-2

Huang, L. C., Niinemets, U., Ma, J. Z., Schrader, J., Wang, R., and Shi, P. J. (2021). Plant age has a minor effect on non-destructive leaf area calculations in moso bamboo (*Phyllostachys edulis*). *Symmetry.* 13:369. doi: 10.3390/sym13030369

Kampfenkel, K., van Montagu, M., and Inzé, D. (1995). Extraction and determination of ascorbate and dehydroascorbate from plant tissue. *Anal. Biochem.* 225, 165–167. doi: 10.1006/abio.1995.1127

Khatun, S., Ali, M. B., Hahn, E. J., and Paek, K. Y. (2008). Copper toxicity in *Withania somnifera*: growth and antioxidant enzymes responses of in vitro grown plants. *Environ. Exp. Bot.* 64, 279–285. doi: 10.1016/j.envexpbot.2008.02.004

Li, M., Liang, D., Pu, F., Ma, F., Hou, C., and Lu, T. (2009). Ascorbate levels and the activity of key enzymes in ascorbate biosynthesis and recycling in the leaves of 22 Chinese persimmon cultivars. *Sci Hortic-Amesterdam* 120, 250–256. doi: 10.1016/j.scienta.2008.10.010

Li, Y., Quinn, B. K., Niinemets, Ü., Schrader, J., Gielis, J., Liu, M., et al. (2022). Ellipticalness index–A simple measure of the complexity of oval leaf shape. *Par. J. Bot.* 54, 2233–2240. doi: 10.30848/PJB2022-6(44)

Li, B., Zhang, J., Yu, Z., Liang, Z., Chen, L., and Acharya, K. (2017). Climate change driven water budget dynamics of a Tibetan inland lake. *Glob. Planet. Chang.* 150, 70–80. doi: 10.1016/j.gloplacha.2017.02.003

Liao, G., Chen, L., He, Y., Li, X., Lv, Z., Yi, S., et al. (2021). Three metabolic pathways are responsible for the accumulation and maintenance of high AsA content in kiwifruit (*Actinidia eriantha*). *BMC Genomics* 22:13. doi: 10.1186/s12864-020-07311-5

Liu, J. X., Wang, H., Feng, K., Li, T., Liu, Y. H., Duan, A. Q., et al. (2022). AgDHAR2, a chloroplast-located dehydroascorbate reductase, modulates the ascorbate accumulation and drought stress response in celery. *Environ. Exp. Bot.* 202:105006.

Lou, L., Li, X., Chen, J., Li, Y., Tang, Y., and Lv, J. (2018). Photosynthetic and ascorbate-glutathione metabolism in the flag leaves as compared to spikes under drought stress of winter wheat (*Triticum aestivum* L.). *PLoS One* 13:e0194625. doi: 10.1371/journal.pone.0194625

Ma, J., Niklas, K. J., Liu, L., Fang, Z., Li, Y., and Shi, P. (2022). Tree size influences leaf shape but does not affect the proportional relationship between leaf area and the product of length and width. *Front. Plant Sci.* 13:850203. doi: 10.3389/fpls.2022.850203

Miyake, C., and Asada, K. (1992). Thylakoid-bound peroxidase in spinach chloroplasts and photoreduction of its primary oxidation product monodehydroascorbate radicals in thylakoids. *Plant Cell Physiol.* 33, 541–553.

Mostofa, M. G., Hossain, M. A., and Fujita, M. (2015). Trehalose pretreatment induces salt tolerance in rice (*Oryza sativa* L.) seedlings: oxidative damage and co-induction of antioxidant defense and glyoxalase systems. *Protoplasma* 252, 461–475. doi: 10.1007/s00709-014-0691-3

Mukarram, M., Choudhary, S., Kurjak, D., Petek, A., and Khan, M. M. A. (2021). Drought: sensing, signalling, effects and tolerance in higher plants. *Physiol. Plant.* 172, 1291–1300. doi: 10.1111/ppl.13423

Nahar, K., Hasanuzzaman, M., Alam, M. M., and Fujita, M. (2015). Glutathione-induced drought stress tolerance in mung bean: coordinated roles of the antioxidant defense and methylglyoxal detoxification systems. *AoB Plants* 7:plv069. doi: 10.1093/aobpla/plv069

Nakano, Y., and Asada, K. (1981). Hydrogen peroxide is scavenged by ascorbate-specific peroxidase in spinach chloroplasts. *Plant Cell Physiol.* 22, 867–880.

Nemeskéri, E., and Helyes, L. (2019). Physiological responses of selected vegetable crop species to water stress. *Agronomy-Basel* 9:447. doi: 10.3390/agronomy9080447

Nemeskéri, E., Molnár, K., Rácz, C., Dobos, A., and Helyes, L. (2019). Effect of water supply on spectral traits and their relationship with the productivity of sweet corns. *Agronomy-Basel* 9:63. doi: 10.3390/agronomy9020063

Omar, S. A., Elsheery, N. I., Kalaji, H. M., Xu, Z. F., Song, S. Q., Carpentier, R., et al. (2013). Dehydroascorbate reductase and glutathione reductase play an important role in scavenging hydrogen peroxide during natural and artificial dehydration of *Jatropha curcas* seeds. *J Plant Biol* 55, 469–480. doi: 10.1007/s12374-012-0276-7

Peng, G., Xiong, Y., Yin, M., Wang, X., Zhou, W., Cheng, Z., et al. (2022). Leaf venation architecture in relation to leaf size across leaf habits and vein types in subtropical woody plants. *Front. Plant Sci.* 13:873036. doi: 10.3389/fpls.2022.873036

Peng, F., Xue, X., You, Q., Sun, J., Zhou, J., Wang, T., et al. (2019). Change in the trade-off between aboveground and belowground biomass of alpine grassland: implications for the land degradation process. *Land Degrad. Dev.* 31, 105–117. doi: 10.1002/ldr.3432

Sairam, R. K., Dharmar, K., Lekshmy, S., and Chinnusamy, V. (2010). Expression of antioxidant defense genes in mung bean (*Vigna radiata* L.) roots under water-logging is associated with hypoxia tolerance. *Acta Physiol. Plant.* 33, 735–744. doi: 10.1007/s11738-010-0598-3

Sarker, U., and Oba, S. (2018). Catalase, superoxide dismutase and ascorbate-glutathione cycle enzymes confer drought tolerance of *Amaranthus tricolor*. *Sci. Rep.* 8:16496. doi: 10.1038/s41598-018-34944-0

Schneider, J. R., Caverzan, A., and Chavarria, G. (2018). Water deficit stress, ROS involvement, and plant performance. *Arch. Agron. Soil Sci.* 65, 1160–1181. doi: 10.1080/03650340.2018.1556789

Shan, C., Wang, B., Sun, H., Gao, S., and Li, H. (2020). H_2S induces NO in the regulation of AsA-GSH cycle in wheat seedlings by water stress. *Protoplasma* 257, 1487–1493. doi: 10.1007/s00709-020-01510-3

Shan, C., Zhang, S., and Ou, X. (2018). The roles of H_2S and H_2O_2 in regulating AsA-GSH cycle in the leaves of wheat seedlings under drought stress. *Protoplasma* 255, 1257–1262. doi: 10.1007/s00709-018-1213-5

Shi, P., Miao, Q., Niinemets, Ü., Liu, M., Li, Y., Yu, K., et al. (2022). Scaling relationships of leaf vein and areole traits versus leaf size for nine Magnoliaceae species differing in venation density. *Am. J. Bot.* 109, 899–909. doi: 10.1002/ajb2.1856

Shi, P., Yu, K., Niinemets, Ü., and Gielis, J. (2021). Can leaf shape be represented by the ratio of leaf width to length? Evidence from nine species of Magnolia and Michelia (Magnoliaceae). *Forests* 12:41. doi: 10.3390/f12010041

Simova-Stoilova, L., Demirevska, K., Kingston-Smith, A., and Feller, U. (2012). Involvement of the leaf antioxidant system in the response to soil flooding in two Trifolium genotypes differing in their tolerance to waterlogging. *Plant Sci.* 183, 43–49. doi: 10.1016/j.plantsci.2011.11.006

Sun, Y., Wang, C., Chen, H. Y. H., and Ruan, H. (2020). Response of plants to water stress: a meta-analysis. *Front. Plant Sci.* 11:978. doi: 10.3389/fpls.2020.00978

Szarka, A., Tomasskovics, B., and Banhegyi, G. (2012). The ascorbate-glutathione-alpha-tocopherol triad in abiotic stress response. *Int. J. Mol. Sci.* 13, 4458–4483. doi: 10.3390/ijms13044458

Takahama, U., and Oniki, T. (1992). Regulations of peroxidase-dependent oxidation of phenolics in the of spinach leaves by ascorbate. *Plant Cell Physiol.* 33, 379–387.

Trenberth, K. E., Dai, A., van der Schrier, G., Jones, P. D., Barichivich, J., Briffa, K. R., et al. (2013). Global warming and changes in drought. *Nat. Clim. Chang.* 4, 17–22. doi: 10.1038/NCLIMATE2067

Turcsányi, E., Lyons, T., Plöchl, M., and Barnes, J. (2000). Does ascorbate in the mesophyll cell walls form the first line of defence against ozone? Testing the concept using broad bean (*Vicia faba* L.). *J. Exp. Bot.* 51, 901–910. doi: 10.1093/jexbot/51.346.901

Wang, H., Chen, Y., Hu, W., Snider, J. L., and Zhou, Z. (2019). Short-term soil-waterlogging contributes to cotton cross tolerance to chronic elevated temperature by regulating ROS metabolism in the subtending leaf. *Plant Physiol. Biochem.* 139, 333–341. doi: 10.1016/j.plaphy.2019.03.038

Wang, P., Lassoie, J. P., Morreale, S. J., and Dong, S. (2015). A critical review of socioeconomic and natural factors in ecological degradation on the Qinghai-Tibetan plateau, China. *Rangel. J.* 37, 1–9. doi: 10.1071/RJ14094

Wang, H., Liu, H., Cao, G., Ma, Z., Li, Y., Zhang, F., et al. (2020). Alpine grassland plants grow earlier and faster but biomass remains unchanged over 35 years of climate change. *Ecol. Lett.* 23, 701–710. doi: 10.1111/ele.13474

Wang, S., Zhou, H., Feng, N., Xiang, H., Liu, Y., Wang, F., et al. (2022). Physiological response of soybean leaves to uniconazole under waterlogging stress at R1 stage. *J. Plant Physiol.* 268:153579. doi: 10.1016/j.jplph.2021.153579

Xu, Y., Dong, S., Gao, X., Wu, S., Yang, M., Li, S., et al. (2022a). Target species rather than plant community tell the success of ecological restoration for degraded alpine meadows. *Ecol. Indic.* 135:108487. doi: 10.1016/j.ecolind.2021.108487

Xu, J., Guo, L., and Liu, L. (2022b). Exogenous silicon alleviates drought stress in maize by improving growth, photosynthetic and antioxidant metabolism. *Environ. Exp. Bot.* 201:104974. doi: 10.1016/j.envexpbot.2022.104974

Yang, K., Wu, H., Qin, J., Lin, C., Tang, W., and Chen, Y. (2014). Recent climate changes over the Tibetan plateau and their impacts on energy and water cycle: A review. *Glob. Planet. Chang.* 112, 79–91. doi: 10.1016/j.gloplacha.2013.12.001

Yu, X. J., Hui, C., Sandhu, H. S., Lin, Z. Y., and Shi, P. J. (2019). Scaling relationships between leaf shape and area of 12 Rosaceae species. *Symmetry* 11:1255. doi: 10.3390/sym11101255

Yu, X., Shi, P., Schrader, J., and Niklas, K. J. (2020). Nondestructive estimation of leaf area for 15 species of vines with different leaf shapes. *AM J BOT-London* 107, 1481–1490. doi: 10.1002/ajb2.1560

Zhan, T., Zhang, Z., Sun, J., Liu, M., Zhang, X., Peng, F., et al. (2020). Meta-analysis demonstrating that moderate grazing can improve the soil quality across China's grassland ecosystems. *Appl. Soil Ecol.* 147:103438. doi: 10.1016/j.apsoil.2019.103438

Zhao, L., Hu, G. J., Zou, D. F., Wu, X. D., Ma, L., Sun, Z., et al. (2019). Permafrost changes and its effects on hydrological processes on Qinghai-Tibet plateau. *China Academic J* 34, 1233–1246. doi: 10.16418/j.issn.1000-3045.2019.11.006

Zupin, M., Sedlar, A., Kidric, M., and Meglic, V. (2017). Drought-induced expression of aquaporin genes in leaves of two common bean cultivars differing in tolerance to drought stress. *J. Plant Res.* 130, 735–745. doi: 10.1007/s10265-017-0920-x

frontiers | Frontiers in Plant Science

TYPE Original Research
PUBLISHED 04 October 2022
DOI 10.3389/fpls.2022.832300

OPEN ACCESS

EDITED BY
Boris Rewald,
University of Natural Resources and Life Sciences Vienna, Austria

REVIEWED BY
Chris Lusk,
University of Waikato, New Zealand
Hendrik Poorter,
Helmholtz Association of German Research Centres (HZ), Germany

*CORRESPONDENCE
Jianhui Xue
jhxue@njfu.edu.cn
Peijian Shi
pjshi@njfu.edu.cn
Julian Schrader
jschrader@posteo.de

SPECIALTY SECTION
This article was submitted to Functional Plant Ecology, a section of the journal Frontiers in Plant Science

RECEIVED 09 December 2021
ACCEPTED 15 September 2022
PUBLISHED 04 October 2022

CITATION
Guo X, Niklas KJ, Li Y, Xue J, Shi P and Schrader J (2022) Diminishing returns: A comparison between fresh mass vs. area and dry mass vs. area in deciduous species.
Front. Plant Sci. 13:832300.
doi: 10.3389/fpls.2022.832300

Diminishing returns: A comparison between fresh mass vs. area and dry mass vs. area in deciduous species

Xuchen Guo[1], Karl J. Niklas[2], Yirong Li[3], Jianhui Xue[1,4*], Peijian Shi[1*] and Julian Schrader[5,6*]

[1]Bamboo Research Institution, College of Biology and the Environment, Nanjing Forestry University, Nanjing, China, [2]School of Integrative Plant Science, Cornell University, Ithaca, NY, United States, [3]College of Life Science, South China Agricultural University, Guangzhou, China, [4]Institute of Botany, Jiangsu Province and Chinese Academy Sciences, Nanjing, China, [5]School of Natural Sciences, Macquarie University, Sydney, NSW, Australia, [6]Biodiversity, Macroecology and Biogeography, University of Göttingen, Göttingen, Germany

"Diminishing returns" in leaf economics occurs when increases in lamina mass (*M*), which can either be represented by lamina dry mass (DM) or fresh mass (FM), fail to produce proportional increases in leaf surface area (*A*), such that the scaling exponent (α) for the *M* vs. *A* scaling relationship exceeds unity (i.e., $\alpha >$ 1.0). Prior studies have shown that FM vs. *A* is better than DM vs *A* in assessing diminishing returns in evergreen species. However, the superiority of FM vs. *A* over DM vs. *A* has been less well examined for deciduous species. Here, we applied reduced major axis protocols to test whether FM vs. *A* is better than DM vs. *A* to describe the *M* vs. *A* scaling relationship, using a total of 4271 leaves from ten deciduous and two evergreen tree species in the Fagaceae and Ulmaceae for comparison. The significance of the difference between the scaling exponents of FM vs. *A* and DM vs. *A* was tested using the bootstrap percentile method. Further, we tested the non-linearity of the FM (DM) vs. *A* data on a log-log scale using ordinary least squares. We found that (i) the majority of scaling exponents of FM vs. *A* and DM vs. *A* were >1 thereby confirming diminishing returns for all 12 species, (ii) FM vs. *A* was more robust than DM vs. *A* to identify the *M* vs. *A* scaling relationship, (iii) the non-linearity of the allometric model was significant for both DM vs. *A* and FM vs. *A*., and (iv) the evergreen species of Fagaceae had significantly higher DM and FM per unit area than other deciduous species. In summary, FM vs. *A* is a more reliable measure than DM vs. *A* when dealing with diminishing returns, and deciduous species tend to invest less biomass in unit leaf light harvesting area than evergreen species.

KEYWORDS
diminishing returns, leaf area, leaf biomass, light-capture, water content

Introduction

Leaves are the primary light-harvesting organs of most vascular land plants. They convert solar irradiance into chemical energy by means of photosynthesis (Rascher and Nedbal, 2006). As such, the biology of leaves provides deep insights into plant economic spectra and ecological strategies (Westoby et al., 2002).

Leaf functional traits (leaf area, leaf mass and leaf water content, etc.) are related to plant growth strategies as well as to ecosystem processes such as primary productivity and nutrient cycling (Garnier et al., 2001; Wright et al., 2004). Scaling relationships of leaf functional traits, such as leaf dimensions and leaf mass, are useful to understand the full spectrum of leaf forms and functions as well as to characterize evolutionary stable leaf forms (Niklas et al., 2007; Shi et al., 2019).

For example, leaf mass (M) and leaf lamina surface area (A) follow a quantifiable scaling relationship described by the power-law function $M = \beta A^{\alpha}$, where β is the normalization constant, and α is the scaling exponent. For many plant species groups, the numerical values of α exceed unity, which indicates that leaf mass increases at a faster rate than leaf area, a phenomenon referred to as "diminishing returns" (Milla and Reich, 2007; Niklas et al., 2007; Sun et al., 2017). A widely accepted explanation is that larger leaves require a disproportionately larger amount of non-photosynthetic tissues, which results in an increased biomass-cost to support leaf area (Niklas, 1994; Niklas et al., 2009; Sack et al., 2012; Shi et al., 2022a). The concept of diminishing returns is important to understand the energy allocation and variation among leaves from different species, which can affect ecosystem processes especially light capture (Westoby and Wright, 2003; Koester et al., 2014). In addition, the phenomenon of diminishing returns between M and A reflects a series of trade-offs, such as biomass allocation to the lamina with respect to biomass allocation to the petiole and lamina midrib (Niklas, 1991; Niklas, 1992; Niinemets et al., 2006).

Previous studies have used leaf dry mass (DM) as a measure of leaf biomass. However, the numerical value of the exponent governing the DM vs. A scaling relationship is not independent of the environment (Pan et al., 2013; Sun et al., 2017), and the water content of the lamina is an additional mechanical load that must be supported by the petiole (Niklas, 1991; Niklas, 1992; Li et al., 2022). Plants must optimize energy allocation among different structures and often allocate more biomass to the compartments responsive to environmental changes (Enquist et al., 2007; Price and Enquist, 2007; Zhang et al., 2011). For example, in some extreme circumstances, such as a windy environment, leaves may increase the proportion of biomass allocation to the lamina support tissues to provide sufficient mechanical stability; or under drought, biomass allocation may be devoted to root growth (Niklas and Enquist, 2002). Consequently, the extent to which leaves manifest diminishing returns is related to the environmental characteristics of a habitat (Takenaka et al., 2001).

In order to study diminishing returns under different habitats, investigators have examined the effects of altitude on the scaling of DM vs. A, because environmental factors, such as temperature or precipitation, can rapidly change over short distances along an elevational gradient (Pan et al., 2013). For example, Li et al. (2008) found that the scaling exponent of DM vs. A always exceeds unity for 93 temperate woody species collected at different elevations. However, Pan et al. (2013) analyzed the scaling relationships between DM and A for 121 vascular plant species along an elevational gradient in a subtropical monsoon forest, and found that the numerical values of the scaling exponent increased significantly with altitude from a numerical value of 0.859 to 1.299, with exponents consistently$<$1 in low altitudes. The disagreement between these two studies can be quantified by the extent of the goodness of fit for the different datasets. In the case of Pan et al. (2013), the value $r^2<0.8$ is significantly smaller than that of $r^2>0.9$ reported by Li et al. (2008), which suggests that DM vs. A might be unreliable for describing the scaling of M vs. A under some circumstances. Thus, investigators have sought to find a substitute for DM to evaluate M vs. A.

Considering that the water in leaves is metabolically essential and that it contributes to the mechanical loads that the petiole (and the secondary and midrib veins) must structurally support, some studies have proposed that FM might be better than DM to assess M vs. A scaling relationships. For example, using FM vs. A as opposed to DM vs. A is statistically more robust when assessing the M vs. A scaling relationship for bamboo leaves (Shi et al., 2015; Lin et al., 2018). Likewise, (Huang et al., 2019a; Huang et al., 2019b) compared the scaling relationship between FM vs. A with that of DM vs. A using 15 broad-leaved species and 12 bamboo species, which found the same phenomenon.

Prior studies have compiled large datasets on the size of individual evergreen leaves tree species, log-transformed both variables of interest, have applied linear regression of the pooled data to compare the difference between FM vs. A and DM vs. A, and have concluded that FM vs. A is more reliable when dealing with "diminishing returns" because FM vs. A has a better goodness of fit compared to DM vs. A (see Huang et al., 2019a; Huang et al., 2019b). However, this approach assumes that the relationship is log-log linear. If the relationship has other forms (e.g., quadratic rather than linear), this assumption has consequences for the estimated slope and the goodness of fit, which may be unpersuasive or inconclusive.

Yet another concern about the assertion that FM vs. A is more reliable when dealing with "diminishing returns" is that most studies have focused on evergreen species. Evergreen species retain their leaves for several years, and prior work has shown a huge range of leaf life spans among evergreen woody species, ranging from a couple of months in some tropical pioneer species to > 20 years in some gymnosperms (Chabot and Hicks, 1982; Reich et al., 1992). Some evergreen species are "leaf-exchangers", dropping most of the previous season's leaves just as the new cohort emerges (Lusk, 2019). Compared to evergreen species, deciduous species shed their leaves at the end of the growing season (Zhang et al., 2017). Thus, deciduous species may not invest as much biomass in leaf area expansion as evergreen species because their leaves are more 'disposable' (Athokpam et al., 2014). Alternatively, deciduous species may invest more biomass in leaf area expansion than evergreen species as their relatively short leaf lifespan requires light harvesting and more energy storage in relatively short time spans (Poorter et al., 2009; Tomlinson et al., 2013). Arguably, the scaling relationship for "diminishing returns" may be different in deciduous and evergreen species.

Here, we examine ten deciduous and two evergreen species to compare the difference between FM vs. *A* and DM vs. *A*, and test the non-linearity of traditional linear regression models. The species examined are from two families, the Fagaceae and Ulmaceae, that contain keystone species in forest ecosystems (Kremer et al., 2012; Fragnière et al., 2021). The taxonomic focus on these two families also permits a comparison of deciduous and evergreen species within a single family (i.e., the Fabaceae), thereby removing the effects of phylogenetic bias.

In these comparisons, we asked two questions: (1) is FM vs. *A* more reliable than DM vs. *A* for the description of diminishing returns in deciduous species?, and (2) does leaf biomass investment strategy differ between deciduous and evergreen species?

Materials and methods

Collection site and plant materials

A total of 4271 mature and undamaged leaves was collected from Nanjing Forestry University (32°07'67"N, 118°81'36"E), Nanjing, Jiangsu Province, China. Given the possible influences of seasons on the scaling exponent of leaf mass vs. *A* for deciduous trees (Liu et al., 2020), leaves were collected in a short time period, from 20 August to 3 September 2020. For each species, >300 leaves were collected in the morning (9:30-11:30 am) from five to ten free standing trees. To reduce water loss during transport, leaves were wrapped in wet paper and then placed in resealable plastic bags (28 cm × 20 cm), and quickly brought back to the laboratory of Nanjing Forestry University (which took less than two hours from the collection site to the laboratory) to measure leaf fresh mass. Table 1 provides the relevant data for the leaves collected for this study. Figure 1 shows representative examples of the investigated leaves for the 12 species.

Leaf image processing

Leaf dry and fresh mass was measured using an electronic balance (ME204/02, Mettler Toledo Company, Greifensee, Switzerland; measurement accuracy 0.0001 g). Leaf dry mass was obtained after drying leaves in a ventilated oven (XMTD–8222; Jinghong Experimental Equipment Co., Ltd., Shanghai, China) at 80°C for at least 72 hours. To estimate leaf area, each fresh leaf was scanned with an Epson photo scanner (V550, Epson, Batam, Indonesia). Adobe Photoshop (version 9.0; Adobe, San Jose, CA, USA) was used to obtain black and white leaf edge images that were saved as bitmap images at a 600-dpi resolution. The protocols of Shi et al. (2018) and Su et al. (2019) were then used to calculate the pixel values of leaf images to obtain the planar coordinates of leaf boundary points. Leaf area was calculated by using the 'bilat' function in the 'biogeom' package (version 1.0.5; Shi et al., 2022b) based on R software (version 4.2.0; R Core Team, 2022).

Statistical methods

A power-law function was used to describe the scaling relationships among DM, FM, and *A*:

TABLE 1 Leaf collection information for the 12 species belonging to two families (Fagaceae and Ulmaceae) from Nanjing Forestry University campus, Nanjing, Jiangsu Province, P. R. China.

Species code	Family	Scientific name	Sampling date	Leaf type
1	Fagaceae	*Cyclobalanopsis glauca* (Thunberg) Oersted	26 August 2020	Evergreen
2	Fagaceae	*Lithocarpus glaber* (Thunb.) Nakai	25 August 2020	Evergreen
3	Fagaceae	*Quercus acutissima* Carr.	21 August 2020	Deciduous
4	Fagaceae	*Quercus aliena* Blume	20 August 2020	Deciduous
5	Fagaceae	*Quercus chenii* Nakai	27 August 2020	Deciduous
6	Fagaceae	*Quercus variabilis* Blume	20 August 2020	Deciduous
7	Ulmaceae	*Aphananthe aspera* (Thunb.) Planch.	2 September 2020	Deciduous
8	Ulmaceae	*Celtis julianae* Schneid.	31 August 2020	Deciduous
9	Ulmaceae	*Celtis sinensis* Pers.	1 September 2020	Deciduous
10	Ulmaceae	*Pteroceltis tatarinowii* Maxim.	3 September 2020	Deciduous
11	Ulmaceae	*Ulmus parvifolia* Jacq.	1 September 2020	Deciduous
12	Ulmaceae	*Zelkova serrata* (Thunb.) Makino	30 August 2020	Deciduous

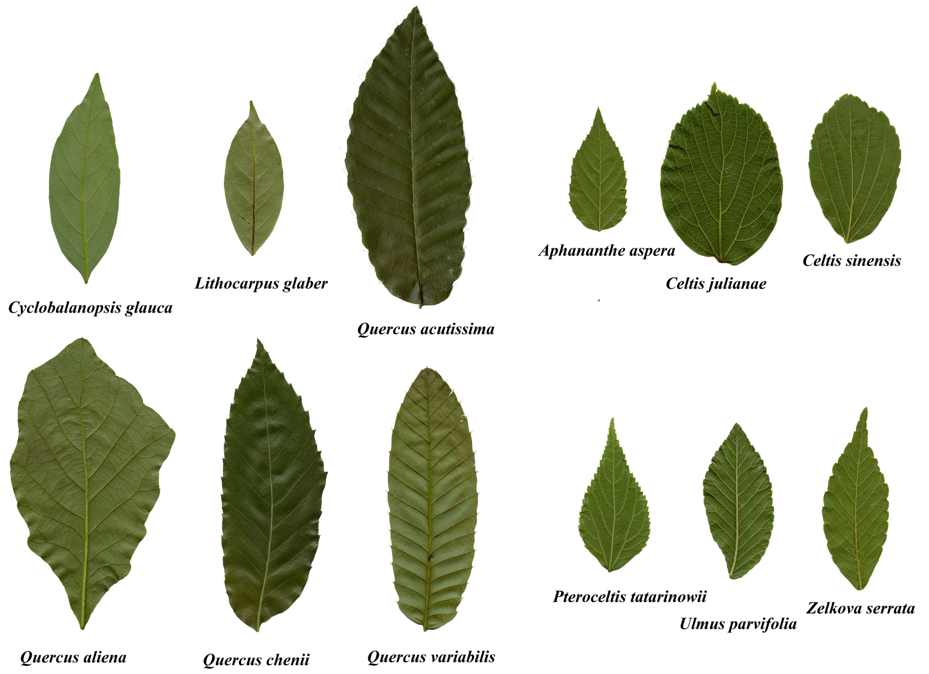

FIGURE 1
Examples of the leaves of the 12 species investigated in this study.

$$Y_1 = \beta Y_2^{\alpha}, \tag{1}$$

where Y_1 and Y_2 represent interdependent variables (e.g., FM and A), β is the normalization constant, and α is the scaling exponent (Niklas, 1994). After log-log transformation, the power-law function was converted into

$$y = \gamma + \alpha x, \tag{2}$$

where $y = \ln(Y_1)$, $x = \ln(Y_2)$, and $\gamma = \ln(\beta)$. Parameters γ and α were estimated by using reduced major axis regression protocols (Niklas, 1994; Smith, 2009). The bootstrap percentile method (based on 3000 bootstrapping replicates) was used to test the significance of the difference in the estimated scaling exponents of y vs. x between any two of the 12 species (Efron and Tibshirani, 1993; Sandhu et al., 2011).

Ordinary least squares regression protocols were used to test the non-linearity of the log-transformed bivariate data. The linearity was rejected if the coefficient (γ_2) of ^{2} of a quadratic model was statistically significant at the 0.05 significance level (see Zhao et al. (2019) for details).

$$y = \gamma_0 + \gamma_1 x + \gamma_2 x^2 \tag{3}$$

The percentage error (PE) was used to evaluate the effect of the non-linear term on the goodness of fit.

$$\mathrm{PE} = \frac{\mathrm{RSS}_{linear} - \mathrm{RSS}_{non\text{-}linear}}{\mathrm{RSS}_{linear}} \times 100\,\%, \tag{4}$$

where RSS_{linear} and $\mathrm{RSS}_{non\text{-}linear}$ were the residual sum of squares of equations 2 and 3, respectively. As a rule of thumb, for two equations with similar model structures, if PE< 5%, the additional parameter (i.e., γ_2) is not relevant.

The significance of differences in DM, FM, A, leaf absolute water content, leaf DM per unit area (LMA), and leaf FM per unit area (LFMA) among the 12 species were determined using the analysis of variance (ANOVA) based on the Tukey's Honest Significant Difference (HSD) test at the 0.05 significance level (Hsu, 1996). All statistical analyses were performed using R (version 4.2.0) (R Core Team, 2022).

Results

Statistically significant log-log DM vs. A and FM vs. A scaling relationships were observed for each of the 12 species (Table 2; Figures S1, S2). The numerical values of the scaling exponent of DM vs. A for 11 out of the 12 species exceeded unity and the lower bounds of the corresponding CIs of the scaling exponents for the 11 species exceeded unity. The only exception was *Aphananthe aspera* (Ulmaceae) whose goodness of fit (r^2 = 0.795) was lower than the majority of the other species. The numerical values of the scaling exponent of FM vs. *A* for all of the 12 species exceeded unity, and the corresponding 95% CIs of the scaling exponents did not include unity. For each species, the goodness of fit for the FM vs. *A* scaling relationship was higher than that for the DM vs. *A* scaling relationship, as reflected by the numerical values of the coefficients of determination (Table 2). For almost half of the species examined, the non-linear term was found to be significant. There were no significant differences between evergreen and deciduous species. The PE value, which designed whether it is worth introducing the non-linear term, was found to be smaller than 5% for each of most data sets (23/24). (Table 2; Figures S1, S2).

Interspecific comparisons among the two scaling exponents (i.e., for DM vs. *A*, and FM vs. *A*) showed that there were significant differences among the 12 species (Figure 2). Although there were slight differences between the interspecific scaling exponents of DM vs. *A* and those of FM vs. *A*, the variation trends were assessed to be the same for the 12 species (Figure 2).

The numerical values of the scaling exponents of DM vs. *A* and of FM vs. *A* and the corresponding CIs for the pooled data were greater than unity. However, the numerical value of the latter was slightly smaller than that of the former (Figure 3). In addition, the coefficient of determination of DM vs. *A* was smaller than that of FM vs. *A*.

The non-linear terms of the allometric model were found to be significant for both DM vs. *A* and FM vs. *A*. However, the PE values were < 5%, which indicated that the non-linear term did not improve the model fit (Figure 3).

There were significant differences in leaf size (as measured by DM, FM, or *A*) among the 12 species. The numerical values of Fagaceae species were generally greater than those of Ulmaceae species (Figures 4A–C). Leaf absolute water content had a similar trend with respect to leaf size, and the leaves of the Fagaceae species tended to have a higher water content (Figure 4D).

There were significant differences in leaf DM per unit area (LMA) and leaf FM per unit area (LFMA) among the 12 species. Two evergreen species, *Cyclobalanopsis glauca* and *Lithocarpus glaber*, had the largest LMA and LFMA values (Figures 4E, F).

Discussion

The leaves of evergreen and deciduous species both conformed to the phenomenon called diminishing returns as

TABLE 2 Statistical parameters for dry mass vs. area and fresh mass vs. area in 12 species.

Species code	n	Diminishing returns	Equation	Slope CI	r^2	$P_{\text{non-linearity}}$	PE (%)
1	364	Dry mass vs. area	$y = -5.268 + 1.159\,x$	(1.115, 1.204)	0.861	<0.05	4.19
		Fresh mass vs. area	$y = -4.313 + 1.111\,x$	(1.085, 1.137)	0.943	<0.05	1.53
2	357	Dry mass vs. area	$y = -4.535 + 1.069\,x$	(1.028, 1.112)	0.855	0.8227	0.01
		Fresh mass vs. area	$y = -3.857 + 1.065\,x$	(1.027, 1.106)	0.881	0.9787	0
3	346	Dry mass vs. area	$y = -5.276 + 1.058\,x$	(1.020, 1.096)	0.867	0.3154	0.29
		Fresh mass vs. area	$y = -4.837 + 1.132\,x$	(1.098, 1.166)	0.925	0.5759	0.09
4	346	Dry mass vs. area	$y = -5.630 + 1.122\,x$	(1.096, 1.150)	0.956	<0.05	1.99
		Fresh mass vs. area	$y = -4.612 + 1.101\,x$	(1.081,1.121)	0.980	<0.05	1.41
5	370	Dry mass vs. area	$y = -5.544 + 1.122\,x$	(1.085,1.159)	0.890	0.7502	0.03
		Fresh mass vs. area	$y = -4.858 + 1.134\,x$	(1.110, 1.158)	0.957	0.888	0.01
6	315	Dry mass vs. area	$y = -5.740 + 1.201\,x$	(1.159, 1.247)	0.891	0.1119	0.81
		Fresh mass vs. area	$y = -4.997 + 1.195\,x$	(1.160, 1.231)	0.935	0.0943	0.89
7	365	Dry mass vs. area	$y = -5.454 + 0.997\,x$	(0.957, 1.039)	0.777	0.6695	0.05
		Fresh mass vs. area	$y = -4.902 + 1.087\,x$	(1.046, 1.131)	0.854	<0.05	1.41
8	369	Dry mass vs. area	$y = -5.673 + 1.159\,x$	(1.116, 1.208)	0.862	<0.05	2.60
		Fresh mass vs. area	$y = -4.573 + 1.098\,x$	(1.071, 1.126)	0.950	<0.05	1.91
9	359	Dry mass vs. area	$y = -5.139 + 1.116\,x$	(1.058, 1.176)	0.653	<0.05	1.68
		Fresh mass vs. area	$y = -4.573 + 1.098\,x$	(1.071, 1.126)	0.758	<0.05	2.68
10	359	Dry mass vs. area	$y = -5.930 + 1.174\,x$	(1.137, 1.213)	0.867	<0.05	2.01
		Fresh mass vs. area	$y = -4.734 + 1.126\,x$	(1.100, 1.151)	0.940	<0.05	5.29
11	363	Dry mass vs. area	$y = -6.176 + 1.520\,x$	(1.464, 1.584)	0.823	0.3377	0.26
		Fresh mass vs. area	$y = -5.028 + 1.442\,x$	(1.399, 1.489)	0.914	0.2457	0.37
12	358	Dry mass vs. area	$y = -5.495 + 1.168\,x$	(1.135, 1.202)	0.920	<0.05	2.44
		Fresh mass vs. area	$y = -4.848 + 1.177\,x$	(1.153, 1.202)	0.959	<0.05	1.39

Species codes associated with binomials are provided in Table 1.

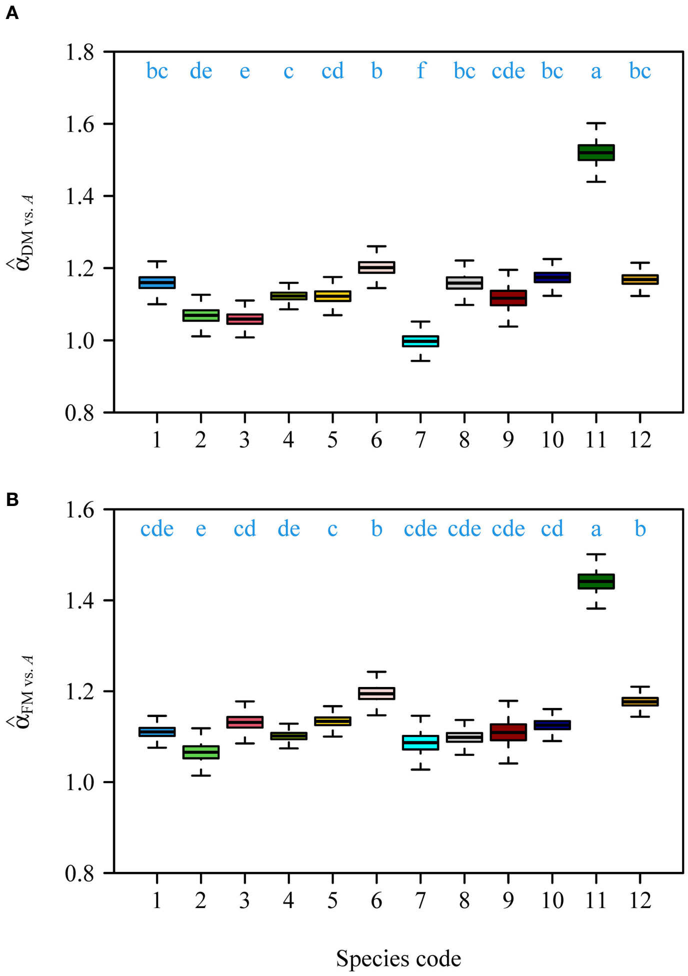

FIGURE 2
Comparisons of the estimated numerical values of the scaling exponents of DM vs. *A* among the 12 species **(A)**, and the estimated numerical values of the scaling exponents of FM vs. *A* among the 12 species **(B)**. The letters on the top of the whiskers signify the significance of the difference in the scaling exponent between any two pairs of the 12 species; the solid segments in the boxes represent the medians of the scaling exponents based on 3000 bootstrapping replications. Species codes associated with their binomials are the same as those in Table 1.

indicated by the numerical values of the exponents of leaf mass (DM or FM) vs. *A* exceeding unity. The exponent of FM vs. *A* was numerically slightly lower than that of DM vs. *A*, likely because the addition of water to the mass of the leaf lamina. An examination or the non-linear response in diminishing returns indicated that the non-linear model was not superior and was less parsimonious compared to the linear model as indicated by higher r^2 and PE values.

No significant difference in DM, FM, and *A* was observed between the ten deciduous and the two evergreen species. However, leaf dry mass per unit area (LMA) and leaf fresh mass per unit area (LFMA) differed between the evergreen and deciduous species. Specifically, the evergreen species had larger mass investments in their per unit leaf area than the other deciduous species.

We conclude therefore that FM vs. *A* is a more reliable than DM vs. *A* for describing leaf scaling relationships of *M* vs. *A* with respect to both the evergreen and deciduous species. The leaf biomass investment strategy between evergreen and deciduous species is slightly different, but they both conformed to diminishing returns. However, it worth noting that the concept of diminishing returns revolves around the investments made in the construction of leaves and not around the mechanical loads that a leaf must support (Niklas et al., 2007). The superiority of the reliability of FM vs. *A* highlights the importance of mechanical support, whereas diminishing returns in the context of DM vs. *A* highlights the importance of carbon allocation (Niklas and Spatz, 2012). With this distinction in mind, we address in the following sections each of the two questions outlined in the Introduction.

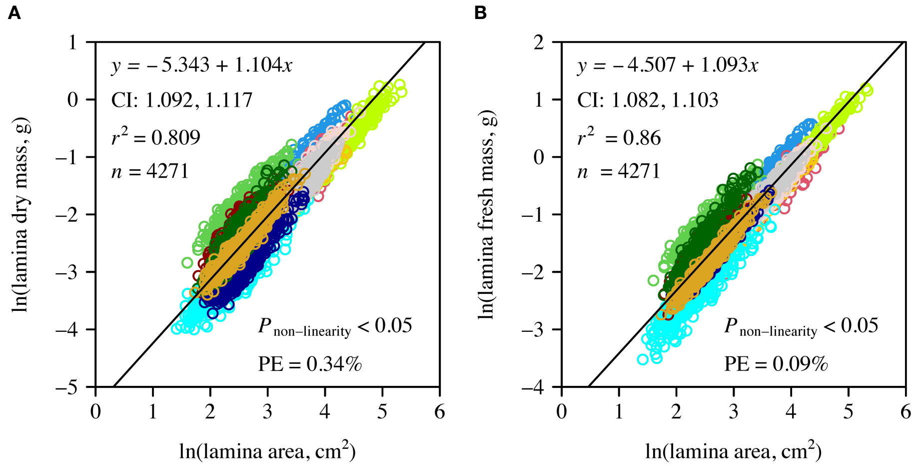

FIGURE 3
Log-log bivariate plots and linear fits to leaf dry mass vs. *A* **(A)**, and to leaf fresh mass vs. *A* **(B)** for the pooled data of the 12 species. Open circles are the observed data; the straight lines are the log-log regression curves.

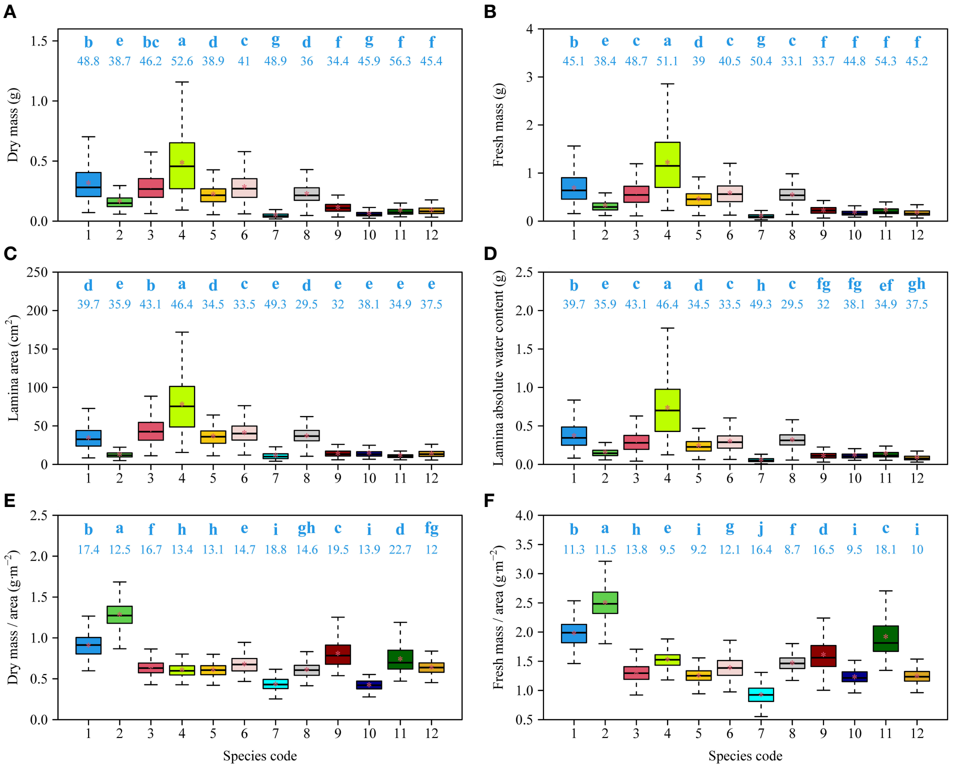

FIGURE 4
Comparisons of dry mass **(A)**, fresh mass **(B)**, lamina area **(C)**, lamina absolute water content **(D)**, ratio of fresh mass to area **(E)**, and ratio of dry mass and area **(F)** among 12 species. The letters on the top of the whiskers of the boxes signify the significance of the difference between any two of 12 species; the numbers on the top of the whiskers of the boxes signify the coefficients of variation of leaf measures; the solid segments and asterisks within the boxes represent the medians and means of each leaf measure based on 3000 bootstrapping replications, respectively. Species codes associated with their binomials are the same as those in Table 1.

Is leaf FM vs. *A* more reliable than DM vs. *A* when assessing diminishing returns

The two evergreen species manifested a FM vs. *A* scaling relationship that was statistically more robust than that of the DM vs. *A* scaling relationship (see also Huang et al., 2019a; Huang et al., 2019b; Liu et al., 2020). Among each of the ten deciduous species and the two evergreen species, the goodness of fit (as gauged by r^2) for the FM vs. *A* scaling relationship was greater than that of DM vs. *A* scaling relationship (Table 2), as reported for other evergreen species (Huang et al., 2019a; Huang et al., 2019b; Liu et al., 2020; Guo et al., 2021).

In prior studies, reduced major axis protocols have been used to assess the log-log bivariate relationships of biologically interrelated variables of interest. However, to date, there are no available methods to test the statistical significance of the non-linear term based on reduced major axis protocols. In the present study, ordinary least squares regression protocols were used to test the significance of the non-linear term (see also Zhao et al., 2019). Although the non-linear terms were found to be significant for the *M* vs. *A* scaling relationship for some datasets, the PE values nevertheless showed that the addition of the non-linear term did not improve the significance of correlations and unnecessarily increased the model complexity and was, therefore, unnecessary and a distraction

It is obvious that relationship between FM and lamina *A* depends on both the leaf water content and the dry mass content across all of the species examined in this study. FM depends on the availability of water in the local environment, whereas leaf dry mass is unresponsive to variations in water availability after leaf expansion (Jiao et al., 2022). For this reason, all of the leaves used in the present study were sampled at the same season and daytime of day in an effort to limit the effect of rainfall on leaf fresh mass and its effect on the r^2 of FM vs. *A*. Because leaf area determines the ability to capture light to a great extent, the leaf biomass invested in the construction of lamina area and thickness is considered to be a trade-off between the ability to capture and utilize light (White and Montes-R, 2005; Jullien et al., 2009; Koester et al., 2014). Thicker leaves tend to have a higher water content, longer palisade cells, and multiple palisade cell layers, which can enhance area-based photosynthesis (Mitchell et al., 1999; Lambers et al., 2008).

Therefore, we conclude that FM vs. *A* is a better measure of leaf performance than DM vs. *A* when considering the scaling of leaf biomass with respect to *A* (Liu et al., 2020).

Does the leaf biomass investment strategy differ between deciduous and evergreen species?

Leaf dry mass, fresh mass, and water content does not differ significantly between the evergreen and deciduous species examined in this study (Figures 4A–C). This indifference might reflect equivalent investments to maintain essential metabolic pathways regardless of leaf life span (Niinemets et al., 2006; Yan et al., 2016). Regardless of the proximate cause(s), we cannot conclusively confirm whether deciduous species invest more or less biomass to leaf area expansion compared to evergreen species.

However, our data indicate that the LMA and FLMA of deciduous species are significantly smaller than those of evergreen species (Figures 4E, F; see also Poorter et al., 2009). LMA is frequently used as a surrogate measure of photosynthetic rate and growth strategy (Wright et al., 2004; Poorter et al., 2009). Typically, photosynthetic activity per leaf area declines with increasing LMA, whereas the concentration of proteins and minerals tends to increase as LMA decreases. This trend is attended by lower concentrations of lignin and other secondary compounds, which leads to increased carbon return rates but also to lower leaf life-span (Lambers and Poorter, 1992; Wright and Westoby, 2002). Compared to deciduous species, evergreen species generally have higher LMA and possess a larger proportion of non-photosynthetically active tissue associated with longer leaf life spans. The evergreen species included in our study occur in shaded environments with low soil moisture that demand long-lasting and thick leaves with high LMA. In contrast, the deciduous species occuy habitats with higher light and water availabilities permitting faster life history strategies expressed by, among other things, low LMA values (see also Poorter et al., 2009). Based on these results, we conclude that deciduous species may invest more biomass in their photosynthetically active tissues per unit leaf area to balance the shorter duration of their investment returns. Noting that evergreen species possess larger LMA and LFMA than deciduous species, we also speculate that these species invest more biomass in the construction of non-photosynthetically active tissues to support their longer duration of investment returns.

Conclusions

The data presented here indicate that FM vs. *A* is more reliable for describing leaf scaling relationships than DM vs. *A* for both evergreen and deciduous species. The FM vs. *A* scaling exponents of the 12 species investigated have 95% CIs numerically greater than unity and a similar trend is observed for DM vs. *A*. Thus, the results are consistent with the phenomenon called “diminishing returns”. The data also indicate that the leaves of evergreen species have higher LMA and LFMA values than the deciduous species within the same family (Fagaceae). These results indicate that the leaf biomass investment strategies of deciduous and evergreen species are slightly different: deciduous species tend to obtain larger light harvesting capabilities by investing less biomass per unit area.

Future research is required to determine if these trends apply to species within other families, particularly families including evergreen and deciduous species.

Data availability statement

The datasets presented in this study can be found in online repositories. The names of the repository/repositories and accession number(s) can be found below: Dryad Data Repository, https://doi.org/10.5061/dryad.kprr4xh4r.

Author contributions

KN, PS, and JS designed this work; YL carried out the experiment; PS analyzed the data; XG and KN wrote the initial draft, and contributed equally to this work; JS, PS and JX commented on and revised the manuscript; all authors read and agree with this manuscript.

Funding

JX was supported by Jiangsu Forestry Science & Technology Innovation and Extension Project (No: LYKJ[2022]02); JS acknowledges funding by the German Research Foundation (DFG) with a research scholarship (No: SCHR1672/1- 1) and by a Macquarie University Research Fellowship.

Acknowledgments

We thank Yabing Jiao, Ülo Niinemets and Kexin Yu for their valuable help in the preparation of this manuscript. We also thank Drs. Boris Rewald and Tiina Tosens for handling our manuscript and two reviewers for providing valuable comments on the earlier version of this manuscript.

Conflict of interest

The authors declare that the research was conducted in the absence of any commercial or financial relationships that could be construed as a potential conflict of interest.

Publisher's note

Supplementary material

The Supplementary Material for this article can be found online at: https://www.frontiersin.org/articles/10.3389/fpls.2022.832300/full#supplementary-material

References

Athokpam, F. D., Garkoti, S. C., and Borah, N. (2014). Periodicity of leaf growth and leaf dry mass changes in the evergreen and deciduous species of southern Assam, India. *Ecol. Res.* 29, 153–165. doi: 10.1007/s11284-013-1105-2

Chabot, B. F., and Hicks, D. J. (1982). The ecology of leaf life spans. *Ann. Rev. Ecol. Syst.* 13, 229–259. doi: 10.1146/annurev.es.13.110182.001305

Efron, B., and Tibshirani, R. J. (1993). *An introduction to the bootstrap* (New York: Chapman and Hall/CRC).

Enquist, B. J., Kerkhoff, A. J., Stark, S. C., Swenson, N. G., McCarthy, M. C., and Price, C. A. (2007). A general integrative model for scaling plant growth, carbon flux, and functional trait spectra. *Nature* 449, 218–222. doi: 10.1038/nature06061

Fragnière, Y., Song, Y., Fazan, L., Manchester, S. R., Garfi, G., and Kozlowski, G. (2021). Biogeographic overview of ulmaceae: Diversity, distribution, ecological preferences, and conservation status. *Plants* 10, 1111. doi: 10.3390/plants10061111

Garnier, E., Laurent, G., Bellmann, A., Debain, S., Berthelier, P., Ducout, B., et al. (2001). Consistency of species ranking based on functional leaf traits. *N. Phytol.* 152, 69–83. doi: 10.1046/j.0028-646x.2001.00239.x

Guo, X., Shi, P., Niinemets, Ü., Hölscher, D., Wang, R., Liu, M., et al. (2021). "Diminishing returns" for leaves of five age-groups of phyllostachys edulis culms. *Am. J. Bot.* 108, 1662–1672. doi: 10.1002/ajb2.1738

Hsu, P. (1996). *Multiple comparisons: Theory and methods* (New York: Chapman and Hall/CRC).

Huang, W., Ratkowsky, D. A., Hui, C., Wang, P., Su, J., and Shi, P. (2019a). Leaf fresh weight versus dry weight: Which is better for describing the scaling relationship between leaf biomass and leaf area for broad-leaved plants? *Forests* 10, 256. doi: 10.3390/f10030256

Huang, W., Su, X., Ratkowsky, D. A., Niklas, K. J., Gielis, J., and Shi, P. (2019b). The scaling relationships of leaf biomass vs. leaf surface area of 12 bamboo species. *Glob. Ecol. Conserv.* 20, e00793. doi: 10.1016/j.gecco.2019.e00793

Jiao, Y., Niklas, K. J., Wang, L., Yu, K., Li, Y., and Shi, P. (2022). Influence of leaf age on the scaling relationships of lamina mass vs. area. *Front. Plant Sci.* 13, 860206. doi: 10.3389/fpls.2022.860206

Jullien, A., Allirand, J.-M., Mathieu, A., Andrieu, B., and Ney, B. (2009). Variations in leaf mass per area according to N nutrition, plant age and leaf position reflect ontogenetic plasticity in winter oilseed rape (*Brassica napus* L.). *Field Crop Res.* 114, 188–197. doi: 10.1016/j.fcr.2009.07.015

Koester, R. P., Skoneczka, J. A., Cary, T. R., Diers, B. W., and Ainsworth, E. A. (2014). Historical gains in soybean (*Glycine max* Merr.) seed yield are driven by linear increases in light interception, energy conversion, and partitioning efficiencies. *J. Exp. Bot.* 65, 3311–3321. doi: 10.1093/jxb/eru187

Kremer, A., Abbott, A. G., Carlson, J. E., Manos, P. S., Plomion, C., Sisco, P., et al. (2012). Genomics of fagaceae. *Tree Genet. Genomes* 8, 583–610. doi: 10.1007/s11295-012-0498-3

Lambers, H., Chapin III, F. S., and Pons, T. L. (2008). *Plant physiological ecology* (2nd Edition) (New York: Springer).

Lambers, H., and Poorter, H. (1992). Inherent variation in growth rate between higher plants: a search for physiological causes and ecological consequences. *Adv. Ecol. Res.* 23, 187–261. doi: 10.1016/S0065-2504(08)60148-8

Lin, S., Shao, L., Hui, C., Song, Y., Reddy, G. V. P., Gielis, J., et al. (2018). Why does not the leaf weight-area allometry of bamboos follow the 3/2-power law? *Front. Plant Sci.* 9, 583. doi: 10.1002/ece3.2407

Li, Y., Shi, P., Niinemets, Ü., Song, Y., Yu, K., Schrader, J., et al. (2022). Diminishing returns among lamina fresh and dry mass, surface area, and petiole fresh mass among nine lauraceae species. *Am. J. Bot.* 109, 377–392. doi: 10.1002/ajb2.1812

Liu, M., Niklas, K. J., Niinemets, Ü., Hölscher, D., Chen, L., and Shi, P. (2020). Comparison of the scaling relationships of leaf biomass versus leaf surface area between spring and summer for two deciduous tree species. *Forests* 11, 1010. doi: 10.3390/f11091010

Li, G., Yang, D., and Sun, S. (2008). Allometric relationships between lamina area, lamina mass and petiole mass of 93 temperate woody species vary with leaf habit, leaf form and altitude. *Funct. Ecol.* 22, 557–564. doi: 10.1111/j.1365-2435.2008.01407.x

Lusk, C. H. (2019). Leaf functional trait variation in a humid temperate forest, and relationships with juvenile tree light requirements. *Peer J.* 7, e6855. doi: 10.7717/peerj.6855

Milla, R., and Reich, P. B. (2007). The scaling of leaf area and mass: The cost of light interception increases with leaf size. *Proc. R. Soc B-Biol. Sci.* 274, 2109–2114. doi: 10.1098/rspb.2007.0417

Mitchell, K. A., Bolstad, P. V., and Vose, J. M. (1999). Interspecific and environmentally induced variation in foliar dark respiration among eighteen southeastern deciduous tree species. *Tree Physiol.* 19, 861–870. doi: 10.1093/treephys/19.13.861

Niinemets, Ü., Portsmuth, A., and Tobias, M. (2006). Leaf size modifies support biomass distribution among stems, petioles and mid-ribs in temperate plants. *N. Phytol.* 171, 91–104. doi: 10.1111/j.1469-8137.2006.01741.x

Niklas, K. J. (1991). Effects of tissue volume and location on the mechanical consequences of dehydration of petioles. *Am. J. Bot.* 78, 361–369. doi: 10.1002/j.1537-2197.1991.tb15198.x

Niklas, K. J. (1992). Petiole mechanics, light interception by lamina, and economy in design. *Oecologia* 90, 518–526. doi: 10.1007/BF01875445

Niklas, K. J. (1994). *Plant allometry: The scaling of form and process* (Chicago: The University of Chicago Press).

Niklas, K. J., and Enquist, B. J. (2002). On the vegetative biomass partitioning of seed plant leaves, stems, and roots. *Am. Nat.* 159, 482–497. doi: 10.1086/339459

Niklas, K. J., and Spatz, H.–C. (2012). *Plant physics* (Chicago: The University of Chicago Press).

Niklas, K. J., Cobb, E. D., Niinemets, Ü., Reich, P. B., Sellin, A., Shipley, B., et al. (2007). "Diminishing returns" in the scaling of functional leaf traits across and within species groups. *Proc. Natl. Acad. Sci. U.S.A.* 104, 8891–8896. doi: 10.1073/pnas.0701135104

Niklas, K. J., Cobb, E. D., and Spatz, H. C. (2009). Predicting the allometry of leaf surface area and dry mass. *Am. J. Bot.* 96, 531–536. doi: 10.3732/ajb.0800250

Pan, S., Liu, C., Zhang, W., Xu, S., Wang, N., Li, Y., et al. (2013). The scaling relationships between leaf mass and leaf area of vascular plant species change with altitude. *PloS One* 8, e76872. doi: 10.1371/journal.pone.0076872

Poorter, H., Niinemets, Ü., Poorter, L., Wright, I. J., and Villar, R. (2009). Causes and consequences of variation in leaf mass per area (LMA): a meta-analysis. *N. Phytol.* 182, 565–588. doi: 10.1111/j.1469-8137.2009.02830.x

Price, C. A., and Enquist, B. J. (2007). Scaling mass and morphology in leaves: an extension of the WBE model. *Ecology* 88, 1132–1141. doi: 10.1890/06-1158

Rascher, U., and Nedbal, L. (2006). Dynamics of photosynthesis in fluctuating light commentary. *Curr. Opin. Plant Biol.* 9, 671–678. doi: 10.1016/j.pbi.2006.09.012

R Core Team (2022) *R: A language and environment for statistical computing* (Vienna: R Foundation for statistical computing). Available at: https://www.r-project.org/ (Accessed 1 July 2022).

Reich, P. B., Walters, M. B., and Ellsworth, D. S. (1992). Leaf life-span in relation to leaf, plant, and stand characteristics among diverse ecosystems. *Ecol. Monogr.* 62, 365–392. doi: 10.2307/2937116

Sack, L., Scoffoni, C., McKown, A. D., Frole, K., Rawls, M., Havran, J. C., et al. (2012). Developmentally based scaling of leaf venation architecture explains global ecological patterns. *Nat. Commun.* 3, 837. doi: 10.1038/ncomms1835

Sandhu, H. S., Shi, P., Kuang, X., Xue, F., and Ge, F. (2011). Applications of the bootstrap to insect physiology. *Fla. Entomol.* 94, 1036–1041. doi: 10.1653/024.094.0442

Shi, P., Gielis, J., Quinn, B. K., Niklas, K. J., Ratkowsky, D. A., Schrader, J., et al. (2022b). *'biogeom': An R package for simulating and fitting natural shapes* (Ann. N.Y. Acad. Sci. in press). doi: 10.1111/nyas.14862

Shi, P., Liu, M., Ratkowsky, D. A., Gielis, J., Su, J., Yu, X., et al. (2019). Leaf area-length allometry and its implications in leaf shape evolution. *Trees Struct. Funct.* 33, 1073–1085. doi: 10.1007/s00468-019-01843-4

Shi, P., Li, Y., Wang, R., and Niklas, K. J. (2021). Leaf data of four families of broad-leaved plants. *Dryad Data Repository*. doi: 10.5061/dryad.kprr4xh4r

Shi, P., Miao, Q., Niinemets, Ü., Liu, M., Li, Y., Yu, K., et al. (2022a). Scaling relationships of leaf vein and areole traits versus leaf size for nine magnoliaceae species differing in venation density. *Am. J. Bot.* 109, 899–909. doi: 10.1002/ajb2.1856

Shi, P., Ratkowsky, D. A., Li, Y., Zhang, L., Lin, S., and Gielis, J. (2018). A general leaf area geometric formula exists for plants – evidence from the simplified gielis equation. *Forests* 9, 714. doi: 10.3390/f9110714

Shi, P., Xu, Q., Sandhu, H. S., Gielis, J., Ding, Y., Li, H., et al. (2015). Comparison of dwarf bamboos (*Indocalamus* sp.) leaf parameters to determine relationship between spatial density of plants and total leaf area per plant. *Ecol. Evol.* 5, 4578–4589. doi: 10.1002/ece3.1728

Smith, R. J. (2009). Use and misuse of the reduced major axis for line-fitting. *Am. J. Phys. Anthropol.* 140, 476–486. doi: 10.1002/ajpa.21090

Sun, J., Fan, R., Niklas, K. J., Zhong, Q., Yang, F., Li, M., et al. (2017). "Diminishing returns" in the scaling of leaf area vs. dry mass in wuyi mountain bamboos, southeast China. *Am. J. Bot.* 104, 993–998. doi: 10.3732/ajb.1700068

Su, J., Niklas, K. J., Huang, W., Yu, X., Yang, Y., and Shi, P. (2019). Lamina shape does not correlate with lamina surface area: An analysis based on the simplified gielis equation. *Glob. Ecol. Conserv.* 19, e00666. doi: 10.1016/j.gecco.2019.e00666

Takenaka, A., Takahashi, K., and Kohyama, T. (2001). Optimal leaf display and biomass partitioning for efficient light capture in an understory palm, *Licuala arbuscula*. *Funct. Ecol.* 15, 660–668. doi: 10.1046/j.0269-8463.2001.00562.x

Tomlinson, K. W., van Langevelde, F., Ward, D., Bongers, F., da Silva, D. A., Prins, H. H. T., et al. (2013). Deciduous and evergreen trees differ in juvenile biomass allometries because of differences in allocation to root storage. *Ann. Bot.* 112, 575–587. doi: 10.1093/aob/mct132

Westoby, M., Falster, D. S., Moles, A. T., Vesk, P. A., and Wright, I. J. (2002). Plant ecological strategies: some leading dimensions of variation between species. *Annu. Rev. Ecol. Syst.* 33, 125–159. doi: 10.1146/annurev.ecolsys.33.010802.150452

Westoby, M., and Wright, I. J. (2003). The leaf size-twig size spectrum and its relationship to other important spectra of variation among species. *Oecologia* 135, 621–628. doi: 10.1007/s00442-003-1231-6

White, J. W., and Montes-R, C. (2005). Variation in parameters related to leaf thickness in common bean (*Phaseolus vulgaris* L.). *Field Crop Res.* 91, 7–21. doi: 10.1016/j.fcr.2004.05.001

Wright, I. J., Reich, P. B., Westoby, M., Ackerly, D. D., Baruch, Z., Bongers, F., et al. (2004). The worldwide leaf economics spectrum. *Nature* 428, 821–827. doi: 10.1038/nature02403

Wright, I. J., and Westoby, M. (2002). Leaves at low versus high rainfall: coordination of structure, lifespan and physiology. *N. Phytol.* 155, 403–416. doi: 10.1046/j.1469-8137.2002.00479.x

Yan, B., Ji, Z., Fan, B., Wang, X., He, G., Shi, L., et al. (2016). Plants adapted to nutrient limitation allocate less biomass into stems in an arid-hot grassland. *N. Phytol.* 221, 1232–1240. doi: 10.1111/nph.13970

Zhang, W., Jia, X., Bai, Y. Y., and Wang, G. (2011). The difference between above- and below-ground self-thinning lines in forest communities. *Ecol. Res.* 26, 819–825. doi: 10.1007/s11284-011-0843-2

Zhang, S., Zhang, J., and Cao, K. (2017). Divergent hydraulic safety strategies in three co-occurring anacardiaceae tree species in a Chinese savanna. *Front. Plant Sci.* 7, 2075. doi: 10.3389/fpls.2016.02075

Zhao, L., Sheppard, L. W., Reid, P. C., Walter, J. A., and Reuman, D. C. (2019). Proximate determinants of taylor's law slopes. *J. Anim. Ecol.* 88, 484–494. doi: 10.1111/1365-2656.12931

frontiers | Frontiers in Plant Science

TYPE Original Research
PUBLISHED 17 October 2022
DOI 10.3389/fpls.2022.996750

OPEN ACCESS

EDITED BY
Runguo Zang,
Chinese Academy of Forestry, China

REVIEWED BY
Jian Liu,
Shandong University, China
Yan Li,
Mianyang Normal University, China

*CORRESPONDENCE
Yao-Bin Song
ybsong@hznu.edu.cn
Ming Dong
dongming@hznu.edu.cn

†These authors have contributed equally to this work and share first authorship

SPECIALTY SECTION
This article was submitted to Functional Plant Ecology, a section of the journal Frontiers in Plant Science

RECEIVED 18 July 2022
ACCEPTED 09 September 2022
PUBLISHED 17 October 2022

CITATION
Li T-X, Shen-Tu X-L, Xu L, Zhang W-J, Duan J-P, Song Y-B and Dong M (2022) Intraspecific and sex-dependent variation of leaf traits along altitude gradient in the endangered dioecious tree *Taxus fuana* Nan Li & R.R. Mill. *Front. Plant Sci.* 13:996750. doi: 10.3389/fpls.2022.996750

Intraspecific and sex-dependent variation of leaf traits along altitude gradient in the endangered dioecious tree *Taxus fuana* Nan Li & R.R. Mill

Tian-Xiang Li†, Xiao-Lu Shen-Tu†, Li Xu, Wei-Jun Zhang, Jun-Peng Duan, Yao-Bin Song* and Ming Dong*

Key Laboratory of Hangzhou City for Ecosystem Protection and Restoration, College of Life and Environmental Sciences, Hangzhou Normal University, Hangzhou, China

Plant intraspecific trait variation (ITV) including sex-dependent differences are matters of many ecological consequences, from individual to ecosystem, especially in endangered and rare species. *Taxus fuana* is an endangered dioecious species with small and isolated populations endemic to the Himalayas region. Little is known about its trait variation between sexes, and among populations. In this study, 18 leaf traits from 179 reproductive trees (males and females) along the altitude (2600-3200m a.s.l.) of the *T. fuana* populations distributed in Gyirong County, Tibet, China, were measured. ITV and sources of variation in leaf traits were assessed. The relationship between leaf traits of males and females and altitude was analyzed separately. Variations in leaf traits of *T. fuana* ranged from 3.1% to 24.2%, with the smallest in leaf carbon content and the largest in leaf thickness to area ratio. On average 78.13% of the variation in leaf traits was from within populations and 21.87% among populations. The trends in leaf width, leaf nitrogen to phosphorus ratio, leaf carbon to nitrogen ratio, leaf carbon isotope ratio, and leaf nitrogen isotope ratio in relation to altitude were the same for males and females. Leaf length to width ratio varied significantly with altitude only in males, while leaf phosphorus content, leaf nitrogen content, and leaf carbon to phosphorus ratio varied significantly with altitude only in females. The correlation coefficients of most leaf traits of females with altitude were larger than that of males. In the relationship between leaf traits, there was a high similarity among males and females, but the altitude accounted for more explanation in females than in males. Our results suggested that the variation in leaf traits of *T. fuana* was small and did not dominate the interspecific competition in the local communities. Adaptation to the altitude gradient of *T. fuana* might be through altering nutrient storage processes and water use efficiency. Adaptation of male and female *T. fuana* to environmental changes showed differences, where the males were more tolerant and the females responded greatly to altitude. The differences in adaptation strategies between male and female *T. fuana* may be detrimental to the maintenance of their populations.

KEYWORDS

altitude, endangered plant, intraspecific trait variation, leaf traits, sex-dependent variation, *Taxus fuana*

Introduction

The earliest study of plant intraspecific trait variation (ITV) could be attributed to the notable novelist and naturalist Johann Wolfgang von Goethe (Stegmann, 2021). However, most early studies in trait-based ecology focused on interspecific variation and only used a mean trait value per species, which assumed smaller trait variation among conspecific individuals (Suding et al., 2008; Shipley et al., 2016). Recent studies found that ITV of some plants could range from 10% to 40% of total variation (Albert et al., 2010; Messier et al., 2010; Siefert et al., 2015; Burton et al., 2017; Gaudard et al., 2019), 25% on average based on a global meta-analysis (Siefert et al., 2015). Another recent meta-analysis showed that the ecological effects of ITV are comparable to species effects (Des Roches et al., 2018). The ecological consequences of ITV have received ever more renewed interest from ecologists (Bolnick et al., 2011), such as population dynamics, interspecific interactions, stability, coexistence, and diversity of ecological communities (Steinmetz et al., 2020). Those findings suggest ITV could not be simply ignored in trait-based ecology (Shipley et al., 2016; Westerband et al., 2021; Rixen et al., 2022).

ITV is thought to be correlated with population size (Steinmetz et al., 2020), which means that populations of endangered species usually have lower ITV compared to widely distributed or common species. Species' trait variation and covariation were thought to contribute to explaining ecological strategies in response to environmental gradients or changes (Jung et al., 2014). For instance, the variability of plant traits with altitude gradient reflects the adaptation of plants to the environment (Mathiasen and Premoli, 2016; de Villemereuil et al., 2018; Rathee et al., 2021). Changes in altitude lead to variations in some other environmental factors (e.g., temperature, light, etc.) that ultimately affect plant trait variability (Körner, 2007; Graae et al., 2012; Hartl-Meier et al., 2014; Sidor et al., 2015). Such trait–environment relationships are important for predicting the responses of global environmental change on individuals and populations of plants (Niinemets et al., 2015; Meng et al., 2017). Meanwhile, higher ITV could stabilize populations from extreme temporal fluctuations in population density and decrease extinction risk (Bolnick et al., 2011). This implies that exploration of ITV of rare and endangered species could contribute to understanding population demography, dynamic, and adaptation to natural and/or anthropogenic disturbances of rare and endangered species in changing environments (Meng et al., 2017; Song et al., 2020a). Therefore, incorporating ITV of rare and endangered species helps to better understand the mechanism for being endangered or threatened and benefits conservation practice (Chown, 2012; Cochrane et al., 2015; Turner et al., 2017; Álvarez-Yépiz et al., 2019). ITV generally includes morphological traits, functional traits, and stoichiometric traits by which to reveal the adaptation strategies of species to heterogeneous environments (Cordell et al., 2001; Elser et al., 2010; Albert et al., 2011; de Bello et al., 2011; Álvarez-Yépiz et al., 2019).

Sexual dimorphism is rather common not only in angiosperm but also in gymnosperm plants (64.6%) based on the latest estimation (Walas et al., 2018), such as Cycadidae, Gnetidae, *Ginkgo*, and some species in Pinidae (e.g. Taxaceae) (Ohri and Rastogi, 2020). The rate of dioecious plants is much higher than monoecious plants in the temperate climate zone (Walas et al., 2018). As for altitude, it has been found that the proportion of dioecious plants decreases with increasing altitude (Lin et al., 2020). Moreover, high altitude tends to exhibit male-biased sexes, while females are more abundant in lower altitude regions, because the relative abundance of environmental conditions is more favorable for the reproduction and survival of females (Ortiz et al., 2002; Juvany and Munné-Bosch, 2015; Retuerto et al., 2018). Due to different reproductive demands and selective pressures, male and female plants usually expressed different physiological, morphological, phenological, and reproductive traits (Obeso, 2002; Song et al., 2016). Studies found that female plants generally have higher photosynthetic rates than males owing to a compensation mechanism for reproductive costs (Obeso, 2002; Wu et al., 2021). In addition, females usually are smaller and grow more slowly than males (Cipollini and Whigham, 1994; Li et al., 2007; Seyedi et al., 2019; Zhang et al., 2019). Accumulating studies on functional sex-related trait differences of dioecious angiosperm plants (e.g.

Populus) responding to stressful biotic and abiotic environmental factors have been conducted under controlled systems (Retuerto et al., 2018; Xia et al., 2020). However, few studies on trait-based ecology incorporated trait variation between genders (Galfrascoli and Calviño, 2020), especially for gymnosperm plants in natural ecosystems across environmental gradients (e.g. altitude).

Taxus fuana Nan Li & R.R. Mill (syn. *Taxus contorta*), is an endangered and dioecious gymnosperm endemic to the Western Himalayas region and grows as a tree or large shrub in the understory of mixed or *Pinus* forests along an altitude gradient ranging from 2600 to 3200 m in Southwest Tibet (China), Nepal, North India, and Pakistan (Shah et al., 2008; Song et al., 2020b). Due to its timber production, traditional medicinal uses, and commercial production of Taxol (i.e. the cancer-inhibitory alkaloid Paclitaxel) like other species of *Taxus*, this species also suffered from heavy anthropologically disturbances (Poudel et al., 2013; Song et al., 2020b). Previous studies found males have higher height, larger diameter, shorter needles, smaller leaf area, and stomata density than females but no differences between sexes in specific leaf area (SLA), leaf nitrogen, and carbon concentration in *T. baccata* (Iszkuło et al., 2009; Cedro and Iszkuło, 2011; Stefanović et al., 2017). However, to date, few studies focused on ITV and sex-dependent variation responding to environmental changes in natural ecosystems, and little is known if there are sexual dimorphisms in terms of leaf functional traits of *T. fuana*.

In this study, we sampled leaf materials and measured 18 leaf traits of *T. fuana* along an altitude gradient (from 2600 m to 3200 m a.s.l.) in Gyirong County, aiming to quantify the ITV and their environmental explanation. Specifically, we address the following scientific questions: 1) What are intraspecific variations (including sex-dependent variations) of leaf traits in *T. fuana*? 2) How do leaf traits of *T. fuana* vary along the altitude gradient? 3) Whether males trees respond differently from female ones along an altitude gradient?

Materials and methods

Study site and sampling

This study was conducted at Gyirong County (28°21′–28°29′ N, 85°13′–85°21′ E, 2600-3200 m a.s.l.), southwest of Tibet in China. The region is a subtropical mountain monsoon climate, with a mean average temperature of 8 - 11°C, and a mean annual precipitation of 800 mm. Based on our field survey, we observed 6 main (sub)populations with total individuals of more than 5000 which showed significantly male-biased populations in this area (Song et al., 2020b).

Among six known populations (Tangbo, Kaire, Guofu, Jilong, Langjiu, and Jipu) (Song et al., 2020b; Li et al., 2022) (Figure 1), individuals of *T. fuana* were randomly selected along an altitude gradient, with the distance between trees ensured to be above 50 m as far as possible. Fresh, mature (fully developed), and healthy leaves (needles) of *T. fuana* were sampled during the growing season (July–August) in 2018. In total, 179 samples were collected, of which 85 were males and 94 were females (The sex of the trees was identified according to whether they had obvious female cone or staminate strobilus). For each tree, we measured diameter at breast height (DBH), tree height, and altitude of the locality.

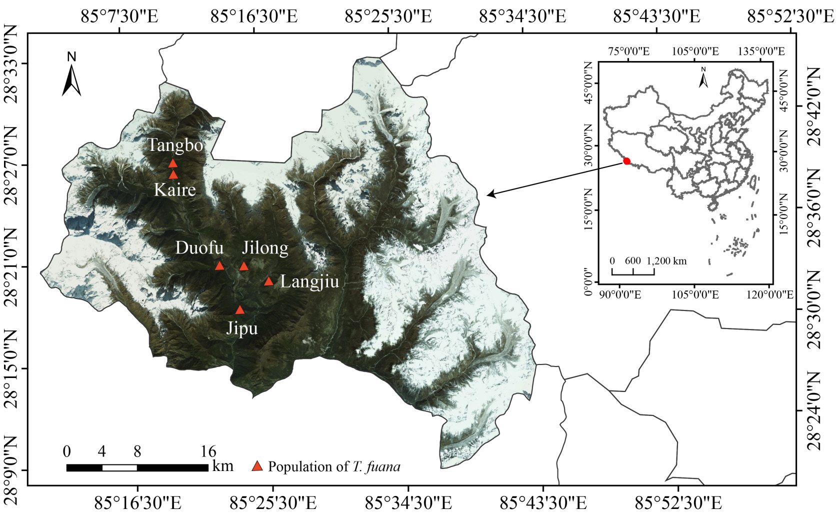

FIGURE 1
Geographical distribution of sampling sites (Li et al., 2022).

Leaf traits measurement

A total of 18 leaf traits were measured and categorized into morphological traits, functional traits, and stoichiometric traits (Pérez-Harguindeguy et al., 2013). For morphological traits, 10 fresh leaves from each tree were randomly selected and the thickness of each leaf was measured with a vernier caliper (0.01 mm), which was used to calculate the mean leaf thickness (LT) (mm) of each tree. Then, those leaves of each tree were separately immersed in water overnight, blotted up water, and measured for water-saturated weight. After that, the same leaf samples were scanned with a photo scanner and weighed after oven-dried at 60°C for 72h. Leaf area (LA) (cm^2), leaf length (LL) (cm), leaf width (LW) (cm), leaf perimeter (LP) (cm) of each sample were accessed from scanned photo with ImageJ (http://imagej.nih.gov/ij/), which also was used to determine leaf length to width ratio [leaf length (cm)/leaf width(cm)] (LLWR) ($cm\ cm^{-1}$), leaf thickness to area ratio [leaf thickness (cm)/leaf area (cm^2)] (LTAR) ($cm\ cm^{-2}$) and leaf profile index [leaf perimeter (cm)/ $\sqrt{LA}$ (cm)] (LPI) ($cm\ cm^{-1}$) (Pérez-Harguindeguy et al., 2013).

For functional traits, the specific leaf area (SLA) ($cm^2\ g^{-1}$) of each sample was calculated as the ratio of sample leaf area to oven-dry weight. Leaf dry matter content (LDMC) ($g\ g^{-1}$) was determined by the ratio of leaf oven-dry weight to water-saturated weight. Leaf carbon (C) and nitrogen (N) content ($mg\ g^{-1}$) was determined using an elemental analyzer (vario MICRO cube; Elemental, Germany) (Hu et al., 2015). Leaf phosphorus content (P) ($mg\ g^{-1}$) was determined by digestion with $HClO_4$-HNO_3 and then measured by Prodigy7 ICP-OES Spectrometer (Leeman, US) (Hu et al., 2019).

For stoichiometric traits, leaf carbon to nitrogen ratio (C:N), leaf carbon to phosphorus ratio (C:P), and leaf nitrogen to phosphorus ratio (N:P) were calculated by the ratio of leaf C to leaf N, leaf C to leaf P and leaf N to leaf P, respectively. Leaf carbon isotope ratio ($\delta^{13}C$) (‰) and leaf nitrogen isotope ratio ($\delta^{15}N$) (‰) were determined using the elemental analyzer coupled to an isotope ratio mass spectrometer (Isoprime100; Isoprime Ltd, Germany) (Hu et al., 2017; Hu et al., 2022; Tan et al., 2022).

Statistical analyses

To describe the variation of *T. fuana* traits, the mean, minimum, maximum, and median values, as well as standard errors, and coefficients of variation (CV) were calculated for each leaf trait (Kumordzi et al., 2014). In order to analyze the intra-population variation of leaf traits, non-parametric multivariate analysis of variance with the "*adonis*" function in the "vegan" package was used to obtain among and within populations variance values for leaf traits, which were used as sources of variation among and within populations (Anderson, 2001). To investigate the overall response of *T. fuana* to environmental heterogeneity caused by altitude changes and the differential performance between males and females, a correlation analysis was conducted.

To explore the interrelationships among leaf traits of male and female *T. fuana*, and the differences between males and females, piecewise structural equation models (piecewiseSEM) were fitted to the leaf traits of male and female *T. fuana*, respectively (Lefcheck, 2016; Liu et al., 2020). Because the differences in light, water and heat conditions at different altitude (Körner, 2007; Moser et al., 2010) may have a greater impact on leaf traits of *T. fuana*, altitude was included as a random effect in the model, and the differences in marginal R^2 (fixed factors only) and conditional R^2 (all factors, including the random effect) were analyzed to assess the effect of altitude in *T. fuana* (Nakagawa and Schielzeth, 2013). Interrelationships among leaf traits were analyzed by standardized path coefficients. The fit of the model was confirmed using Fisher's C test (when $0 \leq$ Fisher's $C \leq 2$ and $0.05< P \leq 1.00$). The model was optimized by eliminating non-significant paths or factors (e.g., tree height, DBH, etc.), and the final model was obtained by comparison of models (Huang et al., 2020). The original model was constructed based on existing knowledge of the interrelationships of leaf traits (Navarro et al., 2010). A $\log_{10}$ transformation of the data was performed before model building. The main R packages involved in the model fitting process were "piecewiseSEM", "nlme", and "lme4" (Pinheiro et al., 2014; Lefcheck, 2016). All analyses were conducted using the statistical software R 4.2.1 (R Core Team, 2022).

Results

The variation of leaf traits in *T. fuana*

There was some variability among the 18 leaf traits of *T. fuana* (Table 1). The coefficients of variation were in the range of 3.1% to 24.2%. The larger variation occurred in leaf area, leaf thickness to area ratio, SLA, leaf P, and leaf C:P, respectively. The leaf thickness to area ratio was the most variable, ranging from 0.601-2.602, and the coefficient of variation was 24.2%. The smaller variation included leaf profile index, leaf C, and leaf $\delta^{13}C$, where the smallest variation was in leaf C, ranging from 460.674 to 527.157 and the coefficient of variation was 3.1%.

The results obtained from non-parametric analysis of variance showed that 78.13% of the 18 leaf traits variation for *T. fuana* could be attributed to differences within populations, while the remaining 21.87% explained variation among populations (Table 2) (F = 9.684, P = 0.001). The results indicated that the variation in leaf traits of *T. fuana* mainly occurred within populations.

TABLE 1 Descriptive statistics of 18 leaf traits in *T. fuana* in six populations.

Leaf traits	Unit	N	Mean	SE	Min	Med	Max	CV (%)
LT	mm	179	0.481	0.004	0.372	0.477	0.642	10.6
LL	cm	179	2.730	0.031	1.658	2.720	4.255	15.3
LW	cm	179	0.197	0.002	0.121	0.196	0.255	11.0
LP	cm	179	6.228	0.068	3.886	6.204	9.520	14.6
LA	cm^2	179	0.562	0.009	0.269	0.551	1.133	22.5
LLWR	cm cm^{-1}	179	13.985	0.138	9.904	14.095	18.348	13.2
LTAR	cm cm^{-2}	179	1.171	0.021	0.601	1.131	2.602	24.2
LPI	cm cm^{-1}	179	8.337	0.033	7.301	8.303	9.330	5.3
SLA	cm^2 g^{-1}	179	79.680	1.332	40.738	77.826	141.937	22.4
LDMC	g g^{-1}	179	0.358	0.003	0.279	0.356	0.474	10.1
Leaf C	mg g^{-1}	179	499.408	1.147	460.674	503.608	527.157	3.1
Leaf N	mg g^{-1}	179	14.880	0.195	8.294	15.011	21.852	17.5
Leaf P	mg g^{-1}	179	1.595	0.028	0.844	1.524	3.493	23.7
Leaf C:N	–	179	34.640	0.486	23.126	33.529	58.770	18.8
Leaf C:P	–	179	328.896	5.437	141.577	327.732	609.256	22.1
Leaf N:P	–	179	9.564	0.123	5.844	9.560	14.572	17.3
Leaf δ^{13}C	‰	179	−28.345	0.087	−31.613	−28.247	−25.282	−4.1
Leaf δ^{15}N	‰	179	0.727	0.127	−2.913	0.632	5.498	232.9

Due to positive and negative values of leaf δ^{15}N, there was a large degree of data dispersion, the CV of leaf δ^{15}N was excluded from the analysis. LT, leaf thickness; LL, leaf length; LW, leaf width; LP, leaf perimeter; LA, leaf area; LLWR, leaf length to width ratio; LTAR, leaf thickness to area ratio; LPI, leaf profile index; SLA, specific leaf area; LDMC, leaf dry matter content; Leaf C, leaf carbon content; Leaf N, leaf nitrogen content; Leaf P, leaf phosphorus content; Leaf C:N, leaf carbon to nitrogen ratio; Leaf C:P, leaf carbon to phosphorus ratio; Leaf N:P, leaf nitrogen to phosphorus ratio; Leaf δ^{13}C, leaf carbon isotope ratio; Leaf δ^{15}N, leaf nitrogen isotope ratio.

Patterns of variation in leaf traits with altitude in *T. fuana*

On the whole, the leaf thickness ($r = -0.149$, $P = 0.047$) (Figure 2A), leaf width ($r = -0.335$, $P < 0.001$) (Figure 2C), leaf N ($r = -0.205$, $P = 0.006$) (Figure 2L), leaf C:P ($r = -0.235$, $P = 0.002$) (Figure 2O), leaf N:P ($r = -0.572$, $P < 0.001$) (Figure 2P) of *T. fuana* were significantly negatively correlated with altitude, whereas the leaf length to width ratio ($r = 0.215$, $P = 0.004$) (Figure 2F), leaf P ($r = 0.283$, $P < 0.001$) (Figure 2M), leaf C:N ($r = 0.279$, $P < 0.001$) (Figure 2N), leaf δ^{13}C ($r = 0.230$, $P = 0.002$) (Figure 2Q), leaf δ^{15}N ($r = 0.243$, $P = 0.001$) (Figure 2R) were significantly positively associated with altitude. The remaining leaf traits were not significantly related to altitude (Figures 2B, D, E, G–K).

In terms of sex, the leaf width (female: $r = -0.338$, $P = 0.001$; male: $r = -0.334$, $P = 0.002$) (Figure 2C) and leaf N:P (female: $r = -0.750$, $P < 0.001$; male: $r = -0.322$, $P = 0.003$) (Figure 2P) of female and male *T. fuana* were significantly negatively correlated with altitude, whereas leaf C:N (female: $r = 0.312$, $P = 0.002$; male: $r = 0.246$; $P = 0.023$) (Figure 2N), leaf δ^{13}C (female: $r = 0.234$, $P = 0.023$; male: $r = 0.235$, $P = 0.030$) (Figure 2Q), and leaf δ^{15}N (female: $r = 0.241$, $P = 0.019$; male: $r = 0.244$, $P = 0.025$) (Figure 2R) were significantly positively correlated with altitude in both female and male. However, the leaf length to width ratio (male: $r = 0.318$, $P = 0.003$) (Figure 2F) showed a significant increase with altitude only in males. In addition, leaf P (female: $r = 0.485$, $P < 0.001$) (Figure 2M) increased significantly with altitude only in females, and leaf N (female: $r = -0.223$, $P = 0.030$) (Figure 2L) and leaf C:P (female: $r = -0.476$, $P < 0.001$) (Figure 2O) decreased significantly with altitude only in females. It was worth noting that the number of leaf traits significantly correlated with altitude in females was higher than that in males, as well as the magnitude of correlation coefficients.

TABLE 2 Non-parametric analysis of variation for 18 leaf traits of *T. fuana* in six populations.

Source of variation	d.f.	Sum of squares	Mean of squares	Percentage of variation	*F*	*P*
Among populations	5	0.1221	0.0244	21.87	9.684	0.001
Within populations	173	0.4362	0.0025	78.13		
Total	178	0.5583				

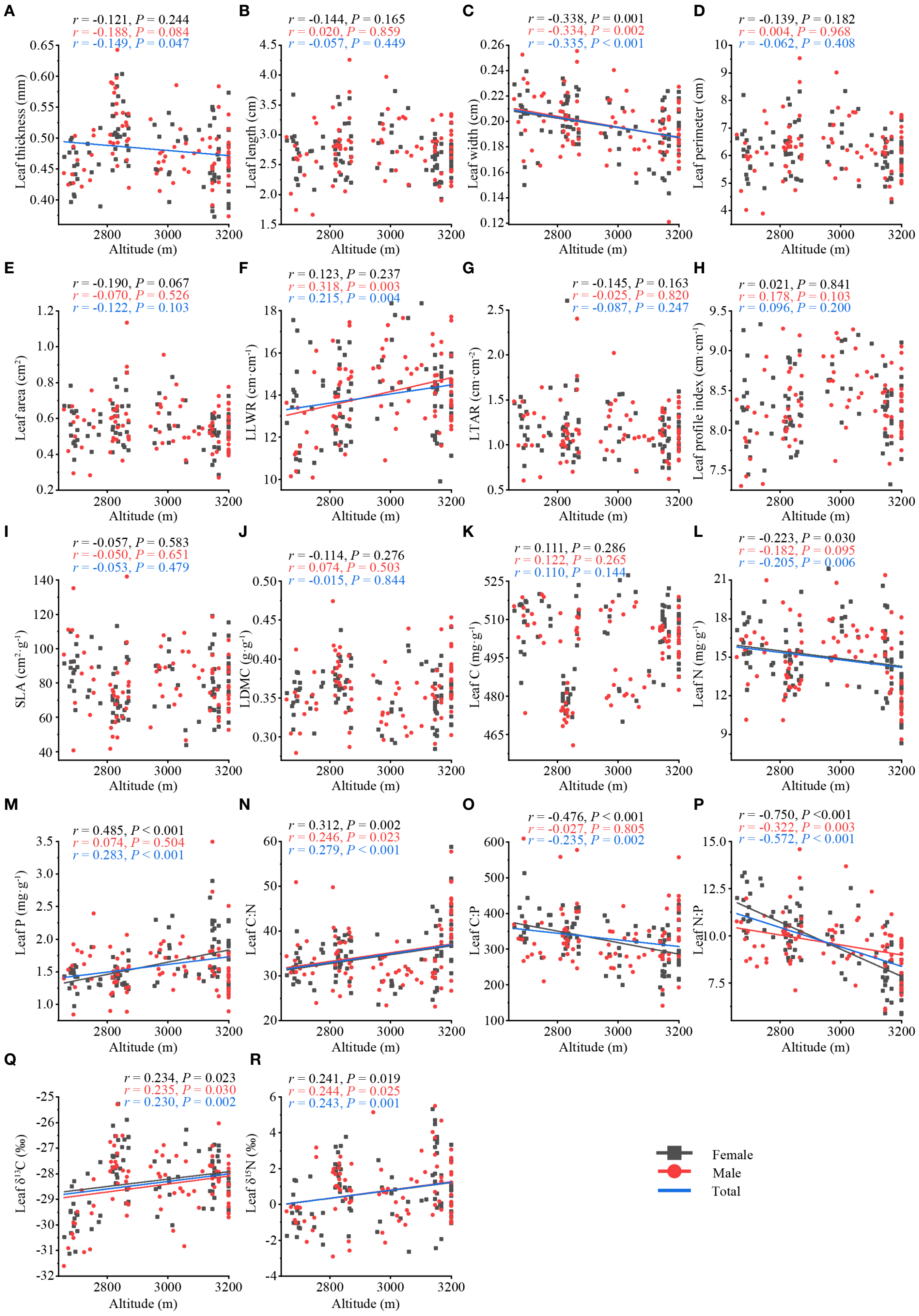

FIGURE 2
Relationship between leaf traits (total, female, male) along altitude in *T. fuana*. Morphological traits **(A–H)**, functional traits **(I–M)**, and stoichiometric traits **(N–R)**. Regression lines were plotted for significant relationships with $P < 0.05$. LLWR, leaf length to width ratio; LTAR, leaf thickness to area ratio; SLA, specific leaf area; LDMC, leaf dry matter content; Leaf C, leaf carbon content; Leaf N, leaf nitrogen content; Leaf P, leaf phosphorus content; Leaf C:N, leaf carbon to nitrogen ratio; Leaf C:P, leaf carbon to phosphorus ratio; Leaf N:P, leaf nitrogen to phosphorus ratio; Leaf δ^{13}C, leaf carbon isotope ratio; Leaf δ^{15}N, leaf nitrogen isotope ratio.

Interrelations between male and female leaf traits in *T. fuana*

Results of the structural equation model revealed that there was a greater similarity in the relationship between male and female leaf traits of *T. fuana* (Figures 3A, B). However, some differences were shown between the two models. As far as the direct effects of leaf traits are concerned, the principal variation in leaf traits between male and female *T. fuana* was manifested by the intervention of the additional leaf length and the relationship between leaf area and leaf C with other leaf traits in males. On the other hand, the path coefficients between leaf traits of male *T. fuana* were relatively larger than those of females.

The two structural equation models in this study differed significantly in the amount of explanation for leaf traits (Table 3). In female *T. fuana*, except for the LDMC, the conditional R^2 (all factors) of the model for leaf traits was above 0.6. The variation of LDMC and leaf area explained by the model was minimum and maximum, respectively, and the conditional R^2 (all factors) was 0.29 and 0.83. Correspondingly, the model of male *T. fuana* explained the variation of leaf $\delta^{15}N$ was minimum, the conditional R^2 (all factors) was 0.29. Among the other leaf traits, there were three leaf traits with conditional R^2 (all factors) reaching 0.8, these were SLA, leaf P, and leaf $\delta^{13}C$. On the whole, the conditional R^2 (all factors) of most leaf traits in male *T. fuana* was greater than that of females. Regarding marginal R^2 (fixed effects), females had lower marginal R^2 (fixed effects) than males except for leaf N. In contrast, the difference between marginal R^2 (fixed effects) and conditional R^2 (all factors) was higher in females than in males overall, which indicated that the random factor "altitude" accounted for more explanation in females than in males, namely, altitude had a higher effect on leaf traits in female *T. fuana* than in males.

Discussion

Extent and sources of leaf trait variation in *T. fuana*

Generally, in most of the ecological studies on functional traits, the mean value of a trait was often taken to represent the whole species while ignoring ITV, which assumed there were few intraspecific variations compared to interspecific variations (Bolnick et al., 2011; de Bello et al., 2011; Shipley et al., 2016). However, numerous important functional traits showed considerable intraspecific variation with potential ecological effects similar to interspecific variation (Albert et al., 2011; Siefert et al., 2015; Moran et al., 2016; Laughlin et al., 2017; He et al., 2021; Rixen et al., 2022). The loss of ITV was even thought to be an important reason for its rareness in some wild species (Severns and Liston, 2008; González-Suárez and Revilla, 2013; Wang et al., 2022). Increasingly, studies found that ITV was probably an important ecological variable (Moran et al., 2016; Derroire et al., 2018; Mougi, 2020; Senthilnathan and Gavrilets, 2021), which played a non-negligible role in species coexistence (Ehlers et al., 2016; Hart et al., 2016; Zhang and Yu, 2018; Wang et al., 2022), interspecific competition (Kostikova et al., 2016; He et al., 2018; Xu et al., 2020), and population maintenance (Deepa, 2009; Bolnick et al., 2011; Raffard et al., 2019), etc. In this study, we found that leaf traits of six populations of *T. fuana* exhibited a certain degree of ITV, and the variation of leaf traits mostly originated from within populations and a small portion from among populations, which may be related to the distribution of *T. fuana* and local community features (Zhang et al., 2020; Li et al., 2022). It was shown that the importance of interspecific trait variation was likely to be greater than that of ITV at the large spatial scales of the study subjects. However, along with decreasing scales, for ITV, their relative importance would continually increase and possibly even emerge similar to that of interspecific trait variation (Messier et al., 2010; Albert et al., 2011; Kumordzi et al., 2014). Other studies had showed that the greater habitat heterogeneity, the more intraspecific and interspecific trait variation would be (Zhang and Yu, 2018; Homeier et al., 2021). The distribution area of *T. fuana* in the Gyirong region was relatively narrow (Song et al., 2020b), hence it showed a certain extent of ITV. Generally, the variation within populations reflects the plasticity and flexibility of the species to adapt to the environment, while the variation among populations reveals the influence of environmental selection (Siefert et al., 2015; Lajoie and Vellend, 2018; Moran et al., 2022). We found a small proportion of the ITV in *T. fuana* originated from among populations, perhaps because of the narrow distribution with little environmental heterogeneity among populations, and then failed to generate a large variation. In addition, the majority of trait variations originating from within populations may be associated with the position of *T. fuana* in the tree layer of the local community (Dan et al., 2020; Song et al., 2020b; Zhang et al., 2020). Plant communities in the Gyirong region were dominated by the tree layer, and strong interspecific competition led to a large plastic variation within the population. Therefore, the interactions between biotic factors in the community were perhaps the primary factors that determined the variation in *T. fuana* leaf traits.

Variation patterns of leaf traits along altitude in *T. fuana*

Plant trait variation is often influenced by climate and topography (Brousseau et al., 2013; Heilmeier, 2019; Dobbert et al., 2021; Joswig et al., 2022), which in general is mainly influenced by climatic factors at the global scale and by topographic factors at the small scale (van Bodegom et al., 2014;

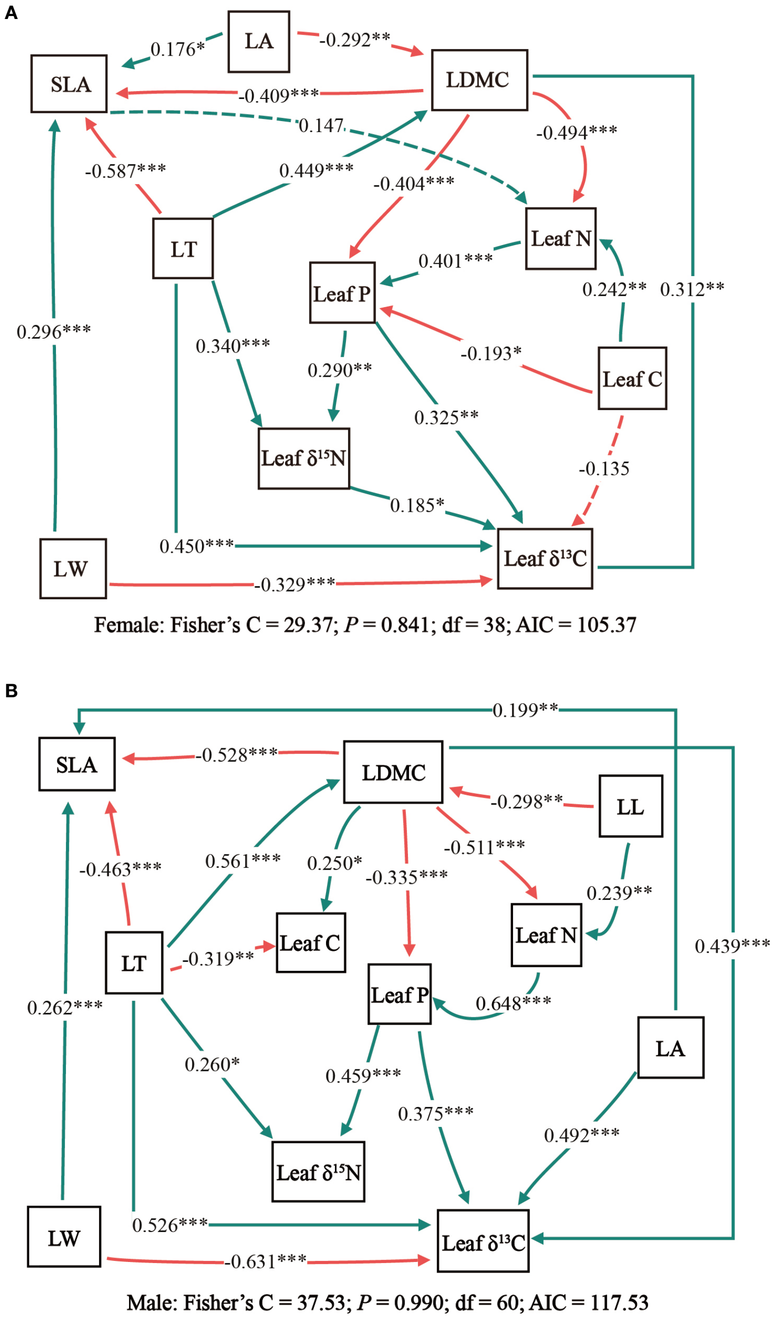

FIGURE 3
The piecewise structural equation models for testing the interrelations of leaf traits in female **(A)** and male **(B)** *T. fuana*. Solid arrows represent significant paths ($P < 0.05$) and dashed arrows represent non-significant paths ($P > 0.05$). The red arrows reflect negative relationships and the green arrows reflect positive relationships. Each path coefficient was standardized. *, **, *** indicated $P < 0.05$, $P < 0.01$, $P < 0.001$, respectively. LT, leaf thickness; LL, leaf length; LW, leaf width; LA, leaf area; SLA, specific leaf area; LDMC, leaf dry matter content; Leaf C, leaf carbon content; Leaf N, leaf nitrogen content; Leaf P, leaf phosphorus content; Leaf $\delta^{13}C$, leaf carbon isotope ratio; Leaf $\delta^{15}N$, leaf nitrogen isotope ratio.

Bruelheide et al., 2018; Myers-Smith et al., 2019; Shao et al., 2019; Zheng et al., 2022). Altitude is a key topographic factor (Graae et al., 2012; Waigwa et al., 2020; Tang et al., 2022), and changes in altitude can lead to changes in temperature (Sidor et al., 2015; Chen et al., 2018), precipitation (Luce et al., 2013; Herrmann et al., 2016), light (Körner, 2007; Thakur et al., 2019), etc., resulting in hydrothermal differences that affect plant traits (Hartl-Meier et al., 2014; Zhang et al., 2022). In this study, we found that the leaf traits of *T. fuana*

TABLE 3 The marginal R^2 and conditional R^2 of the structural equation model in functional traits of female and male *T. fuana*.

Response variable	Female		Male	
	Marginal R^2	Conditional R^2	Marginal R^2	Conditional R^2
SLA	0.75	0.83	0.86	0.87
LDMC	0.22	0.29	0.34	0.47
Leaf P	0.46	0.69	0.69	0.80
Leaf C	–	–	0.08	0.72
Leaf N	0.47	0.67	0.41	0.57
Leaf $\delta^{15}N$	0.12	0.67	0.20	0.29
Leaf $\delta^{13}C$	0.46	0.64	0.49	0.80

Marginal R^2 represents the variance explanation that includes only fixed effects, and conditional R^2 represents the variance explanation that includes both fixed and random effects. "-" indicating the absence of marginal R^2 and conditional R^2 due to the elimination of paths to leaf C during the modification of the model. SLA, specific leaf area; LDMC, leaf dry matter content; Leaf C, leaf carbon content; Leaf N, leaf nitrogen content; Leaf P, leaf phosphorus content; Leaf $\delta^{13}C$, leaf carbon isotope ratio; Leaf $\delta^{15}N$, leaf nitrogen isotope ratio.

showed different trends with altitude. Among them, leaf width became significantly smaller with altitude, while the leaf length did not change significantly with altitude, thus leading to a larger leaf length to width ratio with altitude. This indicated that the leaves of *T. fuana* were more needle-shaped with increasing altitude. It was also found that the leaf thickness decreased slightly with altitude, indicating that the leaves became softer while needle-shaped, which was probably related to the adaptation of *T. fuana* to snowfall and resistance to the tearing by strong winds. As the altitude increases, the likelihood and amount of snowfall become greater (Šípek and Tesař, 2014; Deng et al., 2017). The more needle-shaped and softer leaves would better avoid excessive snow accumulation and reduce damage, as well as resist extreme wind with some advantages (Read and Sanson, 2003; Onoda et al., 2011; Hua et al., 2020). In other aspects, the variation of leaf carbon content with altitude was not significant, thus the significant variation of leaf carbon to nitrogen ratio and leaf carbon to phosphorus ratio with altitude was mainly determined by the change in leaf nitrogen content and leaf phosphorus content, which indicated that the leaf carbon content of *T. fuana* was highly stable in accordance with universality (McGroddy et al., 2004; Elser et al., 2010; Yang and Luo, 2011). The leaf nitrogen content was reduced with increasing altitude, while the leaf phosphorus content showed the opposite trend, which in turn contributed to the reduction of leaf nitrogen to phosphorus ratio with increasing altitude. The leaf nitrogen content, leaf phosphorus content, and leaf nitrogen to phosphorus ratio reflect the nutrient utilization status of plants (Thompson et al., 1997; Reich and Oleksyn, 2004; Chen et al., 2013). The mean value of leaf nitrogen to phosphorus ratio in this study was 9.564, indicating that the growth and development of *T. fuana* were principally limited by nitrogen (Koerselman and Meuleman, 1996; Güsewell et al., 2003; LeBauer and Treseder, 2008). The decrease in nitrogen mineralization rate with increasing altitude probably inhibited the uptake of nitrogen by plants and thus caused a decrease in leaf nitrogen content (Reich and Oleksyn, 2004). In addition, the reduced plant growth and metabolic activities may also lead to lower leaf nitrogen content as the temperature drops with increasing altitude (Elser et al., 2003). In general, plants prefer to accumulate excess nutrients in extreme environments, especially excess leaf phosphorus content to enhance survival (Chapin, 1990; Cordell et al., 2001). Therefore, as the habitat was progressively harsher with increasing altitude, *T. fuana* might improve leaf phosphorus to adapt to the habitat change, especially under nitrogen limitations. This suggested that the environmental heterogeneity caused by altitude change affected the nutrient storage process of *T. fuana*. It was at the same time found that both leaf $\delta^{13}C$ and leaf $\delta^{15}N$ were greater with increasing altitude, which seemed to be related to the temperature and precipitation variability caused by altitude changes (Zhou et al., 2011; Yang et al., 2013; Li et al., 2017). In general, both temperature and precipitation were reduced with increasing altitude, and the reduction of temperature would diminish the diffusion capacity of CO_2 in leaves, which in turn reduced the CO_2 conductance of stomata and increased $\delta^{13}C$ in leaves (Hultine and Marshall, 2000; Diefendorf et al., 2010). Meanwhile, leaf $\delta^{13}C$ was an indicator of plant water use efficiency, and the higher the leaf $\delta^{13}C$, the higher the plant water use efficiency (Pascual et al., 2013; Barbour, 2017). This indicated that the water use efficiency of *T. fuana* gradually improved with increasing altitude and precipitation reduction, which was a manifestation that *T. fuana* adapted to environmental changes. The relationship between leaf $\delta^{15}N$ and altitude was complicated, and the correlation differed with the species and environment in the studies (Liu and Wang, 2009; Gavazov et al., 2016; Wang et al., 2019). It has been shown that plant $\delta^{15}N$ relates more to climate globally, such as negative relation with precipitation and positively correlated with temperature (Amundson et al., 2003). In this study, leaf $\delta^{15}N$ was positively correlated with altitude, and from another perspective, it could be considered to be indirectly negatively correlated with temperature and precipitation, i.e., it is consistent with the relationship of precipitation in the global pattern and opposite to that of temperature. The possible reason was that the increase in altitude would lead to a decrease in precipitation and temperature, but the Gyirong region was more influenced by the warm and humid airflow from the Indian Ocean (Adhikari and Mejia, 2021; Li et al., 2022), so that precipitation might have a more prominent effect on *T. fuana*. Therefore, the leaf $\delta^{15}N$ of *T. fuana* showed a positive trend with altitude. It implied that environmental factors are important drivers affecting the variation of *T. fuana* leaf traits, and their specific roles should be further considered in future studies.

Interrelations and differences between male and female *T. fuana* leaf traits

Differences between dioecious plant traits and their response to environmental changes might detrimentally affect population maintenance (Melnikova et al., 2017; Hultine et al., 2018; LeRoy et al., 2020). In this study, leaf width, leaf nitrogen to phosphorus ratio, leaf carbon to nitrogen ratio, leaf $\delta^{13}C$, and leaf $\delta^{15}N$ showed similar trends with altitude between male *T. fuana* and females, which reflected the similarity in adaptation to altitude changes between genders. Comparing the two structural equation models also exhibited such a situation, i.e., a greater similarity in the relationship between male and female leaf traits. This illustrated the coherence of adaptation strategies between male and female *T. fuana* (Ortiz et al., 2002; Munné-Bosch, 2015; Wang et al., 2018). However, in the correlation coefficients between leaf traits and altitude, females were mostly greater than males. Moreover, females exhibited remarkable performance in terms of stoichiometric characteristics. For instance, in leaf nitrogen content, leaf carbon to phosphorus ratio, and leaf phosphorus content, females reached significant levels with altitude only. Meanwhile, males showed relatively pronounced morphological characteristics, such as in leaf length to width ratio, where males reached significant levels with altitude only. These suggested that female *T. fuana* responded more strongly to altitude, and it can be inferred that the differences are mainly in nutrient utilization, while male *T. fuana* showed more stability to environmental heterogeneity caused by altitude changes (Lei et al., 2017). This might be related to the fact that males are more focused on vegetative growth, i.e. males may devote more resources to vegetative growth and thus have greater tolerance to corresponding environmental changes (Obeso, 2002; Meinzer et al., 2011). This was further illustrated in the performance of structural equation models, where the path coefficients among male leaf traits were mostly larger than the corresponding path coefficients for females (e.g., SLA, LDMC, leaf N, P, etc.). This may be related to the difference in resource absorption between the sexes. Studies showed that female trees allocated higher resources to reproduction than males, while males were likely to devote more resources to vegetative growth (Tognetti, 2012; Hultine et al., 2016; Lei et al., 2017). Therefore, this may result in the leaf traits of males being more closely linked and more tolerant to environmental changes, while females are more susceptible to multiple factors. A similar phenomenon was presented for the explained values (marginal R^2 (fixed effect) and conditional R^2 (all factors)). This suggested that the fixed factors could explain more variation in male *T. fuana* leaf traits than in females, while the random factor (altitude) accounted for a greater amount of explanation in females. Therefore, the inference seems to be that female *T. fuana* was more influenced by other factors or responded more strongly to environmental variability. Males, on the other hand, possess higher stability and could tolerate more environmental changes. This result supports previous studies that males were more adaptable than females and in a more favorable position in population development, which in turn possibly led to male-biased sex in *T. fuana* populations (Song et al., 2020b). Overall, it is inferred that male and female *T. fuana* exhibited greater similarity in their strategies for adapting to environmental changes, but there was also a considerable extent of variation between the male and female.

Conclusions

The analysis revealed that the variance of *T. fuana* leaf traits was at a low level and did not dominate the interspecific competition in the local communities. Altitude was an important factor affecting the variation of *T. fuana* leaf traits. Adaptation of *T. fuana* to altitude gradient probably through altered nutrient storage processes and water use efficiency. The growth and development of *T. fuana* was restricted mainly by nitrogen, and probably adapted to the altitude change by modifying the nutrient storage process and water use efficiency. Male and female *T. fuana* showed differences in their strategies for adapting to environmental variability, where the male *T. fuana* was more tolerant and the females responded more strongly to altitude changes and were more influenced by the environment. The differences in adaptation strategies between male and female *T. fuana* may be detrimental to the maintenance of their populations, besides the environment was an important aspect affecting *T. fuana*, which deserved further consideration in future studies.

Data availability statement

The original contributions presented in the study are included in the article/supplementary files. Further inquiries can be directed to Yao-Bin Song, ybsong@hznu.edu.cn or Ming Dong, dongming@hznu.edu.cn.

Author contributions

Y-BS and MD contributed to the conception of the study. X-LS-T, T-XL, LX, W-JZ, J-PD performed the experiment and collected data. T-XL and X-LS-T analyzed the data. T-XL and

Y-BS wrote the manuscript. All authors contributed to the article and approved the submitted version.

Funding

This research was funded by the National Key Research and Development Program of China, grant numbers 2016YFC0503100; and the National Natural Science Foundation of China, grant number 31670429 and 31400346.

Acknowledgment

We thank Yu-Lu Qin, Wang-Kai Shu, and Jun-Chao Ruan for their help in data collection.

Conflict of interest

The authors declare that the research was conducted in the absence of any commercial or financial relationships that could be construed as a potential conflict of interest.

Publisher's note

References

Adhikari, P., and Mejia, J. F. (2021). Influence of aerosols on clouds, precipitation and freezing level height over the foothills of the Himalayas during the Indian summer monsoon. *Clim. Dyn.* 57, 395–413. doi: 10.1007/s00382-021-05710-2

Albert, C. H., Grassein, F., Schurr, F. M., Vieilledent, G., and Violle, C. (2011). When and how should intraspecific variability be considered in trait-based plant ecology? *Perspect. Plant Ecol. Evol. Syst.* 13, 217–225. doi: 10.1016/j.ppees.2011.04.003

Albert, C. H., Thuiller, W., Yoccoz, N. G., Soudant, A., Boucher, F., Saccone, P., et al. (2010). Intraspecific functional variability: Extent, structure and sources of variation. *J. Ecol.* 98, 604–613. doi: 10.1111/j.1365-2745.2010.01651.x

Álvarez-Yépiz, J. C., Búrquez, A., Martínez-Yrízar, A., and Dovciak, M. (2019). A trait-based approach to the conservation of threatened plant species. *Oryx* 53, 429–435. doi: 10.1017/s003060531800087x

Amundson, R., Austin, A. T., Schuur, E. A. G., Yoo, K., Matzek, V., Kendall, C., et al. (2003). Global patterns of the isotopic composition of soil and plant nitrogen. *Glob. Biogeochem. Cycle* 17, 1031. doi: 10.1029/2002GB001903

Anderson, M. J. (2001). A new method for non-parametric multivariate analysis of variance. *Aust. Ecol.* 26, 32–46. doi: 10.1111/j.1442-9993.2001.01070.pp.x

Barbour, M. M. (2017). Understanding regulation of leaf internal carbon and water transport using online stable isotope techniques. *New Phytol.* 213, 83–88. doi: 10.1111/nph.14171

Bolnick, D. I., Amarasekare, P., Araújo, M. S., Bürger, R., Levine, J. M., Novak, M., et al. (2011). Why intraspecific trait variation matters in community ecology. *Trends Ecol. Evol.* 26, 183–192. doi: 10.1016/j.tree.2011.01.009

Brousseau, L., Bonal, D., Cigna, J., and Scotti, I. (2013). Highly local environmental variability promotes intrapopulation divergence of quantitative traits: An example from tropical rain forest trees. *Ann. Bot.* 112, 1169–1179. doi: 10.1093/aob/mct176

Bruelheide, H., Dengler, J., Purschke, O., Lenoir, J., Jiménez-Alfaro, B., Hennekens, S. M., et al. (2018). Global trait-environment relationships of plant communities. *Nat. Ecol. Evol.* 2, 1906–1917. doi: 10.1038/s41559-018-0699-8

Burton, J. I., Perakis, S. S., McKenzie, S. C., Lawrence, C. E., and Puettmann, K. J. (2017). Intraspecific variability and reaction norms of forest understory plant species traits. *Funct. Ecol.* 31, 1881–1893. doi: 10.1111/1365-2435.12898

Cedro, A., and Iszkuło, G. (2011). Do females differ from males of European yew (*Taxus baccata* L.) in dendrochronological analysis? *Tree-Ring Res.* 67, 3–11. doi: 10.3959/2009-9.1

Chapin, F. (1990). The ecology and economics of storage in plants. *Annu. Rev. Ecol. Syst.* 21, 423–447. doi: 10.1146/annurev.es.21.110190.002231

Chen, Y. H., Han, W. X., Tang, L. Y., Tang, Z. Y., and Fang, J. Y. (2013). Leaf nitrogen and phosphorus concentrations of woody plants differ in responses to climate, soil and plant growth form. *Ecography* 36, 178–184. doi: 10.1111/j.1600-0587.2011.06833.x

Chen, L., Huang, J. G., Ma, Q. Q., Hänninen, H., Rossi, S., Piao, S. L., et al. (2018). Spring phenology at different altitudes is becoming more uniform under global warming in Europe. *Glob. Change Biol.* 24, 3969–3975. doi: 10.1111/gcb.14288

Chown, S. L. (2012). Trait-based approaches to conservation physiology: Forecasting environmental change risks from the bottom up. *Philos. Trans. R. Soc B.* 367, 1615–1627. doi: 10.1111/1365-2656.13462

Cipollini, M. L., and Whigham, D. F. (1994). Sexual dimorphism and cost of reproduction in the dioecious shrub *Lindera benzoin* (Lauraceae). *Am. J. Bot.* 81, 65–75. doi: 10.1002/j.1537-2197.1994.tb15410.x

Cochrane, A., Yates, C. J., Hoyle, G. L., and Nicotra, A. B. (2015). Will among-population variation in seed traits improve the chance of species persistence under climate change? *Glob. Ecol. Biogeogr.* 24, 12–24. doi: 10.1111/geb.12234

Cordell, S., Goldstein, G., Meinzer, F. C., and Vitousek, P. M. (2001). Morphological and physiological adjustment to N and P fertilization in nutrient-limited *Metrosideros polymorpha* canopy trees in Hawaii. *Tree Physiol.* 21, 43–50. doi: 10.1093/treephys/21.1.43

Dan, Z., Li, B. Z., and Yin, Z. J. (2020). Analysis of the characteristics and floristic elements of communities containing *Taxus contorta* Griffith in Zhumulang-Mafeng National Nature Reserve, Tibet. *Plant Sci. J.* 38, 58–67. doi: 10.11913/PSJ.2095-0837.2020.10058

de Bello, F., Lavorel, S., Albert, C. H., Thuiller, W., Grigulis, K., Dolezal, J., et al. (2011). Quantifying the relevance of intraspecific trait variability for functional diversity. *Methods Ecol. Evol.* 2, 163–174. doi: 10.1111/j.2041-210X.2010.00071.x

Deepa, A. (2009). The stabilizing effect of intraspecific genetic variation on population dynamics in novel and ancestral habitats. *Am. Nat.* 174, 255–267. doi: 10.1086/600085

Deng, H. J., Pepin, N. C., and Chen, Y. N. (2017). Changes of snowfall under warming in the Tibetan Plateau. *J. Geophys. Res.-Atmos.* 122, 7323–7341. doi: 10.1002/2017JD026524

Derroire, G., Powers, J. S., Hulshof, C. M., Varela, L. E. C., Healey, J. R., and Sveriges, L. (2018). Contrasting patterns of leaf trait variation among and within species during tropical dry forest succession in Costa Rica. *Sci. Rep.* 8, 285. doi: 10.1038/s41598-017-18525-1

Des Roches, S., Post, D. M., Turley, N. E., Bailey, J. K., Hendry, A. P., Kinnison, M. T., et al. (2018). The ecological importance of intraspecific variation. *Nat. Ecol. Evol.* 2, 57–64. doi: 10.1038/s41559-017-0402-5

de Villemereuil, P., Mouterde, M., Gaggiotti, O. E., and Till-Bottraud, I. (2018). Patterns of phenotypic plasticity and local adaptation in the wide elevation range of the alpine plant *Arabis alpina*. *J. Ecol.* 106, 1952–1971. doi: 10.1111/1365-2745.12955

Diefendorf, A. F., Mueller, K. E., Wing, S. L., Koch, P. L., and Freeman, K. H. (2010). Global patterns in leaf ^{13}C discrimination and implications for studies of past and future climate. *Proc. Natl. Acad. Sci. U. S. A.* 107, 5738–5743. doi: 10.1073/pnas.0910513107

Dobbert, S., Pape, R., and Löffler, J. (2021). How does spatial heterogeneity affect inter- and intraspecific growth patterns in tundra shrubs? *J. Ecol.* 109, 4115–4131. doi: 10.1111/1365-2745.13784

Ehlers, B. K., Damgaard, C. F., and Laroche, F. (2016). Intraspecific genetic variation and species coexistence in plant communities. *Biol. Lett.* 12, 20150853. doi: 10.1098/rsbl.2015.0853

Elser, J. J., Acharya, K., Kyle, M., Cotner, J., Makino, W., Markow, T., et al. (2003). Growth rate-stoichiometry couplings in diverse biota. *Ecol. Lett.* 6, 936–943. doi: 10.1046/j.1461-0248.2003.00518.x

Elser, J. J., Fagan, W. F., Kerkhoff, A. J., Swenson, N. G., and Enquist, B. J. (2010). Biological stoichiometry of plant production: metabolism, scaling and ecological response to global change. *New Phytol.* 186, 593–608. doi: 10.1111/j.1469-8137.2010.03214.x

Galfrascoli, G. M., and Calviño, A. (2020). Secondary sexual dimorphism in a dioecious tree: A matter of inter-plant variability? *Flora* 266, 151595. doi: 10.1016/j.flora.2020.151595

Gaudard, C. A., Robertson, M. P., and Bishop, T. R. (2019). Low levels of intraspecific trait variation in a keystone invertebrate group. *Oecologia* 190, 725–735. doi: 10.1007/s00442-019-04426-9

Gavazov, K., Hagedorn, F., Buttler, A., Siegwolf, R., and Bragazza, L. (2016). Environmental drivers of carbon and nitrogen isotopic signatures in peatland vascular plants along an altitude gradient. *Oecologia* 180, 257–264. doi: 10.1007/s00442-015-3458-4

González-Suárez, M., and Revilla, E. (2013). Variability in life-history and ecological traits is a buffer against extinction in mammals. *Ecol. Lett.* 16, 242–251. doi: 10.1111/ele.12035

Graae, B. J., De Frenne, P., Kolb, A., Brunet, J., Chabrerie, O., Verheyen, K., et al. (2012). On the use of weather data in ecological studies along altitudinal and latitudinal gradients. *Oikos* 121, 3–19. doi: 10.1111/j.1600-0706.2011.19694.x

Güsewell, S., Koerselman, W., and Verhoeven, J. (2003). Biomass N:P ratios as indicators of nutrient limitation for plant populations in wetlands. *Ecol. Appl.* 13, 372–384. doi: 10.1890/1051-0761(2003)013[0372:BNRAIO]2.0.CO;2

Hartl-Meier, C., Zang, C., Dittmar, C., Esper, J., Gottlein, A., and Rothe, A. (2014). Vulnerability of Norway spruce to climate change in mountain forests of the European Alps. *Clim. Res.* 60, 119–132. doi: 10.3354/cr01226

Hart, S. P., Schreiber, S. J., and Levine, J. M. (2016). How variation between individuals affects species coexistence. *Ecol. Lett.* 19, 825–838. doi: 10.1111/ele.12618

He, D., Biswas, S. R., Xu, M. S., Yang, T. H., You, W. H., and Yan, E. R. (2021). The importance of intraspecific trait variability in promoting functional niche dimensionality. *Ecography* 44, 380–390. doi: 10.1111/ecog.05254

He, D., Chen, Y. F., Zhao, K. N., Cornelissen, J. H. C., and Chu, C. J. (2018). Intra- and interspecific trait variations reveal functional relationships between specific leaf area and soil niche within a subtropical forest. *Ann. Bot.* 121, 1173–1182. doi: 10.1093/aob/mcx222

Heilmeier, H. (2019). Functional traits explaining plant responses to past and future climate changes. *Flora* 254, 1–11. doi: 10.1016/j.flora.2019.04.004

Herrmann, S. M., Didan, K., Barreto-Munoz, A., and Crimmins, M. A. (2016). Divergent responses of vegetation cover in Southwestern US ecosystems to dry and wet years at different elevations. *Environ. Res. Lett.* 11, 124005. doi: 10.1088/1748-9326/11/12/124005

Homeier, J., Seeler, T., Pierick, K., and Leuschner, C. (2021). Leaf trait variation in species-rich tropical Andean forests. *Sci. Rep.* 11, 9993. doi: 10.1038/s41598-021-89190-8

Hu, Y. K., Liu, G. F., Pan, X., Song, Y. B., Dong, M., and Cornelissen, J. H. C. (2022). Contrasting nitrogen cycling between herbaceous wetland and terrestrial ecosystems inferred from plant and soil nitrogen isotopes across China. *J. Ecol.* 110, 1259–1270. doi: 10.1111/1365-2745.13866

Hu, Y. K., Pan, X., Liu, G. F., Li, W. B., Dai, W. H., Tang, S. L., et al. (2015). Novel evidence for within-species leaf economics spectrum at multiple spatial scales. *Front. Plant Sci.* 6, 901. doi: 10.3389/fpls.2015.00901

Hu, Y. K., Pan, X., Yang, X. J., Liu, G. F., Liu, X. Y., Song, Y. B., et al. (2019). Is there coordination of leaf and fine root traits at local scales? A test in temperate forest swamps. *Ecol. Evol.* 9, 8714–8723. doi: 10.1002/ece3.5421

Hu, Y. K., Zhang, Y. L., Liu, G. F., Pan, X., Yang, X., Li, W. B., et al. (2017). Intraspecific N and P stoichiometry of *Phragmites australis*: Geographic patterns and variation among climatic regions. *Sci. Rep.* 7, 43018. doi: 10.1038/srep43018

Hua, L., He, P., Goldstein, G., Liu, H., Yin, D., Zhu, S., et al. (2020). Linking vein properties to leaf biomechanics across 58 woody species from a subtropical forest. *Plant Biol.* 22, 212–220. doi: 10.1111/plb.13056

Huang, M. J., Liu, X., and Zhou, S. R. (2020). Asynchrony among species and functional groups and temporal stability under perturbations: Patterns and consequences. *J. Ecol.* 108, 2038–2046. doi: 10.1111/1365-2745.13418

Hultine, K. R., Bush, S. E., Ward, J. K., and Dawson, T. E. (2018). Does sexual dimorphism predispose dioecious riparian trees to sex ratio imbalances under climate change? *Oecologia* 187, 921–931. doi: 10.1007/s00442-018-4190-7

Hultine, K. R., Grady, K. C., Wood, T. E., Shuster, S. M., Stella, J. C., and Whitham, T. G. (2016). Climate change perils for dioecious plant species. *Nat. Plants* 2, 16109. doi: 10.1038/nplants.2016.109

Hultine, K. R., and Marshall, J. D. (2000). Altitude trends in conifer leaf morphology and stable carbon isotope composition. *Oecologia* 123, 32–40. doi: 10.1007/s004420050986

Iszkuło, G., Jasińska, A. K., Giertych, M. J., and Boratyński, A. (2009). Do secondary sexual dimorphism and female intolerance to drought influence the sex ratio and extinction risk of *Taxus baccata*? *Plant Ecol.* 200, 229–240. doi: 10.1007/s11258-008-9447-5

Joswig, J. S., Wirth, C., Schuman, M. C., Kattge, J., Reu, B., Wright, I. J., et al. (2022). Climatic and soil factors explain the two-dimensional spectrum of global plant trait variation. *Nat. Ecol. Evol.* 6, 36–50. doi: 10.1038/s41559-021-01616-8

Jung, V., Albert, C. H., Violle, C., Kunstler, G., Loucougaray, G., and Spiegelberger, T. (2014). Intraspecific trait variability mediates the response of subalpine grassland communities to extreme drought events. *J. Ecol.* 102, 45–53. doi: 10.1111/1365-2745.12177

Juvany, M., and Munné-Bosch, S. (2015). Sex-related differences in stress tolerance in dioecious plants: A critical appraisal in a physiological context. *J. Exp. Bot.* 66, 6083–6092. doi: 10.1093/jxb/erv343

Koerselman, W., and Meuleman, A. F. M. (1996). The vegetation N:P ratio: A new tool to detect the nature of nutrient limitation. *J. Appl. Ecol.* 33, 1441–1450. doi: 10.2307/2404783

Körner, C. (2007). The use of 'altitude' in ecological research. *Trends Ecol. Evol.* 22, 569–574. doi: 10.1016/j.tree.2007.09.006

Kostikova, A., Silvestro, D., Pearman, P. B., and Salamin, N. (2016). Bridging inter- and intraspecific trait evolution with a hierarchical Bayesian approach. *Syst. Biol.* 65, 417–431. doi: 10.1093/sysbio/syw010

Kumordzi, B. B., Nilsson, M. C., Gundale, M. J., and Wardle, D. A. (2014). Changes in local-scale intraspecific trait variability of dominant species across contrasting island ecosystems. *Ecosphere* 5, 26. doi: 10.1890/ES13-00339.1

Lajoie, G., and Vellend, M. (2018). Characterizing the contribution of plasticity and genetic differentiation to community-level trait responses to environmental change. *Ecol. Evol.* 8, 3895–3907. doi: 10.1002/ece3.3947

Laughlin, D. C., Lusk, C. H., Bellingham, P. J., Burslem, D. F. R. P., Simpson, A. H., and Kramer-Walter, K. R. (2017). Intraspecific trait variation can weaken interspecific trait correlations when assessing the whole-plant economic spectrum. *Ecol. Evol.* 7, 8936–8949. doi: 10.1002/ece3.3447

LeBauer, D. S., and Treseder, K. K. (2008). Nitrogen limitation of net primary productivity in terrestrial ecosystems is globally distributed. *Ecology* 89, 371–379. doi: 10.1890/06-2057.1

Lefcheck, J. S. (2016). piecewiseSEM: Piecewise structural equation modelling in R for ecology, evolution, and systematics. *Methods Ecol. Evol.* 7, 573–579. doi: 10.1111/2041-210X.12512

Lei, Y. B., Jiang, Y. L., Chen, K., Duan, B. L., Zhang, S., Korpelainen, H., et al. (2017). Reproductive investments driven by sex and altitude in sympatric *Populus* and *Salix* trees. *Tree Physiol.* 37, 1503–1514. doi: 10.1093/treephys/tpx075

LeRoy, C. J., Ramstack Hobbs, J. M., Claeson, S. M., Moffett, J., Garthwaite, I., Criss, N., et al. (2020). Plant sex influences aquatic-terrestrial interactions. *Ecosphere* 11, e02994. doi: 10.1002/ecs2.2994

Li, M. X., Peng, C. H., Wang, M., Yang, Y. Z., Zhang, K. R., Li, P., et al. (2017). Spatial patterns of leaf δ^{13}C and its relationship with plant functional groups and environmental factors in China. *J. Geophys. Res.-Biogeosci.* 122, 1564–1575. doi: 10.1002/2016JG003529

Li, T. X., Xu, L., Wang, F., Zhang, W. J., Duan, J. P., Shen-Tu, X. L., et al. (2022). Novel evidence from *Taxus fuana* forests for niche-neutral process assembling community. *For. Ecosyst.* 9, 100035. doi: 10.1016/j.fecs.2022.100035

Li, C. Y., Xu, G., Zang, R. G., Korpelainen, H., and Berninger, F. (2007). Sex-related differences in leaf morphological and physiological responses in *Hippophae rhamnoides* along an altitudinal gradient. *Tree Physiol.* 27, 399–406. doi: 10.1093/treephys/27.3.399

Lin, H. Y., Tseng, Y. H., Hsieh, C. F., and Hu, J. M. (2020). Geographical distribution of dioecy and its ecological correlates based on fine-scaled species distribution data from a subtropical island. *Ecol. Res.* 35, 170–181. doi: 10.1111/1440-1703.12068

Liu, W. G., and Wang, Z. (2009). Nitrogen isotopic composition of plant-soil in the loess plateau and its responding to environmental change. *Chin. Sci. Bull.* 54, 272–279. doi: 10.1007/s11434-008-0442-y

Liu, S. G., Wang, H., Tian, P., Yao, X., Sun, H., Wang, Q. K., et al. (2020). Decoupled diversity patterns in bacteria and fungi across continental forest ecosystems. *Soil Biol. Biochem.* 144, 107763. doi: 10.1016/j.soilbio.2020.107763

Luce, C. H., Abatzoglou, J. T., and Holden, Z. A. (2013). The missing mountain water: Slower westerlies decrease orographic enhancement in the Pacific Northwest USA. *Science* 342, 1360–1364. doi: 10.1126/science.1242335

Mathiasen, P., and Premoli, A. C. (2016). Living on the edge: adaptive and plastic responses of the tree *Nothofagus pumilio* to a long-term transplant experiment predict rear-edge upward expansion. *Oecologia* 181, 607–619. doi: 10.1007/s00442-016-3568-7

McGroddy, M. E., Daufresne, T., and Hedin, L. O. (2004). Scaling of C: N: P stoichiometry in forests worldwide: Implications of terrestrial Redfield-type ratios. *Ecology* 85, 2390–2401. doi: 10.1890/03-0351

Meinzer, F. C., Lachenbruch, B., and Dawson, T. E. (2011). *Size- and age-related changes in tree structure and function* (Corvallis: Springer Netherlands). doi: 10.1007/978-94-007-1242-3

Melnikova, N. V., Borkhert, E. V., Snezhkina, A. V., Kudryavtseva, A. V., and Dmitriev, A. A. (2017). Sex-specific response to stress in *Populus*. *Front. Plant Sci.* 8, 1827. doi: 10.3389/fpls.2017.01827

Meng, H., Wei, X., Franklin, S. B., Wu, H., and Jiang, M. (2017). Geographical variation and the role of climate in leaf traits of a relict tree species across its distribution in China. *Plant Biol.* 19, 552–561. doi: 10.1111/plb.12564

Messier, J., McGill, B. J., and Lechowicz, M. J. (2010). How do traits vary across ecological scales? A case for trait-based ecology. *Ecol. Lett.* 13, 838–848. doi: 10.1111/j.1461-0248.2010.01476.x

Moran, N. P., Caspers, B. A., Chakarov, N., Ernst, U. R., Fricke, C., Kurtz, J., et al. (2022). Shifts between cooperation and antagonism driven by individual variation: A systematic synthesis review. *Oikos* 2022, e08201. doi: 10.1111/oik.08201

Moran, E. V., Hartig, F., and Bell, D. M. (2016). Intraspecific trait variation across scales: Implications for understanding global change responses. *Glob. Change Biol.* 22, 137–150. doi: 10.1111/gcb.13000

Moser, L., Fonti, P., Büntgen, U., Esper, J., Luterbacher, J., Franzen, J., et al. (2010). Timing and duration of European larch growing season along altitudinal gradients in the Swiss Alps. *Tree Physiol.* 30, 225–233. doi: 10.1093/treephys/tpp108

Mougi, A. (2020). Natural selection contributes to food web stability. *PLoS One* 15, e227420. doi: 10.1371/journal.pone.0227420

Munné-Bosch, S. (2015). Sex ratios in dioecious plants in the framework of global change. *Environ. Exp. Bot.* 109, 99–102. doi: 10.1016/j.envexpbot.2014.08.007

Myers-Smith, I. H., Thomas, H. J. D., and Bjorkman, A. D. (2019). Plant traits inform predictions of tundra responses to global change. *New Phytol.* 221, 1742–1748. doi: 10.1111/nph.15592

Nakagawa, S., and Schielzeth, H. (2013). A general and simple method for obtaining R^2 from generalized linear mixed-effects models. *Methods Ecol. Evol.* 4, 133–142. doi: 10.1111/j.2041-210x.2012.00261.x

Navarro, T., El Oualidi, J., Taleb, M. S., Pascual, V., Cabezudo, B., and Milla, R. (2010). Leaf patterns, leaf size and ecologically related traits in high Mediterranean mountain on the Moroccan High Atlas. *Plant Ecol.* 210, 275–290. doi: 10.1007/s11258-010-9756-3

Niinemets, U., Keenan, T. F., and Hallik, L. (2015). A worldwide analysis of within-canopy variations in leaf structural, chemical and physiological traits across plant functional types. *New Phytol.* 205, 973–993. doi: 10.1111/nph.13096

Obeso, J. R. (2002). The costs of reproduction in plants. *New Phytol.* 155, 321–348. doi: 10.1046/j.1469-8137.2002.00477.x

Ohri, D., and Rastogi, S. (2020). Sex determination in gymnosperms. *Nucleus* 63, 75–80. doi: 10.1007/s13237-019-00297-w

Onoda, Y., Westoby, M., Adler, P. B., Choong, A. M. F., Clissold, F. J., Cornelissen, J. H. C., et al. (2011). Global patterns of leaf mechanical properties. *Ecol. Lett.* 14, 301–312. doi: 10.1111/j.1461-0248.2010.01582.x

Ortiz, P. L., Arista, M., and Talavera, S. (2002). Sex ratio and reproductive effort in the dioecious *Juniperus communis* subsp. *alpina* (Suter) Čelak. (Cupressaceae) along an altitudinal gradient. *Ann. Bot.* 89, 205–211. doi: 10.1093/aob/mcf028

Pascual, M., Lordan, J., Villar, J. M., Fonseca, F., and Rufat, J. (2013). Stable carbon and nitrogen isotope ratios as indicators of water status and nitrogen effects on peach trees. *Sci. Hortic.* 157, 99–107. doi: 10.1016/j.scienta.2013.04.007

Pérez-Harguindeguy, N., Díaz, S., Garnier, E., Lavorel, S., Poorter, H., Jaureguiberry, P., et al. (2013). New handbook for standardised measurement of plant functional traits worldwide. *Aust. J. Bot.* 61, 167–234. doi: 10.1071/BT12225

Pinheiro, J., Bates, D., Debroy, S., Sarkar, D., and R Core Team (2014). *nlme*: Linear and nonlinear mixed effects model. *R package version* 3, 1–117. Available at: http://CRAN.R-project.org/package=nlme

Poudel, R. C., Gao, L. M., Möller, M., Baral, S. R., Uprety, Y., Liu, J., et al. (2013). Yews (*Taxus*) along the Hindu Kush-Himalayan region: Exploring the ethnopharmacological relevance among communities of Mongol and Caucasian origins. *J. Ethnopharmacol.* 147, 190–203. doi: 10.1016/j.jep.2013.02.031

R Core Team (2022). *R: A language and environment for statistical computing* (Vienna, Austria: R Foundation for Statistical Computing). Available at: https://www.R-project.org/.

Raffard, A., Santoul, F., Cucherousset, J., and Blanchet, S. (2019). The community and ecosystem consequences of intraspecific diversity: A meta-analysis. *Biol. Rev.* 94, 648–661. doi: 10.1111/brv.12472

Rathee, S., Ahmad, M., Sharma, P., Singh, H. P., Batish, D. R., Kaur, S., et al. (2021). Biomass allocation and phenotypic plasticity are key elements of successful invasion of *Parthenium hysterophorus* at high elevation. *Environ. Exp. Bot.* 184, 104392. doi: 10.1016/j.envexpbot.2021.104392

Read, J., and Sanson, G. D. (2003). Characterizing sclerophylly: The mechanical properties of a diverse range of leaf types. *New Phytol.* 160, 81–99. doi: 10.1046/j.1469-8137.2003.00855.x

Reich, P. B., and Oleksyn, J. (2004). Global patterns of plant leaf N and P in relation to temperature and latitude. *Proc. Natl. Acad. Sci. U. S. A.* 101, 11001–11006. doi: 10.1073/pnas.0403588101

Retuerto, R., Sánchez Vilas, J., and Varga, S. (2018). Sexual dimorphism in response to stress. *Environ. Exp. Bot.* 146, 1–4. doi: 10.1016/j.envexpbot.2017.12.006

Rixen, C., Wipf, S., Rumpf, S. B., Giejsztowt, J., Millen, J., Morgan, J. W., et al. (2022). Intraspecific trait variation in alpine plants relates to their elevational distribution. *J. Ecol.* 110, 860–875. doi: 10.1111/1365-2745.13848

Senthilnathan, A., and Gavrilets, S. (2021). Ecological consequences of intraspecific variation in coevolutionary systems. *Am. Nat.* 197, 1–17. doi: 10.1086/711886

Severns, P. M., and Liston, A. (2008). Intraspecific chromosome number variation: A neglected threat to the conservation of rare plants. *Conserv. Biol.* 22, 1641–1647. doi: 10.1111/j.1523-1739.2008.01058.x

Seyedi, N., Costa, C., Máguas, C., and Correia, O. (2019). The contribution of leaf life span to sexual dimorphism in deciduous and evergreen *Pistacia* species under Mediterranean conditions. *Flora* 251, 114–121. doi: 10.1016/j.flora.2019.01.005

Shah, A., Li, D. Z., Gao, L. M., Li, H. T., and Möller, M. (2008). Genetic diversity within and among populations of the endangered species *Taxus fuana* (Taxaceae) from Pakistan and implications for its conservation. *Biochem. Syst. Ecol.* 36, 183–193. doi: 10.1016/j.bse.2007.09.012

Shao, J. J., Yuan, T. F., Li, Z., Li, N., Liu, H. Y., Bai, S. H., et al. (2019). Plant evolutionary history mainly explains the variance in biomass responses to climate warming at a global scale. *New Phytol.* 222, 1338–1351. doi: 10.1111/nph.15695

Shipley, B., de Bello, F., Cornelissen, J. H. C., Laliberté, E., Laughlin, D. C., and Reich, P. B. (2016). Reinforcing loose foundation stones in trait-based plant ecology. *Oecologia* 180, 923–931. doi: 10.1007/s00442-016-3549-x

Sidor, C. G., Popa, I., Vlad, R., and Cherubini, P. (2015). Different tree-ring responses of Norway spruce to air temperature across an altitudinal gradient in the Eastern Carpathians (Romania). *Trees* 29, 985–997. doi: 10.1007/s00468-015-1178-3

Siefert, A., Violle, C., Chalmandrier, L., Albert, C. H., Taudiere, A., Fajardo, A., et al. (2015). A global meta-analysis of the relative extent of intraspecific trait variation in plant communities. *Ecol. Lett.* 18, 1406–1419. doi: 10.1111/ele.12508

Šípek, V., and Tesař, M. (2014). Seasonal snow accumulation in the mid-latitude forested catchment. *Biologia* 69, 1562–1569. doi: 10.2478/s11756-014-0468-3

Song, Y. B., Li, W. B., Dai, W. H., and Dong, M. (2016). Does sex constrain functional clonal traits and their responses to environmental heterogeneity in the stoloniferous herb *Glechoma longituba*? *Flora* 218, 18–23. doi: 10.1016/j.flora.2015.11.004

Song, Y. B., Shen-Tu, X. L., and Dong, M. (2020a). Intraspecific variation of samara dispersal traits in the endangered tropical tree *Hopea hainanensis* (Dipterocarpaceae). *Front. Plant Sci.* 11, 599764. doi: 10.3389/fpls.2020.599764

Song, Y. B., Xu, L., Duan, J. P., Zhang, W. J., Shen-Tu, X. L., Li, T. X., et al. (2020b). Sex ratio and spatial pattern of *Taxus fuana*, a wild plant with extremely small populations in Tibet. *Biodivers. Sci.* 28, 269–276. doi: 10.17520/biods.2019102

Stefanović, M., Nikolić, B., Matić, R., Popović, Z., Vidaković, V., and Bojović, S. (2017). Exploration of sexual dimorphism of *Taxus baccata* L. needles in natural populations. *Trees* 31, 1697–1710. doi: 10.1007/s00468-017-1579-6

Stegmann, U. E. (2021). A willow drawing from 1786: The earliest depiction of intraspecific trait variation in plants? *Ann. Bot.* 127, 411–412. doi: 10.1093/aob/mcaa091

Steinmetz, B., Kalyuzhny, M., and Shnerb, N. M. (2020). Intraspecific variability in fluctuating environments: Mechanisms of impact on species diversity. *Ecology* 101, e3174. doi: 10.1002/ecy.3174

Suding, K. N., Lavorel, S., Chapin, F. S., Cornelissen, J. H. C., Díaz, S., Garnier, E., et al. (2008). Scaling environmental change through the community-level: A trait-based response-and-effect framework for plants. *Glob. Change Biol.* 14, 1125–1140. doi: 10.1111/j.1365-2486.2008.01557.x

Tang, L. L., Morris, W. K., Zhang, M., Shi, F. C., and Vesk, P. A. (2022). Exploring how functional traits modulate species distributions along topographic gradients in Baxian Mountain, North China. *Sci. Rep.* 12, 994. doi: 10.1038/s41598-021-04210-x

Tan, L., Song, Y. B., Fu, R. H., Liu, M., Li, Y., Escudero, M., et al. (2022). Variation of stable carbon and nitrogen isotopes ratio in *Ficus tikoua* and their linkage to its specific pollinator. *Flora* 291, 152073. doi: 10.1016/j.flora.2022.152073

Thakur, D., Rathore, N., and Chawla, A. (2019). Increase in light interception cost and metabolic mass component of leaves are coupled for efficient resource use in the high altitude vegetation. *Oikos* 128, 254–263. doi: 10.1111/oik.05538

Thompson, K., Parkinson, J. A., Band, S. R., and Spencer, R. E. (1997). A comparative study of leaf nutrient concentrations in a regional herbaceous flora. *New Phytol.* 136, 679–689. doi: 10.1046/j.1469-8137.1997.00787.x

Tognetti, R. (2012). Adaptation to climate change of dioecious plants: Does gender balance matter? *Tree Physiol.* 32, 1321–1324. doi: 10.1093/treephys/tps105

Turner, S. R., Lewandrowski, W., Elliott, C. P., Merino-Martín, L., Miller, B. P., Stevens, J. C., et al. (2017). Seed ecology informs restoration approaches for threatened species in water-limited environments: A case study on the short-range Banded Ironstone endemic *Ricinocarpos brevis* (Euphorbiaceae). *Aust. J. Bot.* 65, 661–677. doi: 10.1071/BT17155

van Bodegom, P. M., Douma, J. C., and Verheijen, L. M. (2014). A fully traits-based approach to modeling global vegetation distribution. *Proc. Natl. Acad. Sci. U. S. A.* 111, 13733–13738. doi: 10.1073/pnas.1304551110

Waigwa, A. N., Mwangi, B. N., Wahiti, G. R., Omengo, F., Zhou, Y. D., and Wang, Q. F. (2020). Variation of morphological and leaf stoichiometric traits of two endemic species along the elevation gradient of Mount Kenya, East Africa. *J. Plant Ecol.* 13, 785–792. doi: 10.1093/jpe/rtaa067

Walas, Ł., Mandryk, W., Thomas, P. A., Tyrała-Wierucka, Ż, and Iszkuło, G. (2018). Sexual systems in gymnosperms: A review. *Basic Appl. Ecol.* 31, 1–9. doi: 10.1016/j.baae.2018.05.009

Wang, X., Jiang, Y., Ren, H. Y., Yu, F. H., and Li, M. H. (2019). Leaf and soil $\delta^{15}N$ patterns along elevational gradients at both treelines and shrublines in three different climate zones. *Forests* 10, 557. doi: 10.3390/f10070557

Wang, J. Y., Wang, J. N., Guo, W. H., Li, Y. G., Wang, G. G., and Wu, T. G. (2018). Stoichiometric homeostasis, physiology, and growth responses of three tree species to nitrogen and phosphorus addition. *Trees* 32, 1377–1386. doi: 10.1007/s00468-018-1719-7

Wang, S. T., Xu, Y. Z., Wei, X. Z., and Jiang, M. X. (2022). Do leaf functional traits differ between 20-35-year-old transplanted and wild source populations? A case study involving five endangered tree species. *Nat. Conserv. Res.* 7, 32–41. doi: 10.24189/ncr.2022.016

Westerband, A. C., Funk, J. L., and Barton, K. E. (2021). Intraspecific trait variation in plants: A renewed focus on its role in ecological processes. *Ann. Bot.* 127, 397–410. doi: 10.1093/aob/mcab011

Wu, J. M., Shi, Z. M., Liu, S., Centritto, M., Cao, X. W., Zhang, M. M., et al. (2021). Photosynthetic capacity of male and female *Hippophae rhamnoides* plants along an elevation gradient in eastern Qinghai-Tibetan plateau, China. *Tree Physiol.* 41, 76–88. doi: 10.1093/treephys/tpaa105

Xia, Z. C., He, Y., Yu, L., Lv, R. B., Korpelainen, H., and Li, C. Y. (2020). Sex-specific strategies of phosphorus (P) acquisition in *Populus cathayana* as affected by soil P availability and distribution. *New Phytol.* 225, 782–792. doi: 10.1111/nph.16170

Xu, W. M., Tomlinson, K. W., and Li, J. (2020). Strong intraspecific trait variation in a tropical dominant tree species along an elevational gradient. *Plant Divers.* 42, 1–6. doi: 10.1016/j.pld.2019.10.004

Yang, Y. H., Ji, C. J., Robinson, D., Zhu, B., Fang, H. J., Shen, H. H., et al. (2013). Vegetation and soil ^{15}N natural abundance in alpine grasslands on the Tibetan Plateau: Patterns and implications. *Ecosystems* 16, 1013–1024. doi: 10.1007/s10021-013-9664-1

Yang, Y. H., and Luo, Y. Q. (2011). Carbon: nitrogen stoichiometry in forest ecosystems during stand development. *Glob. Ecol. Biogeogr.* 20, 354–361. doi: 10.1111/j.1466-8238.2010.00602.x

Zhang, Y. Q., Li, Z. C., Song, L. G., Hou, L. Y., and Sun, Q. W. (2020). Natural distribution and community ecological characteristics of *Taxus fuana*. *Acta Ecol. Sin.* 40, 1999–2009. doi: 10.5846/stxb201809282117

Zhang, R., Liu, J. Y., Liu, Q. S., He, H. G., Xu, X., and Dong, T. F. (2019). Sexual differences in growth and defence of *Populus yunnanensis* under drought stress. *Can. J. For. Res.* 49, 491–499. doi: 10.1139/cjfr-2018-0270

Zhang, X. S., Wang, C., and Zhou, C. N. (2022). The variation of functional traits in leaves and current-year twigs of *Quercus aquifolioides* along an altitudinal gradient in Southeastern Tibet. *Front. Ecol. Evol.* 10, 855547. doi: 10.3389/fevo.2022.855547

Zhang, Z. M., and Yu, S. X. (2018). Potential tradeoffs between intraspecific and interspecific trait variations along an environmental gradient in a subtropical forest. *J. Forest. Res.* 29, 1731–1740. doi: 10.1007/s11676-018-0594-9

Zheng, J., Jiang, Y., Qian, H., Mao, Y. J., Zhang, C., Tang, X. X., et al. (2022). Size-dependent and environment-mediated shifts in leaf traits of a deciduous tree species in a subtropical forest. *Ecol. Evol.* 12, e8516. doi: 10.1002/ece3.8516

Zhou, Y. C., Fan, J. W., Zhang, W. Y., Harris, W., Zhong, H. P., Hu, Z. M., et al. (2011). Factors influencing altitudinal patterns of C_3 plant foliar carbon isotope composition of grasslands on the Qinghai-Tibet Plateau, China. *Alp. Bot.* 121, 79–90. doi: 10.1007/s00035-011-0093-5

Frontiers in
Plant Science

Cultivates the science of plant biology and its applications

The most cited plant science journal, which advances our understanding of plant biology for sustainable food security, functional ecosystems and human health.

Discover the latest Research Topics

See more →

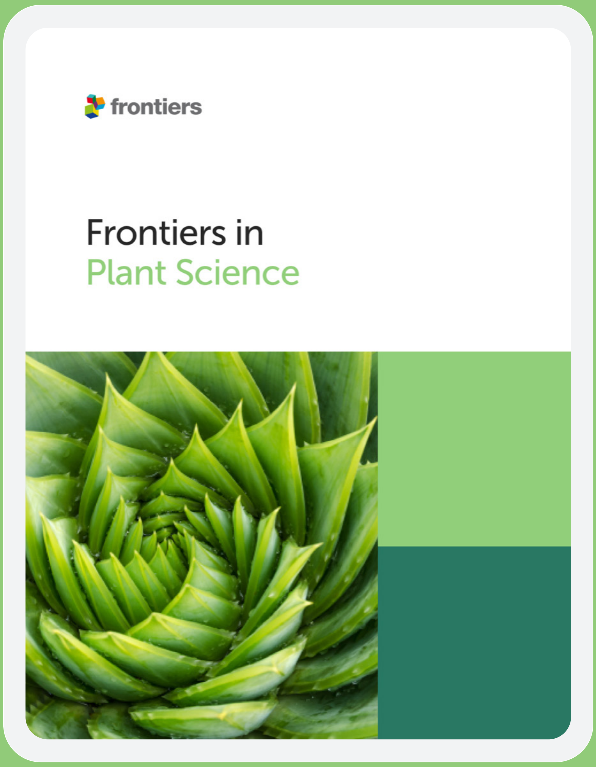

frontiers

Frontiers in
Plant Science

Frontiers
Avenue du Tribunal-Fédéral 34
1005 Lausanne, Switzerland
frontiersin.org

Contact us
+41 (0)21 510 17 00
frontiersin.org/about/contact

frontiers | Research Topics